# UNDERSTANDING THE INTERPLAY BETWEEN THE TUMOR IMMUNE MICROENVIRONMENT AND GENETIC ALTERATIONS IN THORACIC MALIGNANCIES

EDITED BY: Giulia Pasello, Emanuela Felley-Bosco and Jordi Remon
PUBLISHED IN: Frontiers in Oncology

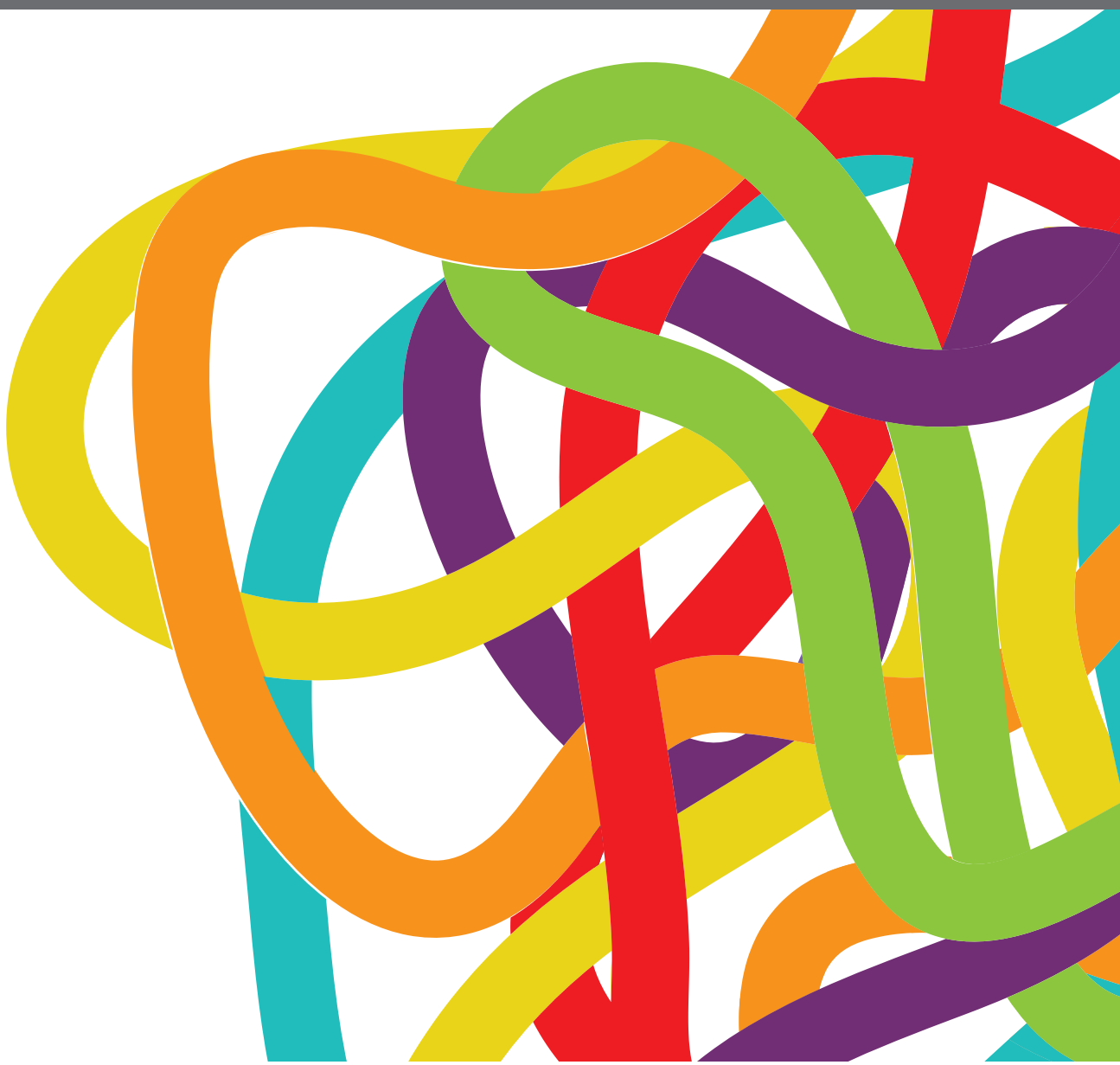

frontiers Research Topics

ISSN 1664-8714
ISBN 978-2-88974-818-1
DOI 10.3389/978-2-88974-818-1

## About Frontiers

Frontiers is more than just an open-access publisher of scholarly articles: it is a pioneering approach to the world of academia, radically improving the way scholarly research is managed. The grand vision of Frontiers is a world where all people have an equal opportunity to seek, share and generate knowledge. Frontiers provides immediate and permanent online open access to all its publications, but this alone is not enough to realize our grand goals.

## Frontiers Journal Series

The Frontiers Journal Series is a multi-tier and interdisciplinary set of open-access, online journals, promising a paradigm shift from the current review, selection and dissemination processes in academic publishing. All Frontiers journals are driven by researchers for researchers; therefore, they constitute a service to the scholarly community. At the same time, the Frontiers Journal Series operates on a revolutionary invention, the tiered publishing system, initially addressing specific communities of scholars, and gradually climbing up to broader public understanding, thus serving the interests of the lay society, too.

## Dedication to Quality

Each Frontiers article is a landmark of the highest quality, thanks to genuinely collaborative interactions between authors and review editors, who include some of the world's best academicians. Research must be certified by peers before entering a stream of knowledge that may eventually reach the public - and shape society; therefore, Frontiers only applies the most rigorous and unbiased reviews.
Frontiers revolutionizes research publishing by freely delivering the most outstanding research, evaluated with no bias from both the academic and social point of view. By applying the most advanced information technologies, Frontiers is catapulting scholarly publishing into a new generation.

## What are Frontiers Research Topics?

Frontiers Research Topics are very popular trademarks of the Frontiers Journals Series: they are collections of at least ten articles, all centered on a particular subject. With their unique mix of varied contributions from Original Research to Review Articles, Frontiers Research Topics unify the most influential researchers, the latest key findings and historical advances in a hot research area! Find out more on how to host your own Frontiers Research Topic or contribute to one as an author by contacting the Frontiers Editorial Office: frontiersin.org/about/contact

# UNDERSTANDING THE INTERPLAY BETWEEN THE TUMOR IMMUNE MICROENVIRONMENT AND GENETIC ALTERATIONS IN THORACIC MALIGNANCIES

Topic Editors:
**Giulia Pasello,** Veneto Institute of Oncology (IRCCS), Italy
**Emanuela Felley-Bosco,** University of Zurich, Switzerland
**Jordi Remon,** Hospital HM Delfos, Spain

**Citation:** Pasello, G., Felley-Bosco, E., Remon, J., eds. (2022). Understanding the Interplay Between the Tumor Immune Microenvironment and Genetic Alterations in Thoracic Malignancies. Lausanne: Frontiers Media SA.
doi: 10.3389/978-2-88974-818-1

# Table of Contents

frontiers in Oncology

EDITORIAL
published: 10 March 2022
doi: 10.3389/fonc.2022.871544

# Editorial: Understanding the Interplay Between the Tumor Immune Microenvironment and Genetic Alterations in Thoracic Malignancies

*Giulia Pasello*[1,2]*, *Jordi Remon*[3] *and Emanuela Felley-Bosco*[4]

[1] Department of Surgery, Oncology and Gastroenterology, University of Padua, Padua, Italy, [2] Medical Oncology 2, Istituto Oncologico Veneto Instituto di Ricerca e Cura a Carattere Scientifico (IOV IRCCS), Padua, Italy, [3] Department of Medical Oncology, Centro Integral Oncológico Clara Campal (HM-CIOCC), Hospital HM Nou Delfos, HM Hospitales, Barcelona, Spain, [4] Laboratory of Molecular Oncology, Department of Thoracic Surgery, University Hospital Zurich, Zurich, Switzerland

**Keywords: tumor immune microenvironment, genetic alteration, lung cancer, mesothelioma, thymic epithelial tumor (TET)**

**Editorial on the Research Topic**

**Understanding the Interplay Between the Tumor Immune Microenvironment and Genetic Alterations in Thoracic Malignancies**

OPEN ACCESS

***Edited and reviewed by:***
*Katy Rezvani,*
*University of Texas MD Anderson Cancer Center, United States*

***Correspondence:**
*Giulia Pasello*
*giulia.pasello@iov.veneto.it;*
*giulia.pasello@unipd.it*

***Specialty section:***
*This article was submitted to Cancer Immunity and Immunotherapy, a section of the journal Frontiers in Oncology*

***Received:*** *08 February 2022*
***Accepted:*** *10 February 2022*
***Published:*** *10 March 2022*

***Citation:***
*Pasello G, Remon J and Felley-Bosco E (2022) Editorial: Understanding the Interplay Between the Tumor Immune Microenvironment and Genetic Alterations in Thoracic Malignancies. Front. Oncol. 12:871544. doi: 10.3389/fonc.2022.871544*

Harnessing immune response to attack tumor cells has proven to be a successful treatment strategy against advanced thoracic malignancies. This immune checkpoint blockade (ICB) strategy with anti-PD-(L)1 and anti-CTLA4 monoclonal antibodies has reported durable responses and has significantly improved the overall survival rates either as monotherapy in selected tumors, or as a combination with immunotherapy and/or chemotherapy in all thoracic malignancies, except thymic epithelial tumors (TET) (1–3). PD-L1 expression in tumor cells is the most robust predictive biomarker for the efficacy of the ICB strategy. Nowadays, an increasing body of literature suggests a crucial role for the tumor microenvironment (TME) in cancer progression and therapeutic responses. Therefore, other potential biomarkers are being explored such as tumor-infiltrating lymphocytes (TILs), tumor-associated macrophages (TAMs), and cancer-associated fibroblasts (CAFs). Likewise, tumor mutational burden and immune-related genetic signatures are being tested with the aim to select those patients most likely to obtain a true benefit from this strategy, and avoid exposure to potential toxicity in patients who will not obtain clinical benefit (Chen et al.). In this Research Topic, a group of international authors discuss the current advances in the study of the interplay between the TME and genetic alterations in thoracic malignancies, such as non-small cell lung cancer (NSCLC), small cell lung cancer (SCLC), pleural mesothelioma (PM), and thymic epithelial tumors (TETs). This Frontiers in Oncology issue includes novel data (Alves et al.; Cao et al.; Chen et al.; Du et al.; Pezzuto et al.; Xu et al.) and review papers (Behrouzfar et al.; Grard et al.; Hiltbrunner et al.; Principe et al.; van Genugten et al.Wadowski et al.).

The predictive and prognostic role of the TME as a whole and the correlation of specific phenotypes with differential gene expressions and clinical-pathological features of lung adenocarcinoma has been recently investigated. The construction of a TME-score on the basis of the genetic signatures involved in T-cell activation, lymphocyte proliferation, and mononuclear cell

proliferation has been suggested as a useful prognostic and predictive tool for patients receiving ICB (Chen et al.).

CD8+ T cells are one of the central effector cells in the immune microenvironment and play a vital role in the development and progression of lung adenocarcinoma (LUAD). Du et al. explored the key genes related to CD8+ T-cell infiltration in 529 LUAD-related samples from TCGA and developed a novel prognosis model based on these genes. The risk score was negatively related to CD8+ T-cell infiltration and correlated with the advanced tumor stage (Du et al.). Clinical applicability of this score could be relevant in the coming future as the adjuvant ICB strategy is accepted in completely resected PD-L1-positive stage II-IIIA NSCLC (4).

The crucial role of T-cell activation and TME modeling in predicting the survival of lung cancer patients has also been highlighted by the work by Cao et al., which showed longer survival in lung cancer patients functionally enriched with platelet endothelial cell adhesion molecule-1, a molecule involved in T-cell response regulation and migration (Cao et al.).

In the coming future it would be relevant to explore the role of potential biomarkers that select patients who cannot obtain benefit from the ICB strategy. As an example, in LUAD, the *STK11* and *KEAP1* mutations confer worse outcomes to immunotherapy among patients with KRAS mutant NSCLC but not among KRAS wild-type LUAD (5). Similarly, Grard et al. reviewed the role of homozygous co-deletion of type I interferons and CDKN2A, due to their co-localization in chromosome 9, in thoracic cancers and its consequences for therapy such as oncolytic therapy. Indeed, this co-deletion has been observed in a large proportion of mesothelioma patients and, together with the status of tumor suppressor BRCA-associated protein 1 (BAP1), is part of the genetic effect on the immune phenotype, as reviewed by Wadowski et al. In this and the complementary review by Hiltbrunner et al., they summarized the different studies documenting immune cells, differential infiltration, and the association with clinical outcome in mesothelioma. CDKN2A encodes for two proteins, p16/INK4A and p14/ARF, and Pezzuto et al. report that mesothelioma with strong immunoreactivity for p14/ARF has a high expression of ICB target PD-L1. It would be interesting to explore nuclear BAP1, which is used as a surrogate for wild-type function (6), in such a context. Indeed, in the TCGA study (7), the researchers found that type-I IFN signaling is associated with the status of BAP1.

Although mesothelioma is the sixth of the 31 most prevalent cancer types with a 38-interferon-stimulated genes signature (8), one aspect that is still underexplored is the priming for viral mimicry induction (9) which has been observed in an experimental model of mesothelioma development (10).

During the course of immunotherapy it will be important to follow immune responses longitudinally (11) and predict outcome, since it allows researchers to stratify patients into responders and non-responders. Principe et al. highlight the potential of doing so using pleural effusion, which is minimally invasive, and therefore easy to implement.

TETs are a heterogenous group of thoracic malignancies, mostly considered cold tumors except B3-thymoma and thymic carcinoma (12), reflecting a different TME according to the histologic subtype, which may negatively impact the tumor mutational burden, affecting ICB efficacy. Xu et al. report that *TP53* mutation is higher in hot TETs and correlates with worse prognosis compared with TETs without *TP53* mutations. Therefore, the genomic profile may have an influence in the immune sensitivity of TETs.

Alterations in microenvironmental metabolic characteristics are recognized as important means for cancer cells to interact with the infiltrating T cells within this TME (13). Molecular imaging has developed a wide array of tracers targeting metabolic pathways to understand metabolic reprogramming in cancer cells, as well as its effects on immune cells. van Genugten et al. provide an overview of currently available molecular imaging tracers for clinical studies and discuss their potential roles in the development of effective ICB strategies.

In the same way, the interconnection between metabolic pathways and immune response regulation has been suggested and a role of metabolic biomarkers as predictors of response to ICB is currently under investigation. Glycogen synthase kinase-3 (GSK3)-beta is a serine/threonine kinase involved in the phosphorylation of different components of the PI3K/AKT pathway as well as in PD-1/PD-L1 expression regulation and CD8+ T-cell activation. Positive expression of this biomarker in NSCLC samples showed a correlation with worse clinical stage and survival as well as with high PTEN but not with PD-L1 expression (Alves et al.).

Beyond genetic alterations in cancer cells, host genetics may influence thoracic cancer risk and pathogenesis and may shape TME features, thus representing a determinant predictor of treatment outcome.

Recent evidence has focused on genome-wide association studies (GWAS), which suggested a polygenic pattern of predisposition to lung cancer in some series (14). Likewise, single-nucleotide polymorphisms, somatic mutations, and epigenetic alterations are involved in TME refining and prediction of response to ICB. Lacking GWAS evidence on uncommon thoracic cancers such as PM and TET lead to *in vivo* models able to mimic human cancer development and finally to the identification of host genetic variants. Among these, the Cross Collaborative MexTAg mouse model offers a wide picture of host genetic make-up predisposing to the risk of asbestos-related mesothelioma and determining TME composition and the biological pathway involved in the immune response (Behrouzfar et al.).

In conclusion, evidence from original works and literature reviews collected within the present topic expands knowledge about the characterization of TME, its prognostic and predictive role in thoracic cancer malignancies, and finally deepens the relationship between the antitumor immune response and genetics of cancer and host. These findings may help clinicians to improve the risk-benefit ratio of treatment with ICB for patients with thoracic malignancies incorporating immune-related signatures in the future design of clinical trials.

## AUTHOR CONTRIBUTIONS

GP: planned the Research Topic, invited coeditors and authors, edited and submitted papers, and finally wrote the editorial. JR and EF-B contributed to author invitation, paper editing and finally editorial writing. All authors contributed to the article and approved the submitted version.

## REFERENCES


1. Remon J, Aldea M, Besse B, Planchard D, Reck M, Giaccone G, et al. Small Cell Lung Cancer: A Slightly Less Orphan Disease After Immunotherapy. *Ann Oncol* (2021) 32(6):698–709. doi: 10.1016/j.annonc.2021.02.025
2. Reck M, Remon J, Hellmann MD. First-Line Immunotherapy for Non-Small-Cell Lung Cancer. *J Clin Oncol* (2022) 40(6):586–97. doi: 10.1200/JCO.21.01497
3. Baas P, Scherpereel A, Nowak AK, Fujimoto N, Peters S, Tsao AS, et al. First-Line Nivolumab Plus Ipilimumab in Unresectable Malignant Pleural Mesothelioma (CheckMate 743): A Multicentre, Randomised, Open-Label, Phase 3 Trial. *Lancet* (2021) 397(10272):375–86. doi: 10.1016/S0140-6736(20)32714-8
4. Felip E, Altorki N, Zhou C, Csoszi T, Vynnychenko I, Goloborodko O, et al. Adjuvant Atezolizumab After Adjuvant Chemotherapy in Resected Stage IB-IIIA Non-Small-Cell Lung Cancer (IMpower010): A Randomised, Multicentre, Open-Label, Phase 3 Trial. *Lancet* (2021) 398(10308):1344–57. doi: 10.1016/S0140-6736(21)02098-5
5. Ricciuti B, Arbour KC, Lin JJ, Vajdi A, Vokes N, Hong L, et al. Diminished Efficacy of Programmed Death-(Ligand)1 Inhibition in STK11- and KEAP1-Mutant Lung Adenocarcinoma Is Affected by KRAS Mutation Status. *J Thorac Oncol* (2022) 17(3):399–410. doi: 10.1016/j.jtho.2021.01.532
6. Carbone M, Adusumilli PS, Alexander HRJr., Baas P, Bardelli F, Bononi A, et al. Mesothelioma: Scientific Clues for Prevention, Diagnosis, and Therapy. *CA Cancer J Clin* (2019) 69(5):402–29. doi: 10.3322/caac.21572
7. Hmeljak J, Sanchez-Vega F, Hoadley KA, Shih J, Stewart C, Heiman DI, et al. Integrative Molecular Characterization of Malignant Pleural Mesothelioma. *Cancer Discov* (2018) 8(12):1548–65. doi: 10.1158/2159-8290.CD-18-0804
8. Liu H, Golji J, Brodeur LK, Chung FS, Chen JT, deBeaumont RS, et al. Tumor-Derived IFN Triggers Chronic Pathway Agonism and Sensitivity to ADAR Loss. *Nat Med* (2019) 25(1):95–102. doi: 10.1038/s41591-018-0302-5
9. Chen R, Ishak CA, De Carvalho DD. Endogenous Retroelements and the Viral Mimicry Response in Cancer Therapy and Cellular Homeostasis. *Cancer Discov* (2021) 11(11):2707–25. doi: 10.1158/2159-8290.CD-21-0506
10. Sun S, Frontini F, Qi W, Hariharan A, Ronner M, Wipplinger M, et al. Endogenous Retrovirus Expression Activates Type-I Interferon Signaling in an Experimental Mouse Model of Mesothelioma Development. *Cancer Lett* (2021) 507:26–38. doi: 10.1016/j.canlet.2021.03.004
11. Isaacs J, Tan AC, Hanks BA, Wang X, Owzar K, Herndon JE2nd, et al. Clinical Trials With Biologic Primary Endpoints in Immuno-Oncology: Concepts and Usage. *Clin Cancer Res* (2022) 28(1):13–22. doi: 10.1158/1078-0432.CCR-21-1593
12. Yamamoto Y, Iwahori K, Funaki S, Matsumoto M, Hirata M, Yoshida T, et al. Immunotherapeutic Potential of CD4 and CD8 Single-Positive T Cells in Thymic Epithelial Tumors. *Sci Rep* (2020) 10(1):4064. doi: 10.1038/s41598-020-61053-8
13. Hanahan D. Hallmarks of Cancer: New Dimensions. *Cancer Discov* (2022) 12(1):31–46. doi: 10.1158/2159-8290.CD-21-1059
14. Kachuri L, Graff RE, Smith-Byrne K, Meyers TJ, Rashkin SR, Ziv E, et al. Pan-Cancer Analysis Demonstrates That Integrating Polygenic Risk Scores With Modifiable Risk Factors Improves Risk Prediction. *Nat Commun* (2020) 11(1):6084. doi: 10.1038/s41467-020-19600-4


**Conflict of Interest:** The authors declare that the research was conducted in the absence of any commercial or financial relationships that could be construed as a potential conflict of interest.

frontiers in Oncology

ORIGINAL RESEARCH
published: 05 March 2021
doi: 10.3389/fonc.2021.581030

# Characterization of Tumor Microenvironment in Lung Adenocarcinoma Identifies Immune Signatures to Predict Clinical Outcomes and Therapeutic Responses

*Donglai Chen[1†], Yifei Wang[2†], Xi Zhang[3,4†], Qifeng Ding[2†], Xiaofan Wang[2], Yuhang Xue[2], Wei Wang[2], Yiming Mao[5*‡], Chang Chen[1*‡] and Yongbing Chen[2*‡]*

[1] Department of Thoracic Surgery, Shanghai Pulmonary Hospital, Tongji University, School of Medicine, Shanghai, China, [2] Department of Thoracic Surgery, The Second Affiliated Hospital of Soochow University, Suzhou, China, [3] Stem Cell Translational Research Center, Tongji Hospital, Tongji University School of Medicine, Shanghai, China, [4] Department of Neurology, Tongji Hospital, Tongji University School of Medicine, Shanghai, China, [5] Department of Thoracic Surgery, Suzhou Kowloon Hospital, Shanghai Jiaotong University School of Medicine, Suzhou, China

**Background and Objective:** Increasing evidence has elucidated the clinicopathological significance of individual TME component in predicting outcomes and immunotherapeutic efficacy in lung adenocarcinoma (LUAD). Therefore, we aimed to investigate whether comprehensive TME-based signatures could predict patient survival and therapeutic responses in LUAD, and to assess the associations among TME signatures, single nucleotide variations and clinicopathological characteristics.

**Methods:** In this study, we comprehensively estimated the TME infiltration patterns of 493 LUAD patients and systematically correlated the TME phenotypes with genomic characteristics and clinicopathological features of LUADs using two proposed computational algorithms. A TMEscore was then developed based on the TME signature genes, and its prognostic value was validated in different datasets. Bioinformatics analysis was used to evaluate the efficacy of the TMEscore in predicting responses to immunotherapy and chemotherapy.

**Results:** Three TME subtypes were identified with no prognostic significance exhibited. Among them, naïve B cells accounted for the majority in TMEcluster1, while M2 TAMs and M0 TAMs took the largest proportion in TMEcluster2 and TMEcluster3, respectively. A total of 3395 DEGs among the three TME clusters were determined, among which 217 TME signature genes were identified. Interestingly, these signature genes were mainly involved in T cell activation, lymphocyte proliferation and mononuclear cell proliferation. With somatic variations and tumor mutation burden (TMB) of the LUAD samples characterized, a genomic landscape of the LUADs was thereby established to visualize the relationships among the TMEscore, mutation spectra and clinicopathological profiles. In addition, the TMEscore was identified as not only a prognosticator for long-term survival

OPEN ACCESS

**Edited by:**
*Emanuela Felley-Bosco, University of Zurich, Switzerland*

**Reviewed by:**
*Can Küçük, Dokuz Eylül University, Turkey*
*Olli Pekka Yli-Harja, Tampere University of Technology, Finland*

***Correspondence:**
*Yongbing Chen*
*chentongt@sina.com*
*Yiming Mao*
*253992240@qq.com*
*Chang Chen*
*chenthoracic@163.com*

*[†]These authors have contributed equally to this work*

*[‡]These authors share senior authorship*

**Specialty section:**
*This article was submitted to Thoracic Oncology, a section of the journal Frontiers in Oncology*

**Received:** *07 July 2020*
**Accepted:** *27 January 2021*
**Published:** *05 March 2021*

**Citation:**
*Chen D, Wang Y, Zhang X, Ding Q, Wang X, Xue Y, Wang W, Mao Y, Chen C and Chen Y (2021) Characterization of Tumor Microenvironment in Lung Adenocarcinoma Identifies Immune Signatures to Predict Clinical Outcomes and Therapeutic Responses. Front. Oncol. 11:581030. doi: 10.3389/fonc.2021.581030*

in different datasets, but also a predictive biomarker for the responses to immune checkpoint blockade (ICB) and chemotherapeutic agents. Furthermore, the TMEscore exhibited greater accuracy than other conventional biomarkers including TMB and microsatellite instability in predicting immunotherapeutic response ($p < 0.001$).

**Conclusion:** In conclusion, our present study depicted a comprehensive landscape of the TME signatures in LUADs. Meanwhile, the TMEscore was proved to be a promising predictor of patient survival and therapeutic responses in LUADs, which might be helpful to the future administration of personalized adjuvant therapy.

**Keywords: lung adenocarcinoma, tumor microenvironment, signature, survival, therapeutic response**

## INTRODUCTION

Lung adenocarcinoma (LUAD) is the commonest histological type of all lung cancers, accounting for approximately 50% of them (1, 2). Nowadays, surgical resection remains as the standard treatment for early-stage LUADs. Meanwhile, chemotherapy plays an important role in LUAD patients at all stages of the disease. Recently, blockade of immune checkpoint has been proved as a promising therapy for patients with LUADs (3, 4) which seems to be an alternative to conventional chemotherapy. Nevertheless, the fact that most patients do not derive any benefit from PD-1/PD-L1 blockade combined with the risk of serious immune-related adverse events (5, 6) and the significant up-front costs, underscore the need for developing accurate tools for predicting therapeutic response to chemotherapy and immune checkpoint blockade (ICB) (7).

Nowadays, an increasing body of literature suggests a crucial role for the tumor microenvironment (TME) in cancer progression and therapeutic responses (8–11). The TME context in LUADs has been reported not only to reflect the potential benefits from treatment (12–14), but also to predict patient survival (15, 16), which includes tumor-infiltrating lymphocytes (e.g., CD8+ T cells, CD4+ T cells), tumor-associated macrophages (TAMs), cancer-associated fibroblasts (CAFs), and other cell types. With the introduction of computational methods to assess the abundance of cells infiltrating in the TME, several studies using these methodologies have explored the clinical utility of TME context (13, 17–19). However, the comprehensive landscape of TME infiltrates and its predictive power for therapeutic responses in LUADs have not been fully investigated.

In our present study, two previously proposed computational algorithms (20, 21) were employed to estimate the fractions of 23 immune and stromal cells based on LUAD gene expression profiles from The Cancer Genome Atlas (TCGA) database. The TME infiltrating patterns of LUAD samples were investigated and correlated with both transcriptomic characteristics and clinicopathological features. Unsupervised clustering was applied to quantify the TME infiltrating patterns which were calculated as a TMEscore. Consequently, the TMEscore was proved to be a promising prognostic biomarker and a robust predictive factor for the therapeutic responses in LUADs.

## MATERIALS AND METHODS

### LUAD Datasets and Preprocessing

The transcriptomic dataset of LUAD from TCGA database was downloaded from the UCSC Xena browser (https://xenabrowser.net/datapages/). LUAD patients without survival information were removed from further evaluation, among whom 499 were available to construct the TMEscore. Data of somatic mutations (MuSE Variant Aggregation and Masking) were downloaded from TCGA database, which included 567 LUAD specimens. Somatic mutation data, transcriptomic data and survival information were available in 493 of the 499 specimens, of which clinical characteristics were accessible in 474. The raw data in TCGA dataset generated from Illumina were processed using the lumi software package according to a previous study (8).

The microarray data (GSE68465) generated by Affymetrix were obtained from the Gene Expression Omnibus (https://www.ncbi.nlm.nih.gov/geo/) (GEO) as a validation dataset, which included 422 LUAD specimens with expression profiles and clinical outcomes available. The raw data for the dataset from Affymetrix were processed using the Range Migration Algorithm (RMA) for background adjustment in the Affy software package (22). The RMA was used to perform background adjustment, quantile normalization, and final summarization of oligonucleotides per transcript using the median polish algorithm. The detailed information of the LUAD datasets is listed in **Supplementary Table 1**.

### Assessment of Infiltrating Cells in TME

To calculate the proportions of immune cells in the LUAD samples, we used the CIBERSORT (cell type identification by estimating relative subset of known RNA transcripts) algorithm (20) and the LM22 gene signature, which allows for highly sensitive and specific discrimination of 22 human immune cell phenotypes (8). CIBERSORT is a deconvolution algorithm that uses a set of reference gene expression values (a signature with 547 genes) considered a minimal representation for each cell type and, based on those values, infers different cell type proportions in tumor samples using support vector regression (8). Gene expression profiles were prepared using standard annotation files, and data were uploaded to the CIBERSORT web portal (http://cibersort.stanford.edu/), with the algorithm run using the

LM22 signature and 1,000 permutations. Proportions of stromal cells were estimated by applying the Microenvironment Cell Populations (MCP)-counter method, which allows for robust quantification of the absolute abundance of immune and stromal cell populations in heterogeneous tissues from transcriptomic data (21).

## Consensus Clustering for TME-Infiltrating Cells

Hierarchical agglomerative clustering (based on Euclidean distance and Ward's linkage) was employed to group the samples with qualitatively different TME cell infiltration patterns. Unsupervised clustering methods (K-means) (23) for dataset analysis were used to identify TME patterns and classify patients for further analysis. A consensus clustering algorithm was applied to determine the number of clusters (8), which was repeated 1000 times to ensure the stability of classification using the ConsensuClusterPlus R package (24).

## Generation and Analysis of TME Gene Signatures

To identify genes associated with TME cell infiltrating patterns, we classified patients into three TMEclusters. Differentially expressed genes (DEGs) among these three groups were determined using the R package limma (25). DEGs among different TME patterns were determined by significance criteria (adjusted $p$ value < 0.05; |logFC|>0.58). An unsupervised clustering method (K-means) for analysis of DEGs was employed to classify patients into two groups for further analysis. TME signature genes were then obtained using the random forest classification algorithm to screen redundant genes. Gene-annotation enrichment analysis using the clusterProfiler R package (26) was performed on TME signature genes. Gene Ontology (GO) terms were identified with a strict cutoff of $p < 0.01$ and false discovery rate (FDR) of less than 0.05.

## Establishment of TME Scores

Cox regression model was applied to assess the prognostic value of each signature gene which was classified according to its Cox coefficient. A method similar to gene expression grade index (24) was used to define the TMEscore of each patient:

$$TMEscore = \Sigma\ log_2(X + 1) - \Sigma\ log_2(Y + 1)$$

where X is the expression level of genes whose Cox coefficient is positive, and Y is the expression level of genes whose Cox coefficient is negative. The cut-off values of each dataset were evaluated based on the association between patient overall survival (OS) and TMEscore in each separate dataset using the survminer package (8). The R package MaxStat (27) which iteratively tests all possible cut points to find the one achieving the maximum rank statistic, was used to dichotomize TMEscore, and patients were then divided into low- and high-TMEscore subgroups.

## Analysis of Tumor Mutation Profiles

Somatic mutation data were obtained from the publicly available TCGA database. Notably, one sample with merely silent mutation was excluded from the aforementioned 493 samples in our analysis. We prepared the Mutation Annotation Format (MAF) of somatic variants, and implemented the R package Maftools (https://bioconductor.org/packages/release/bioc/html/maftools.html) which provides a multiple of analysis modules to perform the visualization process (28) to display somatic landscape. In addition, the R package SomaticSignatures (https://bioconductor.org/packages/release/bioc/html/SomaticSignatures.html) was used to characterize the mutation signatures of the LUAD samples (29). Mutational signatures were extracted using 96 nonnegative components (single-base somatic substitutions and their immediate sequence context) and compared to the validated consensus mutational signatures in the Catalogue Of Somatic Mutations In Cancer (COSMIC) (30), version 2 (https://cancer.sanger.ac.uk/cosmic/signatures_v2) to identify the set of COSMIC mutational signatures in TCGA datasets (31). Moreover, the estimation of TMB in LUAD samples was conducted according to a previous study (32).

## Predictive Value of TMEscore to Estimate Therapeutic Effect

Tumor Immune Dysfunction and Exclusion (TIDE) (http://tide.dfci.harvard.edu/) (33), a computational method to predict ICB response based on melanoma patients who underwent anti-PD-1 or anti-CTLA-4 agent, was used to investigate the predictive value of TMEscore for immunotherapy. TIDE uses a set of gene expression markers to estimate two distinct mechanisms of tumor immune evasion, including dysfunction of tumor infiltrating cytotoxic T lymphocytes (CTL) and exclusion of CTL by immunosuppressive factors (34). Patients with higher TIDE score have a higher chance of antitumor immune escape, thus exhibiting lower response rate of ICB treatment (33). The TIDE score was shown to have a higher accuracy than PD-L1 expression level and tumor mutation burden (TMB) in predicting survival outcome of cancer patients treated with ICB agents (34–37). The R package MaxStat (27) was also employed to dichotomize the TMB level. The R package pRRophetic (38) was used to determine whether TMEscore could accurately predict clinical chemotherapeutic responses.

## Immunohistochemistry Staining

LUAD samples resected from a cohort of chemo- and/or radio-naïve patients (**Supplementary Table 2**) were obtained from the Second Affiliated Hospital of Soochow University, which was approved by the Institutional Review Board (IRB NO.JD-HG-2020-09). The chairperson of the ethics committee waived the need for patient consent. The sections of tumor tissues were firstly deparaffinized and rehydrated. Endogenous peroxidase was then quenched using 10% H2O2 for 10 min at room temperature. Subsequently, nonspecific proteins were blocked with 10% goat serum for 1 h. Afterwards, the sections were rinsed and incubated with anti-BTK (YM0083, Immunoway; diluted 1: 400) overnight at 4°C. The DAB Horseradish Peroxidase Color Development Kit (Beyotime, China) was used for color

development. Finally, the sections were counterstained with hematoxylin and mounted.

As described in our previous study (39), the staining index was calculated as a product of staining intensity (negative = 0, weak = 1, moderate = 2, and strong = 3) multiplied by staining extent (0% = 0, 1%–10% = 1, 11%–50% = 2, and > 50% = 3). A final score of 0–2 indicated low BTK expression, and a score of > 2 indicated high BTK expression.

## Statistical Analysis

For comparisons of two subgroups, unpaired Student t tests was used to estimate statistical significance for normally distributed variables, and Wilcoxon rank-sum test was used for analyzing non-normally distributed variables. To identify significant genes in the DEG analysis, Benjamini-Hochberg method was applied to converting the *p* values to FDRs (40). The Kaplan-Meier method was used to generate survival curves for the subgroups in each dataset, and the Log-rank test was used to determine the statistical significance of differences. The hazard ratios for univariate analyses were calculated using a univariate Cox proportional hazards regression model. A multivariate Cox regression model was used to determine independent prognostic factors. The R package pROC (41) was used to plot and visualize receiver operating characteristic (ROC) curves to calculate the area under the curve (AUC) and confidence intervals to evaluate the diagnostic accuracy of TMB and TMEscore. For comparison of AUCs, likelihood ratio test for two correlated ROC curves was used. All statistical analyses were conducted using R (https://www.r-project.org/) or SPSS software (version 25.0). A two-tailed $p$-value < 0.05 was considered statistically significant.

# RESULTS

## Characterization of TME in LUADs and Distinct Patterns of TME Subtypes

The general flowchart of our study is shown in **Supplementary Figure 1A**. A TCGA dataset comprised of 499 patients with

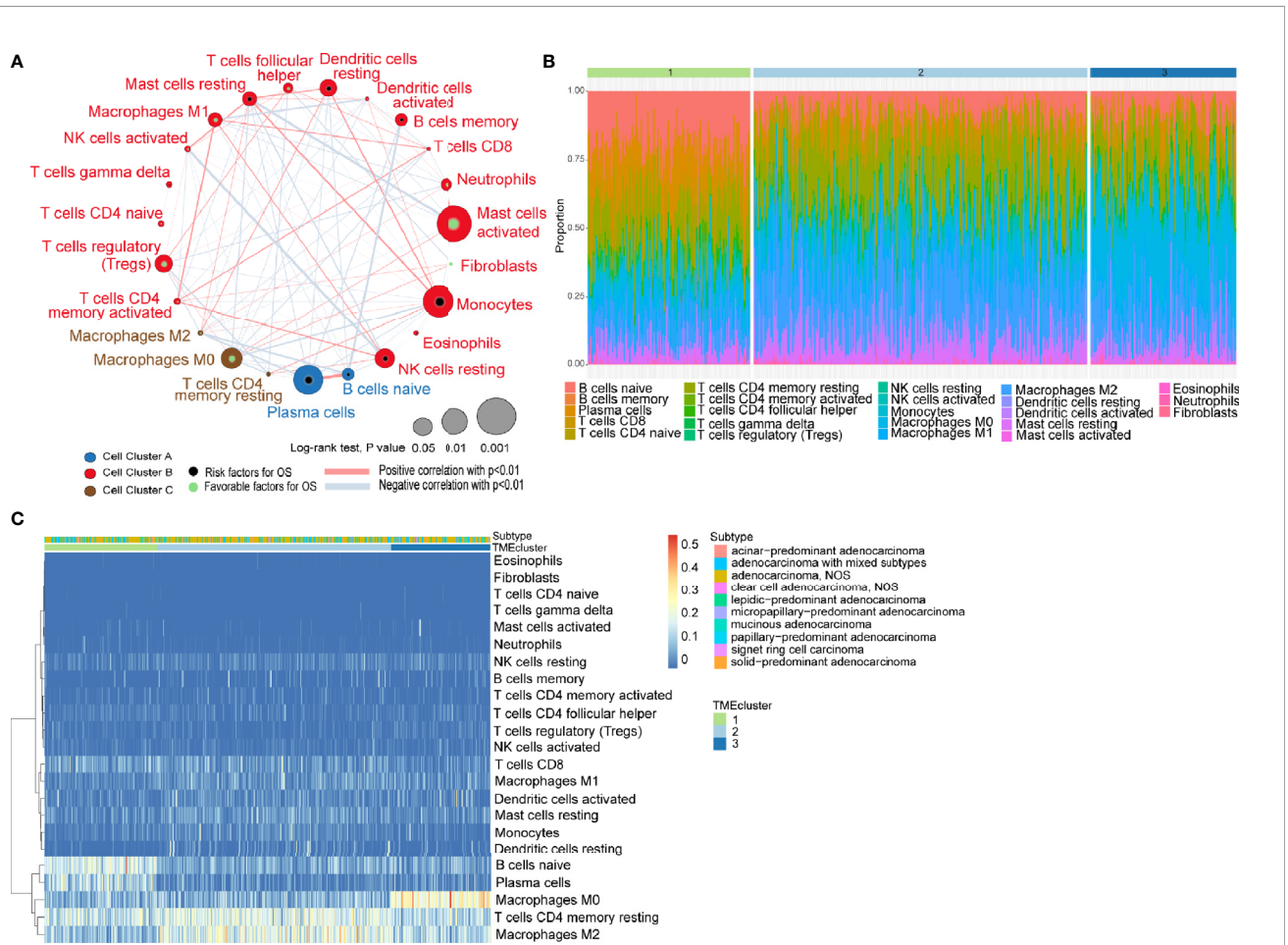


**FIGURE 1** | Characterization of TME in LUADs and distinct patterns of TME subtypes. **(A)** Cellular interaction of tumor microenvironment (TME) cell types in LUADs; **(B)** Barplot showing the specific 23 immune fractions represented by various colors in each TMEcluster; **(C)** Unsupervised clustering of TME cell types and histologic subtypes for LUAD patients.

their transcriptomic data were included in our initial analysis. By applying CIBERSORT algorithm and MCP-counter method, we obtained the proportions of 23 different immune and stromal cells in the 499 samples (**Supplementary Figure 1B**). Meanwhile, a TME cell network was used to depict the comprehensive landscape of tumor-immune cell interactions and their effects on the OS of patients with LUADs (**Figure 1A** and **Supplementary Table 3**).

Unsupervised learning using K-means algorithm was used on the dataset to perform group clustering, which identified $K$=3 according to the elbow method and gap statistic (**Supplementary Figures 2A, B**). To identify the aforementioned optimal cluster number, we assessed clustering stability using the ConsensusClusterPlus R package which displayed the clustering stability using 1,000 iterations of hierarchical clustering. The consensus matrix supported the existence of three robust clusters of LUADs (**Supplementary Figure 2C**). As shown in **Figures 1B, C**, the proportions of infiltrating immune cells and histologic subtypes differ significantly among the three TME subtypes. We found that naïve B cells accounted for the majority in TMEcluster1, while M2 TAMs and M0 TAMs took the largest proportion in TMEcluster2 and TMEcluster3, respectively. However, log-rank test revealed no significant difference in survival among different TMEclusters ($p$ = 0.45) (**Supplementary Figure 2D**).

## Construction and Validation of the TMEscore in Different LUAD Datasets

A total of 3395 DEGs among the three TME clusters were determined by significance criteria (adjusted $p$ value < 0.05; |logFC| > 0.58) as implemented in the R package limma (**Supplementary Figure S3A**). An unsupervised clustering method (K-means) for analysis of DEGs was then employed to classify the patients into two groups (**Supplementary Figure 3B**). Among these DEGs, 217 TME signature genes were obtained using the random forest classification algorithm, on which Gene-annotation enrichment analysis using the clusterProfiler R package (26) was performed. Consequently, the data indicated that these TME signature genes significantly enriched in pathways associated with T cell activation, lymphocyte proliferation and mononuclear cell proliferation (**Supplementary Figure 3C**).

Cox regression model was used to assess the prognostic value of each signature genes according to the Cox coefficient, by which the TMEscore was established for each patient. As shown in **Figure 2A**, the TMEscore could effectively distinguish significantly different OS in the entire cohort. Notably, patients with high TMEscore (n = 120) had significantly better survival than those with low TMEscore (n = 354) ($p$ < 0.0001).

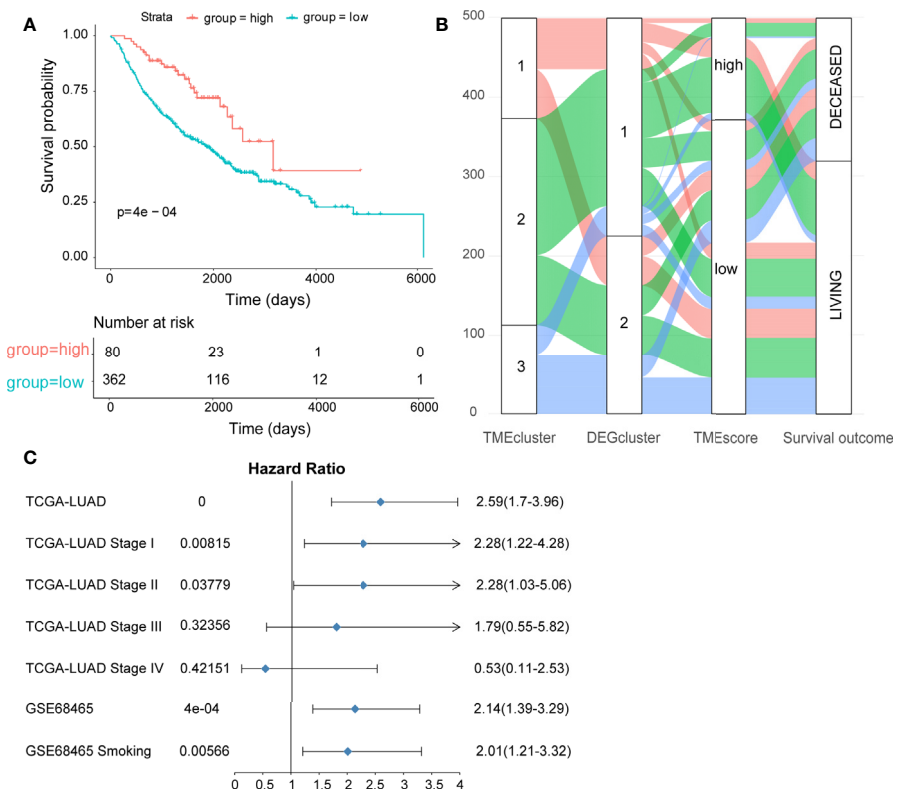


**FIGURE 2** | Construction and validation of the TMEscore in different LUAD datasets. **(A)** Kaplan-Meier curves of high- and low-TMEscore subgroups in the entire TCGA cohort; **(B)** Alluvial diagram showing the relationships among TME subtypes and TMEscore subgroups as well as clinical outcomes; **(C)** Forest plot showing the prognostic value of TMEscore in different datasets.

Additionally, we visualized the relationships of TME subtypes and TMEscore subgroups as well as patient outcomes using an alluvial diagram (**Figure 2B**). Moreover, TMEscore remained efficient in stratifying the patients with early-stage disease (stage I-II) into different OS (**Supplementary Figures 4A, B**), which exhibited its value in the external validation cohort from the GEO database as well (**Supplementary Figure 4C**). To be noted, even for smokers in the validation cohort, significantly different OS was also observed among the subgroups stratified by the TMEscore (**Supplementary Figure 4D**). A forest plot was used to summarize the predictive value of TMEscore in different patient cohorts (**Figure 2C**).

## Association Between TMEscore and Cancer Somatic Genomes

We analyzed the somatic variations of the 492 LUAD samples in TCGA database which revealed missense mutation as the leading type of single nucleotide variant (SNV) (**Supplementary Figure 5A**). Meanwhile, SNV was identified as the major variant in LUADs that occurred more frequently than insertion or deletion (**Supplementary Figure 5B**). In addition, it was observed that C>A was the predominant SNV type in LUADs (**Supplementary Figure 5C**). Besides, we calculated the TMB and showed the mutation type with different colors in LUAD samples (**Supplementary Figures 5D, E**), as well as the top 10 mutated genes in LUADs with ranked percentages (**Supplementary Figure 5F**). We also mapped the landscape of mutation profiles among the three TMEclusters, which characterized the mutation types of the frequently mutated genes (**Supplementary Figure 6**). Waterfall plots were then used to exhibit the mutation profiles of patients with high/low-TMEscore in which various colors with annotations at the bottom represented the different mutation types and TMB levels (**Figures 3A, B**). Meanwhile, boxplots were applied to showing the mutation frequency of each frequently mutated genes in high- and low-TMEscore subgroups, respectively (**Figures 3C, D**).

There are six classes of base substitution—C>A, C>G,C>T, T>A, T>C, T>G(all substitutions are referred to by the pyrimidine of the mutated Watson–Crick base pair)—and as we incorporated information on the bases immediately 5' and 3' to each mutated base, there are 96 possible mutations in this

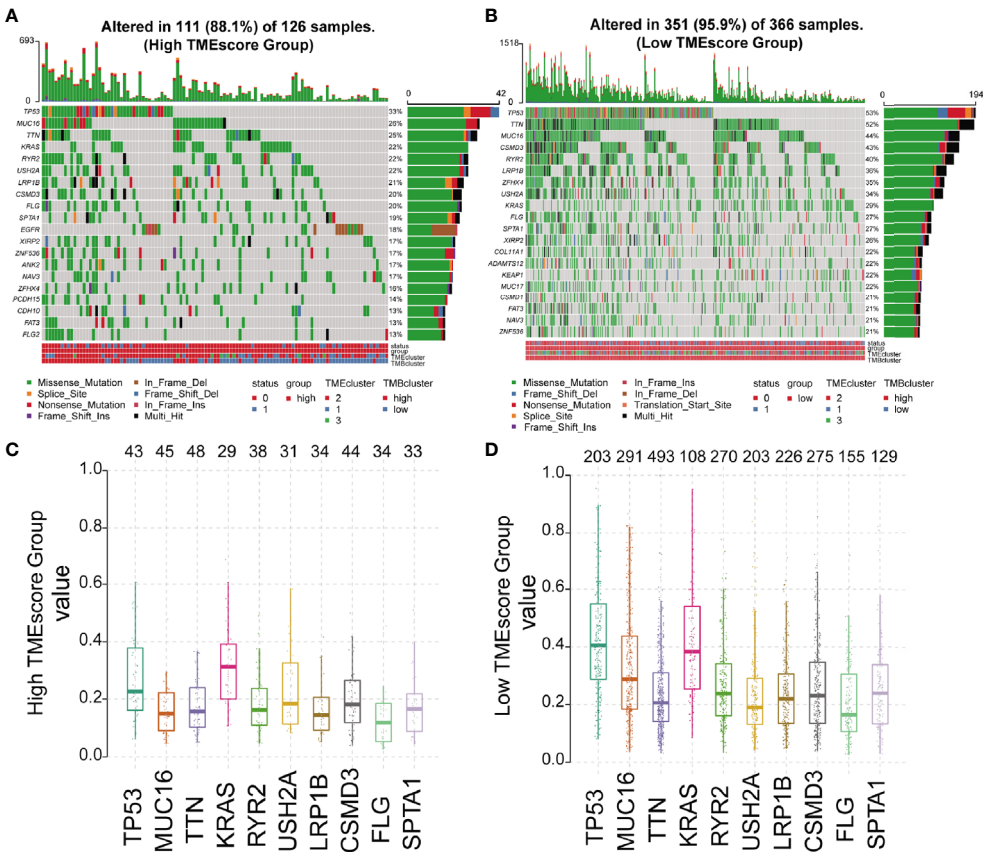


**FIGURE 3** | Mutation profiles of different TMEscore subgroups. **(A, B)** Waterfall plots exhibiting the mutation profiles of patients with high/low-TMEscore in which various colors with annotations at the bottom represented the different mutation types and tumor mutation burden; **(C, D)** Boxplots showing the mutation frequency of the 10 most frequently mutated genes in high- and low-TMEscore subgroups.

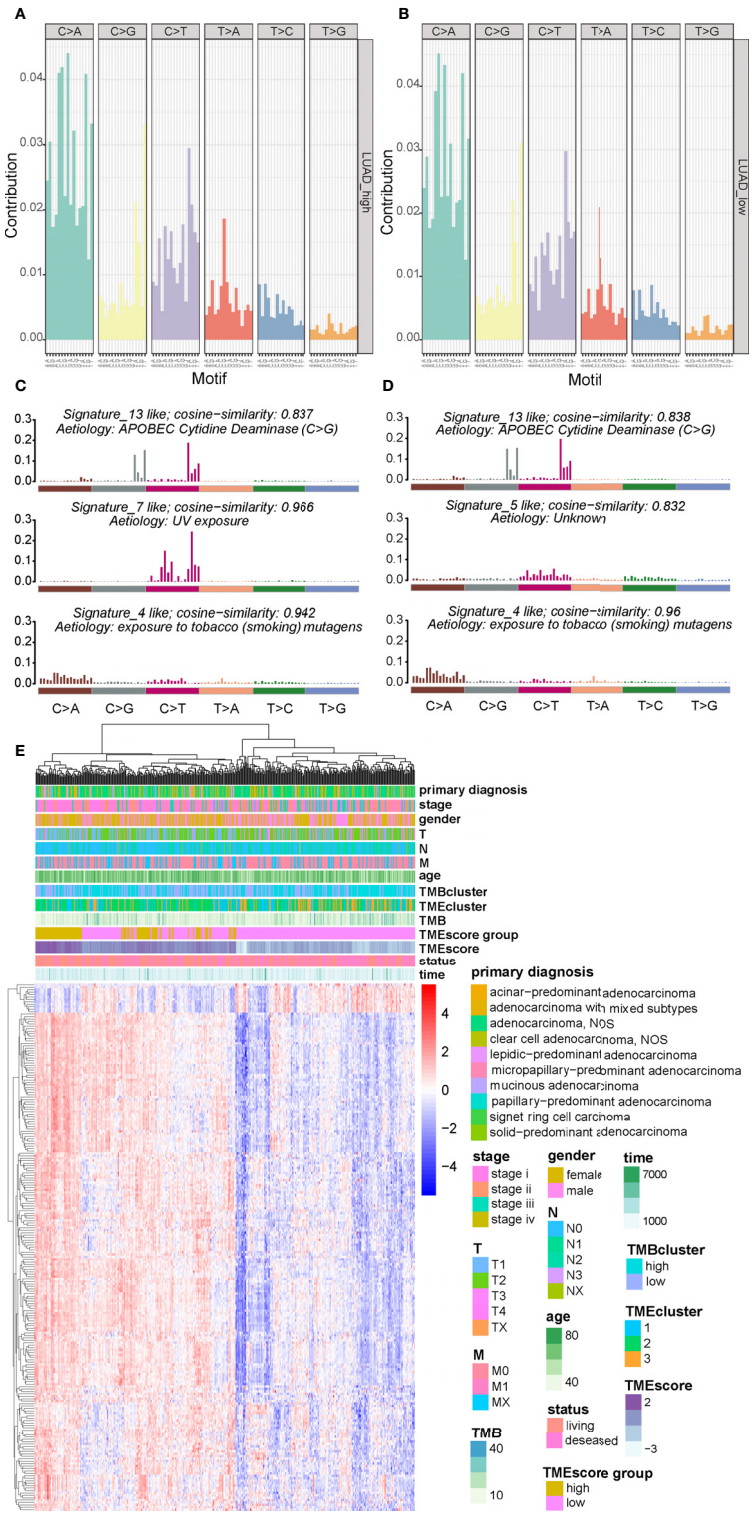


**FIGURE 4** | Visualization of mutational signatures and TME signatures in TME subgroups. **(A, B)** Mutation spectra showing the 96 substitution classification defined by the substitution class and sequence context immediately 3' and 5' to the mutated base in the high- and low-TME subgroups. **(C, D)** Barplot showing the differential mutation signatures between the high- and low-TME subgroups. The y-axis indicates exposure of 96 trinucleotide motifs to overall signature. The plot title indicates best match against validated COSMIC signatures and cosine similarity value along with the proposed etiology. **(E)** Unsupervised analysis and hierarchical clustering of the 217 TME signature genes and their associations with clinicopathological characteristics.

classification (30). This 96 substitution classification is particularly useful for distinguishing mutational signatures that cause the same substitutions but in different sequence contexts (30). A previous study (30) applied this approach to the 30 cancer types and revealed 21 distinct validated mutational signatures. Each mutational signature was characterized by different substitutions and was associated with epidemiological and biological features of particular cancer types. Therefore the frequency distribution of the 96 mutations based on the six classes of base substitution were analyzed in both TMEscore subgroups (**Figures 4A, B**). Moreover, by comparing the extracted signatures from our samples with those in COSMIC, we identified different mutational signatures between the two TMEscore subgroups. The identified signatures in both groups similarly showed a strong resemblance to COSMIC signature 13 and COSMIC signature 4 (**Figures 4C, D**). A high similarity to COSMIC signature 7 was also found in the high-TMEscore subgroup (**Figure 4C**). Meanwhile, a mutational signature similar to COSMIC signature 5 was present in the low-TMEscore subgroup (**Figure 4D**). As reported previously (30), COSMIC signature 13 and COSMIC signature 4 were associated with APOBEC and smoking, respectively, while COSMIC signature 7 was mainly associated with ultraviolet light.

A genomic landscape of the LUADs was thereby plotted by integrating the TMB information and clinical characteristics with TME profiles including the 217 TME signature genes and TMEscore (**Figure 4E**).

## Predictive Value of TMEscore as a Biomarker for Therapeutic Effect

TIDE to evaluate TMEscore as a predictor of immunotherapy, interestingly, no significant difference ($p$ = 0.8) was observed in TIDE score between the high- (n = 120) and low-TMEscore (n = 354) subgroups (**Figure 5A**). However, we observed significantly different PD-L1 expression levels between the high- and low-TMEscore subgroups ($p$ < 0.001) (**Figure 5B**). Since microsatellite instability (MSI), the spontaneous loss or gain of nucleotides from repetitive DNA tracts, is a promising predictive biomarker for patient survival and response to immunotherapy (42, 43), TMEscore was compared between the two subgroups stratified by MSIscore which was calculated by TIDE (44). As shown in **Figure 5C**, TMEscore in the high-MSI subgroup (n=314) was significantly higher than that in the low-MSI one (n = 160) ($p$ < 0.001). Meanwhile, TMEscore in the high-TMB subgroup (n = 257) was significantly lower than that in the low-TMB one (n = 217) ($p$ < 0.001) (**Figure 5D**). Furthermore, the AUC indicated that TMEscore was superior to TMB alone in predicting response to ICB ($p$ < 0.001) which exhibited greater accuracy in combination with TMB (**Figure 5E**). Additionally, comparison of the 50% inhibitory concentration (IC50) of chemotherapy drugs indicated that the low-TMEscore subgroup had higher sensitivity to cisplatin ($p$ = 0.019) (**Figure 6A**) while the high-TMEscore subgroup was prone to the benefits from gemcitabine ($p$ = 0.00042) (**Figure 6B**).

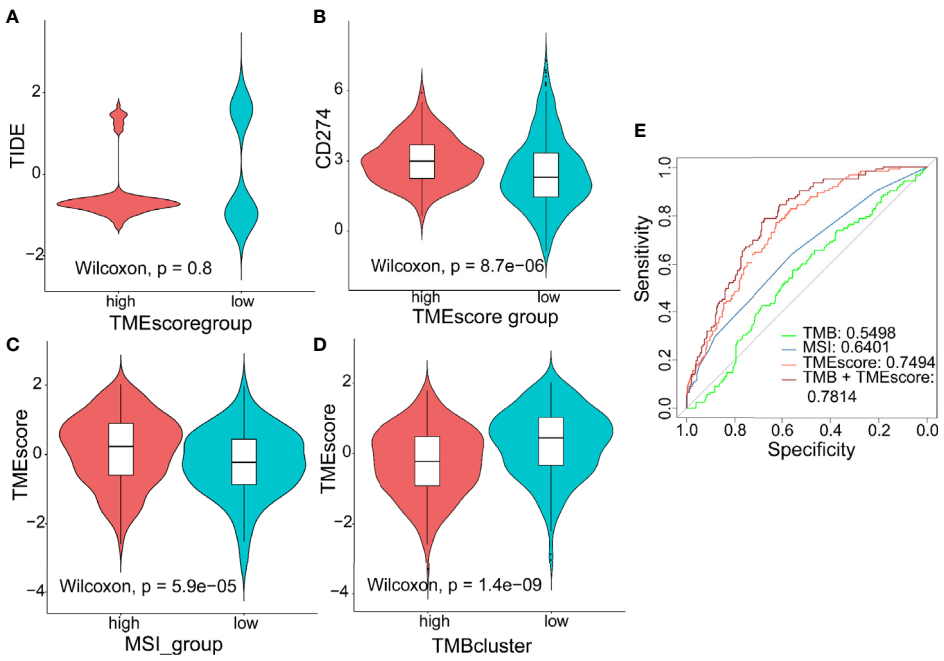


**FIGURE 5** | Predictive value of TMEscore as a biomarker for immunotherapy. **(A, B)** Violin plot showing TIDE score and PD-L1 level between the high- and low-TMEscore subgroups; **(C, D)** Violin plot showing TMEscores in groups with different microsatellite instability (MSI) status and with different TMB levels; **(E)** ROC curves to compare the accuracy of TMB, MSI and TMEscore in predicting responses to immunotherapy.

## DISCUSSION

Our findings indicated that assessment of the immune and stromal statuses *via* the TME signature provided a potent predictor of survival in early-stage patients with LUAD and a promising biomarker for therapeutic responses as well. Based on the DEGs and GO enrichment analysis, we observed that the TME signature genes significantly enriched in pathways mainly associated with lymphocyte activation and proliferation. Moreover, missense mutation was identified as the leading type of SNV which was identified as the major variant in LUADs. Meanwhile, the established TMEscore could stratify the patient cohort from TCGA database into two subgroups with distinct mutation profiles and COSMIC signatures. A genomic landscape of the LUADs was also characterized by integrating the TMB information and clinical characteristics with TME profiles. To our best knowledge, the present study is the first bioinformatics-based study to comprehensively investigate the associations among clinicopathological features, the mutation spectra and the TME profiles of LUADs, which also developed a computational algorithm and demonstrated its predictive value for both ICB and chemotherapeutic agents.

Previously, Yue et al. (45) identified a prognostic gene signature associated with TME, and validated its predictive accuracy for OS in LUAD patients. However, they omitted to analyze whether the signature could predict therapeutic responses to ICB or chemotherapy. In their study, univariate Cox regression analysis was initially employed to screen out 23 prognostic TME-related DEGs. Afterwards, Yue et al. (45) used selection operator (LASSO) and multivariate Cox regression analyses to identify three key genes for constructing a prognostic model, in which the analytical methods were different from ours. Interestingly, there are five common DEGs between their 23 TME-related DEGs and our 217 signature genes, including BTK, CCDC69, CD33, CD52, and LY86. Among the five common DEGs, only BTK was selected out as a signature gene in both their and our studies. We therefore validated the prognostic impacts of the five DEGs using the LUAD cohort from TCGA database (**Supplementary Figures 7A–E**). Additionally, the role of BTK as a prognostic factor was also validated in our domestic cohort using IHC (**Supplementary Figure 7F**). Similar to our data, Bi et al. (46) who performed a study based on TCGA mining also found that BTK was an immune-related gene and a promising prognostic factor for LUAD. Recently, Tan et al. (47) performed a bioinformatics study to characterize the immune landscape of LUADs, in which they divided the patients with LUAD into two immunophenotypes based on the tumor microenvironment. The two immunophenotypes were denoted as the Active Immune Class and Exhausted Immune Class. The former showed significant IFN, T-cells, M1 macrophage signatures, and better prognosis, while the latter presented an exhausted immune response with activated stromal enrichment, M2 macrophage signatures, and immunosuppressive factors such as WNT/transforming growth factor-β. In addition, Tan and his colleagues (47) identified their developed Immune Class as a useful tool to predict the response to ICB. However, merely 32 patients in a metastatic melanoma cohort were included in their prediction of PD-L1 inhibitor response. In addition, the relationships of clinicopathological characteristics and immunophenotypes were not comprehensively characterized, neither were the somatic landscape and COSMIC signatures. Additionally, Huang et al. (48) identified two LUAD subtypes with specific immune and metabolic state based on the bioinformatic analyses of TME, who constructed a TME score to predict TME phenotypes in LUADs. Interestingly, they constructed the TME score using the principal component analysis algorithm based on the TME signature genes, which could represent the signature of the two TME clusters in their study (48). Differently, their TME score was applied to evaluating the expression patterns of immune-associated genes in LUADs,

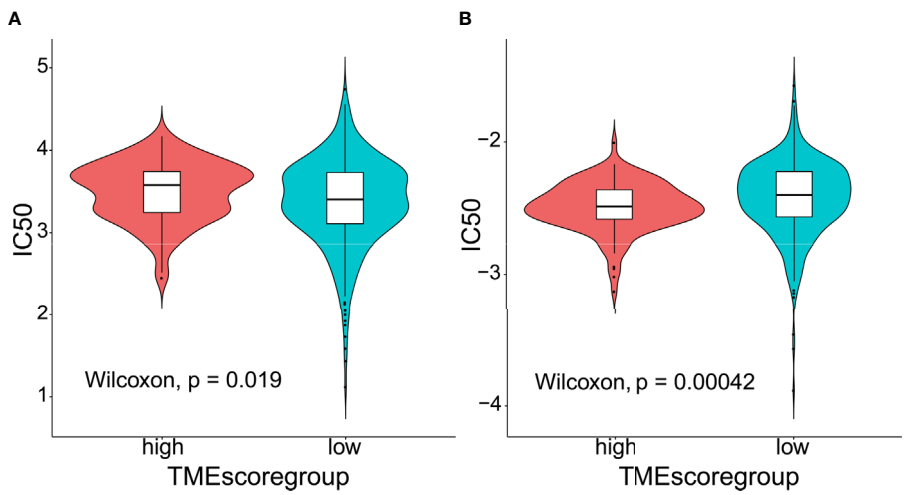


**FIGURE 6** | Predictive value of TMEscore as a biomarker for chemotherapy. **(A)** Violin plot comparing IC50 of cisplatin between the high- and low-TMEscore subgroups; **(B)** Violin plot comparing IC50 of gemcitabine between the high- and low-TMEscore subgroups.

which merely exhibited diagnostic value. It remained unknown whether the TME score raised by Huang et al (48) could accurately predict patient survival and therapeutic responses to ICB or chemotherapy. Meanwhile, the data of somatic variations in LUADs were unavailable in their study.

Hitherto, several bioinformatics studies (34, 47, 49, 50) have identified the immune-related signatures as a prognostic biomarker in LUADs. However, the roles of immunophenotype-derived signatures in predicting response to chemotherapy have not been fully clarified. Notably, a number of clinical investigations (51–53) have highlighted adjuvant chemotherapy as a prognostic factor for improved survival in patients with stage IB LUADs. Under the circumstances, our study not only proved TMEscore as a survival-related predictor, but also identified its potential in stratifying patients with distinct sensitivity to different chemotherapy regimens. According to our analysis, low-TMEscore subgroup had higher sensitivity to cisplatin while high-TMEscore group was more likely to respond to gemcitabine, which offered insights into the administration of personalized adjuvant therapy.

There are some limitations that should not be ignored in our study: 1) lack of domestic sequencing data to validate the associations between the TME infiltrating patterns and clinicopathological characteristics as well as mutation spectra; 2) lack of external validation cohort to confirm the roles of TMEscore in predicting therapeutic responses; 3) possessing predictive power though, the chosen set of signature genes are not necessarily valid in terms of their biological significance. For instance, the differences in IC50 scores between high- and low-TMEscore subgroups in **Figure 6** do not seem to be obvious although statistically significant differences were obtained. It raises the possibility that the observed differences may not be biologically important; however, they are statistically significant due to a large number of samples included in the analyses. More prospective clinical trials are warranted to verify the potentials of TMEscore in predicting patient outcomes and response to both chemotherapeutic agents and ICB.

In conclusion, our present study depicted a comprehensive landscape of the TME signatures in LUADs. Meanwhile, the TMEscore was proved to be a promising predictor of patient survival and therapeutic responses in LUADs, which might be helpful to the future administration of personalized adjuvant therapy.

## DATA AVAILABILITY STATEMENT

The datasets presented in this study can be found in online repositories. The names of the repository/repositories and accession number(s) can be found in the article/**Supplementary Material**.

## ETHICS STATEMENT

Ethical review and approval were not required for the study on human participants in accordance with the local legislation and institutional requirements. Written informed consent for participation was not required for this study in accordance with the national legislation and the institutional requirements.

## AUTHOR CONTRIBUTIONS

DC, YW, XZ, and QD: conceptualization, formal analysis, and writing original draft. XW, YX, and WW: data curation, methodology, and formal analysis. YM: software, methodology, supervision, and reviewing the draft. YC and CC: supervision, reviewing, and editing the draft. All authors contributed to the article and approved the submitted version.

## FUNDING

Jiangsu Key Research and Development Plan (Social Development) Project (BE2020653); Suzhou Key Discipline for Medicine (SZXK201803); Suzhou Key Laboratory of Thoracic Oncology (SZS201907); Municipal Program of People's Livelihood Science and Technology in Suzhou (SS2019061); Discipline Construction Project of the Second Affiliated Hospital of Soochow University (XKTJ-XK202004); Scientific Program of Suzhou Municipal Health and Health Committee (LCZX202004).

## SUPPLEMENTARY MATERIAL

The Supplementary Material for this article can be found online at: https://www.frontiersin.org/articles/10.3389/fonc.2021.581030/full#supplementary-material

**Supplementary Figure 1 |** General flowchart and TME infiltrates of LUAD samples in our study. **(A)** Overview of the study design; **(B)** The specific 23 immune and stromal fractions represented by various colors in each LUAD sample from The Cancer Genome Atlas (TCGA) database.

**Supplementary Figure 2 |** Determination and assessment of different TMEclusters. **(A, B)** Elbow method and gap statistic to determining the optimal number of clusters in the dataset; **(C)** Consensus matrix of the LUAD cohort for *K*=3, displaying the clustering stability using 1000 iterations of hierarchical clustering; **(D)** Kaplan-Meier curves showing the survival stratified by different TMEclusters.

**Supplementary Figure 3 |** Characterization of DEGs among the three TMEclusters and the derived TME signature genes. **(A)** Venn diagram illustrating the number of differentially expressed genes (DEGs) among the three TMEclusters; **(B)** Consensus matrix of DEGs for *K*=2, displaying the clustering stability using 1000 iterations of hierarchical clustering; **(C)** Gene Ontology (GO) enrichment analysis of the TME relevant signature genes. The x axis indicates the number of genes within each GO term.

**Supplementary Figure 4 |** Survival analyses of LUAD patients in different datasets stratified by TMEscore. **(A, B)** Kaplan-Meier curves exhibiting the survival of patient cohort from TCGA dataset with stage I-II disease stratified by TMEscore; **(C)** Kaplan-Meier curves for the two subgroups of patients from the Gene Expression Omnibus (GEO) dataset (GSE68465) stratified by TMEscore;

**(D)** Kaplan-Meier curves for the survival of smokers in the GEO dataset stratified by TMEscore.

**Supplementary Figure 5 |** Summary of the mutation information with statistical calculations. **(A–C)** Classification of mutation types according to different categories, in which missense mutation accounts for the most fraction of SNV, SNV showed more frequency than insertion or deletion, and C>A was the most common of SNV; **(D–E)** tumor mutation burden and variant classification in specific samples; **(F)** the top 10 mutated genes in LUADs.

**Supplementary Figure 6 |** Mutation landscape of the top 10 mutated genes in TCGA LUAD cohort stratified by TME subtypes and its association with histologic subtypes.

**Supplementary Figure 7 |** Survival curves of patient cohorts stratified by TME-related signature genes. **(A–E)** Kaplan-Meier curve showing OS of TCGA cohort stratified by **(A)** BTK, **(B)** LY86, **(C)** CCDC69, **(D)** CD33, and **(E)** CD52 expression, respectively; **(F)** Kaplan-Meier curve showing OS of domestic cohort stratified by BTK expression.

## REFERENCES


1. TCGA Research Network. Comprehensive molecular profiling of lung adenocarcinoma. *Nature* (2014) 511:543–50. doi: 10.1038/nature13385
2. Warth A, Muley T, Meister M, Stenzinger A, Thomas M, Schirmacher P, et al. The Novel Histologic International Association for the Study of Lung Cancer/American Thoracic Society/European Respiratory Society Classification System of Lung Adenocarcinoma Is a Stage-Independent Predictor of Survival. *J Clin Oncol* (2012) 30:1438–46. doi: 10.1200/JCO.2011.37.2185
3. Buttner R, Gosney JR, Skov BG, Adam J, Motoi N, Bloom KJ, et al. Programmed Death-Ligand 1 Immunohistochemistry Testing: A Review of Analytical Assays and Clinical Implementation in Non-Small-Cell Lung Cancer. *J Clin Oncol* (2017) 35:3867–76. doi: 10.1200/JCO.2017.74.7642
4. Dong ZY, Zhong WZ, Zhang XC, Su J, Xie Z, Liu SY, et al. Potential Predictive Value of TP53 and KRAS Mutation Status for Response to PD-1 Blockade Immunotherapy in Lung Adenocarcinoma. *Clin Cancer Res* (2017) 23:3012–24. doi: 10.1158/1078-0432.CCR-16-2554
5. Reck M, Rodriguez-Abreu D, Robinson AG, Hui R, Csoszi T, Fulop A, et al. Pembrolizumab versus Chemotherapy for PD-L1-Positive Non-Small-Cell Lung Cancer. *N Engl J Med* (2016) 375:1823–33. doi: 10.1056/NEJMoa1606774
6. Naidoo J, Page DB, Li BT, Connell LC, Schindler K, Lacouture ME, et al. Toxicities of the anti-PD-1 and anti-PD-L1 immune checkpoint antibodies. *Ann Oncol* (2015) 26:2375–91. doi: 10.1093/annonc/mdv383
7. Matikas A, Zerdes I, Lovrot J, Richard F, Sotiriou C, Bergh J, et al. Prognostic implications of PD-L1 expression in breast cancer: systematic review and meta-analysis of immunohistochemistry and pooled analysis of transcriptomic data. *Clin Cancer Res* (2019) 25:5717–26. doi: 10.1158/1078-0432.CCR-19-1131
8. Zeng D, Li M, Zhou R, Zhang J, Sun H, Shi M, et al. Tumor microenvironment characterization in gastric cancer identifies prognostic and immunotherapeutically relevant gene signatures. *Cancer Immunol Res* (2019) 7:737–50. doi: 10.1158/2326-6066.CIR-18-0436
9. Remark R, Lupo A, Alifano M, Biton J, Ouakrim H, Stefani A, et al. Immune contexture and histological response after neoadjuvant chemotherapy predict clinical outcome of lung cancer patients. *Oncoimmunology* (2016) 5: e1255394. doi: 10.1080/2162402X.2016.1255394
10. Thommen DS, Schreiner J, Muller P, Herzig P, Roller A, Belousov A, et al. Progression of Lung Cancer Is Associated with Increased Dysfunction of T Cells Defined by Coexpression of Multiple Inhibitory Receptors. *Cancer Immunol Res* (2015) 3:1344–55. doi: 10.1158/2326-6066.CIR-15-0097
11. Zhang C, Zhang J, Xu FP, Wang YG, Xie Z, Su J, et al. Genomic Landscape and Immune Microenvironment Features of Preinvasive and Early-Invasive Lung Adenocarcinoma. *J Thorac Oncol* (2019) 14:1912–23. doi: 10.1016/j.jtho.2019.07.031
12. Lavin Y, Kobayashi S, Leader A, Amir ED, Elefant N, Bigenwald C, et al. Innate Immune Landscape in Early Lung Adenocarcinoma by Paired Single-Cell Analyses. *Cell* (2017) 169:750–65.e17. doi: 10.1016/j.cell.2017.04.014
13. Suda K, Kim J, Murakami I, Rozeboom L, Shimoji M, Shimizu S, et al. Innate Genetic Evolution of Lung Cancers and Spatial Heterogeneity: Analysis of Treatment-Naïve Lesions. *J Thorac Oncol* (2018) 13:1496–507. doi: 10.1016/j.jtho.2018.05.039
14. Chen H, Carrot-Zhang J, Zhao Y, Hu H, Freeman SS, Yu S, et al. Genomic and immune profiling of pre-invasive lung adenocarcinoma. *Nat Commun* (2019) 10:5472. doi: 10.1038/s41467-019-13460-3
15. Kinoshita T, Kudo-Saito C, Muramatsu R, Fujita T, Saito M, Nagumo H, et al. Determination of poor prognostic immune features of tumour microenvironment in non-smoking patients with lung adenocarcinoma. *Eur J Cancer* (2017) 86:15–27. doi: 10.1016/j.ejca.2017.08.026
16. Sakai T, Aokage K, Neri S, Nakamura H, Nomura S, Tane K, et al. Link between tumor-promoting fibrous microenvironment and an immunosuppressive microenvironment in stage I lung adenocarcinoma. *Lung Cancer* (2018) 126:64–71. doi: 10.1016/j.lungcan.2018.10.021
17. Donnem T, Kilvaer TK, Andersen S, Richardsen E, Paulsen EE, Hald SM, et al. Strategies for clinical implementation of TNM-Immunoscore in resected nonsmall-cell lung cancer. *Ann Oncol* (2016) 27:225–32. doi: 10.1093/annonc/mdv560
18. Corredor G, Wang X, Zhou Y, Lu C, Fu P, Syrigos KN, et al. Spatial architecture and arrangement of tumor-infiltrating lymphocytes for predicting likelihood of recurrence in early-stage non-small cell lung cancer. *Clin Cancer Res* (2019) 25:1526–34. doi: 10.1158/1078-0432.CCR-18-2013
19. Krysan K, Tran LM, Grimes BS, Fishbein GA, Seki A, Gardner BK, et al. The Immune Contexture Associates with the Genomic Landscape in Lung Adenomatous Premalignancy. *Cancer Res* (2019) 79:5022–33. doi: 10.1158/0008-5472.CAN-19-0153
20. Newman AM, Liu CL, Green MR, Gentles AJ, Feng W, Xu Y, et al. Robust enumeration of cell subsets from tissue expression profiles. *Nat Methods* (2015) 12:453–7. doi: 10.1038/nmeth.3337
21. Becht E, Giraldo NA, Lacroix L, Buttard B, Elarouci N, Petitprez F, et al. Estimating the population abundance of tissue-infiltrating immune and stromal cell populations using gene expression. *Genome Biol* (2016) 17:218. doi: 10.1186/s13059-016-1070-5
22. Gautier L, Cope L, Bolstad B, Irizarry R. affy–analysis of Affymetrix GeneChip data at the probe level. *Bioinformatics* (2004) 20:307–15. doi: 10.1093/bioinformatics/btg405
23. Jabi M, Pedersoli M, Mitiche A, Ben AI. Deep clustering: On the link between discriminative models and K-means. *IEEE Trans Pattern Anal Mach Intell* (2019). doi: 10.1109/TPAMI.2019.2962683
24. Monti S, Tamayo P, Mesirov J, Golub T. Consensus Clustering: A Resampling-Based Method for Class Discovery and Visualization of Gene Expression Microarray Data. *Mach Learn* (2003) 52:91–118. doi: 10.1023/A:1023949509487
25. Ritchie ME, Phipson B, Wu D, Hu Y, Law CW, Shi W, et al. limma powers differential expression analyses for RNA-sequencing and microarray studies. *Nucleic Acids Res* (2015) 43:e47. doi: 10.1093/nar/gkv007
26. Yu G, Wang L-G, Han Y, He Q-Y. clusterProfiler: an R package for comparing biological themes among gene clusters. *OMICS* (2012) 16:284–7. doi: 10.1089/omi.2011.0118
27. Hothorn T. maxstat: Maximally Selected Rank Statistics. R package version 0.7-22. (2015). doi: 10.1158/2326-6066.cir-18-0436
28. Mayakonda A, Lin DC, Assenov Y, Plass C, Koeffler HP. Maftools: efficient and comprehensive analysis of somatic variants in cancer. *Genome Res* (2018) 28:1747–56. doi: 10.1101/gr.239244.118
29. Gehring JS, Fischer B, Lawrence M, Huber W. SomaticSignatures: inferring mutational signatures from single-nucleotide variants. *Bioinformatics* (2015) 31:3673–5. doi: 10.1093/bioinformatics/btv408
30. Alexandrov LB, Nik-Zainal S, Wedge DC, Aparicio SA, Behjati S, Biankin AV, et al. Signatures of mutational processes in human cancer. *Nature* (2013) 500:415–21. doi: 10.1038/nature12477
31. Alexandrov LB, Nik-Zainal S, Wedge DC, Campbell PJ, Stratton MR. Deciphering signatures of mutational processes operative in human cancer. *Cell Rep* (2013) 3:246–59. doi: 10.1016/j.celrep.2012.12.008

32. van Dessel L, van Riet J, Smits M, Zhu Y, Hamberg P, van der Heijden M, et al. The genomic landscape of metastatic castration-resistant prostate cancers reveals multiple distinct genotypes with potential clinical impact. *Nat Commun* (2019) 10:5251. doi: 10.1038/s41467-019-13084-7
33. Jiang P, Gu S, Pan D, Fu J, Sahu A, Hu X, et al. Signatures of T cell dysfunction and exclusion predict cancer immunotherapy response. *Nat Med* (2018) 24:1550–8. doi: 10.1038/s41591-018-0136-1
34. Wang Q, Li M, Yang M, Yang Y, Song F, Zhang W, et al. Analysis of immune-related signatures of lung adenocarcinoma identified two distinct subtypes: implications for immune checkpoint blockade therapy. *Aging* (2020) 12:3312–39. doi: 10.18632/aging.102814
35. Wang S, He Z, Wang X, Li H, Liu XS. Antigen presentation and tumor immunogenicity in cancer immunotherapy response prediction. *eLife* (2019) 8:e49020. doi: 10.7554/eLife.49020
36. Keenan TE, Burke KP, Van Allen EM. Genomic correlates of response to immune checkpoint blockade. *Nat Med* (2019) 25:389–402. doi: 10.1038/s41591-019-0382-x
37. Kaderbhaï C, Tharin Z, Ghiringhelli F. The Role of Molecular Profiling to Predict the Response to Immune Checkpoint Inhibitors in Lung Cancer. *Cancers* (2019) 11:201. doi: 10.3390/cancers11020201
38. Geeleher P, Cox N, Huang RS. pRRophetic: an R package for prediction of clinical chemotherapeutic response from tumor gene expression levels. *PloS One* (2014) 9:e107468. doi: 10.1371/journal.pone.0107468
39. Qiu X, Chen D, Liu Y, Duan S, Zhang F, Zhang Y, et al. Relationship between stromal cells and tumor spread through air spaces in lung adenocarcinoma. *Thorac Cancer* (2019) 10:256–67. doi: 10.1111/1759-7714.12945
40. Benjamini Y, Hochberg Y. Controlling the false discovery rate: a practical and powerful approach to multiple testing. *J R Stat Soc: Ser B (Methodological)* (1995) 57:289–300. doi: 10.1111/j.2517-6161.1995.tb02031.x
41. Robin X, Turck N, Hainard A, Tiberti N, Lisacek F, Sanchez J-C, et al. pROC: an open-source package for R and S+ to analyze and compare ROC curves. *BMC Bioinf* (2011) 12:77. doi: 10.1186/1471-2105-12-77
42. Hause RJ, Pritchard CC, Shendure J, Salipante SJ. Classification and characterization of microsatellite instability across 18 cancer types. *Nat Med* (2016) 22:1342–50. doi: 10.1038/nm.4191
43. Luchini C, Bibeau F, Ligtenberg MJL, Singh N, Nottegar A, Bosse T, et al. ESMO recommendations on microsatellite instability testing for immunotherapy in cancer, and its relationship with PD-1/PD-L1 expression and tumour mutational burden: a systematic review-based approach. *Ann Oncol* (2019) 30:1232–43. doi: 10.1093/annonc/mdz116
44. Fu J, Li K, Zhang W, Wan C, Zhang J, Jiang P, et al. Large-scale public data reuse to model immunotherapy response and resistance. *Genome Med* (2020) 12:21. doi: 10.1186/s13073-020-0721-z
45. Yue C, Ma H, Zhou Y. Identification of prognostic gene signature associated with microenvironment of lung adenocarcinoma. *PeerJ* (2019) 7:e8128. doi: 10.7717/peerj.8128
46. Bi KW, Wei XG, Qin XX, Li B. BTK Has Potential to Be a Prognostic Factor for Lung Adenocarcinoma and an Indicator for Tumor Microenvironment Remodeling: A Study Based on TCGA Data Mining. *Front Oncol* (2020) 10:424:424. doi: 10.3389/fonc.2020.00424
47. Tan Q, Huang Y, Deng K, Lu M, Wang L, Rong Z, et al. Identification immunophenotyping of lung adenocarcinomas based on the tumor microenvironment. *J Cell Biochem* (2020) 121:4569–79. doi: 10.1002/jcb.29675
48. Huang J, Li J, Zheng S, Lu Z, Che Y, Mao S, et al. Tumor microenvironment characterization identifies two lung adenocarcinoma subtypes with specific immune and metabolic state. *Cancer Sci* (2020) 111(6):1876–86. doi: 10.1111/cas.14390
49. Song Q, Shang J, Yang Z, Zhang L, Zhang C, Chen J, et al. Identification of an immune signature predicting prognosis risk of patients in lung adenocarcinoma. *J Transl Med* (2019) 17:70. doi: 10.1186/s12967-019-1824-4
50. Zhang M, Zhu K, Pu H, Wang Z, Zhao H, Zhang J, et al. An Immune-Related Signature Predicts Survival in Patients With Lung Adenocarcinoma. *Front Oncol* (2019) 9:1314. doi: 10.1186/s12967-019-1824-4
51. Hung JJ, Wu YC, Chou TY, Jeng WJ, Yeh YC, Hsu WH. Adjuvant Chemotherapy Improves the Probability of Freedom From Recurrence in Patients With Resected Stage IB Lung Adenocarcinoma. *Ann thoracic Surg* (2016) 101:1346–53. doi: 10.1016/j.athoracsur.2015.10.075
52. Qian F, Yang W, Wang R, Xu J, Wang S, Zhang Y, et al. Prognostic significance and adjuvant chemotherapy survival benefits of a solid or micropapillary pattern in patients with resected stage IB lung adenocarcinoma. *J Thorac Cardiovasc Surg* (2018) 155:1227–35.e2. doi: 10.1016/j.jtcvs.2017.09.143
53. Wang J, Wu N, Lv C, Yan S, Yang Y. Should patients with stage IB non-small cell lung cancer receive adjuvant chemotherapy? A comparison of survival between the 8th and 7th editions of the AJCC TNM staging system for stage IB patients. *J Cancer Res Clin Oncol* (2019) 145:463–9. doi: 10.1007/s00432-018-2801-7


**Conflict of Interest:** The authors declare that the research was conducted in the absence of any commercial or financial relationships that could be construed as a potential conflict of interest.

frontiers in Oncology

ORIGINAL RESEARCH
published: 09 March 2021
doi: 10.3389/fonc.2021.621050

# Glycogen Synthase Kinase-3 Beta Expression Correlates With Worse Overall Survival in Non-Small Cell Lung Cancer—A Clinicopathological Series

*Marclesson Alves[1], Daniela de Paula Borges[2], Aline Kimberly[1,2], Francisco Martins Neto[3], Ana Claudia Oliveira[3], Juliana Cordeiro de Sousa[1,2], Cleto D. Nogueira[1,2], Benedito A. Carneiro[4] and Fabio Tavora[1,2,3]**

[1] Department of Pathology, Federal University of Ceará, Fortaleza, Brazil, [2] Argos Pathology Laboratory, Department of Investigative Pathology, Fortaleza, Brazil, [3] Departments of Patholoy, Oncology and Thoracic Surgery, Messejana Heart and Lung Hospital, Fortaleza, Brazil, [4] Division of Hematology/Oncology, Lifespan Cancer Institute, The Warren Alpert Medical School of Brown University, Providence, RI, United States

OPEN ACCESS

**Edited by:**
Giulia Pasello,
Veneto Institute of Oncology (IRCCS), Italy

**Reviewed by:**
Pasquale Pisapia,
University of Naples Federico II, Italy
Federica Pezzuto,
University of Padua, Italy

***Correspondence:**
Fabio Tavora
ftavora@gmail.com

**Specialty section:**
This article was submitted to Thoracic Oncology, a section of the journal Frontiers in Oncology

**Received:** 24 October 2020
**Accepted:** 27 January 2021
**Published:** 09 March 2021

**Citation:**
Alves M, Borges DP, Kimberly A, Martins Neto F, Oliveira AC, Sousa JC, Nogueira CD, Carneiro BA and Tavora F (2021) Glycogen Synthase Kinase-3 Beta Expression Correlates With Worse Overall Survival in Non-Small Cell Lung Cancer—A Clinicopathological Series. Front. Oncol. 11:621050. doi: 10.3389/fonc.2021.621050

**Background:** Glycogen Synthase Kinase-3 beta (GSK-3β) regulates diverse cell functions including metabolic activity, signaling and structural proteins. GSK-3β phosphorylates target pro-oncogenes and regulates programmed cell death-ligand 1 (PD-L1). This study investigated the correlation between GSK-3β expression and clinically relevant molecular features of lung adenocarcinoma (PDL1 score, PTEN expression and driver mutations).

**Methods:** We evaluated 95 lung cancer specimens from biopsies and surgical resections. Immunohistochemistry was performed to analyze the expression of GSK-3β, PTEN, and PDL1. Epidemiological data, molecular characteristics and staging were evaluated from medical records. The histologic classification was performed by an experienced pulmonary pathologist.

**Results:** Most patients were female (52.6%) and the majority had a positive smoking history. The median age was 68.3 years, with individuals over 60 years accounting for 82.1%. The predominant histological subtype was adenocarcinoma (69.5%), followed by squamous cell carcinoma (20.0%). GSK-3β expression in tumors was cytoplasmic with a dotted pattern and perinuclear concentration, with associated membranous staining. Seven (7.3%) tumors had associated nuclear expression localization. Seventy-seven patients (81.1%) had advanced clinical-stage tumors. GSK-3β was positive in 75 tumors (78%) and GSK3-positive tumors tended to be diagnosed at advanced stages. Among stage III/IV tumors, 84% showed GSK3 positivity (p= 0.007). We identified a statistically significant association between GSK-3β and PTEN in the qualitative analysis (p 0.021); and when comparing PTEN to GSK-3β intensity 2+ (p 0.001) or 3+ expression (> 50%) – p 0.013. GSK-3β positive tumors with a high histological score had a worse overall survival.

**Conclusion:** We identified the histological patterns of GSK-3β expression and evaluated its potential as marker for overall survival, establishing a simple histological score to measure the evaluated status in resected tissues. The use of GSK-3β expression as an immune response biomarker remains a challenge. Future studies will seek to explain the role of its interaction with PTEN.

**Keywords: glycogen synthase kinase-3 beta (GSK-3 beta), lung cancer, non-small cell carcinoma, immunotherapy, programmed death-ligand 1 (PD-L1), phosphatase and tensin homolog deleted on chromosome 10 (PTEN)**

## INTRODUCTION

Lung cancer represents a serious public health problem. In addition to its high incidence, this malignancy has the highest mortality rate worldwide (1). Glycogen synthase kinase-3 (GSK3) is a serine/threonine kinase, initially described as an ATP-Mg-dependent protein phosphatase (2), subdivided into two isoforms: GSK3 α and β (3). GSK3 was initially found to be related to various inflammatory processes, psychiatric disorders, neurodegenerative diseases, diabetes, cardiac dysfunction, autoimmune disorders, and more recently, it has been associated with cancer development (4, 5). It has been shown that GSK3 phosphorylates various components (TSC2, RICTOR, PTEN, and AKT) of the PI3K-AKT signaling network, an essential pathway for cell proliferation. Growth factors, cytokines, and chemokines are some of the signals that stimulate this process (6).

GSK3 is a central regulator of programmed cell death protein-1 (PD-1) expression, and GSK3 inhibition may downregulate PD-1 and enhance CD8+ cytolytic T cell (CTL) function (7). PD-1 and its ligand (PD-L1) are involved in the immune checkpoint pathway mechanism, of which activation promotes negative regulation of anti-tumor actions (8–11). In the same context, immunotherapy has become the new frontier to be explored in the cancer therapeutic arsenal, especially in lung cancer (12) (13). The level of PD-L1 expression measured by immunohistochemistry correlates with treatment response through the immune checkpoint inhibitor (14) (15). However, its quantification can be influenced by numerous variables, such as tumor heterogeneity, prior systemic therapy, radiation therapy, the molecular status of the neoplasia, type of sample analyzed, and different test methods (16).

PTEN negatively regulates the PI3K/AKT pathway, playing an important role in intracellular growth, leading to decreased phosphorylation of AKT substrates, including BAD (BCL-2-associated agonist of cell death) and GSK-3 (17, 18). PTEN functions as a tumor suppressor gene that antagonizes PI3K activity (19). Several mechanisms can identify PTEN loss, such as mutations, deletions, absence of protein expression, and promoter methylation. In lung tumors, the absence of immunohistochemical expression is seen in 30%–50% of cases (20). (**Figure 1**).

Considering these interactions with components of tumor growth pathways, GSK-3β has become a critical molecule to be used in the fight against cancer and the development of new drugs (30). In the search for the improvement and innovation in biomarkers, recognizing its potential to influence carcinogenesis, and considering its role in other inflammatory pathologies, our study analyzed the GSK-3β expression in lung cancer and its correlation with PDL1, the best predictor of response to immunotherapy used in clinical practice.

## MATERIALS AND METHODS

### Patient and Tissue Selection

We sequentially selected 95 patients diagnosed with lung cancer between 2013 and 2019 in the State of Ceará, using available material (paraffin blocks) and follow-up information from an approximate cohort of 450 newly diagnosed patients from the same period. All patients had clinically and pathologically confirmed tumors as primary lung cancer. The Ethics Review Board reviewed and approved this research study. Cases were diagnosed by a single Thoracic Pathologist based on the current WHO criteria (31, 32).The inclusion criteria consisted of non-small cell lung cancer with enough tissue sample (paraffin blocks with tissue containing more than 100 tumor cells after all recuts) and availability for additional immunohistochemical studies. All patients with secondary tumors of the lung were excluded from the study. Epidemiology and clinicopathological characters (such as gender, age, smoking status, comorbidities, TNM stage, survival, molecular mutations) were obtained from medical records or by contacting the patients.

Tumor necrosis was defined as any amount of necrotic tumor, as an area of increased eosinophilia without tumor cell nuclei, only the shadow of membranous tumor cells or with nuclear shrinkage or fragmentation.

### Immunohistochemistry

Immunohistochemistry (IHC) was performed on histological sections of tumors obtained from biopsies or resections. The sections were cut and mounted on electrically charged glass slides. GSK-3β (Cell Signaling, clone 27C10) and PTEN (Clone SP218; Roche Diagnostics Limited, Burgess Hill, UK) IHC analyses were performed on the Ventana® platform (BenchMark ULTRA IHC/ISH Staining Module, Ventana Medical Systems, Tucson, AZ). The PD-L1 IHC analysis (22C3 pharmDx, Agilent, clone 22c3) was recovered using PT-Link (Dako PT100), followed by target recovery with EnVision ™ FLEX pH 6.0 buffer, using the Agilent Technologies®, USA visualization system in Autostainer Link 48® equipment.

GSK-3ß was recorded according to the cytoplasmic and membranous staining intensity as 0 (negative), 1+(weak), 2+ (moderate), and 3+ (strong), and the percentage of stained tumor cells. A final histological score was established ([% of weak

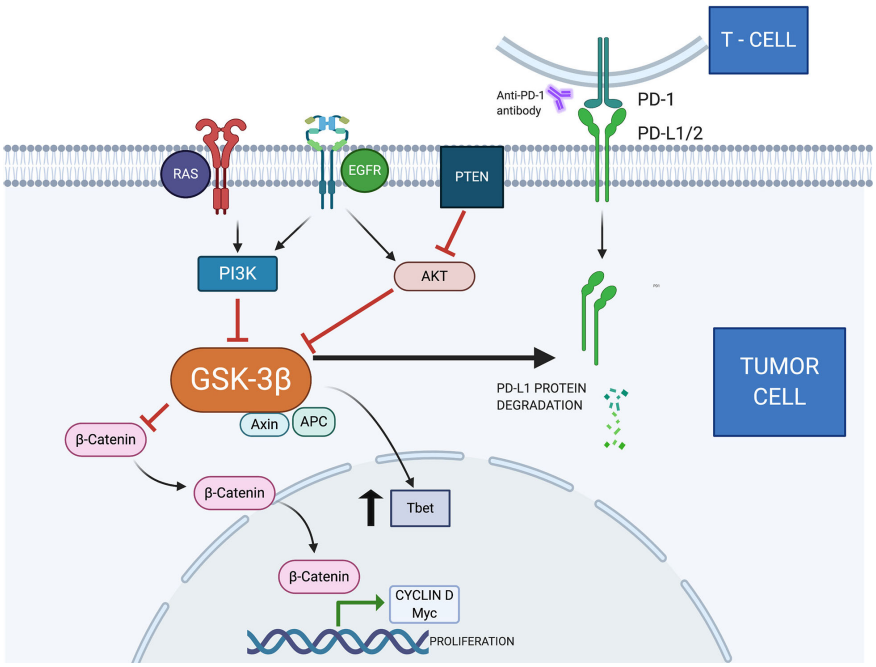


**FIGURE 1** | Several ligands on the cell surface stimulate the production of PIP3 (phosphatidylinositol trisphosphate) by PI3K. These molecules act as a substrate for protein activation, including AKT. This protein phosphorylates GSK3, inhibiting its function (6). The tumor suppressor gene PTEN blocks AKT activity by dephosphorylating PIP3 and PIK3 (21). In addition, Akt can activate the IκB complex (IKK), which phosphorylates IκB, becoming an important stimulus for NFκB (22). The NFkB is translocated to the nucleus, promoting the production of COX-2, an enzyme associated with angiogenesis, invasion, and metastasis (23). A complex consisting of AXIN, APC, and GSK3 is responsible for the destruction and negative regulation of B-catenin (24). The Wnt/β-catenin signaling pathway is related to cell proliferation, stem cell self-renewal, and cell differentiation (25). When active and in accumulation, B-catenin is translocated to the nucleus. Cyclin D1 and C-myc are oncogenes associated with cell proliferation and differentiation. Previous publications demonstrated they are target genes for the Wnt/B-catenin signaling pathway (26). T-box transcription factor protein 21 (TBX21)—also known as Tbet—is present in tumor cells, causing local immune response dysregulation and carcinogenesis (27). GSK3 inhibition promotes increased Tbet transcription (28). Previous reports demonstrated that GSK3 can cause PDL1 degradation by the proteasome pathway (29). GSK3, Glycogen Synthase Kinase-3; PI3K, Phosphatidylinositol-3-kinase; AKT, protein kinase B; MAPK, Mitogen-Activated Protein Kinase; APC, Adenomatous polyposis coli; Axin, Axis inhibitor; NFκB, Nuclear factor-κ light chain enhancer of activated B cells; PTEN, Phosphatase and tensin homolog; COX-2, Cyclooxygenase-2; EGFR, Epidermal growth factor receptor; MyC, Myelocytomatosis—proto oncogene; Tbet, transcription factor T-box expressed in T cells; RAS, Rat sarcoma—oncogene; PD-L1, Programmed death-ligand 1.

staining × 1] + [% of moderate staining × 2] + [% of strong staining × 3]) to determine the overall percentage of GSK-3ß positivity across the entire stained tumor sample, yielding a range from 0 to 300. Any tumor with a score >200 was considered as showing high GSK-3ß expression.

PD-L1 was assessed as membranous positivity in tumor cells, following the Tumor Proportion Score (TPS) as practiced currently (33). We tried different cutoff points to reflect clinical scenarios: <1%, 1%–49%, ≥50%. In investigating the correlation with PTEN, we use yet another method of quantification, characterizing PD-L1 as positive or negative expression if tumor cells had a positivity above 1%.

PTEN protein was considered lost if the cytoplasmic and nuclear staining intensity was markedly decreased or entirely negative across >10% of tumor cells when compared to surrounding benign tissue, which provides internal positive controls. Other molecular data (*EGFR*, *ALK*, *BRAF*, and *KRAS* status) were retrieved from medical records, and correlation with the protein expression findings was attempted.

## Statistical Analysis

Patients were followed for up to 68.3 months (mean follow-up of 18.8 months, SD 14.3 months). Distant metastasis was defined as recurrence at any site other than the abovementioned ones and was confirmed by imaging studies and histopathological evidence, when necessary. Overall survival (OS) was defined as the interval between the initial diagnosis and death (event) or the last follow-up date.

Statistical evaluation was performed by Stata® version 13 statistical software (StataCorp LP, College Station, TX, USA). Initially, a descriptive analysis of the study population variables was performed, calculating absolute and relative frequencies. Subsequently, bivariate analysis was performed using Pearson's or Fisher's chi-square test (when expected values of the contingency table cell were <5), with their respective 95% confidence intervals and statistical significance ($p < 0.05$).

Also, multiple regression was run to predict the overall survival based on the variables age, gender, smoking, histology, treatment (QT), clinic stage, EGFR, PD-L1, and GSK3β

expression. The assumptions of linearity, independence of errors, homoscedasticity, unusual points, and normality of residuals were tested using SPSS 24.0 (SPSS Inc., Chicago, IL, USA).

# RESULTS

## Patient Demographics and Treatment

We evaluated 95 patients with primary lung cancer (90 samples from lung parenchyma and five from pleural tissue). Most patients were female (52.6%), and the majority had a positive smoking history (77.7% of the males and 52% of females). The median age at diagnosis was 68.3 years (range, 32.1–94.9 years), with individuals over 60 years accounting for 82.1%. All data regarding the clinical and pathological factors are presented in **Table 1**.

Seventy-seven patients (81.1%) had advanced clinical-stage tumors at diagnosis (Stages III–IV). Treatment consisted of systemic therapy (including cytotoxic therapy, immunotherapy, or both) in 70.5% patients, lobectomy in 25.2% patients, segmentectomy in 2.1%, and pneumonectomy in 2.1%. Patients following chemotherapy standard protocol represented 85.5% of the cohort, with an additional 25.5% undergoing anti-PD1 immunotherapy regimens. Tyrosine kinase inhibitors corresponded to treatment in 20.2% of cases. Antiangiogenics were found as part of therapy in only 10% of patients. Radiation therapy was administered as a therapeutic modality in 51.1% of patients. It was used to control bone pain, definitive therapy concomitant with chemotherapy, or finally approach brain metastasis. Tumors were in the right upper lobe in 27.4%, followed by the left superior in 25.3%, left inferior in 18.9%, right inferior in 17.9%, and the middle lobe in 5.3%.

## Pathological Classification

The predominant histological subtype was adenocarcinoma (69.5%) followed by squamous cell carcinoma (20.0%). The remainder were unclassifiable non-small cell carcinoma with characteristics of large-cell carcinoma (WHO recommendation). Invasive adenocarcinomas with predominant acinar and solid patterns of growth were the most often identified (39.4% and 37.9%, respectively). There were seven lepidic-predominant (10.6% of adenocarcinomas), one mucinous, and one minimally invasive adenocarcinoma (1.5% each). Most squamous cell carcinomas were moderately differentiated non-keratinizing, tumors, showing the usual histology. Non-small cell, not otherwise specified carcinomas, did not show glandular, squamous or neuroendocrine differentiation either by light microscopy morphology or immunohistochemistry. Tumor necrosis was present at least focally in 40% of cases (38 cases) and showed a strong correlation with solid growth pattern [high-grade, (R=0.335, p=0.012)].

## GSK-3 Beta Protein Expression

GSK-3β was identified in 75 tumors (78%), being considered high in 17 cases (22.7%) and low in 58 cases (77.3%) (**Figures 2** and **3**). There was no difference in GSK-3β positivity when comparing gender, age, or smoking history. GSK-3β-positive tumors were more prevalent in advanced-stage tumors. Among stage III/IV tumors, 84% showed GSK3 positivity, in contrast with 55.6% of stage I/II tumors, with statistical significance in the univariate and multivariate analyses (p = 0.007) (**Table 2**). Interestingly, when evaluating by size alone, we identified a greater number of patients with GSK-3β expression in T1/T2 tumors (95%CI 0.86–1.32, p = 0.523), compared to T3/T4 cancers, but without statistical significance.

We found no statistically significant differences regarding GSK-3β and driver mutations, such as *EGFR*, *ALK*, *ROS1*, or *BRAF* (**Table 1**). Only 11 patients were tested for KRAS mutations. Three cases were KRAS mutated (27.2%), while eight were KRAS wild type (72.8%). There was no direct correlation between GSK-3β expression and PD-L1 positivity or PD-L1 percentage. When considering the PDL1 score most often used in clinical trials and treatment guidelines (negative, 1%–49% and > 50%), no correlation was found. The data is summarized in **Table 1**. Tumor necrosis was also found to be statistically significant with PD-L1 expression regardless of PD-L1 cutoff levels (p<0.001), but there was no correlation between tumor necrosis and GSK-3β expression in the cohort.

Multivariate logistic regression analysis further showed that overall survival was related to EGFR gene mutation (p=0.023), final clinical staging (p=0.033) and GSK-3β expression (p=0.035). These results indicate that the expression of GSK-3β could be potentially a marker of overall prognosis independent of driver mutation status and is correlated with smoking status and clinical stage (**Table 3**).

Of note, we identified a statistical correlation between GSK3 and PTEN (95% CI 0.72–28.73, p = 0.021) with the greater number of PTEN positivity in cases where GSK3 intensity score was = 2 (95%CI 1.04–39.7, p = 0.001) (**Table 2**).

## Survival Analysis

Patients were followed for up to 68.3 months (median 14.1, range 1.0–68.3). Patients with adenocarcinomas survived on average 19.6 months and patients with squamous cell carcinomas, 14.5 months. Solid-predominant tumors had a poor survival rate when compared to the remainder (p<0.01). There was a significant difference when comparing the survival of patients with high GSK expression with patients with low or absent GSK (p<0.0062; **Figure 4**, Kaplan-Meier). We also found a significant difference in survival in patients presenting with higher stage and lymph node metastasis, as expected (p=0.010). There was no statistical difference regarding survival when comparing PDL1, ALK, or EGFR status alone or in combination with GSK-3β. Patients with PTEN positivity had a better overall survival (p=0.026).

# DISCUSSION

Immune manipulation is a chapter of extensive research in oncology. Knowledge about biomarkers predicts better outcomes and results. Our article studied GSK-3 beta protein expression, tumor prognosis, and possible interactions in non-small cell lung cancer. The high expression of GSK-3 was correlated to a worse prognosis, underscoring the importance of studies hypothesizing that blocking GSK can be a potential therapeutic target in non-small lung cancer. After understanding their

**TABLE 1 |** Analysis of clinico-pathologic characteristics of studied population by GSK-3β expression, with bivariate and multivariate analysis.

| | | GSK | | Bivariate | | | Multivariate | | |
|---|---|---|---|---|---|---|---|---|---|
| | **Total N (%)** | **Negative N (%)** | **Positive N (%)** | **RP** | **CI95%** | **P-value** | **RP*** | **CI95%*** | **P-value*** |
| Gender | | | | | | | | | |
| Female | 50 (52.6) | 8 (16.0) | 42 (84.0) | 1.14 | 0.92–1.42 | 0.203 | | | |
| Male | 45 (47.4) | 12 (26.7) | 33 (73.3) | Ref | | | | | |
| Ethnic group | | | | | | | | | |
| Caucasian | 42 (44.2) | 6 (14.3) | 36 (85.7) | Ref | | | 0.73 | 0.41–1.27 | 0.265 |
| African-Brazilian | 2 (2.1) | 2 (100) | – | | | | | | |
| Multiracial | 51 (53.7) | 12 (23.5) | 39 (76.5) | 0.89 | 0.73–1.08 | 0.261 | | | |
| Age (years) | | | | | | | | | |
| <60 | 17 (17.9) | 4 (23.5) | 13 (76.5) | Ref | | | | | |
| ≥60 | 78 (82.1) | 16 (20.5) | 62 (79.5) | 1.04 | 0.78–1.38 | 0.782 | | | |
| Smoking | | | | | | | | | |
| No | 34 (35.8) | 4 (11.8) | 30 (88.2) | Ref | | | 0.43 | 0.12–1.47 | 0.178 |
| Yes | 61 (64.2) | 16 (26.2) | 45 (73.8) | 0.83 | 0.69–1.01 | 0.097 | | | |
| Site (lobe) | | | | | | | | | |
| Inferior Right | 17 (17.9) | 5 (29.4) | 12 (70.6) | Ref | | | | | |
| Inferior Left | 18 (18.9) | 4 (22.2) | 14 (77.8) | 1.10 | 0.74–1.63 | 0.628 | | | |
| Middle | 5 (5.3) | | 5 (100) | | | | | | |
| Superior Right | 26 (27.4) | 6 (23.1) | 20 (76.9) | 1.09 | 0.75–1.58 | 0.642 | | | |
| Superior Left | 24 (25.3) | 5 (20.8) | 19 (79.2) | 1.12 | 0.77–1.62 | 0.529 | | | |
| Histology | | | | | | | | | |
| Adenocarcinoma | 66 (69.5) | 13 (19.7) | 53 (80.3) | 1.34 | 0.79–2.25 | 0.151 | | | |
| Squamous Cell Carcinoma | 19 (20.0) | 3 (158) | 16 (84.2) | 1.40 | 0.82–2.41 | 0.148 | | | |
| Other | 10 (10.5) | 4 (40.0) | 6 (60.0) | Ref | | | | | |
| Adenocarcinoma subtype | | | | | | | | | |
| Acinar | 26 (39.4) | 3 (11.5) | 23 (88.5) | 2.06 | 0.87–4.91 | 0.009 | | | |
| Lepidic | 7 (10.6) | 4 (57.1) | 3 (42.9) | Ref | | | | | |
| Minimally invasive | 1 (1.5) | | 1 (100) | | | | | | |
| Invasive mucinous | 1 (1.5) | | 1 (100) | | | | | | |
| Solid | 25 (37.9) | 5 (20.0) | 20 (80.0) | 1.87 | 0.78–4.49 | 0.053 | | | |
| T (primary tumor) | | | | | | | | | |
| 1 + 2 | 51 (56.7) | 9 (17.6) | 42 (82.4) | 1.07 | 0.86–1.32 | 0.523 | | | |
| 3 + 4 | 39 (43.3) | 9 (23.1) | 30 (76.9) | Ref | | | | | |
| N (regional lymph node) | | | | | | | | | |
| 0 + 1 | 41 (45.1) | 11 (26.8) | 30 (73.2) | Ref | | | | | |
| 2 + 3 | 50 (54.9) | 8 (16.0) | 42 (84.0) | 1.15 | 0.92–1.43 | 0.206 | | | |
| TNM Stage | | | | | | | | | |
| I + II | 18 (18.9) | 8 (44.4) | 10 (55.6) | Ref | | | 4.59 | 1.43–14.72 | 0.010 |
| III + IV | 77 (81.1) | 12 (15.6) | 65 (84.4) | 1.51 | 0.99–2.32 | 0.007 | | | |
| EGFR | | | | | | | | | |
| Inconclusive | 2 (2.1) | 1 (50.0) | 1 (50.0) | Ref | | | | | |
| Negative | 45 (47.4) | 10 (22.2) | 35 (77.8) | 1.55 | 0.38–6.27 | 0.364 | | | |
| Positive | 20 (21.1) | 2 (10.0) | 18 (90.0) | 1.80 | 0.45–7.25 | 0.116 | | | |
| ALK | | | | | | | | | |
| Negative | 55 (57.9) | 11 (20.0) | 44 (80.0) | Ref | | | | | |
| Positive | 6 (6.3) | 1 (16.7) | 5 (83.3) | 1.04 | 0.71–1.52 | 0.845 | | | |
| PDL1 | | | | | | | | | |
| Negative | 62 (65.3) | 14 (22.6) | 48 (77.4) | Ref | | | | | |
| Positive | 29 (30.5) | 5 (17.2) | 24 (82.8) | 1.07 | 0.86–1.32 | 0.559 | | | |
| PDL1 score | | | | | | | | | |
| <1% | 61 (64.2) | 14 (22.9) | 47 (77.1) | | | | | | |
| 1-49% | 17 (17.9) | 3 (17.6) | 14 (82.4) | 1.07 | 0.82–1.38 | 0.639 | | | |
| ≥50% | 13 (13.7) | 2 (15.4) | 11 (84.6) | 1.09 | 0.84–1.44 | 0.547 | | | |
| ROS1 | | | | | | | | | |
| Uncertain | 1 (1.1) | | 1 (100) | | | | | | |
| Inconclusive | 2 (2.1) | 1 (50.0) | 1 (50.0) | Ref | | | | | |
| Negative | 26 (27.4) | 4 (15.4) | 22 (84.6) | 1.69 | 0.42–6.38 | 0.281 | | | |
| BRAF | | | | | | | | | |
| Negative | 15 (15.8) | 4 (26.7) | 11 (13.3) | | | 0.551 | | | |
| Positive | 1 (1.1) | | 1 (100) | | | | | | |

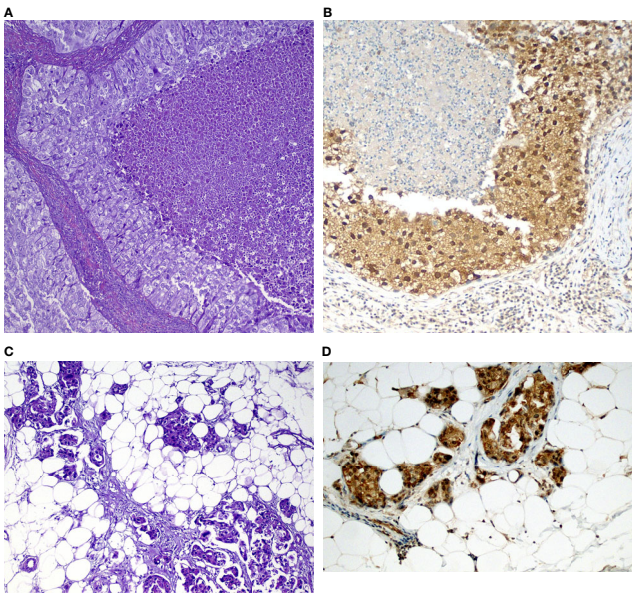


**FIGURE 2** | Examples of tumors and corresponding immunohistochemical stains in **(A)** Solid-predominant adenocarcinoma with tumor necrosis (center) and over atypia; **(B)** GSK-3β expression in the tumor above showing strong (3+) positivity in both nuclei and cytoplasm. Note weak GSK-3β expression in small lymphocytes (arrowheads). **(C)** Acinar adenocarcinoma metastatic to the parietal pleura (adipose tissue) showing **(D)** cytoplasmic staining in tumor cells.

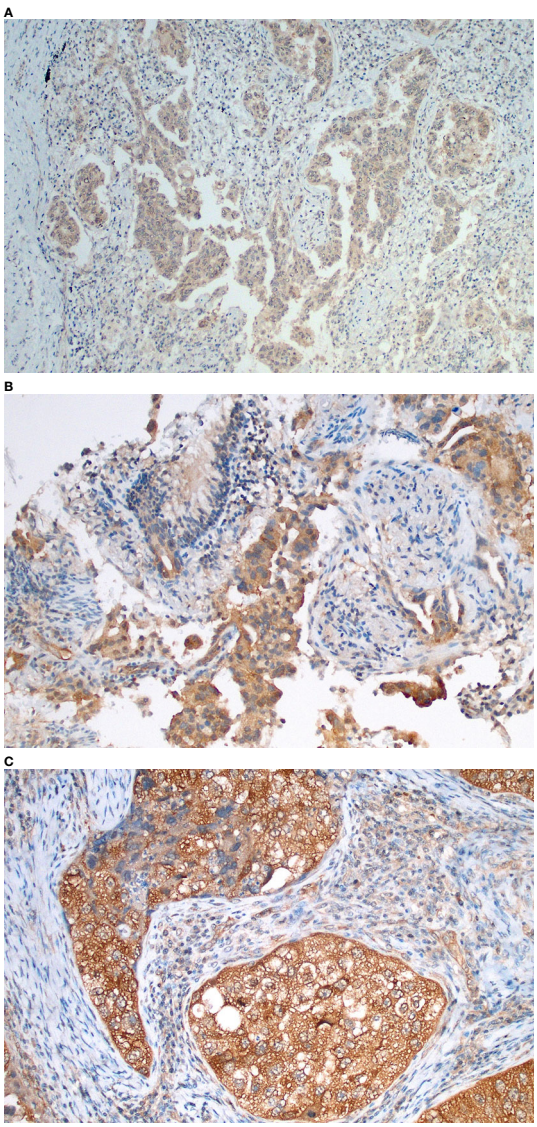


**FIGURE 3** | Immunohistochemical findings of GSK-3β in lung adenocarcinomas, demonstrating semi-quantitative score examples and showing distinct membranous and cytoplasm expression. **(A)** GSK-3β weak (1+) expression in acinar predominant lung adenocarcinoma; **(B)** Moderate expression (2+) in acinar predominant lung adenocarcinoma evaluated in a transbronchial biopsy sample; **(C)** Strong expression in a solid-predominant adenocarcinoma with focal nuclear localization and association with tumor necrosis.

intracellular interactions, GSK3 inhibitors have been researched in the treatment of cancer (34). Many types of drugs have been developed (35) and are being tested in pre-clinical and phase I studies, with promising results (36).

We identified a greater number of advanced-stage III/IV tumors in patients with high GSK3 expression (p=0.007). This translates into a possible more aggressive biological component in this population, or even an association with different genotypes, since higher tumor mutation burden (TMB) has been associated with advanced lung tumors. In contrast, recent studies have shown that tumors with high TMB may respond better to nivolumab and pembrolizumab (37). Somatic mutations can produce neoantigens, immunogenic peptides that activate the immune response. TMB and PDL1 have the same clinical applicability. However, TMB represents a complement and not a substitute for PDL1 (38). Another interesting finding in the current study is the correlation of tumor necrosis and PD-L1 expression. These are in accordance to other studies that showed tumors with higher PD-L1 expression with a greater tendency to necrosis, a more aggressive tumor phenotype and higher proliferation rate (39, 40).

Tumor cells have developed several mechanisms to escape immune surveillance. GSK3 stands out in the regulation of the PD-1/PD-L1 inhibitory checkpoint. This immune activation process can occur through PD-1 interaction or modulation in the tumor molecule PD-L1. Li et al. demonstrated that GSK-3β correlates to PD-L1 and induces phosphorylation-dependent degradation of PD-L1 by b-TrCP (41). The inhibition of GSK3 also acts to promote PD1 downregulation. When associated with anti-PD1 or anti-PDL1 block, it enhances the cytotoxic capacity of T cells (42). Taylor et al. demonstrated that GSK-3 participates in the regulation of PD-1 transcription. GSK-3 inhibition increases Tbet activity, reducing PD-1 transcription, with a further intensification of T lymphocyte cytolytic action (28). Despite the theoretical rationale supporting this association, we did not identify a relationship between PDL1 and GSK-3β scores in our cohort. A recent publication about the positivity of PDL1 in the same region of northeastern Brazil showed that 59.5% of patients were PDL1 negative (43).

**TABLE 2 |** Bivariate analysis and correlations of GSK-3β expression and PTEN status in lung tumors.

| | Total n (%) | PTEN | | Bivariate | | |
|---|---|---|---|---|---|---|
| | | Negative N (%) | Positive N (%) | RP | CI95% | P-value |
| GSK-3β | | | | | | |
| Negative | 7 (25.9) | 6 (85.7) | 1 (14.3) | Ref | | |
| Positive | 20(74.1) | 7 (35.0) | 13(65.0) | 4.55 | 0.72–28.73 | 0.021 |
| GSK Intensity | | | | | | |
| 0 | 7 (25.9) | 6 (85.7) | 1 (14.3) | Ref | | |
| 1 | 6 (22.2) | 4 (66.7) | 2 (33.3) | 2.33 | 0.27–19.8 | 0.416 |
| 2 | 12(44.4) | 1 (8.3) | 11(91.7) | 6.42 | 1.04–39.7 | 0.001 |
| 3 | 2 (7.4) | 2 (100) | | | | |
| GSK score | | | | | | |
| <1% | 7 (25.9) | 6 (85.7) | 1 (14.3) | Ref | | |
| 1%–49% | 6 (22.2) | 3 (50.0) | 3 (50.0) | 3.50 | 0.48–25.4 | 0.164 |
| ≥50% | 14(51.8) | 4 (28.6) | 10(71.4) | 5.00 | 0.79–31.6 | 0.013 |
| PDL1 | | | | | | |
| Negative | 20(76.9) | 8 (40.0) | 12(60.0) | Ref | | |
| Positive | 6 (23.1) | 4 (66.7) | 2 (33.3) | 0.55 | 0.17–1.82 | 0.251 |
| PDL1 score | | | | | | |
| <10% | 22(81.5) | 10 (45.4) | 12(54.6) | Ref | | |
| ≥10% | 5 (18.5) | 3 (60.0) | 2 (40.0) | 0.73 | 0.23–2.29 | 0.557 |
| PDL1 analysis | | | | | | |
| <1% | 21(77.8) | 9 (42.9) | 12(57.1) | 1.42 | 0.46–4.45 | 0.489 |
| 1%–49% | 5 (18.5) | 3 (60.0) | 2 (40.0) | Ref | | |
| ≥50% | 1 (3.7) | 1 (100.0) | | | | |

**TABLE 3 |** Multiple regression to predict overall survival based on clinic variables and GSK-3β expression.

| Variables | Unstandardized Coefficients | | Standardized Coefficients | t | Sig. |
|---|---|---|---|---|---|
| | B | Std. Error | Beta | | |
| Death (Constant) | 3.994 | 0.917 | | 4.353 | 0.000 |
| Age | -0.005 | 0.006 | -0.126 | -0.895 | 0.376 |
| Gender | -0.149 | 0.148 | -0.161 | -1.010 | 0.319 |
| Smoking | 0.147 | 0.146 | 0.155 | 1.006 | 0.321 |
| Histology | 0.111 | 0.150 | 0.119 | 0.741 | 0.463 |
| Treatment | -0.187 | 0.261 | -0.123 | -0.719 | 0.477 |
| PDL1 | -0.200 | 0.142 | -0.203 | -1.411 | 0.167 |
| EGFR | -0.453 | 0.192 | -0.446 | -2.361 | **0.023** |
| Clinic stage | -0.185 | 0.084 | -0.354 | -2.207 | **0.033** |
| GSK-3β | -0.375 | 0.171 | -0.328 | -2.189 | **0.035** |

*Bold text indicates significant differences (p < 0.05).*

Matsuo et al. studied the importance of AKT, mTOR, and GSK3 in the occurrence of lymph node involvement in oral cavity squamous cell carcinomas. Elevated expression of GSK3 and pGSK3-βSer9 was associated with metastasis in cervical lymph nodes (p = 0.004 and p = 0.03) (44) and advanced stages (cTNM), suggesting the relationship of GSK3 with tumor invasion and metastases. In our study, of the few squamous cell carcinomas studied, the expression score of GSK3 was more evident in poorly differentiated tumors and advanced stages. Blocking GSK-3β reduced cell proliferation, stimulated apoptosis, maintained cells in the GO/G1 phase and increased cell invasion. A study published by Zeng et al. focused on the association between GSK3 and survival. The positive expression of GSK3 by immunohistochemistry was also related to a worse prognosis (45). Therefore, the relationship between GSK3 and direct survival has been hypothesized.

Cigarette exposure corresponds to a cluster of toxic substances that promote damage to alveolar cells (46). The mechanisms involved are still not fully understood. Besides, it induces beta-catenin accumulation (47). Nagahori et al. analyzed a polymorphism of the GSK3 gene and its connection with smoking habits. In a cohort of 384 patients, rs334558 was associated with smoking in genotype and allelic frequency (48). Numajiri M et al. also published an article describing the relationship between a polymorphism of the *GSK3* gene and its relationship with nicotine dependence (49). Despite the possible inhibition of GSK3 by smoking, we found no statistical basis for this association in our population (p=0,097).

Anaplastic lymphoma kinase (ALK) is a tyrosine kinase with altered expression in several tumors. In lung cancer, ALK-EML4 rearrangement occurs in about 3%–5% of cases (50), allowing the use of target drugs and achieving better survival results (51). Malagon et al. analyzed the relationship between ALK and GSK3

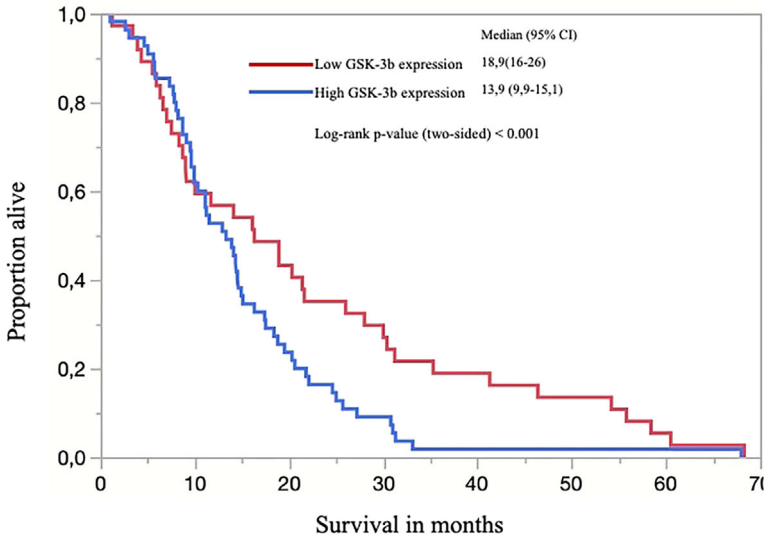


**FIGURE 4** | Kaplan-Meier curve of overall survival (OS) for all patients separated by low (score <200) and high expression of GSK-3β and; the censored events were defined for OS as time to the last known date alive before analysis or date of death.

in neuroblastomas and neural crest cells. They suggest a positive regulation of GSK3 *via* ALK tyrosine kinase (52). McDonnell SRP et al. studied anaplastic large-cell lymphoma, a pediatric disease, in which the NPM-ALK alteration is present in 70%–80% of cases. They revealed that ALK activity acts on the phosphorylation of S9-GSK-3 *via* PI3K/AKT, making GSK3 an important regulator of ALK carcinogenesis (53).

EGFR is a surface receptor, a HER family component, also known as erbB1, HER1, or even as EGFR (54). Its activation triggers intracellular cascades, promoting cell growth and oncogenesis (55). It is especially important in lung tumors, acting as a predictor of response to tyrosine kinase inhibitors (56). Fitzgerald et al. studied the role of EGFR in the intracellular signaling pathways of pancreatic tumors. EGFR activates the Ras/Raf/MEK/ERK pathway. Consequently, it stimulates the ETS transcription factor that binds to the GSK-3beta promoter and induces the expression of GSK-3 and IKK. Subsequently, this regulates the production of NF-kappa-B, leading to gene transcription and cell proliferation (57). This exemplifies a possible relationship between EGFR mutations and GSK3 expression.

In the current study, an additional analysis in a subset of 27 resection samples demonstrated a statistically significant association between GSK-3β and PTEN analysis by immunohistochemistry ($p = 0.021$). This relationship was more evident in cases with strong GSK-3β expression or the expression in > 50% of the tumor. Zhengyu H et al. demonstrated that PTEN overexpression reduces fibroblast proliferation by inhibiting the PI3K/AKT/GSK3 pathway (26). Gao C. et al. showed by measuring the levels of GSK-3β, PTEN, and AKT in breast tumor cell lines, that the PTEN/PI3K/AKT pathway can be regulated by GSK3 (58). PTEN inactivation is associated with lower survival and resistance to systemic treatment (59). These findings underscore the importance of GSK activation in tumor survival and growth regulation (60).

Although previously identified as a tumor suppressor, PTEN is not currently used in clinical practice as a lung cancer biomarker. While active PTEN has anti-tumor action, resulting in better outcomes (18, 61, 62). This is in contrast to our results, which shows a positive correlation. Further research involving GSK3 and PTEN blockers in lung cancer is necessary for better clarification and therapeutic use to manipulate these intracellular checkpoints.

In conclusion, GSK-3β is a molecule involved in multiple signaling pathways. Positive tumor expression was associated with a more advanced tumor stage and worse overall survival in lung cancer. To the best of our knowledge, this is the first study to identify the expression of GSK-3β as a potential marker for overall survival and establish a simple histological score to be measured in resected tissues. The use of GSK-3β expression as an immune response biomarker remains a challenge. Future studies will seek to explain the role of its interaction with PTEN.

## DATA AVAILABILITY STATEMENT

The original contributions presented in the study are included in the article/supplementary material. Further inquiries can be directed to the corresponding author.

## ETHICS STATEMENT

The studies involving human participants were reviewed and approved by Federal University of Ceará. Written informed consent for participation was not required for this study in accordance with the national legislation and the institutional requirements.

## AUTHOR CONTRIBUTIONS

MA, BC, and FT designed the study. DB, AK, and JS performed all molecular studies and immunohistochemical studies. MA and FM reviewed patients charts and follow-up information. Slides were evaluated by pathologists FT, CN, and AO. MA, FT, and BC wrote and reviewed the final manuscript. FT is the lead investigator. All authors contributed to the article and approved the submitted version.

## REFERENCES


1. Siegel RL, Miller KD, Jemal A. Cancer statistics, 2020. *CA Cancer J Clin* (2020) 70(1):7–30. doi: 10.3322/caac.21590
2. Vandenheede JR, Yang SD, Goris J, Merlevede W. ATP x Mg-dependent protein phosphatase from rabbit skeletal muscle. II. Purification of the activating factor and its characterization as a bifunctional protein also displaying synthase kinase activity. *J Biol Chem* (1980) 255(24):11768–74. doi: 10.1016/S0021-9258(19)70200-2
3. Woodgett JR. Molecular cloning and expression of glycogen synthase kinase-3/factor A. *EMBO J* (1990) 9(8):2431–8. doi: 10.1002/j.1460-2075.1990.tb07419.x
4. Beurel E, Grieco SF, Jope RS. Glycogen synthase kinase-3 (GSK3): regulation, actions, and diseases. *Pharmacol Ther* (2015) 148:114–31. doi: 10.1016/j.pharmthera.2014.11.016
5. Jope RS, Yuskaitis CJ, Beurel E. Glycogen synthase kinase-3 (GSK3): inflammation, diseases, and therapeutics. *Neurochem Res* (2007) 32(4-5):577–95. doi: 10.1007/s11064-006-9128-5
6. Hermida MA, Dinesh Kumar J, Leslie NR. GSK3 and its interactions with the PI3K/AKT/mTOR signalling network. *Adv Biol Regul* (2017) 65:5–15. doi: 10.1016/j.jbior.2017.06.003
7. Rudd CE, Chanthong K, Taylor A. Small Molecule Inhibition of GSK-3 Specifically Inhibits the Transcription of Inhibitory Co-receptor LAG-3 for Enhanced Anti-tumor Immunity. *Cell Rep* (2020) 30(7):2075–82.e4. doi: 10.1016/j.celrep.2020.01.076
8. Iwai Y, Terawaki S, Honjo T. PD-1 blockade inhibits hematogenous spread of poorly immunogenic tumor cells by enhanced recruitment of effector T cells. *Int Immunol* (2005) 17(2):133–44. doi: 10.1093/intimm/dxh194
9. Freeman GJ, Long AJ, Iwai Y, Bourque K, Chernova T, Nishimura H, et al. Engagement of the PD-1 immunoinhibitory receptor by a novel B7 family member leads to negative regulation of lymphocyte activation. *J Exp Med* (2000) 192(7):1027–34. doi: 10.1084/jem.192.7.1027
10. Xia L, Liu Y, Wang Y. PD-1/PD-L1 Blockade Therapy in Advanced Non-Small-Cell Lung Cancer: Current Status and Future Directions. *Oncologist* (2019) 24(Suppl 1):S31–41. doi: 10.1634/theoncologist.2019-IO-S1-s05
11. Rotte A. Combination of CTLA-4 and PD-1 blockers for treatment of cancer. *J Exp Clin Cancer Res* (2019) 38(1):255–. doi: 10.1186/s13046-019-1259-z
12. Rosenthal R, Cadieux EL, Salgado R, Bakir MA, Moore DA, Hiley CT, et al. Neoantigen-directed immune escape in lung cancer evolution. *Nature* (2019) 567(7749):479–85. doi: 10.1038/s41586-019-1032-7
13. van den Bulk J, Verdegaal EM, de Miranda NF. Cancer immunotherapy: broadening the scope of targetable tumours. *Open Biol* (2018) 8(6):180037. doi: 10.1098/rsob.180037
14. Gandhi L, Rodriguez-Abreu D, Gadgeel S, Esteban E, Felip E, De Angelis F, et al. Pembrolizumab plus Chemotherapy in Metastatic Non-Small-Cell Lung Cancer. *N Engl J Med* (2018) 378(22):2078–92. doi: 10.1056/NEJMoa1801005
15. Reck M, Rodriguez-Abreu D, Robinson AG, Hui R, Csoszi T, Fulop A, et al. Pembrolizumab versus Chemotherapy for PD-L1-Positive Non-Small-Cell Lung Cancer. *N Engl J Med* (2016) 375(19):1823–33. doi: 10.1056/NEJMoa1606774
16. Bassanelli M, Sioletic S, Martini M, Giacinti S, Viterbo A, Staddon A, et al. Heterogeneity of PD-L1 Expression and Relationship with Biology of NSCLC. *Anticancer Res* (2018) 38(7):3789–96. doi: 10.21873/anticanres.12662
17. Hollander MC, Blumenthal GM, Dennis PA. PTEN loss in the continuum of common cancers, rare syndromes and mouse models. *Nat Rev Cancer* (2011) 11(4):289–301. doi: 10.1038/nrc3037
18. Ma J, Guo X, Zhang J, Wu D, Hu X, Li J, et al. PTEN Gene Induces Cell Invasion and Migration via Regulating AKT/GSK-3beta/beta-Catenin Signaling Pathway in Human Gastric Cancer. *Dig Dis Sci* (2017) 62 (12):3415–25. doi: 10.1007/s10620-017-4764-y
19. Park MK, Yao Y, Xia W, Setijono SR, Kim JH, Vila IK, et al. PTEN self-regulates through USP11 via the PI3K-FOXO pathway to stabilize tumor suppression. *Nat Commun* (2019) 10(1):636. doi: 10.1038/s41467-019-08481-x
20. Alvarez-Garcia V, Tawil Y, Wise HM, Leslie NR. Mechanisms of PTEN loss in cancer: It's all about diversity. *Semin Cancer Biol* (2019) 59:66–79. doi: 10.1016/j.semcancer.2019.02.001
21. Porta C, Paglino C, Mosca A. Targeting PI3K/Akt/mTOR Signaling in Cancer. *Front Oncol* (2014) 4:64. doi: 10.3389/fonc.2014.00064
22. Ghoneum A, Said N. PI3K-AKT-mTOR and NFκB Pathways in Ovarian Cancer: Implications for Targeted Therapeutics. *Cancers (Basel)* (2019) 11 (7):949. doi: 10.3390/cancers11070949
23. Shi G, Li D, Fu J, Sun Y, Li Y, Qu R, et al. Upregulation of cyclooxygenase-2 is associated with activation of the alternative nuclear factor kappa B signaling pathway in colonic adenocarcinoma. *Am J Transl Res* (2015) 7(9):1612–20.
24. Li Vivian SW, Ng Ser S, Boersema Paul J, Low Teck Y, Karthaus Wouter R, Gerlach Jan P, et al. Wnt Signaling through Inhibition of β-Catenin Degradation in an Intact Axin1 Complex. *Cell* (2012) 149(6):1245–56. doi: 10.1016/j.cell.2012.05.002
25. Cheng X, Xu X, Chen D, Zhao F, Wang W. Therapeutic potential of targeting the Wnt/β-catenin signaling pathway in colorectal cancer. *Biomed Pharmacother* (2019) 110:473–81. doi: 10.1016/j.biopha.2018.11.082
26. He Z, Deng Y, Li W, Chen Y, Xing S, Zhao X, et al. Overexpression of PTEN suppresses lipopolysaccharide-induced lung fibroblast proliferation, differentiation and collagen secretion through inhibition of the PI3-K-Akt-GSK3beta pathway. *Cell Biosci* (2014) 4(1):2. doi: 10.1186/2045-3701-4-2
27. Zhang X, Wen X, Feng N, Chen A, Yao S, Ding X, et al. Increased Expression of T-Box Transcription Factor Protein 21 (TBX21) in Skin Cutaneous Melanoma Predicts Better Prognosis: A Study Based on The Cancer Genome Atlas (TCGA) and Genotype-Tissue Expression (GTEx) Databases. *Med Sci Monit* (2020) 26:e923087. doi: 10.12659/MSM.923087
28. Taylor A, Harker JA, Chanthong K, Stevenson PG, Zuniga EI, Rudd CE. Glycogen Synthase Kinase 3 Inactivation Drives T-bet-Mediated Downregulation of Co-receptor PD-1 to Enhance CD8(+) Cytolytic T Cell Responses. *Immunity* (2016) 44(2):274–86. doi: 10.1016/j.immuni.2016.01.018
29. Jiang X-M, Xu Y-L, Huang M-Y, Zhang L-L, Su M-X, Chen X, et al. Osimertinib (AZD9291) decreases programmed death ligand-1 in EGFR-mutated non-small cell lung cancer cells. *Acta Pharmacol Sin* (2017) 38 (11):1512–20. doi: 10.1038/aps.2017.123
30. Sahin I, Eturi A, De Souza A, Pamarthy S, Tavora F, Giles FJ, et al. Glycogen synthase kinase-3 beta inhibitors as novel cancer treatments and modulators of antitumor immune responses. *Cancer Biol Ther* (2019) 20(8):1047–56. doi: 10.1080/15384047.2019.1595283
31. Travis WD. The 2015 WHO classification of lung tumors. *Pathologe* (2014) 35 Suppl 2:188. doi: 10.1007/s00292-014-1974-3
32. Travis WD, Brambilla E, Noguchi M, Nicholson AG, Geisinger K, Yatabe Y, et al. Diagnosis of lung adenocarcinoma in resected specimens: implications of the 2011 International Association for the Study of Lung Cancer/American Thoracic Society/European Respiratory Society classification. *Arch Pathol Lab Med* (2013) 137(5):685–705. doi: 10.5858/arpa.2012-0264-RA
33. Reck M, Rodriguez-Abreu D, Robinson AG, Hui R, Csoszi T, Fulop A, et al. Updated Analysis of KEYNOTE-024: Pembrolizumab Versus Platinum-Based Chemotherapy for Advanced Non-Small-Cell Lung Cancer With PD-L1 Tumor Proportion Score of 50% or Greater. *J Clin Oncol* (2019) 37(7):537–46. doi: 10.1200/JCO.18.00149
34. Maqbool M, Hoda N. GSK3 Inhibitors in the Therapeutic Development of Diabetes, Cancer and Neurodegeneration: Past, Present and Future. *Curr Pharm Des* (2017) 23(29):4332–50. doi: 10.2174/1381612823666170714141450
35. Augello G, Emma MR, Cusimano A, Azzolina A, Montalto G, McCubrey JA, et al. The Role of GSK-3 in Cancer Immunotherapy: GSK-3 Inhibitors as a New Frontier in Cancer Treatment. *Cells* (2020) 9(6):1427. doi: 10.3390/cells9061427

36. Carneiro BA, Cavalcante L, Bastos BR, Powell SF, Ma WW, Sahebjam S, et al. Phase I study of 9-ing-41, a small molecule selective glycogen synthase kinase-3 beta (GSK-3β) inhibitor, as a single agent and combined with chemotherapy, in patients with refractory tumors. *J Clin Oncol* (2020) 38 (15_suppl):3507. doi: 10.1200/JCO.2020.38.15_suppl.3507
37. Yoneda K, Imanishi N, Ichiki Y, Tanaka F. Immune Checkpoint Inhibitors (ICIs) in Non-Small Cell Lung Cancer (NSCLC). *J UOEH* (2018) 40(2):173–89. doi: 10.7888/juoeh.40.173
38. Chan TA, Yarchoan M, Jaffee E, Swanton C, Quezada SA, Stenzinger A, et al. Development of tumor mutation burden as an immunotherapy biomarker: utility for the oncology clinic. *Ann Oncol* (2019) 30(1):44–56. doi: 10.1093/annonc/mdy495
39. Pawelczyk K, Piotrowska A, Ciesielska U, Jablonska K, Gletzel-Plucinska N, Grzegrzolka J, et al. Role of PD-L1 Expression in Non-Small Cell Lung Cancer and Their Prognostic Significance according to Clinicopathological Factors and Diagnostic Markers. *Int J Mol Sci* (2019) 20(4):824. doi: 10.3390/ijms20040824
40. Reiniger L, Teglasi V, Pipek O, Rojko L, Glasz T, Vagvolgyi A, et al. Tumor necrosis correlates with PD-L1 and PD-1 expression in lung adenocarcinoma. *Acta Oncol* (2019) 58(8):1087–94. doi: 10.1080/0284186X.2019.1598575
41. Li CW, Lim SO, Xia W, Lee HH, Chan LC, Kuo CW, et al. Glycosylation and stabilization of programmed death ligand-1 suppresses T-cell activity. *Nat Commun* (2016) 7:12632. doi: 10.1038/ncomms12632
42. Krueger J, Rudd CE, Taylor A. Glycogen synthase 3 (GSK-3) regulation of PD-1 expression and and its therapeutic implications. *Semin Immunol* (2019) 42:101295. doi: 10.1016/j.smim.2019.101295
43. Oliveira A, Silva A, Alves M, Cronemberger E, Carneiro BA, Melo JC, et al. Molecular profile of non-small cell lung cancer in northeastern Brazil. *J Bras Pneumol* (2019) 45(3):e20180181. doi: 10.1590/1806-3713/e20180181
44. Matsuo FS, Andrade MF, Loyola AM, da Silva SJ, Silva MJB, Cardoso SV, et al. Pathologic significance of AKT, mTOR, and GSK3beta proteins in oral squamous cell carcinoma-affected patients. *Virchows Arch* (2018) 472 (6):983–97. doi: 10.1007/s00428-018-2318-0
45. Zeng J, Liu D, Qiu Z, Huang Y, Chen B, Wang L, et al. GSK3β overexpression indicates poor prognosis and its inhibition reduces cell proliferation and survival of non-small cell lung cancer cells. *PLoS One* (2014) 9(3):e91231–e. doi: 10.1371/journal.pone.0091231
46. Bakre SA, Al-Farra TS, Al-Farra S. Diffuse alveolar damage and e-cigarettes: Case report and review of literature. *Respir Med Case Rep* (2019) 28:100935. doi: 10.1016/j.rmcr.2019.100935
47. Gattinoni L, Zhong X-S, Palmer DC, Ji Y, Hinrichs CS, Yu Z, et al. Wnt signaling arrests effector T cell differentiation and generates CD8+ memory stem cells. *Nat Med* (2009) 15(7):808–13. doi: 10.1038/nm.1982
48. Nagahori K, Iwahashi K, Narita S, Numajiri M, Yoshihara E, Nishizawa D, et al. [Association between GSK3beta polymorphisms and the smoking habits in young Japanese]. *Nihon Shinkei Seishin Yakurigaku Zasshi* (2015) 35(3):73–7.
49. Numajiri M, Iwahashi K, Nishizawa D, Ikeda K, Yoshihara E, Ishigooka J. [Haplotype analysis of GSK-3beta gene polymorphisms and smoking behavior]. *Nihon Shinkei Seishin Yakurigaku Zasshi* (2013) 33(4):175–8.
50. Pikor LA, Ramnarine VR, Lam S, Lam WL. Genetic alterations defining NSCLC subtypes and their therapeutic implications. *Lung Cancer* (2013) 82 (2):179–89. doi: 10.1016/j.lungcan.2013.07.025
51. Hida T, Satouchi M, Nakagawa K, Seto T, Matsumoto S, Kiura K, et al. Ceritinib in patients with advanced, crizotinib-treated, anaplastic lymphoma kinase-rearranged NSCLC: Japanese subset. *Jpn J Clin Oncol* (2017) 47 (7):618–24. doi: 10.1093/jjco/hyx045
52. Gonzalez Malagon SG, Liu KJ. ALK and GSK3: Shared Features of Neuroblastoma and Neural Crest Cells. *J Exp Neurosci* (2018) 12:1179069518792499. doi: 10.1177/1179069518792499
53. McDonnell SR, Hwang SR, Basrur V, Conlon KP, Fermin D, Wey E, et al. NPM-ALK signals through glycogen synthase kinase 3beta to promote oncogenesis. *Oncogene* (2012) 31(32):3733–40. doi: 10.1038/onc.2011.542
54. Ciardiello F, Tortora G. EGFR antagonists in cancer treatment. *N Engl J Med* (2008) 358(11):1160–74. doi: 10.1056/NEJMra0707704
55. Normanno N, De Luca A, Bianco C, Strizzi L, Mancino M, Maiello MR, et al. Epidermal growth factor receptor (EGFR) signaling in cancer. *Gene* (2006) 366(1):2–16. doi: 10.1016/j.gene.2005.10.018
56. Liu X, Wang P, Zhang C, Ma Z. Epidermal growth factor receptor (EGFR): A rising star in the era of precision medicine of lung cancer. *Oncotarget* (2017) 8 (30):50209–20. doi: 10.18632/oncotarget.16854
57. Fitzgerald TL, Lertpiriyapong K, Cocco L, Martelli AM, Libra M, Candido S, et al. Roles of EGFR and KRAS and their downstream signaling pathways in pancreatic cancer and pancreatic cancer stem cells. *Adv Biol Regul* (2015) 59:65–81. doi: 10.1016/j.jbior.2015.06.003
58. Wu P, Heins ZJ, Muller J, Katsnelson L, de Bruijn I, Abeshouse AA, et al. Integration and analysis of CPTAC proteomics data in the context of cancer genomics in the cBioPortal. *Mol Cell Proteomics* (2019) 18(9):1893–8. doi: 10.1074/mcp.TIR119.001673
59. Pérez-Ramírez C, Cañadas-Garre M, Molina MÁ, Faus-Dáder MJ, Calleja-Hernández MÁ. PTEN and PI3K/AKT in non-small-cell lung cancer. *Pharmacogenomics* (2015) 16(16):1843–62. doi: 10.2217/pgs.15.122
60. Yang Y, Lei T, Du S, Tong R, Wang H, Yang J, et al. Nuclear GSK3β induces DNA double-strand break repair by phosphorylating 53BP1 in glioblastoma. *Int J Oncol* (2018) 52(3):709–20. doi: 10.3892/ijo.2018.4237
61. Liu X, Zhang P, Xie C, Sham KWY, Ng SSM, Chen Y, et al. Activation of PTEN by inhibition of TRPV4 suppresses colon cancer development. *Cell Death Dis* (2019) 10(6):460. doi: 10.1038/s41419-019-1700-4
62. Tsoyi K, Jang HJ, Nizamutdinova IT, Park K, Kim YM, Kim HJ, et al. PTEN differentially regulates expressions of ICAM-1 and VCAM-1 through PI3K/Akt/GSK-3β/GATA-6 signaling pathways in TNF-α-activated human endothelial cells. *Atherosclerosis* (2010) 213(1):115–21. doi: 10.1016/j.atherosclerosis.2010.07.061


**Conflict of Interest:** The authors declare that the research was conducted in the absence of any commercial or financial relationships that could be construed as a potential conflict of interest.

frontiers in Oncology

ORIGINAL RESEARCH
published: 22 March 2021
doi: 10.3389/fonc.2021.653497

# P14/ARF-Positive Malignant Pleural Mesothelioma: A Phenotype With Distinct Immune Microenvironment

*Federica Pezzuto[1], Francesca Lunardi[1], Luca Vedovelli[1], Francesco Fortarezza[1], Loredana Urso[2], Federica Grosso[3], Giovanni Luca Ceresoli[4], Izidor Kern[5], Gregor Vlacic[5], Eleonora Faccioli[1], Marco Schiavon[1], Dario Gregori[1], Federico Rea[1], Giulia Pasello[2,6†] and Fiorella Calabrese[1*†]*

[1] Department of Cardiac, Thoracic, Vascular Sciences and Public Health, University of Padova, Padova, Italy, [2] Department of Surgery, Oncology and Gastroenterology, University of Padova, Padova, Italy, [3] Azienda Ospedaliera SS Antonio e Biagio e Cesare Arrigo, Mesothelioma and Rare Cancer Unit, Alessandria, Italy, [4] Medical Oncology, Cliniche Humanitas Gavazzeni, Bergamo, Italy, [5] Pathology Laboratory, University Clinic Golnik, Golnik, Slovenia, [6] Department of Oncology, Medical Oncology 2, Istituto Oncologico Veneto IRCCS, Padova, Italy

OPEN ACCESS

**Edited by:**
Marco Lucchi,
University of Pisa, Italy

**Reviewed by:**
Michaela B. Kirschner,
University of Zurich, Switzerland
Luisella Righi,
University of Turin, Italy

***Correspondence:**
Fiorella Calabrese
fiorella.calabrese@unipd.it

†These authors share senior authorship

**Specialty section:**
This article was submitted to Thoracic Oncology, a section of the journal Frontiers in Oncology

**Received:** 14 January 2021
**Accepted:** 01 March 2021
**Published:** 22 March 2021

**Citation:**
Pezzuto F, Lunardi F, Vedovelli L, Fortarezza F, Urso L, Grosso F, Ceresoli GL, Kern I, Vlacic G, Faccioli E, Schiavon M, Gregori D, Rea F, Pasello G and Calabrese F (2021) P14/ARF-Positive Malignant Pleural Mesothelioma: A Phenotype With Distinct Immune Microenvironment. Front. Oncol. 11:653497. doi: 10.3389/fonc.2021.653497

**Introduction:** The CDKN2A gene plays a central role in the pathogenesis of malignant pleural mesothelioma (MPM). The gene encodes for two tumor suppressor proteins, p16/INK4A and p14/ARF, frequently lost in MPM tumors. The exact role of p14/ARF in MPM and overall its correlation with the immune microenvironment is unknown. We aimed to determine whether there is a relationship between p14/ARF expression, tumor morphological features, and the inflammatory tumor microenvironment.

**Methods:** Diagnostic biopsies from 76 chemo-naive MPMs were evaluated. Pathological assessments of histotype, necrosis, inflammation, grading, and mitosis were performed. We evaluated p14/ARF, PD-L1 (tumor proportion score, TPS), and Ki-67 (percentage) by immunohistochemistry. Inflammatory cell components (CD3+, CD4+, CD8+ T lymphocytes; CD20+ B-lymphocytes; CD68+ and CD163+ macrophages) were quantified as percentages of positive cells, distinguishing between intratumoral and peritumoral areas. The expression of p14/ARF was associated with several clinical and pathological characteristics. A random forest-based machine-learning algorithm (Boruta) was implemented to identify which variables were associated with p14/ARF expression.

**Results:** p14/ARF was evaluated in 68 patients who had a sufficient number of tumor cells. Strong positivity was detected in 14 patients (21%) (11 epithelioid and 3 biphasic MPMs). At univariate analysis, p14/ARF-positive epithelioid mesotheliomas showed higher nuclear grade (G3) ($p = 0.023$) and higher PD-L1 expression (≥50%) ($p = 0.042$). The percentages of CD4 and CD163 in peritumoral areas were respectively higher and lower in p14/ARF positive tumors but did not reach statistical significance with our sample size (both $p = 0.066$). The Boruta algorithm confirmed the predictive value of PD-L1 percentage for p14/ARF expression in all histotypes.

**Conclusions:** p14/ARF-positive epithelioid mesotheliomas may mark a more aggressive pathological phenotype (higher nuclear grade and PD-L1 expression). Considering the

results regarding the tumor immune microenvironment, p14/ARF-negative tumors seem to have an immune microenvironment less sensitive to immune checkpoint inhibitors, being associated with low PD-L1 and CD4 expression, and high CD163 percentage. The association between p14/ARF-positive MPMs and PD-L1 expression suggests a possible interaction of the two pathways. Confirmation of our preliminary results could be important for patient selection and recruitment in future clinical trials with anticancer immunotherapy.

**Keywords: immune microenvironment, MPM, p14/ARF, malignant pleural mesothelioma, tumor microenvironment**

## INTRODUCTION

Malignant pleural mesothelioma (MPM), an occupational disease mainly due to asbestos exposure, is characterized by rapidly progressive and diffusely local growth, late metastases and poor prognosis. Asbestos fibers lead to a protracted immune response and make mesothelioma a neoplasm characterized by a clear immune infiltrate (1). In recent years, the awareness of a strict interaction between tumor cells and tumor microenvironment (TME) (2) have offered new therapeutic opportunities with immunotherapeutic agents (3). One such strategy is based on the treatments targeting the programmed cell death pathway (PD-1/PD-L1) (4). Nevertheless, some limitations persist. They are mainly related to the complexity of the TME structure and the mechanisms of resistance and inhibition, likely associated with the complex genetic profiling of the tumor (5).

The genetics of MPM appear extremely intricate and not completely unraveled. The complexity resides mainly in the variety of genetic aberrations that can occur, the crosstalk between genetics and the microenvironment, and the inter-patient and intra-tumoral variability (6).

In MPM, heterogeneity is indeed also an intrinsic aspect of the neoplasia that has its roots in the histological classification into three major histological types (epithelioid, biphasic, and sarcomatoid) (7), confirmed and emphasized by large-scale molecular profiling studies (8, 9). This is principally true for the epithelioid histotype that includes a wide range of architectural patterns and cytological and stromal features, each of which is supposed to be associated with a different behavior (10). In this complex scenario, the identification of a biomarker makes it possible to stratify the population. When associated with a certain clinical course, this would be useful for diagnostic, prognostic and therapeutic purposes.

Major molecular changes lead to altered expression of the genes involved in oncogenic mechanisms, especially the onco-suppressor genes at 9p21 (INK4) and 22q (NF2) foci (8, 9). The 9p21 locus includes the genes cyclin-dependent kinase inhibitor 2B (CDKN2B), cyclin-dependent kinase inhibitor 2A (CDKN2A) and S-methyl-5'-thioadenosine phosphorylase (MTAP). Frequent involvement of the CDKN2A gene in the pathogenesis of MPM has recently been confirmed (8, 9). The gene encodes for two proteins, p16/INK4A and p14/ARF, both acting as tumor suppressors through the regulation of the cell cycle. p14/ARF is involved in cell cycle regulation, mainly inhibiting MDM2 and promoting p53 function that in turn activates p21. This last protein binds and inactivates cyclin-cycline dependent kinase complexes, thus blocking the transition from the G1 to S phases of the cell cycle. The deletion interferes with the p53-MDM2 pathway, leading to accumulation of MDM2 and loss of p53 function with cell cycle deregulation. Even if less common, several p53-independent actions have been attributed to p14/ARF (11). Although p14/ARF deletion or silencing has been found in several solid tumors (12), the role of p14/ARF in the pathogenesis of MPM remains unclear with most evidence dating back to the last decade and being based only on experimental models (13).

In human cell lines, the inactivation/absence of p14/ARF was found to interact with p53 function in case of DNA damage and thus in the apoptotic process (14). p14/ARF (called p19 in mice) alterations were also studied in mouse mesothelioma cells, making mice a feasible model to study molecular features of human MPM (15). Indeed, more recently, p19 status was also studied in *in vivo* experiments, resulting as an important factor for MPM tumorigenesis (16, 17). Interestingly, p14/ARF transfected mesothelioma cells were used to explore new therapeutic approaches, favoring p53 activity and apoptosis, and modulating the cytolytic effects of drugs (18, 19).

Although the role of p14/ARF in tumorigenesis has been widely suggested, its prognostic significance remains unknown (12). Only few studies have clinically evaluated p14/ARF in MPM, achieving inconclusive results (20, 21). In particular the association of p14 with TME has not yet been explored.

Thus, the aim of this study was to investigate p14/ARF expression in MPM and to explore if p14/ARF-positive MPM samples show pathological and immunohistochemical features, with specific focus on immune TME.

## MATERIALS AND METHODS

### Study Population

We retrospectively analyzed biopsies from chemo-naive patients with MPM recruited in three Italian centers and one Slovenian center from 2011 to 2019. Clinical information about patients enrolled in the study were reported and included in an electronic shared data base. Written informed consent was given by all subjects included in the research. The study was approved by the Ethics Committee.

## Histological and Immunohistochemical Evaluation

For histological analyses, tissue samples were fixed in 4% buffered formalin and embedded in paraffin. Each case was classified into epithelioid, biphasic and sarcomatoid, according to the 2015 World Health Organization (WHO) classification (7).

Histological parameters and immunohistochemical evaluations were performed only when biopsies met the following criteria: 1) size adequacy: at least 2 $cm^2$/>60% neoplastic cells.

In epithelioid histotypes, the specific architectural pattern was reported and a nuclear grading system (I-II-III) was performed as originally described by Kadota et al. (22). The proliferative index Ki67 antigen was investigated (1:80, Immunotech, clone MIB-1) and expressed as number of positive cells on total cell number.

Necrosis and inflammation were morphologically evaluated both in intratumoral and peritumoral areas and quantified in percentage over the entire tumor surface. The tumor-infiltrating immune cell analysis was based on the guidelines from the International Immuno-Oncology Biomarkers Working Group (23). Briefly, the tumor-infiltrating immune cell analysis was carried out within the borders of the invasive tumor and areas within the tumor. Areas with necrosis, fibrosis/scar or adjacent normal tissue were excluded.

Inflammatory cells were further classified into lymphocytes (B and T) and macrophages (also considering M2 type). The TME characterization was performed by using the following primary antibodies: anti-CD20 (1:200, Dako, clone L26, CD20CY), anti-CD3 (1:200, Leica, clone NCL-L-CD3-565), anti-CD8 (1:200, Dako, clone C8/144B), anti-CD4 (1:200, Dako, clone 4B12), anti-CD68 (1:200, Dako, clone PG-M1), anti-CD163 (1:200, Novocastra, NCL-L3CD163). Immunoreactivity was expressed as percentage of positive cells with respect to the total number of inflammatory cells.

PD-L1 (1:200, cell signaling, clone E1L3N) was evaluated in neoplastic cells and considered to be positive when it was higher than 1%. In a previous study (2) we used an anti-human Ventana PD-L1 rabbit monoclonal primary antibody (clone SP263, pre-diluted, 1,61 μg/mL). After that, we have started to use PD-L1 (clone E1L3N) following a laboratory validation test that demonstrated a similar rate of positivity of the two antibodies. In tumor cells, PD-L1 was scored as Tumor Proportion Score (TPS). p14/ARF (1:100, Santa Cruz, clone 4C6/4ARF) was defined as positive when neoplastic cells showed strong nuclear or both cytoplasmic and nuclear/staining. In all immunostainings negative controls for non-specific binding were included omitting the primary antibodies.

Immunohistochemistry was performed by using the Bond automated system (Leica Bond III, Leica Microsystems Srl, Wetzlar, Germany).

## Statistical Analysis

Data are expressed as medians (interquartile range). Univariate analyses were conducted with the non-parametric Mann-Whitney U or Kruskal-Wallis tests for continuous variables and Fisher's exact test for categorical variables. Feature selection was implemented using a machine-learning algorithm based on random forest (Boruta). The Boruta algorithm aims to identify all the relevant predictors that impact the outcome of interest (in our case, being in the p14/ARF+ or p14/ARF- group). It implements a random forest on an augmented set of covariates. Additional covariates, called shadow variables, are copies of the original ones obtained by permuting the observations and thus removing any possible association with the outcome. For each explanatory variable, an importance measure is computed, i.e., a Z score, which is the average improvement in the predictive performance of the random forest with the considered explanatory variable divided by its standard deviation. The obtained important predictors are those that show a Z score higher than the one observed for the variable with the maximum Z score among the shadow variables. The procedure is repeated until an importance measure is assigned to each predictor or until the maximum number of random forests is reached. The Boruta R package (24) was used for the analysis. The Boruta feature selection is a heuristic algorithm of machine learning that was used to highlight the most important variables that were able to distinguish the p14/ARF positiveness. The algorithm is based on the random forest algorithm and permits to compare variables randomizing both data and variables in order to obtain independent decision trees that are finally used to produce a decision about the most influencing, group-diving features. Survival was evaluated using Kaplan-Meyer curves and Log-rank test. Moreover, survival curves were also compared with the non-parametric restricted mean survival time as a summary measure of the survival time distribution adjusted for age, sex, and chemotherapy and/or surgery treatments at 6 and 12 months with the survival and survRM2 R packages. Graphs were made with the ggstatsplot R package. R (v. 4.0.3) was used for the analysis (25).

# RESULTS

## Patients

Seventy-six chemo naive MPM patients were enrolled in the study. p14/ARF was evaluable in 68 (89%) MPM samples containing a sufficient number of tumor cells. Most patients were males (51/68, 75%), with a median age of 72 (61.8-76; Q1-Q3) years. A positive history of asbestos exposure was obtained from 62%. According to the Eastern Cooperative Oncology Group (ECOG), performance status (PS) was 0 in 32%, 1 in 62% and 2 in 6%. Median survival was 9.3 (5.5-12.9; Q1-Q3) months. The main clinical data are summarized in **Table 1**.

## Morphological Characteristics, TME/PD-L1 and p14/ARF Expression

Forty-seven cases were epithelioid (69%), 17 biphasic (25%) and 4 sarcomatoid (6%). Epithelioid histotype displayed a solid prevalent growth pattern (25 out of 47, 53%). The majority of epithelioid MPM had mild/moderate nuclear grading (13 cases with G1, 21 G2) while 28% (13 G3) showed severe nuclear grading.

**TABLE 1** | Main clinical features of patients affected by malignant pleural mesothelioma.

| | p14/ARF positive (n = 14) | p14/ARF negative (n = 54) | TOTAL (n = 68) |
|---|---|---|---|
| **Sex [F:M]** | 5:9 | 12:42 | 17:51 |
| **Age [yrs, median (Q1-Q3)]** | 64 (61.2-73.5) | 72.5 (63.0-76.0) | 72.0 (61.8-76.0) |
| **Overall Survival [months, median (Q1-Q3)]** | 9.3 (5.8-11.7) | 9.8 (5.6-14.4) | 9.3 (5.5-12.9) |
| **Asbestos Exposure [%]** | | | |
| **Yes** | 63 | 57 | 62 |
| **No** | 28 | 43 | 32 |
| **Not available** | 9 | 0 | 6 |
| **ECOG PS [%]** | | | |
| **0** | 22 | 35 | 32 |
| **1** | 64 | 61 | 62 |
| **2** | 14 | 4 | 6 |
| **EORTC PrS [median (Q1-Q3)]** | 1.75 (1.5-1.8) | 1.67 (1.15-1.82) | 1.72 (1.15-1.82) |
| **Surgery [%]** | | | |
| **Yes** | 0 | 100 | 22 |
| **No** | 26 | 74 | 78 |
| **Chemotherapy [%]** | | | |
| **Yes** | 22 | 78 | 75 |
| **No** | 43 | 57 | 10 |
| **Not available** | 0 | 100 | 15 |
| **Multimodal Treatment [%]** | | | |
| **Yes** | 0 | 100 | 22 |
| **No** | 26 | 74 | 78 |

*ECOG, Eastern Cooperative Oncology Group; PS, performance status; EORTC, European Organization for Research and Treatment of Cancer; PrS, prognostic score.*

Necrosis was detected in 48 cases (71%) with a median percentage of 10.0 (5.0-18.5; Q1-Q3). Loss of nuclear immunoreactivity of p14/ARF was evident in 54 cases (79%). Strong nuclear expression was mainly detected in epithelioid mesotheliomas (11 out of 14, 79%). In 79% of positive cases cytoplasmic immunoreactivity was detected in addition to the nuclear staining.

TME was evaluable in 68 cases. Inflammation showed a median of 10.0 (5.0-17.5; Q1-Q3), higher in epithelioid than non-epithelioid (14.0 vs 10.0). PD-L1 was expressed in 37 (54%) cases (23 epithelioid and 14 non-epithelioid: 12 biphasic and 2 sarcomatoid). PD-L1 was strongly positive with a TPS ≥ 50% in 17 (25%) cases.

## Relationship Between p14/ARF and Clinicopathological Data

Censored patients were 4 in the p14-positive group and 14 in the negative group. While there was no significant difference in median overall survival (9.3 vs 9.8 months), it was noted that more patients with lack of p14/ARF expression showed survival beyond 10 months. Including chemotherapy, surgery, or their combination as covariates in the survival analysis, the results did not change (**Figure 1**). Restricted mean survival time at 6 and 12 months showed no differences between the two arms adjusted for age and sex: 6 months estimate -0.24 (95% CI -1.02; 0.53, p = 0.536): 12 months estimate -0.34 (95%CI -2.10; 1.71, p = 0.742). p14/ARF expression was correlated with histotype, necrosis, inflammation, all inflammatory cell subtypes and PD-L1 values; at univariate analysis, a significant association was achieved between p14/ARF positivity and high PD-L1 expression in tumor cells (p = 0.015) (**Figure 2**). This strict correlation was also confirmed by the Boruta feature selection that, among all variables evaluated, showed a predictive significance for this parameter (**Figure 3**). Moreover, the percentages of CD4 and CD163 in peritumoral areas were respectively higher and lower (but not significantly) in p14/ARF

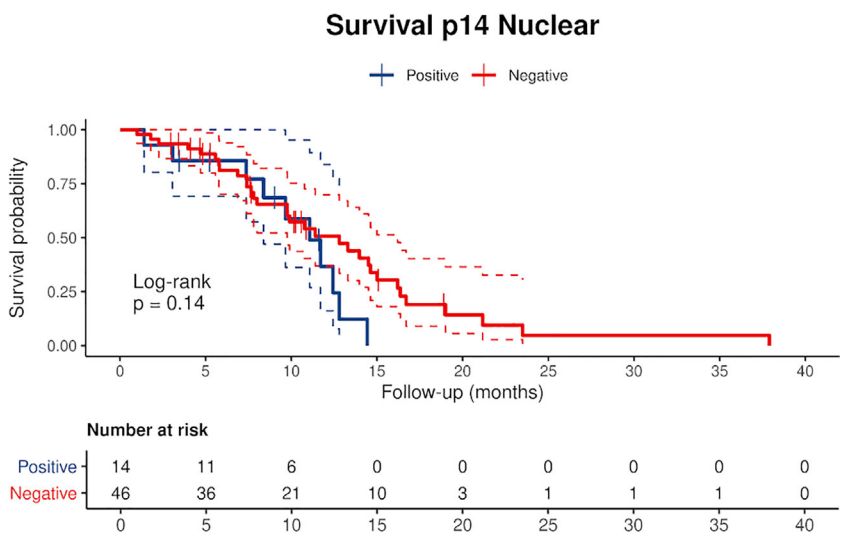


**FIGURE 1** | Kaplan Meier curves of p14/ARF positive and negative cases showing a lower survival rate in patients with p14/ARF expression. Censored patients are depicted as crosses intersecting the curve.

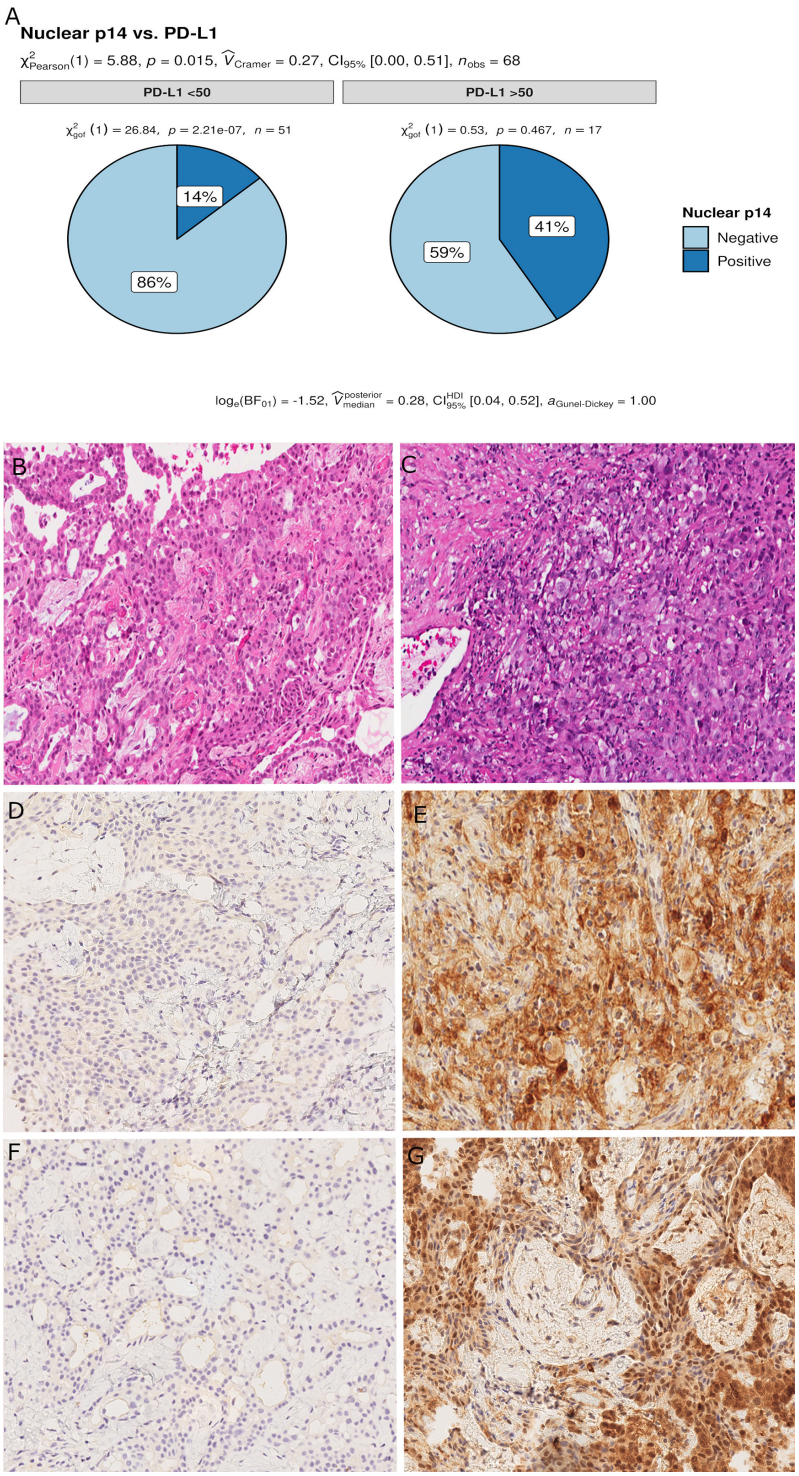


**FIGURE 2** | Pie chart of PD-L1 expression in p14/ARF-positive and negative samples. A higher percentage of PD-L1≥50% was noted in p14/ARF-positive samples than in p14/ARF-negative MPMs **(A)**. Panel figures of two representative cases of p14/ARF-negative **(B, D, F)** and p14/ARF-positive MPM **(C, E, G)**. **(B)** Histology showing trabecular pattern of MPM (hematoxylin and eosin, original magnification x 200). **(D)** Immunohistochemistry for PD-L1: TPS<1% (immunohistochemistry, original magnification x 200). **(F)** Immunohistochemistry for p14/ARF: negative (immunohistochemistry, original magnification x 200). **(C)** Histology showing prevalent solid pattern of MPM (hematoxylin and eosin, original magnification x 200). **(E)** Immunohistochemistry for PD-L1: TPS≥50% (80%) (immunohistochemistry, original magnification x 200). **(G)** Immunohistochemistry for p14/ARF: positive (immunohistochemistry, original magnification x 200).

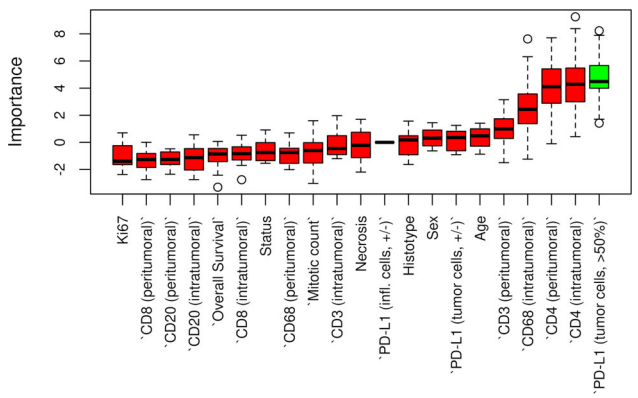


**FIGURE 3** | Boruta feature selection showing predictive significance for PD-L1 expression in p14/ARF positivity. Unfilled circles indicating outliers.

positive tumors (both p = 0.066) (**Figure 4**). The results are summarized in **Table 2**.

For epithelioid MPM, 13 cases (28%) had a high nuclear grade (G3). p14/ARF expression was significantly associated with a higher nuclear grade (p = 0.023) (**Figure 5**). As would be expected since almost all p14/ARF positive MPM samples were epithelioid, a high PD-L1 expression was associated with p14/ARF expression (p = 0.042). No other differences were found between the two groups.

The Boruta feature selection showed that nuclear grade and PD-L1 expression were the two most important variables in determining the p14/ARF status, although significance was not achieved (**Figure 6**).

## DISCUSSION

In the present study, we detected tissue expression of p14/ARF in only 21% of MPM, mainly epithelioid histotype (79%) thus confirming previous studies on MPM that showed a more frequent loss of the CDKN2A gene (10).

An interesting finding of our study was that MPM with p14/ARF expression showed a higher nuclear grading, more extensive necrosis (this parameter also did not reach statistical significance) and a higher PD-L1 TPS value. All these findings seem to characterize more aggressive pathological forms. The CDKN2A locus expresses two partially overlapping transcripts that encode two distinct proteins, namely p14/ARF and p16/INK4a, which present no sequence identity. While several experimental studies showed that both proteins are potent tumor suppressors, the importance of p14/ARF alterations in several human cancers remains unclear (23). Novel data collected in recent years have challenged the traditional and established role of this protein as a tumor suppressor. In particular it has been demonstrated that several tumors retaining p14/ARF expression evolve to metastatic and invasive phenotypes and in humans are associated with a poor prognosis as detected in a subset of our cases (26, 27).

There are only two previous clinical studies that investigated the expression of p14/ARF in MPM which used molecular analysis or immunostaining (20, 21) that did not however allow for univocal interpretation of clinical correlations, particularly the correlation with survival. In our study, Kaplan-Meier curves separated patients with low expression from patients with high expression (**Figure 1**). Curves seem to diverge around 10 months but the different and small numbers of the two groups did not allow a clear evaluation of the two profiles. Restricted mean survival time at 6 and 12 months did not show evidence of different survival in the two groups.

Our findings are apparently in contradiction with those obtained in the study by Walter et al. who reported elevated p14/ARF expression correlated with prolonged survival. However, the authors evaluated p14/ARF using a different methodology: by qPCR.

mRNA is usually translated into protein under the assumption that there is some sort of correlation between level of mRNA and level of protein. However, there may be reasons for the typically poor correlations between mRNA and protein levels, and these reasons may not be mutually exclusive. In particular, low expression of mRNA and protein abundance may be related to the fact that proteins have very different half-lives as the result of varied protein syntheses and degradations. Indeed, protein turnover can vary significantly depending on a number of different conditions. Future more in-depth studies are needed to investigate both *in vitro* and *in vivo* post-transcriptional p14/ARF activity.

In contrast with the exclusively nucleolar localization of p14/ARF observed in most *in vitro* models and in several tumors, abnormal p14/ARF nucleo-cytoplasmic accumulation was found in the majority of our cases. This has been observed in other tumors (27, 28).

It does not seem likely that this is a consequence of nonspecific staining, as a distinct nucleolar signal has been obtained with the same antibody and under the same conditions in other tumor tissues (28). The presence of other nuclear markers (WT1; Ki67) without cytoplasmic spreading demonstrated that our observations are not an artifact related to loss of nuclear integrity. We ignore the significance of nucleocytoplasmic staining—it would be expected that under conditions of massive p14/ARF induction the nucleoplasmic fraction would become detectable as was in many of our cases.

In the present study it was demonstrated that there was an association between p14/ARF and PD-L1 expression in mesothelial cells, which may be explained by the response of neoplastic cells to immune attack. Several experimental and clinical studies have demonstrated that p14/ARF is a critical modulator of the inflammatory response although its exact role in the complex regulation of an inflammatory tumor microenvironment is still unclear. Inflammatory tumor microenvironments contribute to the carcinogenesis and progression of several types of solid and hematologic cancers. PDL-1 is an immune modulatory molecule in cancer cells that

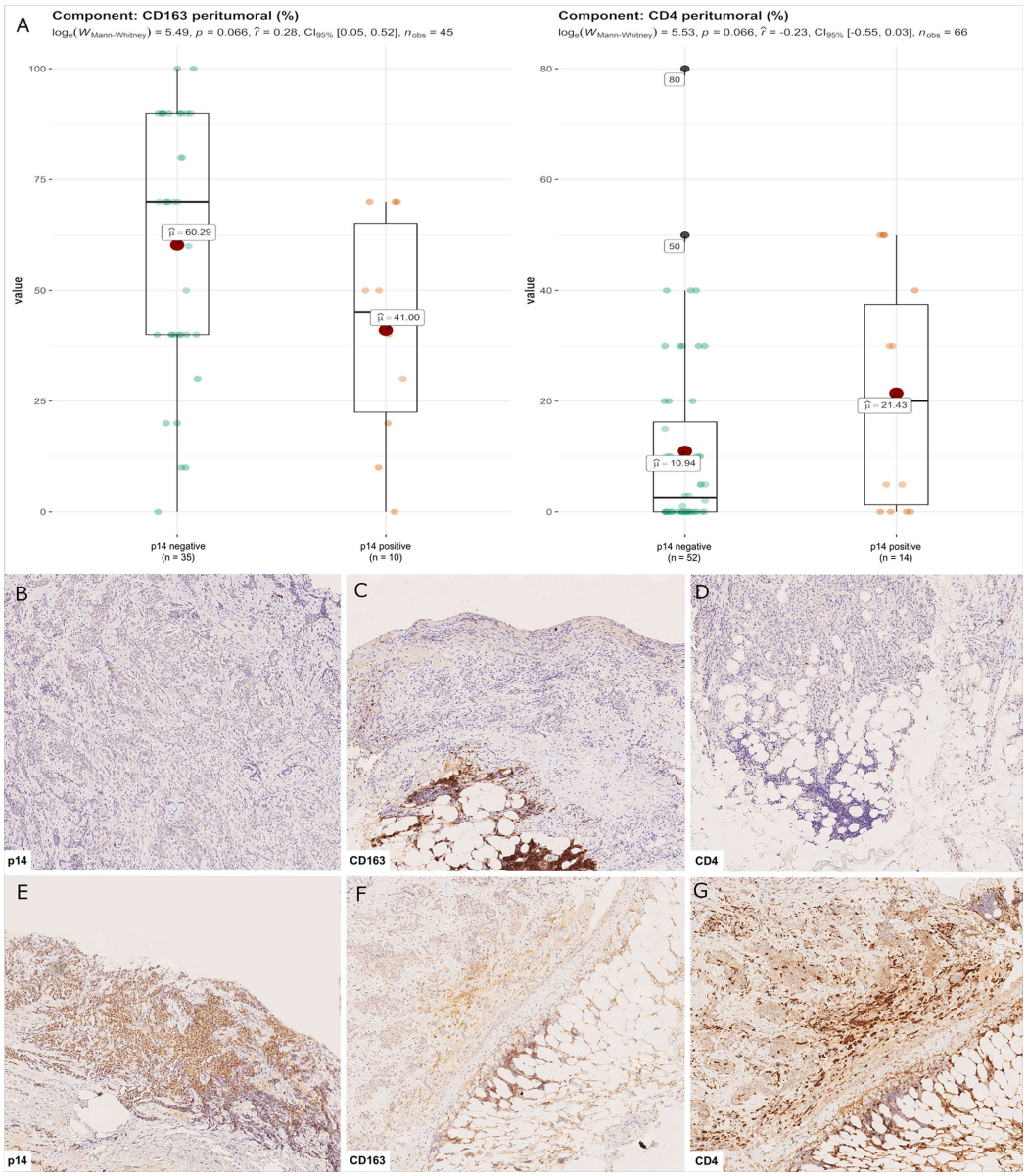


**FIGURE 4** | CD4+ and CD163+ distribution in peritumoral areas. T helper lymphocytes and M2 macrophages were respectively higher and lower in p14/ARF-positive tumors than in negative samples **(A)**. Panel figures of two representative cases of p14/ARF-negative **(B–D)** and p14/ARF-positive MPM **(E–G)**. **(B)** Immunohistochemistry for p14/ARF: negative (immunohistochemistry, original magnification x 70). **(C)** Immunohistochemistry for CD163 showing a high percentage in peritumoral areas (immunohistochemistry, original magnification x 70). **(D)** Immunohistochemistry for CD4 showing a low percentage in peritumoral areas (immunohistochemistry, original magnification x 70). **(E)** Immunohistochemistry for p14/ARF: positive (immunohistochemistry, original magnification x 70). **(F)** Immunohistochemistry for CD163 showing a low percentage in peritumoral areas (immunohistochemistry, original magnification x 70). **(G)** Immunohistochemistry for CD4 showing a high percentage in peritumoral areas (immunohistochemistry, original magnification x 70).

inhibits cytotoxic T cell activity (29) thereby enabling tumor growth (30). Chronic inflammation due to inhaled asbestos in the pleura and/or into the lung has been thought to play a major role in MPM pathogenesis. Recently, the use of immune checkpoint inhibitor (ICI) as single agents or in combination in previously treated and naïve patients has been shown to potentially prolong MPM patient survival even if the value of single agent checkpoint inhibitors is rather limited yielding overall response rates with immunotherapy around 30% (31). Even if more recently the Checkmate-743 study demonstrated a significant improvement in overall survival for the combination of nivolumab and ipilimumab (32), some issues about the expected response and the acceptable toxicity need to be addressed. While the clinical efficacy of ICI has been claimed

**TABLE 2** | Main histological features of malignant pleural mesothelioma distinguishing p14/ARF positive and negative cases.

| | p14/ARF positive (n = 14) | p14/ARF negative (n = 54) | TOTAL (n = 68) | p-value |
|---|---|---|---|---|
| **Histotype (n, %)** | | | | |
| **Epithelioid** | 11 (23%) | 36 (77%) | 47 (69%) | 0.339 |
| **Biphasic** | 3 (18%) | 14 (82%) | 17 (25%) | |
| **Sarcomatoid** | 0 | 4 (100%) | 4 (6%) | |
| **Necrosis [%, median (Q1-Q3)]** | 15.0 (10.0–15.0) | 7.0 (5.0–19.0) | 10.0 (5.0–18.5) | 0.229 |
| **Mitoses [n/mm$^2$, median (Q1-Q3)]** | 4.0 (3.0–4.8) | 3.0 (2.0–5.0) | 3.0 (2.0–5.0) | 0.478 |
| **Proliferative index [%, median (Q1-Q3)]** | 40.0 (25.0, 65.0) | 30.0 (20.0, 52.5) | 30.0 (20.0–57.5) | 0.553 |
| **PD-L1 tumor cells** | | | | |
| **<50%** | 7 (50%) | 44 (81.5%) | 51 (75%) | ***0.015**** |
| **≥50%** | 7 (50%) | 10 (18.5%) | 17 (25%) | |
| **CD8 [%, median (Q1-Q3)]** | | | | |
| **Peritumoral** | 20.0 (15.0–30.0) | 20.0 (8.5–30.0) | 20.0 (10.0–30.0) | 0.614 |
| **Intratumoral** | 20.0 (10.0–30.0) | 20.0 (5.0–50.0) | 20.0 (6.2–50.0) | 0.910 |
| **CD4 [%, median (Q1-Q3)]** | | | | |
| **Peritumoral** | 20.0 (1.2–37.5) | 2.5 (0.0–16.2) | 5.0 (0.0–20.0) | 0.066 |
| **Intratumoral** | 5.0 (0.5–10.0) | 0.0 (0.0–10.0) | 0.0 (0.0–10.0) | 0.174 |
| **CD20 [%, median (Q1-Q3)]** | | | | |
| **Peritumoral** | 25.0 (15.0–40.0) | 20.0 (5.0–40.0) | 20.0 (6.2–40.0) | 0.626 |
| **Intratumoral** | 0.0 (0.0–4.0) | 0.0 (0.0–5.0) | 0.0 (0.0–5.0) | 0.841 |
| **CD20 [%, median (Q1-Q3)]** | | | | |
| **Peritumoral** | 25.0 (15.0–40.0) | 20.0 (5.0–40.0) | 20.0 (6.2–40.0) | 0.626 |
| **Intratumoral** | 0.0 (0.0–4.0) | 0.0 (0.0–5.0) | 0.0 (0.0–5.0) | 0.841 |
| **CD3 [%, median (Q1-Q3)]** | | | | |
| **Peritumoral** | 40.0 (16.2–57.5) | 30.0 (10.0–40.0) | 30.0 (13.8–50.0) | 0.266 |
| **Intratumoral** | 17.5 (10.0–46.2) | 20.0 (5.0–40.0) | 20.0 (5.0–, 42.5) | 0.813 |
| **CD68 [%, median (Q1-Q3)]** | | | | |
| **Peritumoral** | 30.0 (25.0–47.5) | 30.0 (15.0–40.0) | 30.0 (20.0–40.0) | 0.250 |
| **Intratumoral** | 27.5 (20.0–40.0) | 40.0 (20.0–60.0) | 40.0 (20.0–, 60.0) | 0.129 |
| **CD163 [%, median (Q1-Q3)]** | | | | |
| **Peritumoral** | 45.0 (22.5–65.0) | 70.0 (40.0–90.0) | 60.0 (40.0–80.0) | 0.066 |
| **Intratumoral** | 35.0 (22.5–47.5) | 40.0 (30.0–80.0) | 40.0 (30.0–70.0) | 0.192 |

** and bold for statistical significance.*

to correlate with a high tumor mutational burden as in melanoma or NSCLC patients, mesothelioma has consistently been demonstrated to harbor a low mutation burden (10). This may explain the low sensitivity to the ICI targeting PD-1/PDL-1; however, the possible influence of some genes that could have the same efficacy of ICI in MPM patients is also important. A role for p14/ARF in the innate immune response has been previously demonstrated, although the underlying mechanisms are unclear (33–35). The mechanisms include the modulation of angiogenesis, matrix remodeling, and immune suppression (36). In vitro and *in vivo* models have demonstrated a significant influence of p19/ARF in regulating the plasticity and polarization of macrophages. Mice lacking the p19/ARF gene showed a balance with prevalent M2 macrophage phenotypes characterized by the expression of a series of chemokines, cytokines, and proteases that promote immunosuppression (33–36). This seems to be in line with our results as ARF-negative MPM showed higher levels of CD163 than positive MPM.

It could be speculated that p14/ARF and PD-L1 positive mesothelioma characterizes tumor phenotypes with an inflammatory TME that might be more sensitive to the ICI treatment.

There were some limitations of the present study. First, due to the small sample size, the study could be underpowered. Nonetheless, we implemented robust and reliable methods to limit the probability of getting significant results by chance. Moreover, the strength of our research is that all patients included in the current study were chemo-naive and that it overcomes an important selection bias that could influence the evaluation of TME and PD-L1. Concerning p14/ARF immunostaining, there is no standardization for defining p14/ARF positivity. In this regard, further studies are required considering that the absence of a cut-off value may influence the detection rate of positive samples. This is also true for the evaluation of PD-L1 that is not standardized in MM, neither in terms of clones nor type of expression evaluation and threshold.

Finally, although a significant association between PD-L1 and p14/ARF expression was identified, the molecular substrate that influences this association remains unknown. Nonetheless, this study may serve as an important starting point for future genetic and functional studies.

In conclusion, we found an association between p14/ARF-positive MPM and a peculiar MPM phenotype, characterized by a higher nuclear grading, PD-L1 expression, and peculiar inflammatory TME (high number of peritumoral CD4 T-lymphocyte and low number of M2 macrophages). The significant correlation between p14/ARF positive MPM and PD-L1 expression suggests a possible interaction of the two pathways.

There is an urgent need for biomarkers to select the optimal candidates for immunotherapy among MPM patients moreover

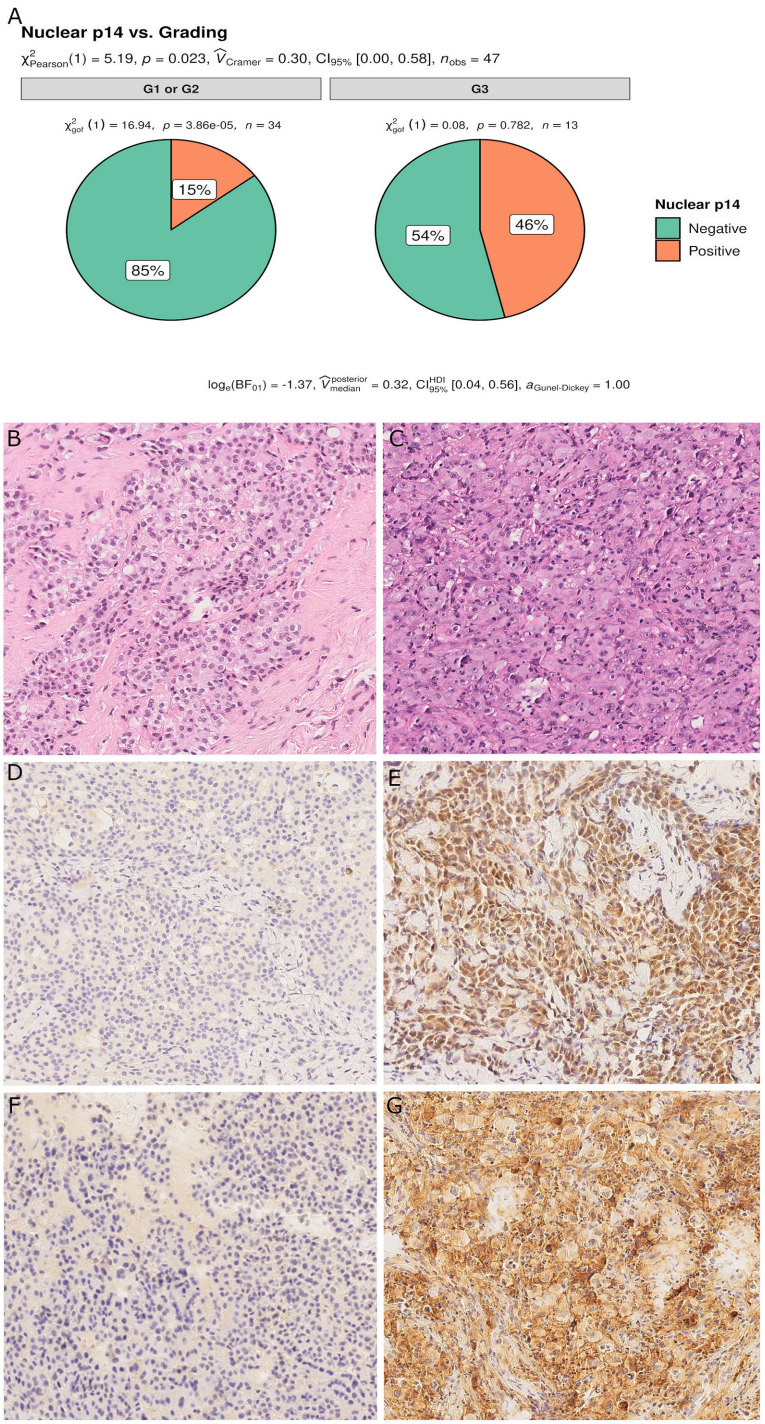


**FIGURE 5** | Pie chart of nuclear grading in p14/ARF-positive and negative samples. p14/ARF-positive samples showed higher nuclear grade (G3) than p14/ARF-negative MPM **(A)**. Panel figures of two representative cases of p14/ARF-negative **(B, D, F)** and p14/ARF positive MPM **(C, E, G)**. **(B)** Histology showing an epithelioid MPM with low nuclear grading (G2 sec. Kadota et al.) (hematoxylin and eosin, original magnification x 200). **(D)** Immunohistochemistry for p14/ARF showing complete negative immunostaining (immunohistochemistry, original magnification x 200). **(F)** Immunohistochemistry for PD-L1: TPS<1% (immunohistochemistry, original magnification x 200). **(C)** Histology showing an epithelioid MPM with high nuclear grading (G3 sec. Kadota et al.) (hematoxylin and eosin, original magnification x 200). **(E)** Immunohistochemistry for p14/ARF showing strong nuclear and cytoplasmic immunostaining in most tumor cells (immunohistochemistry, original magnification x 200). **(G)** Immunohistochemistry for PD-L1: TPS≥50% (immunohistochemistry, original magnification x 200).

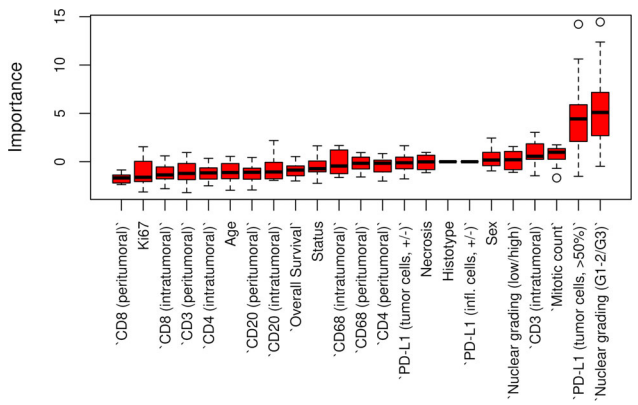


**FIGURE 6** | Boruta feature selection showing the highest importance of nuclear grade and PD-L1 expression among all variables in determining p14/ARF status. Unfilled circles indicating outliers.

in terms of efficacy to the ICI treatment. The confirmation of our preliminary results could be useful for patient selection and recruitment in future clinical trials with anticancer immunotherapy to optimize the benefit and the effectiveness of these drugs in MPM.

## DATA AVAILABILITY STATEMENT

The raw data supporting the conclusions of this article will be made available by the authors, without undue reservation.

## ETHICS STATEMENT

The studies involving human participants were reviewed and approved by Istituto Oncologico Veneto IRCCS, Padova, Italy. The patients/participants provided their written informed consent to participate in this study.

## AUTHOR CONTRIBUTIONS

Conception/design: FP, FL, GP, and FC. Data acquisition: FP, FF, GP, FG, GC, IK, GV, MS, and LU. Data analysis/interpretation: LV and DG. Drafting: FP, FL, GP, LV, and FC. Critical revision: FC, GP, DG, and FR. All authors contributed to the article and approved the submitted version.

## FUNDING

This work was supported by the University of Padova (BIRD197018/19: Influence of tumor microenvironment, metabolic interaction and telomere dysfunction in malignant pleural mesothelioma: translational and preclinical study).

## ACKNOWLEDGMENTS

The authors thank Dr. Judith Wilson for the English revision.

## REFERENCES

1. Chu GJ, van Zandwijk N, Rasko JEJ. The Immune Microenvironment in Mesothelioma: Mechanisms of Resistance to Immunotherapy. *Front Oncol* (2019) 9:1366. doi: 10.3389/fonc.2019.01366
2. Pasello G, Zago G, Lunardi F, Urso L, Kern I, Vlacic G, et al. Malignant pleural mesothelioma immune microenvironment and checkpoint expression: Correlation with clinical-pathological features and intratumor heterogeneity over time. *Ann Oncol* (2018) 29:1258–65. doi: 10.1093/annonc/mdy086
3. Carbone M, Adusumilli PS, Alexander HR, Baas P, Bardelli F, Bononi A, et al. Mesothelioma: Scientific clues for prevention, diagnosis, and therapy. *CA Cancer J Clin* (2019) 69:402–29. doi: 10.3322/caac.21572
4. Lantuejoul S, Le Stang N, Damiola F, Scherpereel A, Galateau-Sallé F. PD-L1 Testing for Immune Checkpoint Inhibitors in Mesothelioma: For Want of Anything Better? *Thorac Oncol* (2017) 12:778–81. doi: 10.1016/j.jtho.2017.03.018
5. Dozier J, Zheng H, Adusumilli PS. Immunotherapy for malignant pleural mesothelioma: Current status and future directions. *Transl Lung Cancer Res* (2017) 6:315–24. doi: 10.21037/tlcr.2017.05.02
6. Abbott DM, Bortolotto C, Benvenuti S, Lancia A, Filippi AR, Stella GM. Malignant pleural mesothelioma: Genetic and microenviromental heterogeneity as an unexpected reading frame and therapeutic challenge. *Cancers (Basel)* (2020) 12:1186. doi: 10.3390/cancers12051186
7. Galateau-Salle F, Churg A, Roggli V, Travis WD. The 2015 world health organization classification of tumors of the pleura: Advances since the 2004 Classification. *J Thorac Oncol* (2015) 10:1243–60. doi: 10.1097/JTO.0000000000000630
8. Hmeljak J, Sanchez-Vega F, Hoadley KA, Shih J, Stewart C, Heiman D, et al. Integrative molecular characterization of malignant pleural mesothelioma. *Cancer Discov* (2018) 8:1548–65. doi: 10.1158/2159-8290.CD-18-0804
9. Bueno R, Stawiski EW, Goldstein LD, Durinck S, De Rienzo A, Modrusan Z, et al. Comprehensive genomic analysis of malignant pleural mesothelioma identifies recurrent mutations, gene fusions and splicing alterations. *Nat Genet* (2016) 48:407–16. doi: 10.1038/ng.3520
10. Nicholson AG, Sauter JL, Nowak AK, Kindler HL, Gill RR, Remy-Jardin M, et al. EURACAN/IASLC Proposals for Updating the Histologic Classification of Pleural Mesothelioma: Towards a More Multidisciplinary Approach. *J Thorac Oncol* (2020) 15:29–49. doi: 10.1016/j.jtho.2019.08.2506
11. Weber JD, Jeffers JR, Rehg JE, Randle DH, Lozano G, Roussel MF, et al. p53-independent functions of the p19(ARF) tumor suppressor. *Cold Spring Harb Symp Quant Biol* (2005) 70:129–37. doi: 10.1101/sqb.2005.70.004
12. Inoue K, Fry E. Aberrant expression of p14 ARF in human cancers: A new biomarker? *Tumor Microenviron* (2018) 1:37–44. doi: 10.4103/tme.tme_24_17
13. Sekido Y. Molecular pathogenesis of malignant mesothelioma. *Carcinogenesis* (2013) 34:1413–9. doi: 10.1093/carcin/bgt166
14. Hopkins-Donaldson S, Belyanskaya AL, Simões-Wüst AP, Sigrist B, Kurtz S, Zangemeister-Wittke U, et al. p53-induced apoptosis occurs in the absence of p14ARF in malignant pleural mesothelioma. *Neoplasia* (2006) 8:551–9. doi: 10.1593/neo.06148
15. Lecomte C, Andujar P, Renier A, Kheuang L, Abramowski V, Mellottee L, et al. Similar tumor suppressor gene alteration profiles in asbestos-induced murine and human mesothelioma. *Cell Cycle* (2005) 4:1862–9. doi: 10.4161/cc.4.12.2300
16. Altomare DA, Menges CW, Xu J, Pei J, Zhang L, Tadevosyan A, et al. Losses of both products of the cdkn2a/arf locus contribute to asbestos-induced mesothelioma development and cooperate to accelerate tumorigenesis. *PloS One* (2011) 6:e18828. doi: 10.1371/journal.pone.0018828
17. Altomare DA, Menges CW, Pei J, Zhang L, Skele-Stump KL, Carbone M, et al. Activated TNF-α/NF-κB signaling via down-regulation of Fas-associated

factor 1 in asbestos-induced mesotheliomas from Arf knockout mice. *Proc Natl Acad Sci U S A* (2009) 106:3420–5. doi: 10.1073/pnas.0808816106
18. Yang CT, You L, Yeh CC, Chang JWC, Zhang F, McCormick F, et al. Adenovirus-mediated p14(ARF) gene transfer in human mesothelioma cells. *J Natl Cancer Inst* (2000) 92:636–41. doi: 10.1093/jnci/92.8.636
19. Yang CT, You L, Uematsu K, Yeh CC, McCormick F, Jablons DM. p14ARF modulates the cytolytic effect of ONYX-015 in mesothelioma cells with wild-type p53. *Cancer Res* (2001) 61:5959–63.
20. Bahnassy AA, Zekri ARN, Abou-Bakr AA, El-Deftar MM, El-Bastawisy A, Sakr MA, et al. Aberrant expression of cell cycle regulatory genes predicts overall and disease free survival in malignant pleural mesothelioma patients. *Exp Mol Pathol* (2012) 93:154–61. doi: 10.1016/j.yexmp.2012.04.001
21. Walter RFH, Mairinger FD, Ting S, Vollbrecht C, Mairinger T, Theegarten D, et al. MDM2 is an important prognostic and predictive factor for platin-pemetrexed therapy in malignant pleural mesotheliomas and deregulation of P14/ARF (encoded by CDKN2A) seems to contribute to an MDM2-driven inactivation of P53. *Br J Cancer* (2015) 112:883–90. doi: 10.1038/bjc.2015.27
22. Kadota K, Suzuki K, Colovos C, Sima CS, Rusch VW, Travis WD, et al. A nuclear grading system is a strong predictor of survival in epitheloid diffuse malignant pleural mesothelioma. *Mod Pathol* (2012) 25:260–71. doi: 10.1038/modpathol.2011.146
23. Hendry S, Salgado R, Gevaert T, Russell PA, John T, Thapa B, et al. Assessing Tumor-Infiltrating Lymphocytes in Solid Tumors: A Practical Review for Pathologists and Proposal for a Standardized Method from the International Immuno-Oncology Biomarkers Working Group: Part 2: TILs in Melanoma, Gastrointestinal Tract Carcinomas, Non-Small Cell Lung Carcinoma and Mesothelioma, Endometrial and Ovarian Carcinomas, Squamous Cell Carcinoma of the Head and Neck, Genitourinary Carcinomas, and Primary Brain Tumors. *Adv Anat Pathol* (2017) 24:311–35. doi: 10.1097/PAP.0000000000000161
24. Kursa MB, Rudnicki WR. Feature selection with the boruta package. *J Stat Software* (2010) 36(11). doi: 10.18637/jss.v036.i11
25. R Core Team (2020). *R: A language and environment for statistical computing. R: A language and environment for statistical computing*. Vienna, Austria: R Foundation for Statistical Computing (2020).
26. Sánchez-Aguilera A, Sánchez-Beato M, García JF, Prieto I, Pollan M, Piris MA. p14ARF nuclear overexpression in aggressive B-cell lymphomas is a sensor of malfunction of the common tumor suppressor pathways. *Blood* (2002) 99:1411–8. doi: 10.1182/blood.v99.4.1411
27. Dominguez G, Silva J, Silva JM, Garca JM, Larrondo FJ, Vargas J, et al. Different expression of P14ARF defines two groups of breast carcinomas in terms of TP73 expression and TP53 mutational status. *Genes Chromosomes Cancer* (2001) 31:99–106. doi: 10.1002/gcc.1123
28. Vestey SB, Sen C, Calder CJ, Perks CM, Pignatelli M, Winters ZE. p14ARF expression in invasive breast cancers and ductal carcinoma in situ-relationships to p53 and Hdm2. *Breast Cancer Res* (2004) 6:R571–85. doi: 10.1186/bcr912
29. Han Y, Liu D, Li L. PD-1/PD-L1 pathway: current researches in cancer. *Am J Cancer Res* (2020) 10:727–42.
30. Chen DS, Mellman I. Oncology meets immunology: The cancer-immunity cycle. *Immunity* (2013) 39:1–10. doi: 10.1016/j.immuni.2013.07.012
31. Okada M, Kijima T, Aoe K, Kato T, Fujimoto N, Nakagawa K, et al. Clinical efficacy and safety of nivolumab: Results of a multicenter, open-label, single-arm, Japanese phase II study in malignant pleural mesothelioma (MERIT). *Clin Cancer Res* (2019) 25:5485–92. doi: 10.1158/1078-0432.CCR-19-0103
32. Baas P, Scherpereel A, Nowak A, Fujimoto N, Peters S, Tsao A, et al. ID:2908 First-Line Nivolumab + Ipilimumab vs Chemotherapy in Unresectable Malignant Pleural Mesothelioma: CheckMate 743. *J Thorac Oncol* (2020) 15:E42. doi: 10.1016/S0140-6736(20)32714-8
33. Través PG, Luqu A, Hortelano S. Tumor suppressor ARF: The new player of innate immunity. *Oncoimmunology* (2012) 1:946–7. doi: 10.4161/onci.19948
34. Herranz S, Través PG, Luque A, Hortelano S. Role of the tumor suppressor ARF in macrophage polarization: Enhancement of the M2 phenotype in ARF-deficient mice. *Oncoimmunology* (2012) 1:1227–38. doi: 10.4161/onci.21207
35. Jiménez-García L, Herranz S, Higueras MA, Luque A, Hortelano S. Tumor suppressor ARF regulates tissue microenvironment and tumor growth through modulation of macrophage polarization. *Oncotarget* (2016) 7:66835–50. doi: 10.18632/oncotarget.11652
36. Través PG, Luque A, Hortelano S. Macrophages, inflammation, and tumor suppressors: ARF, a new player in the game. *Mediators Inflamm* (2012) 2012:568783. doi: 10.1155/2012/568783

**Conflict of Interest:** The authors declare that the research was conducted in the absence of any commercial or financial relationships that could be construed as a potential conflict of interest.

frontiers in Oncology

ORIGINAL RESEARCH
published: 22 March 2021
doi: 10.3389/fonc.2021.587744

# Prognostic Implication of the Expression Level of PECAM-1 in Non-small Cell Lung Cancer

*Shuhui Cao†, Yue Wang†, Jingwen Li, Xuxinyi Ling, Yao Zhang, Yan Zhou* and Hua Zhong**

*Department of Pulmonary, Shanghai Chest Hospital, Shanghai Jiaotong University, Shanghai, China*

**Background:** Lung cancer is a malignant disease that threatens human health. Hence, it is crucial to identify effective prognostic factors and treatment targets. Single-cell RNA sequencing can quantify the expression profiles of transcripts in individual cells.

**Methods:** GSE117570 profiles were downloaded from the Gene Expression Omnibus database. Key ligand-receptor genes in the tumor and the normal groups were screened to identify integrated differentially expressed genes (DEGs) from the GSE118370 and The Cancer Genome Atlas Lung Adenocarcinoma databases. DEGs associated with more ligand-receptor pairs were selected as candidate DEGs for Gene Ontology (GO) functional annotation, Kyoto Encyclopedia of Genes and Genomes (KEGG) pathway analysis, and survival analysis. In addition, we conducted validation immunohistochemical experiments on postoperative specimens of 30 patients with lung cancer.

**Results:** A total of 18 candidate DEGs were identified from the tumor and the normal groups. The analysis of the GO biological process revealed that these DEGs were mainly enriched in wound healing, in response to wounding, cell migration, cell motility, and regulation of cell motility, while the KEGG pathway analysis found that these DEGs were mainly enriched in proteoglycans in cancer, bladder cancer, malaria, tyrosine kinase inhibitor resistance in Epidermal Growth Factor Receptor (EGFR), and the ERBB signaling pathway. Survival analysis showed that a high, rather than a low, expression of platelet endothelial cell adhesion molecule-1 (PECAM-1) was associated with improved survival. Similarly, in postoperative patients with lung cancer, we found that the overall survival of the PECAM-1 high-expression group shows a better trend than the PECAM-1 low-expression group ($p = 0.172$).

**Conclusions:** The candidate DEGs identified in this study may play some important roles in the occurrence and development of lung cancer, especially PECAM-1, which may present potential prognostic biomarkers for the outcome.

**Keywords: non-small cell lung cancer, single-cell RNA-seq, gene expression omnibus database (GEO), the Cancer Genome Atlas (TCGA), PECAM-1 (CD31)**

OPEN ACCESS

***Edited by:***
*Emanuela Felley-Bosco, University of Zurich, Switzerland*

***Reviewed by:***
*Luisella Righi, University of Turin, Italy*
*Long-Fei Wu, Soochow University, China*

****Correspondence:***
*Hua Zhong*
*eddiedong8@hotmail.com*
*Yan Zhou*
*yzhou716@163.com*

*†These authors have contributed equally to this work*

***Specialty section:***
*This article was submitted to Thoracic Oncology, a section of the journal Frontiers in Oncology*

***Received:*** *27 July 2020*
***Accepted:*** *08 February 2021*
***Published:*** *22 March 2021*

***Citation:***
*Cao S, Wang Y, Li J, Ling X, Zhang Y, Zhou Y and Zhong H (2021) Prognostic Implication of the Expression Level of PECAM-1 in Non-small Cell Lung Cancer. Front. Oncol. 11:587744. doi: 10.3389/fonc.2021.587744*

## INTRODUCTION

Lung cancer (LC) is the leading cause of cancer-related deaths among men and the third most common type of cancer among women, accounting for an estimated 2.1 million new cases and ∼1.9 million deaths worldwide in 2018. Non-small cell LC (NSCLC) is the most common type of LC, accounting for about 85% of cases (1). Tumors of NSCLC typically undergo extensive genomic changes. Recently, molecularly targeted therapies and immune checkpoint inhibitors have dramatically improved the survival of patients with genomic changes to somatic cells (2). However, patients with LC often have different outcomes with the same therapy, and resistance to targeted therapies and immunotherapies remains problematic. Hence, the identification of a new biomarker of prognosis is needed.

Single-cell genomics is a powerful tool to explore genetic and functional heterogeneity, reconstruct evolutionary lineages, and detect rare subpopulations (3). Single-cell RNA sequencing (scRNA-seq) of human tumors has revealed new insights into tumor heterogeneity and the identification of different cell subpopulations, which are crucial to elucidate the mechanisms underlying tumorigenesis (4, 5). Furthermore, a better understanding of the gene expression profiles of the tumor microenvironment (TME) may help to improving prognosis and identifying molecular therapeutic targets.

Recently, intra-tumor mutational diversification analysis of LC at the single-cell level has been conducted (2, 6, 7). However, the scRNA-seq analysis has not yet been implemented to compare the gene expression profiles of non-small cell LC with those of normal tissues.

In the present study, the genomic features of LC cells and adjacent normal cells were obtained from GSE117570 and were analyzed to sort and screen key genes coding for ligand receptors. Then, candidate differentially expressed genes (DEGs) from The Cancer Genome Atlas Lung Adenocarcinoma (TCGA-LUAC) and GSE118370 databases were used for an enrichment analysis to identify those associated with crucial ligand-receptor activities to improve the efficacy of individualized treatment regimens for LC.

## MATERIALS AND METHODS

### Patients

This analysis enrolled patients with newly diagnosed, pathologically confirmed NSCLC at the Shanghai Chest Hospital (Shanghai, China) from December 1, 2012 to December 31, 2017. All patients underwent complete resection, and no distant metastases were observed. All patients underwent follow-up of survival once a year. Paraffin-embedded lung adenocarcinoma specimens were obtained from all participants, and clinical, as well as pathological, data were collected. The present study was approved by the Institutional Review Board for Clinical Research of the Shanghai Chest Hospital.

### Data Curation

The GSE117570 and GSE118370 datasets were downloaded from the Gene Expression Omnibus database (https://www.ncbi.nlm.nih.gov/geo/query/acc.cgi). The expression profiles of LC samples were downloaded from TCGA-LUAD database (https://portal.gdc.cancer.gov/).

### Quality Control

The DropletUtils function of the R package was used to characterize the gene expression profiles of individual cells and to filter out any gene with counts of zero for all barcodes (8). Then, further screening was conducted of each cell with $<$100 unique molecular identifiers. The calculateQCMetrics scater package (9) was used to filter cells with $\leq$5% of mitochondrial genes and $\geq$10% of ribosomal genes. The expression matrix of each sample was normalized with the NormalizeData function included with the Seurat package (10).

### Principle Component Analysis (PCA) and *t*-Distributed Stochastic Neighbor Embedding (t-SNE)

The FindVariableFeatures function of the Seurat package was used to screen the top 2,000 genes with the highest standard deviations and defined as high variants. Focusing on high variant genes by downstream analysis helps to highlight biological signals in single-cell data sets. Then, the ScaleData function of the Seurat package was used to linearly scale the expression data. Finally, the RunPCA function of the Seurat package was used for linear dimensionality reduction analysis. After the selection of the principal components with large SDs, the FindNeighbors and FindClusters functions of the Seurat package were used for cell clustering analysis. Later, the RunTSNE function of the Seurat package was used for the non-linear dimensionality reduction analysis *via t*-SNE.

### Marker Gene Identification

The FindAllMarkers function of the Seurat package was used to identify DEGs between each cluster and other cell types [logFC $\geq$ 0.25 (expression ratio of the cell population $\geq$0.25); $p \leq 0.05$] as marker genes. Cell clusters were labeled and visualized according to existing annotations in the CellMarker database (11).

### Screening of DEGs

Genes in TCGA-LUAD and the GSE118370 databases with a significant difference in mean values among all samples (ANOVA; $p \leq 0.05$) were selected for PCA. Samples with appropriate phenotypes were selected for differential expression analysis with the use of GSE118370 chip data with the Limma package and of TCGA sequencing data with the edgeR package after log2 conversion of each sample ($|\log2FC| \geq 0.5849625$). Then, DEGs were collected.

### Ligand Receptor Network Analysis

Based on the ligand-receptor pairing data, related ligand-receptor pairs of various cell types were analyzed, counted, and organized by networks (12).

### Gene Function Enrichment Analysis

Functional enrichment analysis of DEGs was conducted with the use of the Gene Ontology (GO) and the Kyoto Encyclopedia

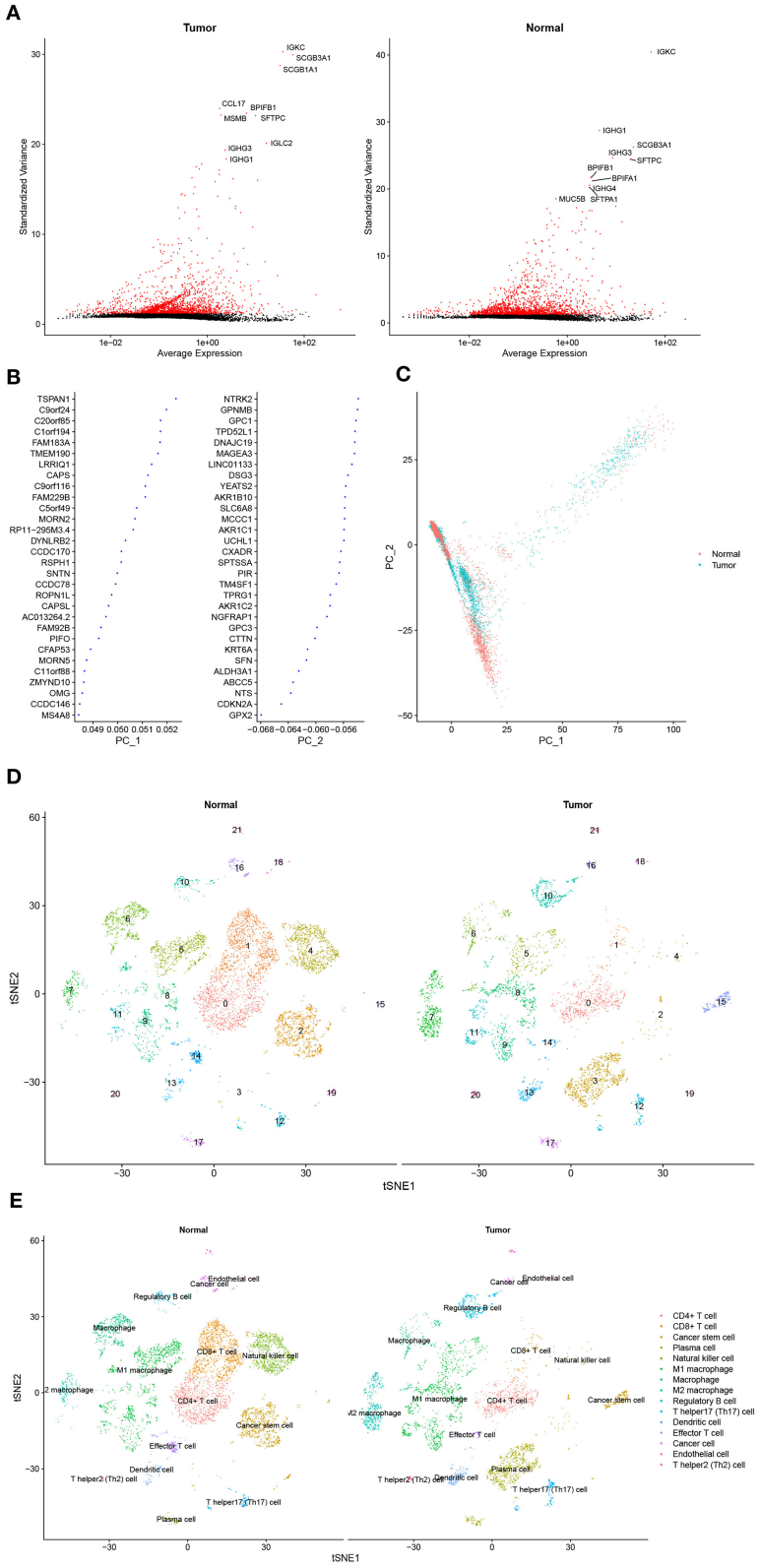


**FIGURE 1 |** Cell cluster compositions of tumor tissues and normal tissues. **(A)** Top 10 genes with the most significant differences in SDs. **(B)** Gene contributions in two principal components (PC), namely PC_1 and PC_2. **(C)** Distribution of cells in two dimensions based on the PC_1 and PC_2 components. **(D,E)**. Cell clusters of *t*-distributed stochastic neighbor embedding (*t*-SNE) and identified marker genes.

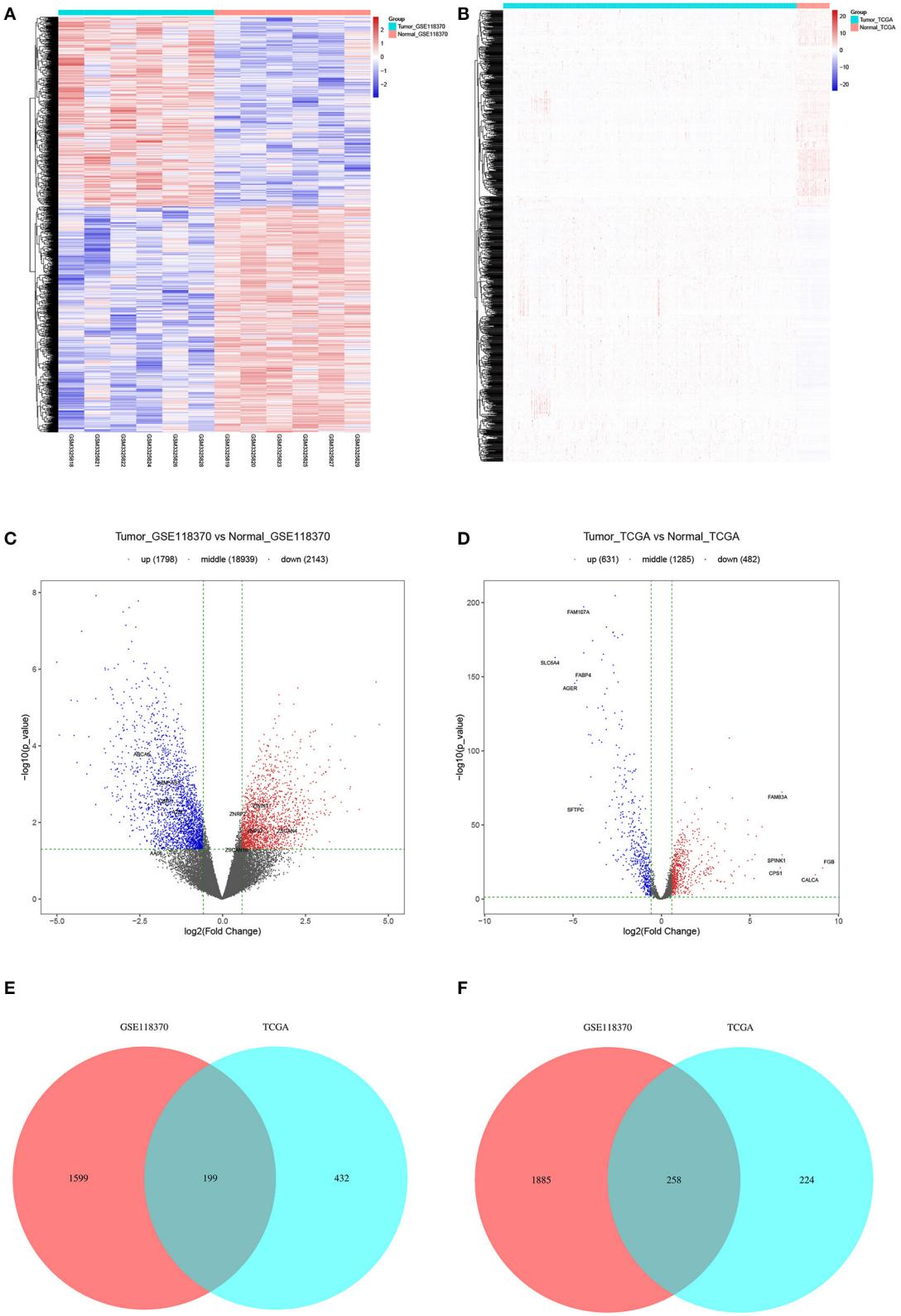


**FIGURE 2 |** Filtering of differentially expression genes (DEGs). **(A,B)** Heat maps of DEGs of **(A)** GSE118370 and **(B)** The Cancer Genome Atlas (TCGA). **(C,D)** Volcano plot of DEGs of **(C)** GSE118370 and **(D)** TCGA. **(E,F)** The intersection of **(E)** upregulated DEGs and **(F)** downregulated DEGs of GSE118370 and TCGA.

of Genes and Genomes (KEGG) biochemical pathway databases (13, 14). The Fisher's exact test was used to determine the specific functions of DEGs. The *p*-value and the false discovery rate were calculated for each DEG. The smaller the *p*-value, the greater the relationship between the functional item and the input gene, as most DEGs in the same group had similar functions.

## Gene Set Enrichment Analysis (GSEA)

Based on the genes included in the GSE118370 database, GSEA was used to compensate for the deficiency of a single gene (15).

## Immunohistochemistry (IHC)

Anti-PEACM1 antibody (1:50, ab28364, Abcam) was used for IHC staining. After the staining was completed, two pathologists independently scored the stained samples according to the staining intensity and the percentage of positively stained cells. The staining intensity was scored as follows: 0 (no staining), 1 (yellow or yellow-brown), and 2 (brown). The percentage of positive cells was scored as follows: 0 (none), 1 (<10%), 2 (10–50%), and 3 (<50%). Then, the relative expression index was calculated by multiplying these two scores; the final score $<$ 3 indicates low expression, and the final score $\geq$ 3 indicates high expression.

## Survival Analysis

According to the TCGA database, we defined the median value of the expression of candidate DEGs in all patients as the cut-off value and performed the Kaplan-Meier Survival analysis and the COX regression analysis by using the survival package. Correlations among the characteristics of patients in different groups were analyzed with the Fisher's exact test and

**TABLE 1 |** Statistic result of differentially expressed genes(DEGs).

| Resources | Platform | Sample size of Tumor | Sample size of Normal | FC | *P*_value | Up | Down |
|---|---|---|---|---|---|---|---|
| GSE118370 | GPL570 | 6 | 6 | 1.5 | 0.05 | 1,798 | 2,143 |
| TCGA | HiSeq | 526 | 59 | 1.5 | 0.05 | 631 | 482 |

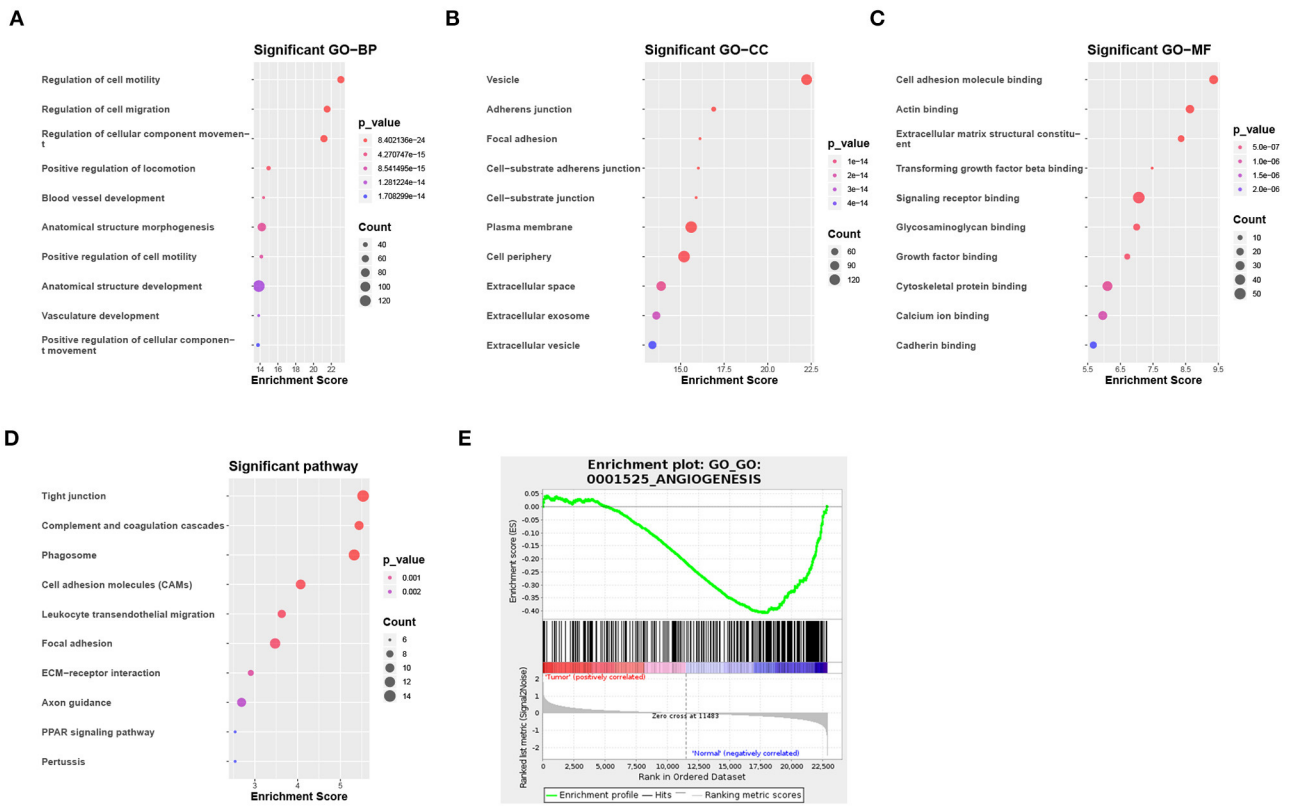


**FIGURE 3 |** Functional enrichment analysis of DEGs. **(A–C)** Enrichment result of downregulated DEGs in **(A)** the biological process (BP), **(B)** the cellular component (CC), and **(C)** the molecular function (MF) pathway of Gene Ontology (GO). **(D)** Enrichment result of downregulated DEGs of the Kyoto Encyclopedia of Genes and Genomes (KEGG) pathway. **(E)** Gene set enrichment analysis result of GO:0001525 (ANGIOGENESIS).

performed using the SPSS software version 22 (IBM Corporation, Chicago, IL).

# RESULTS

## Cell Cluster Compositions of Tumor Tissues and Normal Tissues

Approximately, 11,233 cells from the GSE117570 database passed quality control and were selected for further analysis (**Supplementary Figure 1A**). The top 2,000 genes with the most significant differences in SDs were screened, and the top 10 genes are revealed in **Figure 1A**. The distribution of these genes between the tumor group and the normal group was detected by PCA and *t*-SNE. The top 46 significantly correlated genes are shown in **Supplementary Figure 1B**. We mapped the cells into two dimensions based on the PC_1 and PC_2 components, and other components were calculated with an estimated *p*-value, and the significant components were selected for subsequent analysis (**Figures 1B,C**). To further precisely cluster the populations of cells, *t*-SNE was adopted for the visualization of high dimensional data (**Figure 1D**). In total, 15 distinct cell clusters were identified by clustering analysis and classified based on the top 10 DEGs, which included CD4+T cells, CD8+ T cells, cancer stem cells, plasma cells, natural killer cells, M1 macrophages, macrophages, M2 macrophages, regulatory B cells, T helper 17 (Th17) cells, dendritic cells, effector T cells, cancer cells, endothelial cells, and Th2 cells (**Figure 1E**).

## Filtering and Functional Enrichment Analysis of DEGs

Of the 3,941 DEGs identified in the GSE118370 dataset, 1,798 were up-regulated and 2,143 were downregulated (**Figures 2A,C**; **Table 1**). Of the 1,113 DEGs identified in the TCGA dataset, 631 were upregulated and 482 were downregulated (**Figures 2B,D**; **Table 1**). Of the 457 shared DEGs in the two databases, 199 were upregulated and 258 were downregulated (**Figures 2E,F**). To further investigate cell functional states associated with LC and potential molecular regulators, functional enrichment analyses, including GO and KEGG analyses, of these DEGs were conducted. Three main categories of the GO function analysis [biological process (BP), cellular component (CC), and molecular function (MF)] revealed that the downregulated DEGs were significantly enriched in the following functions: cell motility, cell migration, and cell component movement (GO BP, **Figure 3A**); vesicle (GO CC, **Figure 3B**); and cell adhesion molecule binding, actin binding, and extracellular matrix structural constituent (GO MF, **Figure 3C**). According to the results of the KEGG analysis, the downregulated DEGs were mainly enriched in tight junctions, complement and coagulation cascades, and phagosomes (**Figure 3D**).

To identify the potential functions of the DEGs in the tumor group and the normal group, GSEA was conducted to search GO terms enriched in the GSE118370 dataset (**Figure 3E**). The results showed that some of the genes expressed in the normal group were significantly and negatively correlated with the angiogenesis pathway (GO: 0001525).

## Ligand Receptor Network Analysis

Previous analyses of the ligand-receptor relationships of all marker genes in each cell type were presented as arrow diagrams (**Supplementry Figure 1D**; **Figure 4A**) (11). Finally, screening of nine ligand-receptor pairs with the most interactions identified a distinct network in individual cells (**Figure 4B**).

## Selection and Enrichment Analysis of Candidate DEGs

The DEGs were compared with screened ligand-receptor pairs and the following top 18 transcripts were selected as candidate DEGs: AXL, C1QA, CAV1, CD36, CD93, CDH1, COL1A1, DDR1, EFNB2, ERBB2, ERBB3, GNAI2, HBEGF,

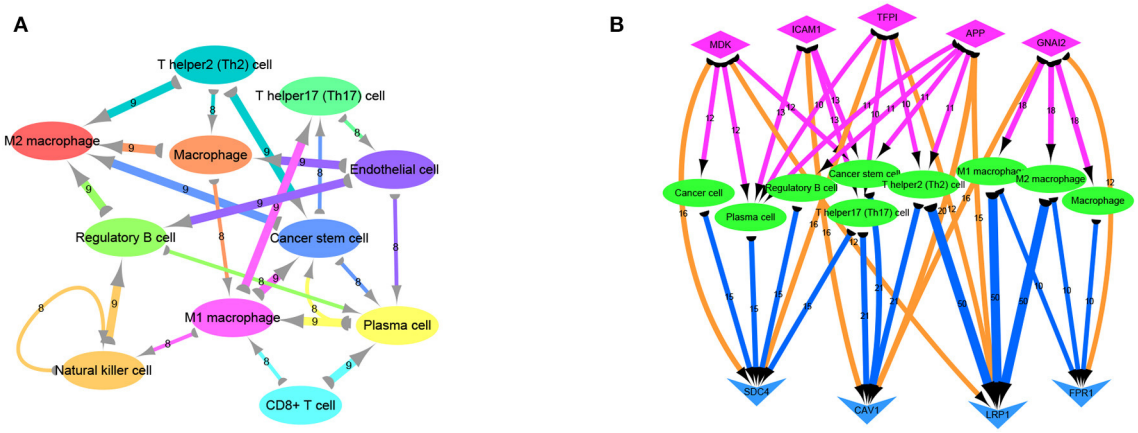


**FIGURE 4 |** Ligand receptor network analysis. **(A)** Network diagram of the detailed relationship between ligand receptors in various cell types. **(B)** Based on the network pairing relationship, the top none most ligand-receptor relationship pairs are selected, and the number of relationships between them with cell group is counted, including SDC4-MDK (16 pairs); SDC4-TFPI (16 pairs); LRP1-MDK (12 pairs); CAV1-ICAM1 (16 pairs); CAV1-APP (20 pairs); CAV1-GNAI2 (16 pairs); LRP1-TFPI (12 pairs); LRP1-APP (15 pairs); FPR1-GNAI2 (12 pairs). Diamond-shaped nodes represent ligands, and the arrows from ligands to cell types means V-shaped nodes represent receptors.

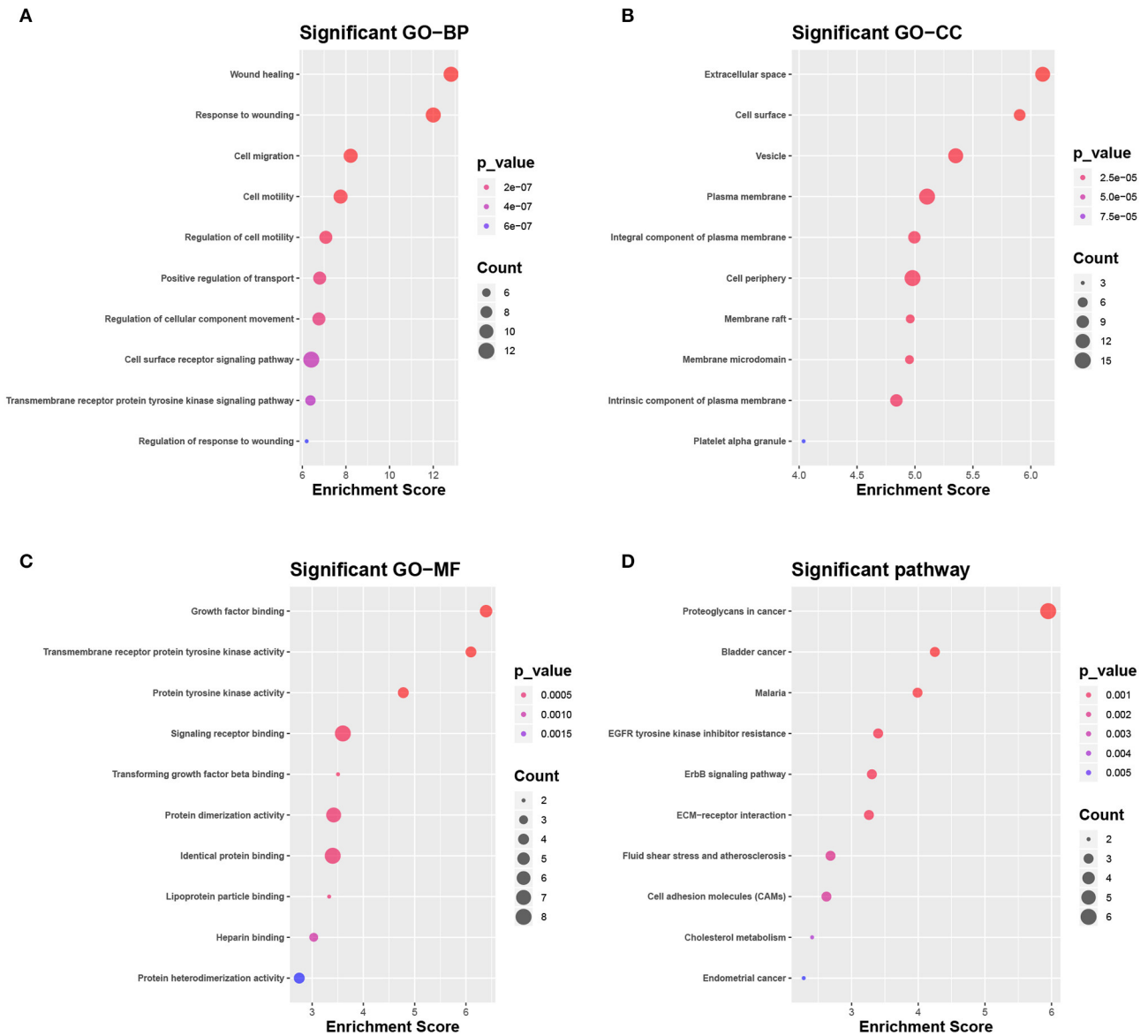


**FIGURE 5 |** Selection and enrichment analysis of candidate DEGs. **(A–C)** Gene function enrichment analysis of candidate DEGs in **(A)** GO BP, **(B)** GO CC, and **(C)** GO MF. **(D)** Gene function enrichment analysis of candidate DEGs in the KEGG pathway.

LPL, MDK, PECAM-1, PROS1, and SDC1. Compared to normal tissues, CDH1, COL1A1, DDR1, ERBB2, ERBB3, MDK, and SDC1 were upregulated in LC, and AXL, C1QA, CAV1, CD36, CD93, EFNB2, GNAI2, HBEGF, LPL, PECAM-1, and PROS1 were downregulated. According to the GO analysis, the candidate DEGs were significantly enriched in wound healing, response to wounding, and cell migration (BP, **Figure 5A**), extracellular space, cell surface, and vesicle (CC, **Figure 5B**), and growth factor binding, transmembrane receptor protein kinase activity, and protein tyrosine activity (MF, **Figure 5C**). According to KEGG analysis, the candidate DEGs were significantly enriched in proteoglycans in cancer, bladder cancer, malaria, tyrosine kinase inhibitor resistance in the EGFR, the ERBB signaling pathway, ECM-receptor interactions, fluid shear stress and atherosclerosis, cell adhesion molecules, and cholesterol metabolism in endometrial cancer (**Figure 5D**).

## Survival Analysis of Candidate DEGs

Further analysis of the expression and clinical information of candidate DEGs in TCGA-LUAD database. We performed survival analysis on half of the patients with high expression levels and half of the patients with low expression levels of candidate DEGs and found that the expression of PECAM-1 had

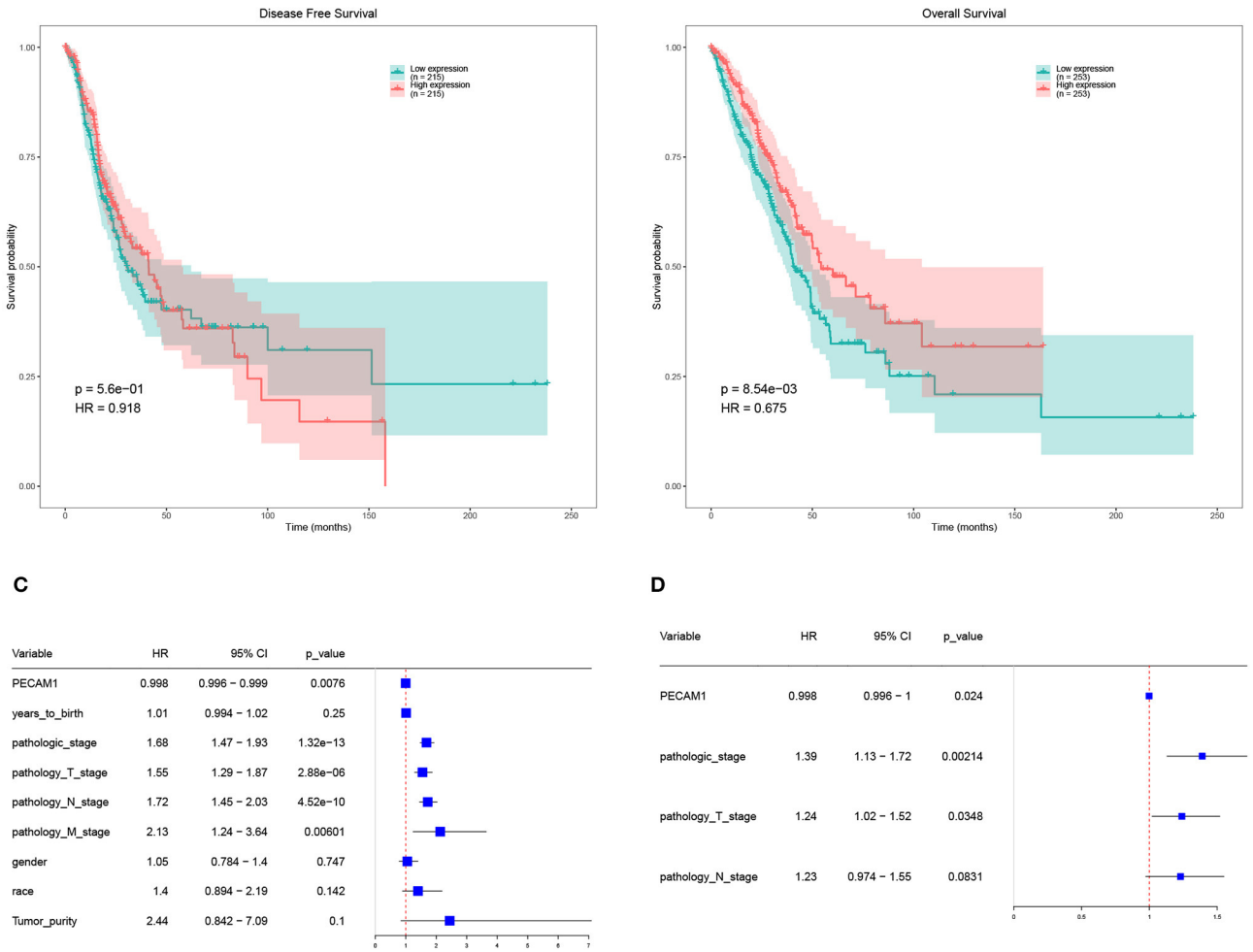


**FIGURE 6 |** Survival analysis of PECAM-1. **(A)** Disease-free survival (DFS) of PECAM-1 expression. **(B)** Overall survival (OS) of PECAM-1 expression. **(C)** Univariate cox analysis of PECAM-1. **(D)** Multivariate cox analysis of PECAM-1.

a significant impact on the survival of patients with LC at the threshold expression value of 8,615 (**Figures 6A–D**).

High expression of PECAM-1 apparently lead to a longer overall survival than its low expression [$p = 0.00854$, hazard ratio (HR) = 0.675, **Figure 6B**]. Univariate Cox analysis showed that PECAM-1 is a protective factor [HR = 0.998, 95% confidence interval (95%CI) = 0.996–0.999, $p = 0.0076$, **Figure 6C**]. Multivariate analysis was used for factors found to be obviously significant in univariate analysis, and the results of multivariate Cox analysis showed that PECAM-1 tended to have a protective effect (HR = 0.998, 95%CI = 0.996–1, $p = 0.0024$, **Figure 6D**).

## Validation of the Prognostic Effect of PECAM-1

First, we collected the paraffin tissue and clinical data of 30 patients with postoperative LUAC (**Table 2**). Then, we performed immunohistochemical tests to validate the expression of PECAM-1 in those paraffin specimens (**Figures 7A,B**). The median follow-up time is 50 months (three patients were lost). The Kaplan–Meier survival analysis of the overall survival of two groups showed that the PECAM-1 high-expression group showed a better survival trend than the PECAM-1 low-expression group, similar to our previous analysis ($p = 0.172$, **Figure 7C**).

# DISCUSSION

In the present study, cell clusters in the tumor group and the normal group were identified. Screening of the top 18 candidate DEGs in two groups identified those expressed predominantly in ligand-receptor pairs with many interactions. Functional enrichment and survival analyses indicated that the candidate DEGs were significantly associated with the prognosis of LC, especially PECAM-1.

**TABLE 2 |** Demographic, clinical, and pathological characteristics of patients with lung adenocarcinoma in the PECAM-1 high-expression group (PECAM-1+) and the PECAM-1 low-expression group (PECAM-1-).

| Parameters | PECAM-1 + | PECAM-1 − | *p*-value |
|---|---|---|---|
| **Age** | | | 1.000 |
| ≥60 | 6 | 5 | |
| <60 | 11 | 8 | |
| **Gender** | | | 0.700 |
| Male | 10 | 9 | |
| Female | 7 | 4 | |
| **Smoking history** | | | 1.000 |
| Non-smoker | 16 | 13 | |
| Smoker | 1 | 0 | |
| **Lymph node metastasis** | | 1.000 | |
| Yes | 8 | 7 | |
| No | 9 | 6 | |
| **TNM stage** | | | 0.783 |
| I | 6 | 3 | |
| II | 5 | 3 | |
| III | 5 | 6 | |
| IV | 1 | 1 | |

Overall, 18 candidate DEGs that participate in many ligand-receptor activities were subjected to scRNA-seq. The GO BP analysis results revealed that these DEGs were mainly enriched in the following top five functions: wound healing, response to wounding, cell migration, cell motility, and regulation of cell motility. Previous studies have demonstrated that the stroma of solid tumors contains a variety of cellular phenotypes and signaling pathways associated with wound healing. For example, tumor stroma is formed by abnormal activation of the wound healing pathways (16, 17). Both wound healing and TME are dependent on changes to deposition of the extracellular matrix, which promotes epithelial–mesenchymal transition and increases the motility of both fibroblasts and tumor cells (18). The GO CC analysis indicated that candidate DEGs enriched in extracellular space, cell surface, and vesicles may have important impacts on exosome production and tumor metastasis (19). The GO MF analysis demonstrated that some of the candidate DEGs were enriched in transmembrane receptor protein kinase activity and protein tyrosine activity, suggesting that the difference in the cellular processes of tumor cells vs. normal cells, such as cell signaling, cell-cell communication, transport, energy transduction, and enzyme activation, may be induced by receptor protein kinases. (20). These results suggest that these DEGs are involved in the establishment of the TME and the migration of LC cells.

The KEGG pathway analysis showed that the identified DEGs were mainly enriched in the following top five pathways: proteoglycans in cancer, bladder cancer, malaria, tyrosine kinase inhibitor resistance in EGFR, and the ERBB signaling pathway. Proteoglycans exert diverse functions in the occurrence of cancer (21–23) and are thought to regulate the phenotype of tumor cells and angiogenesis in tumor metabolism, in addition to promoting the formation of a temporary matrix for tumor growth, thereby affecting cell-cell interactions and cell-matrix interactions and tumor cell signal transduction (21). EGFR and the ERBB pathway are common targets for the treatment of LC (24, 25). The results of the present study showed DEGs have impact on tyrosine kinase inhibitor resistance in EGFR and the ERBB signaling pathway, which provide interesting insights for future studies of tyrosine kinase inhibitors in LC.

There were a lot of research about the 18 candidate DEGs. Expression of CDH1 (E-Cadherin) is associated with physiological signaling pathways, such as cell proliferation, maintenance of cell adhesion, cell polarity, and epithelial–mesenchymal transition. It is considered a risk factor for diffuse gastric and lobular breast cancer (26). COL1A1 expressions are found in most connective tissues and are abundant in bones, corneas, the dermis, and tendons (27). DDR1 is predominantly expressed in epithelial cells and is reported to be involved in the progression of cancer (28). Amplification of ERBB2 is well-described in many kinds of solid cancer and has been established as an important actionable target in multiple cancer types (29). ERBB3 plays an important role in cancer, and the mutation of ERBB is a potential tumor driver (30). MDK is a heparin-binding growth factor and acts as a mediator for the acquisition of critical hallmarks of cancer, including cell growth, survival, metastasis, migration, and angiogenesis (31). The expression of SDC1 often produces malignant phenotypes, which arise from increased cell proliferation and cell growth, cell survival, cell invasion and metastasis, and angiogenesis (32). AXL is a receptor tyrosine kinase expressed in many cancer types and has been associated with therapy resistance and poor clinical prognosis and outcomes (33). C1QA encodes the A-chain polypeptide of serum complement subcomponent C1q, which is associated with lupus erythematosus and glomerulonephritis (34). CAV1 encodes the scaffolding protein, which is the main component of the caveolae plasma membranes found in most cell types (35). CD36 is a scavenger receptor expressed in multiple cell types, and it mediates lipid uptake, immunological recognition, inflammation, molecular adhesion, and apoptosis (36). CD93 is a transmembrane receptor that is upregulated in tumor vessels in many types of cancer, including high-grade glioma (37). EFNB2 is expressed at abnormally high levels in some neoplasms, such as squamous cell carcinoma of the head and neck and colorectal cancer (38). The expression of GNAI2 in CD11c+ cells and IL6 in CD4+/CD11b+ DCs appears to promote colon tumor development in mice (39). HBEGF is a ligand for the EGFR, one of the most commonly amplified receptor tyrosine kinases in glioblastoma, which may be a clinically relevant target (40). LPL has been extensively investigated as a potential risk factor for coronary artery disease (41). PROS1 encodes a vitamin K-dependent plasma protein that functions as a cofactor for the anticoagulant protease, an activated protein C to inhibit blood coagulation. It plays an essential role in the resolution of inflammation (42).

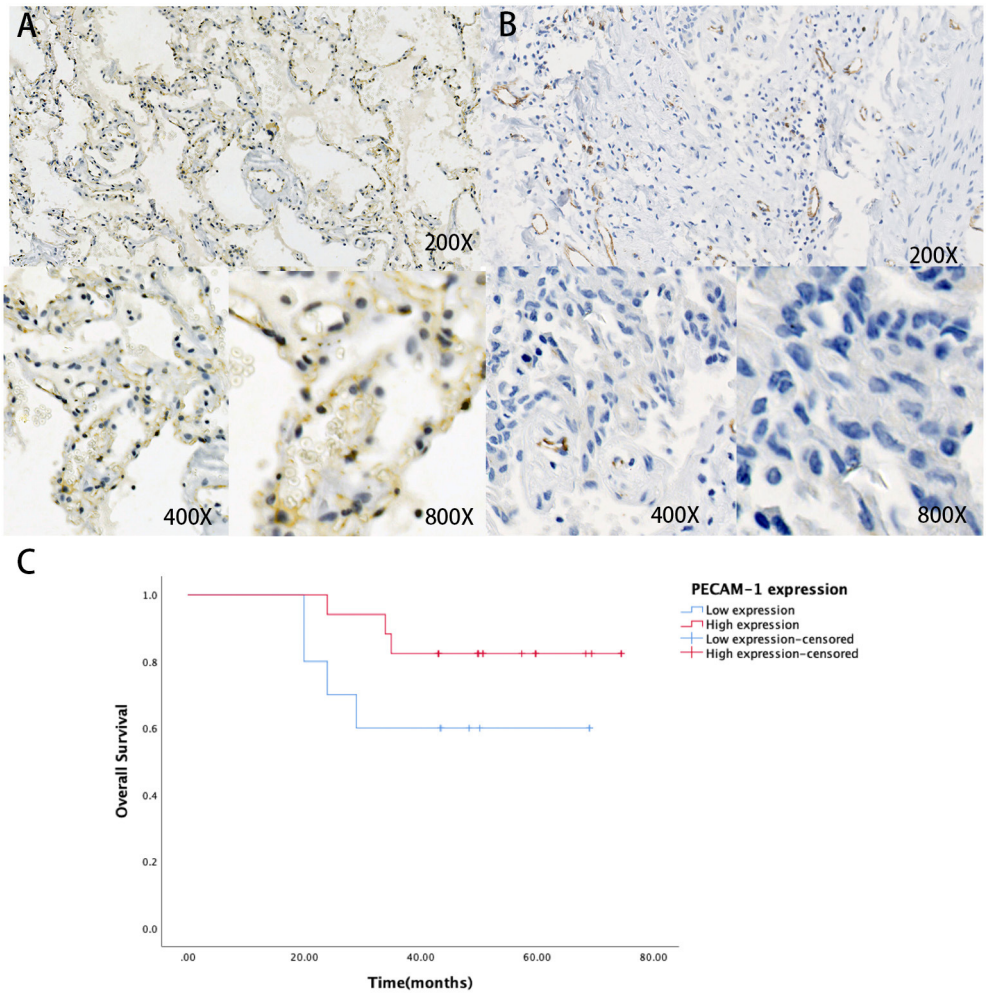


**FIGURE 7 |** The expression of protein PECAM-1 in patients with lung adenocarcinoma. A-B Representative positive **(A)** and negative **(B)** expression of PECAM-1 were examined by immunohistochemistry in lung adenocarcinoma tissues ($n = 30$). Original magnification, ×200 (upper panel), ×400 (lower panel), ×800 (lower panel). **(C)** The association of protein expression of PECAM-1 with OS ($n = 30$).

PECAM-1 (also known as a cluster of differentiation 31, CD31) was primarily identified as an adhesion molecule that plays various roles in cell proliferation, apoptosis, and migration, in addition to cellular immunity. PECAM-1 is expressed by some tumor cells and may contribute to tumor invasion (43, 44). However, the role of PECAM-1 in LC remains unclear (45–50). Giovanna et al. found that PECAM-1 acts as a checkpoint molecule and can negatively regulate FcγR-mediated phagocytosis by monocytes and macrophages, and downregulation of PECAM-1 correlated with decreased survival of chronic lymphocytic leukemia cells (51, 52). Virman et al. found that high expression of PECAM-1 was significantly associated with improved survival.

At present, the research on PECAM-1 is not sufficient, but many studies have shown that PECAM-1 may affect immune regulation. This molecule may play a crucial and complex role in the regulation of T-cell-mediated immune responses, with a large impact on immunity in health and disease (53). Previous studies have found that although the loss of PECAM-1 leads to excessively cytotoxic killing, PECAM-1 also can delay T-cell apoptosis and prolong the action time of T cells (54, 55). Studies have also found that the PECAM-1 protein can promote the endothelial migration of lymphocytes and natural killer cell, which take pivotal roles in eliminating the abnormal cells, such as tumor cells (54, 56, 57). Analysis by our group revealed that a high PECAM-1 expression was associated with better overall survival and is a significant prognostic factor in LC. Although multivariate Cox analysis showed that PECAM-1 was not statistically significant, a suitable cutoff value of PECAM-1 expression may help to indicate better survival of patients with LC. Our research also found that, although it is statistically non-significant, patients with LC with a high PECAM-1 expression had a longer overall survival period, which may be related to the effect of PECAM-1 on the tumor immune microenvironment, promoting the transport of immune

cells and enhancing the role of immune cells. However, the potential impact of PECAM-1-mediated interactions on the development and function of the immune system need to be fully studied.

The results of the present study identified key genes and pathways in LC, which will improve our understanding of the molecular mechanisms underlying the development and progression of LC. Eighteen genes that potentially play pivotal roles in the pathogenesis of LC and may be closely associated with tumor progression, especially PECAM-1, were identified in the present study. In addition, we conducted immunohistochemical analysis on the protein expression of PECAM-1 in lung cancer tissues and analyzed the survival of patients with LC with different PECAM-1 expressions. We found that the PECAM-1 high-expression group has a clear survival advantage, which further shows that PECAM-1 may be a protective prognostic factor.

## DATA AVAILABILITY STATEMENT

Publicly available datasets were analyzed in this study. This data can be found here: the NCBI Gene Expression Omnibus (GSE117570 and GSE118370) and The Cancer Genome Atlas (https://portal.gdc.cancer.gov/) (TCGA LUAD).

## ETHICS STATEMENT

Written informed consent was obtained from the individual(s) for the publication of any potentially identifiable images or data included in this article.

## AUTHOR CONTRIBUTIONS

HZ, YZho, and SC designed the study. SC and YW drafted the manuscript. SC, YW, and JL processed and analyzed data. XL and YZha edited the drafting of the manuscript and drew some pictures. HZ and YZho revised the manuscript. All authors contributed to the article and approved the submitted version.

## FUNDING

This work was supported by the Science and Technology Commission of Shanghai Muncipality (No. 19411970900) and the Shanghai Chest Hospital-Collaborative Innovation Project (Project No.YJXT20190204).

## SUPPLEMENTARY MATERIAL

The Supplementary Material for this article can be found online at: https://www.frontiersin.org/articles/10.3389/fonc.2021.587744/full#supplementary-material

## REFERENCES

1. Herbst RS, Heymach JV, Lippman SM. Lung cancer. *N Engl J Med.* (2008) 359:1367–80. doi: 10.1056/NEJMra0802714
2. Collisson EA, Campbell JD, Brooks AN, Berger AH, Lee W, Chmielecki J, et al. Comprehensive molecular profiling of lung adenocarcinoma. *Nature.* (2014) 511:543–50. doi: 10.1038/nature13385
3. Tanay A, Regev A. Scaling single-cell genomics from phenomenology to mechanism. *Nature.* (2017) 541:331–8. doi: 10.1038/nature21350
4. Patel AP, Tirosh I, Trombetta JJ, Shalek AK, Gillespie SM, Wakimoto H, et al. Single-cell RNA-seq highlights intratumoral heterogeneity in primary glioblastoma. *Science.* (2014) 344:1396–401. doi: 10.1126/science.1254257
5. Lawson DA, Bhakta NR, Kessenbrock K, Prummel KD, Yu Y, Takai K, et al. Single-cell analysis reveals a stem-cell program in human metastatic breast cancer cells. *Nature.* (2015) 526:131–5. doi: 10.1038/nature15260
6. Xiong D, Pan J, Yin Y, Jiang H, Szabo E, Lubet RA, et al. Novel mutational landscapes and expression signatures of lung squamous cell carcinoma. *Oncotarget.* (2018) 9:7424–41. doi: 10.18632/oncotarget.23716
7. Guo X, Zhang Y, Zheng L, Zheng C, Song J, Zhang Q, et al. Global characterization of T cells in non-small-cell lung cancer by single-cell sequencing. *Nat Med.* (2018) 24:978–85. doi: 10.1038/s41591-018-0045-3
8. Lun ATL, Riesenfeld S, Andrews T, Dao TP, Gomes T, Marioni JC. EmptyDrops: distinguishing cells from empty droplets in droplet-based single-cell RNA sequencing data. *Genome Biol.* (2019) 20:63. doi: 10.1186/s13059-019-1662-y
9. McCarthy DJ, Campbell KR, Lun AT, Wills QF. Scater: pre-processing, quality control, normalization and visualization of single-cell RNA-seq data in R. *Bioinformatics.* (2017) 33:1179–86. doi: 10.1093/bioinformatics/btw777
10. Butler A, Hoffman P, Smibert P, Papalexi E, Satija R. Integrating single-cell transcriptomic data across different conditions, technologies, and species. *Nat Biotechnol.* (2018) 36:411–20. doi: 10.1038/nbt.4096
11. Zhang X, Lan Y, Xu J, Quan F, Zhao E, Deng C, et al. CellMarker: a manually curated resource of cell markers in human and mouse. *Nucleic Acids Res.* (2019) 47:D721–8. doi: 10.1093/nar/gky900
12. Ramilowski JA, Goldberg T, Harshbarger J, Kloppmann E, Lizio M, Satagopam VP, et al. A draft network of ligand-receptor-mediated multicellular signalling in human. *Nat Commun.* (2015) 6:7866. doi: 10.1038/ncomms8866
13. Ashburner M, Ball CA, Blake JA, Botstein D, Butler H, Cherry JM, et al. Gene ontology: tool for the unification of biology. The Gene Ontology Consortium. *Nat Genet.* (2000) 25:25–9. doi: 10.1038/75556
14. Kanehisa M, Goto S. KEGG: Kyoto encyclopedia of genes and genomes. *Nucleic Acids Res.* (2000) 28:27–30. doi: 10.1093/nar/28.1.27
15. Subramanian A, Tamayo P, Mootha VK, Mukherjee S, Ebert BL, Gillette MA, et al. Gene set enrichment analysis: a knowledge-based approach for interpreting genome-wide expression profiles. *Proc Natl Acad Sci USA.* (2005) 102:15545–550. doi: 10.1073/pnas.0506580102
16. Dvorak HF. Tumors: wounds that do not heal. Similarities between tumor stroma generation and wound healing. *N Engl J Med.* (1986) 315:1650–9. doi: 10.1056/NEJM198612253152606
17. Foster DS, Jones RE, Ransom RC, Longaker MT, Norton JA. The evolving relationship of wound healing and tumor stroma. *JCI Insight.* (2018) 3:e99911. doi: 10.1172/jci.insight.99911
18. Ge Y, Gomez NC, Adam RC, Nikolova M, Yang H, Verma A, et al. Stem cell lineage infidelity drives wound repair and cancer. *Cell.* (2017) 169:636–50.e614. doi: 10.1016/j.cell.2017.03.042
19. Meldolesi J. Exosomes and ectosomes in intercellular communication. *Curr Biol.* (2018) 28:R435–44. doi: 10.1016/j.cub.2018.01.059
20. Albrecht C, Appert-Collin A, Bagnard D, Blaise S, Romier-Crouzet B, Efremov RG, et al. Transmembrane peptides as inhibitors of protein-protein interactions: an efficient strategy to target cancer cells? *Front Oncol.* (2020) 10:519. doi: 10.3389/fonc.2020.00519
21. Fan S, Liang Z, Gao Z, Pan Z, Han S, Liu X, et al. Identification of the key genes and pathways in prostate cancer. *Oncol Lett.* (2018) 16:6663–9. doi: 10.3892/ol.2018.9491

22. Barash U, Cohen-Kaplan V, Dowek I, Sanderson RD, Ilan N, Vlodavsky I. Proteoglycans in health and disease: new concepts for heparanase function in tumor progression and metastasis. *FEBS J.* (2010) 277:3890–903. doi: 10.1111/j.1742-4658.2010.07799.x
23. Theocharis AD, Skandalis SS, Neill T, Multhaupt HA, Hubo M, Frey H, et al. Insights into the key roles of proteoglycans in breast cancer biology and translational medicine. *Biochim Biophys Acta.* (2015) 1855:276–300. doi: 10.1016/j.bbcan.2015.03.006
24. Singh D, Attri BK, Gill RK, Bariwal J. Review on EGFR inhibitors: critical updates. *Mini Rev Med Chem.* (2016) 16:1134–66. doi: 10.2174/1389557516666160321114917
25. Wang Z. ErbB receptors and cancer. *Methods Mol Biol.* (2017) 1652:3–35. doi: 10.1007/978-1-4939-7219-7_1
26. Shenoy S. CDH1 (E-Cadherin) mutation and gastric cancer: genetics, molecular mechanisms and guidelines for management. *Cancer Manag Res.* (2019) 11:10477–86. doi: 10.2147/CMAR.S208818
27. Marini JC, Forlino A, Bächinger HP, Bishop NJ, Byers PH, Paepe A, et al. Osteogenesis imperfecta. *Nat Rev Dis Primers.* (2017) 3:17052. doi: 10.1038/nrdp.2017.52
28. Yeh YC, Lin HH, Tang MJ. Dichotomy of the function of DDR1 in cells and disease progression. *Biochim Biophys Acta Mol Cell Res.* (2019) 1866:118473. doi: 10.1016/j.bbamcr.2019.04.003
29. Subramanian J, Katta A, Masood A, Vudem DR, Kancha RK. Emergence of ERBB2 mutation as a biomarker and an actionable target in solid cancers. *Oncologist.* (2019) 24:e1303–14. doi: 10.1634/theoncologist.2018-0845
30. Kiavue N, Cabel L, Melaabi S, Bataillon G, Callens C, Lerebours F, et al. ERBB3 mutations in cancer: biological aspects, prevalence and therapeutics. *Oncogene.* (2020) 39:487–502. doi: 10.1038/s41388-019-1001-5
31. Filippou PS, Karagiannis GS, Constantinidou A. Midkine (MDK) growth factor: a key player in cancer progression and a promising therapeutic target. *Oncogene.* (2020) 39:2040–54. doi: 10.1038/s41388-019-1124-8
32. Gharbaran R. Advances in the molecular functions of syndecan-1 (SDC1/CD138) in the pathogenesis of malignancies. *Crit Rev Oncol Hematol.* (2015) 94:1–17. doi: 10.1016/j.critrevonc.2014.12.003
33. Tanaka M, Siemann DW. Gas6/Axl signaling pathway in the tumor immune microenvironment. *Cancers.* (2020) 12:1850. doi: 10.3390/cancers12071850
34. Fonseca MI, Chu SH, Hernandez MX, Fang MJ, Modarresi L, Selvan P, et al. Cell-specific deletion of C1qa identifies microglia as the dominant source of C1q in mouse brain. *J Neuroinflammation.* (2017) 14:48. doi: 10.1186/s12974-017-0814-9
35. Hofmann F, Flockerzi V, Kahl S, Wegener JW. L-type CaV1.2 calcium channels: from *in vitro* findings to *in vivo* function. *Physiol Rev.* (2014) 94:303–26. doi: 10.1152/physrev.00016.2013
36. Wang J, Li Y. CD36 tango in cancer: signaling pathways and functions. *Theranostics.* (2019) 9:4893–908. doi: 10.7150/thno.36037
37. Lugano R, Vemuri K, Yu D, Bergqvist M, Smits A, Essand M, et al. CD93 promotes β1 integrin activation and fibronectin fibrillogenesis during tumor angiogenesis. *J Clin Invest.* (2018) 128:3280–97. doi: 10.1172/JCI97459
38. Zhu F, Dai SN, Xu DL, Hou CQ, Liu TT, Chen QY, et al. EFNB2 facilitates cell proliferation, migration, and invasion in pancreatic ductal adenocarcinoma via the p53/p21 pathway and EMT. *Biomed Pharmacother.* (2020) 125:109972. doi: 10.1016/j.biopha.2020.109972
39. Li ZW, Sun B, Gong T, Guo S, Zhang J, Wang J, et al. GNAI1 and GNAI3 reduce colitis-associated tumorigenesis in mice by blocking IL6 signaling and down-regulating expression of GNAI2. *Gastroenterology.* (2019) 156:2297–312. doi: 10.1053/j.gastro.2019.02.040
40. Shin CH, Robinson JP, Sonnen JA, Welker AE, Yu DX, VanBrocklin MW, et al. HBEGF promotes gliomagenesis in the context of Ink4a/Arf and Pten loss. *Oncogene.* (2017) 36:4610–18. doi: 10.1038/onc.2017.83
41. Xie L, Li YM. Lipoprotein Lipase (LPL) polymorphism and the risk of coronary artery disease: a meta-analysis. *Int J Environ Res Public Health.* (2017) 14:84. doi: 10.3390/ijerph14010084
42. Rothlin CV, Carrera-Silva EA, Bosurgi L, Ghosh S. TAM receptor signaling in immune homeostasis. *Annu Rev Immunol.* (2015) 33:355–91. doi: 10.1146/annurev-immunol-032414-112103
43. Gong G, Lin T, Yuan Y. Integrated analysis of gene expression and DNA methylation profiles in ovarian cancer. *J Ovarian Res.* (2020) 13:30. doi: 10.1186/s13048-020-00632-9
44. Ranamukhaarachchi SK, Modi RN, Han A, Velez DO, Kumar A, Engler AJ, et al. Macromolecular crowding tunes 3D collagen architecture and cell morphogenesis. *Biomater Sci.* (2019) 7:618–33. doi: 10.1039/C8BM01188E
45. Liu XL, Liu LD, Zhang SG, Dai SD, Li WY, Zhang L. Correlation between expression and significance of δ-catenin, CD31, and VEGF of non-small cell lung cancer. *Genet Mol Res.* (2015) 14:13496–503. doi: 10.4238/2015.October.28.10
46. Mohamed SY, Mohammed HL, Ibrahim HM, Mohamed EM, Salah M. Role of VEGF, CD105, and CD31 in the prognosis of colorectal cancer cases. *J Gastrointest Cancer.* (2019) 50:23–34. doi: 10.1007/s12029-017-0014-y
47. Rask L, Høgdall CK, Kjaer SK, Christensen L, Jensen A, Blaakaer J, et al. Association of CD31 and p53 with survival of ovarian cancer patients. *Anticancer Res.* (2019) 39:567–76. doi: 10.21873/anticanres.13149
48. Tzeng HT, Tsai CH, Yen YT, Cheng HC, Chen YC, Pu SW, et al. Dysregulation of Rab37-mediated cross-talk between cancer cells and endothelial cells via thrombospondin-1 promotes tumor neovasculature and metastasis. *Clin Cancer Res.* (2017) 23:2335–45. doi: 10.1158/1078-0432.CCR-16-1520
49. Virman J, Bono P, Luukkaala T, Sunela K, Kujala P, Kellokumpu-Lehtinen LP. VEGFR3, and CD31 as prognostic factors in renal cell cancer. *Anticancer Res.* (2015) 35:921–7.
50. Zhang YY, Kong LQ, Zhu XD, Cai H, Wang CH, Shi WK, et al. CD31 regulates metastasis by inducing epithelial-mesenchymal transition in hepatocellular carcinoma via the ITGB1-FAK-Akt signaling pathway. *Cancer Lett.* (2018) 429:29–40. doi: 10.1016/j.canlet.2018.05.004
51. Gautam S, Fatehchand K, Elavazhagan S, Reader BF, Ren L, Mo X, et al. Reprogramming nurse-like cells with interferon γ to interrupt chronic lymphocytic leukemia cell survival. *J Biol Chem.* (2016) 291:14356–62. doi: 10.1074/jbc.M116.723551
52. Merchand-Reyes G, Robledo-Avila FH, Buteyn NJ, Gautam S, Santhanam R, Fatehchand K, et al. CD31 acts as a checkpoint molecule and is modulated by FcγR-mediated signaling in monocytes. *J Immunol.* (2019) 203:3216–24. doi: 10.4049/jimmunol.1900059
53. Marelli-Berg FM, Clement M, Mauro C, Caligiuri G. An immunologist's guide to CD31 function in T-cells. *J Cell Sci.* (2013) 126(Pt. 11):2343–52. doi: 10.1242/jcs.124099
54. Zocchi MR, Ferrero E, Leone BE, Rovere P, Bianchi E, Toninelli E, et al. CD31/PECAM-1-driven chemokine-independent transmigration of human T lymphocytes. *Eur J Immunol.* (1996) 26:759–67. doi: 10.1002/eji.1830260406
55. Ma L, Mauro C, Cornish GH, Chai J-G, Coe D, Fu H, et al. Ig gene-like molecule CD31 plays a nonredundant role in the regulation of T-cell immunity and tolerance. *Proc Natl Acad Sci USA.* (2010) 107:19461–6. doi: 10.1073/pnas.1011748107
56. Berman ME, Xie Y, Muller WA. Roles of platelet/endothelial cell adhesion molecule-1 (PECAM-1, CD31) in natural killer cell transendothelial migration and beta 2 integrin activation. *J Immunol.* (1996) 156:1515–24.
57. Winneberger J, Schöls S, Lessmann K, Rández-Garbayo J, Bauer AT, Yusuf AM, et al. Platelet endothelial cell adhesion molecule-1 is a gatekeeper of neutrophil transendothelial migration in ischemic stroke. *Brain Behav Immun.* (2020) doi: 10.1016/j.bbi.2020.12.026. [Epub ahead of print].


**Conflict of Interest:** The authors declare that the research was conducted in the absence of any commercial or financial relationships that could be construed as a potential conflict of interest.

frontiers in Oncology

REVIEW
published: 27 April 2021
doi: 10.3389/fonc.2021.672747

# Malignant Pleural Effusions—A Window Into Local Anti-Tumor T Cell Immunity?

*Nicola Principe*[1,2], *Joel Kidman*[1,2], *Richard A. Lake*[1,2], *Willem Joost Lesterhuis*[2,3], *Anna K. Nowak*[1,4], *Alison M. McDonnell*[3] *and Jonathan Chee*[1,2*]

[1] National Centre for Asbestos Related Diseases, Institute for Respiratory Health, University of Western Australia, Nedlands, WA, Australia, [2] School of Biomedical Sciences, University of Western Australia, Crawley, WA, Australia, [3] Telethon Kids Institute, Perth, WA, Australia, [4] School of Medicine, University of Western Australia, Crawley, WA, Australia

The success of immunotherapy that targets inhibitory T cell receptors for the treatment of multiple cancers has seen the anti-tumor immune response re-emerge as a promising biomarker of response to therapy. Longitudinal characterization of T cells in the tumor microenvironment (TME) helps us understand how to promote effective anti-tumor immunity. However, serial analyses at the tumor site are rarely feasible in clinical practice. Malignant pleural effusions (MPE) associated with thoracic cancers are an abnormal accumulation of fluid in the pleural space that is routinely drained for patient symptom control. This fluid contains tumor cells and immune cells, including lymphocytes, macrophages and dendritic cells, providing a window into the local tumor microenvironment. Recurrent MPE is common, and provides an opportunity for longitudinal analysis of the tumor site in a clinical setting. Here, we review the phenotype of MPE-derived T cells, comparing them to tumor and blood T cells. We discuss the benefits and limitations of their use as potential dynamic biomarkers of response to therapy.

**Keywords: malignant pleural effusions (MPE), T cells, immune checkpoint therapy, checkpoint receptors, memory T cells**

OPEN ACCESS

***Edited by:***
*Emanuela Felley-Bosco, University of Zurich, Switzerland*

***Reviewed by:***
*Evelien Smits, University of Antwerp, Belgium*
*Floris Dammeijer, Erasmus Medical Center, Netherlands*

***Correspondence:**
*Jonathan Chee*
*jonathan.chee@uwa.edu.au*

***Specialty section:***
*This article was submitted to Cancer Immunity and Immunotherapy, a section of the journal Frontiers in Oncology*

***Received:*** *26 February 2021*
***Accepted:*** *07 April 2021*
***Published:*** *27 April 2021*

***Citation:***
*Principe N, Kidman J, Lake RA, Lesterhuis WJ, Nowak AK, McDonnell AM and Chee J (2021) Malignant Pleural Effusions—A Window Into Local Anti-Tumor T Cell Immunity? Front. Oncol. 11:672747. doi: 10.3389/fonc.2021.672747*

## MALIGNANT PLEURAL EFFUSION IS A COMPLICATION IN THORACIC CANCERS

A malignant pleural effusion (MPE) is an abnormal accumulation of fluid in the pleural space associated with advanced stage disease and poor clinical outcomes (1, 2). These effusions are present at diagnosis in over 90% of patients with mesothelioma (3) and 40% of patients with advanced lung cancer (1), and are a common feature of metastatic disease to the lung in patients with breast cancer, lymphoma, ovarian and stomach cancers (2, 4). MPEs are an exudative fluid, resulting from increased vascular permeability, inflammation and plasma leakage caused in part by tumor cells blocking the outflow of fluid from the pleural space (5). This build up of fluid leads to symptoms of various severity including breathlessness, chest pain and cough (5), with current therapy consisting largely of palliative measures designed to drain or eliminate the pleural space to prevent

accumulation of fluid (6–9). With the exception of pleurectomy, recurrent MPE can occur throughout disease progression.

As MPE is adjacent to both primary and metastatic lung tumor tissue, it is a unique peri-tumoral environment populated with tumor cells, cytokines, growth factors, enzymes and immune cells (10, 11). MPEs are routinely drained, providing an attractive option to longitudinally study the tumor microenvironment (TME) in thoracic cancers such as mesothelioma, where a major hurdle is the inability to collect serial tumor biopsies. Our review focuses on the adaptive immune cells in MPEs, and how they could inform responses to cancer immunotherapies.

## THERE IS AN URGENT NEED TO DEVELOP BIOMARKERS OF RESPONSE TO IMMUNE CHECKPOINT BLOCKADE

Immune checkpoint blockade (ICB) targeting T cell inhibitory receptors: cytotoxic T lymphocyte associated protein-4 (CTLA-4) and programmed cell death protein-1/ligand-1 (PD-1/PD-L1) have revolutionized cancer treatment. Single or dual agent ICB provides an durable survival benefit in patients with mesothelioma and non-small cell (NSCLC) lung cancer patients (12–15). Four ICB therapies: pembrolizumab, nivolumab, atezolizumab and durvulamab that target the PD-1/PD-L1 pathway are approved first and second-line treatments for patients with advanced NSCLC (16). Combination of ipilimumab (anti-CTLA-4) and nivolumab (anti-PD-1) provides a survival benefit over chemotherapy in malignant pleural mesothelioma (14). Platinum-based chemotherapies may synergize with ICB, with single arm studies showing that combination chemo-immunotherapy reduces tumor burden and shows promising progression-free and overall survival outcomes for mesothelioma (17–19). In addition, complete tumor regression has been observed in some NSCLC (20–22) and SCLC (23–25) patients treated with chemo-immunotherapy. Atezolizumab and durvalumab are also approved in combination with platinum-based chemotherapy for advanced SCLC patients (26). However, these best-case responses are only observed in a minority of patients. ICB is also expensive and can cause severe immune-related toxicities, highlighting the need to develop biomarkers that can accurately predict patient outcomes and inform clinical decisions (27). To date, several predictive biomarkers have been associated with ICB outcomes in some cancers, including intratumoral expression of the inhibitory receptor PD-L1 (28), the tumor mutational landscape (29), immune gene signatures within the TME (30, 31), and the presence of tumor infiltrating lymphocytes (TILs) and their expression of PD-1/PD-L1 (32–35). However, there is no common biomarker that can accurately predict ICB outcomes across different thoracic cancers, and there is a need to develop more nuanced biomarkers of response.

As ICB primarily acts through T cells, in-depth characterization of T cell subsets within the TME, and how they correlate with ICB outcomes, has been extensively investigated. $CD8^+$ T cell subsets characterized by expression of activation/memory associated markers and their T cell receptor (TCR) usage have been linked with outcome to ICB (34, 36–39), highlighting the potential utility of T cell subsets to inform ICB responses. As T cells are also enriched in MPEs, they could offer insight into anti-tumor responses if they accurately reflect TIL phenotype, frequency and function. Longitudinal analysis of MPEs could reveal dynamic changes in the TME without the need for serial biopsies, and aid development of a biomarker of response.

Below, we review studies that have characterized matched MPE, TME and peripheral blood derived T cells, focusing on whether MPE T cells are similar in phenotype, function and specificity to their tumor counterparts. We also review changes in T cells derived from MPEs of patients undergoing ICB, and whether these changes were associated with treatment outcomes. Lastly, we discuss the unique opportunities and challenges a longitudinal study of MPE T cells brings, in terms of improving our understanding of therapeutic mechanisms, and developing a biomarker of response to ICB.

## CELLULAR CHARACTERISTICS OF MALIGNANT PLEURAL EFFUSIONS WITHOUT ICB

MPEs contain multiple cell types including tumor cells, pleural mesothelial cells, and innate and adaptive immune cells (40). Innate immune cells in the MPE include monocytes, macrophages, neutrophils, mast cells, dendritic cells and natural killer cells (41). These cells release cytokines, growth factors and chemokines including monocyte chemotactic protein (MCP-1), vascular endothelial growth factor (VEGF), IL-8, IL-6, IL-1β, interferon gamma (IFN-$\gamma$), tumor necrosis factor alpha (TNF$\alpha$), and transforming growth factor beta (TGFβ) (40, 42–48). These cytokines can be proinflammatory and in some cases protumorigenic, promoting angiogenesis, vascular permeability and protecting cancer cells from apoptosis. MPE have increased lactate dehydrogenase, and a lower pH than non-malignant pleural fluid, suggestive of an immunosuppressive environment (11, 41, 49). The characterization of MPE proteins, cytokine milieu, innate cells, tumor cells, and their relation to overall survival have been extensively reviewed elsewhere (50–52), so this review will focus on T cells.

### MPE Are Enriched With T Cells

The proportion of total T cells in the MPE is greater than in matched peripheral blood samples from both mesothelioma and lung cancer patients (53, 54). $CD4^+$ T cells are the predominant T cell subset in MPE both prior to and after chemotherapy (41, 54–57). Of these $CD4^+$ T cells, an increased proportion of regulatory T cells ($CD4^+CD25^+$) are recruited in MPEs by chemokines and pro-inflammatory cytokines, compared to matched peripheral blood (58–61). Despite this abundance of $CD4^+$ T cells, several studies have shown that the $CD4^+/CD8^+$ T cell ratio in MPEs is similar to matched peripheral blood samples in patients with

mesothelioma (54, 62). For lung cancer patients, $CD8^+$ T cell frequencies were greater in the peripheral blood compared to the MPE for one study (53) but were similar between both compartments in others (41, 63), suggesting $CD8^+$ T cell infiltration in the pleural space may be more cancer or chemotherapy specific.

Several recent studies have examined the effect of chemotherapy on the immune milieu of matched MPE and tumor samples. At baseline, MPEs contain a lower frequency of $CD4^+$ and $CD4^+$ regulatory ($Foxp3^+$) T cells compared to matched NSCLC tumor tissue, whereas $CD8^+$ T cells were increased in the MPE compared to tumor samples (63). After chemotherapy, matched MPEs and tumor tissue from patients with mesothelioma displayed similar proportions of $CD3^+$ T cells, $CD4^+$ helper ($CD25^-$) and $CD4^+$ regulatory ($CD25^+CD127^{lo}$) T cells post-chemotherapy (64), but similarly, $CD8^+$ T cells were greater in the MPE than matched tumor tissue (10, 64). Increased pre- and post-chemotherapy frequencies of $CD4^+$ T cells in MPE and tumors were associated with complete response and improved survival in chemotherapy treated mesothelioma patients (56, 65, 66). Post-chemotherapy regulatory T cell frequencies in tumors negatively associated with survival, but this association was not observed in matched MPE samples (64). Comparison of T cell proportions between tumor and MPE in these studies are limited by small sample sizes, and whether proportions of $CD4^+$ and $CD8^+$ T cells are similar in matched tumor and MPE samples are unknown.

MPEs are typically enriched with $CD4^+$ T cells, particularly regulatory $CD4^+$ T cells. $CD4^+/CD8^+$ T cell ratios in MPEs vary between patients, likely because of patient heterogeneity such as prior treatment, disease stage and amount of fluid drained. The surface phenotype, effector function, and differentiation status of MPE T cells offers further insight into the immune status of the MPE.

## MPE-Derived T Cells Express Inhibitory Checkpoint Receptors

T cells upregulate inhibitory checkpoint receptors in the presence of chronic tumor antigen exposure. Checkpoint receptor signaling inhibits T cell function, and immunosuppressive TMEs exploit these signaling pathways to curtail an effective anti-tumor response. Although CTLA-4 and PD-1 are the most common targets in ICB therapy, other inhibitory checkpoint receptors are expressed on TILs including TIM-3, LAG-3, TIGIT and PD-L1. Increased frequencies of $CD8^+PD\text{-}1^+$ T cells in tumors post anti-PD-1 treatment have been associated with complete and partial responses in NSCLC (34). Hence, the expression of checkpoint receptors on MPE T cells is of great interest because these T cells could be potential targets for ICB, and predictors of response.

The expression of inhibitory receptors on $CD4^+$ and $CD8^+$ T cells in MPE have been reported in multiple studies for mesothelioma and lung cancer. While this varies between patients, ~30% of $CD4^+$ and ~40% of $CD8^+$ T cells express PD-1 in the MPE (56, 62, 63) and these frequencies are greater than in matched peripheral blood T cells (62, 63, 67–70). Inhibitory receptors TIM-3, LAG-3, CTLA-4 and PD-L1 are also expressed on MPE $CD4^+$ and $CD8^+$ T cells at greater proportions than matched peripheral blood samples in mesothelioma and lung cancer patients (56, 62, 63, 67, 69). In addition, regulatory T cells constitutively express the inhibitory receptor TIGIT (71), and display increased expression of CTLA-4 and PD-1 in the MPE compared to peripheral blood (58, 63).

In comparison to tumor tissue, the frequencies of $CD8^+$ T cells expressing PD-1 and TIM-3 are greater than the MPE prior to treatment (63). However, they are similar in frequency between the two compartments post-chemotherapy (64). For $CD4^+$ helper ($Foxp3^-$) T cells and regulatory ($Foxp3^+$) T cells, the expression of PD-1 and TIM-3 are similar between matched MPE and tumor tissue both pre- and post-chemotherapy (63, 64). In addition, the proportion of $CD4^+LAG\text{-}3^+$ and $CD8^+LAG\text{-}3^+$ T cells in MPE after chemotherapy are similar to tumor tissue in one study (64), but not another (56). Co-expression of inhibitory receptors on T cells, in particular PD-1 and TIM-3, indicates further T cell dysfunction which has been reported to be unfavorable for ICB efficacy (37). To date, there is only one report of co-expression of these receptors, which found that the majority of $CD4^+PD\text{-}1^+$ and $CD8^+PD\text{-}1^+$ MPE T cells prior to treatment did not co-express LAG-3 or TIM-3. Less than 2% of $CD8^+$ T cells were $PD\text{-}1^+TIM\text{-}3^+$ and less than 6% of $CD4^+$ T cells were $PD\text{-}1^+LAG\text{-}3^+$ (68), suggesting that most of the $CD8^+$ T cells in the MPE could be amenable to anti-PD-1 therapy.

MPE T cells are similar to TILs in that they both express increased inhibitory checkpoint receptors compared to blood T cells. Although the expression of inhibitory receptors TIM-3, PD-1 or LAG-3 on MPE T cells did not associate with improved survival post chemotherapy (64), inhibitory receptor co-expression on MPE T cells, and their correlation to ICB therapy outcomes are still of interest.

## MPE-Derived $CD8^+$ T Cells Exhibit a Memory Phenotype

A hallmark of antigen-specific T cell responses is their ability to differentiate into memory T cells after activation, and mount a rapid response upon re-exposure to their cognate antigen. Memory $CD8^+$ T cells are loosely classified into effector memory ($T_{EM}$: $CD45RO^+/CD62L^-$, $CD45RA^-CCR7^-$), central memory ($T_{CM}$: $CD45RO^+CD62L^+$, $CD45RA^-CCR7^+$) and resident memory ($T_{RM}$: $CD45RO^+CD103^+$) subsets based on surface expression of differentiation markers and tissue localization. $T_{EM}$ and $T_{CM}$s are generally found circulating in the peripheral blood and lymphatics, whilst $T_{RM}$s are non-circulatory and tissue tropic. Understanding $CD8^+$ memory T cell differentiation status is crucial because inhibitory checkpoint receptors are highly expressed on memory $CD8^+$ T cells in tumors (72–74) and are potential cellular targets of ICB. ICB also drives changes in $CD8^+$ memory T cell differentiation (75). Importantly, tumor infiltration of memory T cell subsets and their gene signatures correlated with ICB response and overall survival in melanoma and lung cancer patients (36, 73). MPE-derived $CD4^+$ and $CD8^+$ T cells in mesothelioma and lung cancer exhibit a memory phenotype prior to treatment. MPEs have increased frequencies of $T_{CM}$ and

$T_{EM}$ cells for both cancer types compared to peripheral blood (53, 57). MPEs also have greater frequencies of $T_{CM}$ but reduced $T_{EM}$ compared to non-malignant pleural fluid (54).

Memory T cell subsets found in MPE are phenotypically similar to subsets found in mesothelioma tumors but there are limited studies on matched samples. Both MPE and tumors have a greater frequency of $T_{EM}$ cells than the circulation (76), suggesting that the proportion of $T_{EM}$ cells in the MPE may reflect the TME. Recent studies have also shone a spotlight on the role of $T_{RMs}$ in tumor immunosurveillance. Increased pre-treatment frequencies of $T_{RMs}$ in tumors associate with improved survival (72, 74), and increase pre- or post-treatment frequencies associate with response to anti-PD-1 therapy in lung cancer patients (73). $CD8^+$ $T_{RMs}$ prior to chemotherapy have been reported in MPE of lung cancer patients, but in lesser proportions compared to matched tumor samples (77). Similar to their tumor counterparts, memory T cell subsets in the MPE could offer a predictor of therapeutic response.

## MPE-Derived $CD8^+$ T Cells Have Impaired Effector Function

$CD8^+$ T cells proliferate and produce effector molecules such as cytotoxic granules (granzyme B, perforin) and proinflammatory cytokines (IFN$\gamma$) to mediate tumor cell killing. The ability of T cells to produce effector molecules *ex vivo* is a measure of T cell effector function. Understanding the effector status of T cells is important as ICB induces activation and proliferation of circulating and intratumoral T cells which correlates with response (78, 79). While MPE $CD8^+$ T cells can produce IFN$\gamma$, granzyme B and perforin *ex vivo*, the frequency of MPE T cells that secrete these molecules is reduced compared to T cells from matched peripheral blood samples (67, 70). Specifically, blood derived effector ($CD45RA^+CD27^-$) T cells have increased perforin secretion than these T cell subsets from the MPE (53). However, these reports have used non-specific stimuli *ex vivo* to measure effector molecule production from MPE and peripheral blood T cells. Antigen-specific assays are required to understand if impairment is restricted to tumor antigen-specific T cells only.

There are limited comparisons of matched MPE-derived T cell and TIL effector function. TILs and matched MPE T cells from advanced NSCLC patients were hypofunctional, with decreased frequency of $CD8^+IFN\gamma^+$ T cells than tumors from patients with early stage NSCLC (80). Impaired effector function of MPE T cells could be due to an immunosuppressive environment characterized by high levels of TGFβ, tumor associated macrophages and myeloid derived suppressor cells (42, 55, 64, 67).

## Different $CD4^+$ T Helper Cell Subsets Are Found in the MPE

Effector $CD4^+$ T cells can differentiate into helper T cell (Th) subtypes which have been identified in MPE from people with lung cancer and mesothelioma. The $CD4^+$ helper T cell subtypes include Th1, Th2, Th17, Th9 and Th22 which are each identified by unique transcriptional signatures, and production of different cytokines (81, 82). ICB induces expansion of effector Th1 and Th17 cells in the TME, therefore it is important to determine if Th subtypes in the MPE is associated with ICB outcomes (83–85).

Th1 cells are pro-inflammatory, secreting IFN$\gamma$ to stimulate effector $CD8^+$ T cell differentiation. Approximately 45% of $CD4^+$ MPE T cells produce IFN$\gamma$indicating a predominant Th1 phenotype in the MPE which is greater in frequency than matched peripheral blood samples (53). In comparison to Th1, Th2 promotes humoral immunity by producing cytokines IL-4, IL-5 and IL-10. The balance of these two subsets in the MPE remains controversial. Some reports suggest the MPE favors the Th2 over the Th1 pathway in comparison to pleural fluid from tuberculosis patients (86, 87). However, IL-4 was detected in the MPE in some studies (86–88) but was below 1% or undetected in others (53, 55, 89). In addition, IL-4 was detected at low levels and IFN$\gamma$was undetected in both paired MPE and mesothelioma tumor supernatant in another study (55).

The role of Th17 cells in the TME also remains controversial. The production of IL-17 has been reported to stimulate recruitment of dendritic cells, NK cells and $CD8^+$ T cells into the TME (90), but also can promote tumor growth through IL-17R signaling (91, 92). Frequencies of Th17 cells are greater in the MPE than peripheral blood and exhibit an $T_{EM}$ phenotype ($CD45RO^+CD45RA$) (93). The proportion of Th17 cells negatively correlated with regulatory T cells in the MPE, suggesting that regulatory T cells inhibited generation and differentiation of Th17 cells in the pleural space (61). For tumor tissue, one study found IL-17 in mesothelioma tumor supernatant but not in matched MPE (55).

In comparison, Th9 and Th22 cells suppress anti-tumor immunity. Both Th9 and Th22 cell proportions in the MPE are greater than the peripheral blood and also express an $T_{EM}$ phenotype ($CD45RO^+CD45RA$) in both compartments (94, 95). Th9 cells produce IL-9 which has been identified to promote tumor angiogenesis (96). Th9 cell frequencies correlate to regulatory T cell frequencies in the MPE, and higher Th9 cells in MPEs associated with poor survival in lung cancer patients (95). There are no reports of Th9 cells in matched MPE and TME. One study suggests that Th9 cells may infiltrate into the MPE from the circulation as CCR7 expression was decreased on Th9 cells in the MPE compared to matched blood (97). Th22 cells produce IL-22 which has been identified to promote migration and proliferation of cancer cells and resist apoptosis and chemotherapy (98). In NSCLC patients, IL-22 was greater in matched tumor tissue than MPE (99), and IL-22 expression in MPE promoted cancer cell migration (94), and protected cancer cells from apoptosis by chemotherapies (99).

Taken together, it is evident that multiple $CD4^+$ T helper subtypes are present in the MPE, but varying frequencies of different subtypes have been reported. Further analysis is required to understand if any of these cell types in the MPE associate with ICB efficacy.

## MPE-Derived $CD8^+$ T Cells Are Clonally Expanded, and Some Are Specific for Tumor Antigens

Importantly, tumor antigen-specific T cells can be found in the MPE. Co-culture of MPE-derived lymphocytes with tumor cells

or known tumor antigens from lung cancer patients resulted in IFNγproduction (41, 69) and CD137 expression (68), suggesting tumor reactivity (100). In addition, tumor reactive MPE-derived $CD8^+$ T cells displayed a memory phenotype with checkpoint expression ($PD\text{-}1^+TIM\text{-}3^-$) (68). However, most studies have included a T cell expansion step prior to assessing tumor reactivity, so the actual proportion of MPE T cells specific for tumor-antigens is unclear.

In addition to screening for reactivity, T cell receptor (TCR) analyses are used to study antigen-specific T cell responses. Individual TCRα/β chains are highly variable across complementarity determining regions (CDR), the regions crucial for antigen-specificity. Antigen-specific clonal expansion can be estimated by quantifying the distribution of TCR variable genes, or CDR sequences. ICB induces a peripheral expansion of TCR clonotypes which correlates to clinical benefit in lung cancer (101, 102). In lung tumors, the TCR repertoire clonality and the number of expanded TCR clones was greater in ICB responders compared to non-responders post-treatment (38).

TCR analyses of matched MPE and blood from lung cancer patients revealed over expression of particular TCRβ variable genes in the MPE compared to matched blood samples (103), suggesting that MPE T cells had undergone clonal expansion. The presence of shared, highly expanded TCR clonotypes in MPE and tumors would greatly support the notion that T cells in both compartments are similar. High throughput TCR sequencing is used in this area, as shared TCRβs have been found in ascites and tumors in other studies (104). We previously reported that $CD4^+PD\text{-}1^+$ MPE T cells consist of distinct, clonally expanded TCRβs from $CD4^+PD\text{-}1^+$ T cells in matched peripheral blood (62). TCR analyses of matched TILs and MPE T cells in thoracic cancers are currently limited, and would greatly inform the similarities in antigen-specificity between the compartments.

## MPE T Cells and TILs Exhibit Phenotypic Similarities, but the Extent of Similarity Is Unclear

The expression of inhibitory checkpoint receptors, enrichment of $CD4^+$ regulatory T cells, presence of $CD8^+$ memory T cells and impaired cytotoxic, effector T cell function in MPEs suggest that they exist in an immunosuppressed environment. They are more similar to TILs than peripheral blood T cells (**Figure 1**). However, there are reported differences in the $CD4^+/CD8^+$ ratios, co-expression patterns of checkpoint receptors, and $CD4^+$ Th subtypes between TILs and MPE T cells. The similarities in antigen-specificity, or TCR usage of T cells between the two compartments are also unknown. Characterizing the phenotypes of T cell clones at both sites would help researchers understand how the MPE or TME shapes the development of these cells. Next, we review how therapies could shape the phenotype of MPE T cells, because such changes could inform biomarker development.

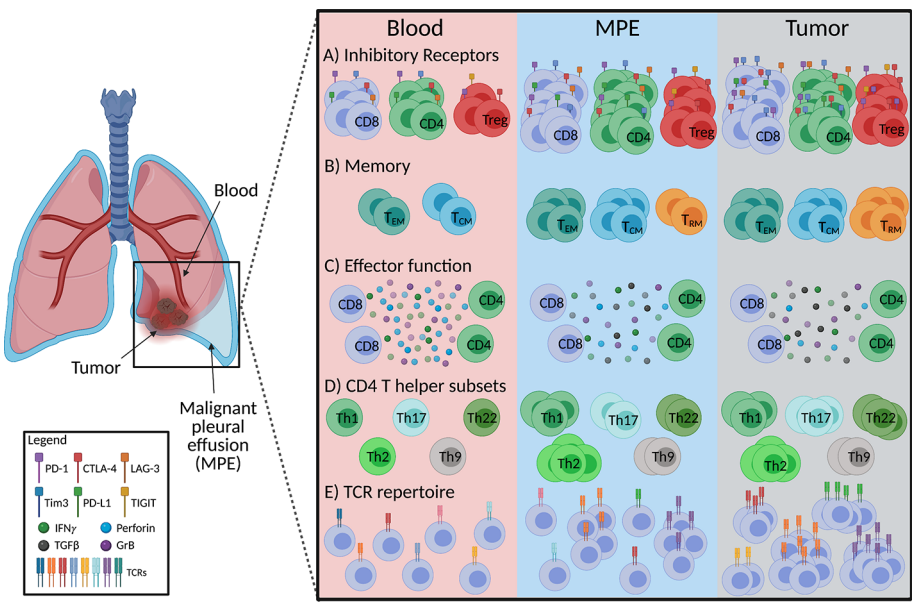


**FIGURE 1** | Schematic diagram summarizing characteristics of MPE-derived T cells in comparison to tumor and peripheral blood in mesothelioma and lung cancer. **(A)** Frequencies of $CD8^+$, $CD4^+$ and $CD4^+$ regulatory (Treg) T cells expressing inhibitory receptors in the MPE are similar to tumor infiltrating T cells, however co-expression of inhibitory receptors on T cells is greater in tumors than MPE. **(B)** MPE and tumor contain greater proportions of effector memory ($T_{EM}$) and central memory ($T_{CM}$) T cells than the circulation with tissue resident memory T cell ($T_{RM}$) frequencies the greatest at the tumor site. **(C)** Production of T cell effector cytokines (IFNγ, granzyme B; GrB, perforin) are similar between the MPE and tumor infiltrating T cells but lower than those in peripheral blood. **(D)** MPE are likely enriched with a Th2 phenotype along with a greater proportion of Th1, Th2, Th17, Th9, Th22 than circulating T cells, while tumors display a greater frequency of Th17 and Th22 than MPE. Th9 between tumor and MPE is undefined. **(E)** MPE contains tumor reactive T cells, implying a more clonal T cell receptor (TCR) repertoire than the peripheral blood. Figure created with BioRender.com.

## CHANGES IN MPE-DERIVED T CELLS FOLLOWING ICB THERAPY

Serial analyses of MPE-derived T cells in patients undergoing ICB are rare, but a study of MPE that developed after ICB has been reported. Ikematsu and colleagues characterized T cells in MPE samples drained from lung cancer patients after ICB. There were greater frequencies of $CD4^+TIM\text{-}3^+$, $CD4^+TIGIT^+$ and $CD8^+PD\text{-}L1^+$ MPE T cells from ICB treated patients compared to MPEs from chemotherapy treated patients (105). However, there were no differences in frequencies of $CD8^+$ and $CD4^+$ MPE T cells expressing PD-1, TIM-3, TIGIT, PD-L1 or IFN$\gamma$between responders and non-responders to anti-PD-1 therapy (105, 106). Interestingly, post treatment frequencies of Th17 ($CD4^+IL\text{-}17^+$) and $CD4^+LAG\text{-}3^+$ T cells in the MPE negatively associated with clinical outcome to anti-PD-1 ICB (105). Two NSCLC patients who became resistant to anti-PD-L1 therapy and developed recurrent MPE had increased frequencies of effector memory ($CCR7^-CD45RA^-$) $CD8^+$ T cells and TIM-3 or CTLA-4 expressing $CD8^+$ and $CD4^+$ T cells cells in the MPE post-treatment, but this was compared to untreated rather than responding patients (107). Together this suggests inhibitory receptor expression increases on MPE T cells in anti-PD-1 and anti-PD-L1 treated patients. There are no studies which have analyzed serial samples of MPE in ICB treated patients.

MPE T cells have been studied in serial samples from patients treated with chemotherapy. Longitudinal analysis of MPE in a mesothelioma patient identified that the percentage of $CD3^+$ T cells decreased in the MPE following 4 cycles of cisplatin-pemetrexed based chemotherapy, producing a partial response (10). When on-treatment changes were examined, the first dose of methotrexate chemotherapy reduced total $CD3^+$ T cells in the MPE but these frequencies returned back to baseline levels after the second dose of methotrexate in NSCLC patients (108). Frequencies of MPE $CD4^+$ T cells increased, regulatory T cells decreased and $CD8^+$ T cells were unchanged following methotrexate. In terms of T cell function, it increased frequencies of MPE-derived IFN$\gamma^+$ and IL-$2^+$ T cells (108). This suggests that the MPE environment is dynamic, and changes in MPE T cells can be shaped by therapies, similar to T cells in other compartments (65, 66, 109–111).

There are very few studies of serial analyses of MPE-derived T cell phenotype, function and antigen-specificity, and how they associate with ICB outcomes. However, those studies inform us of potential T cell phenotypes from TILs and MPEs that are of interest because they could associate with ICB responses (**Table 1**). Serial analysis of MPE T cells in patients undergoing ICB therapies would be greatly informative.

## BENEFITS, OPPORTUNITIES AND CHALLENGES FOR DEVELOPING MPE-DERIVED T CELL BIOMARKERS

The potential of MPE-derived T cells as a biomarker for therapy responses is attractive for several reasons (**Table 2**). Firstly, MPE-derived T cells may be more closely related to TILs than circulating T cells. The presence of memory $CD8^+$ T cells that express inhibitory receptors and $CD4^+$ regulatory T cells in MPEs suggest that T cell responses are suppressed, similar to the TME. Furthermore, the MPE environment also consists of tumor cells, MDSCs and immunosuppressive cytokines that may shape T cell phenotype in a similar manner to the TME. Secondly, because pleural fluid is often serially drained, a dynamic biomarker could be developed. We previously argued that not all determinants of ICB response can be found prior to treatment, and changes in TME or blood that occur early on treatment could offer a more accurate, dynamic biomarker of response. Indeed, changes in T cell repertoire phenotype, diversity, and immune gene signatures early during ICB treatment correlate with ICB responses in murine and clinical studies (36, 75, 116–119). While most studies of tumor and blood suggest that changes in $CD8^+$ T cells correlate with ICB outcomes, other T cell populations in the MPE, such as $CD4^+$ helper T cells, could also be predictive of ICB outcomes. Regular drainage of MPEs provides a unique opportunity to study these dynamic changes. Although this review focuses only on T cells, how MPE-derived T cell frequencies and phenotypes change in

**TABLE 1** | Intratumoral T cell characteristics that associate with clinical benefit to ICB in lung cancer patients.

| T cell characteristic | Cancer | Pre- or post-treatment | ICB | Ref. | Also found in MPE? |
|---|---|---|---|---|---|
| >1% $CD8^+PD\text{-}1^{hi}$ T cells | NSCLC | pre | Nivolumab | (34) | Undefined |
| Low-PD-1-to-CD8 ratio | NSCLC | pre and post | Nivolumab | (112, 113) | Post-treatment: not reported (105) |
| High PD-1 transcripts | NSCLC | pre | Nivolumab | (114) | Undefined |
| $CD8^+PD\text{-}1^{hi,}$ $CD4^+Foxp3^+PD\text{-}L1^{hi}$ | NSCLC | post | Nivolumab | (115) | Undefined |
| High PD-L1 transcripts | NSCLC | pre | Nivolumab | (114) | Undefined |
| High CD8:CD3 ratio | NSCLC | pre and post | Nivolumab | (112, 113) | Undefined |
| >70% $TIM\text{-}3^+IL\text{-}7R^-$ of $CD8^+CD103^+$ $T_{RM}$ | Lung Cancer | pre and post | Nivolumab | (73) | Undefined |
| High IFNγ mRNA | NSCLC | post | Nivolumab | (79) | Undefined |
| High activated CD4 T cell signatures with IFN, Th2, IL-17A, IL-26 related genes | NSCLC | pre | Nivolumab | (114) | Post-treatment $CD4^+IL\text{-}17^+$ T cells associated with no benefit to ICB (105) |
| Increased TCR clonality with expanded TCR clones | NSCLC | post | Nivolumab | (38) | Undefined |

*NSCLC, non-small cell lung cancer.*

**TABLE 2** | Benefits and limitations for using the MPE to develop T cell biomarkers for ICB therapy response.

| Benefits | Limitations |
|---|---|
| • MPE-derived T cells are similar in phenotype to tumor infiltrating lymphocytes (TILs)<br>• Ability to develop a dynamic biomarker as multiple fluid drainage due to MPE recurrence is common for thoracic cancer patients<br>• Opportunity to perform high-throughput sequencing technologies i.e. RNAseq and TCRseq on the anti-tumor immune response where tumor biopsies are limited, particularly in malignant mesothelioma | • Fluid volume, cellularity, number and timing of drainage events varies between patients<br>• External factors such as lung diseases, inflammation and infection could alter MPE-derived T cells<br>• Improved MPE treatment regimens that cause pleural space destruction to prevent fluid recurrence. |

relation to other components in the fluid, such as tumor cell, MDSC numbers, and suppressive cytokine levels is informative for biomarker development.

MPE-derived T cells exhibit memory phenotypes indicative of chronic antigen-specific activation. The antigen-specificity of MPE $T_{EM}$ and $T_{RM}$ cells, and how they change with therapy are of great interest. It is promising that tumor-reactive T cells can be expanded from the MPE, but the overlap in antigen-specificities between TILs and MPE T cells, if any, are unknown. TCR sequencing offers a complementary method to study the extent of clonal overlap between TILs, blood and MPE-derived T cell populations, and to track the changes in antigen-specific

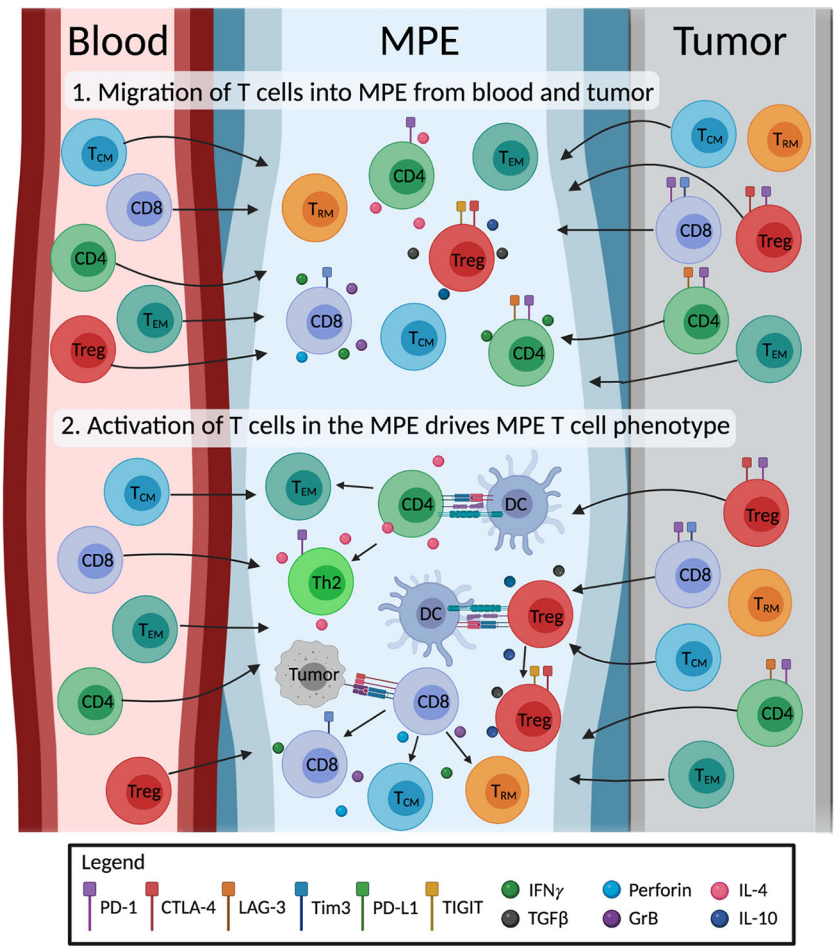


**FIGURE 2** | Illustration of the proposed origin and development of MPE T cells. The impact of the MPE environment on T cell differentiation is unclear. We hypothesize that 1) MPE acts as a sink, containing a mix of T cells originally from the blood and the tumor site. 2) MPE environment including cytokines and other cells (e.g. tumor cells, dendritic cells; DC) drive changes in phenotype of MPE T cells. MPE T cells differentiate into effector subtypes, producing immunostimulatory (IFNγ, perforin, granzyme B; GrB, IL-4) or immunosuppressive (TGF-β, IL-10) cytokines; exhausted T cells expressing inhibitory receptors; and differentiate into memory T cells (i.e. effector ($T_{EM}$), central ($T_{CM}$) and tissue resident ($T_{RM}$) memory T cells). Figure created with BioRender.com.

T cells without prior knowledge of any tumor antigens. The extent in which the MPE environment drives T cell differentiation is unclear. We speculate that MPE consist of T cells that have migrated from the local tumor and blood. However, to what extent the MPE environment changes T cell phenotype is unclear. It is possible that further activation and differentiation of T cells in the MPE drives the distinct phenotypes of MPE-derived T cells (**Figure 2**). Single cell technology is a powerful tool to comprehensively study the interactions of different cells in the MPE, and will greatly help our understanding in this area. The transcriptome and TCRαβ usage of individual T cells can be determined, allowing researchers to match phenotypes to individual T cell clones. These TCRs of interest can be subsequently screened for tumor reactivity. Single cell technology is now used in numerous studies of TMEs, and can be applied to MPE samples.

However, there are some limitations with studying MPEs (**Table 2**). The volume of fluid drained, and cellularity of MPE samples varies between patients (62, 120, 121). In some instances, MPE cell numbers are too few for meaningful downstream analysis, especially for rare T cell subsets. Even though longitudinal analysis can be performed with MPE samples, the number of drainage events vary between patients and the timing of them cannot be predicted. Furthermore, differences in MPE immunophenotype measured over time are not always attributed to tumor or treatment. External factors such as infections and lung inflammation could alter the T cell phenotype and are confounding factors that have to be accounted for (122–124). Lastly, management regimens to treat MPEs including talc pleurodesis and VATS pleurodesis and pleurectomy, which is a palliative therapeutic option for malignant pleural mesothelioma patients, aim to obliterate the pleural space and prevent MPE recurrence. This then eliminates the opportunity to serially sample the MPE for biomarkers of response to therapy.

## CONCLUSIONS AND FUTURE DIRECTIONS

Although the cellular components of MPE have been studied extensively, recent developments in cancer immunotherapy and the need for biomarkers of response have led researchers to focus on MPE T cells. These cells share phenotypic features with TILs, but further study is required to elucidate if MPE T cells are truly reflective of their tumor counterparts. We think that dynamic analyses of MPE T cells in relation to ICB outcomes will lead to a robust and clinically useful ICB response biomarker.

## AUTHOR CONTRIBUTIONS

NP wrote the article and made the figures. JK, WL, RL, AN, AM, and JC critically revised the manuscript. All authors contributed to the article and approved the submitted version.

## FUNDING

NP was supported by Cancer Council WA and UWA Richard Walter Gibbon Medical Research scholarships. JK was supported by icare Dust Diseases Board. WL was supported by a Simon Lee Fellowship, an NHMRC Fellowship, and a Cancer Council WA fellowship. AM was supported by grants and fellowship from Cancer Council WA, Raine Medical Research Foundation and icare Dust Diseases Board. JC was supported by grants and fellowship from the Raine Medical Research Foundation, Cancer Council WA, WA Department of Health, and icare Dust Diseases Board. The National Centre for Asbestos Related Diseases receives funding through the National Health and Medical Research Council Centres of Research Excellence scheme APP1197652.

## REFERENCES

1. Porcel JM, Gasol A, Bielsa S, Civit C, Light RW, Salud A. Clinical Features and Survival of Lung Cancer Patients With Pleural Effusions. *Respirology* (2015) 20(4):654–9. doi: 10.1111/resp.12496
2. Zamboni MM, da Silva CT Jr, Baretta R, Cunha ET, Cardoso GP. Important Prognostic Factors for Survival in Patients With Malignant Pleural Effusion. *BMC Pulm Med* (2015) 15:29. doi: 10.1186/s12890-015-0025-z
3. Cheah HM, Lansley SM, Varano Della Vergiliana JF, Tan AL, Thomas R, Leong SL, et al. Malignant Pleural Fluid From Mesothelioma has Potent Biological Activities. *Respirology* (2017) 22(1):192–9. doi: 10.1111/resp.12874
4. Khaleeq G, Musani AI. Emerging Paradigms in the Management of Malignant Pleural Effusions. *Respir Med* (2008) 102(7):939–48. doi: 10.1016/j.rmed.2008.01.022
5. Lee YC, Light RW. Management of Malignant Pleural Effusions. *Respirology* (2004) 9(2):148–56. doi: 10.1111/j.1440-1843.2004.00566.x
6. Porcel JM, Lui MM, Lerner AD, Davies HE, Feller-Kopman D, Lee YC. Comparing Approaches to the Management of Malignant Pleural Effusions. *Expert Rev Respir Med* (2017) 11(4):273–84. doi: 10.1080/17476348.2017.1300532
7. Davies HE, Mishra EK, Kahan BC, Wrightson JM, Stanton AE, Guhan A, et al. Effect of an Indwelling Pleural Catheter vs Chest Tube and Talc Pleurodesis for Relieving Dyspnea in Patients With Malignant Pleural Effusion: The TIME2 Randomized Controlled Trial. *JAMA* (2012) 307(22):2383–9. doi: 10.1001/jama.2012.5535
8. Thomas R, Fysh ETH, Smith NA, Lee P, Kwan BCH, Yap E, et al. Effect of an Indwelling Pleural Catheter vs Talc Pleurodesis on Hospitalization Days in Patients With Malignant Pleural Effusion: The AMPLE Randomized Clinical Trial. *JAMA* (2017) 318(19):1903–12. doi: 10.1001/jama.2017.17426
9. Muruganandan S, Azzopardi M, Thomas R, Fitzgerald DB, Kuok YJ, Cheah HM, et al. The Pleural Effusion And Symptom Evaluation (Please) Study of Breathlessness in Patients With a Symptomatic Pleural Effusion. *Eur Respir J* (2020) 55(5). doi: 10.1183/13993003.00980-2019
10. Lievense LA, Bezemer K, Cornelissen R, Kaijen-Lambers ME, Hegmans JP, Aerts JG. Precision Immunotherapy; Dynamics in the Cellular Profile of Pleural Effusions in Malignant Mesothelioma Patients. *Lung Cancer* (2017) 107:36–40. doi: 10.1016/j.lungcan.2016.04.015
11. Thomas R, Cheah HM, Creaney J, Turlach BA, Lee YC. Longitudinal Measurement of Pleural Fluid Biochemistry and Cytokines in Malignant Pleural Effusions. *Chest* (2016) 149(6):1494–500. doi: 10.1016/j.chest.2016.01.001
12. Peters S, Gettinger S, Johnson ML, Janne PA, Garassino MC, Christoph D, et al. Phase II Trial of Atezolizumab as First-Line or Subsequent Therapy for Patients With Programmed Death-Ligand 1-Selected Advanced non-Small-Cell Lung Cancer (Birch). *J Clin Oncol* (2017) 35(24):2781–9. doi: 10.1200/JCO.2016.71.9476

13. Hellmann MD, Paz-Ares L, Bernabe Caro R, Zurawski B, Kim S-W, Carcereny Costa E, et al. Nivolumab Plus Ipilimumab in Advanced non–Small-Cell Lung Cancer. *New Engl J Med* (2019) 381(21):2020–31. doi: 10.1056/NEJMoa1910231
14. Baas P, Scherpereel A, Nowak AK, Fujimoto N, Peters S, Tsao AS, et al. First-Line Nivolumab Plus Ipilimumab in Unresectable Malignant Pleural Mesothelioma (CheckMate 743): A Multicentre, Randomised, Open-Label, Phase 3 Trial. *Lancet* (2021) 397(10272):375–86. doi: 10.1016/S0140-6736(20)32714-8
15. Gandhi L, Rodriguez-Abreu D, Gadgeel S, Esteban E, Felip E, De Angelis F, et al. Pembrolizumab Plus Chemotherapy in Metastatic non-Small-Cell Lung Cancer. *N Engl J Med* (2018) 378(22):2078–92. doi: 10.1056/NEJMoa1801005
16. Brahmer JR, Govindan R, Anders RA, Antonia SJ, Sagorsky S, Davies MJ, et al. The Society for Immunotherapy of Cancer Consensus Statement on Immunotherapy for the Treatment of non-Small Cell Lung Cancer (Nsclc). *J Immunother Cancer* (2018) 6(1):75. doi: 10.1186/s40425-018-0382-2
17. Nowak AK, Lesterhuis WJ, Kok PS, Brown C, Hughes BG, Karikios DJ, et al. Durvalumab With First-Line Chemotherapy in Previously Untreated Malignant Pleural Mesothelioma (Dream): A Multicentre, Single-Arm, Phase 2 Trial With a Safety Run-in. *Lancet Oncol* (2020) 21(9):1213–23. doi: 10.1016/S1470-2045(20)30462-9
18. Alley EW, Lopez J, Santoro A, Morosky A, Saraf S, Piperdi B, et al. Clinical Safety and Activity of Pembrolizumab in Patients With Malignant Pleural Mesothelioma (Keynote-028): Preliminary Results From a non-Randomised, Open-Label, Phase 1b Trial. *Lancet Oncol* (2017) 18(5):623–30. doi: 10.1016/S1470-2045(17)30169-9
19. Scherpereel A, Mazieres J, Greillier L, Lantuejoul S, Do P, Bylicki O, et al. Nivolumab or Nivolumab Plus Ipilimumab in Patients With Relapsed Malignant Pleural Mesothelioma (Ifct-1501 Maps2): A Multicentre, Open-Label, Randomised, non-Comparative, Phase 2 Trial. *Lancet Oncol* (2019) 20(2):239–53. doi: 10.1016/S1470-2045(18)30765-4
20. Paz-Ares L, Ciuleanu TE, Cobo M, Schenker M, Zurawski B, Menezes J, et al. First-Line Nivolumab Plus Ipilimumab Combined With Two Cycles of Chemotherapy in Patients With non-Small-Cell Lung Cancer (CheckMate 9la): An International, Randomised, Open-Label, Phase 3 Trial. *Lancet Oncol* (2021) 22(2):198-211. doi: 10.1016/S1470-2045(20)30641-0
21. Faivre-Finn C, Vicente D, Kurata T, Planchard D, Paz-Ares L, Vansteenkiste JF, et al. Brief Report: Four-Year Survival With Durvalumab After Chemoradiotherapy in Stage Iii NSCLC - an Update From the PACIFIC Trial. *J Thorac Oncol* (2021) S1556-0864(21):00022-8. doi: 10.1016/j.jtho.2020.12.015
22. Garassino MC, Cho BC, Kim JH, Mazieres J, Vansteenkiste J, Lena H, et al. Durvalumab as Third-Line or Later Treatment for Advanced non-Small-Cell Lung Cancer (Atlantic): An Open-Label, Single-Arm, Phase 2 Study. *Lancet Oncol* (2018) 19(4):521–36. doi: 10.1016/S1470-2045(18)30144-X
23. Paz-Ares L, Dvorkin M, Chen Y, Reinmuth N, Hotta K, Trukhin D, et al. Durvalumab Plus Platinum–Etoposide Versus Platinum–Etoposide in First-Line Treatment of Extensive-Stage Small-Cell Lung Cancer (Caspian): A Randomised, Controlled, Open-Label, Phase 3 Trial. *Lancet* (2019) 394(10212):1929–39. doi: 10.1016/S0140-6736(19)32222-6
24. Reck M, Bondarenko I, Luft A, Serwatowski P, Barlesi F, Chacko R, et al. Ipilimumab in Combination With Paclitaxel and Carboplatin as First-Line Therapy in Extensive-Disease-Small-Cell Lung Cancer: Results From a Randomized, Double-Blind, Multicenter Phase 2 Trial. *Ann Oncol* (2013) 24(1):75–83. doi: 10.1093/annonc/mds213
25. Ready NE, Ott PA, Hellmann MD, Zugazagoitia J, Hann CL, de Braud F, et al. Nivolumab Monotherapy and Nivolumab Plus Ipilimumab in Recurrent Small Cell Lung Cancer: Results From the CheckMate 032 Randomized Cohort. *J Thorac Oncol* (2020) 15(3):426–35. doi: 10.1016/j.jtho.2019.10.004
26. Mathieu L, Shah S, Pai-Scherf L, Larkins E, Vallejo J, Li X, et al. Fda Approval Summary: Atezolizumab and Durvalumab in Combination With Platinum-Based Chemotherapy in Extensive Stage Small Cell Lung Cancer. *Oncologist* (2021). doi: 10.1002/onco.13752
27. Lesterhuis WJ, Bosco A, Millward MJ, Small M, Nowak AK, Lake RA. Dynamic Versus Static Biomarkers in Cancer Immune Checkpoint Blockade: Unravelling Complexity. *Nat Rev Drug Discovery* (2017) 16(4):264–72. doi: 10.1038/nrd.2016.233
28. Herbst RS, Soria JC, Kowanetz M, Fine GD, Hamid O, Gordon MS, et al. Predictive Correlates of Response to the Anti-PD-L1 Antibody MPDL3280A in Cancer Patients. *Nature* (2014) 515(7528):563–7. doi: 10.1038/nature14011
29. Rizvi NA, Hellmann MD, Snyder A, Kvistborg P, Makarov V, Havel JJ, et al. Cancer Immunology. Mutational Landscape Determines Sensitivity to PD-1 Blockade in non-Small Cell Lung Cancer. *Science* (2015) 348(6230):124–8. doi: 10.1126/science.aaa1348
30. Ayers M, Lunceford J, Nebozhyn M, Murphy E, Loboda A, Kaufman DR, et al. Ifn-Gamma-Related Mrna Profile Predicts Clinical Response to PD-1 Blockade. *J Clin Invest* (2017) 127(8):2930–40. doi: 10.1172/JCI91190
31. Lee HS, Jang HJ, Choi JM, Zhang J, de Rosen VL, Wheeler TM, et al. Comprehensive Immunoproteogenomic Analyses of Malignant Pleural Mesothelioma. *JCI Insight* (2018) 3(7):e98575. doi: 10.1172/jci.insight.98575
32. Yu Y, Zeng D, Ou Q, Liu S, Li A, Chen Y, et al. Association of Survival and Immune-Related Biomarkers With Immunotherapy in Patients With Non-Small Cell Lung Cancer: A Meta-Analysis and Individual Patient-Level Analysis. *JAMA Netw Open* (2019) 2(7):e196879. doi: 10.1001/jamanetworkopen.2019.6879
33. Althammer S, Tan TH, Spitzmuller A, Rognoni L, Wiestler T, Herz T, et al. Automated Image Analysis of NSCLC Biopsies to Predict Response to anti-PD-L1 Therapy. *J Immunother Cancer* (2019) 7(1):121. doi: 10.1186/s40425-019-0589-x
34. Thommen DS, Koelzer VH, Herzig P, Roller A, Trefny M, Dimeloe S, et al. A Transcriptionally and Functionally Distinct PD-1(+) Cd8(+) T Cell Pool With Predictive Potential in non-Small-Cell Lung Cancer Treated With PD-1 Blockade. *Nat Med* (2018) 24(7):994–1004. doi: 10.1038/s41591-018-0057-z
35. Tumeh PC, Harview CL, Yearley JH, Shintaku IP, Taylor EJ, Robert L, et al. Pd-1 Blockade Induces Responses by Inhibiting Adaptive Immune Resistance. *Nature* (2014) 515(7528):568–71. doi: 10.1038/nature13954
36. Sade-Feldman M, Yizhak K, Bjorgaard SL, Ray JP, de Boer CG, Jenkins RW, et al. Defining T Cell States Associated With Response to Checkpoint Immunotherapy in Melanoma. *Cell* (2018) 175(4):998–1013. doi: 10.1016/j.cell.2018.10.038
37. Miller BC, Sen DR, Al Abosy R, Bi K, Virkud YV, LaFleur MW, et al. Subsets of Exhausted Cd8(+) T Cells Differentially Mediate Tumor Control and Respond to Checkpoint Blockade. *Nat Immunol* (2019) 20(3):326–36. doi: 10.1038/s41590-019-0312-6
38. Zhang J, Ji Z, Caushi JX, El Asmar M, Anagnostou V, Cottrell TR, et al. Compartmental Analysis of T-cell Clonal Dynamics as a Function of Pathologic Response to Neoadjuvant Pd-1 Blockade in Resectable non-Small Cell Lung Cancer. *Clin Cancer Res* (2020) 26(6):1327–37. doi: 10.1158/1078-0432.CCR-19-2931
39. Cha E, Klinger M, Hou Y, Cummings C, Ribas A, Faham M, et al. Improved Survival With T Cell Clonotype Stability After Anti-CTLA-4 Treatment in Cancer Patients. *Sci Transl Med* (2014) 6(238):238ra70. doi: 10.1126/scitranslmed.3008211
40. Batra H, Antony VB. Pleural Mesothelial Cells in Pleural and Lung Diseases. *J Thorac Dis* (2015) 7(6):964–80. doi: 10.3978/j.issn.2072-1439.2015.02.19
41. Dhupar R, Okusanya OT, Eisenberg SH, Monaco SE, Ruffin AT, Liu D, et al. Characteristics of Malignant Pleural Effusion Resident Cd8(+) T Cells From a Heterogeneous Collection of Tumors. *Int J Mol Sci* (2020) 21(17):6178. doi: 10.3390/ijms21176178
42. Kaczmarek M, Sikora J. Macrophages in Malignant Pleural Effusions - Alternatively Activated Tumor Associated Macrophages. *Contemp Oncol (Pozn)* (2012) 16(4):279–84. doi: 10.5114/wo.2012.30054
43. Saraya T, Ohkuma K, Watanabe T, Mikura S, Kobayashi F, Aso J, et al. Diagnostic Value of Vascular Endothelial Growth Factor, Transforming Growth Factor-beta, Interleukin-8, and the Ratio of Lactate Dehydrogenase to Adenosine Deaminase in Pleural Effusion. *Lung* (2018) 196(2):249–54. doi: 10.1007/s00408-018-0090-1
44. Lieser EA, Croghan GA, Nevala WK, Bradshaw MJ, Markovic SN, Mansfield AS. Up-Regulation of Pro-Angiogenic Factors and Establishment of Tolerance in Malignant Pleural Effusions. *Lung Cancer* (2013) 82(1):63–8. doi: 10.1016/j.lungcan.2013.07.007

45. Hirayama N, Tabata C, Tabata R, Maeda R, Yasumitsu A, Yamada S, et al. Pleural Effusion Vegf Levels as a Prognostic Factor of Malignant Pleural Mesothelioma. *Respir Med* (2011) 105(1):137–42. doi: 10.1016/j.rmed.2010.10.010
46. Yeh HH, Lai WW, Chen HH, Liu HS, Su WC. Autocrine IL-6-induced Stat3 Activation Contributes to the Pathogenesis of Lung Adenocarcinoma and Malignant Pleural Effusion. *Oncogene* (2006) 25(31):4300–9. doi: 10.1038/sj.onc.1209464
47. Yokoyama A, Maruyama M, Ito M, Kohno N, Hiwada K, Yano S. Interleukin 6 Activity in Pleural Effusion. Its Diagnostic Value and Thrombopoietic Activity. *Chest* (1992) 102(4):1055–9. doi: 10.1378/chest.102.4.1055
48. Giannou AD, Marazioti A, Spella M, Kanellakis NI, Apostolopoulou H, Psallidas I, et al. Mast Cells Mediate Malignant Pleural Effusion Formation. *J Clin Invest* (2015) 125(6):2317–34. doi: 10.1172/JCI79840
49. Nieto JC, Zamora C, Porcel JM, Mulet M, Pajares V, Munoz-Fernandez AM, et al. Migrated T Lymphocytes Into Malignant Pleural Effusions: An Indicator of Good Prognosis in Lung Adenocarcinoma Patients. *Sci Rep* (2019) 9(1):2996. doi: 10.1038/s41598-018-35840-3
50. Murthy P, Ekeke CN, Russell KL, Butler SC, Wang Y, Luketich JD, et al. Making Cold Malignant Pleural Effusions Hot: Driving Novel Immunotherapies. *Oncoimmunology* (2019) 8(4):e1554969. doi: 10.1080/2162402X.2018.1554969
51. Stathopoulos GT, Kalomenidis I. Malignant Pleural Effusion: Tumor-Host Interactions Unleashed. *Am J Respir Crit Care Med* (2012) 186(6):487–92. doi: 10.1164/rccm.201203-0465PP
52. Kassis J, Klominek J, Kohn EC. Tumor Microenvironment: What can Effusions Teach Us? *Diagn Cytopathol* (2005) 33(5):316–9. doi: 10.1002/dc.20280
53. Prado-Garcia H, Aguilar-Cazares D, Flores-Vergara H, Mandoki JJ, Lopez-Gonzalez JS. Effector, Memory and Naive Cd8+ T Cells in Peripheral Blood and Pleural Effusion From Lung Adenocarcinoma Patients. *Lung Cancer* (2005) 47(3):361–71. doi: 10.1016/j.lungcan.2004.07.046
54. Scherpereel A, Grigoriu BD, Noppen M, Gey T, Chahine B, Baldacci S, et al. Defect in Recruiting Effector Memory Cd8+ T-Cells in Malignant Pleural Effusions Compared to Normal Pleural Fluid. *BMC Cancer* (2013) 13:324. doi: 10.1186/1471-2407-13-324
55. Lievense LA, Cornelissen R, Bezemer K, Kaijen-Lambers ME, Hegmans JP, Aerts JG. Pleural Effusion of Patients With Malignant Mesothelioma Induces Macrophage-Mediated T Cell Suppression. *J Thorac Oncol* (2016) 11(10):1755–64. doi: 10.1016/j.jtho.2016.06.021
56. Marcq E, Waele J, Audenaerde JV, Lion E, Santermans E, Hens N, et al. Abundant Expression of TIM-3, Lag-3, PD-1 and PD-L1 as Immunotherapy Checkpoint Targets in Effusions of Mesothelioma Patients. *Oncotarget* (2017) 8(52):89722–35. doi: 10.18632/oncotarget.21113
57. Atanackovic D, Block A, de Weerth A, Faltz C, Hossfeld DK, Hegewisch-Becker S. Characterization of Effusion-Infiltrating T Cells: Benign Versus Malignant Effusions. *Clin Cancer Res* (2004) 10(8):2600–8. doi: 10.1158/1078-0432.CCR-03-0239
58. Chen YQ, Shi HZ, Qin XJ, Mo WN, Liang XD, Huang ZX, et al. Cd4+Cd25+ Regulatory T Lymphocytes in Malignant Pleural Effusion. *Am J Respir Crit Care Med* (2005) 172(11):1434–9. doi: 10.1164/rccm.200504-588OC
59. Qin XJ, Shi HZ, Deng JM, Liang QL, Jiang J, Ye ZJ. Ccl22 Recruits CD4-Positive CD25-Positive Regulatory T Cells Into Malignant Pleural Effusion. *Clin Cancer Res* (2009) 15(7):2231–7. doi: 10.1158/1078-0432.CCR-08-2641
60. Lv M, Xu Y, Tang R, Ren J, Shen S, Chen Y, et al. Mir141-CXCL1-CXCR2 Signaling-Induced Treg Recruitment Regulates Metastases and Survival of non-Small Cell Lung Cancer. *Mol Cancer Ther* (2014) 13(12):3152–62. doi: 10.1158/1535-7163.MCT-14-0448
61. Ye ZJ, Zhou Q, Zhang JC, Li X, Wu C, Qin SM, et al. Cd39+ Regulatory T Cells Suppress Generation and Differentiation of Th17 Cells in Human Malignant Pleural Effusion Via a LAP-dependent Mechanism. *Respir Res* (2011) 12:77. doi: 10.1186/1465-9921-12-77
62. Chee J, Watson MW, Chopra A, Nguyen B, Cook AM, Creaney J, et al. Tumour Associated Lymphocytes in the Pleural Effusions of Patients With Mesothelioma Express High Levels of Inhibitory Receptors. *BMC Res Notes* (2018) 11(1):864. doi: 10.1186/s13104-018-3953-x
63. Kim HR, Park HJ, Son J, Lee JG, Chung KY, Cho NH, et al. Tumor Microenvironment Dictates Regulatory T Cell Phenotype: Upregulated Immune Checkpoints Reinforce Suppressive Function. *J Immunother Cancer* (2019) 7(1):339. doi: 10.1186/s40425-019-0785-8
64. Salaroglio IC, Kopecka J, Napoli F, Pradotto M, Maletta F, Costardi L, et al. Potential Diagnostic and Prognostic Role of Microenvironment in Malignant Pleural Mesothelioma. *J Thorac Oncol* (2019) 14(8):1458–71. doi: 10.1016/j.jtho.2019.03.029
65. Pasello G, Zago G, Lunardi F, Urso L, Kern I, Vlacic G, et al. Malignant Pleural Mesothelioma Immune Microenvironment and Checkpoint Expression: Correlation With Clinical-Pathological Features and Intratumor Heterogeneity Over Time. *Ann Oncol* (2018) 29(5):1258–65. doi: 10.1093/annonc/mdy086
66. Parra ER, Villalobos P, Behrens C, Jiang M, Pataer A, Swisher SG, et al. Effect of Neoadjuvant Chemotherapy on the Immune Microenvironment in non-Small Cell Lung Carcinomas as Determined by Multiplex Immunofluorescence and Image Analysis Approaches. *J Immunother Cancer* (2018) 6(1):48. doi: 10.1186/s40425-018-0368-0
67. Li L, Yang L, Wang L, Wang F, Zhang Z, Li J, et al. Impaired T Cell Function in Malignant Pleural Effusion is Caused by TGF-beta Derived Predominantly From Macrophages. *Int J Cancer* (2016) 139(10):2261–9. doi: 10.1002/ijc.30289
68. Prado-Garcia H, Romero-Garcia S, Puerto-Aquino A, Rumbo-Nava U. The PD-L1/PD-1 Pathway Promotes Dysfunction, But Not "Exhaustion", in Tumor-Responding T Cells From Pleural Effusions in Lung Cancer Patients. *Cancer Immunol Immunother* (2017) 66(6):765–76. doi: 10.1007/s00262-017-1979-x
69. Khanna S, Thomas A, Abate-Daga D, Zhang J, Morrow B, Steinberg SM, et al. Malignant Mesothelioma Effusions Are Infiltrated by CD3(+) T Cells Highly Expressing PD-L1 and the PD-L1(+) Tumor Cells Within These Effusions Are Susceptible to ADCC by the Anti-PD-L1 Antibody Avelumab. *J Thorac Oncol* (2016) 11(11):1993–2005. doi: 10.1016/j.jtho.2016.07.033
70. Hu CY, Zhang YH, Wang T, Chen L, Gong ZH, Wan YS, et al. Interleukin-2 Reverses Cd8(+) T Cell Exhaustion in Clinical Malignant Pleural Effusion of Lung Cancer. *Clin Exp Immunol* (2016) 186(1):106–14. doi: 10.1111/cei.12845
71. Gu FF, Wu JJ, Liu YY, Hu Y, Liang JY, Zhang K, et al. Human Inflammatory Dendritic Cells in Malignant Pleural Effusions Induce Th1 Cell Differentiation. *Cancer Immunol Immunother* (2020) 69(5):779–88. doi: 10.1007/s00262-020-02510-1
72. Djenidi F, Adam J, Goubar A, Durgeau A, Meurice G, de Montpreville V, et al. Cd8+Cd103+ Tumor-Infiltrating Lymphocytes are Tumor-Specific Tissue-Resident Memory T Cells and a Prognostic Factor for Survival in Lung Cancer Patients. *J Immunol* (2015) 194(7):3475–86. doi: 10.4049/jimmunol.1402711
73. Clarke J, Panwar B, Madrigal A, Singh D, Gujar R, Wood O, et al. Single-Cell Transcriptomic Analysis of Tissue-Resident Memory T Cells in Human Lung Cancer. *J Exp Med* (2019) 216(9):2128–49. doi: 10.1084/jem.20190249
74. Ganesan AP, Clarke J, Wood O, Garrido-Martin EM, Chee SJ, Mellows T, et al. Tissue-Resident Memory Features are Linked to the Magnitude of Cytotoxic T Cell Responses in Human Lung Cancer. *Nat Immunol* (2017) 18(8):940–50. doi: 10.1038/ni.3775
75. Kurtulus S, Madi A, Escobar G, Klapholz M, Nyman J, Christian E, et al. Checkpoint Blockade Immunotherapy Induces Dynamic Changes in PD-1(-)CD8(+) Tumor-Infiltrating T Cells. *Immunity* (2019) 50(1):181–94. doi: 10.1016/j.immuni.2018.11.014
76. Klampatsa A, O'Brien SM, Thompson JC, Rao AS, Stadanlick JE, Martinez MC, et al. Phenotypic and Functional Analysis of Malignant Mesothelioma Tumor-Infiltrating Lymphocytes. *Oncoimmunology* (2019) 8(9):e1638211. doi: 10.1080/2162402X.2019.1638211
77. Qu QX, Zhu XY, Du WW, Wang HB, Shen Y, Zhu YB, et al. 4-1bb Agonism Combined With Pd-L1 Blockade Increases the Number of Tissue-Resident Cd8+ T Cells and Facilitates Tumor Abrogation. *Front Immunol* (2020) 11:577. doi: 10.3389/fimmu.2020.00577
78. Mankor JM, Disselhorst MJ, Poncin M, Baas P, Aerts J, Vroman H. Efficacy of Nivolumab and Ipilimumab in Patients With Malignant Pleural Mesothelioma is Related to a Subtype of Effector Memory Cytotoxic T Cells: Translational Evidence From Two Clinical Trials. *EBioMedicine* (2020) 62:103040. doi: 10.1016/j.ebiom.2020.103040

79. Karachaliou N, Gonzalez-Cao M, Crespo G, Drozdowskyj A, Aldeguer E, Gimenez-Capitan A, et al. Interferon Gamma, an Important Marker of Response to Immune Checkpoint Blockade in Non-Small Cell Lung Cancer and Melanoma Patients. *Ther Adv Med Oncol* (2018) 10:1758834017749748. doi: 10.1177/1758834017749748
80. O'Brien SM, Klampatsa A, Thompson JC, Martinez MC, Hwang WT, Rao AS, et al. Function of Human Tumor-Infiltrating Lymphocytes in Early-Stage non-Small Cell Lung Cancer. *Cancer Immunol Res* (2019) 7(6):896–909. doi: 10.1158/2326-6066.CIR-18-0713
81. Yi FS, Zhai K, Shi HZ. Helper T Cells in Malignant Pleural Effusion. *Cancer Lett* (2021) 500:21–8. doi: 10.1016/j.canlet.2020.12.016
82. Chraa D, Naim A, Olive D, Badou A. T Lymphocyte Subsets in Cancer Immunity: Friends or Foes. *J Leukoc Biol* (2019) 105(2):243–55. doi: 10.1002/JLB.MR0318-097R
83. Wei SC, Levine JH, Cogdill AP, Zhao Y, Anang NAS, Andrews MC, et al. Distinct Cellular Mechanisms Underlie Anti-CTLA-4 and Anti-PD-1 Checkpoint Blockade. *Cell* (2017) 170(6):1120–33. doi: 10.1016/j.cell.2017.07.024
84. Liakou CI, Kamat A, Tang DN, Chen H, Sun J, Troncoso P, et al. Ctla-4 Blockade Increases IFNgamma-producing Cd4+Icoshi Cells to Shift the Ratio of Effector to Regulatory T Cells in Cancer Patients. *Proc Natl Acad Sci U S A* (2008) 105(39):14987–92. doi: 10.1073/pnas.0806075105
85. Jiao S, Subudhi SK, Aparicio A, Ge Z, Guan B, Miura Y, et al. Differences in Tumor Microenvironment Dictate T Helper Lineage Polarization and Response to Immune Checkpoint Therapy. *Cell* (2019) 179(5):1177–90 e13. doi: 10.1016/j.cell.2019.10.029
86. Okamoto M, Hasegawa Y, Hara T, Hashimoto N, Imaizumi K, Shimokata K, et al. T-Helper Type 1/T-Helper Type 2 Balance in Malignant Pleural Effusions Compared to Tuberculous Pleural Effusions. *Chest* (2005) 128 (6):4030–5. doi: 10.1378/chest.128.6.4030
87. Oshikawa K, Yanagisawa K, Ohno S, Tominaga S, Sugiyama Y. Expression of ST2 in Helper T Lymphocytes of Malignant Pleural Effusions. *Am J Respir Crit Care Med* (2002) 165(7):1005–9. doi: 10.1164/ajrccm.165.7.2105109
88. Heymann D, L'Her E, Nguyen J-M, Raher S, Canfrère I, Coupey L, et al. Leukaemia Inhibitory Factor (Lif) Production in Pleural Effusions: Comparison With Production of IL-4, Il-8, IL-10 and Macrophage-Colony Stimulating Factor (M-Csf). *Cytokine* (1996) 8(5):410–6. doi: 10.1006/cyto.1996.0056
89. DeLong P, Carroll RG, Henry AC, Tanaka T, Ahmad S, Leibowitz MS, et al. Regulatory T Cells and Cytokines in Malignant Pleural Effusions Secondary to Mesothelioma and Carcinoma. *Cancer Biol Ther* (2005) 4(3):342–6. doi: 10.4161/cbt.4.3.1644
90. Zou W, Restifo NP. T(H)17 Cells in Tumour Immunity and Immunotherapy. *Nat Rev Immunol* (2010) 10(4):248–56. doi: 10.1038/nri2742
91. Bailey SR, Nelson MH, Himes RA, Li Z, Mehrotra S, Paulos CM. Th17 Cells in Cancer: The Ultimate Identity Crisis. *Front Immunol* (2014) 5:276. doi: 10.3389/fimmu.2014.00276
92. Chang SH. T Helper 17 (Th17) Cells and interleukin-17 (Il-17) in Cancer. *Arch Pharm Res* (2019) 42(7):549–59. doi: 10.1007/s12272-019-01146-9
93. Ye Z-J, Zhou Q, Gu Y-Y, Qin S-M, Ma W-L, Xin J-B, et al. Generation and Differentiation of IL-17–producing Cd4+ T Cells in Malignant Pleural Effusion. *J Immunol* (2010) 185(10):6348–54. doi: 10.4049/jimmunol.1001728
94. Ye ZJ, Zhou Q, Yin W, Yuan ML, Yang WB, Xiang F, et al. Interleukin 22-Producing Cd4+ T Cells in Malignant Pleural Effusion. *Cancer Lett* (2012) 326(1):23–32. doi: 10.1016/j.canlet.2012.07.013
95. Ye ZJ, Zhou Q, Yin W, Yuan ML, Yang WB, Xiong XZ, et al. Differentiation and Immune Regulation of IL-9-producing Cd4+ T Cells in Malignant Pleural Effusion. *Am J Respir Crit Care Med* (2012) 186(11):1168–79. doi: 10.1164/rccm.201207-1307OC
96. He J, Wang L, Zhang C, Shen W, Zhang Y, Liu T, et al. Interleukin-9 Promotes Tumorigenesis Through Augmenting Angiogenesis in non-Small Cell Lung Cancer. *Int Immunopharmacol* (2019) 75:105766. doi: 10.1016/j.intimp.2019.105766
97. Bu XN, Zhou Q, Zhang JC, Ye ZJ, Tong ZH, Shi HZ. Recruitment and Phenotypic Characteristics of Interleukin 9-Producing Cd4+ T Cells in Malignant Pleural Effusion. *Lung* (2013) 191(4):385–9. doi: 10.1007/s00408-013-9474-4
98. Hernandez P, Gronke K, Diefenbach A. A Catch-22: Interleukin-22 and Cancer. *Eur J Immunol* (2018) 48(1):15–31. doi: 10.1002/eji.201747183
99. Zhang W, Chen Y, Wei H, Zheng C, Sun R, Zhang J, et al. Antiapoptotic Activity of Autocrine interleukin-22 and Therapeutic Effects of Interleukin-22-Small Interfering RNA on Human Lung Cancer Xenografts. *Clin Cancer Res* (2008) 14(20):6432–9. doi: 10.1158/1078-0432.CCR-07-4401
100. Sneddon S, Rive CM, Ma S, Dick IM, Allcock RJN, Brown SD, et al. Identification of a CD8+ T-Cell Response to a Predicted Neoantigen in Malignant Mesothelioma. *Oncoimmunology* (2020) 9(1):1684713. doi: 10.1080/2162402X.2019.1684713
101. Han J, Duan J, Bai H, Wang Y, Wan R, Wang X, et al. Tcr Repertoire Diversity of Peripheral Pd-1+Cd8+ T Cells Predicts Clinical Outcomes After Immunotherapy in Patients With Non–Small Cell Lung Cancer. *Cancer Immunol Res* (2020) 8(1):146–54. doi: 10.1158/2326-6066.CIR-19-0398
102. Formenti SC, Rudqvist NP, Golden E, Cooper B, Wennerberg E, Lhuillier C, et al. Radiotherapy Induces Responses of Lung Cancer to CTLA-4 Blockade. *Nat Med* (2018) 24(12):1845–51. doi: 10.1038/s41591-018-0232-2
103. Duncan SR, Elias DJ, Roglic M, Pekny KW. Theofilopoulos AN. T-Cell Receptor Biases and Clonal Proliferations in Blood and Pleural Effusions of Patients With Lung Cancer. *Hum Immunol* (1997) 53(1):39–48. doi: 10.1016/S0198-8859(96)00296-0
104. Jang M, Yew PY, Hasegawa K, Ikeda Y, Fujiwara K, Fleming GF, et al. Characterization of T Cell Repertoire of Blood, Tumor, and Ascites in Ovarian Cancer Patients Using Next Generation Sequencing. *Oncoimmunology* (2015) 4(11):e1030561. doi: 10.1080/2162402X.2015.1030561
105. Ikematsu Y, Tanaka K, Yanagihara T, Liu R, Inoue H, Yoneshima Y, et al. Immune Checkpoint Protein and Cytokine Expression by T Lymphocytes in Pleural Effusion of Cancer Patients Receiving anti-PD-1 Therapy. *Lung Cancer* (2019) 138:58–64. doi: 10.1016/j.lungcan.2019.10.011
106. Tseng YH, Ho HL, Lai CR, Luo YH, Tseng YC, Whang-Peng J, et al. Pd-L1 Expression of Tumor Cells, Macrophages, and Immune Cells in Non-Small Cell Lung Cancer Patients With Malignant Pleural Effusion. *J Thorac Oncol* (2018) 13(3):447–53. doi: 10.1016/j.jtho.2017.10.034
107. Koyama S, Akbay EA, Li YY, Herter-Sprie GS, Buczkowski KA, Richards WG, et al. Adaptive Resistance to Therapeutic Pd-1 Blockade is Associated With Upregulation of Alternative Immune Checkpoints. *Nat Commun* (2016) 7:10501. doi: 10.1038/ncomms10501
108. Guo M, Wu F, Hu G, Chen L, Xu J, Xu P, et al. Autologous Tumor Cell-Derived Microparticle-Based Targeted Chemotherapy in Lung Cancer Patients With Malignant Pleural Effusion. *Sci Transl Med* (2019) 11(474): eaat5690. doi: 10.1126/scitranslmed.aat5690
109. Zhang L, Dermawan K, Jin M, Liu R, Zheng H, Xu L, et al. Differential Impairment of Regulatory T Cells Rather Than Effector T Cells by Paclitaxel-Based Chemotherapy. *Clin Immunol* (2008) 129(2):219–29. doi: 10.1016/j.clim.2008.07.013
110. McCoy MJ, Lake RA, van der Most RG, Dick IM, Nowak AK. Post-Chemotherapy T-cell Recovery is a Marker of Improved Survival in Patients With Advanced Thoracic Malignancies. *Br J Cancer* (2012) 107 (7):1107–15. doi: 10.1038/bjc.2012.362
111. Li JY, Duan XF, Wang LP, Xu YJ, Huang L, Zhang TF, et al. Selective Depletion of Regulatory T Cell Subsets by Docetaxel Treatment in Patients With Nonsmall Cell Lung Cancer. *J Immunol Res* (2014) 2014:286170. doi: 10.1155/2014/286170
112. Mazzaschi G, Facchinetti F, Missale G, Canetti D, Madeddu D, Zecca A, et al. The Circulating Pool of Functionally Competent NK and CD8+ Cells Predicts the Outcome of Anti-PD1 Treatment in Advanced Nsclc. *Lung Cancer* (2019) 127:153–63. doi: 10.1016/j.lungcan.2018.11.038
113. Mazzaschi G, Madeddu D, Falco A, Bocchialini G, Goldoni M, Sogni F, et al. Low PD-1 Expression in Cytotoxic Cd8(+) Tumor-Infiltrating Lymphocytes Confers an Immune-Privileged Tissue Microenvironment in NSCLC With a Prognostic and Predictive Value. *Clin Cancer Res* (2018) 24(2):407–19. doi: 10.1158/1078-0432.CCR-17-2156
114. Prat A, Navarro A, Pare L, Reguart N, Galvan P, Pascual T, et al. Immune-Related Gene Expression Profiling After PD-1 Blockade in Non-Small Cell Lung Carcinoma, Head and Neck Squamous Cell Carcinoma, and Melanoma. *Cancer Res* (2017) 77(13):3540–50. doi: 10.1158/0008-5472.CAN-16-3556

115. Wu SP, Liao RQ, Tu HY, Wang WJ, Dong ZY, Huang SM, et al. Stromal PD-L1-Positive Regulatory T Cells and PD-1-Positive Cd8-Positive T Cells Define the Response of Different Subsets of Non-Small Cell Lung Cancer to PD-1/PD-L1 Blockade Immunotherapy. *J Thorac Oncol* (2018) 13(4):521–32. doi: 10.1016/j.jtho.2017.11.132
116. Huang AC, Postow MA, Orlowski RJ, Mick R, Bengsch B, Manne S, et al. T-Cell Invigoration to Tumour Burden Ratio Associated With anti-PD-1 Response. *Nature* (2017) 545(7652):60–5. doi: 10.1038/nature22079
117. Kim K, Park S, Park SY, Kim G, Park SM, Cho JW, et al. Single-Cell Transcriptome Analysis Reveals TOX as a Promoting Factor for T Cell Exhaustion and a Predictor for Anti-PD-1 Responses in Human Cancer. *Genome Med* (2020) 12(1):22. doi: 10.1186/s13073-020-00722-9
118. Julia EP, Mando P, Rizzo MM, Cueto GR, Tsou F, Luca R, et al. Peripheral Changes in Immune Cell Populations and Soluble Mediators After Anti-PD-1 Therapy in non-Small Cell Lung Cancer and Renal Cell Carcinoma Patients. *Cancer Immunol Immunother* (2019) 68(10):1585–96. doi: 10.1007/s00262-019-02391-z
119. Siddiqui I, Schaeuble K, Chennupati V, Fuertes Marraco SA, Calderon-Copete S, Pais Ferreira D, et al. Intratumoral Tcf1(+)Pd-1(+)Cd8(+) T Cells With Stem-Like Properties Promote Tumor Control in Response to Vaccination and Checkpoint Blockade Immunotherapy. *Immunity* (2019) 50(1):195–211.e10. doi: 10.1016/j.immuni.2018.12.021
120. Abouzgheib W, Bartter T, Dagher H, Pratter M, Klump W. A Prospective Study of the Volume of Pleural Fluid Required for Accurate Diagnosis of Malignant Pleural Effusion. *Chest* (2009) 135(4):999–1001. doi: 10.1378/chest.08-2002
121. Carter J, Miller JA, Feller-Kopman D, Ettinger D, Sidransky D, Maleki Z. Molecular Profiling of Malignant Pleural Effusion in Metastatic non-Small-Cell Lung Carcinoma. The Effect of Preanalytical Factors. *Ann Am Thorac Soc* (2017) 14(7):1169–76. doi: 10.1513/AnnalsATS.201609-709OC
122. Biton J, Ouakrim H, Dechartres A, Alifano M, Mansuet-Lupo A, Si H, et al. Impaired Tumor-Infiltrating T Cells in Patients With Chronic Obstructive Pulmonary Disease Impact Lung Cancer Response to PD-1 Blockade. *Am J Respir Crit Care Med* (2018) 198(7):928–40. doi: 10.1164/rccm.201706-1110OC
123. Qama D, Choi WI, Kwon KY. Immune Responses in the Lungs of Patients With Tuberculous Pleural Effusion Without Pulmonary Tuberculosis. *BMC Immunol* (2012) 13:45. doi: 10.1186/1471-2172-13-45
124. Mateu-Jimenez M, Curull V, Pijuan L, Sanchez-Font A, Rivera-Ramos H, Rodriguez-Fuster A, et al. Systemic and Tumor Th1 and Th2 Inflammatory Profile and Macrophages in Lung Cancer: Influence of Underlying Chronic Respiratory Disease. *J Thorac Oncol* (2017) 12(2):235–48. doi: 10.1016/j.jtho.2016.09.137

**Conflict of Interest:** The authors declare that the research was conducted in the absence of any commercial or financial relationships that could be construed as a potential conflict of interest.

frontiers in Oncology

MINI REVIEW
published: 11 June 2021
doi: 10.3389/fonc.2021.684025

# Immune Microenvironment and Genetics in Malignant Pleural Mesothelioma

*Benjamin Wadowski, Raphael Bueno and Assunta De Rienzo* *

*Thoracic Surgery Oncology Laboratory and the International Mesothelioma Program, Division of Thoracic and Cardiovascular Surgery, Brigham and Women's Hospital and Harvard Medical School, Boston, MA, United States*

Malignant pleural mesothelioma (MPM) is a rare and aggressive malignancy with limited therapeutic options beyond surgery and cytotoxic chemotherapy. The success of immune checkpoint inhibition has been found to correlate with expression of immune-related genes such as *CD274* (PD-L1) in lung and other solid cancers. However, only a small subset of MPM patients respond to checkpoint inhibition, and this response has been varied and unpredictable across several clinical trials. Recent advances in next-generation sequencing (NGS) technology have improved our understanding of the molecular features of MPM, also with respect to its genetic signature and how this impacts the immune microenvironment. This article will review current evidence surrounding the interplay between MPM genetics, including epigenetics and transcriptomics, and the immune response.

**Keywords: mesothelioma, genomics, transcriptomics, immune, checkpoint, microenvironment**

OPEN ACCESS

***Edited by:***
*Emanuela Felley-Bosco, University of Zurich, Switzerland*

***Reviewed by:***
*Fonteneau Jean-Francois, U1232 Centre de Recherche en Cancérologie et Immunologie Nantes Angers (CRCINA) (INSERM), France*
*Didier Jean, Institut National de la Santé et de la Recherche Médicale (INSERM), France*

***Correspondence:**
*Assunta De Rienzo*
*aderienzo@bwh.harvard.edu*

***Specialty section:***
*This article was submitted to Cancer Immunity and Immunotherapy, a section of the journal Frontiers in Oncology*

***Received:*** *22 March 2021*
***Accepted:*** *28 May 2021*
***Published:*** *11 June 2021*

***Citation:***
*Wadowski B, Bueno R and De Rienzo A (2021) Immune Microenvironment and Genetics in Malignant Pleural Mesothelioma. Front. Oncol. 11:684025. doi: 10.3389/fonc.2021.684025*

## INTRODUCTION

Malignant pleural mesothelioma (MPM) is a rare and aggressive tumor of the pleural cavity. It affects approximately 3,000 new patients per year in the United States, and median survival following diagnosis ranges from 7 to 13 months (1, 2). First-line treatment consists of cytotoxic chemotherapy either in the neoadjuvant or adjuvant setting (3). Given the success of immune checkpoint inhibition in other solid tumors, the use of these agents is being investigated in MPM. Unfortunately, few MPM patients respond to current checkpoint inhibitor regimens (4, 5) and reliable predictive biomarkers for response are lacking (6). A deeper understanding of the immune microenvironment in MPM is required to improve the way immunotherapy is applied in these patients. In this review, we explore the interplay between the complex molecular features of MPM and the immune response.

## THE IMMUNE MICROENVIRONMENT IN MPM

### Tumor Development

MPM is believed to arise in the context of chronic inflammation (7). It is associated with asbestos exposure in 70-90% of cases (8). Over decades, asbestos or other mineral fibers can cause both direct

cytotoxicity and genotoxicity, generate free radicals, and lead to chronic inflammation through cytokine dysregulation (9, 10). This in turn results in immune activation, propagating the inflammatory environment and contributing to epigenetic and genetic alterations in mesothelial cells, and eventual malignant transformation (11). MPM may also arise in the absence of prolonged inflammation, particularly in young female patients or those with germline variants in genes such as *BRCA1* associated protein 1 (*BAP1*) and BLM RecQ Like Helicase (*BLM*) (12, 13). However, MPM tumorigenesis under these circumstances is rare and remains incompletely understood.

Despite evidence for the typical role of inflammation in MPM oncogenesis, tumor survival requires an element of immune evasion or immunosuppression: the tumor microenvironment is believed to be highly immunosuppressive in MPM (11). Consequently, the composition of the immune cell infiltrate, including macrophage phenotypes and lymphocyte subpopulations, has been investigated in several studies.

## The Immunosuppressive Phenotype

The interactions between myeloid cells, particularly tumor-associated monocytes/macrophages (TAMs), and lymphoid cells regulate the local antitumor immune response. In particular, different macrophage phenotypes can shape the immune microenvironment in divergent ways: classically activated M1 macrophages promote T cell proliferation and antitumor activity, while alternatively activated M2 macrophages exert immunosuppressive effects *via* cytokines such as IL-6 and IL-10 (14). Prevalence, function, and prognostic implications of these cell types have been extensively investigated in MPM (11).

To study the myeloid infiltrate in MPM tumors, Burt and collaborators (15) performed immunohistochemistry (IHC) for CD68, a macrophage surface marker, in 52 MPM tumors. They found that macrophages comprise a significant (27% ± 9%) proportion of tumor area on average. The same group found that the numbers of preoperative circulating monocytes and total white blood cells (WBC) were higher in non-epithelial compared with epithelioid MPM. In addition, higher preoperative monocyte counts were correlated with overall shorter survival in all patients regardless of histology (HR 3.98 [2.64-5.93] $p<0.001$). Successively, Ujiie and collaborators (16) demonstrated that beyond macrophage prevalence, the proportion of M2 macrophages specifically influences prognosis. Within the tumor, monocytes differentiate into immunosuppressive macrophages *via* the CSF1R pathway in response to M-CSF (17, 18) and potentially IL-34 secretion by tumor cells (19). Furthermore, IHC analysis for a panel of immune-related markers was performed on 395 MPM tumors across the histologic spectrum. Shorter survival was associated with increased CD163/CD8 (N=22) and CD163/CD20 (N=48) ratios, which are indicative of an M2 predominance. A separate IHC-based analysis in epithelioid tumors alone showed a similar decrease in survival with higher CD163/CD68 ratio (Pearson r −0.72, $p<0.05$), demonstrating the deleterious effect of M2 polarization (14). Using bulk RNA-seq data, Bueno and collaborators (20) found that the M2 macrophage to T cell ratio based on the expression levels of 41 genes was predictive of reduced overall survival. In addition, the expression levels of the 22 genes associated with M2 macrophage phenotype were estimated to be higher in sarcomatoid tumors confirming previous observations of higher number of macrophages in non-epithelioid tumors.

To characterize the lymphoid infiltrate in MPM, Awad and collaborators (21) utilized a novel method for comprehensive immune profiling using flow cytometry in 43 MPM tumors annotated with programmed death ligand 1 (PD-L1) IHC status. PD-L1–positive and non-epithelioid tumors showed a significantly greater proportion of infiltrating T cells than PD-L1–negative and epithelioid tumors (21). In addition, PD-L1–positive tumors exhibited considerable immunophenotypic variability across samples, with a higher proportion of CD8+ memory T cells ($p = 0.007$), higher CD8+ effector memory T cells ($p = 0.03$), and a lower proportion of CD8+ effector T cells ($p = 0.001$) than the PD-L1 negative tumors. Moreover, PD-L1 expression was shown to be associated with increased CD8 T cell proliferation (based on Ki67+ status) and with increased proportion of Treg infiltration compared to PD-L1 negative tumors (21). This study suggested that the immunophenotypic variability observed across PD-L1 samples may be responsible for the minority of PD-L1–positive mesotheliomas likely to respond to pembrolizumab. Another study by Combaz-Lair and colleagues (22) examined the association between PD-L1 staining, TLR3 expression and immune infiltration by IHC in 58 MPM FFPE specimens. The authors demonstrated, using two different antibodies, that overall PD-L1 expression was increased in sarcomatoid tumors compared with other histologic types. A correlation between PD-L1 expression on infiltrating lymphocytes and PD-L1 expression on tumor cells was also found ($p \leq 0.001$ for both antibody clones). In addition, a correlation between PD-L1 expression on lymphocytes and CD3 and CD8 expression was found, but there was no association between PD-L1 expression and immune infiltrate density identified in this study. Increased PD-L1 expression was associated with reduced unadjusted survival for one clone (SP142, log-rank $p=0.016$) but not the other (E1L3L, log-rank $= 0.022$) (22). A different study characterized 93 treated and 65 chemo-naïve MPM cases by tumor microenvironment (TME) and PD-L1 status, respectively (23). Non-epithelioid tumors showed higher cytotoxic T cell infiltration, higher macrophage infiltration, and lower CD4+ T cell levels than epithelioid tumors; they also showed higher levels of tumor PD-L1 expression. The authors also demonstrated an association of these features with aggressive histopathological characteristics including necrosis and tumor grade. In another IHC analysis of 88 MPM tumors, PD-L1 was expressed regardless of the MPM histologic subtype, but both PD-L1 positive tumors and sarcomatoid MPM showed an increase of stromal CD4+ and CD19+ lymphocytes. In contrast, epithelioid tumors were associated with a higher proportion of CD8+ cells (24).

In addition to their effect on the TIL composition, the relative composition of the lymphoid infiltrate itself was found to be an independent predictor of outcomes. The balance between CD4

and CD8 T cells is key in this respect (24, 25). Fusco and collaborators (24) analyzed 88 MPM tumors. In this study, CD4+ cells correlated with improved prognosis (HR 0.48 [0.24-0.96] p=0.036), while CD8 infiltration correlated with poor prognosis (for low CD8, HR 0.44 [0.27-0.72] p=0.0012). Consequently, a high stromal CD4/CD8 ratio was found to be an independent predictor of longer survival in a multivariate model accounting for histology and PD-L1 status (24). Moreover, associations between tumor infiltrating lymphocytes (TIL) and survival were observed to change in presence of systemic therapy. A separate analysis of 32 MPM specimens, resected post-neoadjuvant chemotherapy, demonstrated that patients with high levels of CD8+ tumor-infiltrating lymphocytes by IHC had longer survival compared with those with low levels (3-year survival: 83% vs. 28%; p = 0.06) (26).

In summary, lymphoid and myeloid cells comprise a significant portion of the MPM microenvironment. Non-epithelioid histologic subtypes often exhibit an immunosuppressive phenotype, which correlates with shorter survival. However, there remains significant variability even among histologically similar tumors and further work is needed to explore how this variability may influence treatment response.

## Genetic and Epigenetic Effects on the Immune Response

The genetic intratumor heterogeneity is crucial for cancer invasion, proliferation and resistance to therapy and is closely related to the TME (27). The epigenetic and genetic landscape of MPM is characterized by frequent chromosomal losses and a relatively low number of somatic mutations compared to other solid tumors (20). Potential relationships between genome-level features and immune microenvironment in MPM have been investigated including associations with epigenetic, structural/chromosomal, and gene-specific alterations.

Epigenetic modifications determine changes in gene expression without altering the DNA sequence. Epigenetic changes have been associated with tumor progression and poor outcomes in a diverse array of tumors (28–30), and in MPM have been linked to alterations of the tumor-infiltrating immune cells. Epigenome-wide association analyses of a cohort of 159 asbestos-exposed patients with MPM identified the methylation of the single-CpG marker, cg03546163, located in the 5' untranslated region of the *FKBP5* gene, as associated to survival (31). This marker showed better performance compared with the traditional inflammation scores, lymphocyte-to-monocyte ratio (32), generally used as a prognostic biomarker in MPM.

A similar study focused on immune system-related genes was conducted comparing 163 MPM patients with 137 healthy controls. Several signatures were identified including significant differential methylation of the CpG regions of *LIME1* (involved in lymphocyte signaling), *CXCR6* (associated with T cell localization), *TOLLIP* (related with IL-1 receptor trafficking), and *TNFAIP6* (involved in inflammation) (33). These data supported the hypothesis that changes in the DNA methylation and in the TME may be associated with asbestos exposure.

Chromosomal instability may result in gross karyotypic alterations. It has been related to cancer immunogenicity (27), and is a common feature of MPM (34, 35). Genome-wide copy number analysis performed in 113 MPM tumors with IHC data for PD-L1, CD4, CD8, and FOXP3 was used to compute the percent genome aberration (PGA) for each sample as total count of base pairs involved in copy number gains or losses divided by the total length of the genome in base pairs (36). Epithelioid tumors showed a significantly higher PGA than non-epithelioid tumors, but PGA did not correlate with PD-L1 status. Samples with lower PGA had significantly higher CD4+ and CD8+ T-cell infiltration indicating that chromosomal instability may be associated with immune infiltration. Chromosomal rearrangements have also been shown to have immunologic implications through expression of neoantigens in MPM (37). Mansfield and collaborators (38) performed mate-pair sequencing, RNA-seq, T cell receptor (TCR)-seq, and major histocompatibility complex (MHC) peptide binding assays to assess structural variants of chromosomes and predict neoantigens using 28 specimens from treatment-naïve MPMs. They identified 1535 chromosomal rearrangements, of which 637 (41.5%) resulted in novel gene fusions, leading to 179 potential novel amino acid sequences potentially drive the expression of neoantigens. In addition, the increase in predicted neoantigens was correlated with clonal expansion of tumor-infiltrating T cells. Spatial heterogeneity in MPM has shown to affect TIL clonality in the context of neoantigenicity. In a study of 6 MPM tumors sampled at three distinct anatomic sites each, increasing neoantigen load correlated with oligoclonal TIL expansion, as well as increased cytotoxic T cell activity. In addition, heterogeneous mutation patterns across sites with associated differences in immune microenvironment signatures were identified (39). A multi-region, longitudinal whole exome and T-cell receptor sequencing analysis was conducted on 69 specimens from nine MPM tumors before and after dasatinib treatment. It was found that mutation profile among sites was relatively homogeneous (>80% concordance), but T-cell clonality varied widely particularly after treatment (40).

Growing data suggest that mutations in specific genes influence the immune response (41). *BAP1* is one of the most frequently mutated genes in MPM (20), and the impact of *BAP1* mutations on the immune system has been investigated. An analysis of 43 MPM tumors found no significant differences in the immune cell infiltration between *BAP1* mutant versus wild-type MPM (21). In peritoneal mesothelioma, a multi-omic analysis of 19 tumors identified an association between inflammatory TME and haploinsufficiency of *BAP1*. Specifically, *BAP1* deleted tumors were found to have strong cytokine signaling and upregulation of the innate immune response based on gene set enrichment analysis. In contrast, tumors displaying intact *BAP1* had upregulation of adaptive immunity and MHC-I/II antigen presentation (42). Furthermore, tumors with deleted *BAP1* showed a lower proportion of plasma cells, natural killer (NK) cells, and B cells but higher mast cell and T cell infiltration, as well as higher expression of genes with a known role in immune checkpoint

modulation *(PD1*, *PD-L1 CD80*, *CTLA4*, *LAG3*, and *ICOS)*, compared with tumor with wild-type BAP1. This finding was not supported by the TCGA analysis in pleural mesothelioma (42).

Single gene mutations may also influence the antitumor response through neoantigen formation and modulation of immune and inflammatory signaling pathways. Bueno and collaborators (20) analyzed somatic alterations in 98 MPMs with paired exome and RNA-seq data and found that 59% of 1,493 mutations resulted in MHC class I-binding peptides. Further, the more frequently mutated genes *BAP1*, *NF2*, and *TP53* each resulted in multiple predicted neoantigens (20). *CDKN2A* is another frequently mutated gene in MPM (20), and is located <1Mb from several interferon genes raising the possibility that prognostically significant loss of *IFN* gene expression may reflect a "passive hitchhiking event" associated with *CDKN2A* deletion in cancer (43). Type I interferon (IFN-I) signaling is known to play a role in antitumor immunity (44). An integrative analysis of the association between *IFN* gene alterations, *CDKN2A* loss, and *in vitro* oncolytic virus sensitivity was performed. A deletion of *IFNB1* was identified in 17/57 (30%) MPM short-term cell lines with homozygous deletion of *CDKN2A*, and *CDKN2A* loss in 17/18 (94%) established cell lines with homozygous deletion *IFNB1*. Utilizing the TCGA database of 87 patients with MPM, homozygous deletions of *IFNA2* and *IFNB1* were found in 18.4% and 9.2% of patients respectively. Furthermore, homozygous deletion of IFN-I genes resulted in more frequent sensitivity of MPM cell lines to oncolytic virus therapy (45). While a link between IFN signaling and immunotherapy response has not been established in MPM, it has been observed in other cancers (43).

### Heterogeneity of Gene Expression Associated With Immune Checkpoints

Checkpoint molecules such as programmed-death 1 (PD-1) and cytotoxic T lymphocyte associated antigen 4 (CTLA4) have been recognized as key regulators of oncologic immune evasion through their role in immunosuppression (46). Protein expression of checkpoint molecules by IHC such as PD-L1 are often used as prognostic biomarkers to guide response to checkpoint inhibition in several solid cancers (47). However, in MPM, similar analyses have shown inconsistent results (6, 48, 49). In contrast, characterization of the immune microenvironment in relation to checkpoint pathways using high-throughput methodologies has led to prognostic insights both in MPM and other solid tumors (50, 51).

Unsupervised analysis of RNA-seq data from 284 MPMs identified a continuum of molecular profiles which correlate with prognosis (50). The majority of variation was found to be related to immune checkpoint and angiogenic pathways. Two profiles were identified to be associated with poor prognosis: one immunologically active characterized by high lymphocyte infiltration and high immune checkpoint expression, and one less activated profile with low lymphocyte infiltration. Both were characterized by high expression of pro-angiogenic genes. In contrast, a "VEGFR2+/VISTA+" profile was associated with better prognosis, despite having also highly angiogenic features. RNA expression of *VISTA*, a negative checkpoint regulator, was found to be highly expressed in epithelioid MPM in a separate well-annotated cohort of 74 untreated MPM specimens (52).

Blum and collaborators (51) performed an extensive multi-omic analysis using several public MPM transcriptomic datasets. Two signatures (E/S scores) were identified to discriminate epithelioid-like and sarcomatoid-like tumors within a continuum or "histo-molecular gradient" of MPM samples with epithelioid and sarcomatoid tumors at the two extremes. They found that expression of most immune checkpoints correlated with increased S-score, including *TNFSF4* and its receptor *TNFRSF4*, *CD80*, and *PD-L2*, as well as *CD274* and *CTLA4*. A positive association was found between the S-score and *IDO1*, an immune modulator. In contrast, the E-score was associated with *TNFSF14* and *VISTA* expression. Tumors with higher S-score were associated with increased T cell and monocyte infiltration, while E-score was associated with increased NK cell infiltration (51).

## DISCUSSION

Tumor-immune interactions are complex regardless of the tumor type. As immune checkpoint inhibition gains importance in the treatment of solid tumors including MPM, greater emphasis is being placed on immune characterization and identification of predictive biomarkers for treatment response. Several studies have tried to characterize the immune TME of MPM and linked it to clinical and genetic features.

In general, MPM displays an immunosuppressive microenvironment mediated by M2 macrophages and characterized by high lymphocyte infiltration (**Table 1**) (15, 25). This immunosuppressive phenotype is more common in non-epithelioid MPM (20) and as a result the degree of overall macrophage infiltration has been associated with shorter survival in non-epithelioid MPM alone (14, 15). Across all histologic subtypes, however, an increasing balance of M2 macrophages relative to lymphocyte infiltration has been shown to be predictive of shorter survival (16, 20). Among lymphocytes, an increased proportion of CD8 relative to CD4 T cells has been associated with shorter survival (16, 24, 25). However, this effect was found to be reversed following neoadjuvant chemotherapy in one early study (26). Post-treatment immunologic alterations remain an area of active study.

Investigations of the effect of checkpoint molecule expression, including PD-L1, are also ongoing. Studies have shown that higher PD-L1 expression is associated with shorter survival (25). Non-epithelioid tumors exhibit higher PD-L1 expression than epithelioid tumors (23), and there is substantial transcriptomic variability among the expression of checkpoint molecules along the epithelial-to-mesenchymal spectrum observed in a large series of MPM transcriptomes (51).

Genetic alterations in MPM have also been associated with different immune subtypes. *BAP1* mutations have been linked to

**TABLE 1** | Summary of key findings.

| Findings | Reference(s) |
|---|---|
| **Myeloid Infiltrate** | |
| Macrophages and lymphocytes comprise a significant portion of the tumor microenvironment | Burt et al. (15); Losi et al. (25) |
| Increased macrophage infiltration predicts shorter survival in non-epithelioid MPM, but not in epithelioid MPM | Burt et al. (15)<br>Cornelissen et al. (14) |
| Non-epithelioid tumors exhibit higher levels of immunosuppressive M2 macrophage-associated gene expression | Bueno et al. (20) |
| Higher proportion of $CD163^+$-M2 macrophages is associated with shorter survival relative to: | |
| • CD8 T cells (CD163/CD8 ratio) | Ujiie et al. (16) |
| • CD20 B cells (CD163/CD20 ratio) | Ujiie et al. (16) |
| • overall T cells (by canonical gene expression profiles) | Bueno et al. (20) |
| **Lymphoid Infiltrate** | |
| PD-L1-positive tumors exhibit higher overall T cell infiltration, CD8 memory T cells, $CD8^+$ cell proliferation, CD4 T cells, and CD19 lymphocytes | Awad et al. (21)<br>Fusco et al. (24) |
| Higher PD-L1 expression is associated with poor prognosis | Combaz-Lair et al. (22)<br>Losi et al. (25) |
| Higher proportion of CD4 T cells is associated with longer survival | Fusco et al. (24); Ujiie et al. (16) |
| Higher proportion of CD8 T cells is associated with shorter survival | Fusco et al. (24); Losi et al. (25) |
| Post-neoadjuvant chemotherapy, high CD8 cells paradoxically demonstrate trend toward longer survival. | Anraku et al. (26) |

upregulation of the local innate immune response in peritoneal mesothelioma (42), but no significant association has been shown for pleural mesothelioma in either TCGA-based or other analyses (52). In MPM, aneuploidy is quite common and the creation of novel gene products through chromosomal rearrangements has significant immune implications (27, 38). Epigenetic alterations have been identified, particularly in peripheral DNA specimens in asbestos-exposed MPM cases, and have been associated in limited contexts with altered inflammatory and immune pathways (33). However, further work is needed to assess for causal relationships between these findings and specific changes in the tumor microenvironment. Gene expression is a widely studied approach to predicting the immunologic behavior of a given tumor. Association of both transcriptomic information and IHC with clinical data has revealed distinct patterns of immune activation or suppression (20, 50–52).

There remain several gaps to be addressed to link genetic signatures to the TME, and especially to predict clinical outcomes and guide therapy. Current and future work with high-resolution sequencing technology will identify unique immune programs to associate the genetic characteristics of individual tumor to specific immune phenotypes. Next-generation sequencing and machine learning are being applied to develop polygenic scoring systems predictive of response to checkpoint therapy. Spatial transcriptomics can reveal crosstalk between tumor cells and adjacent leukocytes, as well as interactions between different immune and stromal cells within the microenvironment. Genotypic inferences can be made from single-cell transcriptomic data, allowing correlation between cell clonality and immune behavior in different regions of a given tumor. As improved murine and *in vitro* tumor models are being developed, immunomodulatory therapeutics can be readily tested on patient-specific tissues leading to personalized medicine. Ultimately, full understanding of the association between immune TME and genetics will lead to improved prognostication and outcomes for patients with MPM.

## AUTHOR CONTRIBUTIONS

Literature review: BW and ADR. All authors contributed to the article and approved the submitted version.

## REFERENCES


1. Beebe-Dimmer JL, Fryzek JP, Yee CL, Dalvi TB, Garabrant DH, Schwartz AG, et al. Mesothelioma in the United States: A Surveillance, Epidemiology, and End Results (Seer)-Medicare Investigation of Treatment Patterns and Overall Survival. *Clin Epidemiol* (2016) 8:743–50. doi: 10.2147/CLEP.S105396
2. Green J, Dundar Y, Dodd S, Dickson R, Walley T. Pemetrexed Disodium in Combination With Cisplatin Versus Other Cytotoxic Agents or Supportive Care for the Treatment of Malignant Pleural Mesothelioma. *Cochrane Database Syst Rev* (2007) 1):CD005574. doi: 10.1002/14651858.CD005574.pub2
3. Ettinger DS, Wood DE, Akerley W, Bazhenova LA, Borghaei H, Camidge DR, et al. NCCN Guidelines Insights: Malignant Pleural Mesothelioma, Version 3.2016. *J Natl Compr Canc Netw* (2016) 14(7):825–36. doi: 10.6004/jnccn.2016.0087
4. Maio M, Scherpereel A, Calabro L, Aerts J, Perez SC, Bearz A, et al. Tremelimumab as Second-Line or Third-Line Treatment in Relapsed Malignant Mesothelioma (DETERMINE): A Multicentre, International, Randomised, Double-Blind, Placebo-Controlled Phase 2b Trial. *Lancet Oncol* (2017) 18(9):1261–73. doi: 10.1016/S1470-2045(17)30446-1
5. Scherpereel A, Mazieres J, Greillier L, Lantuejoul S, Do P, Bylicki O, et al. Nivolumab or Nivolumab Plus Ipilimumab in Patients With Relapsed Malignant Pleural Mesothelioma (IFCT-1501 MAPS2): A Multicentre, Open-Label, Randomised, non-Comparative, Phase 2 Trial. *Lancet Oncol* (2019) 20(2):239–53. doi: 10.1016/S1470-2045(18)30765-4
6. Hassan R, Thomas A, Nemunaitis JJ, Patel MR, Bennouna J, Chen FL, et al. Efficacy and Safety of Avelumab Treatment in Patients With Advanced

Unresectable Mesothelioma: Phase 1b Results From the JAVELIN Solid Tumor Trial. *JAMA Oncol* (2019) 5(3):351–7. doi: 10.1001/jamaoncol.2018.5428
7. Yang H, Bocchetta M, Kroczynska B, Elmishad AG, Chen Y, Liu Z, et al. TNF-Alpha Inhibits Asbestos-Induced Cytotoxicity Via a NF-kappaB-dependent Pathway, a Possible Mechanism for Asbestos-Induced Oncogenesis. *Proc Natl Acad Sci USA* (2006) 103(27):10397–402. doi: 10.1073/pnas.0604008103
8. Attanoos RL, Churg A, Galateau-Salle F, Gibbs AR, Roggli VL. Malignant Mesothelioma and Its non-Asbestos Causes. *Arch Pathol Lab Med* (2018) 142(6):753–60. doi: 10.5858/arpa.2017-0365-RA
9. Choe N, Tanaka S, Kagan E. Asbestos Fibers and Interleukin-1 Upregulate the Formation of Reactive Nitrogen Species in Rat Pleural Mesothelial Cells. *Am J Respir Cell Mol Biol* (1998) 19(2):226–36. doi: 10.1165/ajrcmb.19.2.3111
10. Huang SX, Jaurand MC, Kamp DW, Whysner J, Hei TK. Role of Mutagenicity in Asbestos Fiber-Induced Carcinogenicity and Other Diseases. *J Toxicol Environ Health B Crit Rev* (2011) 14(1-4):179–245. doi: 10.1080/10937404.2011.556051
11. Yap TA, Aerts JG, Popat S, Fennell DA. Novel Insights Into Mesothelioma Biology and Implications for Therapy. *Nat Rev Cancer* (2017) 17(8):475–88. doi: 10.1038/nrc.2017.42
12. Rai K, Pilarski R, Cebulla CM, Abdel-Rahman MH. Comprehensive Review of BAP1 Tumor Predisposition Syndrome With Report of Two New Cases. *Clin Genet* (2016) 89(3):285–94. doi: 10.1111/cge.12630
13. Bononi A, Goto K, Ak G, Yoshikawa Y, Emi M, Pastorino S, et al. Heterozygous Germline BLM Mutations Increase Susceptibility to Asbestos and Mesothelioma. *Proc Natl Acad Sci USA* (2020) 117(52):33466–73. doi: 10.1073/pnas.2019652117
14. Cornelissen R, Lievense LA, Maat AP, Hendriks RW, Hoogsteden HC, Bogers AJ, et al. Ratio of Intratumoral Macrophage Phenotypes is a Prognostic Factor in Epithelioid Malignant Pleural Mesothelioma. *PloS One* (2014) 9(9):e106742. doi: 10.1371/journal.pone.0106742
15. Burt BM, Rodig SJ, Tilleman TR, Elbardissi AW, Bueno R, Sugarbaker DJ. Circulating and Tumor-Infiltrating Myeloid Cells Predict Survival in Human Pleural Mesothelioma. *Cancer* (2011) 117(22):5234–44. doi: 10.1002/cncr.26143
16. Ujiie H, Kadota K, Nitadori JI, Aerts JG, Woo KM, Sima CS, et al. The Tumoral and Stromal Immune Microenvironment in Malignant Pleural Mesothelioma: A Comprehensive Analysis Reveals Prognostic Immune Markers. *Oncoimmunology* (2015) 4(6):e1009285. doi: 10.1080/2162402X.2015.1009285
17. Chene AL, d'Almeida S, Blondy T, Tabiasco J, Deshayes S, Fonteneau JF, et al. Pleural Effusions From Patients With Mesothelioma Induce Recruitment of Monocytes and Their Differentiation Into M2 Macrophages. *J Thorac Oncol* (2016) 11(10):1765–73. doi: 10.1016/j.jtho.2016.06.022
18. Dammeijer F, Lievense LA, Kaijen-Lambers ME, van Nimwegen M, Bezemer K, Hegmans JP, et al. Depletion of Tumor-Associated Macrophages With a CSF-1R Kinase Inhibitor Enhances Antitumor Immunity and Survival Induced by DC Immunotherapy. *Cancer Immunol Res* (2017) 5(7):535–46. doi: 10.1158/2326-6066.CIR-16-0309
19. Blondy T, d'Almeida SM, Briolay T, Tabiasco J, Meiller C, Chene AL, et al. Involvement of the M-CSF/IL-34/CSF-1R Pathway in Malignant Pleural Mesothelioma. *J Immunother Cancer* (2020) 8(1):e000182. doi: 10.1136/jitc-2019-000182
20. Bueno R, Stawiski EW, Goldstein LD, Durinck S, De Rienzo A, Modrusan Z, et al. Comprehensive Genomic Analysis of Malignant Pleural Mesothelioma Identifies Recurrent Mutations, Gene Fusions and Splicing Alterations. *Nat Genet* (2016) 48(4):407–16. doi: 10.1038/ng.3520
21. Awad MM, Jones RE, Liu H, Lizotte PH, Ivanova EV, Kulkarni M, et al. Cytotoxic T Cells in PD-L1-Positive Malignant Pleural Mesotheliomas Are Counterbalanced by Distinct Immunosuppressive Factors. *Cancer Immunol Res* (2016) 4(12):1038–48. doi: 10.1158/2326-6066.CIR-16-0171
22. Combaz-Lair C, Galateau-Salle F, McLeer-Florin A, Le Stang N, David-Boudet L, Duruisseaux M, et al. Immune Biomarkers PD-1/PD-L1 and TLR3 in Malignant Pleural Mesotheliomas. *Hum Pathol* (2016) 52:9–18. doi: 10.1016/j.humpath.2016.01.010
23. Pasello G, Zago G, Lunardi F, Urso L, Kern I, Vlacic G, et al. Malignant Pleural Mesothelioma Immune Microenvironment and Checkpoint Expression: Correlation With Clinical-Pathological Features and Intratumor Heterogeneity Over Time. *Ann Oncol* (2018) 29(5):1258–65. doi: 10.1093/annonc/mdy086
24. Fusco N, Vaira V, Righi I, Sajjadi E, Venetis K, Lopez G, et al. Characterization of the Immune Microenvironment in Malignant Pleural Mesothelioma Reveals Prognostic Subgroups of Patients. *Lung Cancer* (2020) 150:53–61. doi: 10.1016/j.lungcan.2020.09.026
25. Losi L, Bertolini F, Guaitoli G, Fabbiani L, Banchelli F, Ambrosini-Spaltro A, et al. Role of Evaluating Tumorinfiltrating Lymphocytes, Programmed Death1 Ligand 1 and Mismatch Repair Proteins Expression in Malignant Mesothelioma. *Int J Oncol* (2019) 55(5):1157–64. doi: 10.3892/ijo.2019.4883
26. Anraku M, Cunningham KS, Yun Z, Tsao MS, Zhang L, Keshavjee S, et al. Impact of Tumor-Infiltrating T Cells on Survival in Patients With Malignant Pleural Mesothelioma. *J Thorac Cardiovasc Surg* (2008) 135(4):823–9. doi: 10.1016/j.jtcvs.2007.10.026
27. Vitale I, Shema E, Loi S, Galluzzi L. Intratumoral Heterogeneity in Cancer Progression and Response to Immunotherapy. *Nat Med* (2021) 27(2):212–24. doi: 10.1038/s41591-021-01233-9
28. Teixeira VH, Pipinikas CP, Pennycuick A, Lee-Six H, Chandrasekharan D, Beane J, et al. Deciphering the Genomic, Epigenomic, and Transcriptomic Landscapes of Pre-Invasive Lung Cancer Lesions. *Nat Med* (2019) 25(3):517–25. doi: 10.1038/s41591-018-0323-0
29. Li S, Garrett-Bakelman FE, Chung SS, Sanders MA, Hricik T, Rapaport F, et al. Distinct Evolution and Dynamics of Epigenetic and Genetic Heterogeneity in Acute Myeloid Leukemia. *Nat Med* (2016) 22(7):792–9. doi: 10.1038/nm.4125
30. Lin DC, Mayakonda A, Dinh HQ, Huang P, Lin L, Liu X, et al. Genomic and Epigenomic Heterogeneity of Hepatocellular Carcinoma. *Cancer Res* (2017) 77(9):2255–65. doi: 10.1158/0008-5472.CAN-16-2822
31. Cugliari G, Catalano C, Guarrera S, Allione A, Casalone E, Russo A, et al. DNA Methylation of FKBP5 as Predictor of Overall Survival in Malignant Pleural Mesothelioma. *Cancers (Basel)* (2020) 12(11):3470. doi: 10.3390/cancers12113470
32. Papadatos-Pastos D, Roda D, De Miguel Luken MJ, Petruckevitch A, Jalil A, Capelan M, et al. Clinical Outcomes and Prognostic Factors of Patients With Advanced Mesothelioma Treated in a Phase I Clinical Trials Unit. *Eur J Cancer* (2017) 75:56–62. doi: 10.1016/j.ejca.2016.12.026
33. Guarrera S, Viberti C, Cugliari G, Allione A, Casalone E, Betti M, et al. Peripheral Blood Dna Methylation as Potential Biomarker of Malignant Pleural Mesothelioma in Asbestos-Exposed Subjects. *J Thorac Oncol* (2019) 14(3):527–39. doi: 10.1016/j.jtho.2018.10.163
34. Ivanov SV, Miller J, Lucito R, Tang C, Ivanova AV, Pei J, et al. Genomic Events Associated With Progression of Pleural Malignant Mesothelioma. *Int J Cancer* (2009) 124(3):589–99. doi: 10.1002/ijc.23949
35. Zhang M, Luo JL, Sun Q, Harber J, Dawson AG, Nakas A, et al. Clonal Architecture in Mesothelioma is Prognostic and Shapes the Tumour Microenvironment. *Nat Commun* (2021) 12(1):1751. doi: 10.1038/s41467-021-21798-w
36. Thapa B, Salcedo A, Lin X, Walkiewicz M, Murone C, Ameratunga M, et al. The Immune Microenvironment, Genome-wide Copy Number Aberrations, and Survival in Mesothelioma. *J Thorac Oncol* (2017) 12(5):850–9. doi: 10.1016/j.jtho.2017.02.013
37. Mansfield AS, Peikert T, Vasmatzis G. Chromosomal Rearrangements and Their Neoantigenic Potential in Mesothelioma. *Transl Lung Cancer Res* (2020) 9(Suppl 1):S92–S9. doi: 10.21037/tlcr.2019.11.12
38. Mansfield AS, Peikert T, Smadbeck JB, Udell JBM, Garcia-Rivera E, Elsbernd L, et al. Neoantigenic Potential of Complex Chromosomal Rearrangements in Mesothelioma. *J Thorac Oncol* (2019) 14(2):276–87. doi: 10.1016/j.jtho.2018.10.001
39. Kiyotani K, Park JH, Inoue H, Husain A, Olugbile S, Zewde M, et al. Integrated Analysis of Somatic Mutations and Immune Microenvironment in Malignant Pleural Mesothelioma. *Oncoimmunology* (2017) 6(2):e1278330. doi: 10.1080/2162402X.2016.1278330
40. Chen R, Lee WC, Fujimoto J, Li J, Hu X, Mehran R, et al. Evolution of Genomic and T-cell Repertoire Heterogeneity of Malignant Pleural Mesothelioma Under Dasatinib Treatment. *Clin Cancer Res* (2020) 26(20):5477–86. doi: 10.1158/1078-0432.CCR-20-1767
41. Shi Y, Lei Y, Liu L, Zhang S, Wang W, Zhao J, et al. Integration of Comprehensive Genomic Profiling, Tumor Mutational Burden, and PD-L1 Expression to Identify Novel Biomarkers of Immunotherapy in non-Small Cell Lung Cancer. *Cancer Med* (2021) 10(7):2216–31. doi: 10.1002/cam4.3649

42. Shrestha R, Nabavi N, Lin YY, Mo F, Anderson S, Volik S, et al. BAP1 Haploinsufficiency Predicts a Distinct Immunogenic Class of Malignant Peritoneal Mesothelioma. *Genome Med* (2019) 11(1):8. doi: 10.1186/s13073-019-0620-3
43. Ye Z, Dong H, Li Y, Ma T, Huang H, Leong HS, et al. Prevalent Homozygous Deletions of Type I Interferon and Defensin Genes in Human Cancers Associate With Immunotherapy Resistance. *Clin Cancer Res* (2018) 24 (14):3299–308. doi: 10.1158/1078-0432.CCR-17-3008
44. Zitvogel L, Galluzzi L, Kepp O, Smyth MJ, Kroemer G. Type I Interferons in Anticancer Immunity. *Nat Rev Immunol* (2015) 15(7):405–14. doi: 10.1038/nri3845
45. Delaunay T, Achard C, Boisgerault N, Grard M, Petithomme T, Chatelain C, et al. Frequent Homozygous Deletions of Type I Interferon Genes in Pleural Mesothelioma Confer Sensitivity to Oncolytic Measles Virus. *J Thorac Oncol* (2020) 15(5):827–42. doi: 10.1016/j.jtho.2019.12.128
46. Topalian SL, Taube JM, Anders RA, Pardoll DM. Mechanism-Driven Biomarkers to Guide Immune Checkpoint Blockade in Cancer Therapy. *Nat Rev Cancer* (2016) 16(5):275–87. doi: 10.1038/nrc.2016.36
47. Tu L, Guan R, Yang H, Zhou Y, Hong W, Ma L, et al. Assessment of the Expression of the Immune Checkpoint Molecules PD-1, Ctla4, TIM-3 and LAG-3 Across Different Cancers in Relation to Treatment Response, Tumor-Infiltrating Immune Cells and Survival. *Int J Cancer* (2020) 147(2):423–39. doi: 10.1002/ijc.32785
48. Brosseau S, Danel C, Scherpereel A, Mazieres J, Lantuejoul S, Margery J, et al. Shorter Survival in Malignant Pleural Mesothelioma Patients With High PD-L1 Expression Associated With Sarcomatoid or Biphasic Histology Subtype: A Series of 214 Cases From the Bio-MAPS Cohort. *Clin Lung Cancer* (2019) 20 (5):e564–75. doi: 10.1016/j.cllc.2019.04.010
49. Metaxas Y, Rivalland G, Mauti LA, Klingbiel D, Kao S, Schmid S, et al. Pembrolizumab as Palliative Immunotherapy in Malignant Pleural Mesothelioma. *J Thorac Oncol* (2018) 13(11):1784–91. doi: 10.1016/j.jtho.2018.08.007
50. Alcala N, Mangiante L, Le-Stang N, Gustafson CE, Boyault S, Damiola F, et al. Redefining Malignant Pleural Mesothelioma Types as a Continuum Uncovers Immune-Vascular Interactions. *EBioMedicine* (2019) 48:191–202. doi: 10.1016/j.ebiom.2019.09.003
51. Blum Y, Meiller C, Quetel L, Elarouci N, Ayadi M, Tashtanbaeva D, et al. Dissecting Heterogeneity in Malignant Pleural Mesothelioma Through Histo-Molecular Gradients for Clinical Applications. *Nat Commun* (2019) 10 (1):1333. doi: 10.1038/s41467-019-09307-6
52. Hmeljak J, Sanchez-Vega F, Hoadley KA, Shih J, Stewart C, Heiman D, et al. Integrative Molecular Characterization of Malignant Pleural Mesothelioma. *Cancer Discov* (2018) 8(12):1548–65. doi: 10.1158/2159-8290.CD-18-0804

**Conflict of Interest:** RB reports research grants and clinical trials support from MedGenome, Roche, Verastem, Genentech, Merck, Gritstone, Epizyme, Siemens, National Institutes of Health, and Department of Defense. In addition, RB holds 4 patents through Brigham and Women's Hospital and equity in Navigation Sciences.

The remaining authors declare that the research was conducted in the absence of any commercial or financial relationships that could be construed as a potential conflict of interest.

frontiers in Oncology

REVIEW
published: 21 June 2021
doi: 10.3389/fonc.2021.679609

# How to Better Understand the Influence of Host Genetics on Developing an Effective Immune Response to Thoracic Cancers

*Kiarash Behrouzfar*[1,2], *Kimberley Burton*[1,2], *Steve E. Mutsaers*[2,3], *Grant Morahan*[4], *Richard A. Lake*[1] *and Scott A. Fisher*[1,2]*

[1] National Centre for Asbestos Related Diseases (NCARD), University of Western Australia, Nedlands, WA, Australia, [2] School of Biomedical Sciences, University of Western Australia, Nedlands, WA, Australia, [3] Institute for Respiratory Health, University of Western Australia, Nedlands, WA, Australia, [4] Centre for Diabetes Research, Harry Perkins Institute of Medical Research, Nedlands, WA, Australia

OPEN ACCESS

**Edited by:**
*Emanuela Felley-Bosco, University of Zurich, Switzerland*

**Reviewed by:**
*Marie-Claude Jaurand, Institut National de la Santé et de la Recherche Médicale (INSERM), France*
*Daniel Murphy, University of Glasgow, United Kingdom*

***Correspondence:**
*Scott A. Fisher*
*scott.fisher@uwa.edu.au*

**Specialty section:**
*This article was submitted to Cancer Immunity and Immunotherapy, a section of the journal Frontiers in Oncology*

**Received:** *12 March 2021*
**Accepted:** *31 May 2021*
**Published:** *21 June 2021*

**Citation:**
*Behrouzfar K, Burton K, Mutsaers SE, Morahan G, Lake RA and Fisher SA (2021) How to Better Understand the Influence of Host Genetics on Developing an Effective Immune Response to Thoracic Cancers. Front. Oncol. 11:679609. doi: 10.3389/fonc.2021.679609*

Thoracic cancers pose a significant global health burden. Immune checkpoint blockade therapies have improved treatment outcomes, but durable responses remain limited. Understanding how the host immune system interacts with a developing tumor is essential for the rational development of improved treatments for thoracic malignancies. Recent technical advances have improved our understanding of the mutational burden of cancer cells and changes in cancer-specific gene expression, providing a detailed understanding of the complex biology underpinning tumor-host interactions. While there has been much focus on the genetic alterations associated with cancer cells and how they may impact treatment outcomes, how host genetics affects cancer development is also critical and will greatly determine treatment response. Genome-wide association studies (GWAS) have identified genetic variants associated with cancer predisposition. This approach has successfully identified host genetic risk factors associated with common thoracic cancers like lung cancer, but is less effective for rare cancers like malignant mesothelioma. To assess how host genetics impacts rare thoracic cancers, we used the Collaborative Cross (CC); a powerful murine genetic resource designed to maximize genetic diversity and rapidly identify genes associated with any biological trait. We are using the CC in conjunction with our asbestos-induced MexTAg mouse model, to identify host genes associated with mesothelioma development. Once genes that moderate tumor development and progression are known, human homologues can be identified and human datasets interrogated to validate their association with disease outcome. Furthermore, our CC–MexTAg animal model enables in-depth study of the tumor microenvironment, allowing the correlation of immune cell infiltration and gene expression signatures with disease development. This strategy provides a detailed picture of the underlying biological pathways associated with mesothelioma susceptibility and progression; knowledge that is crucial for the rational development of new diagnostic and therapeutic strategies. Here we discuss the influence of host genetics

on developing an effective immune response to thoracic cancers. We highlight current knowledge gaps, and with a focus on mesothelioma, describe the development and application of the CC-MexTAg to overcome limitations and illustrate how the knowledge gained from this unique study will inform the rational design of future treatments of mesothelioma.

**Keywords: thoracic malignancies, tumor immune microenvironment, mesothelioma, Collaborative Cross, MexTAg, host genetics**

## INTRODUCTION

Thoracic cancers including lung cancer (LC), malignant mesothelioma and thymic epithelial tumors (TETs) are among the most lethal cancers (1). In addition to conventional treatment options for thoracic cancers such as surgery, chemotherapy and radiotherapy, immune based treatments including immune checkpoint therapies, have improved treatment outcome for some patients (2, 3).

Cancer immunotherapy aims to restore or enhance the host's immune system to recognize and eliminate cancer cells (4). Although immunotherapies have improved treatment outcomes for some thoracic cancers, success is often limited to a subset of patients, while prognosis for the majority of patients remains dismal (5). This dichotomy in response, highlights the need to better understand interactions between thoracic cancer cells and the host immune system that underpin an effective response to cancer immunotherapy.

Advances in high-throughput sequencing technologies and associated computational analysis pipelines allow us to investigate the interplay between tumor cells and the immune microenvironment (6, 7). These technologies enable us to broaden our knowledge of the immunobiology of tumor-host interactions by identifying immune-related genetic alterations associated with cancer development (6, 7). While genetic alterations associated with immune response in thoracic cancers have been exploited to improve treatment outcome (8, 9), the development of strong, durable responses occurs in a limited subset of patients (10); further highlighting the importance of understanding the role of host genetics, in addition to tumor genetics, in thoracic cancer development, for predicting response to immunotherapies (9, 11–13).

In this review, we discuss how host genetics affects the development of an effective immune response to thoracic cancers. We highlight knowledge gaps in our current understanding and acknowledge the limitations related to identifying host genetic factors associated with thoracic cancer susceptibility and development of effective anti-tumor immunity. Finally, we propose our unique murine model; the MexTAg Collaborative Cross (CC–MexTAg), as a strategy to overcome current limitations of conventional genetic studies in mesothelioma, to improve our knowledge about the impact of host genetics on initiating immune responses and the developing tumor microenvironment.

## HOST GENETIC FACTORS AND THORACIC CANCER SUSCEPTIBILITY

To date, many rare, high penetrance genetic variants such as *BRCA1, BRCA2, TP53, APC, and PTEN* have been associated with a genetic predisposition to cancer (14–16). However, these genetic alterations only account for a small proportion of heritable cancer genetic risk variants (14, 15). In fact, the combination of genetic variation in common low penetrance alleles and rare moderate-risk alleles has been recognized as the major genetic contributors to heritable cancer genetic predisposition (17–19).

Common low-penetrance genetic variants, including single-nucleotide polymorphisms (SNPs), have been identified by GWAS (20). These genetic studies determine the frequency of SNPs in patients compared to healthy individuals (20). More than 450 genetic variants associated with increased cancer risk for breast, prostate, colorectal and lung cancer have been identified; supporting the polygenic pattern of susceptibility in these cancers (18).

### Lung Cancer

Lung cancer is the most prevalent thoracic cancer, and chromosomal positions 15q25, 5p15.33 and 6p21 have been identified as susceptibility loci (21, 22). However, whether 15q25 is truly an independent susceptibility locus for lung cancer remains contentious, as genetic variants of nicotinic acetylcholine receptor (CHRNA) genes, which have been strongly associated with nicotine dependence and smoking behavior (23–26), are also present at this loci. Furthermore, genetic variants in 15q25 are mainly frequent in European populations and not Asian populations (23). Other independent susceptibility loci, 6p21 and 5p15, show significant levels of genetic polymorphisms associated with lung cancer risk in Asian populations, including Japanese and Korean. However, there are different risk variants within 6p21 locus observed between Asian and European populations (27).

A large meta-analysis of GWAS on Chinese and European populations identified 19 susceptibility loci significantly associated with non-small cell lung cancer (NSCLC) risk (28). Using identified genetic factors, this study proposed the polygenic risk score (PRS) strategy as an effective risk indicator of lung cancer, independent from age and smoking pack-year (28). However, the utility of the PRS strategy may be limited, as it was only used to predict lung cancer risk among the Chinese

population, not in other cohorts comprised of different ethnicity and effect size for genetic variants (28). Furthermore, most genetic variants were only associated with a small improvement in the prediction of lung cancer risk, and were not any greater than major risk factors such as smoking and age (29–31).

### Malignant Mesothelioma

Malignant mesothelioma is a relatively rare thoracic cancer, inextricably linked to asbestos exposure. The relatively low number of samples available for study means that conventional genetic studies are often underpowered (1). Consequently, despite using separate and well–characterized cohorts of control and mesothelioma patients, numerous GWAS studies have failed to identify common genetic risk factors that can be considered broadly associated with mesothelioma (32–34).

Germline mutations in *BAP1* and some DNA repair genes have been considered as predisposing genetic factors associated with mesothelioma development (34–36). However, these genetic risk factors are not specific for mesothelioma alone and can predispose people to other cancers such as uveal melanoma (37).

### Thymic Epithelial Tumors

Thymic epithelial tumors (TETs) are rare thoracic cancers arising from epithelial cells of the thymus, and can be categorized as either thymomas or thymic carcinomas (38). Our current knowledge of the etiology and genomic alterations of TETs remains limited, and like mesothelioma, the small number of patients available for study often restricts the power of conventional genetic analyses (39, 40). Although we could not find any published GWAS associated with any form of TETs, Wang et. al., identified mutated *TP53* as the most frequent genetic alteration in TET patients (40). The authors used comparative sequence analysis to show a higher mutation incidence in epigenetic regulatory genes in thymic carcinoma compared to thymoma patients (40). Additionally, a study by Cortes–Ledesma et. al., demonstrated a strong causal relationship between the loss of the highly-specialized DNA repair enzyme tyrosyl-DNA phosphodiesterase 2 (*TDP2*) and increased thymic-derived cancer predisposition in ataxia telangiectasia affected individuals (41).

## THE IMPORTANCE OF HOST GENETICS IN CANCER SUSCEPTIBILITY: SHAPING OF THE TUMOR IMMUNE MICROENVIRONMENT

The tumor microenvironment (TME) consists of a variety of immune cells, endothelial cells, fibroblasts and associated tissue cells, and develops in part from the dynamic interactions between the developing tumor and the surrounding host tissue (42). One way to describe how host-tumor interactions play a significant role in shaping the tumor microenvironment, is through the impact on 'field effect' around the tumor (43). In the context of cancer development, the term 'field effect' refers to pre-neoplastic cellular and molecular changes that arise as a consequence of long–term exposure to environmental carcinogens in morphologically healthy tissues, promoting a 'field of susceptibility' to neoplasia initiation and progression (44). For instance, the presence of a high burden and pervasive positive selection of somatic driver mutations has been identified in normal human skin (45). In a cohort of patients undergoing blepharoplasty, positively selected 'driver' mutations were found in 18–32% of normal skin cells taken from 234 biopsies of sun-exposed eyelid epidermis. These data suggest that the frequency of driver mutations in physiologically normal skin cells is surprisingly high, with multiple driver mutations in cancer associated genes found in many 'normal' cells that had not yet acquired malignant potential. These findings raise the question as to what combination of intrinsic (additional mutations) or extrinsic (host genetics/anti–tumor immunity) changes are required for cellular transformation to proceed?

In addition to driver mutations, epigenetic alterations including DNA methylation and histone modifications can play a role in establishing a field effect contributing to cancer development (46, 47). A number of studies have indicated the influence of an epigenetic field effect around the tumor by identifying aberrant DNA methylation profiles in both tumor and normal adjacent tissues (48–52).

## THE EFFECT OF KNOWN HOST GENETIC FACTORS ON TUMOR IMMUNE MICROENVIRONMENT OF THORACIC CANCERS

The influence of host genetics on the development of thoracic cancers remains poorly understood. Shen et. al., performed enrichment analysis of GWAS data to identify shared genomic regions and pathways between host genetic variants and somatic mutations in lung cancer (53). They identified an association between the SNP rs36600 at 22q12.2 and somatic mutations within *ARID1A* (53), a member of the SWI/SNF chromatin remodeling complexes associated with many cancers (54). Mutations in *ARID1A* and *ARID1B* are also associated with improved response to NSCLC patients receiving immune checkpoint blockade (ICB) therapy (55). Elevation of the tumor mutational burden, enhanced antigen presentation and cellular immunity, and increased PD-L1 expression, are all correlated with the presence of ARID1A and ARID1B mutations; suggesting that mutated ARID1A and ARID1B could serve as novel biomarkers to predict sensitivity and prognosis to ICB in advanced NSCLC patients (55). Additionally, rare missense variants in genes encoding SWI/SNF chromatin remodeling components and genes encoding the histone methyl transferases, *SETD2* and *SETDB1*, were identified in a cohort of Japanese mesothelioma patients (56).

Furthermore, *TRB*:rs1964986 and *IDO1*:rs10108662 have been identified as the two most significant SNPs associated with the risk of disease recurrence and death respectively in

early stage lung cancer (57). When assessing the functionality of T cells between low and high-risk groups relative to healthy controls (57), high-risk subjects exhibited lower cytotoxicity and reduced granulation of T cells, as demonstrated by increased expression of T cell inhibitory checkpoint gene Indoleamine 2, 3-dioxygenase (*IDO1*) and decreased expression of the T cell cytotoxicity genes *IL2*, Perforin 1 (*PRF*) and Granzyme B (*GZMB*). These data support the hypothesis that mutations of host immune genes affect the TME and thus, prognosis of NSCLC *via* suppression of T cell antitumor immunity (57).

Additionally, epigenetic alterations of tissues derived from NSCLC patients revealed the upregulation of *CTLA4*, *PDCD1 via* hypomethylation in tumors *versus* non-tumor tissues (58). Effects of epigenetic alterations in shaping immune tumor microenvironment was also demonstrated by strong correlation between site-specific DNA methylation of CpG markers of cancers and transcription of genes associated with immune infiltration (59).

In contrast to NSCLC, there are limited published studies that investigate the role of host genetic factors in shaping the tumor immune microenvironment of mesothelioma and TETs. Costa et. al., identified lower expression of miR-320 in mesothelioma tumors compared to normal tissues by performing differential miRNA expression analysis on 14 formalin-fixed paraffin-embedded tumors and six normal controls (60). They also identified an association between p53-induced expression of miR-320, miR-200a and miR-34a with reduced expression of *PD-L1* in mesothelioma cell lines (60). These data indicate defective p53-induced miRNA response as a possible contributor to immune evasion in mesothelioma by increasing tumor *PD-L1* expression (60). Reduced expression of major histocompatibility complex (*MHC*) and autoimmune regulator (*AIRE*) genes has been associated with defective T cell maturation in thymoma patients (61, 62) and as such, the reduced expression of *MHC* and *AIRE* were proposed as genetic alterations explaining the association between thymomas and autoimmune disorders (61).

More recently, a number of studies have significantly advanced our understanding of the molecular biology of mesothelioma (63–67). Through the application of next generation sequencing technologies and innovative bioinformatic analyses, these studies have demonstrated the complex heterogeneity within and between tumors; expanding the classic epithelioid, biphasic and sarcomatoid paradigm to at least 4 distinct molecular subtypes, with a molecular gradient along the epithelial-to mesenchymal transition spectrum separating the two extreme epithelioid-like and mesenchymal-like groups (63, 65–67). Additionally, the NSG approach has further advanced our knowledge of the key mutational events associated with mesothelioma, linking a number of unique cancer signaling pathways with mesothelioma (64, 65). However, despite these advances, our understanding of how host genetics impacts mesothelioma onset remains underdeveloped.

In summary, studies investigating the role of immune related genetic factors in NSCLC have identified suggestive genetic variants capable of shaping the tumor immune microenvironment and affecting cellular immunity. However, there are a limited number of studies identifying immune related genetic factors in mesothelioma and TETs, highlighting the dearth in our knowledge of, and ability to identify how host genetic factors shape the immune tumor microenvironment of rare thoracic cancers.

## OVERCOMING LIMITATIONS FOR IDENTIFYING HOST GENETIC FACTORS ASSOCIATED WITH THORACIC CANCERS

GWAS have been used to identify susceptibility loci in common cancers such as breast, prostate, colorectal and lung cancer (22, 68), but they have been less effective for rare cancers including mesothelioma (32). In fact, the suitability of GWAS for rare cancers is often restricted by the relatively small number of patients available for studies; thus any identified genetic variants are often limited to the study cohort and not likely to have a significant influence on disease outcome (32, 34, 68–71). Furthermore, the absence of standardized protocols for collecting environmental exposure data in addition to the lack of accurate, consistent and defined phenotypic data to match with genomic information, are additional potential limitations for human genetic studies of thoracic cancers (72–74).

To overcome these limitations, mouse models that can faithfully mimic human cancer development, in a well-controlled and modulated environment are needed for identifying translatable host genetic variants (75). Moreover, such mouse models need to be sufficiently genetically diverse to maximize the chance of genetic polymorphisms associated with cancer development. The ideal mouse model would enable rapid identification of genes associated with cancer homologous to human genetic studies (7).

## ADVANCEMENTS IN RECOMBINANT INBRED MOUSE MODELS FOR HOST GENETIC STUDIES OF THORACIC CANCERS

Recombinant inbred (RI) mice are generated by breeding two or more different mouse strains to genetic stability (76). Historically, RI mice have been used to identify genomic regions, referred to as quantitative trait loci (QTLs), that are associated with particular disease phenotypes (77). The main advantage to using RI mouse strains compared to classical simple (F2) cross breeding is their improved reproducibility due to the ability to test a phenotype in any number of individuals with the same defined genetic constitution (77). The use of RI mice allows unknown genes to be integrated into the known genetic map by comparing the inheritance pattern of an unknown gene or trait in a panel of RI strains with that of known markers. Therefore, these models have been widely used as a robust and rapid method of gene mapping of polygenic traits and diseases (77).

## USE OF CLASSICAL AND TRADITIONAL RECOMBINANT INBRED MOUSE MODELS

Classical mouse genetic studies identified *Kras2* as a major lung cancer susceptibility locus using the F2 progeny of A/J (susceptible) and C3H/He (resistant) mouse strains in a urethane-induced lung cancer model (78). Similarly, experiments involving the progeny of BALB/c and SWR/J mouse strains identified *Par2* and *Par4* as modifier loci that specifically affected tumor initiation, progression and lung tumor multiplicity (79). Additional, whole-genome linkage disequilibrium analysis on 25 inbred mouse strains identified 63 markers including *Kras* and *Pas1* loci, supporting the association of *Kras* loci with lung cancer susceptibility (80). Traditionally, bi-parental RI mouse strains were used for identifying susceptibility loci of diseases with polygenic pattern of inheritance (78, 81, 82). However, the usefulness of traditional bi-parental RI mouse strains in genetic studies is limited by the inherent low genetic diversity associated with using only two parental genomes, which have large 'identical by descent' (IBD) regions in which both parental strains have the same alleles (83). Such IBD regions are 'blind spots', having little or no variation, thus limiting the potential for gene mapping (84).

## THE COLLABORATIVE CROSS (CC)

The Collaborative cross (CC) is a powerful mouse genetic resource, comprising hundreds of independent RI mouse strains developed from eight founder strains selected to maximize genetic diversity (84–86). The CC harnesses 90% of the common allelic diversity of the entire mouse species (84) and has enhanced mapping ability due to the much greater degree of polymorphisms derived from the eight diverse founder strains, rather than the two somewhat similar strains used in conventional RI mapping, as well as the greater number of strains available. Conventional mapping of simple Mendelian traits requires approximately 100 backcrossed mice to obtain 1 cM (approximately 2 megabase pairs; Mbp) resolution. The same resolution can be obtained by testing ~26 BXD RI strains. In contrast, with as few as 70 CC strains, mapping resolution can be less than 40 thousand bp, i.e. approximately to the single gene level (85) and even achieve down-to-the-base resolution (87). Thus, the CC allows mapping of loci with unprecedented accuracy. The CC has been successfully used to study diseases with polygenic inheritance such as melanoma, prostate cancer, diabetes and osteoporosis (86, 88–91). It is also powerful in allowing development of novel disease models (92).

The application of the CC to understanding cancer has been best studied for melanoma and skin cancer. A series of investigations made several important discoveries, such as that every stage of melanoma progression was subject to control by genetic variation (88); that UV–induced and spontaneous cancers were mediated by different genetic mechanisms (93) the specific mutation causing nevus development was identified (94); and the molecular mechanism for giant congenital nevi was defined (95).

## USING GENETICALLY ENGINEERED MOUSE MODELS FOR STUDYING THE IMPACT OF HOST GENETICS ON THORACIC CANCER DEVELOPMENT

Numerous genetically engineered mice models have been developed for modelling and studying genetic heterogeneity of human malignancies (96). Recent technical advances in the manipulation and sequencing of mouse genomes has promoted the use of mouse models as an experimentally tractable system for testing hypotheses generated from human genetic studies (96). Such engineered models have also allowed the identification of novel candidate mechanisms linking the impact of host genetics and cancer development (96, 97). As the development and use of genetically engineered mouse models is time-consuming and expensive, the generation of models with high tumor penetrance and short cancer latency are often favored, as they are more viable in terms of research time and cost (75, 98).

*Kras2*$^{LA2}$ and *Trp53*$^{\text{LSL-R172H/þ}}$ mice are the most common used models in host genetic studies of lung cancer (96, 99, 100). However, mice with mutations in *Kras2* and *Trp53* are highly predisposed to other cancers (101, 102) and cancer development can be triggered by spontaneous oncogene recombination events; thus these models are not necessarily lung cancer specific and therefore some mechanisms of carcinogenesis may not accurately recapitulate human disease (99, 100).

There are many excellent mouse models for mesothelioma research that mimic the genetic defects found in human disease. Knockout (KO) mouse models with heterozygous mutations in *Bap1, CDKN2A*, neurofibromin 2 (*Nf2*), or *p53* have been used to study the effect of genetic alterations on asbestos-induced mesothelioma susceptibility (103–112). These studies demonstrate significantly higher incidence of mesothelioma in the presence, or absence of asbestos in mice with *Bap*$^{(+/-)}$ and *Nf2*$^{(+/-)}$ mutations compared to wild-type (wt) mice (103–112). However, all animal models have their limitations. While some conditional KO models demonstrate increased mesothelioma incidence, they also have moderate to high levels of unrelated (non-mesothelioma) cancers; presumable a consequence of off-target deletion of key tumor suppressor genes (105, 108, 110). However, recently published CRE-mediated conditional KO models only develop disease in CRE-expressing tissues (109, 113). Mesothelioma incidence in *Bap1*$^{(+\backslash-)}$ mice ranged between 36-60% depending on asbestos doses (41, 106). However, while *Bap1*$^{(+\backslash-)}$ mice develop mesothelioma, they also develop other cancers such as uveal and cutaneous melanoma (37). Furthermore, *Bap1*$^{(+\backslash-)}$ mice develop mesothelioma after exposure to doses of asbestos fibers that are unlikely to induce mesothelioma in wt mice (106).

## ASBESTOS INDUCED MESOTHELIOMA MexTAg MOUSE MODEL

There is no absolute consensus over which is the best model system for studying mesothelioma; some groups prefer to use conditional knockout models, as they replicate the genetic deletions observed in human disease, while others prefer alternative models that require asbestos induction and have limited unrelated cancer development. We developed the transgenic C57BL/6 MexTAg mouse model expressing SV40 large T antigen directed to mesothelial cells by use of cell-type specific mesothelin promoter as a tool for the pre-clinical evaluation of asbestos-induced mesothelioma (114). Importantly, MexTAg mice develop mesothelioma with similar pathology to humans, but only after asbestos exposure (115). Furthermore, MexTAg mice have high disease incidence (> 85%) and are less likely to develop unrelated tumors compared to wild type mice or some heterozygous or conditional knockout models (103–112). Comparing gene expression profiles of MexTAg mice and wt mesothelioma with their counterpart normal mesothelial cells, exhibits overlapping gene expression profiles, suggesting a similar overall mechanism of mesothelioma development in transgenic MexTAg mice (116). Expression of the TAg transgene does not affect the overall mechanism of mesothelioma development, but rather phenocopies *p16* loss (117) and as a consequence onset of disease is more rapid, significantly increasing the incidence and rate of mesothelioma development compared to wt mice (114).

## USING THE CC-MexTAg MOUSE MODEL TO ASSESS THE IMPACT OF HOST GENETICS ON THE DEVELOPING ANTI-TUMOR IMMUNE RESPONSE TO MESOTHELIOMA

To investigate how host genetics might impact asbestos related disease development (ARD), it is important to use a model in which only ARD (and not unrelated tumors) occur and high incidence. We developed the MexTAg Collaborative Cross to investigate how a hosts' genetic background influences the development of mesothelioma in asbestos-exposed individuals. Combining the genetic diversity inherent in the CC with the high incidence of asbestos–induced disease and rare onset of unrelated spontaneous tumors of MexTAg mice, provides an ideal model to define with unprecedented accuracy the genes and associated pathways that affect susceptibility and resistance to disease. In this model, the F1 progeny of CC x MexTAg mice (CC–MexTAg mice) are exposed to asbestos and monitored for up to 18 months, or until asbestos related disease (ARD) developed and progressed to a clearly defined endpoint. ARD phenotypic traits such as overall survival, disease latency and progression for each CC–MexTAg group, can be analyzed using the GeneMiner™ bioinformatic portal (87), where candidate modifier genes are mapped with ARD phenotype as a quantitative trait. Genome wide scans defined chromosomal locations of peak SNPs associated with each of the characterized ARD phenotypes. To date, we have generated and asbestos-exposed over 2500 individual CC–MexTAg mice progeny of 72 unique CC strains. At the time of writing 55 CC–MexTAg groups that have completed the observation period. These preliminary data indicate greater than 3-fold variation in median overall survival. This shows the power of the CC approach, given that the parental MexTAg mice survive 365 days. An additional 20 CC–MexTAg groups remain under study, and we envisage accrual of complete data by late 2021.

Importantly, the development of the CC–MexTAg model has not only enabled data collection on numerous ARD phenotypic traits, but has enabled the generation of a large repository of tumor samples and tumor-derived cell lines, collected from animals that are either relatively resistant or highly sensitive to asbestos-induced cancer. Given recent insights provided by the CheckMate 743 study demonstrating for the first time first-line immune checkpoint blockade (nivolumab plus ipilimumab) provided a significant and clinically meaningful improvement in overall survival *versus* platinum plus pemetrexed chemotherapy for mesothelioma (118), this unique biological resource can be exploited for comprehensive genetic and immunohistological analysis on tumors collected from CC-MexTAg mice (**Figure 1**). The CCMT biobank will complement many of the recent 'multi-omic' informed human mesothelioma datasets, helping to overcome some of the limitations associated with conventional genetic studies aimed at identifying the role of host genetic factors associated with the development and immunological control of rare thoracic cancers like mesothelioma.

We believe this strategy will not only allow identification of host modifier genes associated with ARD development, but when correlated with data on immune microenvironment will help elucidate what is required to generate an effective immune response to asbestos induced cancers. In addition, our strategy provides a rational approach that could be applied to other thoracic cancers by taking advantage of the power of CC to define a protective host genetic background.

## SUMMARY AND CONCLUDING REMARKS

Thoracic cancers are a leading cause of death worldwide. While advances have been made in our understanding of how genetic alternations impact cancer development and treatment outcomes for common thoracic malignancies like lung cancer, our knowledge remains limited for less common cancers such as mesothelioma and TETs. Moreover, there is a paucity in our understanding of the complex biological interplay between the tumor and the immune microenvironment. Understanding how the host immune system interacts with a developing tumor is essential for the rational development of new or improved treatment regimens for thoracic malignancies. An often overlooked characteristic of the tumor host interaction, is the influence a hosts' background genetics has on tumor development and how this affects treatment response. While previous conventional genomic studies are often limited to more common cancers, recent technical advances in computation biology, combined with the use of 'system genetics' approaches, now provide

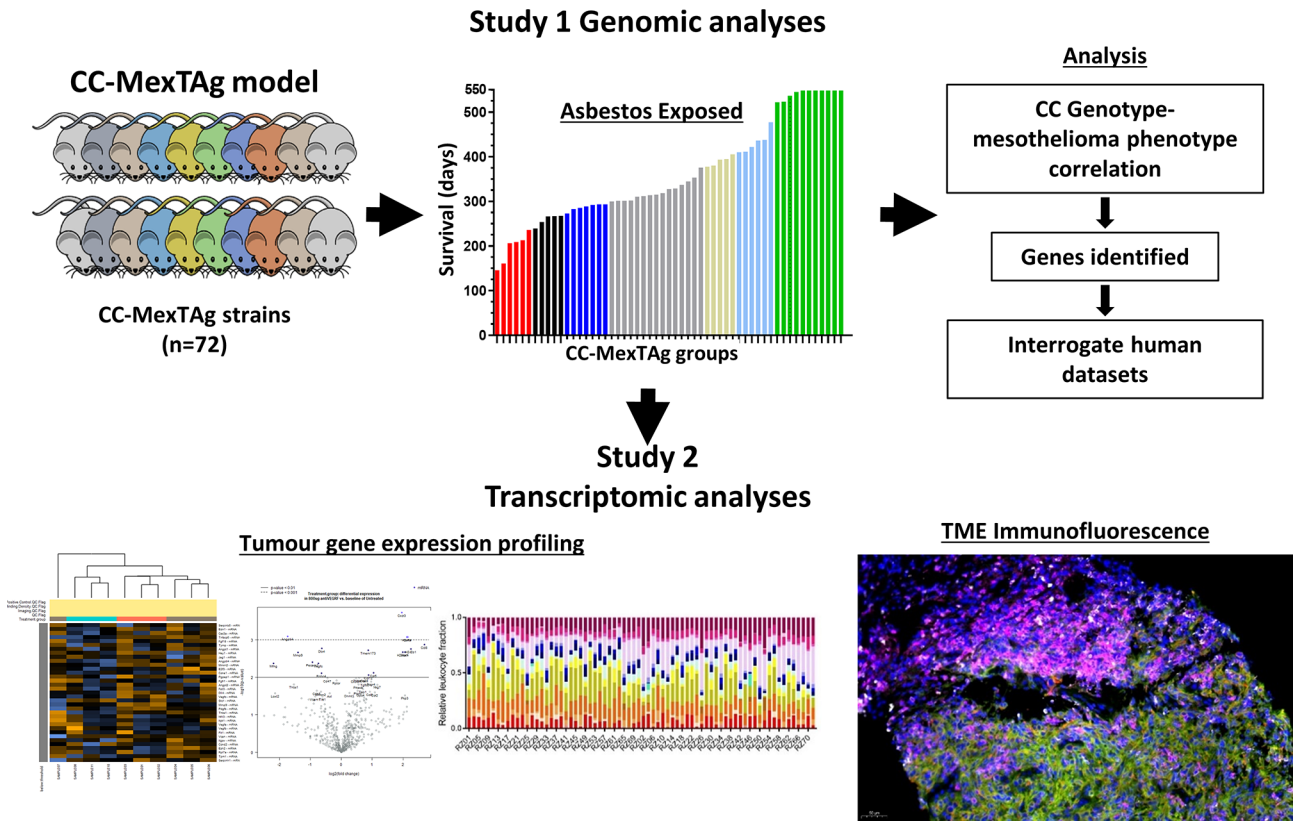


**FIGURE 1** | A schematic of the CC-MexTAg experimental design. *The generation of CC-MexTAg mice and their exposure to asbestos (Study 1):* Briefly, candidate modifier genes will be mapped with mesothelioma-free survival, as a quantitative trait using the GeneMiner Bioinformatics pipeline. Genome wide scans will be used to define chromosomal locations of peak single nucleotide polymorphism (SNPs) associated with each of the characterized mesothelioma phenotypes, such as disease progression, latency, overall survival, and mesothelioma incidence. *Gene expression analysis and immunofluorescence analysis of tumors collected from CC-MexTAg mice exposed to asbestos (Study 2):* Comprehensive analyses of gene expression profiles and immune cell infiltrate of the tumor microenvironment will be performed to identify any differences between distinct CC-MexTAg groups. These data will be correlated back to phenotypic data from Study 1, to build a broader understanding of the impact of host genetics on asbestos related disease development.

a framework for investigating more rare thoracic malignancies such as mesothelioma and TETs. To address these issues, we have developed the MexTAg Collaborative cross to identify host genes that affect asbestos-related disease. The CC-MexTAg mouse model embraces a systems genetics approach, linking the power of CC's defined host background genetics, with gene expression analysis and unparalleled detailed spatial assessment of the immunological milieu of asbestos-induced mesothelioma. This unique model allows rapid identification of key host modifier genes and a comprehensive genomic and histopathological analyses of biological pathways associated with asbestos-induced mesothelioma development. These data can then be validated by interrogating the numerous data sets produced from current human genetic studies.

In conclusion, the CC-MexTAg mouse model, particularly in combination with contemporaneous tumor expression data, will provide a detailed picture of the role of modifier genes and their biological pathways associated with immune response in mesothelioma. Such data is essential to help identify potential druggable and translatable targets for the development of better treatment options and developing an effective anti-tumor immune response in malignant mesothelioma patients.

## AUTHOR CONTRIBUTIONS

SF, KBe, SM and RK contributed to conception and design of the review. SF, KBu and KBe performed, collected and analyzed CC–MexTAg data. KBe and SF wrote the first draft of the manuscript. RK, SM, KBu, and GM wrote sections of the manuscript. All authors contributed to the article and approved the submitted version.

## FUNDING

The CC-MexTAg research program has been supported with funding from The US Department of Defense (CDMRP Ideas Award; CA170299), The National Health and Medical Research Council of Australia (APP1163861) and Insurance and Care NSW (icare).

## REFERENCES


1. Siesling S, van der Zwan JM, Izarzugaza I, Jaal J, Treasure T, Foschi R, et al. Rare Thoracic Cancers, Including Peritoneum Mesothelioma. *Eur J Cancer* (2012) 48(7):949–60. doi: 10.1016/j.ejca.2012.02.047
2. Duruisseaux M, Rouquette I, Adam J, Cortot A, Cazes A, Gibault L, et al. Efficacy of PD-1/PD-L1 Immune Checkpoint Inhibitors and PD-L1 Testing in Thoracic Cancers. *Ann Pathol* (2017) 8(1):61–78. doi: 10.1016/j.annpat.2016.12.009
3. Facchinetti F, Marabelle A, Rossi G, Soria J-C, Besse B, Tiseo M. Moving Immune Checkpoint Blockade in Thoracic Tumors Beyond NSCLC. *J Thorac Oncol* (2016) 11(11):1819–36. doi: 10.1016/j.jtho.2016.05.027
4. Gasparri ML, Ruscito I, Taghavi K, Farooqi AA, Papadia A, Focaccetti C, et al. The Immunobiology of Cancer: From Tumor Escape to Cancer Immunoediting Towards Immunotherapy in Gynecologic Oncology. In: Farooqi A, Ismail M. eds. *Molecular Oncology: Underlying Mechanisms and Translational Advancements*. Cham: Springer (2017). p. 193–204. doi: 10.1007/978-3-319-53082-6_9
5. Byers LA, Rudin CM. Small Cell Lung Cancer: Where do We Go From Here? *Cancer* (2015) 121(5):664–72. doi: 10.1002/cncr.29098
6. Kiyotani K, Park J-H, Inoue H, Husain A, Olugbile S, Zewde M, et al. Integrated Analysis of Somatic Mutations and Immune Microenvironment in Malignant Pleural Mesothelioma. *Oncoimmunology* (2017) 6(2):e1278330. doi: 10.1080/2162402X.2016.1278330
7. Li H, Auwerx J. Mouse Systems Genetics as a Prelude to Precision Medicine. *Trends Genet* (2020) 36(4):259–72. doi: 10.1016/j.tig.2020.01.004
8. Izzi V, Masuelli L, Tresoldi I, Foti C, Modesti A, Bei R. Immunity and Malignant Mesothelioma: From Mesothelial Cell Damage to Tumor Development and Immune Response-Based Therapies. *Cancer Lett* (2012) 322(1):18–34. doi: 10.1016/j.canlet.2012.02.034
9. Freudenstein D, Litchfield C, Caramia F, Wright G, Solomon BJ, Ball D, et al. Tp53 Status, Patient Sex, and the Immune Response as Determinants of Lung Cancer Patient Survival. *Cancers* (2020) 12(6):1535. doi: 10.3390/cancers12061535
10. Topalian SL, Hodi FS, Brahmer JR, Gettinger SN, Smith DC, McDermott DF, et al. Safety, Activity, and Immune Correlates of Anti–PD-1 Antibody in Cancer. *N Engl J Med* (2012) 366(26):2443–54. doi: 10.1056/NEJMoa1200690
11. Wang E, Uccellini L, Marincola FM. A Genetic Inference on Cancer Immune Responsiveness. *Oncoimmunology* (2012) 1(4):520–5. doi: 10.4161/onci.19531
12. Sui X, Ma J, Han W, Wang X, Fang Y, Li D, et al. The Anticancer Immune Response of anti-PD-1/PD-L1 and the Genetic Determinants of Response to anti-PD-1/PD-L1 Antibodies in Cancer Patients. *Oncotarget* (2015) 6(23):19393. doi: 10.18632/oncotarget.5107
13. Lim YW, Chen-Harris H, Mayba O, Lianoglou S, Wuster A, Bhangale T, et al. Germline Genetic Polymorphisms Influence Tumor Gene Expression and Immune Cell Infiltration. *Proc Natl Acad Sci* (2018) 115(50):E11701–10. doi: 10.1073/pnas.1804506115
14. Chubb D, Broderick P, Dobbins SE, Frampton M, Kinnersley B, Penegar S, et al. Rare Disruptive Mutations and Their Contribution to the Heritable Risk of Colorectal Cancer. *Nat Commun* (2016) 7(1):1–7. doi: 10.1038/ncomms11883
15. Yurgelun MB, Kulke MH, Fuchs CS, Allen BA, Uno H, Hornick JL, et al. Cancer Susceptibility Gene Mutations in Individuals With Colorectal Cancer. *J Clin Oncol* (2017) 35(10):1086. doi: 10.1200/JCO.2016.71.0012
16. AlDubayan SH, Giannakis M, Moore ND, Han GC, Reardon B, Hamada T, et al. Inherited DNA-Repair Defects in Colorectal Cancer. *Am J Hum Genet* (2018) 102(3):401–14. doi: 10.1016/j.ajhg.2018.01.018
17. Khera AV, Chaffin M, Aragam KG, Haas ME, Roselli C, Choi SH, et al. Genome-Wide Polygenic Scores for Common Diseases Identify Individuals With Risk Equivalent to Monogenic Mutations. *Nat Genet* (2018) 50(9):1219–24. doi: 10.1038/s41588-018-0183-z
18. Sud A, Kinnersley B, Houlston RS. Genome-Wide Association Studies of Cancer: Current Insights and Future Perspectives. *Nat Rev Cancer* (2017) 17(11):692–704. doi: 10.1038/nrc.2017.82
19. Frank SA. Genetic Predisposition to Cancer—Insights From Population Genetics. *Nat Rev Genet* (2004) 5(10):764–72. doi: 10.1038/nrg1450
20. Stadler ZK, Thom P, Robson ME, Weitzel JN, Kauff ND, Hurley KE, et al. Genome-Wide Association Studies of Cancer. *J Clin Oncol* (2010) 28(27):4255. doi: 10.1200/JCO.2009.25.7816
21. Wang Y, McKay JD, Rafnar T, Wang Z, Timofeeva MN, Broderick P, et al. Rare Variants of Large Effect in BRCA2 and CHEK2 Affect Risk of Lung Cancer. *Nat Genet* (2014) 46(7):736–41. doi: 10.1038/ng.3002
22. Timofeeva MN, Hung RJ, Rafnar T, Christiani DC, Field JK, Bickeböller H, et al. Influence of Common Genetic Variation on Lung Cancer Risk: Meta-Analysis of 14 900 Cases and 29 485 Controls. *Hum Mol Genet* (2012) 21(22):4980–95. doi: 10.1093/hmg/dds334
23. McKay JD, Hung RJ, Han Y, Zong X, Carreras-Torres R, Christiani DC, et al. Large-Scale Association Analysis Identifies New Lung Cancer Susceptibility Loci and Heterogeneity in Genetic Susceptibility Across Histological Subtypes. *Nat Genet* (2017) 49(7):1126–32. doi: 10.1038/ng.3892
24. Kaur-Knudsen D, Nordestgaard BG, Bojesen SE. CHRNA3 Genotype, Nicotine Dependence, Lung Function and Disease in the General Population. *Eur Respir J* (2012) 40(6):1538–44. doi: 10.1183/09031936.00176811
25. Pérez-Morales R, González-Zamora A, González-Delgado MF, Calleros Rincón EY, Olivas Calderon EH, Martínez-Ramírez OC, et al. Chrna3 rs1051730 and CHRNA5 rs16969968 Polymorphisms Are Associated With Heavy Smoking, Lung Cancer, and Chronic Obstructive Pulmonary Disease in a Mexican Population. *Ann Hum Genet* (2018) 82(6):415–24. doi: 10.1111/ahg.12264
26. Wang Y, Broderick P, Matakidou A, Eisen T, Houlston RS. Role of 5p15. 33 (Tert-CLPTM1L), 6p21. 33 and 15q25. 1 (Chrna5-CHRNA3) Variation and Lung Cancer Risk in Never-Smokers. *Carcinogenesis* (2010) 31(2):234–8. doi: 10.1093/carcin/bgp287
27. Miki D, Kubo M, Takahashi A, Yoon K-A, Kim J, Lee GK, et al. Variation in TP63 Is Associated With Lung Adenocarcinoma Susceptibility in Japanese and Korean Populations. *Nat Genet* (2010) 42(10):893–6. doi: 10.1038/ng.667
28. Dai J, Lv J, Zhu M, Wang Y, Qin N, Ma H, et al. Identification of Risk Loci and a Polygenic Risk Score for Lung Cancer: A Large-Scale Prospective Cohort Study in Chinese Populations. *Lancet Respir Med* (2019) 7(10):881–91. doi: 10.1016/S2213-2600(19)30144-4
29. Bossé Y, Amos CI. A Decade of GWAS Results in Lung Cancer. *Cancer Epidemiol Biomarkers Prev* (2018) 27(4):363–79. doi: 10.1158/1055-9965.EPI-16-0794
30. Sampson JN, Wheeler WA, Yeager M, Panagiotou O, Wang Z, Berndt SI, et al. Analysis of Heritability and Shared Heritability Based on Genome-Wide Association Studies for 13 Cancer Types. *JNCI: J Natl Cancer Inst* (2015) 107(12):djv279. doi: 10.1093/jnci/djv279
31. Lichtenstein P, Holm NV, Verkasalo PK, Iliadou A, Kaprio J, Koskenvuo M, et al. Environmental and Heritable Factors in the Causation of Cancer—Analyses of Cohorts of Twins From Sweden, Denmark, and Finland. *N Engl J Med* (2000) 343(2):78–85. doi: 10.1056/NEJM200007133430201
32. Cadby G, Mukherjee S, Musk AWB, Reid A, Garlepp M, Dick I, et al. A Genome-Wide Association Study for Malignant Mesothelioma Risk. *Lung Cancer* (2013) 82(1):1–8. doi: 10.1016/j.lungcan.2013.04.018
33. Tunesi S, Ferrante D, Mirabelli D, Andorno S, Betti M, Fiorito G, et al. Gene–Asbestos Interaction in Malignant Pleural Mesothelioma Susceptibility. *Carcinogenesis* (2015) 36(10):1129–35. doi: 10.1093/carcin/bgv097
34. Matullo G, Guarrera S, Betti M, Fiorito G, Ferrante D, Voglino F, et al. Genetic Variants Associated With Increased Risk of Malignant Pleural Mesothelioma: A Genome-Wide Association Study. *PLoS One* (2013) 8(4):e61253. doi: 10.1371/journal.pone.0061253
35. Dianzani I, Gibello L, Biava A, Giordano M, Bertolotti M, Betti M, et al. Polymorphisms in DNA Repair Genes as Risk Factors for Asbestos-Related Malignant Mesothelioma in a General Population Study. *Mutat Res/Fundam Mol Mech Mutagen* (2006) 599(1-2):124–34. doi: 10.1016/j.mrfmmm.2006.02.005
36. Testa JR, Cheung M, Pei J, Below JE, Tan Y, Sementino E, et al. Germline BAP1 Mutations Predispose to Malignant Mesothelioma. *Nat Genet* (2011) 43(10):1022–5. doi: 10.1038/ng.912
37. Carbone M, Ferris LK, Baumann F, Napolitano A, Lum CA, Flores EG, et al. BAP1 Cancer Syndrome: Malignant Mesothelioma, Uveal and Cutaneous

Melanoma, and Mbaits. *J Trans Med* (2012) 10(1):179. doi: 10.1186/1479-5876-10-179
38. Travis WD, Brambilla E, Burke AP, Marx A, Nicholson AG. Introduction to the 2015 World Health Organization Classification of Tumors of the Lung, Pleura, Thymus, and Heart. *J Thorac Oncol* (2015) 10(9):1240–2. doi: 10.1097/JTO.0000000000000663
39. Girard N. Thymic Tumors: Relevant Molecular Data in the Clinic. *J Thorac Oncol* (2010) 5(10):S291–S5. doi: 10.1097/JTO.0b013e3181f209b9
40. Wang Y, Thomas A, Lau C, Rajan A, Zhu Y, Killian JK, et al. Mutations of Epigenetic Regulatory Genes Are Common in Thymic Carcinomas. *Sci Rep* (2014) 4:7336. doi: 10.1038/srep07336
41. Álvarez-Quilón A, Terrón-Bautista J, Delgado-Sainz I, Serrano-Benítez A, Romero-Granados R, Martínez-García PM, et al. Endogenous Topoisomerase II-mediated DNA Breaks Drive Thymic Cancer Predisposition Linked to ATM Deficiency. *Nat Commun* (2020) 11(1):1–14. doi: 10.1038/s41467-020-14638-w
42. Whiteside TL. The Tumor Microenvironment and Its Role in Promoting Tumor Growth. *Oncogene* (2008) 27(45):5904–12. doi: 10.1038/onc.2008.271
43. Stearman RS, Dwyer-Nield L, Grady MC, Malkinson AM, Geraci MW. A Macrophage Gene Expression Signature Defines a Field Effect in the Lung Tumor Microenvironment. *Cancer Res* (2008) 68(1):34–43. doi: 10.1158/0008-5472.CAN-07-0988
44. Lochhead P, Chan AT, Nishihara R, Fuchs CS, Beck AH, Giovannucci E, et al. Etiologic Field Effect: Reappraisal of the Field Effect Concept in Cancer Predisposition and Progression. *Modern Pathol* (2015) 28(1):14–29. doi: 10.1038/modpathol.2014.81
45. Martincorena I, Roshan A, Gerstung M, Ellis P, Van Loo P, McLaren S, et al. Tumor Evolution. High Burden and Pervasive Positive Selection of Somatic Mutations in Normal Human Skin. *Science* (2015) 348(6237):880–6. doi: 10.1126/science.aaa6806
46. Klutstein M, Moss J, Kaplan T, Cedar H. Contribution of Epigenetic Mechanisms to Variation in Cancer Risk Among Tissues. *Proc Natl Acad Sci U S A* (2017) 114(9):2230–4. doi: 10.1073/pnas.1616556114
47. Bezu L, Wu Chuang A, Liu P, Kroemer G, Kepp O. Immunological Effects of Epigenetic Modifiers. *Cancers* (2019) 11(12):1911. doi: 10.3390/cancers11121911
48. Yang B, Bhusari S, Kueck J, Weeratunga P, Wagner J, Leverson G, et al. Methylation Profiling Defines an Extensive Field Defect in Histologically Normal Prostate Tissues Associated With Prostate Cancer. *Neoplasia* (2013) 15(4):399–408. doi: 10.1593/neo.13280
49. Yang B, Etheridge T, McCormick J, Schultz A, Khemees TA, Damaschke N, et al. Validation of an Epigenetic Field of Susceptibility to Detect Significant Prostate Cancer From non-Tumor Biopsies. *Clin Epigenet* (2019) 11(1):168. doi: 10.1186/s13148-019-0771-5
50. Pereira AL, Magalhaes L, Moreira FC, Reis-das-Merces L, Vidal AF, Ribeiro-Dos-Santos AM, et al. Epigenetic Field Cancerization in Gastric Cancer: microRNAs as Promising Biomarkers. *J Cancer* (2019) 10(6):1560–9. doi: 10.7150/jca.27457
51. Sugai T, Yoshida M, Eizuka M, Uesugii N, Habano W, Otsuka K, et al. Analysis of the DNA Methylation Level of Cancer-Related Genes in Colorectal Cancer and the Surrounding Normal Mucosa. *Clin Epigenet* (2017) 9:55. doi: 10.1186/s13148-017-0352-4
52. Daniunaite K, Sestokaite A, Kubiliute R, Stuopelyte K, Kettunen E, Husgafvel-Pursiainen K, et al. Frequent DNA Methylation Changes in Cancerous and Noncancerous Lung Tissues From Smokers With non-Small Cell Lung Cancer. *Mutagenesis* (2020) 35(5):373–9. doi: 10.1093/mutage/geaa022
53. Wang Y, Wang C, Zhang J, Zhu M, Zhang X, Li Z, et al. Interaction Analysis Between Germline Susceptibility Loci and Somatic Alterations in Lung Cancer. *Int J Cancer* (2018) 143(4):878–85. doi: 10.1002/ijc.31351
54. Bitler BG, Fatkhutdinov N, Zhang R. Potential Therapeutic Targets in ARID1A-mutated Cancers. *Expert Opin Ther Targets* (2015) 19(11):1419–22. doi: 10.1517/14728222.2015.1062879
55. Sun D, Tian L, Zhu Y, Wo Y, Liu Q, Liu S, et al. Subunits of ARID1 Serve as Novel Biomarkers for the Sensitivity to Immune Checkpoint Inhibitors and Prognosis of Advanced non-Small Cell Lung Cancer. *Mol Med* (2020) 26(1):1–9. doi: 10.1186/s10020-020-00208-9
56. Yoshikawa Y, Emi M, Nakano T, Gaudino G. Mesothelioma Developing in Carriers of Inherited Genetic Mutations. *Trans Lung Cancer Res* (2020) 9 (Suppl 1):S67. doi: 10.21037/tlcr.2019.11.15
57. Wang Q, Gu J, Wang L, Chang DW, Ye Y, Huang M, et al. Genetic Associations of T Cell Cancer Immune Response-Related Genes With T Cell Phenotypes and Clinical Outcomes of Early-Stage Lung Cancer. *J ImmunoTher Cancer* (2020) 8(2):e000336. doi: 10.1136/jitc-2019-000336
58. Marwitz S, Scheufele S, Perner S, Reck M, Ammerpohl O, Goldmann T. Epigenetic Modifications of the Immune-Checkpoint Genes CTLA4 and PDCD1 in non-Small Cell Lung Cancer Results in Increased Expression. *Clin Epigenet* (2017) 9:51. doi: 10.1186/s13148-017-0354-2
59. Bacolod MD, Barany F, Fisher PB. Can CpG Methylation Serve as Surrogate Markers for Immune Infiltration in Cancer? *Adv Cancer Res* (2019) 143:351–84. doi: 10.1016/bs.acr.2019.03.007
60. Costa C, Indovina P, Mattioli E, Forte IM, Iannuzzi CA, Luzzi L, et al. P53-Regulated miR-320a Targets PDL1 and Is Downregulated in Malignant Mesothelioma. *Cell Death Dis* (2020) 11(9):1–15. doi: 10.1038/s41419-020-02940-w
61. Weksler B, Lu B. Alterations of the Immune System in Thymic Malignancies. *J Thorac Oncol* (2014) 9(9):S137–42. doi: 10.1097/JTO.0000000000000299
62. Lippner EA, Lewis DB, Robinson WH, Katsumoto TR. Paraneoplastic and Therapy-Related Immune Complications in Thymic Malignancies. *Curr Treat Options Oncol* (2019) 20(7):62. doi: 10.1007/s11864-019-0661-2
63. Wadowski B, De Rienzo A, Bueno R. The Molecular Basis of Malignant Pleural Mesothelioma. *Thorac Surg Clin* (2020) 30(4):383–93. doi: 10.1016/j.thorsurg.2020.08.005
64. Hmeljak J, Sanchez-Vega F, Hoadley KA, Shih J, Stewart C, Heiman D, et al. Integrative Molecular Characterization of Malignant Pleural Mesothelioma. *Cancer Discov* (2018) 8(12):1548–65. doi: 10.1158/2159-8290.CD-18-1181
65. Bueno R, Stawiski EW, Goldstein LD, Durinck S, De Rienzo A, Modrusan Z, et al. Comprehensive Genomic Analysis of Malignant Pleural Mesothelioma Identifies Recurrent Mutations, Gene Fusions and Splicing Alterations. *Nat Genet* (2016) 48(4):407–16. doi: 10.1038/ng.3520
66. Blum Y, Meiller C, Quetel L, Elarouci N, Ayadi M, Tashtanbaeva D, et al. Dissecting Heterogeneity in Malignant Pleural Mesothelioma Through Histo-Molecular Gradients for Clinical Applications. *Nat Commun* (2019) 10(1):1333. doi: 10.1038/s41467-019-09307-6
67. Blum Y, Jaurand MC, De Reynies A, Jean D. Unraveling the Cellular Heterogeneity of Malignant Pleural Mesothelioma Through a Deconvolution Approach. *Mol Cell Oncol* (2019) 6(4):1610322. doi: 10.1080/23723556.2019.1610322
68. Liang B, Ding H, Huang L, Luo H, Zhu X. GWAS in Cancer: Progress and Challenges. *Mol Genet Genomics* (2020) 295(3):537–61. doi: 10.1007/s00438-020-01647-z
69. Pharoah PDP, Tsai Y-Y, Ramus SJ, Phelan CM, Goode EL, Lawrenson K, et al. GWAS Meta-Analysis and Replication Identifies Three New Susceptibility Loci for Ovarian Cancer. *Nat Genet* (2013) 45(4):362–70. doi: 10.1038/ng.2564
70. de Maturana EL, Rava M, Anumudu C, Saez O, Alonso D, Malats N. Bladder Cancer Genetic Susceptibility. A Systematic Review. *Bladder Cancer* (2018) 4 (2):215–26. doi: 10.3233/BLC-170159
71. Need AC, Goldstein DB. Next Generation Disparities in Human Genomics: Concerns and Remedies. *Trends Genet* (2009) 25(11):489–94. doi: 10.1016/j.tig.2009.09.012
72. Murphy S, Churchill S, Bry L, Chueh H, Weiss S, Lazarus R, et al. Instrumenting the Health Care Enterprise for Discovery Research in the Genomic Era. *Genome Res* (2009) 19(9):1675–81. doi: 10.1101/gr.094615.109
73. Galvan A, Ioannidis JP, Dragani TA. Beyond Genome-Wide Association Studies: Genetic Heterogeneity and Individual Predisposition to Cancer. *Trends Genet* (2010) 26(3):132–41. doi: 10.1016/j.tig.2009.12.008
74. Song W, Huang H, Zhang C-Z, Bates DW, Wright A. Using Whole Genome Scores to Compare Three Clinical Phenotyping Methods in Complex Diseases. *Sci Rep* (2018) 8(1):1–10. doi: 10.1038/s41598-018-29634-w
75. Olson B, Li Y, Lin Y, Liu ET, Patnaik A. Mouse Models for Cancer Immunotherapy Research. *Cancer Discov* (2018) 8(11):1358–65. doi: 10.1158/2159-8290.CD-18-0044

76. Nisbet NW. Some Aspects of Immunological Tolerance Investigated by Parent to F1 Hybrid Parabiosis in Mice. *Transplantation* (1971) 11(3):318–24. doi: 10.1097/00007890-197103000-00012
77. Flint J, Eskin E. Genome-Wide Association Studies in Mice. *Nat Rev Genet* (2012) 13(11):807–17. doi: 10.1038/nrg3335
78. Festing MFW, Yang A, Malkinson AM. At Least Four Genes and Sex are Associated With Susceptibility to Urethane-Induced Pulmonary Adenomas in Mice. *Genet Res* (1994) 64(2):99–106. doi: 10.1017/S0016672300032705
79. Manenti G, Gariboldi M, Fiorino A, Zanesi N, Pierotti MA, Dragani TA. Genetic Mapping of Lung Cancer Modifier Loci Specifically Affecting Tumor Initiation and Progression. *Cancer Res* (1997) 57(19):4164–6.
80. Wang D, Lemon WJ, You M. Linkage Disequilibrium Mapping of Novel Lung Tumor Susceptibility Quantitative Trait Loci in Mice. *Oncogene* (2002) 21(44):6858–65. doi: 10.1038/sj.onc.1205886
81. Wakana S, Sugaya E, Naramoto F, Yokote N, Maruyama C, Jin W, et al. Gene Mapping of SEZ Group Genes and Determination of Pentylenetetrazol Susceptible Quantitative Trait Loci in the Mouse Chromosome. *Brain Res* (2000) 857(1-2):286–90. doi: 10.1016/S0006-8993(99)02406-3
82. Williams RW, Bennett B, Lu L, Gu J, DeFries JC, Carosone–Link PJ, et al. Genetic Structure of the LXS Panel of Recombinant Inbred Mouse Strains: A Powerful Resource for Complex Trait Analysis. *Mamm Genome* (2004) 15 (8):637–47. doi: 10.1007/s00335-004-2380-6
83. Threadgill DW, Miller DR, Churchill GA, de Villena FP-M. The Collaborative Cross: A Recombinant Inbred Mouse Population for the Systems Genetic Era. *ILAR J* (2011) 52(1):24–31. doi: 10.1093/ilar.52.1.24
84. Roberts A, Pardo-Manuel de Villena F, Wang W, McMillan L, Threadgill DW. The Polymorphism Architecture of Mouse Genetic Resources Elucidated Using Genome-Wide Resequencing Data: Implications for QTL Discovery and Systems Genetics. *Mamm Genome* (2007) 18(6-7):473–81. doi: 10.1007/s00335-007-9045-1
85. Churchill GA, Airey DC, Allayee H, Angel JM, Attie AD, Beatty J, et al. The Collaborative Cross, a Community Resource for the Genetic Analysis of Complex Traits. *Nat Genet* (2004) 36(11):1133–7. doi: 10.1038/ng1104-1133
86. Morahan G, Balmer L, Monley D. Establishment of "The Gene Mine": A Resource for Rapid Identification of Complex Trait Genes. *Mamm Genome* (2008) 19(6):390–3. doi: 10.1007/s00335-008-9134-9
87. Ram R, Mehta M, Balmer L, Gatti DM, Morahan G. Rapid Identification of Major-Effect Genes Using the Collaborative Cross. *Genetics* (2014) 198 (1):75–86. doi: 10.1534/genetics.114.163014
88. Ferguson B, Ram R, Handoko HY, Mukhopadhyay P, Muller HK, Soyer HP, et al. Melanoma Susceptibility as a Complex Trait: Genetic Variation Controls All Stages of Tumor Progression. *Oncogene* (2015) 34(22):2879–86. doi: 10.1038/onc.2014.227
89. Patel SJ, Molinolo AA, Gutkind S, Crawford NP. Germline Genetic Variation Modulates Tumor Progression and Metastasis in a Mouse Model of Neuroendocrine Prostate Carcinoma. *PLoS One* (2013) 8(4): e61848. doi: 10.1371/journal.pone.0061848
90. Yang CH, Mangiafico SP, Waibel M, Loudovaris T, Loh K, Thomas HE, et al. E2f8 and Dlg2 Genes Have Independent Effects on Impaired Insulin Secretion Associated With Hyperglycaemia. *Diabetologia* (2020) 63 (7):1333–48. doi: 10.1007/s00125-020-05137-0
91. Yuan J, Tickner J, Mullin BH, Zhao J, Zeng Z, Morahan G, et al. Advanced Genetic Approaches in Discovery and Characterization of Genes Involved With Osteoporosis in Mouse and Human. *Front Genet* (2019) 10:288. doi: 10.3389/fgene.2019.00288
92. Weerasekera LY, Balmer LA, Ram R, Morahan G. Characterization of Retinal Vascular and Neural Damage in a Novel Model of Diabetic Retinopathy. *Invest Ophthalmol Vis Sci* (2015) 56(6):3721–30. doi: 10.1167/iovs.14-16289
93. Ferguson B, Handoko HY, Mukhopadhyay P, Chitsazan A, Balmer L, Morahan G, et al. Different Genetic Mechanisms Mediate Spontaneous *Versus* UVR-Induced Malignant Melanoma. *Elife* (2019) 8:e42424. doi: 10.7554/eLife.42424
94. Chitsazan A, Ferguson B, Ram R, Mukhopadhyay P, Handoko HY, Gabrielli B, et al. A Mutation in the Cdon Gene Potentiates Congenital Nevus Development Mediated by NRAS(Q61K). *Pigment Cell Melanom Res* (2016) 29(4):459–64. doi: 10.1111/pcmr.12487
95. Chitsazan A, Ferguson B, Villani R, Handoko HY, Mukhopadhyay P, Gabrielli B, et al. Keratinocyte Sonic Hedgehog Upregulation Drives the Development of Giant Congenital Nevi Via Paracrine Endothelin-1 Secretion. *J Invest Dermatol* (2018) 138(4):893–902. doi: 10.1016/j.jid.2017.10.032
96. Walrath JC, Hawes JJ, Van Dyke T, Reilly KM. Genetically Engineered Mouse Models in Cancer Research. *Adv Cancer Res* (2010) 106:113–64. doi: 10.1016/S0065-230X(10)06004-5
97. Gurumurthy CB, Lloyd KCK. Generating Mouse Models for Biomedical Research: Technological Advances. *Dis Models Mech* (2019) 12(1): dmm029462. doi: 10.1242/dmm.029462
98. Kersten K, de Visser KE, van Miltenburg MH, Jonkers J. Genetically Engineered Mouse Models in Oncology Research and Cancer Medicine. *EMBO Mol Med* (2017) 9(2):137–53. doi: 10.15252/emmm.201606857
99. Johnson L, Mercer K, Greenbaum D, Bronson RT, Crowley D, Tuveson DA, et al. Somatic Activation of the K-ras Oncogene Causes Early Onset Lung Cancer in Mice. *Nature* (2001) 410(6832):1111–6. doi: 10.1038/35074129
100. Kasinski AL, Slack FJ. miRNA-34 Prevents Cancer Initiation and Progression in a Therapeutically Resistant K-ras and p53-induced Mouse Model of Lung Adenocarcinoma. *Cancer Res* (2012) 72(21):5576–87. doi: 10.1158/0008-5472.CAN-12-2001
101. Gormally E, Vineis P, Matullo G, Veglia F, Caboux E, Le Roux E, et al. TP53 and KRAS2 Mutations in Plasma DNA of Healthy Subjects and Subsequent Cancer Occurrence: A Prospective Study. *Cancer Res* (2006) 66(13):6871–6. doi: 10.1158/0008-5472.CAN-05-4556
102. Tang FH, Hsieh TH, Hsu CY, Lin HY, Long CY, Cheng KH, et al. KRAS Mutation Coupled With p53 Loss is Sufficient to Induce Ovarian Carcinosarcomas in Mice. *Int J Cancer* (2017) 140(8):1860–9. doi: 10.1002/ijc.30591
103. Testa JR, Berns A. Preclinical Models of Malignant Mesothelioma. *Front Oncol* (2020) 10:101. doi: 10.3389/fonc.2020.00101
104. Kukuyan AM, Sementino E, Kadariya Y, Menges CW, Cheung M, Tan Y, et al. Inactivation of Bap1 Cooperates With Losses of Nf2 and Cdkn2a to Drive the Development of Pleural Malignant Mesothelioma in Conditional Mouse Models. *Cancer Res* (2019) 79(16):4113–23. doi: 10.1158/0008-5472.CAN-18-4093
105. Fleury-Feith J, Lecomte C, Renier A, Matrat M, Kheuang L, Abramowski V, et al. Hemizygosity of Nf2 is Associated With Increased Susceptibility to Asbestos-Induced Peritoneal Tumours. *Oncogene* (2003) 22(24):3799–805. doi: 10.1038/sj.onc.1206593
106. Napolitano A, Pellegrini L, Dey A, Larson D, Tanji M, Flores EG, et al. Minimal Asbestos Exposure in Germline BAP1 Heterozygous Mice Is Associated With Deregulated Inflammatory Response and Increased Risk of Mesothelioma. *Oncogene* (2016) 35(15):1996–2002. doi: 10.1038/onc.2015.243
107. Shamseddin M, Obacz J, Garnett MJ, Rintoul RC, Francies HE, Marciniak SJ. Use of Preclinical Models for Malignant Pleural Mesothelioma. *Thorax* (2021) thoraxjnl-2020-216602. doi: 10.1136/thoraxjnl-2020-216602
108. Kadariya Y, Cheung M, Xu J, Pei J, Sementino E, Menges CW, et al. Bap1 Is a Bona Fide Tumor Suppressor: Genetic Evidence From Mouse Models Carrying Heterozygous Germline Bap1 Mutations. *Cancer Res* (2016) 76 (9):2836–44. doi: 10.1158/0008-5472.CAN-15-3371
109. Badhai J, Pandey GK, Song JY, Krijgsman O, Bhaskaran R, Chandrasekaran G, et al. Combined Deletion of Bap1, Nf2, and Cdkn2ab Causes Rapid Onset of Malignant Mesothelioma in Mice. *J Exp Med* (2020) 217(6):e20191257. doi: 10.1084/jem.20191257
110. Jongsma J, van Montfort E, Vooijs M, Zevenhoven J, Krimpenfort P, van der Valk M, et al. A Conditional Mouse Model for Malignant Mesothelioma. *Cancer Cell* (2008) 13(3):261–71. doi: 10.1016/j.ccr.2008.01.030
111. Robinson C, Solin JN, Lee YCG, Lake RA, Lesterhuis WJ. Mouse Models of Mesothelioma: Strengths, Limitations and Clinical Translation. *Lung Cancer Manage* (2014) 3(5):397–410. doi: 10.2217/lmt.14.27
112. Xu J, Kadariya Y, Cheung M, Pei J, Talarchek J, Sementino E, et al. Germline Mutation of Bap1 Accelerates Development of Asbestos-Induced Malignant Mesothelioma. *Cancer Res* (2014) 74(16):4388–97. doi: 10.1158/0008-5472.CAN-14-1328
113. Farahmand P, Gyuraszova K, Rooney C, Raffo-Iraolagoitia XL, Johnson E, Chernova T, et al. Asbestos Accelerates Disease Onset in a Genetic Model of Malignant Pleural Mesothelioma. *BioRxiv* (2020). doi: 10.1101/2020.06.16.154815

114. Robinson C, Van Bruggen I, Segal A, Dunham M, Sherwood A, Koentgen F, et al. A Novel SV40 Tag Transgenic Model of Asbestos-Induced Mesothelioma: Malignant Transformation is Dose Dependent. *Cancer Res* (2006) 66(22):10786–94. doi: 10.1158/0008-5472.CAN-05-4668
115. Robinson C, Walsh A, Larma I, O'Halloran S, Nowak AK, Lake RA. MexTAg Mice Exposed to Asbestos Develop Cancer That Faithfully Replicates Key Features of the Pathogenesis of Human Mesothelioma. *Eur J Cancer* (2011) 47(1):151–61. doi: 10.1016/j.ejca.2010.08.015
116. Robinson C, Dick IM, Wise MJ, Holloway A, Diyagama D, Robinson BWS, et al. Consistent Gene Expression Profiles in MexTAg Transgenic Mouse and Wild Type Mouse Asbestos-Induced Mesothelioma. *BMC Cancer* (2015) 15 (1):983. doi: 10.1186/s12885-015-1953-y
117. De Luca A, Baldi A, Esposito V, Howard CM, Bagella L, Rizzo P, et al. The Retinoblastoma Gene Family pRb/p105, p107, pRb2/p130 and Simian Virus-40 Large T-Antigen in Human Mesotheliomas. *Nat Med* (1997) 3(8):913–6. doi: 10.1038/nm0897-913
118. Baas P, Scherpereel A, Nowak AK, Fujimoto N, Peters S, Tsao AS, et al. First-Line Nivolumab Plus Ipilimumab in Unresectable Malignant Pleural Mesothelioma (CheckMate 743): A Multicentre, Randomised, Open-Label, Phase 3 Trial. *Lancet* (2021) 397(10272):375–86. doi: 10.1016/S0140-6736(20)32714-8

**Conflict of Interest:** The authors declare that the research was conducted in the absence of any commercial or financial relationships that could be construed as a potential conflict of interest.

frontiers in Oncology

REVIEW
published: 23 June 2021
doi: 10.3389/fonc.2021.660039

# Tumor Immune Microenvironment and Genetic Alterations in Mesothelioma

*Stefanie Hiltbrunner[1,2†], Laura Mannarino[3†], Michaela B. Kirschner[4], Isabelle Opitz[4], Angelica Rigutto[1,2], Alexander Laure[1,2], Michela Lia[5], Paolo Nozza[6], Antonio Maconi[7], Sergio Marchini[3], Maurizio D'Incalci[3], Alessandra Curioni-Fontecedro[1,2‡] and Federica Grosso[5,8*‡]*

[1] Department of Medical Oncology and Hematology, University Hospital Zurich, Zurich, Switzerland, [2] Comprehensive Cancer Center Zurich, University of Zurich, Zurich, Switzerland, [3] Department of Oncology, Istituto di Ricerche Farmacologiche Mario Negri Istituto di Ricovero e Cura a Carattere Scientifico (IRCCS), Milano, Italy, [4] Department of Thoracic Surgery, University Hospital Zurich, Zurich, Switzerland, [5] Mesothelioma Unit, Azienda Ospedaliera SS. Antonio e Biagio e Cesare Arrigo, Alessandria, Italy, [6] Department of Pathology, Azienda Ospedaliera SS. Antonio e Biagio e Cesare Arrigo, Alessandria, Italy, [7] Infrastruttura Ricerca Formazione Innovazione (IRFI), Dipartimento Attività Integrate Ricerca e Innovazione (DAIRI), Azienda Ospedaliera SS. Antonio e Biagio e Cesare Arrigo, Alessandria, Italy, [8] Translational Medicine, Dipartimento Attività Integrate Ricerca e Innovazione (DAIRI), Azienda Ospedaliera SS. Antonio e Biagio e Cesare Arrigo, Alessandria, Italy

Malignant pleural mesothelioma (MPM) is a rare and fatal disease of the pleural lining. Up to 80% of the MPM cases are linked to asbestos exposure. Even though its use has been banned in the industrialized countries, the cases continue to increase. MPM is a lethal cancer, with very little survival improvements in the last years, mirroring very limited therapeutic advances. Platinum-based chemotherapy in combination with pemetrexed and surgery are the standard of care, but prognosis is still unacceptably poor with median overall survival of approximately 12 months. The genomic landscape of MPM has been widely characterized showing a low mutational burden and the impairment of tumor suppressor genes. Among them, *BAP1* and *BLM* are present as a germline inactivation in a small subset of patients and increases predisposition to tumorigenesis. Other studies have demonstrated a high frequency of mutations in DNA repair genes. Many therapy approaches targeting these alterations have emerged and are under evaluation in the clinic. High-throughput technologies have allowed the detection of more complex molecular events, like chromotripsis and revealed different transcriptional programs for each histological subtype. Transcriptional analysis has also paved the way to the study of tumor-infiltrating cells, thus shedding lights on the crosstalk between tumor cells and the microenvironment. The tumor microenvironment of MPM is indeed crucial for the pathogenesis and outcome of this disease; it is characterized by an inflammatory response to asbestos exposure, involving a variety of chemokines and suppressive immune cells such as M2-like macrophages and regulatory T cells. Another important feature of MPM is the dysregulation of microRNA expression, being frequently linked to

OPEN ACCESS

**Edited by:**
*Giulia Pasello, Veneto Institute of Oncology (IRCCS), Italy*

**Reviewed by:**
*Luana Calabro', Siena University Hospital, Italy*
*Ana Teresa Amaral, Institute of Biomedicine of Seville (IBIS), Spain*

***Correspondence:**
*Federica Grosso*
*federica.grosso@ospedale.al.it*

*[†]These authors share first authorship*

*[‡]These authors share last authorship*

**Specialty section:**
*This article was submitted to Cancer Immunity and Immunotherapy, a section of the journal Frontiers in Oncology*

**Received:** *28 January 2021*
**Accepted:** *25 May 2021*
**Published:** *23 June 2021*

**Citation:**
*Hiltbrunner S, Mannarino L, Kirschner MB, Opitz I, Rigutto A, Laure A, Lia M, Nozza P, Maconi A, Marchini S, D'Incalci M, Curioni-Fontecedro A and Grosso F (2021) Tumor Immune Microenvironment and Genetic Alterations in Mesothelioma. Front. Oncol. 11:660039. doi: 10.3389/fonc.2021.660039*

cancer development and drug resistance. This review will give a detailed overview of all the above mentioned features of MPM in order to improve the understanding of this disease and the development of new therapeutic strategies.

**Keywords: mesothelioma, tumor microenvironment, genetic alterations, immunotherapy, targeted therapy**

## INTRODUCTION

Malignant pleural mesothelioma (MPM) is an aggressive malignancy of the pleural lining with limited treatment options. It is strongly associated with exposure to fibrous material such as asbestos. Due to the long latency period of up to 40 years and the ongoing use of asbestos in developing countries, the cases are still rising. Patients with MPM have a very short median overall survival of around 12 months after diagnosis and are treated with a combination of surgery, radiotherapy and chemotherapy. Pharmacological treatment has not changed for years consisting in the combination of cisplatin with pemetrexed and/or bevacizumab in some cases. Studies performed so far deciphered the genomic, transcriptional and epigenomic landscape of MPM, highlighting a complex and not yet known scenario. Very recently, the combination of two immune checkpoint inhibitors showed an improvement in overall survival compared to standard chemotherapy in first line. Nevertheless, current therapies have not improved, there is no second line therapy available and inclusion into clinical trials is currently the best option. The tumor microenvironment (TME) of mesothelioma consists of a wide variety of innate and adaptive immune cell subtypes, stromal and endothelial cells and has been characterized as a highly inflammatory TME favoring treatment with immune checkpoint inhibitors. On the other hand, mesothelioma is considered a non-immunogenic cancer due to a low tumor mutational burden and paucity of activated T cells. Thus, the understanding of the crosstalk and interactions of immune, stromal and tumor cells is of major importance for the development of novel therapies and the discovery of new therapeutic targets.

## INFLAMMATORY TUMOR MICROENVIRONMENT

Inhaled mineral fibers traveling to the visceral pleura and deposition of mineral fibers in the pleural lining leads to a permanent innate stimuli with subsequent chronic inflammation, production of oxygen radicals and necrotic cell death of mesothelial cells. Asbestos fibers are biopersistent and non-degradable, which plays an important role in their carcinogenic potential (1). Mesothelial cells exposed to asbestos fibers secrete C-C chemokine ligand 2 (CCL2), which attracts macrophages to the site (2). Reactive-oxygen species induce DNA damage and mutations in mesothelial cells (3) leading to necrotic cell death and to the production and release of damage-associated molecular patterns (DAMPs) including High Mobility Group Box 1 protein (HMGB1). HMGB1 is translocated from the nucleus to the cytoplasm and secreted into the extracellular space, where it can bind to its receptors TLR2, TLR4 and receptor for Advanced Glycation Endproducts (RAGE). The binding of HMGB1 to mesothelial cells enhances their proliferation and migration capacity. The release of HMGB1 also promotes autophagy, allowing a higher fraction of mesothelial cells to survive asbestos exposure. HMGB1 silencing was shown to inhibit autophagy and to increase asbestos-induced mesothelial cell death, thereby decreasing asbestos induced transformation (4) (**Figure 1**). The importance of HMGB1 in cancerous transformation was also studied in a mouse mesothelioma model, where the investigators demonstrated that inhibition of HMGB1 binding to its receptors led to decreased tumor growth (5, 6) again pointing out the importance of this mediator in MPM progression. In addition, serum concentrations of HMGB1 are also significantly higher in mesothelioma patients compared to healthy controls, indicating its significance in tumor development (7).

Recruited macrophages phagocyte asbestos fibers leading to secretion of proinflammatory mediators such as TNF-α, supporting carcinogenesis and cancer cells survival (8). On the other hand, asbestos itself can also activate the inflammasome, a multiprotein complex part of the innate immune system, leading to activation of caspase-1 and cleavage of pro-IL-1β to IL-1β (9). IL-1β released by tumor-associated macrophages (TAMs) and its binding to IL-1R on mesothelial cells can be part of the malignant phenotype inducing cell survival and proliferation (10). Furthermore, production of TNF-α and IL-1β by macrophages can also be induced through the inflammatory environment and the presence of extracellular HMGB1, which protects mesothelial cells from asbestos-induced cell death (11, 12). TNF-α released by macrophages signals through NF-κB in mesothelial cells and supports their survival to asbestos exposure (13). Thus, TNF-α and IL-1β are important players in the transformation of non-tumorigenic mesothelial cells (14). Interestingly, HMGB1 was also shown to play an important role in epithelial to mesenchymal transition (EMT) as it led to upregulation of the EMT markers vimentin and α-smooth muscle actin (12). HMGB1 can also reduce expression of E-cadherins, an epithelial marker and upregulates mesenchymal markers promoting EMT (12). Altogether, this indicates the importance of HMGB1, TNF-α and IL-1β in mediating mesothelioma malignant transformation and progression (**Figure 1**).

The mesothelioma tumor microenvironment consists of a complex structure of stromal cells, immune cells and vasculature. All of these components result in a heterogeneous plethora of possible mesothelioma phenotypes, making this disease very difficult to treat. The immune compartment is characterized by the presence of many regulatory and inhibitory cells such as regulatory T cells, type 2 macrophages and myeloid-derived suppressor cells (MDSC). Immune infiltrates also include T and B cells, NK cells, dendritic cells (DC) and neutrophils.

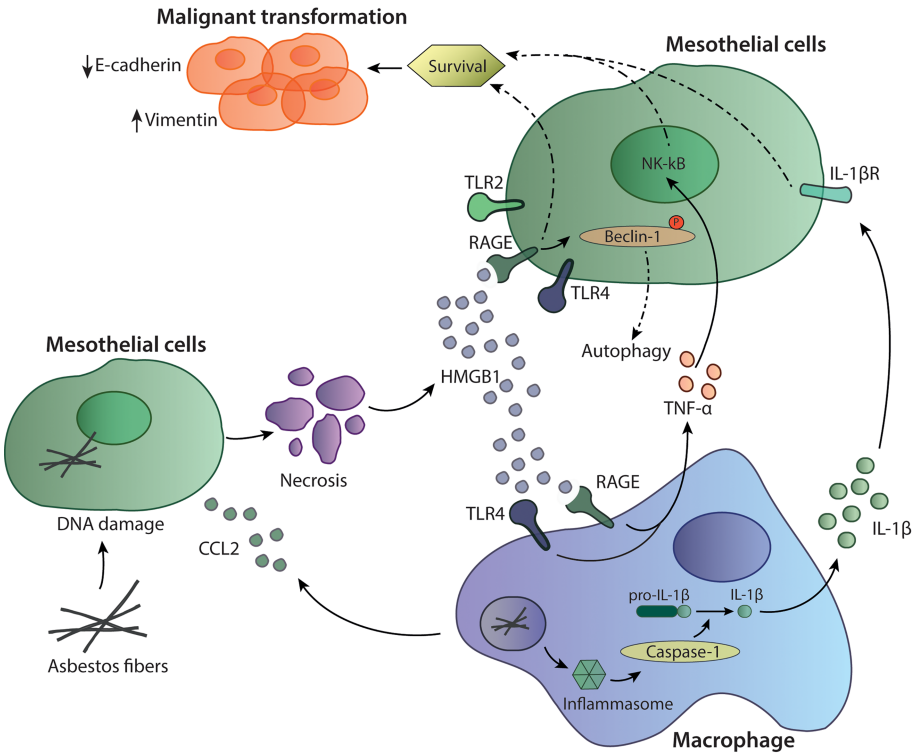


**FIGURE 1** | Mechanisms of asbestos-induced carcinogenesis. Asbestos fibers reach the mesothelial cells where they can induce cell death and the release of inflammatory mediators such as HMGB1 and CCL2. The recruited macrophages are activated through HMGB1 binding to TLR4 and RAGE to induce TNF-α or by inflammasome activation through asbestos fibers. Activation of caspase-1 and cleavage of pro-IL-1β to the active form IL-1β can lead to further survival signals in mesothelial cells. HMGB1 can also bind to TLR4 and RAGE expressed on mesothelial cells supporting survival of those cells.

## NK Cells

Innate lymphoid cells (ILC) such as natural killer (NK) cells can be found in mesothelioma tumors, however, in a very small proportion (15, 16). NK cells are innate immune cells and belong to the innate lymphoid cell family (17), with high cytotoxic capacity and without the need for antigen-specific stimulation (18). NK cells are often characterized to have impaired effector functions in different solid tumors due to local immunosuppressive microenvironment leading to hampering of effector functions (19). However, little is known about the role of NK cells in mesothelioma or their possible engagement for mesothelioma therapy.

MPM tumors are infiltrated with NK cells shown by mRNA expression analysis of specific NK cell makers, which were even higher expressed in MPM compared to other cancers. However, the presence of the NK cell markers was not linked to better overall survival (20).

Similar results were obtained with staining for CD56 by immunohistochemistry (IHC) of a tissue-microarray in both epithelioid and non-epithelioid subgroups (16). In addition, different studies report different results about the expression of inhibitory or activating molecules on NK cells. A study by Nishimura et al. described that NK cells isolated from the blood of mesothelioma patients had lower cytotoxic activity compared to NK cells from healthy individuals and showed a reduced expression of the activating receptor NKp46 but normal levels of another activating receptor NKG2D (21). Another study described a higher frequency of $CD56^{bright}$ and a lower frequency of $CD56^{dim}$ NK cells in mesothelioma patients compared to healthy controls. Interestingly, treatment with anti-CTLA-4 immune checkpoint inhibitor changed this ratio from a higher frequency of $CD56^{dim}$ to a more physiological level of healthy controls (20).

Pleural effusion of MPM patients is often used to study the presence and function of different immune cells. NK cells isolated from pleural effusion show high expression of the immune checkpoint molecules T cell immunoglobulin and mucin-domain containing-3 (TIM-3) and lymphocyte activation gene-3 (LAG-3), whereas both molecules are expressed to the highest levels on NK cells and to a lesser extent on CD4 and CD8 T cells (22). Interestingly, LAG-3 is not expressed on MPM tumor cells (23). Here, the investigators claim that effusions are more often present in an inflammatory context, which could influence the expression of suppressive immune checkpoint molecules as they have shown that the early activation marker CD69 is significantly correlated with the expression of TIM-3. Another explanation could be that matching pleural effusion and tumor tissue do not reflect each

other's immune cell composition (24). Nevertheless, differences in effusion and tumor samples could also be due to different analysis methods (22). Furthermore, NK cells in pleural effusion from MPM patients are functional and produce high amounts of TNF-α and INF-γ upon stimulation (25) but have also an impaired expression of perforin, which can be restored by IL-2 stimulation *in vitro*. However, incubation of NK cells with pleural effusion completely abrogated the activation status of the NK cells, indicating the presence of inhibitory cytokines in the pleural effusion (26) (**Figure 2**). Similar results were obtained in a study performed by Vacca et al., they also described NK cells from pleural effusion from different cancer patients (including mesothelioma patients) as functionally capable to produce cytokines, perforin and granzyme A and B and to perform cytotoxic functions upon *in vitro* stimulation with IL-2. Furthermore, NK cells express normal levels of activating receptor including NKp30, NKp44, NKG2D, and DNAM-1 after stimulation. This suggests a possibility for reactivation of NK cells and no expression of an anergic phenotype as described in other studies (27). However, the functional capacities of NK cells in human tumors were not investigated and it is currently unclear if they are in a state of exhaustion or can perform effector functions normally. A mouse syngenic mesothelioma model using the AE17 cell line, reveals that depletion of NK cells with an anti-asialo GM1 antibody did not influence tumor growth (28). Current data about NK cells in MPM tumors does not correlate to overall survival, nevertheless, more data is needed to understand their functional effector capacity and their exhaustion profile intratumorally and the possibility to target them with therapeutic approaches.

## NKT Cells

Natural killer T (NKT) cells are a distinct population of T cells recognizing glycolipids presented on the non-classical class I-like molecule CD1d in contrast to normal T cells, which recognize peptide fragments presented on MHC molecules (29, 30). NKT cells have lytic activity, but their main function lies in the production and secretion of a wide variety of cytokines. Upon activation, they can produce high amounts of Th1 or Th2 cytokines, which can lead to bystander activation of NK cells, CD8 T cells and dendritic cells.

Little is known about the function of NKT cells in the tumor microenvironment of patients with MPM. Altomare et al. investigated the presence of NKT cells in the blood of MPM patients. Here, they showed that MPM patients have a higher frequency of circulating NKT cells compared to healthy volunteers, whereas there were no differences in their ability to produce IFN-γ and IL-4 (31) (**Figure 2**). NKT cells have been mainly studied in the context of mesothelioma mouse models and as a therapeutic target, since they can easily be activated by artificial glycolipids. In the pleural effusion of a MPM mouse model, NKT cells are present, express high levels of the activation

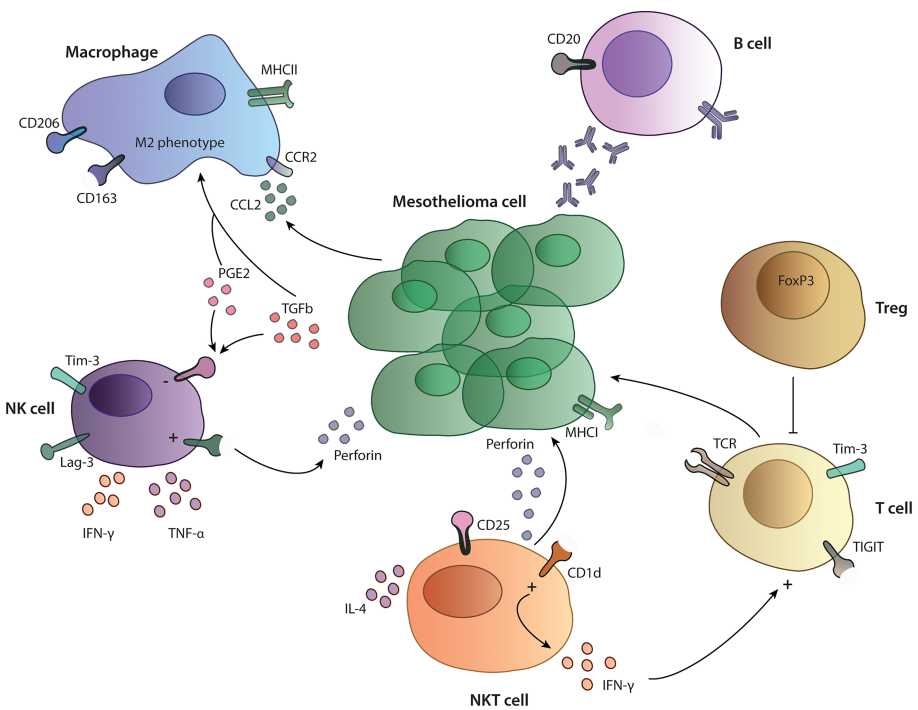


**FIGURE 2** | Tumor microenvironment in mesothelioma. Overview on the functionality and interactions of different immune cells studied in MPM patients. NK cells and T cells express inhibitory receptors such as TIM-3, LAG-3 and TIGIT and are influenced by a suppressive cytokines (PGE2, TGF-β) and the presence of Treg cells in performing their cytotoxic functions. Macrophages show a M2-like phenotype with expression of CD206 and CD163 on their surface. B cells in the TME produce specific antibodies against cancer cells, participating in the anti-tumor immune response.

marker CD25 and produce large amounts of INF-γ. In the same model, activation of NKT cells through administration of glycolipids led to prolonged survival in the treated groups (32, 33), indicating that these cells have an anti-tumor phenotype and can activate other cytotoxic cells. More studies are needed in order to understand the possibility to use them as a therapeutic target in MPM.

## Macrophages

Macrophages are innate immune cells specialized in phagocytosis, engulfing and digestion of invading organisms and cell debris and play an important role in tissue homeostasis. Monocytes are recruited from the blood to the TME through locally produced chemokines and become TAMs and, in patients' blood, increased amounts of circulating monocytes and a low lymphocyte to monocyte ratio have been reported to negatively correlate with overall survival (34, 35). TAMs can be divided into two subset depending on their function and marker expression. M1 macrophages are proinflammatory macrophages and have strong capacity to kill invading pathogens and contribute as well to tissue destruction. M2 macrophages are important mediators in tissue remodeling, allergic diseases and angiogenesis. Nevertheless, macrophages are a functionally diverse and plastic group and can reverse their polarization from M2 to M1 depending on the chemokine environment (36–38).

Various cytokines can induce differentiation of monocytes and macrophages into TAMs, such as CCL2, C–C chemokine ligand 4 (CCL4), C–C chemokine ligand 5 (CCL5) and C-X-C motif chemokine ligand 12 (CXCL12) secreted by MPM cells (39, 40). CCL2, the most studied TAM-associated chemokine, recruits immune cells such as T cells, macrophages and dendritic cells through binding to CCR2 on the cells to the inflammatory site (41). CCL2 is upregulated in pleural effusion and serum from MPM patients compared to benign pleural effusion or pleural effusion from other malignancies and serum from healthy volunteers, respectively (42–44). Interestingly, CCL2 levels also correlate with the tumor stage, indicating an important role of macrophages in disease progression (42). Other chemokine receptors like CXCR1, CXCR4, CCR5, and CCR7 are infrequently expressed on mesothelioma cells isolated from pleural effusion of MPM patients (45). Therefore, those chemokine pathways might only play a role in a subset of MPM patients.

Activation of the colony stimulating factor-1 receptor (CSF-1R) through M-CSF or IL-34 can induce differentiation of monocytes to macrophages (46). Incubation of monocytes with pleural effusion from MPM patients or supernatant from MPM cell cultures resulted in a $CD14^{mid}CD163^{high}$ M2 immunosuppressive macrophage phenotype (47) (**Figure 2**). It has been shown that pleural effusions from MPM patients contain M-CSF and that they can induce differentiation of monocytes to M2-like macrophages in a CSF-1R dependent manner (48). M2 macrophages themselves can induce proliferation of MPM cells and induce treatment resistance to chemotherapies (47). Another study from Cioce et al. showed that autocrine CSF-1R signaling through AKT and β-catenin is a crucial signaling pathway for chemotherapy resistance and survival (49). Thus, the CSF1R/AKT axis represents an interesting target for further therapeutic development.

Other important factors for the differentiation of monocytes and macrophages like prostaglandin E2 (PGE2) and Transforming Growth Factor β (TGF-β) are present in pleural effusion and in the supernatant of MPM tumor cell lines (50, 51). PGE2 is an immunosuppressive factor in the TME and can induce a suppressive phenotype in macrophages with high suppressive capacity on T cell proliferation (52). The human monocytic cell line THP-1 activated with lipopolysaccharide (LPS), developed an immunosuppressive phenotype when co-cultured with the MPM cell line Mero84. An increased production of immunosuppressive cytokines like PGE2 and IL-10 was produced by macrophages with a shift towards M2 phenotype (53).

A very close interplay has been described between the production of TGF-β and priorities of macrophages in several settings. TGF-β is a critical cytokine in tissue homeostasis and can have pleiotropic functions in cancer. It can inhibit proliferation of cancer cells but also induce tumor progression and metastasis, thereby function as a tumor promoting cytokine (54). TGF-β concentrations in pleural effusions are significantly higher in MPM patients compared to those from primary lung cancer patients and they correlate with disease stage and tumor volume (55–58). Patients with high TGF-β concentrations in pleural effusions have significantly shorter survival, however, circulating serum TGF-β concentrations do not have a predictive value (58).

Upon production of the above mentioned chemokines, monocytes then become TAMs. TAMs have been widely described to express a pro-tumoral M2 phenotype, but recent studies suggest that they might have M1 and M2 properties at the same time (38, 59). M2 macrophages are considered to promote tumor growth, proliferation and invasiveness. Increased TAM levels correlate with poor survival, bad prognosis and increased metastasis potential in different tumors (60–63). In the human MPM tumor microenvironment, TAMs account for the majority of tumor infiltrating cells with about 25-40% of total immune infiltrates (23, 64). TAMs in MPM express an immunosuppressive M2 phenotype with high levels of the surface molecules CD163, CD206 and Interleukin 4 receptor α. Independent on the histological subtype, MPM is generally heavily infiltrated with macrophages without any correlation with tumor stage, but interestingly with survival in the non-epithelioid group (34) (**Table 1**). This could be due to presence of more immunosuppressive cytokines supporting the pro-tumoral role of infiltrated macrophages. A study by Marcq et al. showed a correlation between $CD68^+$ macrophages with the presence of $CD4^+FoxP3^+$ regulatory T cells, accounting for a downregulation of the adaptive immune response and support of an immunosuppressive TME, which could explain partially the difference between the prognostic differences in survival (23). Nevertheless, the prognostic value of macrophages and in particular M2 macrophages has led to divergent conclusions, depending on the different studies and datasets, while certain

**TABLE 1** | Summary of publications of overall survival correlated with immune infiltrates.

| Number of cases | Histology | Cell Subset | Survival | Ref |
|---|---|---|---|---|
| 667 | Epithelioid and non-epithelioid group | Circulating monocytes | Negative correlation with overall survival | |
| | Non-epithelioid group | CD68+ macrophages | Negative correlation with overall survival | (34) |
| 230 | Epithelioid group | CD163+ macrophages | No correlation with overall survival | |
| | Epithelioid group | CD163+/CD8+ ratio | Negative correlation with overall survival | (39) |
| | Epithelioid group | CD68+ or CD163+ in stroma | Negative correlation with overall survival | |
| 49 | All histology, 75% epithelioid | M2 macrophages (CD68+, CD208+, Arginase-1+) | No correlation with overall survival | (65) |
| 67 | Epithelioid 49%, non-epithelioid 51% | CD68+ macrophages | No correlation with overall survival | (66) |
| 8 | Epithelioid group | CD163+/CD68+ ratio | Negatively correlated with overall survival | (67) |
| 32 | Epithelioid and non-epithelioid group | CD8+ T cells | Correlation with better survival | (68) |
| 44 | Epithelioid and non-epithelioid group | CD8+ T cells | Correlation with longer survival | (69) |
| 302 | Epithelioid group | CD4+ T cells | Correlation with better survival | |
| | Non-epithelioid group | CD8+ T cells | Correlation with better survival | (16) |
| | Epithelioid and non-epithelioid group | CD4+ FoxP3+ regulatory T cells | High expression is correlated with poorer survival | |
| 93 | Epithelioid and non-epithelioid group | CD4+ T cells | Correlation with better survival | |
| | Epithelioid and non-epithelioid group | CD8+ T cells | Negatively correlated with overall survival | (66) |
| 302 | Epithelioid group | CD20+ | Correlation with better survival | (16) |
| 93 | Epithelioid group | CD20+ | Correlation with better survival | (66) |
| 230 | Epithelioid group | CD20+ | Correlation with better survival | (39) |
| 88 | Epithelioid and non-epithelioid group-PD-L1$^+$ | CD20+ | Negatively correlated with survival | (70) |

studies report a significance others do not (16, 34, 65–67) (**Table 1**). In order to further dissect the role of these cells in MPM, an orthotopic mouse model of MPM was used, where a tumor promoting effect of macrophages was described: mice with a high tumor burden had higher numbers of macrophages/monocytes in the pleural effusion as well as higher percentages of M2 suppressive macrophages (71). In another orthotopic, syngenic murine peritoneal mesothelioma model, the tumor burden, measured by tumor growth rates, invasiveness and number of metastasis was significantly reduced when macrophages were depleted in these mice (72). Both studies indicate TAMs as a negative prognostic factor for tumor progression in mice.

In conclusion, MPM seems to alter the myeloid cell differentiation program by tumor-derived factors, which contributes to tumor suppression and a pro-tumoral immune response. TAMs and monocytes could be a potential target to alter this effect and induce an anti-tumoral immune response.

## Myeloid-Derived Suppressor Cells

Myeloid-derived suppressor cells (MDSC) represent a pathological status of monocytes and neutrophils and are present in different pathological conditions. MDSC represent a small proportion of tumor infiltrating cells in MPM, below 10%, but with important pro-tumoral functions (65). MDSC promote tumor development and progression through different mechanisms, they have the ability to suppress T cells, remodel the TME, support EMT and angiogenesis (73, 74). MDSC are a heterogeneous group of myeloid cells but can be roughly divided in two groups, the granulocytic (Gr-MDSC) and the monocytic (M-MDSC) subset (74).

In MPM, the two populations of MDSCs can be found in the TME; the granulocytic like subtype expressing $CD15^{high}$/$CD33^{low}$ and the monocytic like subtype expressing $CD15^{low}$/$CD33^{high}$ (15, 67, 75, 76). Gr-MDSCs are recruited to the tumor site through G-CSF and GM-CSF released by MPM tumor cells and further differentiate into an immunosuppressive phenotype within the tumor (75, 77, 78). In MPM, MDSCs inhibit proliferation of $CD8^+$ T cells through secretion of immunosuppressive molecules like reactive oxygen species (ROS), nitric oxide (NO) and kynurenine (75, 79, 80). High amounts of tumor infiltrating MDSCs significantly decrease progression free survival and overall survival in MPM patients (65).

Targeting MDSC in murine model of mesothelioma leads to reduced numbers of intra-tumoral MDSC with reduced capability to produce ROS and to reduce tumor growth (81). Targeting MDSC in MPM patients might represent a way to reduce intra-tumoral immune suppression and enhance immunotherapy regimes in future.

## T Cells

T cells play an important role in anti-cancer immunity in solid tumors and overall survival is closely linked to the presence of tumor infiltrating lymphocytes (TILs) across different tumor

types (82). The approval of immune checkpoint inhibitors targeting CTLA-4 or the PD-1/PD-L1 interaction and their enormous clinical success in different malignancies (83, 84) further points out the importance of T cells in controlling cancer cells. In MPM $CD3^+$ T cells are highly abundant in the TME and the presence of $CD8^+$ TILs is a favorable marker for prognosis (68, 69). However, 60 to 80% of the cases analyzed are usually MPM tumors with an epithelioid subtype, and only few cases with the most aggressive sarcomatoid form are included. Sarcomatoid tumors show fewer $CD4^+$ and $CD8^+$ T cells in the tumor and are characterized by a loss of Th1 features such as T-bet (marker for Th1 polarization) and granzyme B expression, which are required for an efficacious anti-tumor immune response. In addition, the sarcomatoid subtype does not express HLA class I molecules leading to escape of T cell mediated cytotoxicity (17). Another study compared the epithelioid group with a non-epithelioid group (sarcomatoid and biphasic) and linked immune markers with outcome: high $CD4^+$ counts in the epithelioid subset was associated with better prognosis, in contrary, in the non-epithelioid subsets, high $CD8^+$ counts were associated with better prognosis, in both, high expression of FoxP3 was correlated to poorer survival (16, 66) (**Table 1**). Infiltration of T cells also varies between PD-L1 high and low expressing tumors. PD-L1 high tumors have more $CD45^+$ cells infiltrated compared to PD-L1 low tumors, and significantly more $CD3^+$ cells including $CD4^+$ and $CD8^+$ and regulatory T cells and express more co-inhibitory receptors such as TIM-3. Nevertheless, there is also a huge variability between patients, which could account for the differences in responses to immunotherapies (15, 85). Thus, the presence of TILs and the expression of PD-L1 are not sufficient to predict responses to such therapies, but rather the whole immune-context, including the presence of suppressive cells and inhibitory receptors might predict outcome. Other important factors for response to immunotherapy in MPM patients are the effector functions of TILs. On the one hand, cytotoxic T cells in MPM express more T cell immunoglobulin and ITIM domain (TIGIT) and TIM-3 compared to T cells from health lung tissue and had a minor ability to produce IFN-γ upon stimulation (86) (**Figure 2**). On the other hand, patients with MPM do have approximately double the amount of regulatory T cells (Tregs) cells in the periphery compared to healthy control. Tregs are important in sustaining peripheral tolerance and preventing autoimmune disease by suppressing other cells. The balance between effector T and B cells and Tregs is crucial for the quality and magnitude of the immune response. Nevertheless, the presence of Tregs can also block required anti-tumor immune responses (87) and their presence in tumors is associated with poorer prognosis in different malignancies (88). In a study from Klampatsa et al. around 12.8% of all $CD4^+$ T cells in the MPM tissue are positive for FoxP3 compared to 2.2% from healthy lung tissue. In addition, there were significantly more Tregs in the tumor compared to the blood (86, 89). In a murine MPM model Tregs were also shown to be crucial for cancer progression, depleting Tregs with an anti-CD25 antibody led to reduced tumor growth (90).

## PD-L1 AND OTHER IMMUNE CHECKPOINT INHIBITORS

Immune checkpoints have drawn attention during the last years due to the development of antibodies blocking the interaction of PD-1 and PD-L1 and its extraordinary success in cancer therapy. The PD-L1/PD-1 axis leads to inactivation of T cells. In the context of cancer, T cells are continuously exposed to tumor antigens, which leads to a state of dysfunctionality and unresponsiveness called exhaustion. Blocking the PD-L1/PD-1 axis with therapeutic antibodies reactivates T cells against cancer. PD-L1 is expressed in mesothelioma tumors, however, the positivity rate very much depends on the study, the cohort and the assay performed for analysis (23, 91–93). A recent overview analysis of four different antibodies used to stain for PD-L1 gave an incoherent picture over the different assays. The use of reliable antibodies and standardization of staining methods are important features in order to receive comparable studies (94). In MPM, high PD-L1 expression is associated with histology and is higher expressed in sarcomatoid/biphasic subtypes (66, 92, 95). In the recently published PROMISE-MESO trial, 48.9% of the patient had less than 1% PD-L1 expression, 28.2% had 1-20% and 18.5% more than 20% PD-L1 expression (96). Another study described 73% to be positive (> 1%) and 27% negative (<1%) (97). Inaguma et al. describe 33% of MPM to be positive and 67% negative. In addition, high PD-L1 expression is negatively correlated with overall survival (85, 95, 98). Importantly, PD-L1 expression is not only restricted to TME but also on tumor cells of the pleural effusions (99); therefore, further investigations with detailed analysis of abundance and localization of expression are warranted.

Recent studies have identified a wide range of other immune checkpoint molecules beside PD1/PD-L1, which could be suitable for cancer treatment, in particular TIM-3, LAG-3, TIGIT and V-domain Ig suppressor of T cell activation (VISTA). TIM-3 plays a major role in controlling the function of NK and T cells. Upregulation of TIM-3 on peripheral immune cells and its cognate ligand galectin-9 on tumor cells inhibits immune responses. Galectin-9 is expressed on MPM tumors where it can suppress T cell response (65). Furthermore, a higher number of $TIM\text{-}3^+$ cells in peripheral NK and T cell populations correlate with a poor prognosis in many solid tumor types (20). In MPM, T cells in pleural effusion express inhibitory molecules such as PD-1, TIM-3, LAG-3 and have a higher diversity of TCR clones compared to blood of the same patient (65, 100). Interestingly, the *LAG-3* gene is higher expressed on mesothelioma tumors compared to lung adenocarcinoma, while *PD-L1* gene is higher expressed is lung adenocarcinoma (101). Understanding differences in the TME of various solid tumors can open up new options for more personalized immunotherapeutic approaches. A recent study defines a subgroup of patients co-expressing inhibitory molecules TIM-3, PD-L1, CTLA-4 and LAG-3 where this expression is associated with a shorter survival (102). Another immune checkpoint molecule, VISTA, is a negative regulator of T cell activation and it is highly expressed on myeloid cells. Similar to

PD-L1, VISTA can support the conversion of naïve T cells to FoxP3$^+$ regulatory T cells (103, 104). In MPM, VISTA is highly expressed on the epithelioid subtype but to a lesser extent on more aggressive subtypes. Interestingly, it is also expressed on normal and reactive mesothelium (105). In contrary to PD-L1 patients with high VISTA expression had a better overall survival, moreover, patients with concurrent high expression of VISTA and VEGFR2 survive almost five times longer compared to patients with low expression (102, 106).

## B CELLS

B cells are essential cells of the adaptive immune system and function as antigen presenting cells (APC) thereby contributing to T cell activation, differentiation and polarization. B cells also play an important role in promoting the formation of tumor-associated tertiary lymphoid structures (TLS), areas for B cell maturation and isotype switching (107). The presence of B cells in the tumor can be a prognostic factor in different malignancies (108). In MPM, only few studies addressed the function and importance of B cells in the tumor and in pleural effusion. Krishnan et al. showed high levels of tumor-specific antibodies in murine models of mesothelioma treated with immunotherapy compared with untreated controls. In addition, disease eradication in all treated animals and complete failure of the treatment in B cell-deficient mice have been demonstrated (109). These findings line up with previous preclinical data, which showed increased levels of IgM and IgG after anti-CD40 antibody treatment and during tumor regression in mice (110). This data suggests that antibodies generated upon treatment play an important role in the tumor immunity and are essential for tumor responses (**Figure 2**). Besides high levels of antibodies, Jackman et al. showed an increased percent of B cells in the tumor as well as in the secondary lymphoid organs. In contrast, the number of T cells and of the other cells of the immune system (e.g., macrophages, NK, granulocytes) remained low (110). In a previous study, high antibody titers against four tumor-associated antigens (GeneX, THBS-2, STUB-1 and IFT88) were identified in the *sera* of MPM patients. In particular, high levels of antibodies against two of those antigens, GeneX and THBS-2, were detected in almost all MPM patients, with a decrease after surgical resection (111). These findings represent another example of the existence of a specific humoral immune response in MPM patients: antibodies produced by tumor infiltrating B cells can be used as a tumor marker for diagnosis and follow up. The association of high B cell numbers in the tumor with survival has been recently described. Different studies showed that high counts of CD20$^+$ cells in patients with epithelioid mesothelioma positively correlated with survival, however, this was not the case in the non-epithelioid subgroup (16, 39, 66) (**Table 1**). In contrast, another study identified elevated B cell numbers in the sarcomatoid subgroup (70). In addition, in PD-L1$^{neg}$ MPMs B cells are considered a good prognostic factor, whereas in PD-L1$^+$ MPMs, CD20$^+$ infiltrates are associated with a poorer outcome (70) (**Table 1**). Patil et al. classified MPM cases into three different subgroups, based on immune profiles: one subgroup showed higher expression of B cell markers and antigen presentation-related genes compared with the other ones (91). This indicates that B cell infiltration is not a constant feature in all MPM cases and cannot be considered as a hallmark as, sometimes it is rarely detectable (76). Nevertheless, in some patients increased levels of B cells constitute a window of opportunity to develop novel immunotherapies and to identify novel MPM targeting receptors. Through bulk RNA-Seq data analysis from MPM tissue, the BCR sequence can be identified to generate candidate antibodies binding to MPM target cells. Another new approach to produce high-affinity antibodies involves the isolation of memory B cells from peripheral blood of the donors, when immortalized, such B cells stably secrete monoclonal antigen-specific antibodies, which could be used as further therapeutic agents (112). More research is needed to better understand the role of B cells in MPM but based on these premises, this cell population can be considered an important candidate for the development of new therapies.

## GENETIC ALTERATIONS PREDISPOSING TO MESOTHELIOMA

As previously described, the role of external agents in inducing mesothelioma is mainly attributable to the chronic inflammation guided by *HMGB1*, NF-kB and the PIK3CA pathway. Meanwhile, clinical studies of large cohorts of individuals and the improvement of genome wide sequencing technologies have helped the identification of an increased number of oncological diseases associated with germline mutations (113). These genes mainly encode for tumor suppressor proteins involved in cell cycle regulation, apoptosis and DNA repair pathways; being involved in cancer development, they are called cancer susceptibility genes (113). The identification of these genes have paved the way for the development of targeted therapeutic approaches as well as for cancer prevention and surveillance (114, 115). The most common inherited cancer risk factor associated with MPM is the aberration of BRCA1 Associated Protein 1 (*BAP1*), a deubiquitinating enzyme located on chromosome *3p21.1* acting as tumor suppressor gene (116, 117). *BAP1* is involved in different biological pathways, such as DNA replication, apoptosis, regulation of gene transcription, deubiquitation of histones and DNA repair (116, 117). Germline defects of *BAP1* are responsible for the BAP1-tumor predisposition syndrome (BAP1-TPDS) including the occurrence of renal cell carcinoma, uveal melanoma, cholangiocarcinoma and mesothelioma. High frequency of germline mutations of *BAP1* were demonstrated to cause mesothelioma in 2001, when an epidemic spread of cases was reported in a village in Cappadocia (113, 118). These results were further confirmed by other groups: in 2018, Betti et al. reported a frequency of 7.7% of pathogenic germline variants in a cohort of 39 patients (119), while Pastorino et al. reported a frequency of 30.7% in a cohort of 52 patients affected by malignant mesothelioma (120).

*BAP1* alterations occur in one mutant allele and are inherited as autosomal dominant mutations: a study of germline-mutated mesothelioma showed 43.1% of relatives carried the same mutation of their probands (120). The peculiarity of mesotheliomas carrying *BAP1* defects is a higher frequency in non- or low-exposure to asbestos as reported by Pastorino et al (120). These alterations are more frequently detected in young adults with MPM: 4% in patients older than 75 years and 20% in the ones of 55 years of age or younger (121). Among the three histotypes of MPM, such as epithelioid, sarcomatoid, and biphasic, BAP1-germline mutations are found more frequently in the epithelioid and this correlates with a better prognosis (113, 115).

Today, the assessment of *BAP1* status has become part of the diagnostic routine of mesothelioma allowing to distinguish between benign and malignant mesothelial cells and to identify biphasic mesothelioma (116). However, the implementation of sequencing technologies with more extensive studies will uncover molecular features associated with mesothelioma onset. Interestingly, a recent study has revealed that *BAP1* is not the only cancer-susceptibility-gene predisposing to mesothelioma. Bononi et al. have shown that heterozygous mutations in the Bloom syndrome gene (*BLM*), a gene involved in the DNA repair, promote the development of mesothelioma and the risk is further increased by exposure to asbestos (122).

These results suggest the importance of early detection of cancer risk factors in the population *via* tailored screening programs in order to prevent cancer development.

## THE ROLE OF THE DNA REPAIR

The DNA damage response (DDR) consists of a complex network of genes that respond to different types of DNA damages, such as Double Strand Breaks (DSBs) and Single Strand Breaks (SSBs), being organized in pathways as homologous recombination (HR), non-homologous end-joining (NHEJ), mismatch repair (MMR) and nucleotide excision repair (NER). Defects in one or more pathways lead to genomic instability and promote tumorigenesis and cancer progression (123, 124).

DDR has been an attractive therapeutic target upon the discovery of synthetic lethality, which occurs when the inefficiency of a DNA repair system causes the recruitment of other DNA damage pathways. This concept has first been applied to HR genes like *BRCA1/2* due to their interaction with the poly(ADP-ribose) polymerase (PARP), a family of proteins that are activated in the presence of DNA damage and stabilize the replication machinery during repair (123). Thus, a new category of drugs called PARP-inhibitors (PARPi) have been developed to target the rescue of DNA repair pathway and lead to genomic instability and cell death (123). Among the most studied PARPi there are talazoparib, rucaparib, niraparib, olaparib and veliparib; although being first intended to target tumor lacking functional *BRCA1/2*, their action has been expanded to a larger category of Homologous Recombination Deficiency (HRD) tumors, that comprise other HR genes like *ATM*, *ATR*, *RAD51*, *BARD1 (*124).

Evidence reported in several works has shown a high percentage of germline mutations in MPM occurring in DNA repairing genes. Betti et al. tested a panel of 94 cancer predisposing genes and found mutations in *PALB2*, *BRCA1/2*, *FANC1*, *ATM*, *SLX4*, *FANCC*, *FANCF*, *PMS1* and *XPC* covering almost the 10% of all tested patients (118). Most of these genes were involved in specific DNA repair mechanisms like HR, MMR and NER. A similar result was further confirmed by Panou et al. that reported an improved survival in patients with MPM bearing DNA repairing defects (121). A study by Guo et al. addressed the role of DNA repair genes in the pathogenesis of MPM and identified mutations in novel target genes like *MSH3*, *BARD1* and *RECQL4* that have not been previously described (125). A recent review by Fuso Nerini et al. confirmed that considering different studies performed on MPM, the DNA repair pathways are among the most frequently affected (124).

In this context, the use of PARPi in mesothelioma has been encouraged, however preliminary data do not allow a clear conclusion of PARPi effectiveness (124) (**Table 2**). In fact, while some studies have shown combinatorial treatment with cisplatin and olaparib is effective in mesothelioma cells with a defective HR (137), another study has demonstrated that olaparib has limited anti-tumor activity also in *BAP1* mutated patients (NCT03531840). Other clinical trials are still ongoing (NCT03207347, NCT03654833) and will help clarify the effects of PARPi in mesothelioma.

One of the main concern about DNA damage and mesothelioma has been the assessment of the role of *BAP1* in sensing cells to PARPi. The role of *BAP1* in the DDR is due to its interaction with *BRCA1* and *BARD1*, however this association is far to be completely understood and need further investigation (116). A recent study exploited the sensitivity to PARPi in

**TABLE 2** | Druggable targets in mesothelioma.

| Molecular Feature | Drug | References |
|---|---|---|
| BAP1 | PARPi (olaparib, niraparib, rucaparib) | NCT03531840, NCT03207347, NCT03654833 |
| MGMT low, SFLN11 high | PARPi (talazoparib) + temozolomide | (126) |
| ALK fusion | ALK inhibitors | (127) |
| BAP1 *wt* and KDM6A | tazemetostat | (128) |
| NF2 | FAK inhibitors, everolimus | (129, 130) |
| PTCH1 | vismogedib | (131) |
| TERT | telomerase inhibitors (MST-312) | (132) |
| DNA repair and TME | lurbinectedin | (133) |
| BCL2, BCL-XL | BH3-mimetics, survivin inhibitor(YM155), bortezomib, trabectedin | (134) |
| HDAC | vorinostat | (135) |
| STAT1 | fludarabine (F-araA), risedronic acid (RIS) | (136) |

patient-derived mesothelioma cells (126). They showed that response to PARPi is independent on *BAP1* mutational status. Conversely, they demonstrated that PARPi sensitivity, especially to talazoparib in combination with temozolomide, is mainly related to the combination of low expression levels of O-6-Methylguanine-DNA methyltransferase (*MGMT*) and high expression levels of Schlafen 11 (*SLFN11*) (126) (**Table 2**). Overall, this evidence suggests that targeting the DDR in MPM is still an attractive strategy, most of all in a context of combined therapy; however, more preclinical studies are needed to exploit other combinations and unravel molecular mechanisms and drug-interactions that could lead to improved patients outcome.

## THERAPEUTIC IMPLICATIONS OF GENOMICS AND TRANSCRIPTOMICS EVIDENCES

The *-omics* field in the study of cancer pathology has evolved rapidly in the last decades. The improvement of high-throughput technologies and computational approaches have made a big step forward in cancer characterization and drug-response investigation becoming crucial in the context of translational research.

Genomic and transcriptomic studies have improved the molecular characterization of MPM and set new hypothesis for therapeutic approaches. The first genomic studies from Bueno et al. in 2016 analyzed 211 transcriptomes and 216 whole exomes of mesotheliomas, while Hmeljak et al. in 2018 analyzed 74 samples from The Cancer Genome Atlas (TCGA) by the integration of the exome and the transcriptome (105, 138). Both studies confirmed frequent mutations in the *CDKN2A*, *NF2*, *TP53*, *LATS2*, and *SETD2* genes and a low mutational burden with less than two non-synonymous mutations per megabase (Mb). Bueno et al. identified other genomic aberrations such as gene fusions and splice alterations in the most relevant genes like *NF2*, *BAP1* and *SETD2 (*138*).* Both studies assessed a somatic copy-number alteration (SCNA) landscape with more copy losses than amplifications that included *BAP1*, *NF2*, *CDKN2B*, *LATS2*, as a further confirmation that MPM development is driven primarily by loss of tumor suppressor genes than by activation of classic oncogenic drivers (105, 138).

The pivotal role of *BAP1* in mesothelioma is confirmed also at the somatic level, since 60% of cases present a second hit (120), even if the percentage could be even higher since studies performed so far have used next generation sequencing (NGS) approaches that lacked the identification of large deletions, while assessment from different platforms, like IHC and multiplex ligation–dependent probe amplification (MLPA) have increased detection perfomances (116). Somatic *BAP1* mutations preferentially affect the epithelioid subtype and correlate to better prognosis (116).

Recently, a work by Zhang et al. has depicted a detailed picture of MPM genomic features. Indeed, the study of intratumor heterogeneity of MPM through an exome sequencing approach has shown that most MPMs follow a linear evolution with BAP1 being the most frequent ancestral mutation and NF2 arising mainly as a late event. Moreover, a minority of patients presented a branched evolution that was associated with a higher tumor lymphocyte infiltration and antigen burden, suggesting a possible sensitivity to immunotherapy (139).

Aberrant copy number alterations in *CDKN2A* and *p16* arm identified with sequencing approaches were confirmed in other studies through fluorescent *in-situ* hybridization (FISH) and IHC and they were associated with higher asbestos fiber exposure (140).

Somatic mutations in *CDKN2A*, *NF2*, *BAP1* were also reported in cases of malignant peritoneal mesothelioma, with *CDKN2A* less frequent as compared to pleural mesothelioma (141). Interestingly, the same work reported gene fusions such as EWSR1-ATF1 and FUS-ATF1 and *ALK* rearrangements that are hardly found in pleural mesothelioma and seem to be specific for young women as compared to *ALK-wild type* patients but might respond to targeted treatment (127, 141, 142) (**Table 2**). Two recent studies have reported novel somatic mutations in *RDX* and *MXRA5* genes, independently (143, 144). In Torricelli et al. *RDX* and *MXRA5* are present in 42% and 40.6% of the cohort, respectively and authors stated that *MXRA5* is specific for the biphasic histotype together with *NOD2 (*143). The same genes were also described in the RAMES study where *RDX* and *MXRA5* represented the 42% and 23% of MPMs, respectively, however in this case *MXRA5* was identified in both epithelioid and non-epithelioid histotypes (144). Moreover, the same gene is reported to be significantly correlated to longer survival rate in a cohort of epithelioid only MPMs (145). Therefore, although the correlation of *MXRA5* to histopathologic or clinical features needs further interpretation, more studies on this gene and *RDX* are warranted.

The extensive work of the genomic studies presented so far have defined various genetic features of mesothelioma, but, to date, they have no role in patient stratification and treatment. Interestingly, more insights in MPM molecular characterization have emerged from transcriptomic studies. The first molecular classification in epithelioid, sarcomatoid, and biphasic, was proposed in 2016 with the identification of 400 most variable genes within the groups, 189 upregulated and 241 downregulated, which also correlated with survival (138). Specifically, the epithelioid subtype presented up-regulation of *UPK3B*, *ELMO3, CLDN15* while *LOXL2* and *VIM* were up-regulated in the sarcomatoid subtype, thus showing a key difference in EMT regulation in the two groups. Using a data-integration approach Hmeljak et al. came to the same histotype classification, however, they stressed a relevant issue: since MPM transcriptomic can be used for histotype stratification, it is possible to use it even further for prognosis within a single histotype. For example, although the epithelioid histotype has a better survival rate than sarcomatoid, even within this subgroup it is possible to identify different clinical courses. Guided from this hypothesis, a cluster of patients with epithelioid subtype with poor prognosis was identified and associated with higher *AURKA* mRNA expression (105). Previously, the association of

*AURKA* expression to a worse prognosis was detected by Borchert et al (137). This evidence suggests that for a further improvement in MPM therapeutic approaches it is essential to consider integrated data analysis, such as the combination of genomic and transcriptomic features.

## EXTENSIVE CHROMOSOMAL BREAKAGE: A NEW IDENTIFIED FEATURE IN MESOTHELIOMA

As previously stated, mesothelioma presents as a tumor with low mutational burden with a median of 23 mutations per biopsy specimen (146) with ~1.2 mutations per Mb (105, 138). This finding identifies mesothelioma as an atypical tumor, since it is known that exposure to carcinogens and environmental pollution characterize tumors with a highly compromised genomic landscape and high mutational burden. However, latest development of sequencing technologies have revealed hidden aspects in cancer malignancies that have not been previously investigated, such as chromotripsis. The word chromotripsis derives from "chromo" which stands for chromosome and "tripsi" which means breaking into small pieces (147) and refers to a mutational phenomenon of DNA breakage from a single event that spreads into hundreds of catastrophic chromosomal damages (148). Accumulated DNA damages lead to the formation of micronuclei, usually containing single chromosome, that are disrupted during cell cycle and spread genetic material in the cells (146). Pieces of chromosomes can be included in the nuclei during mitosis, and this generates chromosome rearrangements and fusions (149) (**Figure 3**). Recent studies have addressed this topic in malignant mesothelioma. With the intent to provide reliable cell line models of mesothelioma, Oey et al. have characterized the genome of tumors and tumor-derived cell lines through whole genome sequencing (151). Here, the authors have identified recurrent events of high chromosomal instability like chromoanagenesis and chromotripsis. Interestingly, inter- and intra-chromosomal rearrangements affected genes like *CDKN2A*, one of the most frequently mutated in mesothelioma and *KDM6A*, a gene that has been associated with sensitivity to enhancer of zeste homolog 2 (EZH2) inhibitors, like tazemetostat (151, 153). This finding might have important implications, as *BAP1*-lacking mesotheliomas have demonstrated sensitivity to EZH2 inhibitors (128) (**Table 2**).

A more recent study addressed chromotripsis in mesothelioma through a new approach (150) called Mate-pair sequencing (Mpseq). Mpseq generates larger sequencing fragments and can detect chromosomal rearrangements and large insertion/deletion (150). Mansfield et al. found rearrangements that lead to *CDKN2A, BAP1* and *NF2* chromosomal instabilities. In particular, they have evaluated the MESO cohort of TCGA and identified chromotripsis events in 69% of patients, mostly occurring in tumor suppressor genes and non-coding DNA (150).

Results obtained in other cancers have shown that chromotripsis contributes to oncogene amplification, thus promoting cancer progression (152, 154). Among them, those harboring telomerase reverse transcriptase (*TERT*) gains have shown higher prevalence for chromothripsis (149) and this can be linked to mesothelioma with TERT-impairment that present poorer prognosis. This evidence suggests that chromotripsis is a specific genomic feature of mesothelioma and that future studies should include investigations of this complex event, especially for therapeutic developments. To this, chromotripsis has been recently associated with the development of drug-resistance in cancer through a mechanism that involves the repairing systems of the DNA *via* PARP and the NHEJ pathway (152). In addition, the notion of mesothelioma as a low mutated tumor should be reconsidered since most studies have defined the mutational burden in relation to only nucleotide changes, however the previously discussed findings suggest to consider genomic and structural rearrangements as well. Indeed, an increased expression of neoantigens resulting from these catastrophic events in mesothelioma correlate with clonal expansion of tumor-infiltrating T cells (150) suggesting a possible role in response to immunotherapy (**Figure 3**). All together, these discoveries indicate that the group of MPM presenting chromotripsis could benefit from combinatorial drug treatment, including PARPi or immunotherapy, that are worth being further exploited.

## NOVEL MOLECULAR TARGETS FOR THERAPEUTIC STRATEGIES

Following *BAP1*, the second most frequent mutated gene in mesothelioma is the neurofibromatosis type 2 (*NF2*) which encodes the protein merlin (138). This protein plays a role in the Hippo and the mTOR pathways, other than being involved in EMT (155). In mesothelioma, *NF2* is found mostly as a biallelic inactivation. As reported by Sato et al. preclinical *in vivo* studies have shown the central role of *NF2* in sensitizing tissue to asbestos and developing mesothelioma (129). In other studies, conducted on patients cohort, it has emerged that impairment of the *NF2* gene is more frequent in the sarcomatoid subtype rather than the epithelioid and this correlates with worst prognosis (129, 138). To date, NF2 alterations represent a possible target for treatment such as drugs aiming at interfering with its function in extracellular matrix signal transduction. Up to date, studies are mainly based on preclinical models, cell lines or xenograft; however, promising results suggest further developments. To this, the initial studies investigating FAK inhibitors as VS-4718, or YAP and mTOR inhibitors in MPM lead to positive results in preclinical studies but not in clinical trials (129) (**Table 2**). Others showed the antagonistic relationship between FAK and Wnt pathways in malignant mesothelioma: dysregulated Wnt signaling is associated with invasion and resistance to apoptosis, while FAK signaling promotes invasion and EMT (130). The most interesting outcome has been reached with the development of K-975, a small molecule that inhibits the transcriptional enhanced associate domain (TEAD) protein that belongs to the Hippo

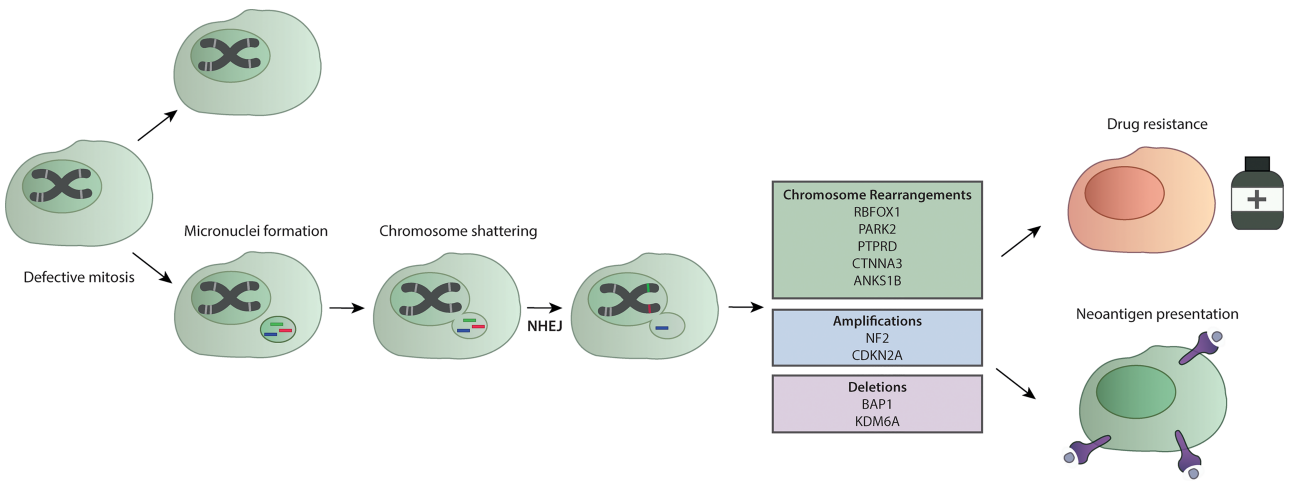


**FIGURE 3** | Chromotripsis in mesothelioma. A defective mitosis process leads to the formation of micronuclei. Further replication leads to chromosome shattering and the addition of genetic material through the NHEJ. This process forms chromosome rearrangements that in MPM interest genes like *RBFOX1, PARK2, PTPRD, CTNNA3* and *ANK51B*, and are linked to amplification of key MPM genes like *NF2* and *CDKN2A*, or the loss of genetic material of *BAP1* and *KDM6A* (113, 150, 151). Amplification of oncogenes due to chromotripsis has been recently associated with drug resistance (152). The extensive chromosomal breakage upon chromotripsis events leads to neoantigen presentation that can make cells more sensitive to immunotherapy (150).

pathway. K-975 showed a potent inhibitory effect on the proliferation of MPM cell lines, with a greater activity on NF2-non-expressing cells (156). Overall, these studies suggest that *NF2* could be considered as a potential target for MPM warranting further investigations.

Recently, the involvement of the Hedgehog pathway in MPM has been investigated. Here, in a patient diagnosed with epithelioid MPM, a mutation in *PTCH1* was identified (131). This gene is involved in the Hedgehog pathway and is druggable by vismodegib, already approved for the treatment of basal cell carcinoma (BCC) (**Table 2**). Despite the patient underwent several lines of treatment, vismodegib led to a very good partial response which lasted for over two years. The lack of genomic testing throughout the course of chemotherapy does not allow understanding whether the *PTCH1* mutation was acquired under pharmacological pressure; still, this result suggests an interesting novel target in MPM.

Pirker et al. investigated the role of *TERT* promoter in mesothelioma (132). They found that mutations in *TERT* are prevalently associated with non-epithelioid subtype and to poor survival. In accordance with this evidence, *TERT* mutations are mutually exclusive with *BAP1*, which is more frequent in the epithelioid subtype and correlates with better prognosis, as previously discussed. An interesting aspect is that cell lines derived from tumors with mutated *TERT* present a more stable genome, e.g., in the number of gains or losses, in comparison to wild type ones, with a specific imbalance in chromosomes 1, 5q, 9p, 7, 14, and 20. These evidences brought to test telomerase inhibitors like MST-312 MPM, however with moderate effects (132) (**Table 2**).

BCL-2 is a family protein involved in tumorigenesis of different cancer types. It consists of BCL-2, BCL-XL, BCL-W, MCL-1 and BFL-1 proteins. In mesothelioma, overexpression of *BCL-2* was found in 20% of cell lines and in 24% of a tumor samples, while the expression of *BCL-XL* and *MCL-1* was identified as a general feature of mesothelioma, suggesting their critical role as pro-survival factors (134). As BCL-2 proteins act directly on the apoptosis pathway downstream from *TP53*, this makes its targeting an interesting therapeutic approach (134). Preclinical studies have been performed in mesothelioma cell lines using direct or indirect targeting of BCL2 and BCL-XL: both in cell lines and *in vivo* models this treatment was able to induce an apoptotic effect. This has paved the way to the development of BH3-mimetics a novel class of compound that mimic the interaction of BCL-2 protein through their BH3 domain. In mesothelioma, BH3-mimetics have been used in combination with YM155, a survivin inhibitor, or bortezomib, with an increased apoptotic effect in comparison to controls (**Table 2**). These drugs have also been used in combination with trabectedin, a marine compound, showing that *BCL-2* mRNA expression inversely correlated with response to the treatment (134).

The marine-derived drug trabectedin has been already tested in MPM, although without any efficacy. In fact, the ATREUS trial, where this drug was administered as second line therapy in epithelioid MPM and as a first or second line in non-epithelioid subtype, showed poor efficacy of trabectedin and high liver toxicity that did not justify further use of this drug (157). However, lurbinectedin, an analogue of trabectedin, has shown promising results in a phase II clinical trial, where it was administered as a second or third line therapy in MPM patients (133) (**Table 2**). Lurbinectedin was efficacious independently on the MPM histotype and previous treatment. Further investigations to understand which patients might

benefit from this drug are needed; however, the possible dual effect of lurbinectedin on both tumor cells and microenvironment might open new therapeutic venues for this disease (158).

In a recent work Dell'Anno et al. have used a drug repositioning approach to screen five MPM cell lines with 1170 FDA-approved drugs (136). They identified fludarabine (F-araA) and risedronic acid (RIS) as effective in MPM through a mechanism of inhibition of STAT1 expression and nucleic acids synthesis. Although promising, these results are yet limited by the use of only five cell lines without molecular characterization of these cells. Further studies including diverse and deeply characterized models are needed to successfully develop treatments for MPM.

## THE ROLE OF MICRORNA DYSREGULATION

In the past 20 years it has become increasingly clear that microRNAs are important players in the regulation of physiological processes within the cells, and that their dysregulation can be a major driver of malignant transformation and tumor progression (159, 160). Following the first description of a direct link between the loss of expression of a specific microRNA and cancer in 2002 (161), many studies followed investigating both the oncogenic and tumor suppressive potential of microRNAs. Hence, to date we know of many microRNAs that are involved in several processes linked to cancer development and progression, from regulation of cell proliferation and cell cycle processes to EMT and involvement in cancer immune escape (160, 162–164).

While still somewhat understudied in MPM, the studies available thus far, have shown that microRNAs play an important role in the biology of MPM, and represent valuable biomarker candidates (165, 166).

Considering that MPM is a diseases characterized by the loss of tumor suppressors, it is not surprising that this is also reflected on microRNA level with the majority of dysregulated microRNAs being lost, while only a limited number has been shown to be upregulated in MPM (165–167). The first study investigating dysregulation of microRNAs in MPM was performed by Guled et al. in 2009, who could show differential expression of microRNAs in MPM tissue compared to normal pericardial mesothelium, but also differential expression between the different histological subtypes of MPM (168). This study was shortly after followed by a study from Busacca et al. on MPM cell lines compared to immortalized mesothelial cells, which showed that the microRNAs with the greatest differential expression between MPM and normal cells, also discriminated between histopathological subtypes when investigated in tumor samples (169).

While the dysregulated microRNAs identified in these early studies were not functionally investigated, the obtained data strongly hinted towards a relevant role for microRNAs in MPM biology. The first studies providing functional data on dysregulated microRNAs, investigated the effect of re-expression of miR-29c-5p (miR-29c*) (170) and miR-31 (171), and in both cases, re-expression using microRNA mimics resulted in reduced proliferation and invasion of MPM cell lines, supporting a tumor suppressive role of these microRNAs. Following these initial studies, further tumor suppressor microRNAs were investigated in MPM such as miR-145 (172) and miR-205 (173), both of which are likely to alter EMT *via* targeting OCT4 and ZEB1/2 respectively. One of most comprehensively investigated tumor suppressive microRNAs in MPM is probably the miR-15~107 super family, and here in particular the family member miR-16. Reid et al. have shown that the members of this microRNA superfamily are quite consistently lost in MPM tissue compared to normal pleura, as well as in MPM cell lines (174). *In vitro* analyses then revealed that re-expression of miR-16-5p resulted in reduced cell proliferation and colony forming ability, as well as induction of apoptosis and a G0/G1 cell cycle arrest in MPM cell lines, but not in the non-malignant mesothelial cell line MeT-5A. These observed effects were most likely brought about by the downregulation of miR-16-5p target genes *BCL2* and *CCND1*. In addition, re-expression of miR-16 resulted in sensitization of cells to pemetrexed and gemcitabine, suggesting an additional role of the miR-15~107 family in response to antimetabolite chemotherapy. Most importantly, mouse experiments, in which miR-16 was systemically delivered to the tumor cells using (EnGenic) minicells resulted in significant tumor growth inhibition *in vivo*. Based on these data, a phase I clinical trial was performed in MPM and non-small cell lung cancer (NSCLC) patients, which apart from reaching its goal of proving safety of the miR-16 replacement therapy approach also showed in one patient a remarkable metabolic and radiological response to the treatment (175, 176). In a more recent study, the same group has now shown that miR-16-5p is a regulator of PD-L1 expression, hence also linking this tumor suppressor to response to immune checkpoint inhibition (177). While miR-16-5p is the most comprehensively investigated tumor, suppressive microRNA linked to MPM biology, other microRNAs such as miR-193a-3p (178), miR-137-5p (179), miR-126 (180, 181), miR-34b/c (182, 183), and miR-215-5p (184) have also promising anti-proliferative and anti-tumor activity, when re-expressed *in vitro* or *in vivo*.

Compared to the tumor suppressive microRNAs, which have been investigated relatively frequently in MPM, studies of oncogenic microRNAs are much rarer, also due to the fact that not many microRNAs have been found to be consistently overexpressed in MPM tumor tissue. One example however are miR-182-5p and miR-183-5p, which inhibition using microRNA inhibitors results in reduced proliferation and invasion (185).

Taken together, the available expression and functional studies highlight that microRNA dysregulation, in particular the loss of tumor suppressive microRNAs, is likely to represent an important contributor to MPM biology, and therefore to the development and progression of this devastating disease. Considering the encouraging data obtained from *in vivo* microRNAs replacement studies and early clinical trials, additional research efforts in this area are certainly warranted.

Especially also in light of the recent development of mRNA-based vaccines against COVID-19, the field of RNA-based vaccines has significantly advanced, possibly also opening additional avenues for delivery of microRNAs to cancer cells in order to replace lost tumor suppressors.

In addition to their important role in contributing to MPM biology, microRNAs have in recent years also been investigated for their biomarker potential both in tumor tissue and in blood (165, 166). Regarding the diagnostic value of tumor microRNA expression, the first published study by Gee et al. performed microRNA profiling in MPM tissue and pleural metastases from lung adenocarcinomas (186). This study identified in particular low expression of members of the miR-220 family as potential diagnostic factors for differentiating MPM and pleural metastases. A subsequent study by Benjamin et al., then investigated microRNA expression in a larger set of MPM and adenocarcinomas of the lung or pleura, and identified in addition to members of the miR-200 family, also members of the miR-192 family as potential diagnostic markers (187). Based on this data, a microRNAs expression signature was generated and independently validated in a small set of patients. The signature consisting of miR-192, -193-5p and -200c showed high accuracy (95%) in discriminating MPM from adenocarcinomas, and was subsequently marketed by Rosetta Genomics. While additional candidates such as miR-126, -143, -145 and -652 have been proposed (188, 189), none of the microRNAs or diagnostic signatures described here has been followed up extensively, hence none of them is in routine clinical use.

Similarly, several studies have been undertaken investigating the prognostic value of microRNAs in MPM. Among the most promising candidates is the tumor suppressive microRNA miR-29c-5p, which expression is not only associated with the histological subtype (higher in epithelioid), but also significantly associated with survival (170). Similarly, the tumor suppressor miR-31 has recently also been proposed to hold prognostic potential, with lower expression being associated with longer survival (190). Furthermore, in a study investigating specimens from patients undergoing extrapleural pneumonectomy, a signature consisting of 6 microRNAs, the so-called miR-Score, was identified, which was able to separate patients with good and poor prognosis with an accuracy of 87% (191). However, similar to the diagnostic candidates, independent validation studies are lacking.

An attractive alternative to microRNA expression in tissue samples is the presence of microRNAs in the circulation. Other than longer RNA species, microRNAs show remarkable stability in the blood of patients due to the fact that they are mainly bound to lipoproteins or encapsulated into extracellular vesicles. With this in mind, a small number of studies has been published proposing for example low levels of miR-103 in whole blood (192, 193), low levels of miR-126 (181, 188, 194) in serum, low level of miR-132 in plasma (195) or high levels of miR-625-3p (196) in plasma or serum to be associated with the presence of MPM, and allowed to discriminate those patients from healthy controls and asbestos-exposed individuals. While these studies again provide first evidence of the biomarker potential of microRNAs in the circulation, large independent validation studies undertaken by independent research groups are usually missing, and none of the candidates is yet ready for routine clinical application.

## EPIGENETIC ALTERATIONS AS PROMISING PROGNOSTIC BIOMARKERS

In addition to the above mentioned specific alterations of DNA or RNA in MPM, great interest is now being paid to the epigenome, that includes post-translational modifications that ultimately impact on gene expression not encoded by the DNA (197). Epigenetics modifications play an important role in the regulation of gene expression and include DNA methylation, histone modifications and chromatin remodeling. Dysfunction of these mechanism have been linked to tumorigenesis, cancer progression and metastasis (198, 199).

Due to the lack of druggable molecular targets, the level of investigation in MPM disease has moved so far. DNA methylation associated with tumor-suppressor genes and mechanisms involving histone modifications have been described and linked to MPM phenotypes and histological subtypes (198). DNA methylation provokes gene silencing by adding a methyl group to the fifth carbon of the cytosine base, with a process that mainly occurs in promoter regions, thus modifying the expression of the associated genes, or on repetitive DNA elements, such as LINE1, causing chromatin modifications (200). Although DNA methylation patterns are fairly stable markers of differentiated tissues that regulate specific gene expression, changes in the methylation profile can occur due to aging, exposure to environmental stimuli and chronic inflammation (200, 201). In particular, accumulation levels of DNA methylation has been associated with higher cancer risk and cancer onset (202). The investigation of the DNA methylation profiles can be carried on at the tumor level, otherwise it is possible to search specific markers in the circulating peripheral blood. Studies conducted in malignant mesothelioma tumors have identified hypermethylated regions in *TMEM30B*, *KAZALD1* and *MAPK13* (203). DNA methyltransferases (*DNMT1*, *DNMT3a* and *DNMT3b*) were hypermethylated in mesothelioma cells in comparison to normal pleura, a result that was further confirmed in the TCGA cohort (203). More recently, through genome-wide methylation array technology Guarrera et al. analyzed the methylome of 163 MPM cases whose exposure to asbestos was previously assessed in comparison to control samples (202). Here, the authors identified differential profiles of DNA methylation, 98% of which comprised hypomethylated single-CpG. These genomic regions were mainly associated with genes involved in immune systems processes. These profiles were not histotype-specific, a part from the couple *CXCR6* and *FYCO1* which had lower methylation level in biphasic mesotheliomas than epithelioid. However, the striking result was the most significant hypomethylated CpG in 7p22.2 associated with the Forkhead Box K1 (*FOXK1*), a transcription factor involved in pathways like development and metabolism, and, most of all, directly interacting with *BAP1*. It has been suggested that the dephosporylation of *FOXK1* transactivated CCL-2 gene and

promotes the activation of TAMs (204). These recent evidences push to go further in the investigation of these markers, especially considering their involvement in the immune system processes that make them a likely target for immunotherapy.

The identification of DNA methylation as a marker in blood has also been explored so far. The most studied gene is mesothelin encoding the mesothelin-related peptide (SMRP) which is generally methylated in the normal pleura, while it is modified in MPM. However, it has a low sensitivity to be considered as a good marker for MPM (204). This led Santarelli et al. to identify a new marker for asbestos-exposed mesotheliomas (194). Thrombomodulin (TM) expression is silenced in malignant mesothelioma through a mechanism that involved the methylation of TM promoter by the recruitment of PARP1. Since the methylation of TM promoter has been associated with survival and given the role of PARP1 in the methylation mechanism, this marker may be of interest for further investigation for therapeutic development. In 2019, Cugliari et al. analyzed the peripheral blood of 159 MPMs and identified the CpG dinucleotide cg03546163 region associated with the gene *FKBP5* as a significant marker for prognosis (205). This is very interesting as *FKBP5* increases chemosensitivity to the AKT pathway, which is druggable in mesothelioma as previously described.

Other epigenetic modifications involve the acetylation and methylation of histones. A study by Goto et al. has identified a high expression of state of histone H3 lysine methylation (H3K27me3) mark (206). Interestingly, high expression marks of H3K27me3 have been associated with overexpression of EZH2 (207). This last has been found as a marker of poor prognosis in mesothelioma (207). Moreover, preclinical studies have shown that loss of function in BAP1 make cells sensitive to the inhibitors of EZH2. Among them, tazemetostat, a first-in-class small-molecule inhibitor of EZH2 received approval from the FDA in January 2020 for the treatment of locally advanced or metastatic sarcoma (207), while an ongoing clinical trial named NCT02860286 has shown antitumor activity of tazemetostat in a cohort of 74 patients lacking BAP1 (128). However, the use of drugs targeting the epigenome has already been attempted in mesothelioma with negative results. In fact, in the phase III VANTAGE-014 trial the efficacy of vorinostat, a histone deacetylase inhibitor, was tested against placebo with no improvement in overall survival (135) (**Table 2**). As claimed by Garassino et al., the main biases of this study were the random selection of patients irrespective of clinicopathological features and the rapid development into a phase III trial (208). These results do not undermine the use of drugs targeting the epigenome, instead they underline the necessity to improve patients' stratification previous to enrollment into clinical trials. In summary, the investigation of potentially reversible modifications like the epigenetics markers seem to be relevant in MPM, and, when identified through liquid biopsy, they could represent a novel and promising approach for diagnosis and monitoring of cancer progression.

## CONCLUSION

In this review, we have covered multiple aspects of mesothelioma microenvironment that have played and will play an important role for immunotherapeutic approaches. To this, targeting the TME with anti-PD1 (nivolumab) and anti-CTLA-4 (ipilimumab) has revealed as the most effective strategy in this disease with few therapeutic options (209). In addition, genomic and transcriptomic have allowed the identification of druggable features, currently under evaluation alone or in combination with immunotherapies. Moreover, microRNAs expression has shown a role in a better understanding of the biology of MPM, and promising preliminary data suggests a possible application in the clinic for diagnosis and monitoring as epigenetic studies.

In conclusion, a comprehensive knowledge of MPM biological aspects is crucial for a deeper understanding of such complex disease and for the improvement of patients' outcome.

## AUTHOR CONTRIBUTIONS

SH and LM: conceptualization, original draft preparation, and writing. AC-F and FG: conceptualization, original draft preparation, writing, and supervision. MK: conceptualization and writing. All the authors: review and editing. All authors contributed to the article and approved the submitted version.

## ACKNOWLEDGMENTS

We would like to thank Fondazione Buzzi and Stiftung für angewandte Krebsforschung.

## REFERENCES

1. Donaldson K, Murphy FA, Duffin R, Poland CA. Asbestos, Carbon Nanotubes and the Pleural Mesothelium: A Review of the Hypothesis Regarding the Role of Long Fibre Retention in the Parietal Pleura, Inflammation and Mesothelioma. *Part Fibre Toxicol* (2010) 7:5. doi: 10.1186/1743-8977-7-5
2. Tanaka S, Choe N, Iwagaki A, Hemenway DR, Kagan E. Asbestos Exposure Induces MCP-1 Secretion by Pleural Mesothelial Cells. *Exp Lung Res* (2000) 26:241–55. doi: 10.1080/019021400404528
3. Xu A, Wu LJ, Santella RM, Hei TK. Role of Oxyradicals in Mutagenicity and DNA Damage Induced by Crocidolite Asbestos in Mammalian Cells. *Cancer Res* (1999) 59:5922–6.
4. Xue J, Patergnani S, Giorgi C, Suarez J, Goto K, Bononi A, et al. Asbestos Induces Mesothelial Cell Transformation *Via* HMGB1-Driven Autophagy. *Proc Natl Acad Sci USA* (2020) 117:25543–52. doi: 10.1073/pnas.2007622117
5. Jube S, Rivera ZS, Bianchi ME, Powers A, Wang E, Pagano I, et al. Cancer Cell Secretion of the DAMP Protein HMGB1 Supports Progression in Malignant Mesothelioma. *Cancer Res* (2012) 72:3290–301. doi: 10.1158/0008-5472.CAN-11-3481
6. Mukherjee A, Vasquez KM. Targeting Chromosomal Architectural HMGB Proteins Could be the Next Frontier in Cancer Therapy. *Cancer Res* (2020) 80:2075–82. doi: 10.1158/0008-5472.CAN-19-3066
7. Napolitano A, Antoine DJ, Pellegrini L, Baumann F, Pagano I, Pastorino S, et al. HMGB1 and Its Hyperacetylated Isoform are Sensitive and Specific

Serum Biomarkers to Detect Asbestos Exposure and to Identify Mesothelioma Patients. *Clin Cancer Res* (2016) 22:3087–96. doi: 10.1158/1078-0432.CCR-15-1130
8. Padmore T, Stark C, Turkevich LA, Champion JA. Quantitative Analysis of the Role of Fiber Length on Phagocytosis and Inflammatory Response by Alveolar Macrophages. *Biochim Biophys Acta Gen Subj* (2017) 1861:58–67. doi: 10.1016/j.bbagen.2016.09.031
9. Wen H, Ting JP-Y, O'Neill LAJ. A Role for the NLRP3 Inflammasome in Metabolic Diseases–did Warburg Miss Inflammation? *Nat Immunol* (2012) 13:352–7. doi: 10.1038/ni.2228
10. Horio D, Minami T, Kitai H, Ishigaki H, Higashiguchi Y, Kondo N, et al. Tumor-Associated Macrophage-Derived Inflammatory Cytokine Enhances Malignant Potential of Malignant Pleural Mesothelioma. *Cancer Sci* (2020) 111:2895–906. doi: 10.1111/cas.14523
11. Yang H, Rivera Z, Jube S, Nasu M, Bertino P, Goparaju C, et al. Programmed Necrosis Induced by Asbestos in Human Mesothelial Cells Causes High-Mobility Group Box 1 Protein Release and Resultant Inflammation. *Proc Natl Acad Sci USA* (2010) 107:12611–6. doi: 10.1073/pnas.1006542107
12. Qi F, Okimoto G, Jube S, Napolitano A, Pass HI, Laczko R, et al. Continuous Exposure to Chrysotile Asbestos Can Cause Transformation of Human Mesothelial Cells *Via* HMGB1 and TNF-α Signaling. *Am J Pathol* (2013) 183:1654–66. doi: 10.1016/j.ajpath.2013.07.029
13. Yang H, Bocchetta M, Kroczynska B, Elmishad AG, Chen Y, Liu Z, et al. TNF-Alpha Inhibits Asbestos-Induced Cytotoxicity *Via* a NF-KappaB-Dependent Pathway, A Possible Mechanism for Asbestos-Induced Oncogenesis. *Proc Natl Acad Sci USA* (2006) 103:10397–402. doi: 10.1073/pnas.0604008103
14. Wang Y, Faux SP, Hallden G, Kirn DH, Houghton CE, Lemoine NR, et al. Interleukin-1beta and Tumour Necrosis Factor-Alpha Promote the Transformation of Human Immortalised Mesothelial Cells by Erionite. *Int J Oncol* (2004) 25:173–8. doi: 10.3892/ijo.25.1.173
15. Awad MM, Jones RE, Liu H, Lizotte PH, Ivanova EV, Kulkarni M, et al. Cytotoxic T Cells in PD-L1-Positive Malignant Pleural Mesotheliomas Are Counterbalanced by Distinct Immunosuppressive Factors. *Cancer Immunol Res* (2016) 4:1038–48. doi: 10.1158/2326-6066.CIR-16-0171
16. Chee SJ, Lopez M, Mellows T, Gankande S, Moutasim KA, Harris S, et al. Evaluating the Effect of Immune Cells on the Outcome of Patients With Mesothelioma. *Br J Cancer* (2017) 117:1341–8. doi: 10.1038/bjc.2017.269
17. Tazzari M, Brich S, Tuccitto A, Bozzi F, Beretta V, Spagnuolo RD, et al. Complex Immune Contextures Characterise Malignant Peritoneal Mesothelioma: Loss of Adaptive Immunological Signature in the More Aggressive Histological Types. *J Immunol Res* (2018) 2018:5804230. doi: 10.1155/2018/5804230
18. Vivier E, Raulet DH, Moretta A, Caligiuri MA, Zitvogel L, Lanier LL, et al. Innate or Adaptive Immunity? The Example of Natural Killer Cells. *Science* (2011) 331:44–9. doi: 10.1126/science.1198687
19. Platonova S, Cherfils-Vicini J, Damotte D, Crozet L, Vieillard V, Validire P, et al. Profound Coordinated Alterations of Intratumoral NK Cell Phenotype and Function in Lung Carcinoma. *Cancer Res* (2011) 71:5412–22. doi: 10.1158/0008-5472.CAN-10-4179
20. Sottile R, Tannazi M, Johansson MH, Cristiani CM, Calabró L, Ventura V, et al. NK- and T-Cell Subsets in Malignant Mesothelioma Patients: Baseline Pattern and Changes in the Context of Anti-CTLA-4 Therapy. *Int J Cancer* (2019) 145:2238–48. doi: 10.1002/ijc.32363
21. Nishimura Y, Kumagai-Takei N, Matsuzaki H, Lee S, Maeda M, Kishimoto T, et al. Functional Alteration of Natural Killer Cells and Cytotoxic T Lymphocytes Upon Asbestos Exposure and in Malignant Mesothelioma Patients. *BioMed Res Int* (2015) 2015:238431. doi: 10.1155/2015/238431
22. Marcq E, Waele JD, Audenaerde JV, Lion E, Santermans E, Hens N, et al. Abundant Expression of TIM-3, LAG-3, PD-1 and PD-L1 as Immunotherapy Checkpoint Targets in Effusions of Mesothelioma Patients. *Oncotarget* (2017) 8:89722–35. doi: 10.18632/oncotarget.21113
23. Marcq E, Siozopoulou V, De Waele J, van Audenaerde J, Zwaenepoel K, Santermans E, et al. Prognostic and Predictive Aspects of the Tumor Immune Microenvironment and Immune Checkpoints in Malignant Pleural Mesothelioma. *Oncoimmunology* (2017) 6:e1261241. doi: 10.1080/2162402X.2016.1261241
24. Lievense LA, Bezemer K, Cornelissen R, Kaijen-Lambers MEH, Hegmans JPJJ, Aerts JGJV. Precision Immunotherapy; Dynamics in the Cellular Profile of Pleural Effusions in Malignant Mesothelioma Patients. *Lung Cancer* (2017) 107:36–40. doi: 10.1016/j.lungcan.2016.04.015
25. Tumino N, Martini S, Munari E, Scordamaglia F, Besi F, Mariotti FR, et al. Presence of Innate Lymphoid Cells in Pleural Effusions of Primary and Metastatic Tumors: Functional Analysis and Expression of PD-1 Receptor. *Int J Cancer* (2019) 145:1660–8. doi: 10.1002/ijc.32262
26. Bosi A, Zanellato S, Bassani B, Albini A, Musco A, Cattoni M, et al. Natural Killer Cells From Malignant Pleural Effusion Are Endowed With a Decidual-Like Proangiogenic Polarization. *J Immunol Res* (2018) 2018:2438598. doi: 10.1155/2018/2438598
27. Vacca P, Martini S, Garelli V, Passalacqua G, Moretta L, Mingari MC. NK Cells From Malignant Pleural Effusions are Not Anergic But Produce Cytokines and Display Strong Antitumor Activity on Short-Term IL-2 Activation. *Eur J Immunol* (2013) 43:550–61. doi: 10.1002/eji.201242783
28. Jackaman C, Lansley S, Allan JE, Robinson BWS, Nelson DJ. IL-2/CD40-Driven NK Cells Install and Maintain Potency in the Anti-Mesothelioma Effector/Memory Phase. *Int Immunol* (2012) 24:357–68. doi: 10.1093/intimm/dxs005
29. Rossjohn J, Pellicci DG, Patel O, Gapin L, Godfrey DI. Recognition of CD1d-Restricted Antigens by Natural Killer T Cells. *Nat Rev Immunol* (2012) 12:845–57. doi: 10.1038/nri3328
30. Bendelac A, Savage PB, Teyton L. The Biology of NKT Cells. *Annu Rev Immunol* (2007) 25:297–336. doi: 10.1146/annurev.immunol.25.022106.141711
31. Altomare E, Fallarini S, Biaggi G, Gattoni E, Botta M, Lombardi G. Increased Frequency of Circulating Invariant Natural Killer T Cells in Malignant Pleural Mesothelioma Patients. *Cancer Biol Ther* (2012) 13:702–11. doi: 10.4161/cbt.20553
32. Tagawa T, Wu L, Anraku M, Yun Z, Rey-McIntyre K, de Perrot M. Antitumor Impact of Interferon-γ Producing CD1d-Restricted NKT Cells in Murine Malignant Mesothelioma. *J Immunother* (2013) 36:391–9. doi: 10.1097/CJI.0b013e3182a801f2
33. Wu L, Yun Z, Tagawa T, de la Maza L, Wu MO, Yu J, et al. Activation of CD1d-restricted Natural Killer T Cells can Inhibit Cancer Cell Proliferation During Chemotherapy by Promoting the Immune Responses in Murine Mesothelioma. *Cancer Immunol Immunother* (2014) 63:1285–96. doi: 10.1007/s00262-014-1597-9
34. Burt BM, Rodig SJ, Tilleman TR, Elbardissi AW, Bueno R, Sugarbaker DJ. Circulating and Tumor-Infiltrating Myeloid Cells Predict Survival in Human Pleural Mesothelioma. *Cancer* (2011) 117:5234–44. doi: 10.1002/cncr.26143
35. Tanrikulu AC, Abakay A, Komek H, Abakay O. Prognostic Value of the Lymphocyte-to-Monocyte Ratio and Other Inflammatory Markers in Malignant Pleural Mesothelioma. *Environ Health Prev Med* (2016) 21:304–11. doi: 10.1007/s12199-016-0530-6
36. Davis MJ, Tsang TM, Qiu Y, Dayrit JK, Freij JB, Huffnagle GB, et al. Macrophage M1/M2 Polarization Dynamically Adapts to Changes in Cytokine Microenvironments in Cryptococcus Neoformans Infection. *mBio* (2013) 4:e00264–00213. doi: 10.1128/mBio.00264-13
37. Goerdt S, Orfanos CE. Other Functions, Other Genes: Alternative Activation of Antigen-Presenting Cells. *Immunity* (1999) 10:137–42. doi: 10.1016/s1074-7613(00)80014-x
38. Mantovani A, Sozzani S, Locati M, Allavena P, Sica A. Macrophage Polarization: Tumor-Associated Macrophages as a Paradigm for Polarized M2 Mononuclear Phagocytes. *Trends Immunol* (2002) 23:549–55. doi: 10.1016/s1471-4906(02)02302-5
39. Ujiie H, Kadota K, Nitadori J-I, Aerts JG, Woo KM, Sima CS, et al. The Tumoral and Stromal Immune Microenvironment in Malignant Pleural Mesothelioma: A Comprehensive Analysis Reveals Prognostic Immune Markers. *Oncoimmunology* (2015) 4:e1009285. doi: 10.1080/2162402X.2015.1009285
40. Fujii M, Toyoda T, Nakanishi H, Yatabe Y, Sato A, Matsudaira Y, et al. TGF-β Synergizes With Defects in the Hippo Pathway to Stimulate Human Malignant Mesothelioma Growth. *J Exp Med* (2012) 209:479–94. doi: 10.1084/jem.20111653
41. Gschwandtner M, Derler R, Midwood KS. More Than Just Attractive: How CCL2 Influences Myeloid Cell Behavior Beyond Chemotaxis. *Front Immunol* (2019) 10:2759. doi: 10.3389/fimmu.2019.02759
42. Kishimoto T, Fujimoto N, Ebara T, Omori T, Oguri T, Niimi A, et al. Serum Levels of the Chemokine CCL2 are Elevated in Malignant Pleural Mesothelioma Patients. *BMC Cancer* (2019) 19:1204. doi: 10.1186/s12885-019-6419-1

43. Gueugnon F, Leclercq S, Blanquart C, Sagan C, Cellerin L, Padieu M, et al. Identification of Novel Markers for the Diagnosis of Malignant Pleural Mesothelioma. *Am J Pathol* (2011) 178:1033–42. doi: 10.1016/j.ajpath.2010.12.014
44. Blanquart C, Gueugnon F, Nguyen J-M, Roulois D, Cellerin L, Sagan C, et al. CCL2, Galectin-3, and SMRP Combination Improves the Diagnosis of Mesothelioma in Pleural Effusions. *J Thorac Oncol* (2012) 7:883–9. doi: 10.1097/JTO.0b013e31824c9272
45. Davidson B, Dong HP, Holth A, Berner A, Risberg B. Chemokine Receptors are Infrequently Expressed in Malignant and Benign Mesothelial Cells. *Am J Clin Pathol* (2007) 127:752–9. doi: 10.1309/LN2075V7C8K31CH8
46. Boulakirba S, Pfeifer A, Mhaidly R, Obba S, Goulard M, Schmitt T, et al. IL-34 and CSF-1 Display an Equivalent Macrophage Differentiation Ability But a Different Polarization Potential. *Sci Rep* (2018) 8:256. doi: 10.1038/s41598-017-18433-4
47. Chéné A-L, d'Almeida S, Blondy T, Tabiasco J, Deshayes S, Fonteneau J-F, et al. Pleural Effusions From Patients With Mesothelioma Induce Recruitment of Monocytes and Their Differentiation Into M2 Macrophages. *J Thorac Oncol* (2016) 11:1765–73. doi: 10.1016/j.jtho.2016.06.022
48. Blondy T, d'Almeida SM, Briolay T, Tabiasco J, Meiller C, Chéné A-L, et al. Involvement of the M-CSF/IL-34/CSF-1R Pathway in Malignant Pleural Mesothelioma. *J Immunother Cancer* (2020) 8:e000182. doi: 10.1136/jitc-2019-000182
49. Cioce M, Canino C, Goparaju C, Yang H, Carbone M, Pass HI. Autocrine CSF-1R Signaling Drives Mesothelioma Chemoresistance *Via* AKT Activation. *Cell Death Dis* (2014) 5:e1167. doi: 10.1038/cddis.2014.136
50. Zhang F, Wang H, Wang X, Jiang G, Liu H, Zhang G, et al. TGF-β Induces M2-like Macrophage Polarization *Via* SNAIL-Mediated Suppression of a Pro-Inflammatory Phenotype. *Oncotarget* (2016) 7:52294–306. doi: 10.18632/oncotarget.10561
51. Gratchev A. TGF-β Signalling in Tumour Associated Macrophages. *Immunobiology* (2017) 222:75–81. doi: 10.1016/j.imbio.2015.11.016
52. Lievense LA, Cornelissen R, Bezemer K, Kaijen-Lambers MEH, Hegmans JPJJ, Aerts JGJV. Pleural Effusion of Patients With Malignant Mesothelioma Induces Macrophage-Mediated T Cell Suppression. *J Thorac Oncol* (2016) 11:1755–64. doi: 10.1016/j.jtho.2016.06.021
53. Izzi V, Chiurchiù V, D'Aquilio F, Palumbo C, Tresoldi I, Modesti A, et al. Differential Effects of Malignant Mesothelioma Cells on THP-1 Monocytes and Macrophages. *Int J Oncol* (2009) 34:543–50. doi: 10.3892/ijo_00000180
54. Seoane J, Gomis RR. Tgf-β Family Signaling in Tumor Suppression and Cancer Progression. *Cold Spring Harb Perspect Biol* (2017) 9(12):a022277. doi: 10.1101/cshperspect.a022277
55. Kumar-Singh S, Weyler J, Martin MJ, Vermeulen PB, Van Marck E. Angiogenic Cytokines in Mesothelioma: A Study of VEGF, FGF-1 and -2, and TGF Beta Expression. *J Pathol* (1999) 189:72–8. doi: 10.1002/(SICI)1096-9896(199909)189:1<72::AID-PATH401>3.0.CO;2-0
56. DeLong P, Carroll RG, Henry AC, Tanaka T, Ahmad S, Leibowitz MS, et al. Regulatory T Cells and Cytokines in Malignant Pleural Effusions Secondary to Mesothelioma and Carcinoma. *Cancer Biol Ther* (2005) 4:342–6. doi: 10.4161/cbt.4.3.1644
57. Maeda J, Ueki N, Ohkawa T, Iwahashi N, Nakano T, Hada T, et al. Transforming Growth Factor-Beta 1 (TGF-Beta 1)- and Beta 2-Like Activities in Malignant Pleural Effusions Caused by Malignant Mesothelioma or Primary Lung Cancer. *Clin Exp Immunol* (1994) 98:319–22. doi: 10.1111/j.1365-2249.1994.tb06144.x
58. Stockhammer P, Ploenes T, Theegarten D, Schuler M, Maier S, Aigner C, et al. Detection of TGF-β in Pleural Effusions for Diagnosis and Prognostic Stratification of Malignant Pleural Mesothelioma. *Lung Cancer* (2020) 139:124–32. doi: 10.1016/j.lungcan.2019.11.013
59. Solinas G, Germano G, Mantovani A, Allavena P. Tumor-Associated Macrophages (TAM) as Major Players of the Cancer-Related Inflammation. *J Leukoc Biol* (2009) 86:1065–73. doi: 10.1189/jlb.0609385
60. Pollard JW. Trophic Macrophages in Development and Disease. *Nat Rev Immunol* (2009) 9:259–70. doi: 10.1038/nri2528
61. Bingle L, Brown NJ, Lewis CE. The Role of Tumour-Associated Macrophages in Tumour Progression: Implications for New Anticancer Therapies. *J Pathol* (2002) 196:254–65. doi: 10.1002/path.1027
62. Tsutsui S, Yasuda K, Suzuki K, Tahara K, Higashi H, Era S. Macrophage Infiltration and Its Prognostic Implications in Breast Cancer: The Relationship With VEGF Expression and Microvessel Density. *Oncol Rep* (2005) 14:425–31. doi: 10.3892/or.14.2.425
63. Condeelis J, Pollard JW. Macrophages: Obligate Partners for Tumor Cell Migration, Invasion, and Metastasis. *Cell* (2006) 124:263–6. doi: 10.1016/j.cell.2006.01.007
64. Minnema-Luiting J, Vroman H, Aerts J, Cornelissen R. Heterogeneity in Immune Cell Content in Malignant Pleural Mesothelioma. *Int J Mol Sci* (2018) 19(4):1041. doi: 10.3390/ijms19041041
65. Salaroglio IC, Kopecka J, Napoli F, Pradotto M, Maletta F, Costardi L, et al. Potential Diagnostic and Prognostic Role of Microenvironment in Malignant Pleural Mesothelioma. *J Thorac Oncol* (2019) 14:1458–71. doi: 10.1016/j.jtho.2019.03.029
66. Pasello G, Zago G, Lunardi F, Urso L, Kern I, Vlacic G, et al. Malignant Pleural Mesothelioma Immune Microenvironment and Checkpoint Expression: Correlation With Clinical-Pathological Features and Intratumor Heterogeneity Over Time. *Ann Oncol* (2018) 29:1258–65. doi: 10.1093/annonc/mdy086
67. Cornelissen R, Lievense LA, Maat AP, Hendriks RW, Hoogsteden HC, Bogers AJ, et al. Ratio of Intratumoral Macrophage Phenotypes is a Prognostic Factor in Epithelioid Malignant Pleural Mesothelioma. *PloS One* (2014) 9:e106742. doi: 10.1371/journal.pone.0106742
68. Anraku M, Cunningham KS, Yun Z, Tsao M-S, Zhang L, Keshavjee S, et al. Impact of Tumor-Infiltrating T Cells on Survival in Patients With Malignant Pleural Mesothelioma. *J Thorac Cardiovasc Surg* (2008) 135:823–9. doi: 10.1016/j.jtcvs.2007.10.026
69. Yamada N, Oizumi S, Kikuchi E, Shinagawa N, Konishi-Sakakibara J, Ishimine A, et al. CD8+ Tumor-Infiltrating Lymphocytes Predict Favorable Prognosis in Malignant Pleural Mesothelioma After Resection. *Cancer Immunol Immunother* (2010) 59:1543–9. doi: 10.1007/s00262-010-0881-6
70. Fusco N, Vaira V, Righi I, Sajjadi E, Venetis K, Lopez G, et al. Characterization of the Immune Microenvironment in Malignant Pleural Mesothelioma Reveals Prognostic Subgroups of Patients. *Lung Cancer* (2020) 150:53–61. doi: 10.1016/j.lungcan.2020.09.026
71. Colin DJ, Cottet-Dumoulin D, Faivre A, Germain S, Triponez F, Serre-Beinier V. Experimental Model of Human Malignant Mesothelioma in Athymic Mice. *Int J Mol Sci* (2018) 19(7):1881. doi: 10.3390/ijms19071881
72. Miselis NR, Wu ZJ, Van Rooijen N, Kane AB. Targeting Tumor-Associated Macrophages in An Orthotopic Murine Model of Diffuse Malignant Mesothelioma. *Mol Cancer Ther* (2008) 7:788–99. doi: 10.1158/1535-7163.MCT-07-0579
73. Gao D, Joshi N, Choi H, Ryu S, Hahn M, Catena R, et al. Myeloid Progenitor Cells in the Premetastatic Lung Promote Metastases by Inducing Mesenchymal to Epithelial Transition. *Cancer Res* (2012) 72:1384–94. doi: 10.1158/0008-5472.CAN-11-2905
74. Umansky V, Blattner C, Gebhardt C, Utikal J. The Role of Myeloid-Derived Suppressor Cells (MDSC) in Cancer Progression. *Vaccines (Basel)* (2016) 4(4):36. doi: 10.3390/vaccines4040036
75. Khanna S, Graef S, Mussai F, Thomas A, Wali N, Yenidunya BG, et al. Tumor-Derived GM-CSF Promotes Granulocyte Immunosuppression in Mesothelioma Patients. *Clin Cancer Res* (2018) 24:2859–72. doi: 10.1158/1078-0432.CCR-17-3757
76. Hegmans JPJJ, Hemmes A, Hammad H, Boon L, Hoogsteden HC, Lambrecht BN. Mesothelioma Environment Comprises Cytokines and T-Regulatory Cells That Suppress Immune Responses. *Eur Respir J* (2006) 27:1086–95. doi: 10.1183/09031936.06.00135305
77. Rikimaru T, Ichikawa Y, Ogawa Y, Higuchi E, Kinosita M, Oizumi K, et al. Production of Granulocyte Colony-Stimulating Factor by Malignant Mesothelioma. *Eur Respir J* (1995) 8:183–4. doi: 10.1183/09031936.95.08010183
78. Fujiwara A, Higashiyama M, Kanou T, Okami J, Tokunaga T, Tomita Y, et al. Granulocyte-Colony Stimulating Factor (G-CSF) Producing Malignant Pleural Mesothelioma: Report of a Case. *Thorac Cancer* (2015) 6:105–9. doi: 10.1111/1759-7714.12140
79. Jackaman C, Yeoh TL, Acuil ML, Gardner JK, Nelson DJ. Murine Mesothelioma Induces Locally-Proliferating IL-10(+)TNF-α(+)CD206(-)CX3CR1(+) M3 Macrophages That Can Be Selectively Depleted by

Chemotherapy or Immunotherapy. *Oncoimmunology* (2016) 5:e1173299. doi: 10.1080/2162402X.2016.1173299
80. Zhao Y, Wu T, Shao S, Shi B, Zhao Y. Phenotype, Development, and Biological Function of Myeloid-Derived Suppressor Cells. *Oncoimmunology* (2016) 5:e1004983. doi: 10.1080/2162402X.2015.1004983
81. Veltman JD, Lambers MEH, van Nimwegen M, Hendriks RW, Hoogsteden HC, Aerts JGJV, et al. COX-2 Inhibition Improves Immunotherapy and is Associated With Decreased Numbers of Myeloid-Derived Suppressor Cells in Mesothelioma. Celecoxib Influences MDSC Function. *BMC Cancer* (2010) 10:464. doi: 10.1186/1471-2407-10-464
82. Fridman WH, Pagès F, Sautès-Fridman C, Galon J. The Immune Contexture in Human Tumours: Impact on Clinical Outcome. *Nat Rev Cancer* (2012) 12:298–306. doi: 10.1038/nrc3245
83. Borghaei H, Paz-Ares L, Horn L, Spigel DR, Steins M, Ready NE, et al. Nivolumab Versus Docetaxel in Advanced Nonsquamous Non-Small-Cell Lung Cancer. *N Engl J Med* (2015) 373:1627–39. doi: 10.1056/NEJMoa1507643
84. Brahmer J, Reckamp KL, Baas P, Crinò L, Eberhardt WEE, Poddubskaya E, et al. Nivolumab Versus Docetaxel in Advanced Squamous-Cell Non-Small-Cell Lung Cancer. *N Engl J Med* (2015) 373:123–35. doi: 10.1056/NEJMoa1504627
85. Thapa B, Salcedo A, Lin X, Walkiewicz M, Murone C, Ameratunga M, et al. The Immune Microenvironment, Genome-Wide Copy Number Aberrations, and Survival in Mesothelioma. *J Thorac Oncol* (2017) 12:850–9. doi: 10.1016/j.jtho.2017.02.013
86. Klampatsa A, O'Brien SM, Thompson JC, Rao AS, Stadanlick JE, Martinez MC, et al. Phenotypic and Functional Analysis of Malignant Mesothelioma Tumor-Infiltrating Lymphocytes. *Oncoimmunology* (2019) 8:e1638211. doi: 10.1080/2162402X.2019.1638211
87. Sakaguchi S, Yamaguchi T, Nomura T, Ono M. Regulatory T Cells and Immune Tolerance. *Cell* (2008) 133:775–87. doi: 10.1016/j.cell.2008.05.009
88. Shang B, Liu Y, Jiang S, Liu Y. Prognostic Value of Tumor-Infiltrating FoxP3 + Regulatory T Cells in Cancers: A Systematic Review and Meta-Analysis. *Sci Rep* (2015) 5:15179. doi: 10.1038/srep15179
89. McCoy MJ, Nowak AK, van der Most RG, Dick IM, Lake RA. Peripheral CD8(+) T Cell Proliferation is Prognostic for Patients With Advanced Thoracic Malignancies. *Cancer Immunol Immunother* (2013) 62:529–39. doi: 10.1007/s00262-012-1360-z
90. Needham DJ, Lee JX, Beilharz MW. Intra-Tumoural Regulatory T Cells: A Potential New Target in Cancer Immunotherapy. *Biochem Biophys Res Commun* (2006) 343:684–91. doi: 10.1016/j.bbrc.2006.03.018
91. Patil NS, Righi L, Koeppen H, Zou W, Izzo S, Grosso F, et al. Molecular and Histopathological Characterization of the Tumor Immune Microenvironment in Advanced Stage of Malignant Pleural Mesothelioma. *J Thorac Oncol* (2018) 13:124–33. doi: 10.1016/j.jtho.2017.09.1968
92. Cedrés S, Ponce-Aix S, Zugazagoitia J, Sansano I, Enguita A, Navarro-Mendivil A, et al. Analysis of Expression of Programmed Cell Death 1 Ligand 1 (PD-L1) in Malignant Pleural Mesothelioma (MPM). *PloS One* (2015) 10:e0121071. doi: 10.1371/journal.pone.0121071
93. Inaguma S, Lasota J, Wang Z, Czapiewski P, Langfort R, Rys J, et al. Expression of ALCAM (CD166) and PD-L1 (CD274) Independently Predicts Shorter Survival in Malignant Pleural Mesothelioma. *Hum Pathol* (2018) 71:1–7. doi: 10.1016/j.humpath.2017.04.032
94. Watanabe T, Okuda K, Murase T, Moriyama S, Haneda H, Kawano O, et al. Four Immunohistochemical Assays to Measure the PD-L1 Expression in Malignant Pleural Mesothelioma. *Oncotarget* (2018) 9:20769–80. doi: 10.18632/oncotarget.25100
95. Mansfield AS, Roden AC, Peikert T, Sheinin YM, Harrington SM, Krco CJ, et al. B7-H1 Expression in Malignant Pleural Mesothelioma is Associated With Sarcomatoid Histology and Poor Prognosis. *J Thorac Oncol* (2014) 9:1036–40. doi: 10.1097/JTO.0000000000000177
96. Popat S, Curioni-Fontecedro A, Dafni U, Shah R, O'Brien M, Pope A, et al. A Multicentre Randomised Phase III Trial Comparing Pembrolizumab Versus Single-Agent Chemotherapy for Advanced Pre-Treated Malignant Pleural Mesothelioma: The European Thoracic Oncology Platform (ETOP 9-15) PROMISE-meso Trial. *Ann Oncol* (2020) 31:1734–45. doi: 10.1016/j.annonc.2020.09.009
97. Losi L, Bertolini F, Guaitoli G, Fabbiani L, Banchelli F, Ambrosini-Spaltro A, et al. Role of Evaluating Tumor–Infiltrating Lymphocytes, Programmed Death−1 Ligand 1 and Mismatch Repair Proteins Expression in Malignant Mesothelioma. *Int J Oncol* (2019) 55:1157–64. doi: 10.3892/ijo.2019.4883
98. Jin L, Gu W, Li X, Xie L, Wang L, Chen Z. PD-L1 and Prognosis in Patients With Malignant Pleural Mesothelioma: A Meta-Analysis and Bioinformatics Study. *Ther Adv Med Oncol* (2020) 12:1758835920962362. doi: 10.1177/1758835920962362
99. Khanna S, Thomas A, Abate-Daga D, Zhang J, Morrow B, Steinberg SM, et al. Malignant Mesothelioma Effusions Are Infiltrated By CD3+ T Cells Highly Expressing PD-L1 and the PD-L1+ Tumor Cells Within These Effusions Are Susceptible to ADCC by the Anti-PD-L1 Antibody Avelumab. *J Thorac Oncol* (2016) 11:1993–2005. doi: 10.1016/j.jtho.2016.07.033
100. Chee J, Watson MW, Chopra A, Nguyen B, Cook AM, Creaney J, et al. Tumour Associated Lymphocytes in the Pleural Effusions of Patients With Mesothelioma Express High Levels of Inhibitory Receptors. *BMC Res Notes* (2018) 11(1):864. doi: 10.1186/s13104-018-3953-x
101. Wu C, Mairinger F, Casanova R, Batavia AA, Leblond A-L, Soltermann A. Prognostic Immune Cell Profiling of Malignant Pleural Effusion Patients by Computerized Immunohistochemical and Transcriptional Analysis. *Cancers (Basel)* (2019) 11(12):1953. doi: 10.3390/cancers11121953
102. Alcala N, Mangiante L, Le-Stang N, Gustafson CE, Boyault S, Damiola F, et al. Redefining Malignant Pleural Mesothelioma Types as a Continuum Uncovers Immune-Vascular Interactions. *EBioMedicine* (2019) 48:191–202. doi: 10.1016/j.ebiom.2019.09.003
103. Lines JL, Pantazi E, Mak J, Sempere LF, Wang L, O'Connell S, et al. VISTA is An Immune Checkpoint Molecule for Human T Cells. *Cancer Res* (2014) 74:1924–32. doi: 10.1158/0008-5472.CAN-13-1504
104. Wang L, Pino-Lagos K, de Vries VC, Guleria I, Sayegh MH, Noelle RJ. Programmed Death 1 Ligand Signaling Regulates the Generation of Adaptive Foxp3+CD4+ Regulatory T Cells. *Proc Natl Acad Sci USA* (2008) 105:9331–6. doi: 10.1073/pnas.0710441105
105. Hmeljak J, Sanchez-Vega F, Hoadley KA, Shih J, Stewart C, Heiman D, et al. Integrative Molecular Characterization of Malignant Pleural Mesothelioma. *Cancer Discovery* (2018) 8:1548–65. doi: 10.1158/2159-8290.CD-18-0804
106. Muller S, Victoria Lai W, Adusumilli PS, Desmeules P, Frosina D, Jungbluth A, et al. V-Domain Ig-containing Suppressor of T-Cell Activation (VISTA), a Potentially Targetable Immune Checkpoint Molecule, Is Highly Expressed in Epithelioid Malignant Pleural Mesothelioma. *Mod Pathol* (2020) 33:303–11. doi: 10.1038/s41379-019-0364-z
107. Sautès-Fridman C, Petitprez F, Calderaro J, Fridman WH. Tertiary Lymphoid Structures in the Era of Cancer Immunotherapy. *Nat Rev Cancer* (2019) 19:307–25. doi: 10.1038/s41568-019-0144-6
108. Ladányi A, Kiss J, Mohos A, Somlai B, Liszkay G, Gilde K, et al. Prognostic Impact of B-Cell Density in Cutaneous Melanoma. *Cancer Immunol Immunother* (2011) 60:1729–38. doi: 10.1007/s00262-011-1071-x
109. Krishnan S, Bakker E, Lee C, Kissick HT, Ireland DJ, Beilharz MW. Successful Combined Intratumoral Immunotherapy of Established Murine Mesotheliomas Requires B-cell Involvement. *J Interferon Cytokine Res* (2015) 35:100–7. doi: 10.1089/jir.2014.0054
110. Jackaman C, Cornwall S, Graham PT, Nelson DJ. CD40-Activated B Cells Contribute to Mesothelioma Tumor Regression. *Immunol Cell Biol* (2011) 89:255–67. doi: 10.1038/icb.2010.88
111. Shigematsu Y, Hanagiri T, Kuroda K, Baba T, Mizukami M, Ichiki Y, et al. Malignant Mesothelioma-Associated Antigens Recognized by Tumor-Infiltrating B Cells and the Clinical Significance of the Antibody Titers. *Cancer Sci* (2009) 100:1326–34. doi: 10.1111/j.1349-7006.2009.01181.x
112. Nicolini F, Bocchini M, Angeli D, Bronte G, Delmonte A, Crinò L, et al. Fully Human Antibodies for Malignant Pleural Mesothelioma Targeting. *Cancers (Basel)* (2020) 12(4):915. doi: 10.3390/cancers12040915
113. Carbone M, Adusumilli PS, Alexander HR, Baas P, Bardelli F, Bononi A, et al. Mesothelioma: Scientific Clues for Prevention, Diagnosis, and Therapy. *CA Cancer J Clin* (2019) 69:402–29. doi: 10.3322/caac.21572
114. McGee RB, Nichols KE. Introduction to Cancer Genetic Susceptibility Syndromes. *Hematol Am Soc Hematol Educ Program* (2016) 2016:293–301. doi: 10.1182/asheducation-2016.1.293
115. Pastorino L, Andreotti V, Dalmasso B, Vanni I, Ciccarese G, Mandalà M, et al. Insights Into Genetic Susceptibility to Melanoma by Gene Panel Testing: Potential Pathogenic Variants in ACD, Atm, BAP1, and POT1. *Cancers* (2020) 12:1007. doi: 10.3390/cancers12041007

116. Carbone M, Harbour JW, Brugarolas J, Bononi A, Pagano I, Dey A, et al. Biological Mechanisms and Clinical Significance of BAP1 Mutations in Human Cancer. *Cancer Discovery* (2020) 10:1103–20. doi: 10.1158/2159-8290.CD-19-1220
117. Hong JH, Chong ST, Lee P-H, Tan J, Heng HL, Ishak NDB, et al. Functional Characterisation Guides Classification of Novel BAP1 Germline Variants. *NPJ Genomic Med* (2020) 5:1–10. doi: 10.1038/s41525-020-00157-6
118. Betti M, Casalone E, Ferrante D, Aspesi A, Morleo G, Biasi A, et al. Germline Mutations in DNA Repair Genes Predispose Asbestos-Exposed Patients to Malignant Pleural Mesothelioma. *Cancer Lett* (2017) 405:38–45. doi: 10.1016/j.canlet.2017.06.028
119. Betti M, Aspesi A, Ferrante D, Sculco M, Righi L, Mirabelli D, et al. Sensitivity to Asbestos Is Increased in Patients With Mesothelioma and Pathogenic Germline Variants in BAP1 or Other DNA Repair Genes. *Genes Chromosomes Cancer* (2018) 57:573–83. doi: 10.1002/gcc.22670
120. Pastorino S, Yoshikawa Y, Pass HI, Emi M, Nasu M, Pagano I, et al. A Subset of Mesotheliomas With Improved Survival Occurring in Carriers of BAP1 and Other Germline Mutations. *J Clin Oncol* (2018) 36(35):JCO2018790352. doi: 10.1200/JCO.2018.79.0352
121. Panou V, Gadiraju M, Wolin A, Weipert CM, Skarda E, Husain AN, et al. Frequency of Germline Mutations in Cancer Susceptibility Genes in Malignant Mesothelioma. *J Clin Oncol* (2018) 36:2863–71. doi: 10.1200/JCO.2018.78.5204
122. Bononi A, Goto K, Ak G, Yoshikawa Y, Emi M, Pastorino S, et al. Heterozygous Germline BLM Mutations Increase Susceptibility to Asbestos and Mesothelioma. *PNAS* (2020) 117:33466–73. doi: 10.1073/pnas.2019652117
123. Pilié PG, Tang C, Mills GB, Yap TA. State-of-the-Art Strategies for Targeting the DNA Damage Response in Cancer. *Nat Rev Clin Oncol* (2019) 16:81–104. doi: 10.1038/s41571-018-0114-z
124. Fuso Nerini I, Roca E, Mannarino L, Grosso F, Frapolli R, D'Incalci M. Is DNA Repair a Potential Target for Effective Therapies Against Malignant Mesothelioma? *Cancer Treat Rev* (2020) 90:102101. doi: 10.1016/j.ctrv.2020.102101
125. Guo R, DuBoff M, Jayakumaran G, Kris MG, Ladanyi M, Robson ME, et al. Novel Germline Mutations in DNA Damage Repair in Patients With Malignant Pleural Mesotheliomas. *J Thorac Oncol* (2020) 15:655–60. doi: 10.1016/j.jtho.2019.12.111
126. Rathkey D, Khanal M, Murai J, Zhang J, Sengupta M, Jiang Q, et al. Sensitivity of Mesothelioma Cells to PARP Inhibitors Is Not Dependent on BAP1 But Is Enhanced by Temozolomide in Cells With High-Schlafen 11 and Low-O6-Methylguanine-DNA Methyltransferase Expression. *J Thorac Oncol* (2020) 15:843–59. doi: 10.1016/j.jtho.2020.01.012
127. Hung YP, Dong F, Watkins JC, Nardi V, Bueno R, Dal Cin P, et al. Identification of ALK Rearrangements in Malignant Peritoneal Mesothelioma. *JAMA Oncol* (2018) 4:235–8. doi: 10.1001/jamaoncol.2017.2918
128. Zauderer MG, Szlosarek PW, Le Moulec S, Popat S, Taylor P, Planchard D, et al. Safety and Efficacy of Tazemetostat, an Enhancer of Zeste-Homolog 2 Inhibitor, in Patients With Relapsed or Refractory Malignant Mesothelioma. *JCO* (2020) 38:9058–8. doi: 10.1200/JCO.2020.38.15_suppl.9058
129. Sato T, Sekido Y. NF2/Merlin Inactivation and Potential Therapeutic Targets in Mesothelioma. *Int J Mol Sci* (2018) 19(4):988. doi: 10.3390/ijms19040988
130. Wörthmüller J, Rüegg C. The Crosstalk Between FAK and Wnt Signaling Pathways in Cancer and Its Therapeutic Implication. *Int J Mol Sci* (2020) 21:9107. doi: 10.3390/ijms21239107
131. Popat S, Sharma B, MacMahon S, Nicholson AG, Sharma RK, Schuster K, et al. Durable Response to Vismodegib in PTCH1 F1147fs Mutant Relapsed Malignant Pleural Mesothelioma: Implications for Mesothelioma Drug Treatment. *JCO Precis Oncol* (2021) 5:39–43. doi: 10.1200/PO.20.00260
132. Pirker C, Bilecz A, Grusch M, Mohr T, Heidenreich B, Laszlo V, et al. Telomerase Reverse Transcriptase Promoter Mutations Identify a Genomically Defined and Highly Aggressive Human Pleural Mesothelioma Subgroup. *Clin Cancer Res* (2020) 26:3819–30. doi: 10.1158/1078-0432.CCR-19-3573
133. Metaxas Y, Früh M, Eboulet EI, Grosso F, Pless M, Zucali PA, et al. Lurbinectedin as Second- or Third-Line Palliative Therapy in Malignant Pleural Mesothelioma: An International, Multi-Centre, Single-Arm, Phase II Trial (SAKK 17/16). *Ann Oncol* (2020) 31:495–500. doi: 10.1016/j.annonc.2019.12.009
134. Arulananda S, Lee EF, Fairlie WD, John T. The Role of BCL-2 Family Proteins and Therapeutic Potential of BH3-Mimetics in Malignant Pleural Mesothelioma. *Expert Rev Anticancer Ther* (2020) 21(4):413–24. doi: 10.1080/14737140.2021.1856660
135. Krug LM, Kindler HL, Calvert H, Manegold C, Tsao AS, Fennell D, et al. Vorinostat in Patients With Advanced Malignant Pleural Mesothelioma Who Have Progressed on Previous Chemotherapy (VANTAGE-014): A Phase 3, Double-Blind, Randomised, Placebo-Controlled Trial. *Lancet Oncol* (2015) 16:447–56. doi: 10.1016/S1470-2045(15)70056-2
136. Dell'Anno I, Martin SA, Barbarino M, Melani A, Silvestri R, Bottaro M, et al. Drug-Repositioning Screening Identified Fludarabine and Risedronic Acid as Potential Therapeutic Compounds for Malignant Pleural Mesothelioma. *Invest New Drugs* (2020) 39(3):644–57. doi: 10.1007/s10637-020-01040-y
137. Borchert S, Wessolly M, Schmeller J, Mairinger E, Kollmeier J, Hager T, et al. Gene Expression Profiling of Homologous Recombination Repair Pathway Indicates Susceptibility for Olaparib Treatment in Malignant Pleural Mesothelioma *In Vitro*. *BMC Cancer* (2019) 19:108. doi: 10.1186/s12885-019-5314-0
138. Bueno R, Stawiski EW, Goldstein LD, Durinck S, De Rienzo A, Modrusan Z, et al. Comprehensive Genomic Analysis of Malignant Pleural Mesothelioma Identifies Recurrent Mutations, Gene Fusions and Splicing Alterations. *Nat Genet* (2016) 48:407–16. doi: 10.1038/ng.3520
139. Zhang M, Luo J-L, Sun Q, Harber J, Dawson AG, Nakas A, et al. Clonal Architecture in Mesothelioma Is Prognostic and Shapes the Tumour Microenvironment. *Nat Commun* (2021) 12:1751. doi: 10.1038/s41467-021-21798-w
140. Kettunen E, Savukoski S, Salmenkivi K, Böhling T, Vanhala E, Kuosma E, et al. CDKN2A Copy Number and p16 Expression in Malignant Pleural Mesothelioma in Relation to Asbestos Exposure. *BMC Cancer* (2019) 19:507. doi: 10.1186/s12885-019-5652-y
141. Hung YP, Dong F, Torre M, Crum CP, Bueno R, Chirieac LR. Molecular Characterization of Diffuse Malignant Peritoneal Mesothelioma. *Modern Pathol* (2020) 33:2269–79. doi: 10.1038/s41379-020-0588-y
142. Rüschoff JH, Gradhand E, Kahraman A, Rees H, Ferguson JL, Curioni-Fontecedro A, et al. STRN-ALK Rearranged Malignant Peritoneal Mesothelioma With Dramatic Response Following Ceritinib Treatment. *JCO Precis Oncol* (2019) 3:PO.19.00048. doi: 10.1200/PO.19.00048
143. Torricelli F, Lococo F, Di Stefano TS, Lorenzini E, Piana S, Valli R, et al. Deep Sequencing Analysis Identified a Specific Subset of Mutations Distinctive of Biphasic Malignant Pleural Mesothelioma. *Cancers* (2020) 12:2454. doi: 10.3390/cancers12092454
144. Pagano M, Ceresoli LG, Zucali PA, Pasello G, Garassino M, Grosso F, et al. Mutational Profile of Malignant Pleural Mesothelioma (MPM) in the Phase Ii RAMES Study. *Cancers* (2020) 12:2948. doi: 10.3390/cancers12102948
145. Torricelli F, Saxena A, Nuamah R, Neat M, Harling L, Ng W, et al. Genomic Analysis in Short- and Long-Term Patients With Malignant Pleura Mesothelioma Treated With Palliative Chemotherapy. *Eur J Cancer* (2020) 132:104–11. doi: 10.1016/j.ejca.2020.03.002
146. Carbone M, Yang H, Gaudino G. Does Chromothripsis Make Mesothelioma an Immunogenic Cancer? *J Thorac Oncol* (2019) 14:157–9. doi: 10.1016/j.jtho.2018.11.006
147. Stephens PJ, Greenman CD, Fu B, Yang F, Bignell GR, Mudie LJ, et al. Massive Genomic Rearrangement Acquired in a Single Catastrophic Event During Cancer Development. *Cell* (2011) 144:27–40. doi: 10.1016/j.cell.2010.11.055
148. Tubio JMC, Estivill X. Cancer: When Catastrophe Strikes a Cell. *Nature* (2011) 470:476–7. doi: 10.1038/470476a
149. Voronina N, Wong JKL, Hübschmann D, Hlevnjak M, Uhrig S, Heilig CE, et al. The Landscape of Chromothripsis Across Adult Cancer Types. *Nat Commun* (2020) 11:2320. doi: 10.1038/s41467-020-16134-7
150. Mansfield AS, Peikert T, Vasmatzis G. Chromosomal Rearrangements and Their Neoantigenic Potential in Mesothelioma. *Transl Lung Cancer Res* (2020) 9:S92–9. doi: 10.21037/tlcr.2019.11.12
151. Oey H, Daniels M, Relan V, Chee TM, Davidson MR, Yang IA, et al. Whole-Genome Sequencing of Human Malignant Mesothelioma Tumours and Cell Lines. *Carcinogenesis* (2019) 40:724–34. doi: 10.1093/carcin/bgz066
152. Shoshani O, Brunner SF, Yaeger R, Ly P, Nechemia-Arbely Y, Kim DH, et al. Chromothripsis Drives the Evolution of Gene Amplification in Cancer. *Nature* (2020) 591(7848):137–41. doi: 10.1038/s41586-020-03064-z

153. van Haaften G, Dalgliesh GL, Davies H, Chen L, Bignell G, Greenman C, et al. Somatic Mutations of the Histone H3K27 Demethylase Gene UTX in Human Cancer. *Nat Genet* (2009) 41:521–3. doi: 10.1038/ng.349
154. Cortés-Ciriano I, Lee JJ-K, Xi R, Jain D, Jung YL, Yang L, et al. Comprehensive Analysis of Chromothripsis in 2,658 Human Cancers Using Whole-Genome Sequencing. *Nat Genet* (2020) 52:331–41. doi: 10.1038/s41588-019-0576-7
155. Wadowski B, De Rienzo A, Bueno R. The Molecular Basis of Malignant Pleural Mesothelioma. *Thorac Surg Clin* (2020) 30:383–93. doi: 10.1016/j.thorsurg.2020.08.005
156. Kaneda A, Seike T, Danjo T, Nakajima T, Otsubo N, Yamaguchi D, et al. The Novel Potent TEAD Inhibitor, K-975, Inhibits YAP1/TAZ-TEAD Protein-Protein Interactions and Exerts an Anti-Tumor Effect on Malignant Pleural Mesothelioma. *Am J Cancer Res* (2020) 10:4399–415.
157. Cortinovis D, Grosso F, Carlucci L, Zucali PA, Pasello G, Tiseo M, et al. Trabectedin in Malignant Pleural Mesothelioma: Results From the Multicentre, Single Arm, Phase II Atreus Study. *Clin Lung Cancer* (2020) S1525-7304(20)30222-9. doi: 10.1016/j.cllc.2020.06.028
158. Barreca M, Spanò V, Montalbano A, Cueto M, Díaz Marrero AR, Deniz I, et al. Marine Anticancer Agents: An Overview With a Particular Focus on Their Chemical Classes. *Mar Drugs* (2020) 18(12):619. doi: 10.3390/md18120619
159. Garzon R, Calin GA, Croce CM. MicroRNAs in Cancer. *Annu Rev Med* (2009) 60:167–79. doi: 10.1146/annurev.med.59.053006.104707
160. Peng Y, Croce CM. The Role of MicroRNAs in Human Cancer. *Signal Transduct Target Ther* (2016) 1:15004. doi: 10.1038/sigtrans.2015.4
161. Calin GA, Dumitru CD, Shimizu M, Bichi R, Zupo S, Noch E, et al. Frequent Deletions and Down-Regulation of Micro- RNA Genes miR15 and miR16 at 13q14 in Chronic Lymphocytic Leukemia. *Proc Natl Acad Sci USA* (2002) 99:15524–9. doi: 10.1073/pnas.242606799
162. Behl T, Kumar C, Makkar R, Gupta A, Sachdeva M. Intercalating the Role of MicroRNAs in Cancer: As Enemy or Protector. *Asian Pac J Cancer Prev* (2020) 21:593–8. doi: 10.31557/APJCP.2020.21.3.593
163. Yi M, Xu L, Jiao Y, Luo S, Li A, Wu K. The Role of Cancer-Derived microRNAs in Cancer Immune Escape. *J Hematol Oncol* (2020) 13:25. doi: 10.1186/s13045-020-00848-8
164. Si W, Shen J, Zheng H, Fan W. The Role and Mechanisms of Action of microRNAs in Cancer Drug Resistance. *Clin Epigenet* (2019) 11:25. doi: 10.1186/s13148-018-0587-8
165. Reid G. MicroRNAs in Mesothelioma: From Tumour Suppressors and Biomarkers to Therapeutic Targets. *J Thorac Dis* (2015) 7:1031–40. doi: 10.3978/j.issn.2072-1439.2015.04.56
166. Birnie KA, Prêle CM, Thompson PJ, Badrian B, Mutsaers SE. Targeting microRNA to Improve Diagnostic and Therapeutic Approaches for Malignant Mesothelioma. *Oncotarget* (2017) 8:78193–207. doi: 10.18632/oncotarget.20409
167. Reid G, Johnson TG, van Zandwijk N. Manipulating microRNAs for the Treatment of Malignant Pleural Mesothelioma: Past, Present and Future. *Front Oncol* (2020) 10:105. doi: 10.3389/fonc.2020.00105
168. Guled M, Lahti L, Lindholm PM, Salmenkivi K, Bagwan I, Nicholson AG, et al. CDKN2A, NF2, and JUN Are Dysregulated Among Other Genes by miRNAs in Malignant Mesothelioma -a miRNA Microarray Analysis. *Genes Chromosomes Cancer* (2009) 48:615–23. doi: 10.1002/gcc.20669
169. Busacca S, Germano S, De Cecco L, Rinaldi M, Comoglio F, Favero F, et al. MicroRNA Signature of Malignant Mesothelioma With Potential Diagnostic and Prognostic Implications. *Am J Respir Cell Mol Biol* (2010) 42:312–9. doi: 10.1165/rcmb.2009-0060OC
170. Pass HI, Goparaju C, Ivanov S, Donington J, Carbone M, Hoshen M, et al. hsa-miR-29c* Is Linked to the Prognosis of Malignant Pleural Mesothelioma. *Cancer Res* (2010) 70:1916–24. doi: 10.1158/0008-5472.CAN-09-3993
171. Ivanov SV, Goparaju CMV, Lopez P, Zavadil J, Toren-Haritan G, Rosenwald S, et al. Pro-Tumorigenic Effects of miR-31 Loss in Mesothelioma. *J Biol Chem* (2010) 285:22809–17. doi: 10.1074/jbc.M110.100354
172. Cioce M, Ganci F, Canu V, Sacconi A, Mori F, Canino C, et al. Protumorigenic Effects of mir-145 Loss in Malignant Pleural Mesothelioma. *Oncogene* (2014) 33:5319–31. doi: 10.1038/onc.2013.476
173. Fassina A, Cappellesso R, Guzzardo V, Dalla Via L, Piccolo S, Ventura L, et al. Epithelial-Mesenchymal Transition in Malignant Mesothelioma. *Mod Pathol* (2012) 25:86–99. doi: 10.1038/modpathol.2011.144
174. Reid G, Pel ME, Kirschner MB, Cheng YY, Mugridge N, Weiss J, et al. Restoring Expression of miR-16: A Novel Approach to Therapy for Malignant Pleural Mesothelioma. *Ann Oncol* (2013) 24:3128–35. doi: 10.1093/annonc/mdt412
175. Kao SC, Fulham M, Wong K, Cooper W, Brahmbhatt H, MacDiarmid J, et al. A Significant Metabolic and Radiological Response After a Novel Targeted MicroRNA-based Treatment Approach in Malignant Pleural Mesothelioma. *Am J Respir Crit Care Med* (2015) 191:1467–9. doi: 10.1164/rccm.201503-0461LE
176. van Zandwijk N, Pavlakis N, Kao SC, Linton A, Boyer MJ, Clarke S, et al. Safety and Activity of microRNA-loaded Minicells in Patients With Recurrent Malignant Pleural Mesothelioma: A First-in-Man, Phase 1, Open-Label, Dose-Escalation Study. *Lancet Oncol* (2017) 18:1386–96. doi: 10.1016/S1470-2045(17)30621-6
177. Kao SC, Cheng YY, Williams M, Kirschner MB, Madore J, Lum T, et al. Tumor Suppressor Micrornas Contribute to the Regulation of PD-L1 Expression in Malignant Pleural Mesothelioma. *J Thorac Oncol* (2017) 12:1421–33. doi: 10.1016/j.jtho.2017.05.024
178. Williams M, Kirschner MB, Cheng YY, Hanh J, Weiss J, Mugridge N, et al. miR-193a-3p is a Potential Tumor Suppressor in Malignant Pleural Mesothelioma. *Oncotarget* (2015) 6:23480–95. doi: 10.18632/oncotarget.4346
179. Johnson TG, Schelch K, Cheng YY, Williams M, Sarun KH, Kirschner MB, et al. Dysregulated Expression of the MicroRNA miR-137 and Its Target YBX1 Contribute to the Invasive Characteristics of Malignant Pleural Mesothelioma. *J Thorac Oncol* (2018) 13:258–72. doi: 10.1016/j.jtho.2017.10.016
180. Tomasetti M, Re M, Monaco F, Gaetani S, Rubini C, Bertini A, et al. MiR-126 in Intestinal-Type Sinonasal Adenocarcinomas: Exosomal Transfer of MiR-126 Promotes Anti-Tumour Responses. *BMC Cancer* (2018) 18:896. doi: 10.1186/s12885-018-4801-z
181. Tomasetti M, Staffolani S, Nocchi L, Neuzil J, Strafella E, Manzella N, et al. Clinical Significance of Circulating miR-126 Quantification in Malignant Mesothelioma Patients. *Clin Biochem* (2012) 45:575–81. doi: 10.1016/j.clinbiochem.2012.02.009
182. Kubo T, Toyooka S, Tsukuda K, Sakaguchi M, Fukazawa T, Soh J, et al. Epigenetic Silencing of microRNA-34b/c Plays an Important Role in the Pathogenesis of Malignant Pleural Mesothelioma. *Clin Cancer Res* (2011) 17:4965–74. doi: 10.1158/1078-0432.CCR-10-3040
183. Ueno T, Toyooka S, Fukazawa T, Kubo T, Soh J, Asano H, et al. Preclinical Evaluation of microRNA-34b/c Delivery for Malignant Pleural Mesothelioma. *Acta Med Okayama* (2014) 68:23–6. doi: 10.18926/AMO/52140
184. Singh A, Bhattacharyya N, Srivastava A, Pruett N, Ripley RT, Schrump DS, et al. Microrna-215-5p Treatment Suppresses Mesothelioma Progression *Via* the MDM2-p53-Signaling Axis. *Mol Ther* (2019) 27:1665–80. doi: 10.1016/j.ymthe.2019.05.020
185. Suzuki R, Amatya VJ, Kushitani K, Kai Y, Kambara T, Takeshima Y. miR-182 and Mir-183 Promote Cell Proliferation and Invasion by Targeting FOXO1 in Mesothelioma. *Front Oncol* (2018) 8:446. doi: 10.3389/fonc.2018.00446
186. Gee GV, Koestler DC, Christensen BC, Sugarbaker DJ, Ugolini D, Ivaldi GP, et al. Downregulated microRNAs in the Differential Diagnosis of Malignant Pleural Mesothelioma. *Int J Cancer* (2010) 127:2859–69. doi: 10.1002/ijc.25285
187. Benjamin H, Lebanony D, Rosenwald S, Cohen L, Gibori H, Barabash N, et al. A Diagnostic Assay Based on microRNA Expression Accurately Identifies Malignant Pleural Mesothelioma. *J Mol Diagn* (2010) 12:771–9. doi: 10.2353/jmoldx.2010.090169
188. Santarelli L, Strafella E, Staffolani S, Amati M, Emanuelli M, Sartini D, et al. Association of MiR-126 With Soluble Mesothelin-Related Peptides, a Marker for Malignant Mesothelioma. *PloS One* (2011) 6:e18232. doi: 10.1371/journal.pone.0018232
189. Andersen M, Grauslund M, Ravn J, Sørensen JB, Andersen CB, Santoni-Rugiu E. Diagnostic Potential of miR-126, miR-143, miR-145, and miR-652 in Malignant Pleural Mesothelioma. *J Mol Diagn* (2014) 16:418–30. doi: 10.1016/j.jmoldx.2014.03.002
190. Matsumoto S, Nabeshima K, Hamasaki M, Shibuta T, Umemura T. Upregulation of microRNA-31 Associates With a Poor Prognosis of Malignant Pleural Mesothelioma With Sarcomatoid Component. *Med Oncol* (2014) 31:303. doi: 10.1007/s12032-014-0303-2

191. Kirschner MB, Cheng YY, Armstrong NJ, Lin RCY, Kao SC, Linton A, et al. MiR-score: A Novel 6-microRNA Signature That Predicts Survival Outcomes in Patients With Malignant Pleural Mesothelioma. *Mol Oncol* (2015) 9:715–26. doi: 10.1016/j.molonc.2014.11.007
192. Weber DG, Casjens S, Johnen G, Bryk O, Raiko I, Pesch B, et al. Combination of MiR-103a-3p and Mesothelin Improves the Biomarker Performance of Malignant Mesothelioma Diagnosis. *PloS One* (2014) 9: e114483. doi: 10.1371/journal.pone.0114483
193. Weber DG, Johnen G, Bryk O, Jöckel K-H, Brüning T. Identification of miRNA-103 in the Cellular Fraction of Human Peripheral Blood as a Potential Biomarker for Malignant Mesothelioma–A Pilot Study. *PloS One* (2012) 7:e30221. doi: 10.1371/journal.pone.0030221
194. Santarelli L, Staffolani S, Strafella E, Nocchi L, Manzella N, Grossi P, et al. Combined Circulating Epigenetic Markers to Improve Mesothelin Performance in the Diagnosis of Malignant Mesothelioma. *Lung Cancer* (2015) 90:457–64. doi: 10.1016/j.lungcan.2015.09.021
195. Weber DG, Gawrych K, Casjens S, Brik A, Lehnert M, Taeger D, et al. Circulating miR-132-3p as a Candidate Diagnostic Biomarker for Malignant Mesothelioma. *Dis Markers* (2017) 2017:9280170. doi: 10.1155/2017/9280170
196. Kirschner MB, Cheng YY, Badrian B, Kao SC, Creaney J, Edelman JJB, et al. Increased Circulating miR-625-3p: A Potential Biomarker for Patients With Malignant Pleural Mesothelioma. *J Thorac Oncol* (2012) 7:1184–91. doi: 10.1097/JTO.0b013e3182572e83
197. Jin B, Li Y, Robertson KD. DNA Methylation. *Genes Cancer* (2011) 2:607–17. doi: 10.1177/1947601910393957
198. Yoshikawa Y, Kuribayashi K, Minami T, Ohmuraya M, Kijima T. Epigenetic Alterations and Biomarkers for Immune Checkpoint Inhibitors–Current Standards and Future Perspectives in Malignant Pleural Mesothelioma Treatment. *Front Oncol* (2020) 10:554570. doi: 10.3389/fonc.2020.554570
199. Park JW, Han J-W. Targeting Epigenetics for Cancer Therapy. *Arch Pharm Res* (2019) 42:159–70. doi: 10.1007/s12272-019-01126-z
200. Ferrari L, Carugno M, Mensi C, Pesatori AC. Circulating Epigenetic Biomarkers in Malignant Pleural Mesothelioma: State of the Art and Critical Evaluation. *Front Oncol* (2020) 10:445. doi: 10.3389/fonc.2020.00445
201. Takeshima H, Ushijima T. Accumulation of Genetic and Epigenetic Alterations in Normal Cells and Cancer Risk. *NPJ Precis Oncol* (2019) 3:1–8. doi: 10.1038/s41698-019-0079-0
202. Guarrera S, Viberti C, Cugliari G, Allione A, Casalone E, Betti M, et al. Peripheral Blood DNA Methylation as Potential Biomarker of Malignant Pleural Mesothelioma in Asbestos-Exposed Subjects. *J Thorac Oncol* (2019) 14:527–39. doi: 10.1016/j.jtho.2018.10.163
203. McLoughlin KC, Kaufman AS, Schrump DS. Targeting the Epigenome in Malignant Pleural Mesothelioma. *Transl Lung Cancer Res* (2017) 6:350–65. doi: 10.21037/tlcr.2017.06.06
204. Nakatsumi H, Matsumoto M, Nakayama KI. Noncanonical Pathway for Regulation of CCL2 Expression by An mTORC1-FOXK1 Axis Promotes Recruitment of Tumor-Associated Macrophages. *Cell Rep* (2017) 21:2471–86. doi: 10.1016/j.celrep.2017.11.014
205. Cugliari G, Catalano C, Guarrera S, Allione A, Casalone E, Russo A, et al. Dna Methylation of FKBP5 as Predictor of Overall Survival in Malignant Pleural Mesothelioma. *Cancers (Basel)* (2020) 12(11):3470. doi: 10.3390/cancers12113470
206. Goto Y, Shinjo K, Kondo Y, Shen L, Toyota M, Suzuki H, et al. Epigenetic Profiles Distinguish Malignant Pleural Mesothelioma From Lung Adenocarcinoma. *Cancer Res* (2009) 69:9073–82. doi: 10.1158/0008-5472.CAN-09-1595
207. Cakiroglu E, Senturk S. Genomics and Functional Genomics of Malignant Pleural Mesothelioma. *Int J Mol Sci* (2020) 21(17):6342. doi: 10.3390/ijms21176342
208. Garassino MC, Marsoni S. A Lesson From Vorinostat in Pleural Mesothelioma. *Lancet Oncol* (2015) 16:359–60. doi: 10.1016/S1470-2045(15)70084-7
209. Baas P, Scherpereel A, Nowak AK, Fujimoto N, Peters S, Tsao AS, et al. First-Line Nivolumab Plus Ipilimumab in Unresectable Malignant Pleural Mesothelioma (CheckMate 743): A Multicentre, Randomised, Open-Label, Phase 3 Trial. *Lancet* (2021) 397(10272):375–86. doi: 10.1016/S0140-6736(20)32714-8


**Conflict of Interest:** The authors declare that the research was conducted in the absence of any commercial or financial relationships that could be construed as a potential conflict of interest.

## GLOSSARY

| | |
|---|---|
| ADCC | antibody-dependent cellular cytotoxicity |
| APC | antigen presenting cells |
| BAP1-TPDS | BAP1-tumor predisposition syndromes |
| BLM | Bloom syndrome gene |
| CCL2 | C-C chemokine ligand 2 |
| CCL4 | C–C chemokine ligand 4 |
| CCL5 | C–C chemokine ligand 5 |
| CSF-1R | colony stimulating factor-1 receptor |
| CXCL12 | C-X-C Motif Chemokine Ligand 12 |
| DAMPs | damage-associated molecular patterns |
| DC | dendritic cells |
| DDR | DNA damage response |
| DSBs | Double Strand Breaks |
| EMT | epithelial to mesenchymal transition |
| EZH2 | enhancer of zeste homolog 2 |
| FISH | fluorescent in-situ hybridization |
| FOXK1 | Forkhead Box K1 |
| Gr-MDSC | granulocytic myeloid-derived suppressor cells |
| H3K27me3 | histone H3 lysine methylation |
| HMGB1 | high mobility group protein B1 |
| HR | Homologous recombination |
| HRD | Homologous Recombination Deficiency |
| IHC | immunohistochemistry |
| ILC | Innate lymphoid cells |
| LAG-3 | lymphocyte activation gene-3 |
| M-MDSC | monocytic myeloid-derived suppressor cells |
| MDSC | myeloid-derived suppressor cells |
| MGMT | O6-methylguanine-DNA methyltransferase |
| MLPA | multiplex ligation–dependent probe amplification |
| MMR | Mismatch Repair |
| MPM | malignant pleural mesothelioma |
| Mpseq | Mate-pair sequencing |
| NER | Nucleotide Excision Repair |
| NF2 | neurofibromatosis type 2 |
| NFKB | Nuclear Factor Kappa B |
| NGS | next generation sequencing |
| NHEJ | non-homologous end-joining |
| NK | natural killer |
| NKT | Natural killer T |
| NO | nitric oxide |
| NSCLC | non-small cell lung cancer |
| PARP | poly(ADP-ribose) polymerase |
| PARPi | PARP-inhibitors |
| PGE2 | prostaglandin E2 |
| RAGE | receptor for Advanced Glycation Endproducts |
| ROS | reactive oxygen species |
| SCNA | somatic copy-number alteration |
| SLFN11 | Schlafen 11 |
| SMRP | mesothelin-related peptide |
| SSBs | Single Strand Breaks |
| TAMs | tumor-associated macrophages |
| TCGA | The Cancer Genome Atlas |
| TEAD | transcriptional enhanced associate domain |
| TERT | telomerase reverse transcriptase |
| TGF-β | Transforming Growth Factor β |
| TIGIT | T cell immunoglobulin and ITIM domain |
| TILs | tumor infiltrating lymphocytes |
| TIM-3 | T cell immunoglobulin and mucin-domain containing-3 |
| TLS | tertiary lymphoid structures |
| TM | Thrombomodulin |
| TME | tumor microenvironment |
| Treg | Regulatory T cells |
| VISTA | V-domain Ig suppressor of T cell activation |
| αGC | glycolipid α-galactosylceramide |

frontiers in Oncology

MINI REVIEW
published: 24 June 2021
doi: 10.3389/fonc.2021.695770

# Homozygous Co-Deletion of Type I Interferons and *CDKN2A* Genes in Thoracic Cancers: Potential Consequences for Therapy

*Marion Grard*[1,2†], *Camille Chatelain*[1,2†], *Tiphaine Delaunay*[1,2], *Elvire Pons-Tostivint*[1,2,3], *Jaafar Bennouna*[1,2,3] *and Jean-François Fonteneau*[1,2*]

[1] Université de Nantes, Inserm, CRCINA, Nantes, France, [2] Labex IGO, Immunology Graft Oncology, Nantes, France, [3] CHU de Nantes, oncologie thoracique et digestive, Université de Nantes, Nantes, France

Homozygous deletion (HD) of the tumor suppressor gene *CDKN2A* is the most frequent genetic alteration in malignant pleural mesothelioma and is also frequent in non-small cell lung cancers. This HD is often accompanied by the HD of the type I interferons (IFN I) genes that are located closed to the *CDKN2A* gene on the p21.3 region of chromosome 9. IFN I genes encode sixteen cytokines (IFN-α, IFN-β…) that are implicated in cellular antiviral and antitumor defense and in the induction of the immune response. In this review, we discuss the potential influence of IFN I genes HD on thoracic cancers therapy and speak in favor of better taking these HD into account in patients monitoring.

**Keywords: lung cancer, mesothelioma, type I interferon, CDKN2A (p16), homozygous deletion, immunotherapy, STING**

OPEN ACCESS

***Edited by:***
*Emanuela Felley-Bosco, University of Zurich, Switzerland*

***Reviewed by:***
*Yoshitaka Sekido, Aichi Cancer Center, Japan*
*Steven Albelda, University of Pennsylvania, United States*

****Correspondence:***
*Jean-François Fonteneau*
*jean-francois.fonteneau@inserm.fr*

*†These authors have contributed equally to this work and share first authorship*

***Specialty section:***
*This article was submitted to Thoracic Oncology, a section of the journal Frontiers in Oncology*

***Received:*** *15 April 2021*
***Accepted:*** *07 June 2021*
***Published:*** *24 June 2021*

***Citation:***
*Grard M, Chatelain C, Delaunay T, Pons-Tostivint E, Bennouna J and Fonteneau J-F (2021) Homozygous Co-Deletion of Type I Interferons and CDKN2A Genes in Thoracic Cancers: Potential Consequences for Therapy. Front. Oncol. 11:695770. doi: 10.3389/fonc.2021.695770*

## FREQUENT HOMOZYGOUS CO-DELETION OF THE *CDKN2A* TUMOR SUPPRESSOR GENE AND THE IFN I GENES IN THORACIC CANCERS

Non-small cell lung cancer (NSCLC) is the most common cause of cancer death worldwide often due to long-term tobacco smoking. Malignant pleural mesothelioma (MPM) is a rare cancer that is mainly due to asbestos exposure. As other cancers, some genomic alterations are found in NSCLC and MPM tumor cells, especially in locus containing tumor suppressor genes. These alterations are in part responsible for the disease.

In MPM cells, the most frequent genomic alteration is the homologous deletion (HD) in the p21.3 region of chromosome 9 (1–6). These HDs are variable in length but they mainly overlap at the level of the cyclin-dependent kinase inhibitor 2A (*CDKN2A*) tumor suppressor gene located in this region (**Figures 1A, B**). Fluorescence *in situ* hybridization (FISH) studies reported that *CDKN2A* gene HDs are found in 60 to 80% of patients (3–6). Copy number alteration study from The Cancer Genome Atlas (TCGA) reported a lower frequency of 44% of patients with *CDKN2A* gene HD in MPM (**Figure 1B**) (7). However, TCGA study is performed on tumor biopsies that often contain non-malignant cells. These non-malignant cells may mask *CDKN2A* gene HD that are only present in tumor cells. Thus, some patients with *CDKN2A* gene HD were probably not detected in the TCGA study.

In NSCLC, *CDKN2A* gene HDs were also identified in the 1990s (8–10). They were then found more frequently in a subset of patient with intact retinoblastoma (rb) pathway (11). FISH studies on 85 and 19 NSCLC patients reported *CDKN2A* gene HD in 21 and 29% of patients respectively (12, 13), and FISH study on 31 squamous cell carcinoma (SqCC) patients reported them in 16% (14). TCGA study on 1144 NSCLC patients (660 lung adenocarcinoma and 484 lung SqCC) reported *CDKN2A* gene HD in 21% of patients (**Figure 1C**) (15).

The *CDKN2A* gene encodes several proteins, notably $p16^{INK4a}$ and $p14^{arf}$ that are implicated in the regulation of the cell cycle. $p16^{INK4a}$ binds to cyclin-dependent kinase 4 and 6 (CDK4/6) and inhibits its capacity with cyclin D1 to phosphorylate rb protein and the translocation of the transcription factor E2F from the cytoplasm to the nucleus (16). In absence of $p16^{INK4a}$, E2F translocates to the nucleus and allows the transition from G1 phase to S phase of the cell cycle. $p14^{arf}$ also acts as a tumor suppressor *via* the p53 pathway and its absence favors the entry in the cell cycle.

Close to *CDKN2A* gene, *CDKN2B* and *MTAP* are two other genes that are often co-deleted with *CDKN2A* in MPM (**Figure 1B**) and NSCLC (**Figure 1C**). *CDKN2B* encode the $p15^{Ink4b}$ protein that interacts with CDK4/6 and inhibits its activation by cyclin D and thus acts as a tumor suppressor (17). *MTAP* encodes the S-methyl-5'-thioadenosine phosphorylase (MTAP) implicated in the polyamine metabolism (18).

Further downstream from *CDKN2A* and *MTAP* in the p21.3 region of human chromosome 9, a cluster of 16 genes encodes the type I interferons (IFN I): IFN-β, IFN-ε, IFN-ω and 13 IFN-α (**Figure 1A**) (19). *IFNB1* is the furthest gene from *CDKN2A*. In the 1990s, IFN I genes HDs were identified in a fraction of NSCLC and MPM patients with *CDKN2A* gene HD (1, 2, 8, 20). We recently reported that in 78 short-term–cultured MPM cell lines, 57 (73%) and 18 (23%) cell lines harbors *CDKN2A* and *IFNBI* genes HD respectively, whereas in TCGA study performed on 82 patients, these percentage where smaller, probably due to non-malignant cells contamination (44 and 9%) (**Figure 1B**) (21). Thus, about 10 to 20% of mesothelioma patients present HD of all the IFN I genes. In NSCLC, the TCGA study on 1,144 patients reported 21 and 7% of patients with *CDKN2A* and *IFNBI* gene HDs respectively (**Figure 1C**). Interestingly, NSCLC patients with IFN I and *CDKN2A* gene

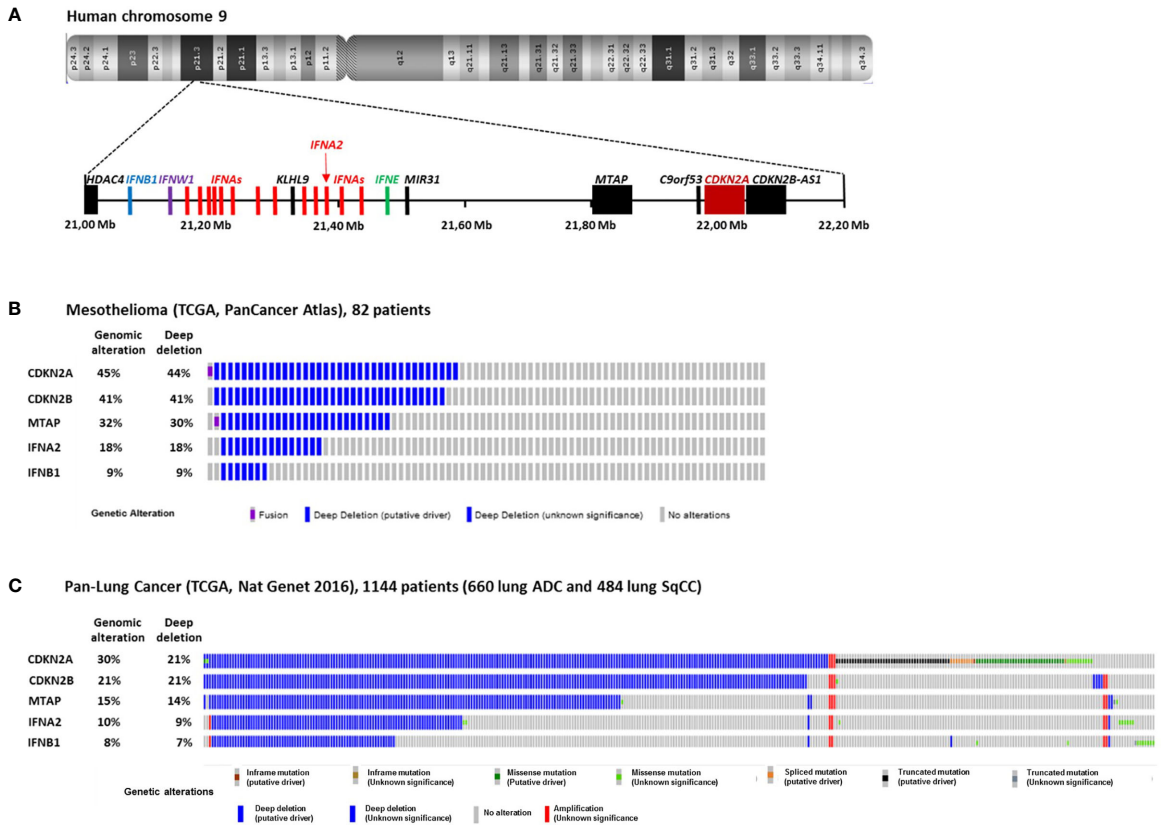


**FIGURE 1** | Homozygous Deletions in the p21.3 region of chromosome 9 in MPM and NSCLC. **(A)** Schematic representation of genes present in the p21.3 region of chromosome 9 between positions 21,000,000 and 22,200,000 drawn from UCSC Genome Browser (https://genome.ucsc.edu/). **(B)** Oncoprint representation of *CDKN2A*, *CDKN2B*, *MTAP*, *IFNA2* and *IFNB1* genomic alterations found in tumor samples of 82 MPM patients. Oncoprint was performed with cbioportals website (http://www.cbioportal.org/) using TCGA Pancancer atlas data. **(C)** Oncoprint representation of *CDKN2A*, *CDKN2B*, *MTAP*, *IFNA2* and *IFNB1* genomic alterations found in tumor samples of 1144 NSCLC patients. Oncoprint was performed with cbioportals website (http://www.cbioportal.org/) using TCGA Pan lung cancer data. Only the patients with at least one genomic alteration in the five genes are shown. ADC, adenocarcinoma; SqCC, squamous cell carcinoma.

HDs have a significantly worst disease free survival than patients with only *CDKN2A* gene HD (22), suggesting a tumor suppressor role for IFN I genes in this cancer.

## THE TYPE I INTERFERON RESPONSE IN THORACIC CANCERS

Type I interferon (IFN I) response is key in antiviral immune response (**Figure 2**). The IFN I response allows infected and immune cells to report *via* IFN-α and -β secretion the presence of the virus to neighboring cells and to the immune system *via* the IFN-α/-β receptor (IFNAR) which is expressed by virtually all somatic cells (23). The presence of viral genome or intermediaries of its replication is detected by cytoplasmic pattern recognition receptors (PRR) and lead to the production of IFN I *via* two main pathways: the stimulator of interferon genes protein (STING) pathway for DNA viruses and the mitochondrial antiviral-signaling protein (MAVS) pathway for RNA viruses (23, 24). IFN I are also produced by immune cells notably *via* Toll like receptor (TLR) activation, especially plasmacytoid dendritic cells (pDC) (25). IFN-β is expressed by all nucleated cells in response to infection, whereas the IFN-α are mainly produced by immune cells. Among IFN-α, IFN-α2 was the first cytokines to be approved in clinics for cancer treatment in 1986 and is the most studied (26).

Cells exposed to IFN I express hundreds of IFN-stimulated genes (ISGs). Many ISGs encode proteins that induce a state of anti-viral resistance. These antiviral proteins act by blocking the different stages of the viral cycle, from the entry of the virus, through the inhibition of its replication, to the release of its progeny by the infected cell (23, 27). The IFN I also play a crucial role in the induction and the regulation of the antiviral adaptive immune response, notably by favoring antigen cross-priming by dendritic cells (28, 29). However, during chronic infection, prolonged IFN I response can have deleterious effects by inducing immune dysfunctions (30).

IFN I response is often induced during cancer development and treatments. Several pathways are involved in this induction. Presence of mitochondrial or nuclear DNA in the cytoplasm of tumor cells can induce the secretion of IFN I *via* the STING pathway (31–39). Expression of endogenous retrovirus (ERV) under the form of dsRNA due to epigenetic deregulation in tumor cells can also trigger the expression of IFN I *via* the MAVS pathway (35, 40–44). Non-malignant cells from the tumor microenvironment, such as phagocytic cells notably dendritic cells (DC), can also produce IFN I *via* activation of the STING pathway after engulfment of dead tumor cells. This occurs due to

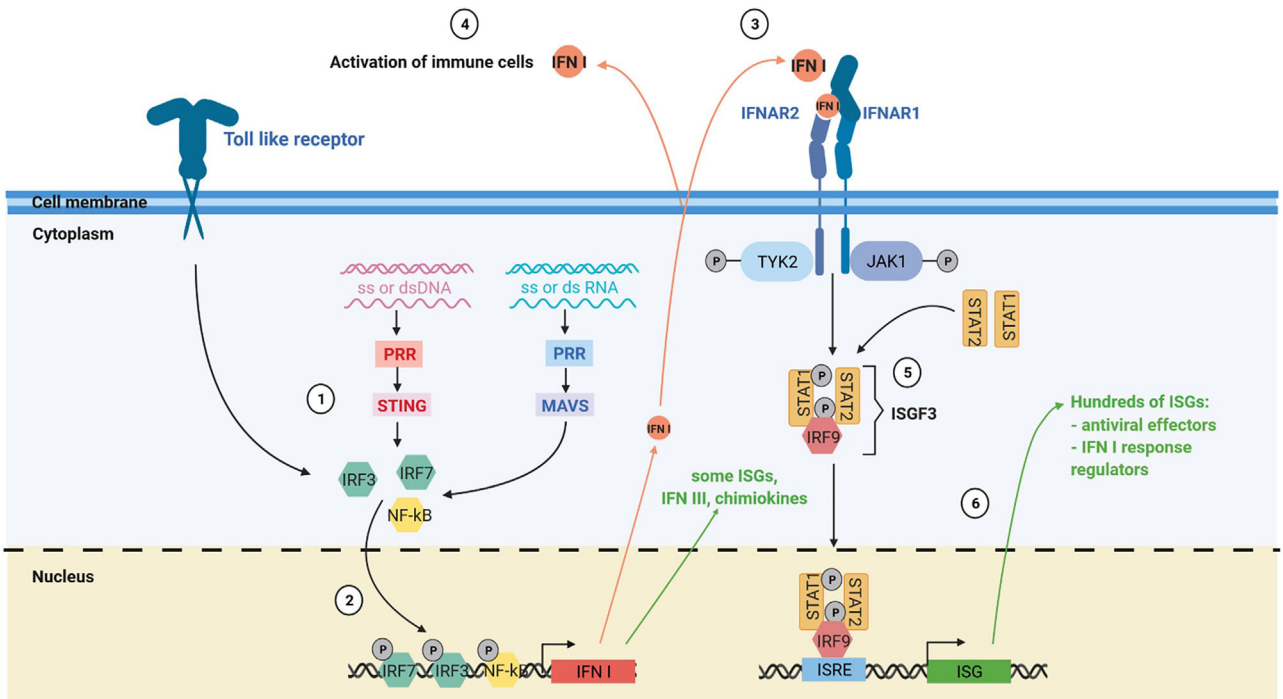


**FIGURE 2** | The IFN I response. (1) The IFN I response is triggered by different stimuli such as ssDNA, dsDNA, ssRNA and dsRNA *via* the toll like receptors, the MAVS and the STING pathway. (2) Activation of these pathways induces the nuclear translocation of transcription factors such as IRF3, IRF7 and NF-kB that trigger IFN I production and expression of some interferon stimulated genes (ISGs). (3) Secreted IFN I trigger IFNAR signaling on neighboring cells, notably immune cells. (4) IFN I and other soluble factors of the IFN I response activate the immune response. (5) Activation of IFNAR signaling by IFN I leads to the formation of the interferon stimulated gene factor 3 complex. (6) This complex translocates to the nucleus and activates numerous ISGs with antiviral, immunomodulatory and regulatory functions. PRR, pattern recognition receptors.

accumulation of DNA from engulfed dead tumor cells in DC cytoplasm (39, 45–47). A recent analysis of 31 cancer types in TCGA database by Liu et al. shows that, lung adenocarcinoma, MPM and SqCC are the 3rd, 6th and 8th respectively in the intensity of an IFN I signature based on the expression of 38 ISGs (35). Globally, IFN I signature correlates with the degree of immune cells infiltration, but some tumors with an interferon signature and with no immune cells infiltration were also found.

IFN I signaling is able to modulate the expressions of hundreds of genes (27). This signaling pathway also induces expression of noncoding RNAs including long noncoding RNAs, miRNA and ERV RNA (27, 41, 48). Due to its potential toxicity and inflammatory effects, IFN I production and signaling are tightly regulated by numerous positive and negative regulators, many of which are ISGs (49). Thus, induction of IFN I response in tumors has multiple complex effects that are rather unfavorable to tumor development. The IFN I can restrict tumor growth by reducing proliferation of tumor cells, inducing their apoptosis, limiting their migratory capacity and inhibiting angiogenesis (50, 51). Furthermore, they increase antigen presentation by HLA molecules, stimulate the innate and adaptive antitumor immune response and inhibit CD4+ regulatory T cells (30, 50, 52–56). IFN I were shown to play an important role in tumor immuno-editing in mouse models of chemically-induced and transposable tumors (57). They signal tumor cells to the immune system. They are necessary for the priming of anti-tumor T cell response as the abrogation of IFN I signaling in CD8+ dendritic cells blocks their capacity to cross-present antigens in mouse (54, 55). They also participate in the activation of anti-tumor NK cell response (56). Induction of anti-tumor NK and T cell responses lead to the secretions of the type II interferon-gamma (IFN-γ) that will further shapes the immunogenicity and the immunosuppressive microenvironment of the tumor with the IFN I (58). Indeed, IFN I are also involved in setting up the immunosuppressive tumor environment by inducing the expression of numerous inhibitory molecules such as PD1 and PDL1 that block CD8+ T cell cytotoxicity (30, 50, 58). IFN I can also induce Indoleamine 2,3-dioxygenase (IDO) expression that reduces locally the amount of tryptophan needed for T cell functions and favors their differentiation in Treg (59). Thus, the IFN I in tumors play a dual role by stimulating the innate and adaptive immune response and inducing feedback mechanisms to control its magnitude.

IFN I in NSCLC modulates numerous pathways implicated in proliferation, survival and apoptosis of tumor cells including JAK/STAT, Src kinases, Vav proto-oncogene, PTEN/PI3-K/AKT, Crk proteins and MAP kinase signaling pathways (51). Several recent studies reported that a constitutive activation of the IFN I response in lung tumors correlates with tumor inflammation and immune checkpoint inhibitors efficacy (60–62). Furthermore, DNA damages and dysfunctions of the DNA damage response are inducers of the IFN I response and have been linked to immune checkpoint efficiency (37, 63). The renewed interest in IFN I response also comes from the observation that they are necessary for the radiotherapy abscopal response (64–67), and that they participate in the induction of the antitumor immune response by chemotherapy (68). This is also due to the identification of new potential immune checkpoint such as ADAR and Trex1 which are ISG that functions as negative regulators of the IFN I response by inactivating the nucleic acids that stimulate this response (35, 40, 65, 66). By blocking ADAR or Trex function, IFN I response is amplified which promotes the antitumor immune response. Thus, there is still a great interest to adapt treatments or find new therapeutic strategies to activate the IFN I response locally especially in cold tumors with no or low immune cells infiltrate.

## POTENTIAL CONSEQUENCES OF IFN I GENES HD FOR THORACIC CANCERS THERAPY

Given the central role of IFN I response in tumor immune surveillance, the frequent loss of all copies of IFN I genes that accompanied *CDKN2A* gene HD in tumor cells likely plays a role in tumor immune escape. In NSCLC, like in other cancers, patients with only *CDKN2A* gene HD have a longer survival compared to patients with IFN I and *CDKN2A* genes HD (22). Thus, IFN I genes act as tumor suppressors genes in malignant cells. Beside this study of Ye et al., nothing is known on the prognostic value and immunotherapy biomarker potential of IFN I genes HD in NSCLC, MPM and other cancers. These deletions were described as early as the mid-1990s and yet they have not been well documented. It may be because they were discovered in studies focusing on the *CDKN2A* tumor suppressor gene HD. Furthermore, reports that IFN I treatment in NSCLC and MPM has limited clinical benefit at that time, may have decrease the interest of studying IFN I gene HD. Finally, most studies on the role of IFN I on antitumor immune response were performed with IFNARko mouse models that are easier to obtain than mouse models ko for all IFN I genes. These IFNARko models are instrumental to understand the role of IFN I signaling on tumor cells and the different subtypes of immune cells but are less suitable to study the source of the IFN I production.

Questions arise regarding presence of IFN I genes HD in tumor cells. There are several potential cellular sources of IFN I secretion in tumors, that are basically tumor and immune cells. Thus, the first question is the role of IFN I production by tumor cells and if absence of this production is compensated by other cellular sources. Several recent studies suggest that triggering of the tumor cells IFN I production play a role in the induction of the anti-tumor immune response.

Kitajima et al. reported that the lack of response to immune checkpoint blockade (ICB) of patients with KRAS-LKB1–mutant lung cancers is due to the inhibition of STING expression *via* the loss of LKB1 (62). They show that KRAS-LKB1–mutant tumor cells are not able to sense cytoplasmic dsDNA *via* the STING pathway, and to produce IFN I in response. In consequence, T cells infiltration and PD-L1 expression in KRAS-LKB1-mutant tumors is reduced and ICB therapy is ineffective.

Demaria's team showed that triggering of tumor cell IFN I response is necessary for induction of anti-tumor immune

response by radiotherapy (64, 65). They first reported that abscopal response in mouse is abrogated when cancer cells in the irradiated tumor do not express cGAS/STING or overexpress the exonuclease Trex1 (65). Irradiation induces the presence of cytoplasmic DNA that triggers the IFN-β production *via* the STING pathway and lead to the expression of the ISG Trex1. This ISG is an exonuclease that degrades DNA in the cytoplasm and thus decreases IFN I response by tumor cells and triggering of the antitumor immune response. By inactivating Trex1 in tumor cells, the IFN I response induced by irradiation is increased, as well as the antitumor immune response. Thus, tumor cell IFN I response is essential for abscopal effect of radiation in that mouse model. Demaria's team then showed that combination of radiotherapy and anti-CTLA4 blockade in NSCLC patients that have failed anti-CTLA4 alone or in combination with chemotherapy, induced IFN-β in the blood and an antitumor T cell response in responding patients (64).

These studies highlight the important role on the antitumor immune response of triggering the IFN I response *via* the STING pathway in tumor cells. However, IFN I response in tumor cells can also be induced by the sensing of endogenous dsRNA *via* the MAVS pathway and that also plays a role in the stimulation of the antitumor immune response (35, 40–44). Best evidences come from the study of an ISG, the adenosine deaminase acting on RNA (ADAR) that acts on the MAVS pathway like Trex1 does on the STING pathway (35, 40). The ADAR protein, by converting A to I, disrupts the normal A:U pairing which destabilizes the dsRNA into ssRNA. dsRNA edited by ADAR are no longer able to trigger the IFN I response by the dsRNA cytoplasmic sensor Mda5. Thus like Trex1, ADAR inactivates the stimuli at the origin of the IFN I production by tumor cells. In a mouse model, Ishizuka et al. reported that loss of *ADAR1* in tumor cells overcomes the resistance to immune checkpoint inhibitors by increasing the IFN I response *via* the MAVS pathway and, thus, the inflammation of the tumor microenvironment (40). This results was confirmed by Liu et al., that show that both, the MAVS and the STING pathway are needed to maintain the IFN I response in tumor cells that have lost ADAR (35).

Altogether these studies on the STING and the MAVS pathway show that triggering of the IFN I response in tumor cells is central to inflame the microenvironment. However, it does not establish clearly that IFN I production by tumor cells is required. Indeed, in these studies, the MAVS or the STING pathway is inactivated. This inactivation impairs IFN I production and also the expression of lots of other genes. Indeed, when the MAVS or the STING pathway are triggered, activated transcription factors such as IRF3 and NF-kB not only induce IFN I production, but also the expression of many other genes with many being ISG (**Figure 2**). In MPM cell lines that have lost IFN I genes, exposition to attenuated measles virus still resulted in the induction of expression of a small subset of genes (21). Among these genes, some may play a role in the inflammation of the microenvironment, such as the chemokines CCL5, CXCL10 and CXCL11, or the type III interferons. Thus, triggering of the IFN I response in tumor cells that have lost IFN I genes may still conserve a certain capacity to inflame the microenvironment. By studying patients with IFN I genes HD tumors, we would better understand the IFN I contribution of tumor cells versus non-malignant cells in cancer development and therapies. We would also better define the contribution of IFN I versus other cytokines/chemokines induced by the triggering of the MAVS or the STING pathway.

IFN I genes HD may also be interesting for new cancer therapies such as antitumor virotherapy using oncolytic replicative viruses. We studied the replication and oncolytic activity of the attenuated Schwarz strain of measles virus (MV) on 22 human MPM cell lines and four types of healthy cell (fibroblasts, mesothelial, endothelial and lung epithelial cells) (69). We found that the healthy cells and seven MPM cell lines were resistant to MV replication due to a protective functional IFN I response. The 15 others MPM cell lines were permissive to MV replication and lysis due to a defective IFN I response. Among these 15 cell lines, 11 were unable to produce IFN I when exposed to MV. We showed later that eight of these 11 cell lines have lost both copies of the IFN I genes (21). The three others cells line have at least one copy of IFN I genes but are not able to produce IFN I in response to the virus suggesting another type of defects of the IFN I response in these MPM cells lines (69). These 11 MV-sensitive MPM cell lines that are unable to produce IFN I in response to MV become MV-resistant if exposed to exogenous IFN I, suggesting that IFNAR signaling is functional in these cell lines. The four other MV-sensitive MPM cell lines were able to produce IFN I in response to MV, but unable to control viral replication suggesting a defect of the IFN I response in IFNAR signaling. This defective IFNAR signaling has been previously reported in tumor cells of some patients with MPM (70). It has been associated to mark decrease of IFNAR, IRF9 and PKR expression and to tumor sensitivity to an oncolytic vesicular stomatitis virus. These studies illustrate the diversity of defects found in the IFN I response from one patients to another in MPM. Such converging selection of tumor cells with a deficient IFN I response highlights the tumor suppressive role of this response.

Other questions are still pending regarding IFN I genes HD. These HD are diverse in length (**Figure 2**). For some patients, only a part of IFN I genes are lost and *IFNB1* gene that encodes IFN-β is preserved (**Figure 1**). Consequences of these partial losses are also to define. During tumor development, do these HD appear concomitantly to *CDKN2A* HD or do they appear later conferring an additional advantage to the tumor variant that carries them? The best techniques for detecting IFN I genes HD is probably FISH assay that can be performed cost effectively on paraffin-embedded tissue and allow to identify homozygous and hemizygous deletions at the single cell level (71). It can also be performed by polymerase chain reaction-based techniques or whole exome sequencing on tumor biopsies, but large amount of non-malignant cells in the biopsy may hide the deletions.

With the success of cancer immunotherapy and recent advances in understanding the IFN I tumor suppressor role, IFN I genes HD should be studied and taken into account in the monitoring of MPM and NSCLC patients. This would likely lead to new strategies and improvements of immunotherapy.

## AUTHOR CONTRIBUTIONS

Literature review: MG, CC, and JFF. All authors contributed to the article and approved the submitted version.

## FUNDING

This work was supported by "La Ligue Régionale Grand Ouest contre le Cancer" (CSIRGO: CD16, CD22, CD44, CD49, CD72, CD79 and CD85), "La Ligue Nationale contre le Cancer", "L'association ARSMESO44 ", "La fondation ARC", L'Agence Nationale pour la Recherche (ANR-16-CE18-0016), and "LabEX IGO program supported by the National Research Agency *via* the investment of the future program ANR-11-LABX-0016-01". TD was supported by a grant from Ligue contre le Cancer.

## ACKNOWLEDGMENTS

We thank Dr. Didier Jean for his insightful discussion. **Figure 2** was created with BioRender.com.

## REFERENCES

1. Cheng JQ, Jhanwar SC, Klein WM, Bell DW, Lee WC, Altomare DA, et al. p16 Alterations and Deletion Mapping of 9p21-p22 in Malignant Mesothelioma. *Cancer Res* (1994) 54(21):5547–51.
2. Xio S, Li D, Vijg J, Sugarbaker DJ, Corson JM, Fletcher JA. Codeletion of p15 and p16 in Primary Malignant Mesothelioma. *Oncogene* (1995) 11(3):511–5.
3. Cheng YY, Yuen ML, Rath EM, Johnson B, Zhuang L, Yu TK, et al. CDKN2A and MTAP Are Useful Biomarkers Detectable by Droplet Digital PCR in Malignant Pleural Mesothelioma: A Potential Alternative Method in Diagnosis Compared to Fluorescence in Situ Hybridisation. *Front Oncol* (2020) 10:579327. doi: 10.3389/fonc.2020.579327
4. Illei PB, Rusch VW, Zakowski MF, Ladanyi M. Homozygous Deletion of CDKN2A and Codeletion of the Methylthioadenosine Phosphorylase Gene in the Majority of Pleural Mesotheliomas. *Clin Cancer Res* (2003) 9(6):2108–13.
5. Hwang HC, Sheffield BS, Rodriguez S, Thompson K, Tse CH, Gown AM, et al. Utility of BAP1 Immunohistochemistry and p16 (Cdkn2a) FISH in the Diagnosis of Malignant Mesothelioma in Effusion Cytology Specimens. *Am J Surg Pathol* (2016) 40(1):120–6. doi: 10.1097/PAS.0000000000000529
6. Marshall K, Jackson S, Jones J, Holme J, Lyons J, Barrett E, et al. Homozygous Deletion of CDKN2A in Malignant Mesothelioma: Diagnostic Utility, Patient Characteristics and Survival in a UK Mesothelioma Centre. *Lung Cancer* (2020) 150:195–200. doi: 10.1016/j.lungcan.2020.10.020
7. Hmeljak J, Sanchez-Vega F, Hoadley KA, Shih J, Stewart C, Heiman D, et al. Integrative Molecular Characterization of Malignant Pleural Mesothelioma. *Cancer Discovery* (2018) 8(12):1548–65. doi: 10.1158/2159-8290.CD-18-0804
8. Dreyling MH, Bohlander SK, Adeyanju MO, Olopade OI. Detection of CDKN2 Deletions in Tumor Cell Lines and Primary Glioma by Interphase Fluorescence in Situ Hybridization. *Cancer Res* (1995) 55(5):984–8.
9. Kamb A, Gruis NA, Weaver-Feldhaus J, Liu Q, Harshman K, Tavtigian SV, et al. A Cell Cycle Regulator Potentially Involved in Genesis of Many Tumor Types. *Science* (1994) 264(5157):436–40. doi: 10.1126/science.8153634
10. Nobori T, Miura K, Wu DJ, Lois A, Takabayashi K, Carson DA. Deletions of the Cyclin-Dependent Kinase-4 Inhibitor Gene in Multiple Human Cancers. *Nature* (1994) 368(6473):753–6. doi: 10.1038/368753a0
11. Shapiro GI, Edwards CD, Kobzik L, Godleski J, Richards W, Sugarbaker DJ, et al. Reciprocal Rb Inactivation and p16INK4 Expression in Primary Lung Cancers and Cell Lines. *Cancer Res* (1995) 55(3):505–9.
12. Okami K, Cairns P, Westra WH, Linn JF, Ahrendt SA, Wu L, et al. Detailed Deletion Mapping at Chromosome 9p21 in Non-Small Cell Lung Cancer by Microsatellite Analysis and Fluorescence in Situ Hybridization. *Int J Cancer* (1997) 74(6):588–92. doi: 10.1002/(sici)1097-0215(19971219)74:6<588::aid-ijc5>3.0.co;2-q
13. Panani AD, Maliaga K, Babanaraki A, Bellenis I. Numerical Abnormalities of Chromosome 9 and p16CDKN2A Gene Deletion Detected by FISH in non-Small Cell Lung Cancer. *Anticancer Res* (2009) 29(11):4483–7.
14. Dessy E, Rossi E, Berenzi A, Tironi A, Benetti A, Grigolato P. Chromosome 9 Instability and Alterations of p16 Gene in Squamous Cell Carcinoma of the Lung and in Adjacent Normal Bronchi: FISH and Immunohistochemical Study. *Histopathology* (2008) 52(4):475–82. doi: 10.1111/j.1365-2559.2008.02969.x
15. Campbell JD, Alexandrov A, Kim J, Wala J, Berger AH, Pedamallu CS, et al. Distinct Patterns of Somatic Genome Alterations in Lung Adenocarcinomas and Squamous Cell Carcinomas. *Nat Genet* (2016) 48(6):607–16. doi: 10.1038/ng.3564
16. Burkhart DL, Sage J. Cellular Mechanisms of Tumour Suppression by the Retinoblastoma Gene. *Nat Rev Cancer* (2008) 8(9):671–82. doi: 10.1038/nrc2399
17. Kim WY, Sharpless NE. The Regulation of INK4/ARF in Cancer and Aging. *Cell* (2006) 127(2):265–75. doi: 10.1016/j.cell.2006.10.003
18. Urso L, Cavallari I, Sharova E, Ciccarese F, Pasello G, Ciminale V. Metabolic Rewiring and Redox Alterations in Malignant Pleural Mesothelioma. *Br J Cancer* (2020) 122(1):52–61. doi: 10.1038/s41416-019-0661-9
19. Diaz MO. The Human Type I Interferon Gene Cluster. *Semin Virol* (1995) 6 (3):143–9. doi: 10.1006/smvy.1995.0019
20. Mead LJ, Gillespie MT, Irving LB, Campbell LJ. Homozygous and Hemizygous Deletions of 9p Centromeric to the Interferon Genes in Lung Cancer. *Cancer Res* (1994) 54(9):2307–9.
21. Delaunay T, Achard C, Boisgerault N, Grard M, Petithomme T, Chatelain C, et al. Frequent Homozygous Deletions of Type I Interferon Genes in Pleural Mesothelioma Confer Sensitivity to Oncolytic Measles Virus. *J Thorac Oncol* (2020) 15(5):827–42. doi: 10.1016/j.jtho.2019.12.128
22. Ye Z, Dong H, Li Y, Ma T, Huang H, Leong HS, et al. Prevalent Homozygous Deletions of Type I Interferon and Defensin Genes in Human Cancers Associate With Immunotherapy Resistance. *Clin Cancer Res* (2018) 24 (14):3299–308. doi: 10.1158/1078-0432.CCR-17-3008
23. Schneider WM, Chevillotte MD, Rice CM. Interferon-Stimulated Genes: A Complex Web of Host Defenses. *Annu Rev Immunol* (2014) 32:513–45. doi: 10.1146/annurev-immunol-032713-120231
24. Iwasaki A. A Virological View of Innate Immune Recognition. *Annu Rev Microbiol* (2012) 66:177–96. doi: 10.1146/annurev-micro-092611-150203
25. Brubaker SW, Bonham KS, Zanoni I, Kagan JC. Innate Immune Pattern Recognition: A Cell Biological Perspective. *Annu Rev Immunol* (2015) 33:257–90. doi: 10.1146/annurev-immunol-032414-112240
26. Paul F, Pellegrini S, Uze G. Ifna2: The Prototypic Human Alpha Interferon. *Gene* (2015) 567(2):132–7. doi: 10.1016/j.gene.2015.04.087
27. Schoggins JW. Interferon-Stimulated Genes: What Do They All do? *Annu Rev Virol* (2019) 6(1):567–84. doi: 10.1146/annurev-virology-092818-015756
28. Crouse J, Kalinke U, Oxenius A. Regulation of Antiviral T Cell Responses by Type I Interferons. *Nat Rev Immunol* (2015) 15(4):231–42. doi: 10.1038/nri3806
29. Schiavoni G, Mattei F, Gabriele L. Type I Interferons as Stimulators of DC-Mediated Cross-Priming: Impact on Anti-Tumor Response. *Front Immunol* (2013) 4:483. doi: 10.3389/fimmu.2013.00483
30. Snell LM, McGaha TL, Brooks DG. Type I Interferon in Chronic Virus Infection and Cancer. *Trends Immunol* (2017) 38(8):542–57. doi: 10.1016/j.it.2017.05.005
31. Mackenzie KJ, Carroll P, Martin CA, Murina O, Fluteau A, Simpson DJ, et al. cGAS Surveillance of Micronuclei Links Genome Instability to Innate Immunity. *Nature* (2017) 548(7668):461–5. doi: 10.1038/nature23449

32. McArthur K, Whitehead LW, Heddleston JM, Li L, Padman BS, Oorschot V, et al. BAK/BAX Macropores Facilitate Mitochondrial Herniation and mtDNA Efflux During Apoptosis. *Science* (2018) 359(6378):eaao6047. doi: 10.1126/science.aao6047
33. Harding SM, Benci JL, Irianto J, Discher DE, Minn AJ, Greenberg RA. Mitotic Progression Following DNA Damage Enables Pattern Recognition Within Micronuclei. *Nature* (2017) 548(7668):466–70. doi: 10.1038/nature23470
34. Marcus A, Mao AJ, Lensink-Vasan M, Wang L, Vance RE, Raulet DH. Tumor-Derived Cgamp Triggers a STING-Mediated Interferon Response in Non-Tumor Cells to Activate the NK Cell Response. *Immunity* (2018) 49 (4):754–63.e4. doi: 10.1016/j.immuni.2018.09.016
35. Liu H, Golji J, Brodeur LK, Chung FS, Chen JT, deBeaumont RS, et al. Tumor-Derived IFN Triggers Chronic Pathway Agonism and Sensitivity to ADAR Loss. *Nat Med* (2019) 25(1):95–102. doi: 10.1038/s41591-018-0302-5
36. Vanpouille-Box C, Demaria S, Formenti SC, Galluzzi L. Cytosolic DNA Sensing in Organismal Tumor Control. *Cancer Cell* (2018) 34(3):361–78. doi: 10.1016/j.ccell.2018.05.013
37. Mouw KW, Goldberg MS, Konstantinopoulos PA, D'Andrea AD. Dna Damage and Repair Biomarkers of Immunotherapy Response. *Cancer Discovery* (2017) 7(7):675–93. doi: 10.1158/2159-8290.CD-17-0226
38. Yamazaki T, Kirchmair A, Sato A, Buque A, Rybstein M, Petroni G, et al. Mitochondrial DNA Drives Abscopal Responses to Radiation That Are Inhibited by Autophagy. *Nat Immunol* (2020) 21(10):1160–71. doi: 10.1038/s41590-020-0751-0
39. Ahn J, Xia T, Konno H, Konno K, Ruiz P, Barber GN. Inflammation-Driven Carcinogenesis is Mediated Through STING. *Nat Commun* (2014) 5:5166. doi: 10.1038/ncomms6166
40. Ishizuka JJ, Manguso RT, Cheruiyot CK, Bi K, Panda A, Iracheta-Vellve A, et al. Loss of ADAR1 in Tumours Overcomes Resistance to Immune Checkpoint Blockade. *Nature* (2019) 565(7737):43–8. doi: 10.1038/s41586-018-0768-9
41. Canadas I, Thummalapalli R, Kim JW, Kitajima S, Jenkins RW, Christensen CL, et al. Tumor Innate Immunity Primed by Specific Interferon-Stimulated Endogenous Retroviruses. *Nat Med* (2018) 24(8):1143–50. doi: 10.1038/s41591-018-0116-5
42. Panda A, de Cubas AA, Stein M, Riedlinger G, Kra J, Mayer T, et al. Endogenous Retrovirus Expression is Associated With Response to Immune Checkpoint Blockade in Clear Cell Renal Cell Carcinoma. *JCI Insight* (2020) 5 (11):e137569. doi: 10.1172/jci.insight.121522
43. Roulois D, Loo Yau H, Singhania R, Wang Y, Danesh A, Shen SY, et al. Dna-Demethylating Agents Target Colorectal Cancer Cells by Inducing Viral Mimicry by Endogenous Transcripts. *Cell* (2015) 162(5):961–73. doi: 10.1016/j.cell.2015.07.056
44. Sun S, Frontini F, Qi W, Hariharan A, Ronner M, Wipplinger M, et al. Endogenous Retrovirus Expression Activates Type-I Interferon Signaling in an Experimental Mouse Model of Mesothelioma Development. *Cancer Lett* (2021) 507:26–38. doi: 10.1016/j.canlet.2021.03.004
45. Woo SR, Fuertes MB, Corrales L, Spranger S, Furdyna MJ, Leung MY, et al. STING-Dependent Cytosolic DNA Sensing Mediates Innate Immune Recognition of Immunogenic Tumors. *Immunity* (2014) 41(5):830–42. doi: 10.1016/j.immuni.2014.10.017
46. Barber GN. STING: Infection, Inflammation and Cancer. *Nat Rev Immunol* (2015) 15(12):760–70. doi: 10.1038/nri3921
47. Xu MM, Pu Y, Han D, Shi Y, Cao X, Liang H, et al. Dendritic Cells But Not Macrophages Sense Tumor Mitochondrial DNA for Cross-priming Through Signal Regulatory Protein Alpha Signaling. *Immunity* (2017) 47(2):363–73.e5. doi: 10.1016/j.immuni.2017.07.016
48. Suarez B, Prats-Mari L, Unfried JP, Fortes P. LncRNAs in the Type I Interferon Antiviral Response. *Int J Mol Sci* (2020) 21(17):6447. doi: 10.3390/ijms21176447
49. Arimoto KI, Miyauchi S, Stoner SA, Fan JB, Zhang DE. Negative Regulation of Type I IFN Signaling. *J Leukoc Biol* (2018) 103:1099–116. doi: 10.1002/JLB.2MIR0817-342R
50. Zhou L, Zhang Y, Wang Y, Zhang M, Sun W, Dai T, et al. A Dual Role of Type I Interferons in Antitumor Immunity. *Adv Biosyst* (2020) 4(11):e1900237. doi: 10.1002/adbi.201900237
51. Galani V, Kastamoulas M, Varouktsi A, Lampri E, Mitselou A, Arvanitis DL. Ifns-Signaling Effects on Lung Cancer: An Up-to-Date Pathways-Specific Review. *Clin Exp Med* (2017) 17(3):281–9. doi: 10.1007/s10238-016-0432-3
52. Zitvogel L, Galluzzi L, Kepp O, Smyth MJ, Kroemer G. Type I Interferons in Anticancer Immunity. *Nat Rev Immunol* (2015) 15(7):405–14. doi: 10.1038/nri3845
53. Vidal P. Interferon Alpha in Cancer Immunoediting: From Elimination to Escape. *Scand J Immunol* (2020) 91(5):e12863. doi: 10.1111/sji.12863
54. Diamond MS, Kinder M, Matsushita H, Mashayekhi M, Dunn GP, Archambault JM, et al. Type I Interferon is Selectively Required by Dendritic Cells for Immune Rejection of Tumors. *J Exp Med* (2011) 208 (10):1989–2003. doi: 10.1084/jem.20101158
55. Fuertes MB, Kacha AK, Kline J, Woo SR, Kranz DM, Murphy KM, et al. Host Type I IFN Signals are Required for Antitumor CD8+ T Cell Responses Through CD8{alpha}+ Dendritic Cells. *J Exp Med* (2011) 208(10):2005–16. doi: 10.1084/jem.20101159
56. Swann JB, Hayakawa Y, Zerafa N, Sheehan KC, Scott B, Schreiber RD, et al. Type I IFN Contributes to NK Cell Homeostasis, Activation, and Antitumor Function. *J Immunol* (2007) 178(12):7540–9. doi: 10.4049/jimmunol.178.12.7540
57. Dunn GP, Bruce AT, Sheehan KC, Shankaran V, Uppaluri R, Bui JD, et al. A Critical Function for Type I Interferons in Cancer Immunoediting. *Nat Immunol* (2005) 6(7):722–9. doi: 10.1038/ni1213
58. Benci JL, Xu B, Qiu Y, Wu TJ, Dada H, Twyman-Saint Victor C, et al. Tumor Interferon Signaling Regulates a Multigenic Resistance Program to Immune Checkpoint Blockade. *Cell* (2016) 167(6):1540–54.e12. doi: 10.1016/j.cell.2016.11.022
59. Lemos H, Mohamed E, Huang L, Ou R, Pacholczyk G, Arbab AS, et al. Sting Promotes the Growth of Tumors Characterized by Low Antigenicity Via IDO Activation. *Cancer Res* (2016) 76(8):2076–81. doi: 10.1158/0008-5472.CAN-15-1456
60. Della Corte CM, Sen T, Gay CM, Ramkumar K, Diao L, Cardnell RJ, et al. Sting Pathway Expression Identifies Nsclc With an Immune-Responsive Phenotype. *J Thorac Oncol* (2020) 15(5):777–91. doi: 10.1016/j.jtho.2020.01.009
61. Thompson JC, Hwang WT, Davis C, Deshpande C, Jeffries S, Rajpurohit Y, et al. Gene Signatures of Tumor Inflammation and Epithelial-to-Mesenchymal Transition (EMT) Predict Responses to Immune Checkpoint Blockade in Lung Cancer With High Accuracy. *Lung Cancer* (2020) 139:1–8. doi: 10.1016/j.lungcan.2019.10.012
62. Kitajima S, Ivanova E, Guo S, Yoshida R, Campisi M, Sundararaman SK, et al. Suppression of STING Associated With LKB1 Loss in KRAS-Driven Lung Cancer. *Cancer Discovery* (2019) 9(1):34–45. doi: 10.1158/2159-8290.CD-18-0689
63. Ricciuti B, Recondo G, Spurr LF, Li YY, Lamberti G, Venkatraman D, et al. Impact of DNA Damage Response and Repair (Ddr) Gene Mutations on Efficacy of PD-(L)1 Immune Checkpoint Inhibition in Non-Small Cell Lung Cancer. *Clin Cancer Res* (2020) 26(15):4135–42. doi: 10.1158/1078-0432.CCR-19-3529
64. Formenti SC, Rudqvist NP, Golden E, Cooper B, Wennerberg E, Lhuillier C, et al. Radiotherapy Induces Responses of Lung Cancer to CTLA-4 Blockade. *Nat Med* (2018) 24(12):1845–51. doi: 10.1038/s41591-018-0232-2
65. Vanpouille-Box C, Alard A, Aryankalayil MJ, Sarfraz Y, Diamond JM, Schneider RJ, et al. DNA Exonuclease Trex1 Regulates Radiotherapy-Induced Tumour Immunogenicity. *Nat Commun* (2017) 8:15618. doi: 10.1038/ncomms15618
66. Diamond JM, Vanpouille-Box C, Spada S, Rudqvist NP, Chapman JR, Ueberheide BM, et al. Exosomes Shuttle Trex1-Sensitive IFN-Stimulatory dsDNA From Irradiated Cancer Cells to Dcs. *Cancer Immunol Res* (2018) 6 (8):910–20. doi: 10.1158/2326-6066.CIR-17-0581
67. Skoulidis F, Goldberg ME, Greenawalt DM, Hellmann MD, Awad MM, Gainor JF, et al. Stk11/Lkb1 Mutations and PD-1 Inhibitor Resistance in KRAS-Mutant Lung Adenocarcinoma. *Cancer Discov* (2018) 8(7):822–35. doi: 10.1158/2159-8290.CD-18-0099
68. Yum S, Li M, Chen ZJ. Old Dogs, New Trick: Classic Cancer Therapies Activate Cgas. *Cell Res* (2020) 30(8):639–48. doi: 10.1038/s41422-020-0346-1
69. Achard C, Boisgerault N, Delaunay T, Roulois D, Nedellec S, Royer PJ, et al. Sensitivity of Pleural Mesothelioma to Oncolytic Measles Virus Depends on

Defects of the Type I Interferon Response. *Oncotarget* (2015) 6(42):44892–904. doi: 10.18632/oncotarget.6285

70. Saloura V, Wang LC, Fridlender ZG, Sun J, Cheng G, Kapoor V, et al. Evaluation of an Attenuated Vesicular Stomatitis Virus Vector Expressing Interferon-Beta for Use in Malignant Pleural Mesothelioma: Heterogeneity in Interferon Responsiveness Defines Potential Efficacy. *Hum Gene Ther* (2010) 21(1):51–64. doi: 10.1089/hum.2009.088
71. Husain AN, Colby TV, Ordonez NG, Allen TC, Attanoos RL, Beasley MB, et al. Guidelines for Pathologic Diagnosis of Malignant Mesothelioma 2017 Update of the Consensus Statement From the International Mesothelioma Interest Group. *Arch Pathol Lab Med* (2018) 142(1):89–108. doi: 10.5858/arpa.2017-0124-RA

**Conflict of Interest:** The authors declare that the research was conducted in the absence of any commercial or financial relationships that could be construed as a potential conflict of interest.

frontiers in Oncology

ORIGINAL RESEARCH
published: 08 July 2021
doi: 10.3389/fonc.2021.667148

# Frequent Genetic Alterations and Their Clinical Significance in Patients With Thymic Epithelial Tumors

*Song Xu[1,2*†], Xiongfei Li[1,2†], Hongyi Zhang[3†], Lingling Zu[2], Lingqi Yang[1,2], Tao Shi[4], Shuai Zhu[1,2], Xi Lei[1,2], Zuoqing Song[1,2] and Jun Chen[1,2*]*

[1] Department of Lung Cancer Surgery, Tianjin Medical University General Hospital, Tianjin, China, [2] Tianjin Key Laboratory of Lung Cancer Metastasis and Tumor Microenvironment, Lung Cancer Institute, Tianjin Medical University General Hospital, Tianjin, China, [3] Department of Thoracic Surgery, Gansu Provincial Hospital, Lanzhou, China, [4] Precision Medicine Center, Tianjin Medical University General Hospital, Tianjin, China

OPEN ACCESS

**Edited by:**
Giulia Pasello,
Veneto Institute of Oncology (IRCCS), Italy

**Reviewed by:**
Madhu M. Ouseph,
Cornell University, United States
Anja Roden,
Mayo Clinic, United States

***Correspondence:**
Song Xu
xusong198@hotmail.com
Jun Chen
huntercj2004@yahoo.com

[†]These authors have contributed equally to this work

**Specialty section:**
This article was submitted to Thoracic Oncology, a section of the journal Frontiers in Oncology

**Received:** 12 February 2021
**Accepted:** 18 June 2021
**Published:** 08 July 2021

**Citation:**
Xu S, Li X, Zhang H, Zu L, Yang L, Shi T, Zhu S, Lei X, Song Z and Chen J (2021) Frequent Genetic Alterations and Their Clinical Significance in Patients With Thymic Epithelial Tumors. Front. Oncol. 11:667148. doi: 10.3389/fonc.2021.667148

**Purpose:** Thymic epithelial tumors (TETs) are relatively rare neoplasms, including thymomas (types A, AB, B1, B2, and B3) and thymic carcinomas (TCs). The current knowledge about the biological properties of TETs is limited due to their low incidence. This study aimed to detect genetic alterations in TETs using next-generation sequencing (NGS) and explore their clinical significance in survival.

**Methods:** Tumor tissues and clinical data were collected from 34 patients with resected TETs in the Tianjin Medical University General Hospital between January 2011 and January 2019, and 56 cancer-associated genes were analyzed. The data of 123 TETs were retrieved from TCGA, and the information on their clinical and somatic mutations was explored.

**Results:** The cohort comprised 34 TETs including 17 thymomas and 17 TCs. The NGS results indicated that 73.08% of TCs+type B3 TETs and 37.50% of non-TCs+type B3 TETs each exhibited gene mutations. For patients with type B3/C, TP53 was the most frequent mutation (19.23%), followed by CDKN2A (11.54%). Similarly, in 123 TETs from the TCGA cohort, TP53 mutations were more frequent in patients with type B3/C than in patients with non-type B3/C (11.53% *vs* 3.09%). Further, patients with TET with TP53 mutations in the present cohort and the TCGA cohort had a worse prognosis compared with those without TP53 mutations.

**Conclusions:** Gene mutation profiles between TCs+type B3 TETs and non-TCs+type B3 TETs were significantly different. The presence of TP53 mutations was more frequent in TCs+type B3 TETs than in non-TCs+type B3 TETs, which was associated with a worse prognosis.

**Keywords: gene mutations, thymic epithelial tumors, NGS, TP53, TCGA**

## INTRODUCTION

Thymic epithelial tumors (TETs) are relatively rare neoplasms originating from the epithelial cells of the thymus, but they are the most common type among tumors of the anterior mediastinum (1, 2). TETs include a heterogeneous group of rare tumors. The World Health Organization (WHO) and the Masaoka–Koga stage classification are used for the histological classification and clinical staging of these tumors (3, 4). According to the WHO 2015 criteria, TETs are classified into thymomas (types A, AB, B1, B2, and B3) and thymic carcinomas (TCs) depending on the morphology of epithelial cells and the relative amount of thymocytes (3, 4). The overall incidence of TETs is 0.13 per 100,000 person-years in the US; however, it is higher among Asians (2). Previous studies have shown that patients with TETs have an elevated risk of developing a subsequent secondary tumor, indicating that certain genetic risk factors might be involved in the etiology of TET (2–4). The current knowledge about the biological properties of TETs is limited due to the low incidence. In particular, significant variability exists in the prognosis of TETs, indicating a complex heterogeneity among them. Previous studies investigated the etiology of TETs at the molecular level and mutations in EGFR, HER2, KIT, KRAS, and TP53 (5–13). However, discrepancies are found in the category and frequency of mutations in different studies.

The present study aimed to explore the genetic alterations and the possible therapeutic targets of TETs using next-generation sequencing (NGS) technology with 56 cancer-related hotspot genes. The correlation between gene mutations was analyzed using pathological classification, Masaoka–Koga stage classification, TNM stage, and overall survival (OS). In addition, the data on somatic mutations of TETs were retrieved from The Cancer Genome Atlas (TCGA) database and used to validate the findings. Finally, the literature was reviewed, and the genetic phenotypes of TETs were summarized. Thus, a better understanding of the molecular consequences of gene mutations might have therapeutic implications and support the personalized approach for the management of TETs.

## MATERIALS AND METHODS

### Ethical Approval

The study was conducted following the ethical principles stated in the Declaration of Helsinki for medical research involving human participants. All participants provided written informed consent, and the ethical review board approved the study protocol for clinical research at the Tianjin Medical University General Hospital.

### Study Design

All patients who underwent surgical treatment or suffered from previous pathologically confirmed TETs at the Tianjin Medical University General Hospital between January 2011 and January 2019 were included in the study. Their clinicopathological characteristics are shown in **Table 1**. The pathological types and clinical staging were based on the 2015 WHO criteria and the Masaoka–Koga system (3, 4). Patients with TETs from the TCGA cohort ($n$ = 123) were also employed in the present study

**TABLE 1** | Clinicopathological characteristics of study population from TCGA and our data.

| | | Our data | | | TCGA data | | |
|---|---|---|---|---|---|---|---|
| | | Type A, AB, B1, B2 (n=8) * | Type B3 (n=9) | Type C (n=17) | Type A, AB, B1, B2 (n=97) * | Type B3 (n=15) | Type C (n=11) |
| **Gender** | Male | 6 | 8 | 13 | 53 | 6 | 4 |
| | Female | 2 | 1 | 4 | 44 | 9 | 7 |
| **Age** | Median | 58.5 | 54 | 55 | 57.5 | 62 | 65 |
| | Range | 33-73 | 39-60 | 16-66 | 17-84 | 40-71 | 44-78 |
| **Smoking status** | Smoker | 3 | 3 | 8 | NP | NP | NP |
| | Non-smoker | 5 | 6 | 9 | NP | NP | NP |
| **Masaoka stage** | I | 3 | 0 | 0 | NP | NP | NP |
| | II | 3 | 5 | 1 | NP | NP | NP |
| | III | 2 | 4 | 10 | NP | NP | NP |
| | IV | 0 | 0 | 6 | NP | NP | NP |
| **TNM stage** | I | 8 | 6 | 2 | NP | NP | NP |
| | II | 0 | 0 | 4 | NP | NP | NP |
| | III | 0 | 3 | 7 | NP | NP | NP |
| | IV | 0 | 0 | 4 | NP | NP | NP |
| **Neoadjuvant therapy** | CT | 0 | 0 | 0 | 2 | 0 | 0 |
| | RT | 0 | 1 | 0 | | | |
| | CT+RT | 0 | 0 | 0 | | | |
| **Adjuvant therapy** | CT | 0 | 1 | 6 | 26 | 8 | 5 |
| | RT | 1 | 6 | 1 | 1 | 0 | 2 |
| | CT+RT | 0 | 0 | 5 | 0 | 2 | 1 |

*CT, hemotherapy; RT, radiotherapy; NP, Not provided.*
**including mixed type, A/B1, B1/B2.*

to verify the findings. For the TCGA cohort, multidimensional data of gene expression and clinical information were obtained from cBioPortal (http://www.cbioportal.org/public-portal/). The gene mutation profile in both the cohorts was analyzed, and the prognostic values of TP53 and cyclin-dependent kinase inhibitor 2A (CDKN2A) were explored.

## Next-Generation Sequencing

DNA from the TETs was extracted using a QiAamp DNA FFPE tissue kit (Qiagen), and the DNA quality was evaluated according to the extent of DNA degradation. DNA extracted from the TET tissues was used for targeted capture sequencing of 56 cancer-associated genes (Lung core TM 56 genes; Burning Rock Biotech; **Supplementary Table 1**).

The concentration of the DNA samples was measured using the Qubit dsDNA assay to ensure that the genomic DNA was larger than 100 ng. The DNA was fragmented (average DNA fragment size of 180–220 bp), followed by hybridization with capture probe baits, hybrid selection with magnetic beads, and PCR amplification. A high-sensitivity DNA assay using a bioanalyzer was then used to assess the quality and size range. The available indexed samples were then sequenced using a NextSeq 500 bioanalyzer (Illumina, CA, USA) with paired-end reads. Flexbar software (version 2.7.0) was used for analyzing the raw data obtained from the NextSeq 500 runs to generate FASTQ data, trim the adapter sequences, and filter and remove the poor-quality reads (14). The sequencing depth was ~1000 units, and Varscan (v. 2.3) was used to call single-nucleotide variations and insertions/deletions with MAPQ >60, base quality >30, and allele frequency (AF) >1% (15).

True mutations were defined as variants that comprised >3 nonduplicated or >5 nonduplicated paired reads. The FASTQ data were mapped to the human genome (hg19) using BWAaligner 0.7.10 (http://bio-bwa.sourceforge.net/). Local alignment optimization, variant calling, and annotation were performed using GATK version 3.2 (https://www.broadinstitute.org/gatk/). DNA translocation analysis was performed using both Tophat2 (http://ccb.jhu.edu/software/tophat/index.shtml) and Factera version 1.4.3 (http://factera.stanford.edu). In the final step, to eliminate erroneous base calling and generate final mutation, variation frequency (>0.5%) was used and manual verification was performed using integrative Genomics Viewer version 2.3.72 (16–18).

## Mutation Prediction

PolyPhen-2 is an online prediction tool which could predict possible impact of amino acid changes of human proteins. We used PolyPhen-2 to predict the mutational consequence of missense mutations (16, 19). Three outcomes were used to show the prediction results: benign, possibly damaging, and probably damaging.

## Literature Review

Two individual researchers conducted platform searches on PubMed. Literature retrieval was performed through a combined search of the subject terms ("MeSH" on PubMed).

All available studies on patients with TETs who underwent NGS, which were published in English until May 01, 2021, were included, and the inclusion and exclusion criteria were listed. The inclusion criteria were as follows: (1) pathologically confirmed TETs, including thymomas and thymic carcinomas and (2) NGS performed for thymic epithelial tumors. The exclusion criteria were as follows: (1) studies with a design of literature review, systematic review, basic research, letter to editors, diagnostic study, and so on, (2) studies using the PCR sequencing method, and (3) studies using repeated patient cohorts with another study. No limitations were imposed on the nationalities of the participants.

## Statistical Analysis

The gene mutation status was compared with the patient's clinicopathological characteristics using the Fisher's exact test and the Wilcoxon–Mann–Whitney test. Survival analysis was calculated using the Kaplan–Meier method to perform the log-rank test and two stage hazard rate comparison when the curves crossed using softwares GraphPad Prism 7.0 (GraphPad Software, CA, USA) and R version 3.6.1 (cran.r-project.org) (20). A two-sided statistically significant cutoff was set at $P < 0.05$.

# RESULTS

## Population Study

A total of 17 thymoma (type A, $n = 3$; type AB, $n = 2$; typeB1, $n = 2$; type B1/B2, $n = 1$; type B3, $n = 9$) and 17TCs were collected in this study. The distributions of sex and age were similar between the two groups. The patients with TCs+type B3 TETs presented with an advanced Masaoka–Koga stage compared with the other types (**Table 1**). For patients with TETs from the TCGA cohort, 123 patients underwent whole-genome sequencing, including 97 patients with types A, AB, B1, and B2, 15 patients with type B3, and 11 patients with TCs. However, some information such as smoking status and Masaoka–Koga stage was not provided (**Table 1**).

## Genetic Mutations in TETs

All 34 TETs underwent genetic mutation analysis with a panel of 56 cancer-related genes. Among the 34 TETs, 22 tumors were detected with at least one gene mutation (non-TCs+type B3 TETs, $n = 3$; type B3, $n = 6$; TCs, $n = 13$), and the most frequent gene mutations were TP53 ($n = 5$), MTOR ($n = 3$), BRCA1 ($n = 3$), NF1 ($n = 3$), CDKN2A ($n = 3$), and PTCH1 ($n = 3$) (**Figure 1**). Seven out of 26 patients with TCs+type B3 TETs and 5 out of 8 patients with type A/B1/B2 thymoma had no detected gene mutations. The mutation percentages were 73.08% for patients with types TCs+type B3 TETs and 37.50% for patients with types A/B1/B2 (**Figure 2A**). In addition, the number of mutated genes was significantly higher in patients with type TCs+type B3 TETs than in patients with type A/B1/B2 thymoma (typeTCs+type B3 TETs = 33 *vs* type A + B1/B2 = 7) (**Figure 2B**). For patients with types A and B1/B2 thymoma ($n = 9$), seven gene mutations, including MTOR, BRCA1, APC, NF1, HRAS, NTRK3, and PTCH1, were detected, and each gene appeared only once in patients with non-TCs+type B3 TETs (**Figure 2C**). For patients with type B3/C ($n = 26$), 33 gene mutations were found and the most frequent mutations were TP53 ($n = 5$), followed by CDKN2A ($n = 3$), MTOR ($n = 2$), NF1 ($n = 2$), BRCA1 ($n = 2$), PTCH1 ($n = 2$), CDK4 ($n = 2$),

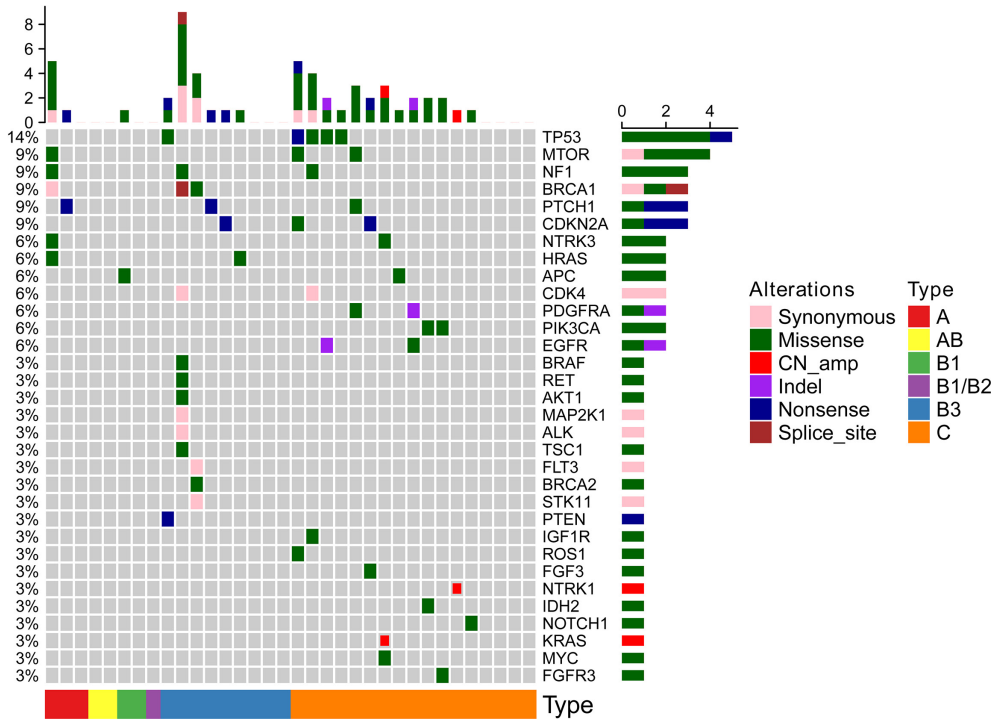


**FIGURE 1** | The mutational results of all 34 TETs in our cohort.

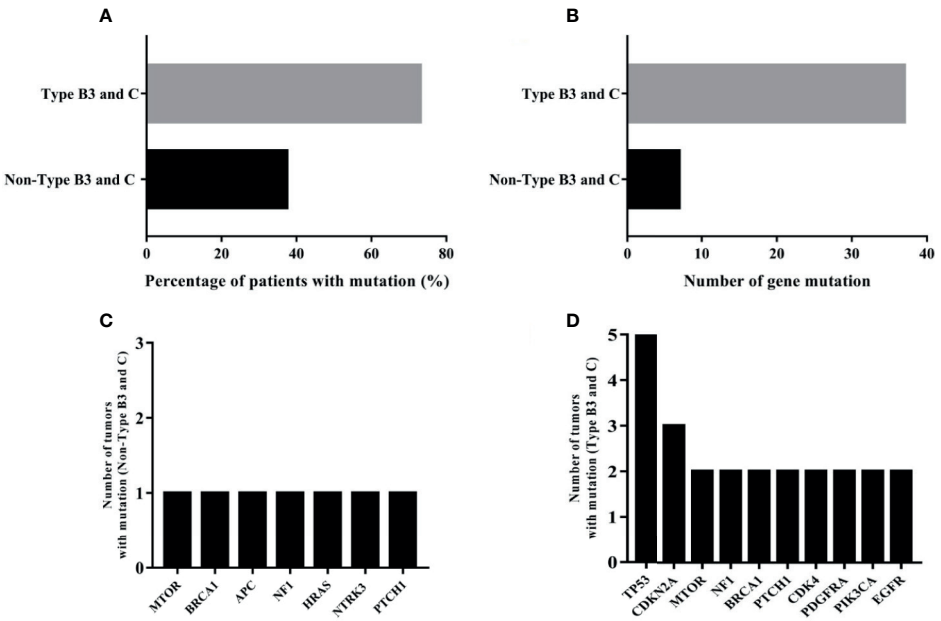


**FIGURE 2** | The analysis of mutational results of TETs in our cohort; **(A)**: the mutation percentage in type B3 and C and non-type B3 and C TET patients; **(B)**: the number of mutated genes in type B3 and C and non-type B3 and C TET patients; **(C)**: the numbers of tumors with mutation of seven genes in type A and B1/B2 thymomas; **(D)**: ten most frequently mutational genes in type B3/C TETs patients.

PDGFRA ($n$ = 2), PIK3CA ($n$ = 2), and EGFR ($n$ = 2) (**Figure 2D**). Importantly, all TP53 or CDKN2A mutations were seen in type TCs +type B3 TETs only (**Figure 1**). There are 18 patients with missense mutations. The prediction results of PolyPhen-2 were showed in the **Supplementary Figure 2** which indicated that all of TP53 missense mutations in our cohort were probably damaging.

The mutations in the 6 most frequently mutated genes in the cohort were further validated using a cohort of 123 patients with TETs from the TCGA database. The mutation types are shown in **Supplementary Figure 1**. TP53 was also the most frequent mutation in the TCGA cohort similar to that in the cohort. CDKN2A ($n$ = 6) was a highly frequent mutation, followed by NF1 ($n$ = 3), MTOR ($n$ = 1), BRCA1 ($n$ = 1), and PTCH1 ($n$ = 1). The mutation characteristics of the six genes are listed in **Table 2**.

Among the 123 patients with TETs from the TCGA cohort, the most frequent gene mutations were GTF2I ($n$ = 49), HRAS ($n$ = 10), TTN ($n$ = 8), MUC16 ($n$ = 6), UNC93B1 ($n$ = 5), MUC4 ($n$ = 5), NPIPA2 ($n$ = 4), TP53 ($n$ = 4), ZNF208 ($n$ = 3), and BCOR ($n$ = 3) (**Supplementary Table 2**). Also, the top 10 highly frequent somatic gene mutations in patients with non-TCs+type B3 TETs and type TCs+type B3 TETs were also listed and compared (**Figure 2** and **Supplementary Tables 3** and **4**). In the TCGA cohort, TP53 had the highest gene mutation in patients with TCs+type B3 TETs compared with non-TCs+type B3 TETs, which was concordant with that in the cohort.

Furthermore, the basic characteristics of TP53 somatic mutations in patients from the present cohort and the TCGA cohort were summarized. Most TP53 somatic mutations were missense mutations, while nonsense and deletion mutations were detected once in the present cohort and TCGA cohort, respectively (**Table 3**).

## Survival Analysis

The gene with the highest frequency of mutations among patients with TETs from the TCGA cohort, including TP53, CDKN2A, and NF1, were selected, and their roles in the prognosis of patients with TETs were investigated. In the cohort of patients with thymoma from the hospital, the most frequent mutation was TP53. All patients with TP53 mutations were classified as Masaoka–Koga stage III or IV and received postoperative radiotherapy or chemotherapy. Using log-rank tests or two stage hazard rate comparison, the study found that the patients with TP53 mutations in the cohort of the hospital showed a significantly shorter disease-free survival (DFS) and overall survival (OS) compared with those without TP53 mutation (**Figure 3**). In addition, patients with CDKN2A (a tumor suppressor gene) mutations in the present cohort exhibited a trend of poor survival compared with those without CDKN2A mutations. However, the difference was not significant, probably due to limited patient numbers (**Supplementary Figure 3A**). The survival analysis between NF1(+) and NF1(−) TETs was also performed, and the

**TABLE 2** | Thymic epithelial tumor patients with high frequent gene alterations (somatic mutation and copy number alterations) in our cohort and TCGA data.

| | | Percentage (No.) | Type | Mutation classification |
|---|---|---|---|---|
| **TP53** | Our data | 14.3% (5) | Type B3, n=1 | Missense variant, n=4 |
| | | | Type C, n=4 | Nonsense variant, n=1 |
| | TCGA data | 5% (6) | Type A, n=1 | Missense variant, n=3 |
| | | | Type AB, n=1 | Deletion variant, n=1 |
| | | | Type B2, n=1 | CN-del, n=2 |
| | | | Type B3, n=1 | |
| | | | Type C, n=2 | |
| **MTOR** | Our data | 8.6% (3) | Type A, n=1 | Missense variant, n=3 |
| | | | Type C, n=2 | |
| | TCGA data | 0.8% (1) | Type C, n=1 | Missense variant, n=1 |
| **BRCA1** | Our data | 8.6% (3) | Type A, n=1 | Missense variant, n=1 |
| | | | Type B3, n=2 | Splice-site, n=1 |
| | | | | Synonymous variant,n=1 |
| | TCGA data | 0.8% (1) | Type C, n=1 | CN-amp, n=1 |
| **NF1** | Our data | 8.6% (3) | Type A, n=1 | Missense variant, n=3 |
| | | | Type C, n=1 | |
| | TCGA data | 2.4% (3) | Type A, n=2 | Missense variant, n=2 |
| | | | Type C, n=1 | Nonsense variant, n=1 |
| **CDKN2A** | Our data | 8.6% (3) | Type B3, n=1 | Missense variant, n=1 |
| | | | Type C, n=2 | Nonsense variant, n=2 |
| | TCGA data | 5% (6) | Type A, n=1 | Deletion variant, n=1 |
| | | | Type AB, n=1 | CN-del, n=5 |
| | | | Type B3, n=2 | |
| | | | Type C, n=2 | |
| **PTCH1** | Our data | 8.6% (3) | Type A, n=1 | Missense variant, n=1 |
| | | | Type B3, n=1 | Nonsense variant, n=2 |
| | | | Type C, n=1 | |
| | TCGA data | 0.8% (1) | Type AB, n=1 | Missense variant, n=1 |

*CN-amp, Copy number variation-amplification.*
*CN-del, Copy number variation-deletion.*
*Total patient number: Our data, n=35; TCGA data, n=123.*

**TABLE 3** | Frequency of different TP53 somatic mutations in Thymoma patients from our and TCGA cohort.

| Our cohort | | | TCGA | | |
|---|---|---|---|---|---|
| **AA change** | **Type** | **#Mut** | **AA change** | **Type** | **#Mut** |
| G244D | Missense | 1 | D281Afs*64 | Deletion | 1 |
| E349* | Nonsense | 1 | R273C | Missense | 1 |
| R282P | Missense | 1 | L194R | Missense | 1 |
| F113C | Missense | 1 | R248L | Missense | 1 |
| R248L | Missense | 1 | | | |

**stop codon.*
*#Frequency of mutations.*

results indicated that the NF1(–) TETs had a better survival rate (**Supplementary Figure 4**).

In addition, this study also investigated TP53, CDKN2A, and NF1 mutations and explored the relationship between individual gene mutations and DFS and OS in patients in the TCGA cohort. Further, 50% of TP53 mutations and 66.7% of CDKN2A mutations were of TCs+type B3 TETs (**Table 2**). The study confirmed, using the TCGA dataset, significantly shorter DFS and OS for TETs with TP53 mutations (**Figure 3**) and a trend of shorter DFS and OS for TETs with CDKN2A mutations (**Supplementary Figure 3B**). NF1 mutation indicated significantly poor survival in patients with TETs from the present cohort; however, NF1 mutation had no correlation with the prognosis of patients with thymoma in the TCGA cohort (**Supplementary Figure 4**). Moreover, the study also investigated the relationship between nine other most frequent gene mutations from the TCGA dataset and the prognosis of thymoma. However, none of the other gene mutations in the TCGA cohort exhibited a significant correlation with the prognosis of patients with thymoma (**Supplementary Figure 5**).

## DISCUSSION

The underlying molecular and genetic mechanisms of TETs are yet to be fully elucidated due to their low incidence and histological heterogeneity compared with other thoracic malignancies (8–12). The findings of previous studies on the molecular characteristics of TETs have been inconsistent, and very few studies focused on the genetic alterations in Asian patients (6–10, 12, 17, 21).

The present study, based on an NGS 56–cancer gene panel, found that TETs with types AB1 and B2 exhibited a remarkable difference in somatic gene mutations compared with

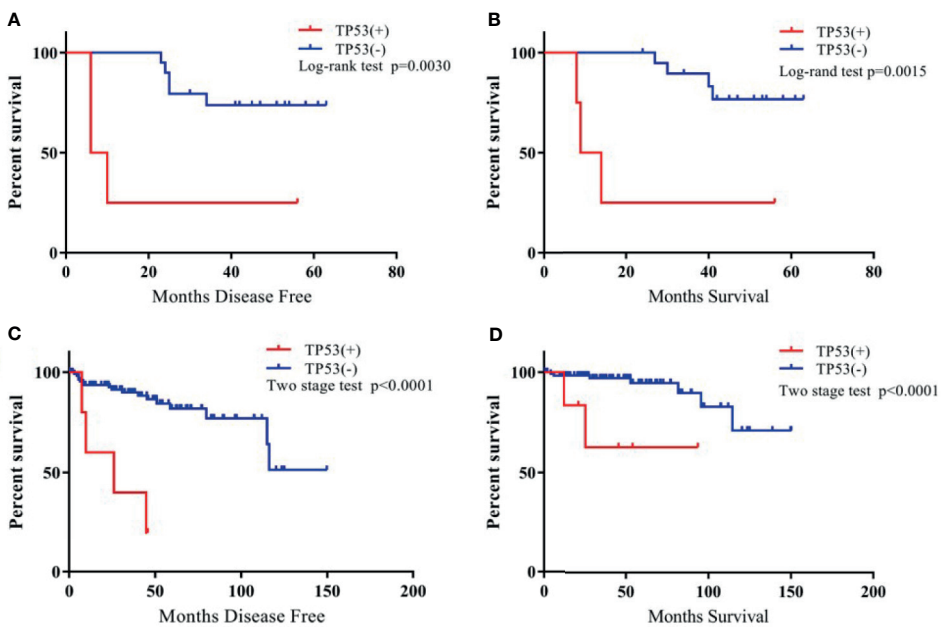


**FIGURE 3** | The Kaplan-Meier survival curve of TP53(+) *vs.* TP53(-) TET patients. **(A)**: TP53(+) *vs*. TP53 (-) TET patients of DFS in our cohort; **(B)**: TP53(+) *vs.* TP53 (-) TET patients of OS in our cohort; **(C)**: TP53 (+) *vs.* TP53 (-) TET patients of DFS in TCGA cohort; **(D)**: TP53 (+) *vs*. TP53 (-) TET patients of OS in TCGA cohort.

types B3 and C, in terms of mutation percentage and frequency. TP53 was the most frequent gene mutation in all 34 patients with TETs from the present cohort, and more importantly, TP53 and CDKN2A mutations were detected only in patients with types B3 and C. Although the sequencing methods and profiling in the TCGA cohort and the present cohort were not exactly the same, TP53 and CDKN2A mutations were found to be more common in patients with TCs+type B3 TETs (TP53, 50%; CDKN2A, 66.7%, in TCs+type B3 TETs) in the TCGA cohort. Survival analysis from both the TCGA cohort and the present cohort demonstrated that TP53 mutations indicated a significantly worse prognosis in patients with TETs, and previous studies also proved this (22–24). The patients with CDKN2A mutations also exhibited a trend of poor survival compared with those without CDKN2A mutations; however, this difference was not significant. Previous studies reported the mutation frequency of CDKN2A in thymic carcinomas were 11%-35% and most of them were truncating mutation (22, 23, 25). Further studies with larger sample sizes are

**TABLE 4** | Gene mutation analysis of TETs from previously published literature.

| Case | Author | Year | Type | N0 | Mutation | Sequencing Method | Country |
|---|---|---|---|---|---|---|---|
| 1 | Chen et al. (26) | 2020 | Thymoma | 50 | MAP3K1 (98%), TGFBR2 (96%), KMT2C (94%), ARID1A (92%), PRKDC (90%) | Next-generation sequencing for 315 genes | China |
| | | | Thymic carcinoma | 5 | ARID1A (100%), KMT2C (100%), MAP3K1 (100%) | | |
| 2 | Thompson et al. (27) | 2020 | Thymoma | 3 | HRAS (33.3%) | Next-generation sequencing for 1385 genes | USA |
| 3 | Sakane et al. (28) | 2019 | Thymoma | 33 | HRAS (3.0%); PIK3CA (6.1%); AKT1 (3.0%) | Single-base extension multiplex assay | Japan |
| | | | Thymic carcinoma | 54 | KRAS (11.1%); HRAS (5.6%); TP53 (9.3%); EGFR (3.7%); PIK3CA (1.9%); NRAS (1.9%); AKT1 (1.9%) | | |
| 4 | Enkner et al. (29) | 2017 | Type A thymoma | 18 | HRAS (16.7%) | Next-generation sequencing for 50 genes | Austria |
| | | | Type B3 thymoma | 19 | SMARCB (5.3%); STK11 (5.3%) | | |
| | | | Thymic carcinoma | 35 | TP53 (25.7%); CDKN2A (11.4%); FGFR3 (5.7%); KIT (5.7%); ALK (2.9%); ATM (2.9%); ERBB4 (2.9%); NRAS (2.9%); | | |
| 5 | Saito et al. (30) | 2017 | Thymic carcinoma | 10 | TET2 (30%); CACNA1A (30%); HTT (20%); MYNN (20%); OR5T2 (20%); ARID1B (20%); CYLD (20%); SETD2 (20%); | Whole exome sequencing | Japan |
| 6 | Asao et al. (31) | 2016 | Thymic carcinoma | 52 | TP53 (7.7%), KRAS (3.8%), FBXW7 (3.8%), NRAS (1.9%), | Next-generation sequencing for 50 genes | Japan |
| 7 | Song et al. (32) | 2016 | Thymoma | 37 | EGFR (2.7%), PIK3CA (2.7%); | Next-generation sequencing for 22 genes | China |
| | | | Thymic carcinoma | 15 | PIK3CA (6.7%) | | |
| 8 | Moreira et al. (25) | 2015 | Type B3 thymoma | 6 | BCOR (50%); MLL3 (16.7%) | Next generation sequencing | USA |
| | | | Thymic carcinoma | 15 | TP53 (26.7%), SMAD4 (13.3%), and CYLD (13.3%), KDM6A (20%), SETD2 (13.3%), MLL3 (13.3%), MLL2 (13.3%). | | |
| 9 | Petrini et al. (33) | 2014 | Thymoma | 38 | GTF2I (42.1%); TP53 (5.3%); ALK (5.3%); PPP2RIA (5.3%) | Exome sequencing or 197-gene assay | USA |
| | | | Thymic carcinoma | 16 | TP53 (25%); CYLD (18.8%); BAP (12.5%); PBRM (12.5%); CDKN2A (12.5%) | | |
| 10 | Shitara et al. (34) | 2014 | Thymic carcinoma | 12 | NF1 (16.7%); 8.3% for HRAS, PBRM1, DDR2, ASXL1, CDK8, CDKN2A, DCC, IGF1R, IKBKE, KAT6B, KDM6A, KIT, KMT2A, KMT2D, NKX2-1, PAX5, PDGFRA, PKHD1, ROS1, RUNX1T1, SMARCA4, TET1, TP53; | Ion Torrent next-generation sequencing for 409 cancer-related genes | Japan |
| 11 | Wang et al. (30) | 2014 | Thymoma | 31 | 3.2% for ASXL1, DCC, EGFR, ERG, HRAS, MAGI1, PDGFRA, PRCC, PTGS2, RUNX1, SDHA, SETD2, SRC, TET2, TP53 | Massively parallel sequencing of 197 cancer-related genes. | USA |
| | | | Thymic carcinoma | 47 | TP53 (25.5%); BAP1 (10.6%); CYLD (8.5%); KIT (8.5%); DNMT3A (8.5%); SETD2 (8.5%); TET3 (6.4%); 4.3% for ASXL1, BRCA2, CDKN2A, DCC, SMARCA4 and WT1. | | |
| 12 | Girard et al. (35) | 2009 | Thymoma | 38 | KRAS (2.6%); HRAS (2.6%) | Array-based comparative genomic hybridization. | USA |
| | | | Thymic carcinoma | 7 | KIT (28.6%); KRAS (14.3%) | | |
| 13 | Asselta et al. (36) | 2021 | Thymic carcinoma | 15 | FGFR3(33.3%);CDKN2A(20%);SMARCB1(13.3%); 6.6% for ATM, NRAS, SRC, APC, KIT, MET | Next-generation sequencing for 50 genes | Italy |
| 14 | Massoth et al. (37) | 2020 | Thymoma | 242 | KMT2A-MAML2 Fusion (4%) | Next-generation sequencing | USA |
| 15 | Sakane et al. (38) | 2021 | Thymic carcinoma | 54 | TP53 (18.5%), KIT (7.4%), and PDGFRA (5.6%) | Next-generation sequencing for 50 genes | Japan |

necessary to validate the role of CDKN2A mutations in the prognosis of TETs.

A comprehensive literature review was performed, and the genetic sequencing data were summarized to further explore the molecular and biological mechanisms of TETs. The clinical characteristics and high-frequency gene mutations are listed in **Table 4**, comprising 15 studies that included 797 TETs (465 thymomas and 332 thymic carcinomas) (25–39). All 15 studies were published between 2009 and 2020, and DNA-based NGS with different gene panel sizes was used. As shown in **Table 4**, as the number of genes for sequencing increased, more gene mutations were detected. In 6 out of 15 studies, TP53 was the most frequent mutation in thymic carcinomas, and the mutation frequency ranged from 7.7% to 26.7%. However, the mutation of TP53 in thymomas was rare. This was consistent with the findings of the present study that TP53 was the gene mutation with the highest mutation frequency (23.5%) in TCs.

The malignant potential of type B3 TETs, especially in an advanced stage, shows a poor prognosis, even similar to that of TCs. Hence, TCs+type B3 TETs were classified together in the present study. The sequencing analysis indicated that the gene mutations and frequency differed between TCs+type B3 TETs and non-TCs+type B3 TETs. Previous studies also focused on the difference between thymomas and TCs. However, most of these studies classified type B3 and types A/B1/B2 together, not with TCs Only a study by Enkner et al. separated type B3 from other thymomas (types A/B1/B2) and reported that the mutations between type TCs+type B3 TETs and non-TCs+type B3 TETs were very different (29). Other studies that compared the molecular mechanisms between type B3 TETs and TCs found comparable gene mutations with similar frequencies. The present genetic analysis found that types B3 and TCs exhibited similar gene mutations, including TP53. Hence, placing type B3 and TCs together was suggested to be more appropriate. Previous studies reported that TP53 mutations in TETs were associated with more aggressive behavior (5, 12, 13, 17, 40).

In the present cohort and the TCGA cohort, patients with TETs having TP53 mutations had significantly poorer survival compared with those without TP53 mutations. HRAS mutations, which were detected in TETs in the present study, were detected in previous studies as well. According to the literature review, five studies reported that the mutations of HRAS in TETs and their frequencies were very inconsistent, ranging from the lowest of 2.6% to the highest of 33.3% (27–30, 34, 35). Furthermore, four studies reported that the frequency of CDKN2A mutations ranged from 4.3% to 12.5%. This study confirmed that CDKN2A was a common mutation in the present cohort, with a frequency of 11.8% in thymic carcinomas, which was similar to that in previous studies. The study also found that TETs with CDKN2A mutations exhibited a trend of poor survival compared with those without CDKN2A mutations; however, this was not statistically significant, probably due to the small sample size.

The effect of CDKN2A on the prognosis of TETs needs further investigation. Another gene with a relatively frequent mutation in TETs was NF1, with mutation frequencies of 8.6% and 5% in the present cohort and the TCGA cohort, respectively. However, Shitara reported that 16.7% of the TETs exhibited NF1 mutations in their cohort study (34). The difference in sample size and histological distribution might have resulted in this discrepancy.

In TCGA cohort we found that GTF2I is the gene mutation with the highest mutation frequency in TETs. Previous studies also reported that GTF2I is the most frequently mutated gene in thymomas especially in type A and type AB TETs, however its frequency is lower than other types thymomas and thymic carcinomas (41–43). It was reported that thymomas had a unique GTF2I mutation Leu404His which was not found in other tumors (42). TETs with GTF2I mutation had better prognosis and our analysis also demonstrated the similar trend (41).

Moreover, this study had some limitations. First, the gene panel of NGS was relatively too small to thoroughly explore the genetic mechanism of TETs. In addition, previous studies also reported some gene mutations with a high frequency, which were not seen in the present cohort, such as GTF2I, CYLD, SMAD4, and a few others. However, the function and value of these genes in the prognosis of TETs are unknown and need to be further investigated. Finally, the sample sizes in the present cohort and the TCGA cohort were small, especially given the heterogeneous histology of TETs.

## CONCLUSION

Our study found that the gene mutations between TCs+type B3 TETs and non-TCs+type B3 TETs were drastically different. The mutations in TP53 were more frequent in type B3/C TETs, indicating a worse prognosis. Targeted therapy against TP53 might be an effective strategy for treating thymic carcinomas. However, further validation is needed through prospective clinical studies with a larger sample size.

## DATA AVAILABILITY STATEMENT

The original contributions presented in the study are included in the article/**Supplementary Material**. Further inquiries can be directed to the corresponding authors.

## ETHICS STATEMENT

The studies involving human participants were reviewed and approved by Tianjin Medical University General Hospital. The patients/participants provided their written informed consent to participate in this study.

## AUTHOR CONTRIBUTIONS

SX, XFL, and HZ retrieved and analyzed all of the data in the study. SX, XFL, HZ, LZ, SZ, XL, LY, TS, and ZS revised the manuscript for important intellectual contents. SX and JC

designed, checked, and supervise all study process. All authors contributed to the article and approved the submitted version.

## FUNDING

The present study was funded by the National Natural Science Foundation of China (No. 81772464) and Tianjin Science and Technology Plan Project (19ZXDBSY00060).

## SUPPLEMENTARY MATERIAL

The Supplementary Material for this article can be found online at: https://www.frontiersin.org/articles/10.3389/fonc.2021.667148/full#supplementary-material

**Supplementary Figure 1 |** Six genes alterations in TCGA.

**Supplementary Figure 2 |** The heatmap of mutations prediction via PolyPhen-2.

**Supplementary Figure 3 |** The Kaplan-Meier survival curve of CDKN2A(+) vs. CDKN2A(-) TET patients. A: CDKN2A(+) vs. CDKN2A(-) TET patients of DFS in our cohort; B: CDKN2A(+) vs. CDKN2A(-) TET patients of OS in our cohort; C: CDKN2A (+) vs. CDKN2A(-) TET patients of DFS in TCGA cohort; B: CDKN2A(+) vs. CDKN2A (-) TET patients of OS in TCGA cohort.

**Supplementary Figure 4 |** The Kaplan-Meier survival curve of NF1(+) vs. NF1 (-) TET patients. A: NF1 (+) vs. NF1 (-) TET patients of DFS in our cohort; B: NF1 (+) vs. NF1 (-) TET patients of OS in our cohort; C: NF1 (+) vs. NF1 (-) TET patients of DFS in TCGA cohort; B: NF1 (+) vs. NF1 (-) TET patients of OS in TCGA cohort.

**Supplementary Figure 5 |** The Kaplan-Meier survival curve of GTF2I(+) vs. GTF2I (-), HRAS(+) vs. HRAS(-), MUC4(+) vs. MUC4(-), MUC16(+) vs. MUC16(-), TTN(+) vs. TTN(-), UNC93B1(+) vs. UNC93B1(-), BCOR(+) vs. BCOR(-), NPIPA2(+) vs. NPIPA2(-), ZNF208(+) vs. ZNF208(-) TET patients in TCGA cohort.

**Supplementary Table 1 |** The lists of 56 cancer-associated genes.

**Supplementary Table 2 |** The gene somatic mutation distribution of TCGA all types of TETs patients.

**Supplementary Table 3 |** The gene somatic mutation distribution of TCGA type B3 and C patients.

**Supplementary Table 4 |** The gene somatic mutation distribution of TCGA non-B3 and C patients.

## REFERENCES

1. Kelly RJ, Petrini I, Rajan A, Wang Y, Giaccone G. Thymic Malignancies: From Clinical Management to Targeted Therapies. *J Clin Oncol: Off J Am Soc Clin Oncol* (2011) 29(36):4820–7. doi: 10.1200/jco.2011.36.0487
2. Engels EA, Pfeiffer RM. Malignant Thymoma in the United States: Demographic Patterns in Incidence and Associations With Subsequent Malignancies. *Int J Cancer* (2003) 105(4):546–51. doi: 10.1002/ijc.11099
3. Travis WD, Brambilla E, Burke AP, Marx A, Nicholson AG. Introduction to The 2015 World Health Organization Classification of Tumors of the Lung, Pleura, Thymus, and Hear. *J Thoracic Oncol: Off Publ Int Assoc Study Lung Cancer* (2015) 10(9):1240–2. doi: 10.1097/jto.0000000000000663
4. Koga K, Matsuno Y, Noguchi M, Mukai K, Asamura H, Goya T, et al. A Review of 79 Thymomas: Modification of Staging System and Reappraisal of Conventional Division Into Invasive and non-Invasive Thymoma. *Pathol Int* (1994) 44(5):359–67. doi: 10.1111/j.1440-1827.1994.tb02936.x
5. Moreira AL, Won HH, McMillan R, Huang J, Riely GJ, Ladanyi M, et al. Massively Parallel Sequencing Identifies Recurrent Mutations in TP53 in Thymic Carcinoma Associated With Poor Prognosis. *J Thoracic Oncol: Off Publ Int Assoc Study Lung Cancer* (2015) 10(2):373–80. doi: 10.1097/jto.0000000000000397
6. Weissferdt A, Lin H, Woods D, Tang X, Fujimoto J, Wistuba II, et al. HER Family Receptor and Ligand Status in Thymic Carcinoma. *Lung Cancer (Amsterdam Netherlands)* (2012) 77(3):515–21. doi: 10.1016/j.lungcan.2012.05.108
7. Sasaki H, Yano M, Fujii Y. Evaluation of Kras Gene Mutation and Copy Number in Thymic Carcinomas and Thymomas. *J Thoracic Oncol: Off Publ Int Assoc Study Lung Cancer* (2010) 5(10):1715–6. doi: 10.1097/JTO.0b013e3181f1cab3
8. Girard N, Shen R, Guo T, Zakowski MF, Heguy A, Riely GJ, et al. Comprehensive Genomic Analysis Reveals Clinically Relevant Molecular Distinctions Between Thymic Carcinomas and Thymomas. *Clin Cancer Res: An Off J Am Assoc Cancer Res* (2009) 15(22):6790–9. doi: 10.1158/1078-0432.ccr-09-0644
9. Yoh K, Nishiwaki Y, Ishii G, Goto K, Kubota K, Ohmatsu H, et al. Mutational Status of EGFR and KIT in Thymoma and Thymic Carcinoma. *Lung Cancer (Amsterdam Netherlands)* (2008) 62(3):316–20. doi: 10.1016/j.lungcan.2008.03.013
10. Ströbel P, Hartmann M, Jakob A, Mikesch K, Brink I, Dirnhofer S, et al. Thymic Carcinoma With Overexpression of Mutated KIT and the Response to Imatinib. *New Engl J Med* (2004) 350(25):2625–6. doi: 10.1056/nejm200406173502523
11. Pan CC, Chen PC, Wang LS, Lee JY, Chiang H. Expression of Apoptosis-Related Markers and HER-2/Neu in Thymic Epithelial Tumours. *Histopathology* (2003) 43(2):165–72. doi: 10.1046/j.1365-2559.2003.01663.x
12. Hirabayashi H, Fujii Y, Sakaguchi M, Tanaka H, Yoon HE, Komoto Y, et al. P16ink4, pRB, P53 and Cyclin D1 Expression and Hypermethylation of CDKN2 Gene in Thymoma and Thymic Carcinoma. *Int J Cancer* (1997) 73(5):639–44. doi: 10.1002/(sici)1097-0215(19971127)73:5<639::aid-ijc5>3.0.co;2-y
13. Tateyama H, Eimoto T, Tada T, Mizuno T, Inagaki H, Hata A, et al. P53 Protein Expression and P53 Gene Mutation in Thymic Epithelial Tumors. An Immunohistochemical and DNA Sequencing Study. *Am J Clin Pathol* (1995) 104(4):375–81. doi: 10.1093/ajcp/104.4.375
14. Dodt M, Roehr JT, Ahmed R, Dieterich C. FLEXBAR-Flexible Barcode and Adapter Processing for Next-Generation Sequencing Platform. *Biology* (2012) 1(3):895–905. doi: 10.3390/biology1030895
15. Koboldt DC, Zhang Q, Larson DE, Shen D, McLellan MD, Lin L, et al. VarScan 2: Somatic Mutation and Copy Number Alteration Discovery in Cancer by Exome Sequencing. *Genome Res* (2012) 22(3):568–76. doi: 10.1101/gr.129684.111
16. Thorvaldsdóttir H, Robinson JT, Mesirov JP. Integrative Genomics Viewer (IGV): High-Performance Genomics Data Visualization and Exploration. *Briefings Bioinf* (2013) 14(2):178–92. doi: 10.1093/bib/bbs017
17. Weissferdt A, Wistuba II, Moran CA. Molecular Aspects of Thymic Carcinoma. *Lung Cancer (Amsterdam Netherlands)* (2012) 78(2):127–32. doi: 10.1016/j.lungcan.2012.08.002
18. Robinson JT, Thorvaldsdóttir H, Winckler W, Guttman M, Lander ES, Getz G, et al. Integrative Genomics Viewer. *Nat Biotechnol* (2011) 29(1):24–6. doi: 10.1038/nbt.1754
19. Robinson JT, Thorvaldsdóttir H, Wenger AM, Zehir A, Mesirov JP. Variant Review With the Integrative Genomics Viewe. *Cancer Res* (2017) 77(21):e31–e4. doi: 10.1158/0008-5472.can-17-0337
20. Qiu P, Sheng J. A Two-Stage Procedure for Comparing Hazard Rate Functions. *J R Stat Soc* (2008) 70:191–208. doi: 10.1111/j.1467-9868.2007.00622.x
21. Suzuki E, Sasaki H, Kawano O, Endo K, Haneda H, Yukiue H, et al. Expression and Mutation Statuses of Epidermal Growth Factor Receptor in Thymic Epithelial Tumors. *Japan J Clin Oncol* (2006) 36(6):351–6. doi: 10.1093/jjco/hyl028
22. Oberndorfer F, Müllauer L. Genomic Alterations in Thymoma-Molecular Pathogenesis? *J Thoracic Dis* (2020) 12(12):7536–44. doi: 10.21037/jtd.2019.12.52

23. Enkner F, Pichlhöfer B, Zaharie AT, Krunic M, Holper TM, Janik S, et al. Molecular Profiling of Thymoma and Thymic Carcinoma: Genetic Differences and Potential Novel Therapeutic Targets. *Pathol Oncol Res* (2017) 23(3):551–64. doi: 10.1007/s12253-016-0144-8
24. Moreira AL, Won HH, McMillan R, Huang J, Riely GJ, Ladanyi M, et al. Massively Parallel Sequencing Identifies Recurrent Mutations in TP53 in Thymic Carcinoma Associated With Poor Prognosis. *J Thorac Oncol* (2015) 10(2):373–80. doi: 10.1097/jto.0000000000000397
25. Moreira AL, Won HH, McMillan R, Huang J, Riely GJ, Ladanyi M, et al. Massively Parallel Sequencing Identifies Recurrent Mutations in TP53 in Thymic Carcinoma Associated With Poor Prognosis. *J Thoracic Oncol: Off Publ Int Assoc Study Lung Cancer* (2015) 10(2):373–80. doi: 10.1097/JTO.0000000000000397
26. Chen K, Che J, Zhang X, Jin R, Xiang J, Han D, et al. Next-Generation Sequencing in Thymic Epithelial Tumors Uncovered Novel Genomic Aberration Sites and Strong Correlation Between TMB and MSH6 Single Nucleotide Variations. *Cancer Lett* (2020) 476:75–86. doi: 10.1016/j.canlet.2020.02.001
27. Thompson LDR, Gagan J, Washington A, Miller RT, Bishop JA. Biphenotypic Branchioma: A Better Name Than Ectopic Hamartomatous Thymoma for a Neoplasm With HRAS Mutation. *Head Neck Pathol* (2020) 14(4):884–8. doi: 10.1007/s12105-020-01132-4
28. Sakane T, Murase T, Okuda K, Saida K, Masaki A, Yamada T, et al. A Mutation Analysis of the EGFR Pathway Genes, RAS, EGFR, PIK3CA, AKT1 and BRAF, and TP53 Gene in Thymic Carcinoma and Thymoma Type A/B3. *Histopathology* (2019) 75(5):755–66. doi: 10.1111/his.13936
29. Enkner F, Pichlhöfer B, Zaharie AT, Krunic M, Holper TM, Janik S, et al. Molecular Profiling of Thymoma and Thymic Carcinoma: Genetic Differences and Potential Novel Therapeutic Target. *Pathol Oncol Res* (2017) 23(3):551–64. doi: 10.1007/s12253-016-0144-8
30. Saito M, Fujiwara Y, Asao T, Honda T, Shimada Y, Kanai Y, et al. The Genomic and Epigenomic Landscape in Thymic Carcinoma. *Carcinogenesis* (2017) 38(11):1084–91. doi: 10.1093/carcin/bgx094
31. Asao T, Fujiwara Y, Sunami K, Kitahara S, Goto Y, Kanda S, et al. Medical Treatment Involving Investigational Drugs and Genetic Profile of Thymic Carcinoma. *Lung Cancer (Amsterdam Netherlands)* (2016) 93:77–81. doi: 10.1016/j.lungcan.2016.01.004
32. Song Z, Yu X, Zhang Y. Rare Frequency of Gene Variation and Survival Analysis in Thymic Epithelial Tumors. *OncoTarg Ther* (2016) 9:6337–42. doi: 10.2147/OTT.S108749
33. Petrini I, Meltzer PS, Kim I-K, Lucchi M, Park K-S, Fontanini G, et al. A Specific Missense Mutation in GTF2I Occurs at High Frequency in Thymic Epithelial Tumors. *Nat Genet* (2014) 46(8):844–9. doi: 10.1038/ng.3016
34. Shitara M, Okuda K, Suzuki A, Tatematsu T, Hikosaka Y, Moriyama S, et al. Genetic Profiling of Thymic Carcinoma Using Targeted Next-Generation Sequencing. *Lung Cancer (Amsterdam Netherlands)* (2014) 86(2):174–9. doi: 10.1016/j.lungcan.2014.08.020
35. Girard N, Shen R, Guo T, Zakowski MF, Heguy A, Riely GJ, et al. Comprehensive Genomic Analysis Reveals Clinically Relevant Molecular Distinctions Between Thymic Carcinomas and Thymomas. *Clin Cancer Res: An Off J Am Assoc Cancer Res* (2009) 15(22):6790–9. doi: 10.1158/1078-0432.CCR-09-0644
36. Asselta R, Di Tommaso L, Perrino M, Destro A, Giordano L, Cardamone G, et al. Mutation Profile and Immunoscore Signature in Thymic Carcinomas: An Exploratory Study and Review of the Literature. *Thorac Cancer* (2021) 12 (9):1271–8. doi: 10.1111/1759-7714.13765
37. Massoth LR, Hung YP, Dias-Santagata D, Onozato M, Shah N, Severson E, et al. Pan-Cancer Landscape Analysis Reveals Recurrent KMT2A-MAML2 Gene Fusion in Aggressive Histologic Subtypes of Thymom. *JCO Precis Oncol* (2020) 4:PO.19.00288. doi: 10.1200/PO.19.00288
38. Sakane T, Sakamoto Y, Masaki A, Murase T, Okuda K, Nakanishi R, et al. Mutation Profile of Thymic Carcinoma and Thymic Neuroendocrine Tumor by Targeted Next-Generation Sequencin. *Clin Lung Cancer* (2021) 22(2):92–9. doi: 10.1016/j.cllc.2020.11.010. e4.
39. Wang Y, Thomas A, Lau C, Rajan A, Zhu Y, Killian JK, et al. Mutations of Epigenetic Regulatory Genes are Common in Thymic Carcinomas. *Sci Rep* (2014) 4:7336–. doi: 10.1038/srep07336
40. Muller PA, Vousden KH. P53 Mutations in Cancer. *Nat Cell Biol* (2013) 15 (1):2–8. doi: 10.1038/ncb2641
41. Petrini I, Meltzer PS, Kim IK, Lucchi M, Park KS, Fontanini G, et al. A Specific Missense Mutation in GTF2I Occurs at High Frequency in Thymic Epithelial Tumors. *Nat Genet* (2014) 46(8):844–9. doi: 10.1038/ng.3016
42. Radovich M, Pickering CR, Felau I, Ha G, Zhang H, Jo H, et al. The Integrated Genomic Landscape of Thymic Epithelial Tumors. *Cancer Cell* (2018) 33 (2):244–58. doi: 10.1016/j.ccell.2018.01.003. e10.
43. Feng Y, Lei Y, Wu X, Huang Y, Rao H, Zhang Y, et al. GTF2I Mutation Frequently Occurs in More Indolent Thymic Epithelial Tumors and Predicts Better Prognosis. *Lung Cancer* (2017) 110:48–52. doi: 10.1016/j.lungcan.2017.05.020


**Conflict of Interest:** The authors declare that the research was conducted in the absence of any commercial or financial relationships that could be construed as a potential conflict of interest.

frontiers in Oncology

ORIGINAL RESEARCH
published: 28 September 2021
doi: 10.3389/fonc.2021.693353

# Identification of Key Genes Related to CD8+ T-Cell Infiltration as Prognostic Biomarkers for Lung Adenocarcinoma

*Minjun Du, Yicheng Liang, Zixu Liu, Xingkai Li, Mei Liang, Boxuan Zhou and Yushun Gao* *

*Department of Thoracic Surgery, National Cancer Center/National Clinical Research Center for Cancer/Cancer Hospital, Chinese Academy of Medical Sciences and Peking Union Medical College, Beijing, China*

**Background:** CD8+ T cells are one of the central effector cells in the immune microenvironment. CD8+ T cells play a vital role in the development and progression of lung adenocarcinoma (LUAD). This study aimed to explore the key genes related to CD8+ T-cell infiltration in LUAD and to develop a novel prognosis model based on these genes.

**Methods:** With the use of the LUAD dataset from The Cancer Genome Atlas (TCGA), the differentially expressed genes (DEGs) were analyzed, and a co-expression network was constructed by weighted gene co-expression network analysis (WGCNA). Combined with the CIBERSORT algorithm, the gene module in WGCNA, which was the most significantly correlated with CD8+ T cells, was selected for the subsequent analyses. Key genes were then identified by co-expression network analysis, protein–protein interactions network analysis, and least absolute shrinkage and selection operator (Lasso)-penalized Cox regression analysis. A risk assessment model was built based on these key genes and then validated by the dataset from the Gene Expression Omnibus (GEO) database and multiple fluorescence *in situ* hybridization experiments of a tissue microarray.

**Results:** Five key genes (MZT2A, ALG3, ATIC, GPI, and GAPDH) related to prognosis and CD8+ T-cell infiltration were identified, and a risk assessment model was established based on them. We found that the risk score could well predict the prognosis of LUAD, and the risk score was negatively related to CD8+ T-cell infiltration and correlated with the advanced tumor stage. The results of the GEO database and tissue microarray were consistent with those of TCGA. Furthermore, the risk score was higher significantly in tumor tissues than in adjacent lung tissues and was correlated with the advanced tumor stage.

**Conclusions:** This study may provide a novel risk assessment model for prognosis prediction and a new perspective to explore the mechanism of tumor immune microenvironment related to CD8+ T-cell infiltration in LUAD.

**Keywords: lung adenocarcinoma, immune microenvironment, CD8+ T cell, bioinformatics analysis, multiplex immunohistochemistry**

OPEN ACCESS

***Edited by:***
*Giulia Pasello, Veneto Institute of Oncology (IRCCS), Italy*

***Reviewed by:***
*Azhar Ali, National University of Singapore, Singapore*
*Valerio Gristina, University of Palermo, Italy*

***Correspondence:**
*Yushun Gao*
*gaoyspumc@163.com*

***Specialty section:***
*This article was submitted to Thoracic Oncology, a section of the journal Frontiers in Oncology*

***Received:*** *10 April 2021*
***Accepted:*** *06 September 2021*
***Published:*** *28 September 2021*

***Citation:***
*Du M, Liang Y, Liu Z, Li X, Liang M, Zhou B and Gao Y (2021) Identification of Key Genes Related to CD8+ T-Cell Infiltration as Prognostic Biomarkers for Lung Adenocarcinoma. Front. Oncol. 11:693353. doi: 10.3389/fonc.2021.693353*

## INTRODUCTION

Lung adenocarcinoma (LUAD) is the most common type of lung cancer, accounting for 40% of all lung cancers (1–3). In recent years, the development of immunotherapy has changed the landscape of non-small cell lung cancer (NSCLC) therapy (4–6). Notably, the immunotherapy effects mainly rely on the immune responses, which are significantly influenced by the tumor microenvironment (7, 8). CD8+ T cells are central effector cells in the tumor microenvironment, and previous studies have reported that highly infiltrating CD8+ T cells are beneficial to prognosis in most tumors, including LUAD (9–14). However, the mechanism of CD8+ T-cell infiltration in the tumor microenvironment in LUAD is still unclear. Therefore, identifying novel biomarkers related to CD8+ T-cell infiltration may help explore the immune infiltration mechanism in LUAD.

With the rapid development of bioinformatics, new tools have arisen to identify novel biomarkers (15–21). For example, weighted gene co-expression network analysis (WGCNA) is an effective tool that mines related patterns between genes to identify relevant modules and hub genes in cancer (16), and it has been widely used to find biomarkers at the transcriptional level (17, 18). Another bioinformatics tool, namely, Cell Type Identification by Estimating Relative Subsets of RNA Transcripts (CIBERSORT), is used to quantify the cellular composition of immune cells using a deconvolution algorithm based on gene expression data (19). This algorithm has been successfully used to approximate the level of immune cell infiltration in various cancers, such as prostate cancer and renal cancer (20, 21).

Previously, many studies have focused on exploring the immune-genomic biomarkers, which may direct immunotherapy. For example, tumor mutational burden (TMB) may be a preferable choice for directing the first-line immuno-oncology agent management of advanced non-oncogene-addicted NSCLC patients (22, 23). However, fewer studies are focusing on exploring prognostic biomarkers from the aspect of immune cell infiltration, which could be used not only to estimate prognosis but also to direct immunotherapy. In this study, to identify the hub genes related to CD8+ T immune cell infiltration and potential biomarkers of LUAD, we first used WGCNA to obtain differentiated gene expression modules based on gene expression data in The Cancer Genome Atlas (TCGA) database. The CIBERSORT algorithm was used to calculate the T-cell compositions of the samples. Those important modules and hub genes related to CD8+ T-cell infiltration were identified by correlation analysis of the WGCNA and CIBERSORT algorithm results. Furthermore, the immune and clinical characteristics of the hub genes were verified, and a risk score model based on the hub genes was built, which were significantly related to the prognosis of LUAD after least absolute shrinkage and selection operator (Lasso) regression analysis and multivariable Cox analysis. The model's performance was evaluated using receiver operating characteristic (ROC) curves, calibration curve, and stratification analysis. Gene Expression Omnibus (GEO) datasets were then conducted for external validation. Furthermore, we performed multiple fluorescence *in situ* hybridization of 98 LUAD tissues and 82 adjacent tissues to further verify the results of bioinformatics analysis. This is the first time that the WGCNA and CIBERSORT algorithm were used to identify the relevant biomarkers of infiltration of CD8+ T cells in LUAD and to further build a LUAD prognosis prediction model.

## MATERIALS AND METHODS

### Data Collection

Expression and clinical data (478 cases of LUAD and 51 normal lung tissues) were downloaded from UCSC TCGA (https://gdc.xenahubs.net/download/TCGA-LUAD.htseq_counts.tsv.gz; https://gdc.xenahubs.net/download/TCGA-LUAD.GDC_phenotype.tsv.gz; https://gdc-hub.s3.us-east-1.amazonaws.com/download/TCGA-LUAD.survival.tsv). The Ensembl database (http://www.ensembl.org/info/data/ftp/index.html) was used for downloading human gtf files (Homo_sapiens.GRCh38.99.gtf.gz) and acquiring symbol data. The validation dataset (GSE72094) containing 393 cases of LUAD was downloaded from the GEO database through the R package "GEOquery."

### Analysis of the Differential Gene Expression

Differentially expressed gene (DEG) analysis was performed using the R package "edgeR" and visualized by volcano plot and heatmap. The heatmap and the volcano plot were done with the R packages "pheatmap" and "EnhancedVolcano," respectively. The threshold of DEGs was set at $|\log FC| > 1$ and false discovery rate $< 0.05$.

### Co-Expression Network Construction by Weighted Gene Co-Expression Network Analysis

With the use of the R package "WGCNA," a weight co-expression network was constructed based on the expression value of 8,807 DEGs (16). According to Pearson's correlation value between paired genes, a similarity matrix containing the expression levels of individual transcripts was built. Then, based on the equation, adjacency between the paired genes = $|\text{Pearson's correlation between the paired genes}|^{\beta}$, the similarity matrix was converted into an adjacency matrix. The parameter $\beta$ could amplify differences of correlation between genes. When $\beta = 4$, the adjacency matrix was converted into a topological overlap matrix. Finally, we used a bottom-up algorithm to classify genes with similar expression patterns into different modules.

### Construction of Module Feature Relationships

With the use of the R package "CIBERSORT," the proportions of 22 types of immune cells in the samples were deduced according to the expressions of genes. The expression of signature genes was extracted to form a signature gene expression matrix. Combined with the known immune cell signature, the immune cell proportions of samples were calculated using "CIBERSORT," and finally, the proportions of relevant subtypes of T cells were extracted. Furthermore, the correlations between genes of modules in WGCNA and the subtypes of T cells were calculated by

Pearson's test. The modules most significantly correlated with CD8+ T cells were selected for the subsequent analyses.

## Enrichment Analysis of Functions and Signaling Pathways

The enrichment of functions and signaling pathways of genes in the identified hub module was conducted using the R package "clusterProfiler," and the threshold was p-value <0.05 and q-value <0.2. After the enrichment pathways were determined, a bubble map was plotted.

## Identification of Hub Genes Associated With Infiltration of CD8+ T Cells and Prognosis

To further determine the central nodes in the modules related to immune cell infiltration, we imported the co-expression network of relevant modules of WGCNA into Cytoscape (https://cytoscape.org/) and then screened the genes with high nodes according to a different degree. Furthermore, approximately one-third of the total genes in the modules were selected as hub genes according to the threshold of degree = 260. Meanwhile, all genes in the hub module were imported into the STRING database (https://string-db.org/), and then a protein–protein interaction (PPI) network was constructed. The network was imported into Cytoscape to search central nodes, and approximately one-third of the total genes were selected as hub genes when the degree = 5. Finally, a Venn plot integrated the WGCNA and STRING database results to identify the hub genes. After acquiring the hub genes, we used univariate Cox regression analyses to preliminarily screen the hub genes associated with the prognosis, and the genes with statistical significance ($p < 0.05$) underwent Lasso-penalized Cox regression analysis for further dimension reduction. Genes with statistical significance ($p < 0.05$) in Lasso-penalized Cox regression analysis were considered key hub genes associated with CD8+ T-cell infiltration and selected for the subsequent analyses.

## Construction and Validation of a Prognostic Risk Model

Based on key hub genes associated with CD8+ T-cell infiltration, a prognostic risk model was constructed. The risk score was calculated as follows: risk score = ($\beta_A \times$ gene A expression) + ($\beta_B \times$gene B expression) ··· + ($\beta_N \times$ gene N expression). To evaluate the model's performance, the "survival" package was used to draw a calibration curve, and the "survivalROC" package was used to draw ROC curves. An area under the ROC curve (AUC) >0.6 was considered as a good performance of the model. Patients were divided into high-risk or low-risk groups according to the median value of the risk score, and the Kaplan–Meier method with log-rank test was used to test the prognostic significance of the risk score. $p < 0.05$ was considered statistically significant.

The prognostic model was then validated by the GSE72094 dataset from the GEO database. The risk scores of samples were calculated as the formula shown above. The ROC curve and the calibration curve were drawn to evaluate the performance, as well as the Kaplan–Meier method and the log-rank test were used to compare the prognostic significance between the high-risk group and the low-risk group. Because EGFR mutation status is critical in LUAD, we estimated the prognostic model in wild-type and mutation-type EGFR samples in the construction and validation cohorts.

## Correlation Between Key Hub Genes and Subtypes of Immune Cells

The correlations of key hub genes and immune cell subtypes were calculated online using the TIMER database (http://timer.cistrome.org/). Then, together with the correlation data, a heatmap was plotted to show the correlations, and scatter diagrams were shown for different key hub genes.

## External Validations of Protein Expression by Multicolor Immunofluorescence

The lung cancer tissue array with 82 pairs of matched cancerous and adjacent tissues, as well as an additional 16 cases of cancer tissues (HLugA180Su07), was obtained from Shanghai Outdo Biotech. To assess the expressions of key hub genes, multicolor immunofluorescence (mIHC) was performed using an Opal 7-color fluorescent IHC kit (PerkinElmer) combined with automated quantitative analysis (AQUA; Genoptix). First, the concentrations and order of the five antibodies were optimized, and a spectral library was built based on single-stained slides. The slides were first deparaffinized with xylene and ethanol, and antigen retrieval was done using a microwave. After incubation with freshly made 3% $H_2O_2$ for 10 min, the tissues were blocked in a blocking buffer for another 10 min at room temperature. Then the tissues were incubated with the primary antibodies, followed by secondary horseradish peroxidase (HRP) antibodies (Cell Signaling Technology) and an opal working solution (Akoya Biosciences). Primary antibodies recognizing the following antigens were used: MZT2A (1:20; Abcam), ALG3 (1:25; Abcam), GAPDH (1:1,500; Abcam), GPI (1:3,000; Abcam), and ATIC (1:200; Abcam). The slides were then mounted with ProLong Gold Antifade Reagent with DAPI and scanned using a confocal microscope (LEICA, Japan). Fluorescence images were acquired using a Vectra 2 intelligent slide analysis system using Vectra 2.0.8 (PerkinElmer). The mean fluorescence intensities (MFIs) of MZT2A, ALG3, GAPDH, GPI, and ATIC were measured.

## Immunohistochemistry of CD8+ T Cell

The distribution of CD8+ T cells in the lung cancer tissue array (HLugA180Su07) was evaluated by immunohistochemistry staining. The tissue array was incubated in a dry oven at 63°C for approximately 1 h, deparaffinized in xylene, and then rehydrated with graded ethanol solutions. After antigen retrieval, the array was incubated with a primary antibody against CD8 (DAKO, IR623) overnight at 4°C in a humidified chamber, followed by incubation at room temperature for 30 min with the secondary antibody (Envision+/HRP, Rabbit, DAKO). Subsequently, the tissue array was incubated with a 3,3′-diaminobenzidine (DAB) solution for 5 min. Finally, the tissue array was counterstained with hematoxylin. The immunostained slide was evaluated by two experienced pathologists blinded to clinicopathological characteristics, and the percentage of CD8 positive cells was annotated.

## Subgroup Analysis to Evaluate the Performance of the Model

To test the performance of the model, the risk score in different subgroups of age, sex, T stage, N stage, etc., was evaluated in TCGA dataset, GEO dataset, and the external validation dataset. Moreover, the Kaplan–Meier method and log-rank test were used to evaluate the performance of prognosis prediction in different subgroups. Differences in risk scores between different clinical characteristics were analyzed by GraphPad Prism 7.0. A Student's t-test was used for comparison between two groups. ANOVA was used for comparison between three or more groups. $p < 0.05$ was considered statistically significant.

# RESULTS

## The Clinical Characteristics of The Cancer Genome Atlas Cohort

After exclusion of those cases with deficient clinical information, 529 cases were included in this study. Of these, 478 were cancer tissues and 51 were normal tissues. The clinical characteristics are shown in **Supplementary Table 1**. The flowchart of this study is shown in **Figure 1**.

## Identification of Differentially Expressed Genes and Construction of Gene Co-Expression Network

After comparing the expressions of LUAD tissues with those of normal tissues in TCGA-LUAD cohort, we identified 8,807 DEGs, including 2,172 upregulated genes and 6,635 downregulated genes (**Figures 2A, B**). The gene co-expression network was then constructed using the 8,807 DEGs. $\beta = 4$ (scale-free $R_2 > 0.85$) was set as the soft-threshold power to build a scale-free network (**Figure 2D**). Furthermore, we used the dynamic hybrid cutting method to construct a hierarchical clustering tree. Each leaf on the tree represented an individual gene, and genes with similar expression data were gathered to form a tree branch representing a gene module. Eleven modules were generated (**Figures 2C, E**).

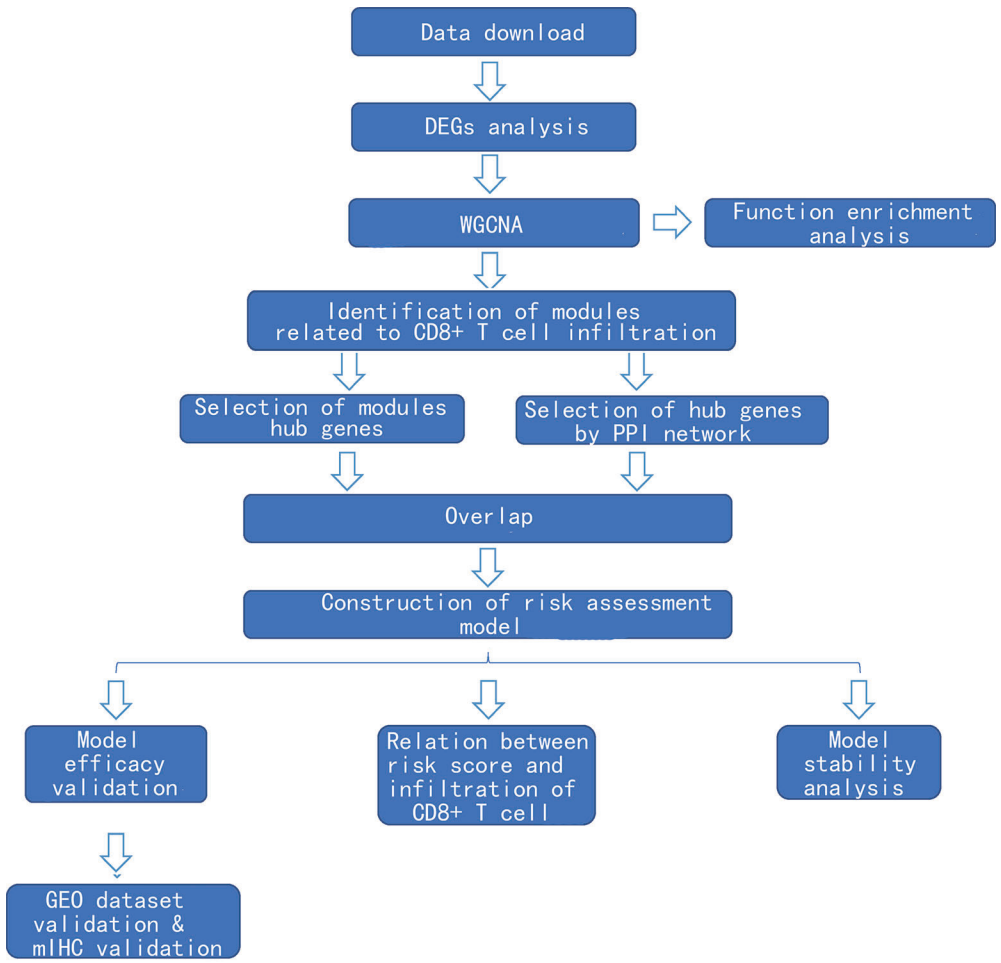


**FIGURE 1** | Flowchart of the study.

## Identification of Key Module Related to CD8+ T-Cell Infiltration

The proportion of immune cells in each sample was calculated based on gene expression by CIBERSORT. Seven T-cell subtypes were included: CD8+ T cells, CD4 naive T cells, CD4 memory resting T cells, CD4 memory activated T cells, follicular helper T cells, regulatory T cells (Tregs), and gamma delta T cells. Significantly, no CD4 naive T cells and gamma delta T cells were found. The proportion of each T cell subtype was extracted as the phenotype data, and its associations with the WGCNA modules were analyzed. The highest correlations were found between genes in the pink modules (275 genes) and CD8+ T cells ($R^2 = 0.22$, $p < 0.01$). Hence, the genes in the pink modules were used in the subsequent analyses (**Figure 3**).

## Function Enrichment Analysis

In the pink module, 275 genes were analyzed by Gene Ontology (GO) and Kyoto Encyclopedia of Genes and Genomes (KEGG) function enrichment analyses. GO analysis showed that the main enriched pathways were RNA metabolic processes, glucose metabolic processes, mitochondrial matrix, mitochondrial inner membrane, heterogeneous enzymatic activity, and tRNA catalytic activity (**Figures 4A–C**). The main pathways found enriched by KEGG were sugar metabolism and arginine/proline metabolism, and the enriched functions were mainly related to cell respiration (**Figure 4D**).

## Identification and Validation of Hub Genes Related to CD8+ T-Cell Infiltration

The genes in the pink module were imported into Cytoscape to build a co-expression network (**Figure 5A**), and a total of 93 hub genes were obtained at degree >260 (**Figure 5B**). One hundred forty-eight interactions with the proteins encoded by the genes of the pink module were identified by the PPI network, and then 46 hub proteins were selected at the degree >5 (**Figure 5C**). By overlapping the genes in Cytoscape and the PPI network, we acquired 117 hub genes related to CD8+ T-cell infiltration (**Figure 5D**). Of them, VARS (originating from the PPI network) does not belong to the pink module or DEGs and thus was excluded from the subsequent analysis. Finally, 116 hub genes associated with CD8+ T-cell infiltration were obtained.

## Identification of Prognosis-Related Key Genes and Construction of a Risk Assessment Model

To identify prognosis-related genes from the hub genes, 116 genes were subjected to univariable Cox regression analysis. In total, 34 genes were found significantly associated with the prognosis (**Figure 6A**). We then used Lasso-penalized Cox regression analysis and identified five genes independently correlated with prognosis (**Figure 6B**). Based on the expressions and correlation coefficients of these five genes, a risk assessment model was established, where Risk Score = MZT2A * 0.035 + ALG3 * 0.084 + ATIC * 0.104 + GPI * 0.125 + GAPDH * 0.134 (**Figure 6C**).

## Validation of Risk Assessment Model

Patients were divided into high-risk and low-risk groups, with the median score at 6.53. The patients with the high-risk group showed a poorer 5-year overall survival (OS) compared with the patients in the low-risk group (low-risk *vs.* high-risk = 44.6% *vs.* 31.0%, $p < 0.01$) (**Figure 7A**). The ROC curves showed that the AUC of OS at 5-year was 0.643, which suggests that the prediction of the risk model has a good performance (**Figure 7B**). The calibration curve of the model suggested that the predicted 5-year OS closely correlated with the actual 5-year OS (**Figure 7C**). The subgroup analysis of the risk model suggested that the model had a good prediction performance in patients with wild-type EGFR status or mutation-type EGFR status (**Figures 7D–I**).

The GSE72094 dataset was used to validate the risk model (**Supplementary Table 2**). After scoring, the cases were divided into high-risk and low-risk groups, with the median score at 5.34. The result of the Kaplan–Meier curve was similar to that of TCGA cohort (**Figure 8A**). Furthermore, the calibration curve, ROC curve, and the AUC (0.62) implied that this risk model had good prediction performance in the external dataset (**Figures 8B, C**). We also assessed the model in the patients with wild-type or mutation-type EGFR status. The results showed that the prognosis of the low-risk group did not have a significant difference from that of the high-risk group in the mutation-type cohort, which may be caused by the small sample size. However, the performance of the model in the wild-type cohort was good (**Figures 8D–I**).

Since our bioinformatics analysis was based on RNA sequences, we performed a multicolor immunofluorescence (mIHC) experiment on 98 LUAD tissues and 82 adjacent tissues from the protein perspective to validate the model. The follow-up time of the cohort was 1–94 months, and the median follow-up time was 39 months (interquartile range: 15–57). The median survival time was 50 months. The baseline characteristics of the cohort are shown in **Supplementary Table 3**. The expressions of five proteins were primarily located in the cytoplasm (**Figure 9**). We calculated the risk score based on fluorescence intensities and then divided the cohort into the low-risk group and high-risk group according to the median risk score. The results showed that the prognosis of the high-risk group was significantly poorer than that of the low-risk group (**Figure 10A**). The ROC curve, the calibration curve, and the AUC = 0.655 showed good performance (**Figures 10B, C**). In the subgroup analysis of EGFR status, the wild-type EGFR cohort showed similar results with the overall cohort. However, the mutation-type EGFR cohort results did not show significant differences between the prognosis of the high-risk group and the low-risk group. In addition, the performance of the risk model was poor, which may be caused by the small sample size (**Figures 10D–I**). We found that the risk score was significantly higher in the advanced T stage, N stage, and TNM stage. Furthermore, we found that the risk score was significantly negatively correlated to the infiltration of CD8+ T cells, which validated our bioinformatics analysis (**Figure 11A**). The distribution of CD8+ T cells is shown in **Figures 11B–E**.

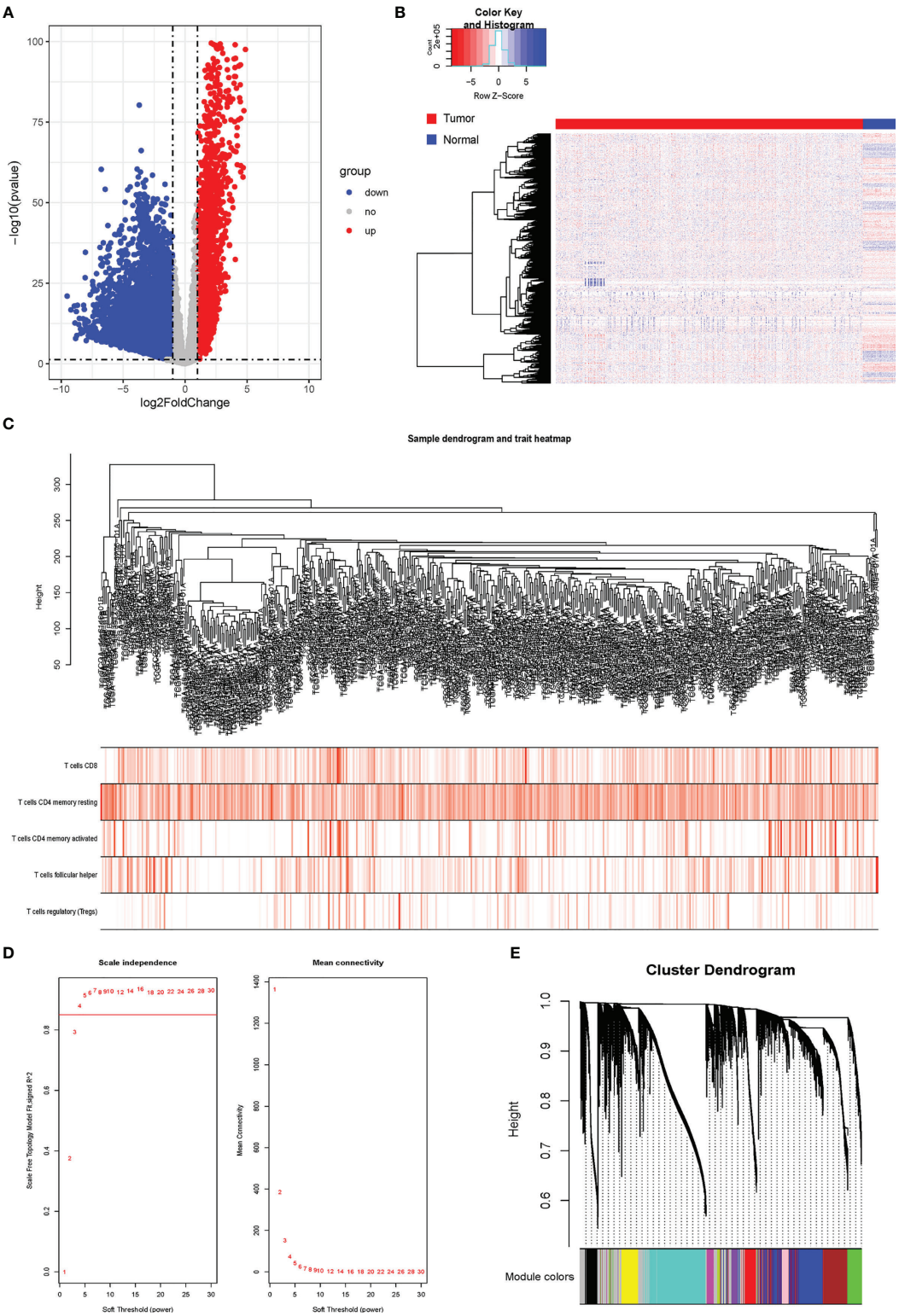


**FIGURE 2** | Analysis of DRGs and WGCNA. **(A)** Volcano plot of differential genes. **(B)** Heatmap of DEGs. **(C)** Sample clustering of WGCNA. **(D)** Screening with soft threshold. **(E)** Clustering of DEGs. DRG, differentially regulated gene; WGCNA, weighted gene co-expression network analysis; DEG, differentially expressed gene.

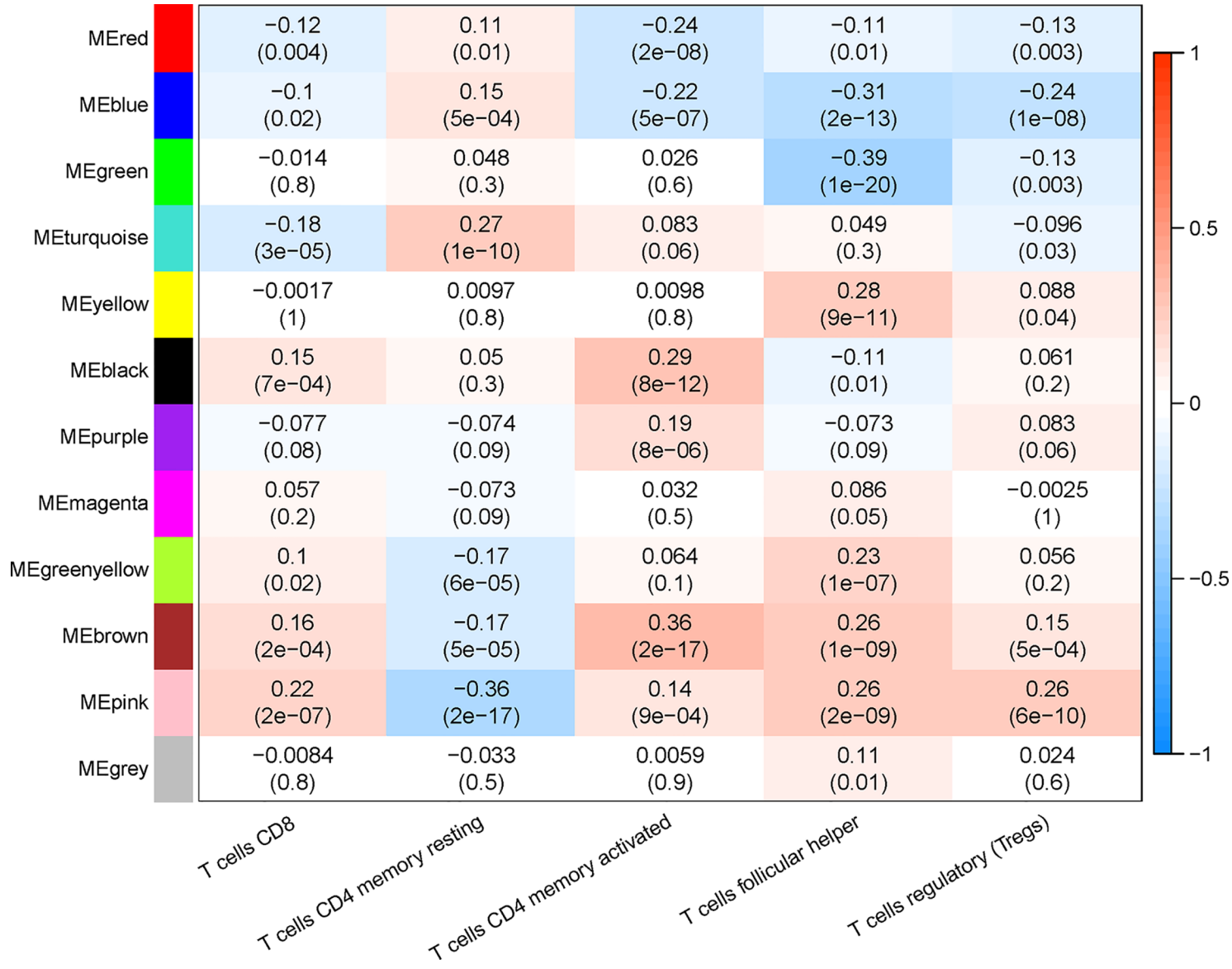


**FIGURE 3** | Correlation between infiltration of subtypes of T cells and different gene modules.

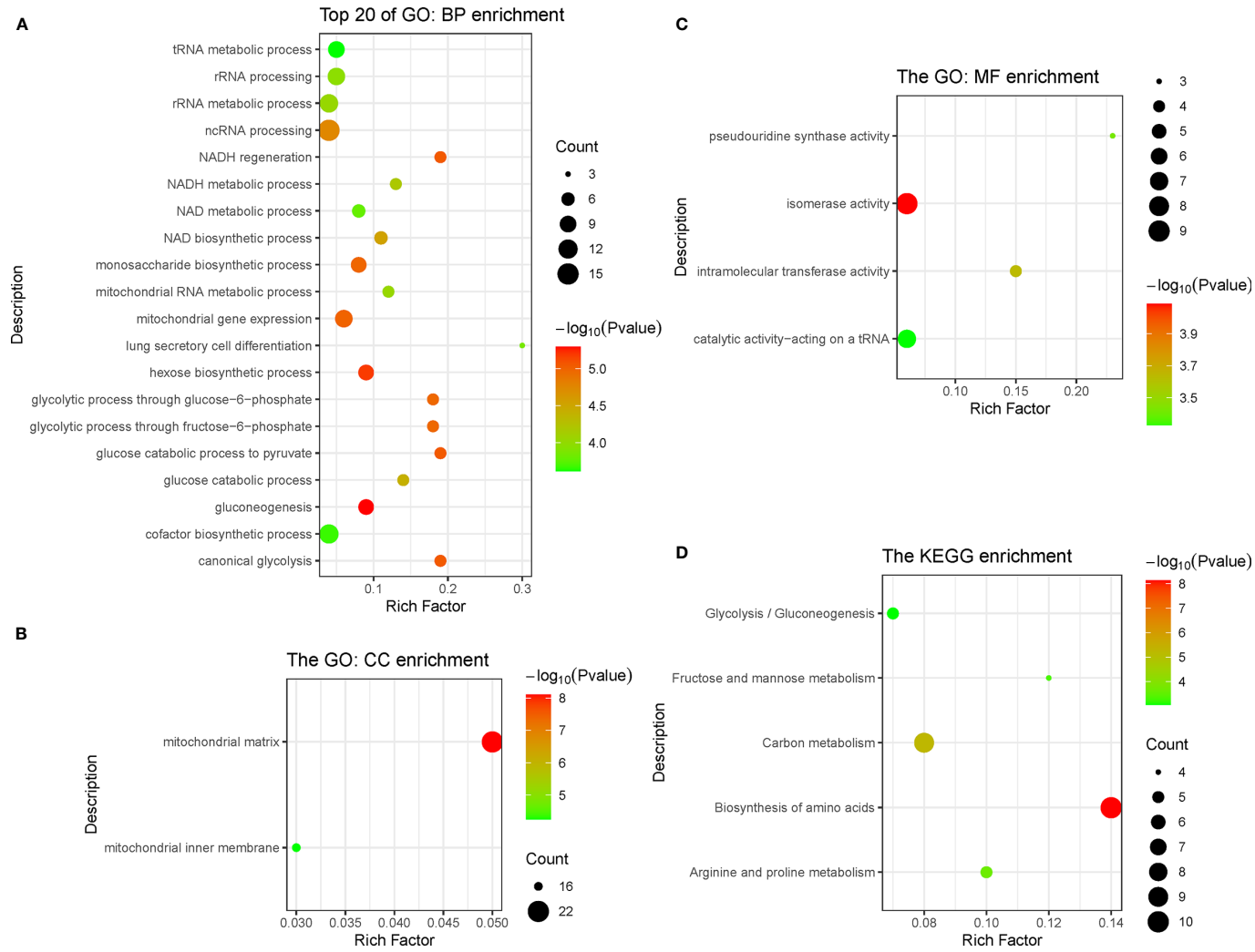


**FIGURE 4** | Function enrichment analysis of genes in pink module, including three types of GO enrichment analysis **(A–C)** and KEGG enrichment analysis **(D)**. GO, Gene Ontology; KEGG, Kyoto Encyclopedia of Genes and Genomes.

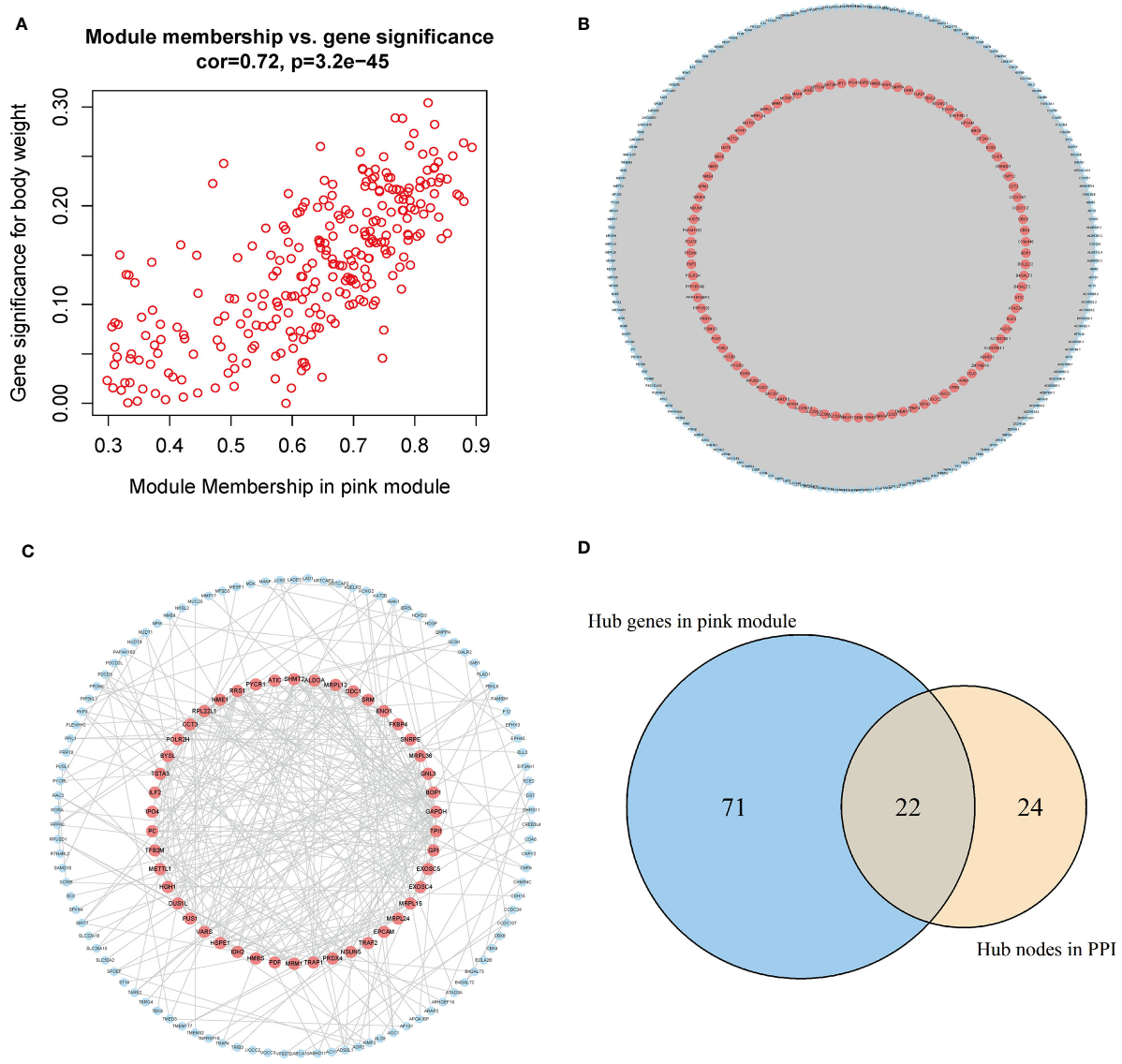


**FIGURE 5** | Acquisition of hub genes related to immune cell infiltration. **(A)** Correlation scatter diagram between pink genes and phenotypes of immune cell infiltration. **(B)** Pink gene co-expression network (red: the screened hub genes). **(C)** PPI network (red: the screened hub proteins). **(D)** Venn map from the two types of screening. PPI, protein–protein interaction.

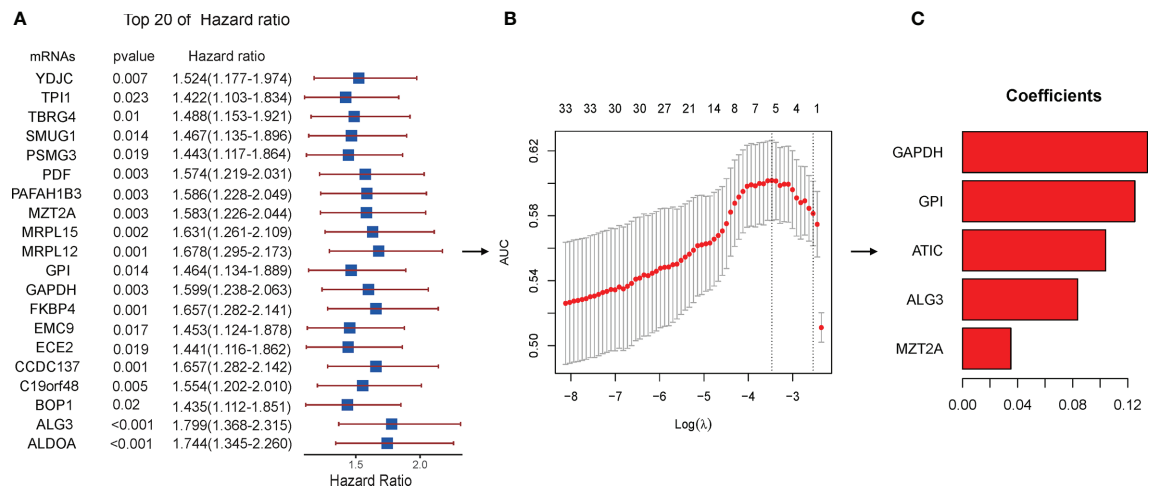


**FIGURE 6** | Lasso regression with the Cox single-factor regression results. **(A)** Top 20 genes of HR obtained from batched Cox single-factor regression. **(B)** Results of lambda screening. **(C)** Statistics of regression coefficients with the significantly related genes obtained from Lasso regression. Lasso, least absolute shrinkage and selection operator.

## Correlation Analysis Between Genes in the TIMER Database and Subtypes of Immune Cells

The relationship between the key genes and CD8+ T cells was calculated online based on the TIMER database. Except for the lack of information on MZT2A, the remaining four genes were negatively correlated with CD8+ T cells significantly, according to both the XCELL algorithm and EPIC algorithm. Especially, the correlation coefficient of GAPDH with CD8+ T cells is −0.23 according to the XCELL algorithm ($p < 0.01$) and is −0.33

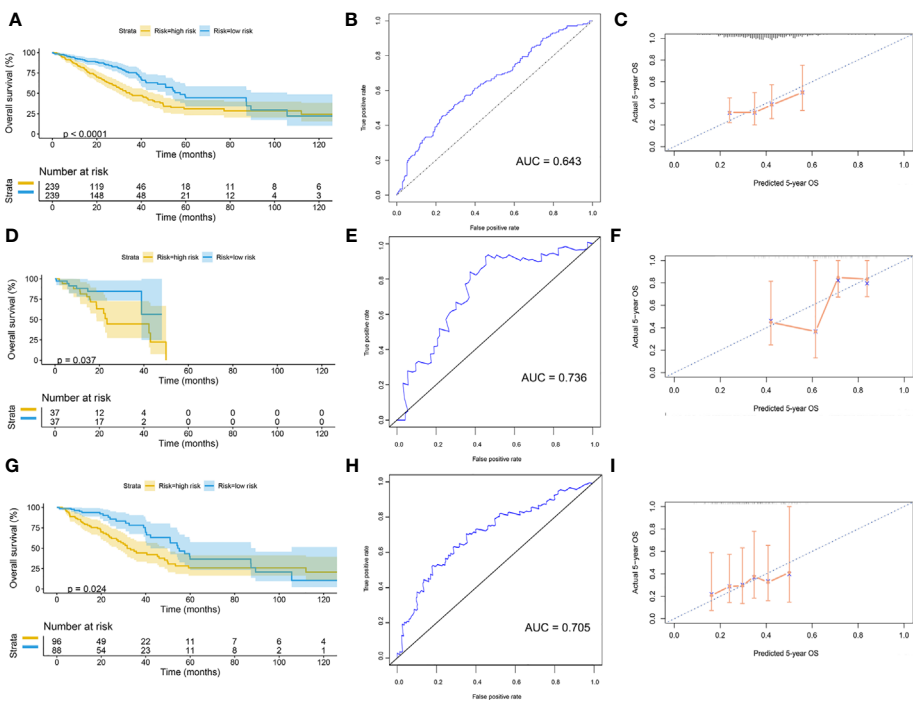


**FIGURE 7** | Validation of model by TCGA cohort. **(A)** Kaplan–Meier curve of overall cohort. **(B)** ROC curve of overall cohort. **(C)** Calibration curve of overall cohort. **(D)** Kaplan–Meier curve of mutation-type cohort. **(E)** ROC curve of mutation-type cohort. **(F)** Calibration curve of mutation-type cohort. **(G)** Kaplan–Meier curve of wild-type cohort. **(H)** ROC curve of wild-type cohort. **(I)** Calibration curve of wild-type cohort. TCGA, The Cancer Genome Atlas; ROC, receiver operating characteristic.

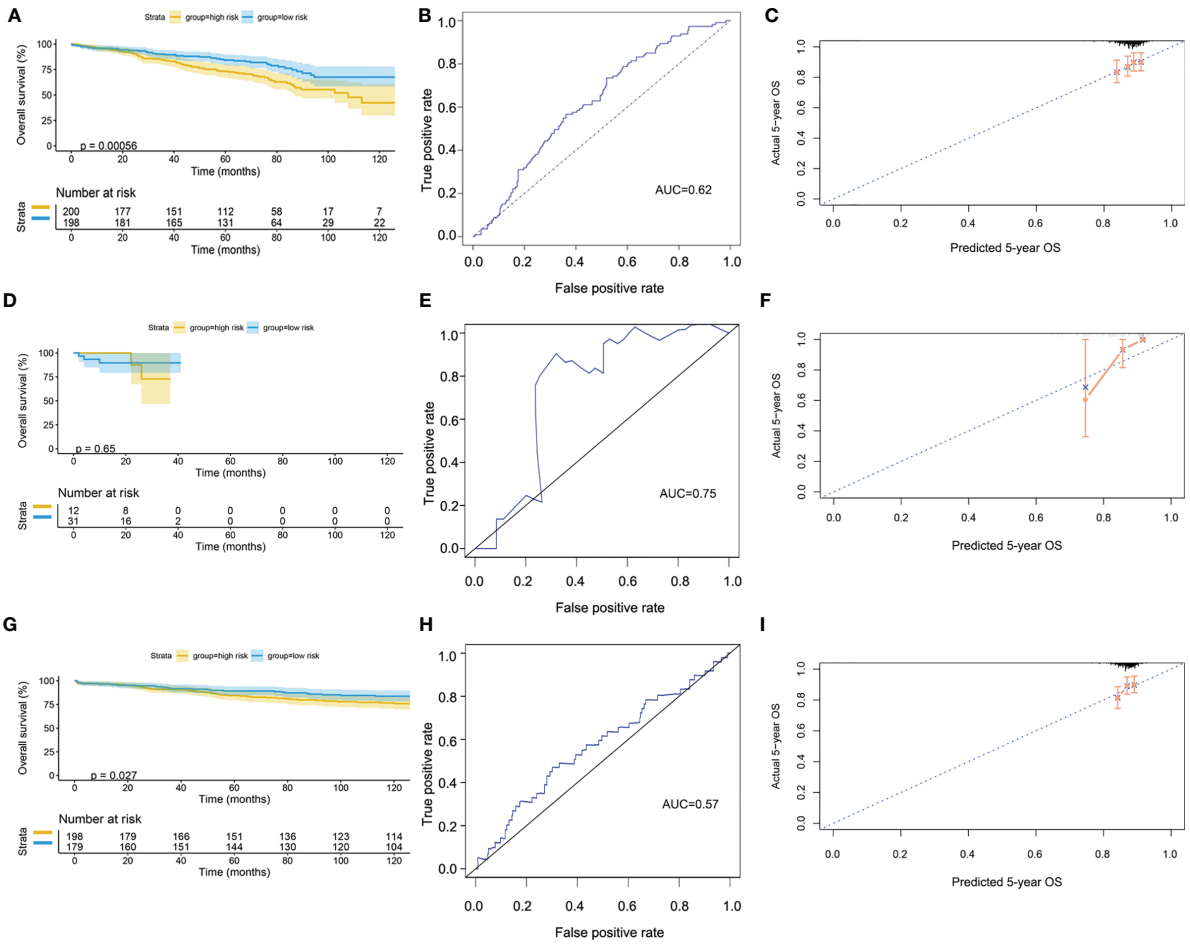


**FIGURE 8** | Validation of model by GEO cohort. **(A)** Kaplan–Meier curve of overall cohort. **(B)** ROC curve of overall cohort. **(C)** Calibration curve of overall cohort. **(D)** Kaplan–Meier curve of mutation-type cohort. **(E)** ROC curve of mutation-type cohort. **(F)** Calibration curve of mutation-type cohort. **(G)** Kaplan–Meier curve of wild-type cohort. **(H)** ROC curve of wild-type cohort. **(I)** Calibration curve of wild-type cohort. GEO, Gene Expression Omnibus; ROC, receiver operating characteristic.

according to the EPIC algorithm ($p < 0.01$). These results implied that the expression of those genes might be negatively correlated with the infiltration of CD8+ T cells. The heatmap of key genes is shown in **Figure 12**.

## Subgroup Analysis

The Kaplan–Meier curves were plotted in subgroups of data from TCGA database, including age, gender, T stage, N stage, M stage, and TNM stage. Although the prognosis of the high-risk group and the low-risk group was not significantly different in the age <60 group or the N0 group, the high-risk group had a poor prognosis in other subgroups (**Figure 13**). Similarly, the model underwent subgroup analysis with the GEO and mIHC cohorts, and the same results were found (**Figures 14**, **15**).

The differences of risk scores among age, gender, M stage, N stage, T stage, and TNM stage were tested in TCGA cohort. The results showed that the risk scores were higher in men, M1 stage, N2 or N3 stage, T3 or T4 stage, and TNM stage III or IV (**Supplementary Figure 1**). Similarly, differences in risk scores were detected in the GEO cohort and the mIHC cohort. The results showed that the advanced TNM stage had a higher score. Furthermore, the distribution of the risk scores between different EGFR statuses was tested in the GEO cohort, and the results showed that the risk scores were significantly higher in the wild type. However, in the mIHC cohort, we found that the risk score distribution in EGFR status was not significantly different. Hence, whether these five genes are related to EGFR status needs further exploration (**Supplementary Figures 2**, **3**).

# DISCUSSION

LUAD is the most common type of lung cancer (24). Nowadays, surgery combined with chemotherapy, targeted therapy, or immunotherapy is the primary treatment strategy for most LUAD patients (25–29). For non-oncogene advanced LUAD, chemo-immunotherapy is an essential treatment strategy. In recent years, several reports found that the immune microenvironment plays a

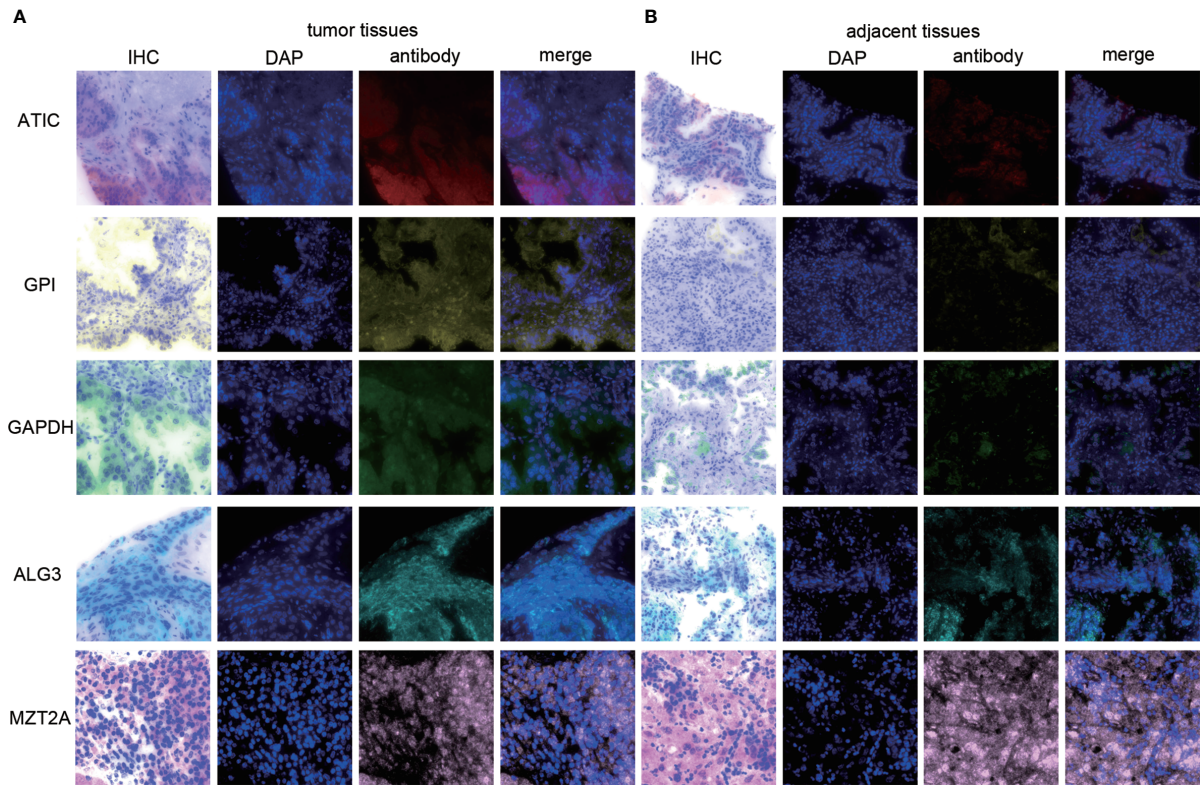


**FIGURE 9** | The expression of ATIC, GPI, GAPDH, ALG3, and MZT2A. **(A)** The expression of five proteins in tumor tissues. **(B)** The expression of five proteins in adjacent tissues.

critical role in it. CD8+ T cells are the central effector cells of anti-tumor immunity (30–33). Identification of the key genes related to the infiltration of CD8+ T cells may offer new insights for research on the mechanism of tumor immunotherapy.

This work analyzed the expressions of 529 LUAD-related samples (478 cancer tissues and 51 paracancerous tissues) from TCGA database. As a result, 8,807 DEGs were identified, including 2,172 upregulated genes and 6,635 downregulated genes. We constructed a co-expression network by WGCNA and then identified the gene module most significantly correlated with CD8+ T cells combining with the CIBERSORT algorithm based on the DEGs. Subsequently, we identified five key genes (MZT2A, ALG3, ATIC, GPI, and GAPDH) related to prognosis and CD8+ T-cell infiltration through a co-expression network PPI network analysis and Lasso-penalized Cox regression analysis.

MZT2A (Mitotic Spindle Organizing Protein 2A) is a protein–encoding gene, but very little research is available on this gene. Recently, Wang et al. reported that MZT2A mRNA and protein levels were overexpressed in NSCLC and associated with poor NSCLC prognosis. Upregulation of MZT2A could promote NSCLC cell viability and invasion by overexpressing LGALS3BP *via* the MTZ2A MOZART2 domain and Akt phosphorylation (34). However, mechanisms on how MZT2A influences tumor prognosis and CD8+ T-cell infiltration should be further explored.

ALG3 (α-1,3-mannose glycosyl transferase) belongs to the ALG family and is located on the chromosomal region 3q27.1. ALG3 upregulation is related to lymph node metastasis of esophageal squamous cell carcinoma (35) and the proliferation of cervical cancer cells (36). ALG3 expression is higher in NSCLC tissues than in normal tissues and is associated with a higher T stage, lymph node metastasis, tissue differentiation, and prognosis (37). Similar to MZT2A, there are no reports on the relationship between ALG3 and CD8+ T-cell infiltration, which we will further explore.

ATIC (5-aminoimidazole-4-carboxamide ribonucleotide formyltransferase/IMP cyclohydrolase) encodes a bifunctional protein and catalyzes the last two steps in *de novo* synthesis of purines. ATIC is overexpressed in hepatic cell carcinoma and is associated with a poor prognosis in patients (38). The fused protein between ATIC and anaplasia lymphoma kinase (ALK, a common oncogene) was discovered in lymphoma patients (39, 40). Interestingly, frame-shift mutations and missense mutations of ATIC were found in a case of radiation sensitivity, and biochemical research showed that purine biosynthesis involving ATIC might help with DNA damage repair (41). Hence, these results imply that ATIC may be

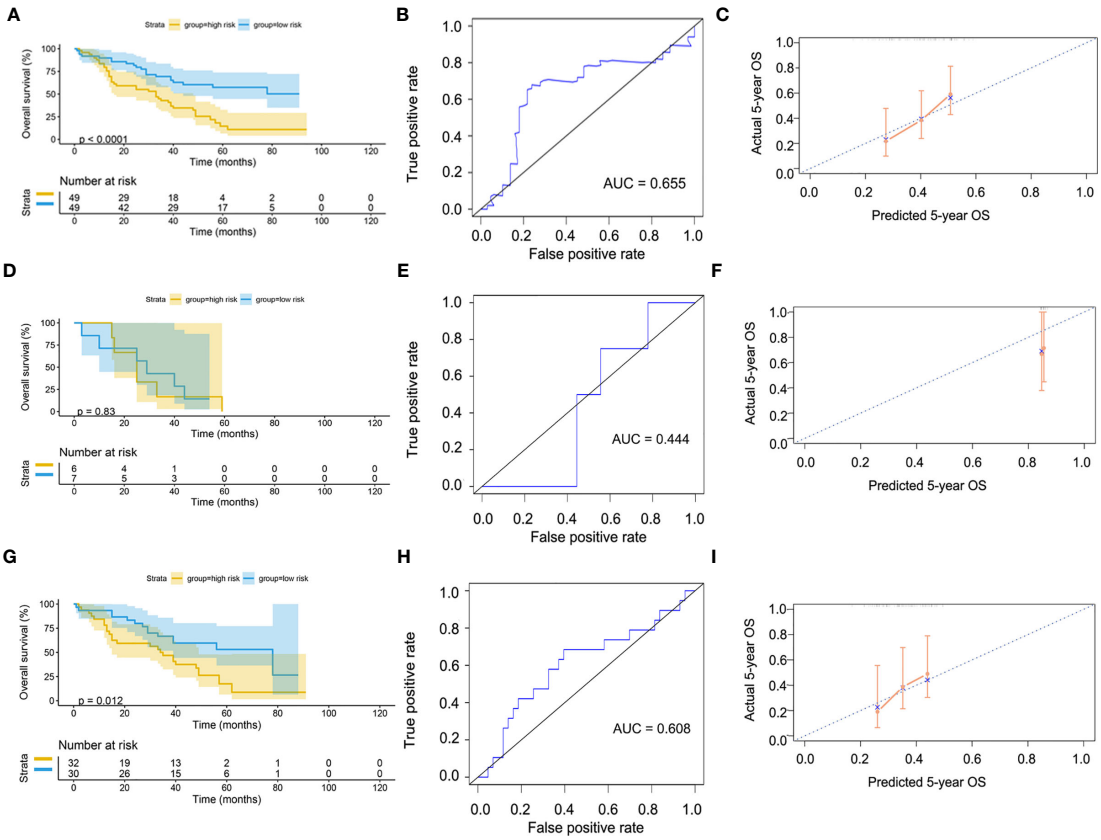


**FIGURE 10** | Validation of model by mIHC cohort. **(A)** Kaplan–Meier curve of overall cohort. **(B)** ROC curve of overall cohort. **(C)** Calibration curve of overall cohort. **(D)** Kaplan–Meier curve of mutation-type cohort. **(E)** ROC curve of mutation-type cohort. **(F)** Calibration curve of mutation-type cohort. **(G)** Kaplan–Meier curve of wild-type cohort. **(H)** ROC curve of wild-type cohort. **(I)** Calibration curve of wild-type cohort. ROC, receiver operating characteristic.

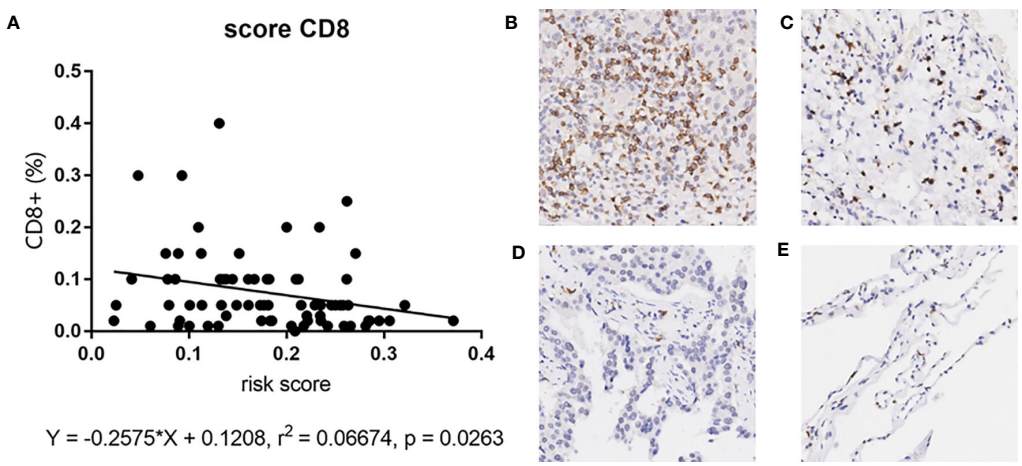


**FIGURE 11** | **(A)** The correlation between risk score and CD8+ T cell in mIHC cohort. **(B–E)** The distribution of CD8+ T cell in tumor tissues and adjacent tissues. High positive rate in tumor tissues **(A)** and adjacent tissues **(B)**. Low positive rate in tumor tissues **(C)** and adjacent tissues **(D)**.

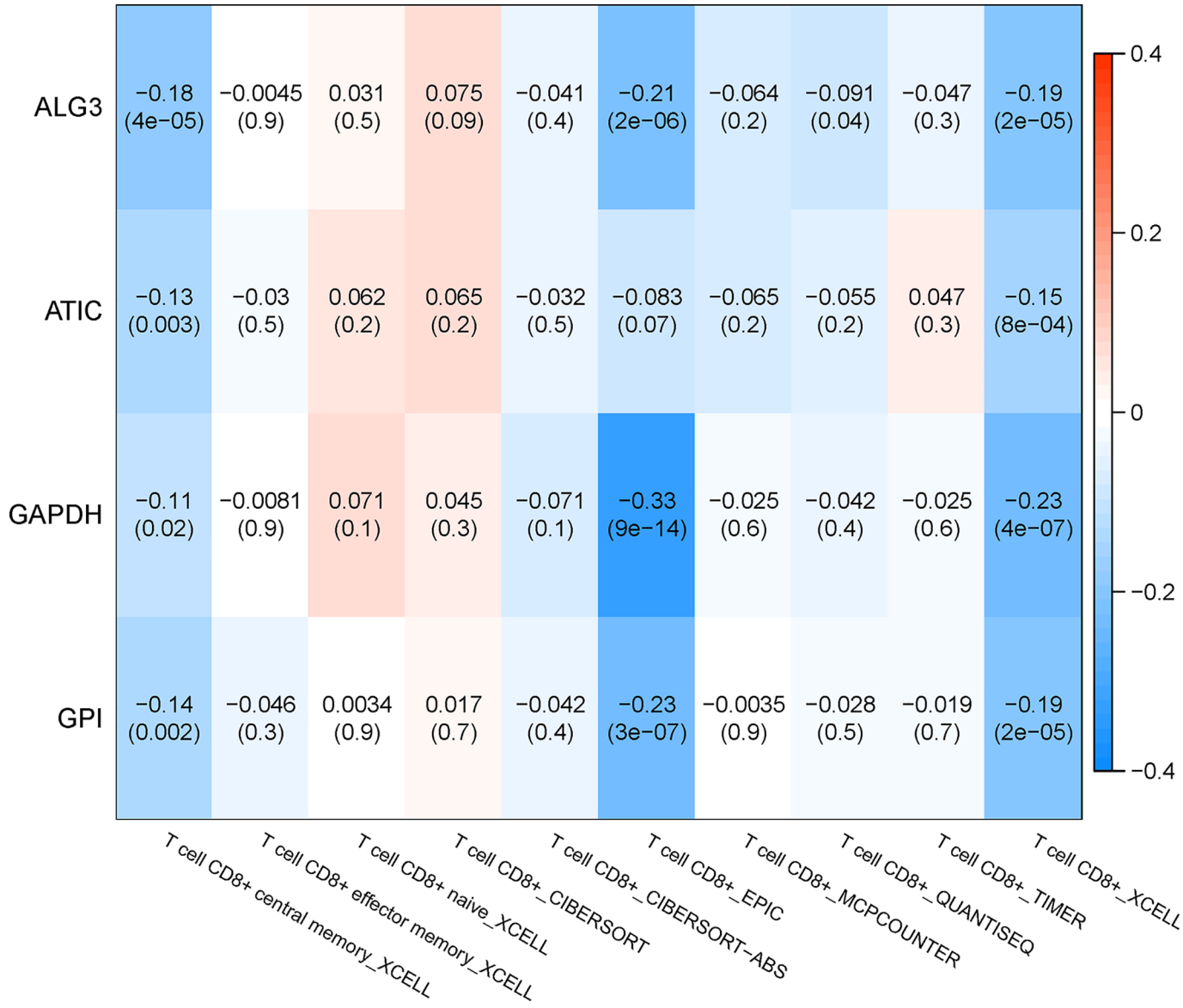


**FIGURE 12** | Correlation analysis between genes in the TIMER database and subtypes of immune cells.

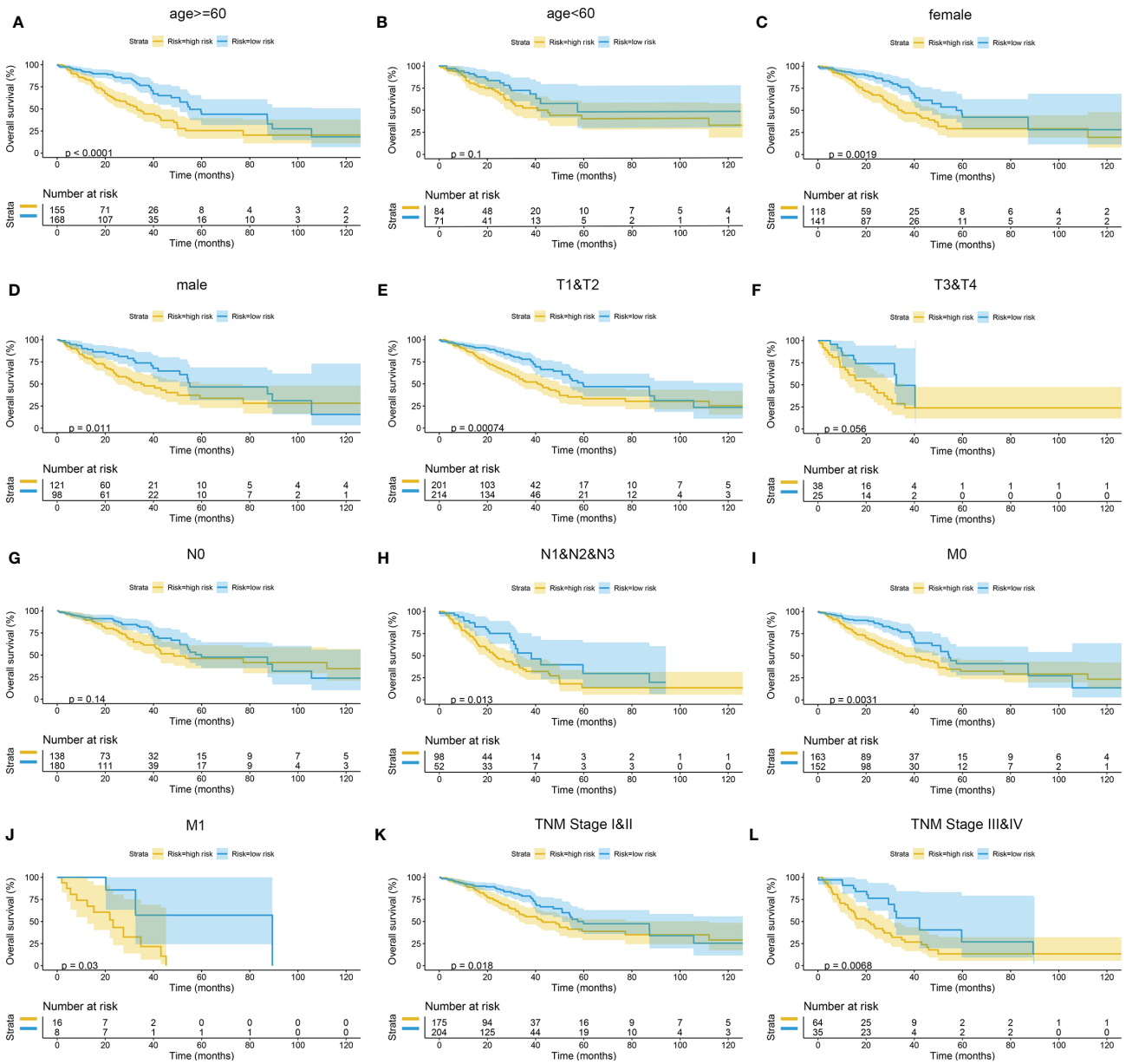


**FIGURE 13** | Subgroup survival analysis of TCGA cohort. **(A)** Age ≥ 60. **(B)** Age < 60. **(C)** Female. **(D)** Male. **(E)** Stages T1 and T2. **(F)** Stages T3 and T4. **(G)** Stage N0. **(H)** Stages N1, N2, and N3. **(I)** Stage M0. **(J)** Stage M1. **(K)** TNM stages I and II. **(L)** TNM stages III and IV. TCGA, The Cancer Genome Atlas.

involved in tumorigenesis and may influence the survival of cancer cells. Additional research would be needed to explore the mechanism of ATIC and its relationship with CD8+ T-cell infiltration.

GPI (glucose-6-phosphate isomerase) is an enzyme that participates in the glycolysis pathway. GPI is a cytoplast dimer that can catalyze the conversion from glucose-6-phosphate to fructose-6-phosphate. GPI is a protein similar to the autocrine movement factors involved in the migration and invasion of tumor cells and angiogenesis (42). In various cancers, the expression of GPI is induced by c-Myc, and HIF-1 is overexpressed at the same time (43, 44). HIF-1 can induce GBE1 upregulation, which would decrease CCL5 and CXCL10 secretion, hindering the recruitment of CD8+ T lymphocytes (45, 46). GPI can also induce the protein expression of matrix metalloproteinase-3 and thereby promote the invasiveness of tumors (47). GPI, which is overexpressed in renal cancer, plays a role in tumor progression and is negatively correlated with the clinical prognosis of patients (48). However, the role of GPI in lung cancer has not been investigated to date.

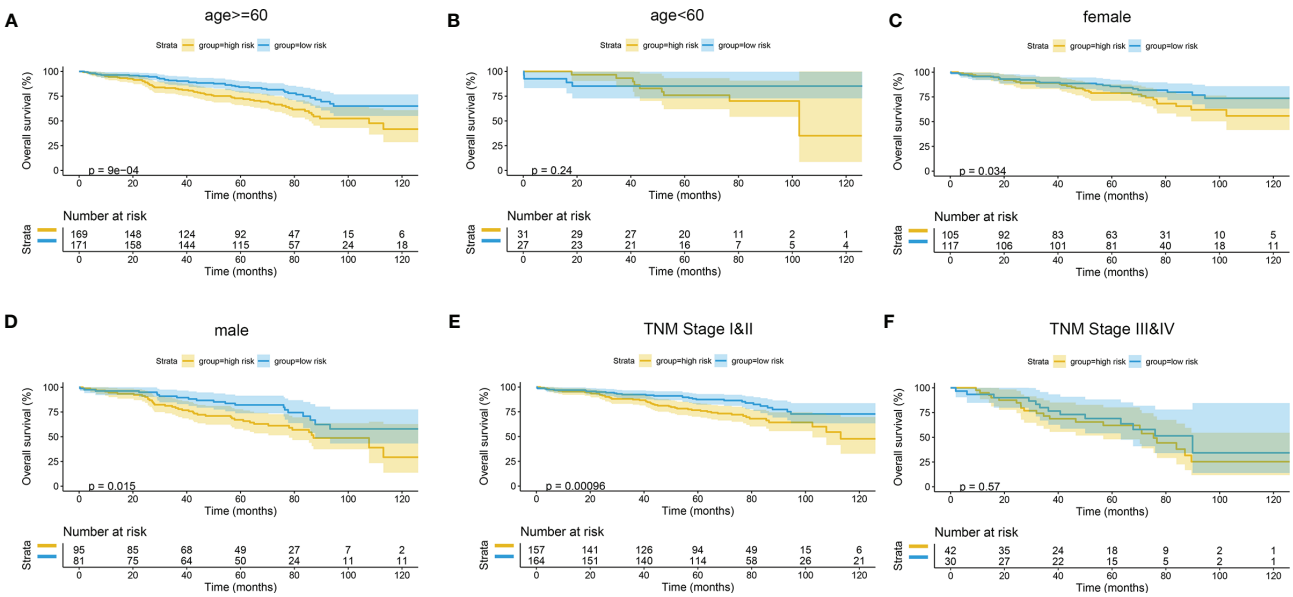


**FIGURE 14** | Subgroup survival analysis of GEO cohort. **(A)** Age ≥ 60. **(B)** Age < 60. **(C)** Female. **(D)** Male. **(E)** TNM stages I and II. **(F)** TNM stages III and IV. GEO, Gene Expression Omnibus.

GAPDH (glyceraldehyde-3-phosphate dehydrogenase) is one of the housekeeping proteins, and the mechanism of its anaerobic conversion to glucose critically regulates tissue regeneration and tumor growth (49, 50). Cancer cells can persistently survive under metabolic stress, anoxia, or starvation; and their glycolysis capacity must be improved by the Warburg effect, such as to improve the activity of enzymes involved in this function. Herein, the total glycolysis flux rate is precisely decided by the conversion stage from GALP (glyceraldehyde-3-phosphate) to biphosphoglyceride and is regulated by the activity of GAPDH (51). As an essential factor in the speed-limiting step of glycolysis, it plays a pivotal role in the energy metabolism of cancer cells. Hence, increased GAPDH activity will increase glycolysis rate and promote tumor growth, leading to poor prognosis (52). Anoxia is one of the major phenomena during tumor growth and activates the HIF-1α transcription factor to upregulate GAPDH expression (53, 54). In addition, upregulation of GAPDH may enhance HIF-1α transcription and activity, restricting the recruitment of CD8+ T lymphocytes (45, 46, 55). Moreover, the high activity of GAPDH increased the mobility of cancer cells, and epithelial–mesenchymal transition (EMT) markers are significantly associated. Colon cancer cell chromatin immune precipitation experiments proved the direct interaction between GAPDH and SPI transcripts, leading to the upregulation of the main regulatory factor in EMT, the zinc finger protein SNAI1 (Snail) (56–58). The initiation of GAPDH synthesis may be a protection mechanism for tumor cells to regulate metabolism and improve survival under anoxic conditions. Therefore, our results indicate that the expression of GAPDH may influence prognosis.

Based on these five genes, we established a risk score model. We found that the risk score could reasonably predict the prognosis of LUAD, and it was negatively related to the CD8+ T-cell infiltration and correlated with the advanced tumor stage. These results implied that these five genes might play a role in the infiltration of CD8+ T cells into the immune microenvironment. Among these genes, GAPDH and GPI may influence the infiltration of CD8+ T cells through the HIF-1/GBE1 pathway (45, 46, 55). Furthermore, the risk score was significantly upregulated in tumor tissues and correlated with advanced tumor stage. The validation of the overall cohort results by GEO dataset and the cohort of tissue microarray was consistent with the results of TCGA. Because the EGFR status is critical in LUAD, we also performed the subgroup analysis of the EGFR status. The performance of the risk model in both wild type and mutation type was good in TCGA cohort, as well as in the GEO cohort. However, the prediction accuracy is deficient in patients with mutation-type EGFR status in the mIHC cohort due to the small sample size. In a future study, we will increase the sample size of patients with mutation-type EGFR status to verify the risk model.

Nevertheless, this study also has some limitations. First, the mechanisms about how the genes affect the infiltration of CD8+ T cells were not explored in this report, but they will be investigated in a future study. Secondly, we constructed a risk score model that depended on gene expression but did not consider gene mutation, methylation, or other genetic events that can affect the occurrence and progression of cancers. In a subsequent study, we may consider more genetic modification to make our risk model more accurate. Finally, a large-sample

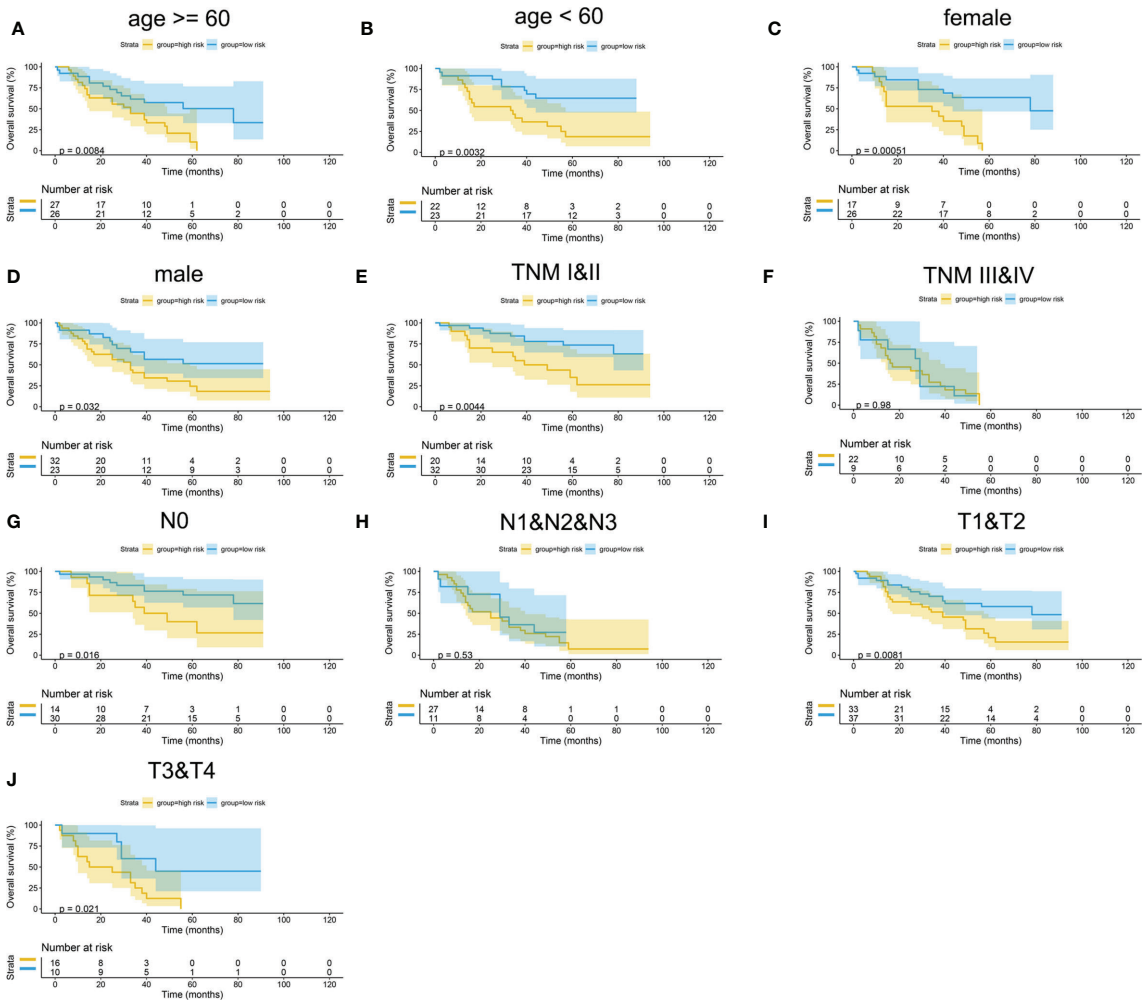


**FIGURE 15** | Subgroup survival analysis of mIHC cohort. **(A)** Age ≥ 60. **(B)** Age < 60. **(C)** Female. **(D)** Male. **(E)** TNM stages I and II. **(F)** TNM stages III and IV. **(G)** Stage N0. **(H)** Stages N1, N2, and N3. **(I)** Stages T1 and T2. **(J)** Stages T3 and T4.

prospective study is needed to further validate the clinical applicability of the risk score.

## CONCLUSIONS

In conclusion, this study may provide a novel risk assessment model for prognosis prediction and a new prospect for exploring the mechanism of tumor immune microenvironment related to CD8+ T-cell infiltration in LUAD.

## DATA AVAILABILITY STATEMENT

The original contributions presented in the study are included in the article/**Supplementary Material**. Further inquiries can be directed to the corresponding author.

## ETHICS STATEMENT

The study was approved by the ethics committee of National Cancer Center, Cancer Hospital, Chinese Academy of Medical Sciences and Peking Union Medical College, and all enrolled patients had given written informed consent to participate in this study.

## AUTHOR CONTRIBUTIONS

MD: conceptualization (lead), formal analysis (Lead), methodology (lead), and writing—original draft (lead). YL: methodology (equal), project administration (equal), supervision (equal), validation (equal), and writing—original draft (lead). ZL: data curation (equal), resources (equal), and writing—original draft

(supporting). XL: validation (equal) and writing—original draft (supporting). ML: validation (equal) and writing—original draft (supporting). BZ: supervision (supporting). YG: funding acquisition (lead), project administration (lead), and writing—review and editing (lead). All authors contributed to the article and approved the submitted version.

## FUNDING

This work was supported by the National Key R&D Program of China (Grant No. 2020YFE0202200).

## SUPPLEMENTARY MATERIAL

The Supplementary Material for this article can be found online at: https://www.frontiersin.org/articles/10.3389/fonc.2021.693353/full#supplementary-material

**Supplementary Figure 1 |** Differences of risk score in subgroup of TCGA cohort. **(A)** age; **(B)** T stage; **(C)** N stage; **(D)** M stage; **(E)** sex; **(F)** TNM stage.

**Supplementary Figure 2 |** Differences of risk score in subgroup of GEO cohort. **(A)** sex; **(B)** age; **(C)** TNM stage; **(D)** EGFR status.

**Supplementary Figure 3 |** Differences of risk score in subgroup of mIHC cohort. **(A)** sex; **(B)** age; **(C)** T stage; **(D)** N stage; **(E)** EGFR status; **(F)** ALK status; **(G)** TNM stage.

## REFERENCES


1. Siegel R, Miller K, Fuchs H, Jemal A. Cancer Statistics, 2021. *CA Cancer J Clin* (2021) 71(1):7–33. doi: 10.3322/caac.21654
2. Noguchi M, Morikawa A, Kawasaki M, Matsuno Y, Yamada T, Hirohashi S, et al. Small Adenocarcinoma of the Lung. Histologic Characteristics and Prognosis. *Cancer* (1995) 75(12):2844–52. doi: 10.1002/1097-0142(19950615)75:12<2844::aid-cncr2820751209>3.0.co;2-#
3. Zappa C, Mousa S. Non-Small Cell Lung Cancer: Current Treatment and Future Advances. *Transl Lung Cancer Res* (2016) 5(3):288–300. doi: 10.21037/tlcr.2016.06.07
4. Sacher A, Gandhi L. Biomarkers for the Clinical Use of PD-1/PD-L1 Inhibitors in Non-Small-Cell Lung Cancer: A Review. *JAMA Oncol* (2016) 2(9):1217–22. doi: 10.1001/jamaoncol.2016.0639
5. Cai L, Sun Y, Wang K, Guan W, Yue J, Li J, et al. The Better Survival of MSI Subtype Is Associated With the Oxidative Stress Related Pathways in Gastric Cancer. *Front Oncol* (2020) 10:1269. doi: 10.3389/fonc.2020.01269
6. Chen D, Mellman IJN. Elements of Cancer Immunity and the Cancer-Immune Set Point. *Nature* (2017) 541:321–30. doi: 10.1038/nature21349
7. Tian Y, Zhai X, Yan W, Zhu H, Yu J. Clinical Outcomes of Immune Checkpoint Blockades and the Underlying Immune Escape Mechanisms in Squamous and Adenocarcinoma NSCLC. *Cancer Med* (2021) 10:3–14. doi: 10.1002/cam4.3590
8. Augustin R, Delgoffe G, Najjar YJC. Characteristics of the Tumor Microenvironment That Influence Immune Cell Functions: Hypoxia, Oxidative Stress, Metabolic Alterations. *Cancers (Basel)* (2020) 12:3802. doi: 10.3390/cancers12123802
9. Galon J, Costes A, Sanchez-Cabo F, Kirilovsky A, Mlecnik B, Lagorce-Pagès C, et al. Type, Density, and Location of Immune Cells Within Human Colorectal Tumors Predict Clinical Outcome. *Science* (2006) 313:1960–4. doi: 10.1126/science.1129139
10. Mahmoud S, Paish E, Powe D, Macmillan R, Grainge M, Lee A, et al. Tumor-Infiltrating CD8+ Lymphocytes Predict Clinical Outcome in Breast Cancer. *J Clin Oncol* (2011) 29:1949–55. doi: 10.1200/JCO.2010.30.5037
11. Sharma P, Shen Y, Wen S, Yamada S, Jungbluth A, Gnjatic S, et al. CD8 Tumor-Infiltrating Lymphocytes Are Predictive of Survival in Muscle-Invasive Urothelial Carcinoma. *Proc Natl Acad Sci USA* (2007) 104:3967–72. doi: 10.1073/pnas.0611618104
12. Donnem T, Hald S, Paulsen E, Richardsen E, Al-Saad S, Kilvaer T, et al. Stromal CD8+ T-Cell Density—A Promising Supplement to TNM Staging in Non-Small Cell Lung Cancer. *Clin Cancer Res* (2015) 21:2635–43. doi: 10.1158/1078-0432.Ccr-14-1905
13. Al-Shibli K, Donnem T, Al-Saad S, Persson M, Bremnes R, Busund L. Prognostic Effect of Epithelial and Stromal Lymphocyte Infiltration in Non-Small Cell Lung Cancer. *Clin Cancer Res* (2008) 14:5220–7. doi: 10.1158/1078-0432.CCR-08-0133
14. Fu X, Xu M, Zhang H, Li Y, Li Y, Zhang C. Staphylococcal Enterotoxin C2 Mutant-Directed Fatty Acid and Mitochondrial Energy Metabolic Programs Regulate CD8 T Cell Activation. *J Immunol* (2020) 205:2066–76. doi: 10.4049/jimmunol.2000538
15. Lin T, Gu J, Qu K, Zhang X, Ma X, Miao R, et al. A New Risk Score Based on Twelve Hepatocellular Carcinoma-Specific Gene Expression Can Predict the Patients' Prognosis. *Aging (Albany NY)* (2018) 10:2480–97. doi: 10.18632/aging.101563
16. Langfelder P, Horvath S. WGCNA: An R Package for Weighted Correlation Network Analysis. *BMC Bioinf* (2008) 9:559. doi: 10.1186/1471-2105-9-559
17. Niemira M, Collin F, Szalkowska A, Bielska A, Chwialkowska K, Reszec J, et al. Molecular Signature of Subtypes of Non-Small-Cell Lung Cancer by Large-Scale Transcriptional Profiling: Identification of Key Modules and Genes by Weighted Gene Co-Expression Network Analysis (WGCNA). *Cancers (Basel)* (2019) 12:37. doi: 10.3390/cancers12010037
18. Liu H, Sun Y, Tian H, Xiao X, Zhang J, Wang Y, et al. Characterization of Long Non-Coding RNA and Messenger RNA Profiles in Laryngeal Cancer by Weighted Gene Co-Expression Network Analysis. *Aging (Albany NY)* (2019) 11:10074–99. doi: 10.18632/aging.102419
19. Newman A, Liu C, Green M, Gentles A, Feng W, Xu Y, et al. Robust Enumeration of Cell Subsets From Tissue Expression Profiles. *Nat Methods* (2015) 12:453–7. doi: 10.1038/nmeth.3337
20. Zhao S, Lehrer J, Chang S, Das R, Erho N, Liu Y, et al. The Immune Landscape of Prostate Cancer and Nomination of PD-L2 as a Potential Therapeutic Target. *J Natl Cancer Inst* (2019) 111:301–10. doi: 10.1093/jnci/djy141
21. Zhang S, Zhang E, Long J, Hu Z, Peng J, Liu L, et al. Immune Infiltration in Renal Cell Carcinoma. *Cancer Sci* (2019) 110:1564–72. doi: 10.1111/cas.13996
22. Galvano A, Gristina V, Malapelle U, Pisapia P, Pepe F, Barraco N, et al. The Prognostic Impact of Tumor Mutational Burden (TMB) in the First-Line Management of Advanced Non-Oncogene Addicted Non-Small-Cell Lung Cancer (NSCLC): A Systematic Review and Meta-Analysis of Randomized Controlled Trials. *ESMO Open* (2021) 6:100124. doi: 10.1016/j.esmoop.2021.100124
23. Pepe F, Pisapia P, Gristina V, Rocco D, Micheli M, Micheli P, et al. Tumor Mutational Burden on Cytological Samples: A Pilot Study. *Cancer Cytopathol* (2021) 129:460–7. doi: 10.1002/cncy.22400
24. Travis W, Brambilla E, Noguchi M, Nicholson A, Geisinger K, Yatabe Y, et al. International Association for the Study of Lung Cancer/American Thoracic Society/European Respiratory Society International Multidisciplinary Classification of Lung Adenocarcinoma. *Thorac Oncol* (2011) 6:244–85. doi: 10.1097/JTO.0b013e318206a221
25. Oser M, Niederst M, Sequist L, Engelman JA. Transformation From Non-Small-Cell Lung Cancer to Small-Cell Lung Cancer: Molecular Drivers and Cells of Origin. *Lancet Oncol* (2015) 16:e165–72. doi: 10.1016/S1470-2045(14)71180-5
26. Blandin Knight S, Crosbie P, Balata H, Chudziak J, Hussell T, Dive C. Progress and Prospects of Early Detection in Lung Cancer. *Open Biol* (2017) 7:170070. doi: 10.1098/rsob.170070
27. Deng W, Xu T, Xu Y, Wang Y, Liu X, Zhao Y, et al. Survival Patterns for Patients With Resected N2 Non-Small Cell Lung Cancer and Postoperative Radiotherapy: A Prognostic Scoring Model and Heat Map Approach. *J Thorac Oncol* (2018) 13:1968–74. doi: 10.1016/j.jtho.2018.08.2021
28. Herskovic A, Mauer E, Christos P, Nagar H. Role of Postoperative Radiotherapy in Pathologic Stage IIIA (N2) Non-Small Cell Lung Cancer in

a Prospective Nationwide Oncology Outcomes Database. *J Thorac Oncol* (2017) 12:302–13. doi: 10.1016/j.jtho.2016.09.135
29. Kris M, Gaspar L, Chaft J, Kennedy E, Azzoli C, Ellis P, et al. Adjuvant Systemic Therapy and Adjuvant Radiation Therapy for Stage I to IIIA Completely Resected Non-Small-Cell Lung Cancers: American Society of Clinical Oncology/Cancer Care Ontario Clinical Practice Guideline Update. *J Clin Oncol* (2017) 35:2960–74. doi: 10.1200/JCO.2017.72.4401
30. Adams N, Grassmann S, Sun JC. Clonal Expansion of Innate and Adaptive Lymphocytes. *Nat Rev Immunol* (2020) 20:694–707. doi: 10.1038/s41577-020-0307-4
31. van der Leun A, Thommen D, Schumacher TN. CD8 T Cell States in Human Cancer: Insights From Single-Cell Analysis. *Nat Rev Cancer* (2020) 20(4):218–32. doi: 10.1038/s41568-019-0235-4
32. Butterfield LJB. Cancer Vaccines. *BMJ* (2015) 350:h988. doi: 10.1136/bmj.h988
33. Appay V, Douek D, Price DA. CD8+ T Cell Efficacy in Vaccination and Disease. *Nat Med* (2008) 14:623–8. doi: 10.1038/nm.f.1774
34. Wang H, Jiang X, Cheng Y, Ren H, Hu Y, Zhang Y, et al. MZT2A Promotes NSCLC Viability and Invasion by Increasing Akt Phosphorylation *via* the MOZART2 Domain. *Cancer Sci* (2021) 112:2210–22. doi: 10.1111/cas.14900
35. Shi Z, Jiang Y, Hao J, Zhang Y, Zhang T, Shang L, et al. Identification of Putative Target Genes for Amplification Within 11q13.2 and 3q27.1 in Esophageal Squamous Cell Carcinoma. *Clin Transl Oncol* (2014) 16:606–15. doi: 10.1007/s12094-013-1124-z
36. Choi Y, Bae S, Kim Y, Lee H, Kim Y, Park T, et al. Gene Expression Profiles in Squamous Cell Cervical Carcinoma Using Array-Based Comparative Genomic Hybridization Analysis. *Int J Gynecol Cancer* (2007) 17:687–96. doi: 10.1111/j.1525-1438.2007.00834.x
37. Ke S, Qiu H, Chen J, Shi W, Han C, Gong Y, et al. ALG3 Contributes to the Malignancy of Non-Small Cell Lung Cancer and Is Negatively Regulated by Mir-98-5p. *Pathol Res Pract* (2020) 216:152761. doi: 10.1016/j.prp.2019.152761
38. Li M, Jin C, Xu M, Zhou L, Li D, Yin YJC, et al. Bifunctional Enzyme ATIC Promotes Propagation of Hepatocellular Carcinoma by Regulating AMPK-Mtor-S6 K1 Signaling. *Cell Commun Signal* (2017) 15:52. doi: 10.1186/s12964-017-0208-8
39. Trinei M, Lanfrancone L, Campo E, Pulford K, Mason D, Pelicci P, et al. A New Variant Anaplastic Lymphoma Kinase (ALK)-Fusion Protein (ATIC-ALK) in a Case of ALK-Positive Anaplastic Large Cell Lymphoma. *Cancer Res* (2000) 60:793–8.
40. van der Krogt J, Bempt M, Ferreiro J, Mentens N, Jacobs K, Pluys U, et al. Anaplastic Lymphoma Kinase-Positive Anaplastic Large Cell Lymphoma With the Variant RNF213-, ATIC- and TPM3-ALK Fusions Is Characterized by Copy Number Gain of the Rearranged ALK Gene. *Haematologica* (2017) 102:1605–16. doi: 10.3324/haematol.2016.146571
41. Liu X, Paila U, Teraoka S, Wright J, Huang X, Quinlan A, et al. Identification of ATIC as a Novel Target for Chemoradiosensitization. *Int J Radiat Oncol Biol Phys* (2018) 100:162–73. doi: 10.1016/j.ijrobp.2017.08.033
42. Funasaka T, Yanagawa T, Hogan V, Raz A. Regulation of Phosphoglucose Isomerase/Autocrine Motility Factor Expression by Hypoxia. *FASEB J* (2005) 19:1422–30. doi: 10.1096/fj.05-3699com
43. Semenza GL. HIF-1 Mediates Metabolic Responses to Intratumoral Hypoxia and Oncogenic Mutations. *J Clin Invest* (2013) 123:3664–71. doi: 10.1172/JCI67230
44. Pusapati R, Daemen A, Wilson C, Sandoval W, Gao M, Haley B, et al. Mtorc1-Dependent Metabolic Reprogramming Underlies Escape From Glycolysis Addiction in Cancer Cells. *Cancer Cell* (2016) 29:548–62. doi: 10.1016/j.ccell.2016.02.018
45. Li L, Yang L, Fan Z, Xue W, Shen Z, Yuan Y, et al. Hypoxia-Induced GBE1 Expression Promotes Tumor Progression Through Metabolic Reprogramming in Lung Adenocarcinoma. *Signal Transduct Target Ther* (2020) 5:54. doi: 10.1038/s41392-020-0152-8
46. Li L, Yang L, Cheng S, Fan Z, Shen Z, Xue W, et al. Lung Adenocarcinoma-Intrinsic GBE1 Signaling Inhibits Anti-Tumor Immunity. *Mol Cancer* (2019) 18:108. doi: 10.1186/s12943-019-1027-x
47. Itoh Y. Membrane-Type Matrix Metalloproteinases: Their Functions and Regulations. *Matrix Biol* (2015) 44–46:207–23. doi: 10.1016/j.matbio.2015.03.004
48. Lucarelli G, Rutigliano M, Sanguedolce F, Galleggiante V, Giglio A, Cagiano S, et al. Increased Expression of the Autocrine Motility Factor Is Associated With Poor Prognosis in Patients With Clear Cell-Renal Cell Carcinoma. *Medicine (Baltimore)* (2015) 94:e2117. doi: 10.1097/MD.0000000000002117
49. Yang J, Ren B, Yang G, Wang H, Chen G, You L, et al. The Enhancement of Glycolysis Regulates Pancreatic Cancer Metastasis. *Cell Mol Life Sci* (2020) 77:305–21. doi: 10.1007/s00018-019-03278-z
50. Woolbright B, Ayres M, Taylor JA. Metabolic Changes in Bladder Cancer. *Urol Oncol* (2018) 36:327–37. doi: 10.1016/j.urolonc.2018.04.010
51. Shestov A, Liu X, Ser Z, Cluntun A, Hung Y, Huang L, et al. Quantitative Determinants of Aerobic Glycolysis Identify Flux Through the Enzyme GAPDH as a Limiting Step. *Elife* (2014) 9(3):e03342. doi: 10.7554/eLife.03342
52. Brzozowa-Zasada M, Kurek J, Piecuch A, Stęplewska KJP. Correlation Study of GAPDH, Bcl-2, and Bax Protein Immunoexpression in Patients With Colorectal Adenocarcinoma. *Prz Gastroenterol* (2018) 13:322–31. doi: 10.5114/pg.2018.79813
53. Mikuriya K, Kuramitsu Y, Ryozawa S, Fujimoto M, Mori S, Oka M, et al. Expression of Glycolytic Enzymes Is Increased in Pancreatic Cancerous Tissues as Evidenced by Proteomic Profiling by Two-Dimensional Electrophoresis and Liquid Chromatography-Mass Spectrometry/Mass Spectrometry. *Int J Oncol* (2007) 30:849–55. doi: 10.3892/ijo.30.4.849
54. Higashimura Y, Nakajima Y, Yamaji R, Harada N, Shibasaki F, Nakano Y, et al. Up-Regulation of Glyceraldehyde-3-Phosphate Dehydrogenase Gene Expression by HIF-1 Activity Depending on Sp1 in Hypoxic Breast Cancer Cells. *Arch Biochem Biophys* (2011) 509:1–8. doi: 10.1016/j.abb.2011.02.011
55. Chiche J, Pommier S, Beneteau M, Mondragón L, Meynet O, Zunino B, et al. GAPDH Enhances the Aggressiveness and the Vascularization of Non-Hodgkin's B Lymphomas *via* NF-Kb-Dependent Induction of HIF-1α. *Leukemia* (2015) 29:1163–76. doi: 10.1038/leu.2014.324
56. Schneider M, Knuesting J, Birkholz O, Heinisch J, Scheibe RJB. Cytosolic GAPDH as a Redox-Dependent Regulator of Energy Metabolism. *BMC Plant Biol* (2018) 18:184. doi: 10.1186/s12870-018-1390-6
57. Liu K, Tang Z, Huang A, Chen P, Liu P, Yang J, et al. Glyceraldehyde-3-Phosphate Dehydrogenase Promotes Cancer Growth and Metastasis Through Upregulation of SNAIL Expression. *Int J Oncol* (2017) 50:252–62. doi: 10.3892/ijo.2016.3774
58. Hao L, Zhou X, Liu S, Sun M, Song Y, Du S, et al. Elevated GAPDH Expression Is Associated With the Proliferation and Invasion of Lung and Esophageal Squamous Cell Carcinomas. *Proteomics* (2015) 15:3087–100. doi: 10.1002/pmic.201400577

**Conflict of Interest:** The authors declare that the research was conducted in the absence of any commercial or financial relationships that could be construed as a potential conflict of interest.

**Publisher's Note:** All claims expressed in this article are solely those of the authors and do not necessarily represent those of their affiliated organizations, or those of the publisher, the editors and the reviewers. Any product that may be evaluated in this article, or claim that may be made by its manufacturer, is not guaranteed or endorsed by the publisher.

frontiers in Oncology

REVIEW
published: 07 January 2022
doi: 10.3389/fonc.2021.786089

# Imaging the Rewired Metabolism in Lung Cancer in Relation to Immune Therapy

*Evelien A. J. van Genugten[1], Jetty A. M. Weijers[1], Sandra Heskamp[1], Manfred Kneilling[2,3], Michel M. van den Heuvel[4], Berber Piet[4], Johan Bussink[5†], Lizza E. L. Hendriks[6] and Erik H. J. G. Aarntzen[1*]*

[1] Department of Medical Imaging, Radboud University Medical Centre (Radboudumc), Nijmegen, Netherlands, [2] Department of Preclinical Imaging and Radiopharmacy, Werner Siemens Imaging Center, Eberhard Karls University, Tuebingen, Germany, [3] Department of Dermatology, Eberhard Karls University, Tuebingen, Germany, [4] Department of Respiratory Diseases, Radboudumc, Nijmegen, Netherlands, [5] Radiotherapy and OncoImmunology Laboratory, Department of Radiation Oncology, Radboudumc, Netherlands, [6] Department of Pulmonary Diseases, GROW – School for Oncology and Developmental Biology, Maastricht University Medical Centre (UMC), Maastricht, Netherlands

OPEN ACCESS

**Edited by:**
Jordi Remon,
Hospital HM Delfos, Spain

**Reviewed by:**
Kumar Pichumani,
Houston Methodist Research Institute, United States
David Akhavan,
University of Kansas Medical Center, United States

***Correspondence:**
Erik H. J. G. Aarntzen
erik.aarntzen@radboudumc.nl

**†ORCID:**
Johan Bussink
orcid.org/0000-0002-5751-4796

**Specialty section:**
This article was submitted to Cancer Immunity and Immunotherapy, a section of the journal Frontiers in Oncology

**Received:** 30 September 2021
**Accepted:** 10 December 2021
**Published:** 07 January 2022

**Citation:**
van Genugten EAJ, Weijers JAM, Heskamp S, Kneilling M, van den Heuvel MM, Piet B, Bussink J, Hendriks LEL and Aarntzen EHJG (2022) Imaging the Rewired Metabolism in Lung Cancer in Relation to Immune Therapy. Front. Oncol. 11:786089. doi: 10.3389/fonc.2021.786089

Metabolic reprogramming is recognized as one of the hallmarks of cancer. Alterations in the micro-environmental metabolic characteristics are recognized as important tools for cancer cells to interact with the resident and infiltrating T-cells within this tumor microenvironment. Cancer-induced metabolic changes in the micro-environment also affect treatment outcomes. In particular, immune therapy efficacy might be blunted because of somatic mutation-driven metabolic determinants of lung cancer such as acidity and oxygenation status. Based on these observations, new onco-immunological treatment strategies increasingly include drugs that interfere with metabolic pathways that consequently affect the composition of the lung cancer tumor microenvironment (TME). Positron emission tomography (PET) imaging has developed a wide array of tracers targeting metabolic pathways, originally intended to improve cancer detection and staging. Paralleling the developments in understanding metabolic reprogramming in cancer cells, as well as its effects on stromal, immune, and endothelial cells, a wave of studies with additional imaging tracers has been published. These tracers are yet underexploited in the perspective of immune therapy. In this review, we provide an overview of currently available PET tracers for clinical studies and discuss their potential roles in the development of effective immune therapeutic strategies, with a focus on lung cancer. We report on ongoing efforts that include PET/CT to understand the outcomes of interactions between cancer cells and T-cells in the lung cancer microenvironment, and we identify areas of research which are yet unchartered. Thereby, we aim to provide a starting point for molecular imaging driven studies to understand and exploit metabolic features of lung cancer to optimize immune therapy.

**Keywords: tumor microenvironment, lung cancer, T-cells (or lymphocytes), immunotherapy, metabolism, molecular imaging**

## 1 INTRODUCTION

Metabolic reprogramming is one of the hallmarks of cancer (1, 2), and the many ways by which cancer cells manipulate their metabolic micro-environment are increasingly being understood. Excellent and comprehensive reviews approaching this topic from the angle of specific cancer types such as non-small cell lung cancer (NSCLC) (3, 4) and head and neck cancer (HNSCC) (5) or from the most common metabolic substrates – oxygen (6), essential nutrients/amino acids (7), lipids/free fatty acids (8), acetate (9) or genetic drivers (10–13) - are available from recent literature.

Alterations in the tumor microenvironmental (TME) metabolites are recognized as important tools for cancer cells to interact with supportive cells in their direct vicinity (14). These supportive cells include endothelial cells, inducing angiogenesis when activated by increased demands for oxygen (15, 16) or cancer-associated fibroblasts driving glycolysis (5, 17). Also, tumor-associated macrophages can modulate glucose metabolism in the TME in favor of cancer progression (18). Interactions between cancer cells and supportive cells are reciprocal in nature (18) and the derivative metabolic phenotypes result from underlying oncogenic mutations (11, 19), pathology (20, 21) as well as from tissue of origin (22). Lung cancer frequently harbors mutations which directly affect cellular glucose metabolism and associated metabolic pathways, as reviewed previously (4). In addition to STK11/LKB1 mutations (23, 24), mutations in the PI3K (phosphoinositide-3-kinase)-AKT-mTOR (mammalian target of rapamycin) pathway (23), the oncogenes RAS, c-MYC, and master regulator HIF-1α (hypoxia inducible factor-1α), or the tumor suppressor gene TP53 are known to reprogram lung cancer metabolism.

By modulating metabolic pathways and depriving the TME from essential nutrients, cancer cells create unfavorable conditions for invading adaptive immune cells (20, 25–27). To execute their effector functions, T-cells should undergo rapid metabolic reprogramming (28, 29), which mainly involves upregulation of aerobic glycolysis by CD28 co-stimulation, acting through PI3K and Akt pathways (30, 31), very much alike the Warburg effect in cancer cells (32). Yet on the longer term, a sustainable memory T-cell response requires a distinct metabolic profile that relies on oxidative phosphorylation and intact mitochondrial function to prevent T-cell exhaustion (33–35). **Figure 1** introduces the main potential sources of energy available in the TME, which will be discussed in this review, and the preference of cancer cells and T-cells to perform glycolysis or oxidative phosphorylation, respectively. Glucose metabolism therefore illustrates that nutrient availability represents a highly conserved fundamental framework to guide decisions on cell survival or apoptosis (36), a process which is continuously taking place in the TME. Next to glucose metabolism, other basal metabolic pathways involving amino acids (7) like glutamine (37) and lipids (8, 38, 39) are reported to affect T-cell immunity.

Cancer-induced metabolic changes in the TME not only favor cancer progression and immune suppression but can also be a limiting factor concerning treatment efficacy. The most studied example in lung cancer is the adverse role of lack of oxygen availability blunting radiotherapy efficacy (40–42). Similarly, blocking adaptive metabolic pathways renders standard chemotherapy more effective in lung cancer (43, 44). Also, development of resistance to targeted therapies is related to plasticity in metabolic pathways associated with Kirsten rat sarcoma viral oncogene homolog (KRAS) mutations in NSCLC (45, 46), a vulnerability which can be exploited in combination treatments (47). More recently, the metabolic determinants of immune checkpoint inhibition are being understood (48). For example, glucose consumption by cancer cells might be a metabolic adaptation to restrict T-cell effector function (26, 49). Furthermore, blocking programmed death ligand-1 (PD-L1) on cancer cells reduces their glycolysis rate by inhibition of mTOR-related pathways, which would permit T-cells to exploit

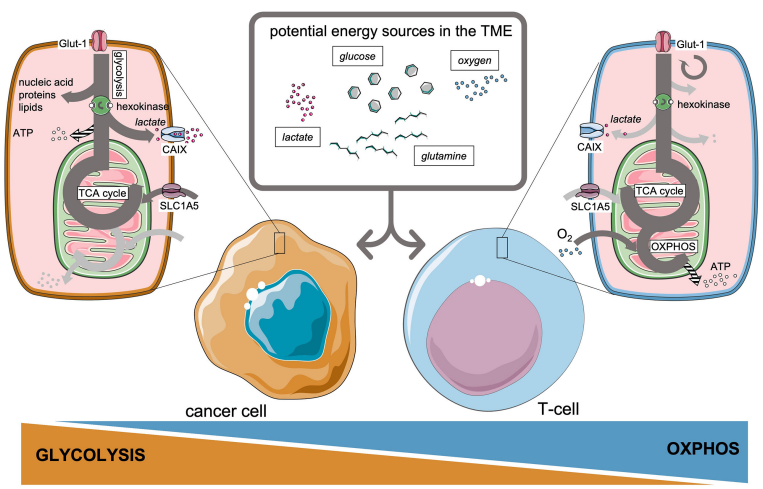


**FIGURE 1** | Preferential metabolic pathways and potential energy sources available in the tumor microenvironment for cancer cells and T-cells.

their glycolytic capacity and restore IFN-γ production (26). Acknowledging the intertwined roles of immune checkpoint molecules, both on cancer cells and T-cells, in immune signaling and regulation of cellular metabolism, this is now an active area of research (50, 51). Ongoing onco-immunology studies on checkpoint inhibitors search to utilize the effect of checkpoint molecule inhibition on cancer cell metabolism, as adjunct to enhancing immune cell function (52, 53).

In addition, onco-immunological treatment strategies emerge that employ the metabolic vulnerabilities of cancer cells, especially at the level of mitochondria (54–58). These strategies include enzymatic drugs that interfere with dominant metabolic pathways in the TME (59), such as metformin, atovaquone, glucose (60), indoleamine 2,3-dioxygenase (IDO inhibitors), glutamine inhibitors (37) and AKT-mTOR inhibitors (27). The efficacy of mitochondrial targeting drugs indicates that oxidative phosphorylation remains important for adenosine-triphosphate (ATP) production in a multitude of tumors, including NSCLC (61, 62).

Tumor senescence represents another important tumor suppressor mechanism (63), apart from apoptosis, embanking cancer cell proliferation as well as malignant progression. Tumor senescence implies stable cell-cycle arrest induced by cellular stress associated with alterations in gene expression patterns, a metabolic shift towards a more glycolytic state and a proinflammatory secretory phenotype (64, 65). Multiple anticancer therapies such as chemotherapy, radiotherapy and cancer immunotherapies are applicable to induce irreversible tumor senescence. Thus, tumor senescence has to be taken into account as an essential component in the treatment of cancer.

PET imaging has developed a wide array of tracers targeting metabolic pathways, originally intended to improve cancer detection and staging (66, 67). Paralleling the developments in understanding metabolic reprogramming in cancer cells, as well as its effects on T-cells, a wave of additional imaging tracers has been published (68, 69) (**Figure 2**).

Definitively, imaging can contribute to more effective anti-cancer therapies (70–72), as it assesses functional processes with high sensitivity and, if applied longitudinally, can monitor treatment effects on an individual patient basis. This adds important insights to immunohistochemistry that can provide a detailed but static insight in the expression of transporters, enzymes and other molecular markers involved in metabolic pathways. Although the methodology allows quantitative assessment of these functional processes this is limited to accessible lesions and hampered by sampling errors. In addition, molecular imaging facilitates evaluation of intra-tumoral regional differences, a critical aspect for the net treatment efficacy (73) which cannot be assessed with invasive sampling procedures such as biopsies. As metabolic adaptation of T-cells can have tissue-specific determinants (74) which might differ from *in vitro* experiments (75), the wide field of view of PET imaging is a critical asset in this domain of research.

However, molecular imaging tools that probe metabolic processes are yet under-utilized in the perspective of immune therapy development. In this review, we provide an overview of currently available PET imaging tools for clinical studies and discuss their potential roles in the development of effective immune therapeutic strategies in lung cancer. We report on ongoing efforts that include PET/CT to understand the outcomes of interactions between lung cancer and T-cells in the tumor microenvironment, and we identify areas of research which are yet unchartered. Thereby, we aim to provide a starting point for molecular imaging driven studies to understand and exploit metabolic features of tumor environment to optimize immune therapy.

## 2 GLUCOSE METABOLISM

### 2.1 Glucose Metabolism in Cancer Cells

The most studied metabolic phenomenon in cancer is its tendency to increase its' rate of glycolysis in adjunct to oxidative phosphorylation, despite the presence of sufficient levels of oxygen in the TME. This feature of cancer metabolism is called the Warburg effect, named after the German scientist who first described this (76). Although glycolysis is less efficient in producing ATP, it does generate increased levels of additional metabolites for the biosynthesis of ribose, glycosylation precursors, amino acids, and lipids (77, 78).

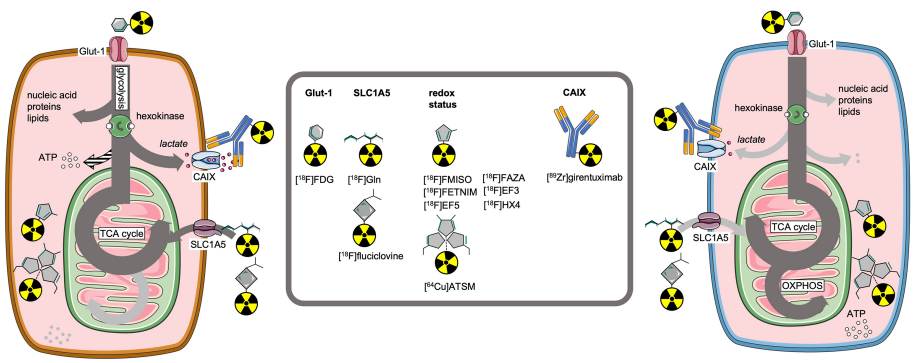


**FIGURE 2** | Molecular imaging tracers to visualize key receptors and pathways involved in cell metabolism.

Inefficient ATP production would only be problematic in scarcity of nutrients, which is in general not the case in cancer. Therefore 'aerobic glycolysis' means a survival advantage for cancer cells in terms of increased anabolism and avoidance of oxidizing precious carbon-carbon bonds (79).

To meet their greatly enhanced demand for glucose under conditions of 'aerobic glycolysis', cancer cells have upregulated levels of the key glucose transporter 1 (Glut-1) on cell membranes (10) and associated hexokinases. Hexokinases are enzymes that phosphorylate six-carbon sugars, primarily glucose, by transferring a phosphate group from ATP to its' substrate. As phosphorylation charges the hexoses, it is trapped intracellularly and available for further metabolic processes, resulting in a stable down-slope gradient that drives glucose transport into the cell. For this reason, hexokinase activity is the rate limiting step for most metabolic pathways involving glucose. The isoform hexokinase II (or hexokinase B) is the dominant isoform in many cell types (80), including most cancers, and located at the outer mitochondrial membrane to have direct access to ATP (81). Upregulation of aerobic glycolysis results in an increase of pyruvate, which is further metabolized into lactate (77). Intracellular lactate is transported out of the cell, along with protons, *via* monocarboxylate transporters (e.g., MCT-1 and MCT-4) into the TME. In addition to lactate shuttles, intracellular acidification is prevented by carbonic anhydrase 9 (CAIX), a transmembrane metalloenzyme that facilitates secretion of acids produced under oxidative stress. Indeed, it has long been noticed that tumors often have an acidic environment (82).

## 2.2 Regulation of Metabolic Reprogramming in Lung Cancer

Metabolic reprogramming in cancer is partly due to oncogenic activation of signal transduction pathways and transcription factors, HIF-1α is a master regulator of glycolysis and the pentose phosphate pathway (20, 83, 84). In lung cancer, oncogenes and pathways divert intracellular glucose flux towards increased usage of glucose into the hexosamine biosynthesis, required for protein glycosylation and pentose phosphate pathway [reviewed in (4)]. Well-studied signaling pathways, including PI3K/Akt/mTOR and RAS/RAF/MEK/MAPK, with high prevalence in lung cancer, associate with increased glycolysis as well as metabolic plasticity, by initiating compensatory mechanisms and facilitating alternative metabolic sources, e.g., amino acids, nucleotides or fatty acid biosynthesis and macropinocytosis. At a transcriptional level, the transcription factor nuclear factor erythroid-2-related factor (NFE2L2/Nrf2) is identified as one of the main regulators of metabolic reprogramming in lung cancer, and its activity is associated with poor survival (85).

Epigenetic mechanisms also contribute to the regulation of gene expression involved in cancer metabolism (86). Disruption of the epigenome is present in cancer cells, including DNA methylation, histone proteins and histone modification enzymes, as well as proteins that regulate the function of metabolic enzymes (87). Reciprocally, activity of histone and DNA modifying enzymes regulates the expression of metabolism-associated genes, leading to a complex interplay between metabolism and epigenetic during cancer progression (88). Understanding the relation between metabolism, signaling pathways and epigenetics may open new avenues for anti-cancer immune therapy (89), which will be discussed later.

## 2.3 How Glucose Consumption by Cancer Cells Affects T-Cells

Upon activation, naïve T-cells also undergo metabolic adaptation to meet the increased bioenergetic demands associated with proliferation and effector function (29, 90–93). In contrast to static cancer cells, which can thus invest in creating a favorable metabolic niche, effector T-cells migrate through the body and are merely passengers who need to adapt to changing environmental conditions, from well-supplied lymph nodes and spleen to rather oxygen and nutrient deprived cancer lesions (94). In general, nutrient competition between cells strongly influences cell fate (36, 95) and function (90). More recently, this interplay between cancer cells and immune cells has been reviewed (51, 96, 97). Aerobic glycolysis is not required for activation or proliferation during early stages of T-cell activation (98), however, it is essential for optimal T-cell effector function in the TME (99, 100). *In vitro* models previously demonstrated that cancer cells outcompete T-cells for glucose, directly restricting cytokine mediated anti-cancer immunity (101). Also *in vivo*, tumor infiltrating CD8+ T-cells face restricted glucose availability, which consequently hampers increased rate of glycolysis by restricted mTOR activity and thus reduced IFN-γ production (98, 102).

In addition to direct competition for glucose, limiting the magnitude of aerobic glycolysis in T-cells, high lactate excretion by cancer cells further suppresses T-cell effector functions (103–105), directly correlated it to reduced survival rates in e.g., head and neck cancer (106). The acidic TME inhibits both T-cell trafficking and cytotoxicity (102, 103, 107) and sheds new light on the role of lactate as immune metabolic mediator (14). The enzyme lactate dehydrogenase A (LDHA) which converts pyruvate into lactate, not only plays a central role in cancer cell aerobic glycolytic capacity but exerts similar function in T-cell function through PI3K signaling (31, 108).

The costimulatory molecule CD28 on T-cells, ligating to CD80 during antigen-specific activation, induces this PI3K signaling (30), resulting in increased expression of Glut-1. By facilitating glycolysis increase, CD28 signaling prepares T-cells to anticipate on changing metabolic demands associated with sustained effector functions. This necessary metabolic switch is furthermore under the control of inhibitory members of the CD28 superfamily (mainly PD-1 expression), with the intend to delicately control T-cell activation (97, 109–111). PD-1 on T-cells is mostly studied as an exhaustion marker, induced by chronic antigen exposure and endurable stages of activation. Its increased expression on T-cells indicates a critical stage of T-cell development, at the verge of going in retraction and clearance (109, 112). The expression of PD-L1, by cancer cells and myeloid derived suppressor cells in the TME not only suppresses

cytotoxic effector function of T-cells, but it also entangles the metabolic reprogramming of T-cells *via* ligation of PD-1. PD-1 ligation suppresses the ability of T-cells to perform glycolysis and glutaminolysis, thus pushing T-cells further towards retraction. Therefore, one of the effects of therapeutic monoclonal antibodies targeting CTLA-4 (interacting with CD28) and PD-L1 (interacting with PD-1), is allowing T-cells to maintain their increased glycolytic and glutaminolytic capacity to execute anti-cancer effector functions in the TME (113, 114).

## 2.4 Imaging Targets Related to Glucose Metabolism

The most widely applied tracer to image the upregulation of glycolysis is 2'-deoxy-2'-[$^{18}$F]fluoro-D-glucose ([$^{18}$F]FDG). [$^{18}$F]FDG is extensively used for the detection of primary tumors, metastases and recurrences, and monitoring responses to anti-cancer treatments (115–117). [$^{18}$F]FDG uptake by glycolytic cancer cells is directly related to upregulated levels Glut-1 transporters (118) and hexokinases activity (119). Consequently, levels of [$^{18}$F]FDG uptake also correlate with increased levels of derivates of the glycolytic pathway; pyruvate and lactate (120).

### 2.4.1[$^{18}$F]FDG to Characterize the Tumor Immune Microenvironment

Given the reciprocal relation of glucose metabolism between cancer cells and T-cells, several studies investigated the relation between [$^{18}$F]FDG-uptake, as parameter for glycolysis in the TME, and expression levels of immune checkpoint molecules and presence of CD8+ T-cells. Independent of the well-known higher [$^{18}$F]FDG-uptake in squamous cell histological subtypes as compared to adenocarcinoma in NSCLC (20), some studies found a trend towards higher $SUV_{max}$ and $SUV_{mean}$ in lung cancers with increasing numbers of CD8+ T-cell numbers and increased expression of PD-1 (121). Not surprisingly, CD8+ T-cells and PD-1 expression were highly intercorrelated and overlapping their positive correlation with [$^{18}$F]FDG-uptake. However, there was no such relation between [$^{18}$F]FDG-uptake and presence of tumor-associated macrophages, measured by CD68 staining, or PD-L1 expression (**Figure 3**). Others did find a positive relation between [$^{18}$F]FDG uptake and PD-L1 expression on immunohistochemistry in patients with NSCLC (122–124). High maximum [$^{18}$F]FDG uptake in NSCLC seemed prognostic for poor disease free survival (121), but it might be predictive for a favorable response to immune checkpoint inhibition (125).

In contrast, high levels of [$^{18}$F]FDG uptake by cancers cells, corresponding with upregulated expression of glycolysis-related genes, was correlated with reduced numbers of CD8+ T-cells, increased T-cell exhaustion gene signatures and higher levels of PD-L1 in NSCLC by others (126), which potentially can stratify patients for subsequent immune checkpoint inhibition. This negative trend has also been observed in HNSCC using a systems biology approach, correlating omics data with histopathological data; CD8+ T-cell numbers were inversely correlated with HIF-1α and EGFR regulated aerobic glycolysis (127). This was confirmed by a similar approach in HNSCC demonstrating reduced numbers and activation status of CD8+ T-cells as well as myeloid cells with increasing [$^{18}$F]FDG uptake (128), and renal cell carcinoma (129, 130).

### 2.4.2 [$^{18}$F]FDG to Monitor Response to Immune Checkpoint Inhibition

Decrease in [$^{18}$F]FDG uptake in melanoma, renal cell or lymphoma lesions within 3 months after start of immune checkpoint inhibition was correlated with a favorable clinical outcome at 1 year (131). Several additional studies confirmed the role of [$^{18}$F]FDG to monitor response to immune checkpoint inhibition in patients with advanced melanoma treated with CTLA-4 inhibitors

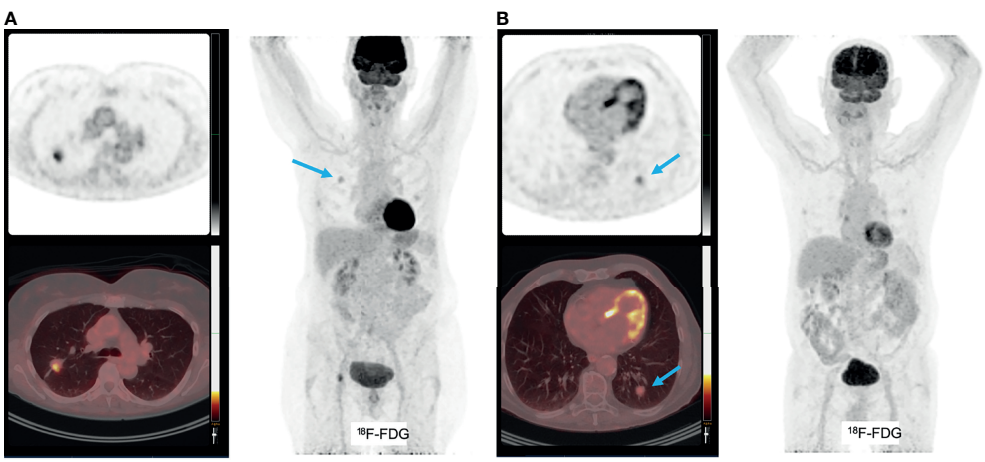


**FIGURE 3** | **(A)** patient with pT2bN0 well-differentiated primary adenocarcinoma of the right upper lobe, with markedly increased [$^{18}$F]FDG uptake **(A)**. This tumor was PD-L1 negative. Molecular analyses: mutations found in KRAS (p.G13C), BRAF (p.G464V) and STK11, no amplifications, no micro-satelite instability. An additional example of a patient with pT1bN0 well-differentiated primary adenocarcinoma of the left lower lobe, with faint [$^{18}$F]FDG uptake **(B)**. This tumor was PD-L1 negative and molecular analyses detected mutations in KRAS (p.G12A), no amplifications and no micro-satellite instability.

(132–134) and advanced NSCLC patients under PD-1 inhibition (124) These studies suggest that [$^{18}$F]FDG may serve as a predictor of response of immune checkpoint inhibition (132, 133), as long as immune therapy related response patterns are taken into account, e.g. appearance of new lesions or initial limited increase in tumor burden not per se define progression (135, 136). At this moment several clinical trials are ongoing with [$^{18}$F]FDG as a biomarker of therapeutic responses to immunotherapy in various cancer types, including thoracic cancer (NCT02608528), NSCLC (NCT02753569 and NCT04082988), and melanoma (NCT04272658). These current studies, generally hinting at a conventional role for [$^{18}$F]FDG PET/CT to assess cancer responses to immune therapy, presumably demonstrates that in the TME cancer cell glycolysis largely outcompetes glycolysis by tumor-infiltrating immune cells.

However, early signs of increased T-cell activity, by upregulated [$^{18}$F]FDG-uptake as a surrogate for increased glycolysis, at sites distant from the TME are readily visualized using [$^{18}$F]FDG PET imaging (137). Immune related adverse events like thyroiditis are associated with favorable clinical outcome (131). In addition, systemic immune activation, linked to increased glycolysis in hematopoietic bone marrow and secondary lymphoid organs such as the spleen, show a positive correlation with favorable response to immune checkpoint inhibition (138–141).

# 3 OXYGEN AVAILABILITY

## 3.1 How Oxygen Availability Affects Cancer Cells

Glycolysis, even when increased, contributes relatively little to cellular ATP content; its majority is provided by oxidative phosphorylation in mitochondria, which requires oxygen in the electron transport chain (142). Although oxygen availability is only limiting mitochondrial electron transport chain at very low levels (<0.07% oxygen) (143, 144), its lowering levels are sensed carefully. Through HIF1a activation, hypoxia promotes glycolysis in addition to increasing oxidative phosphorylation (145, 146). Imbalances in oxygen levels occur in a range of physiological conditions, e.g., wound healing (147), and disease conditions, e.g. chronic obstructive pulmonary disorders (148). In cancer however, the chaotic tissue vascularization results in *chronic* diffusion-limited hypoxia as well as *acute* perfusion limited hypoxia (15). Enduring long-term hypoxia results in additional oxidative stress caused by increased levels of reactive oxygen species (ROS) produced from mitochondrial complex III in cancer cells (149, 150) Excessive levels of intracellular ROS can cause oxidative damage to intracellular lipids, protein and DNA, which might reciprocally drive diversification of cancer phenotypes (151) but at a given point culminates in cell cycle arrest and apoptosis (152).

## 3.2 Lung Cancers' Response to Hypoxia

Intracellular oxygen homeostasis is regulated by the hypoxia-inducible factor (HIF), a heterodimer that is composed of two subunits HIF-1α and HIF-1β (153). HIF-1α transcriptional activation is triggered by short-term hypoxia of 2–24 h with oxygen tensions <0.1% oxygen, while the isoform HIF-2α activation occurs under milder hypoxic conditions (<5% oxygen). Under *normoxic* conditions, HIF-1α is degraded under control of the von Hippel-Lindau (VHL) protein. Under *hypoxic* conditions, HIF-1α is stabilized and binds to HIF-1β before translocating to the nucleus to bind the hypoxia response elements (HRE) that targets genes involved in intracellular acid-base balances, such as carbonic anhydrase IX (CAIX) (154). Furthermore, it induces transcription of genes involved in glycolysis (including Glut-1, hexokinases (155, 156)), angiogenesis and proliferation (157). While HIF initiates increase in glycolysis, the glycolytic products pyruvate and lactate in their turn induce HIF-1α accumulation, indicative of a sustained feed-forward mechanism driving tumor metabolism towards glycolysis (158, 159).

Another result of HIF-1α upregulation is increased expression of CAIX as is described above (160) and MCT-4 (161). The interaction of CAIX with MCT-1 and MCT-4 is linked to acidification of the TME (162) and associated with poorer prognosis (163) and immune suppression (164). However, whether CAIX expression can serve as a surrogate for tumor hypoxia is debatable (165) and clinical studies on CAIX expression in lung cancer are scarce.

As VEGF is the main mediator of angiogenesis in many types of cancer to cater to chronic hypoxic conditions and as VEGF is under control of HIF signaling, it is also aberrantly expressed in lung cancer (166), in particular in adenocarcinoma (167). The level of VEGF expression is correlated with micro-vessel density and development of hypoxia and is involved in the so-called secondary vascular growth phase (168–170). It is suggested that, although VEGF expression stimulates angiogenesis, the disorganized and immature features of newly formed blood vessels in fact sustain the presence of intra-tumoral regions of hypoxia (171). Consequently, VEGF expression is in most studies correlated to a worse survival in NSCLC (172).

In parallel to oxidative stress, oncogenic mutations in lung cancer can also induce HIF activation, e.g., phosphatase and tensin homolog (PTEN), PI3K/Akt/mTOR pathway (152, 173), or epigenetic alterations (174, 175). As a consequence of increased HIF-1α signaling, PD-L1 expression on lung cancer cells increases (176–179).

## 3.3 How Oxygen Availability Affects T-Cells

On a general note, cancer cells show a greater metabolic plasticity than effector T-cells and have evolved to manipulate the host TME to their benefit, which enables them to utilize a variety of alternative metabolic pathways and substrates also under hypoxic conditions. Consequently, these alternative metabolic pathways often come with side-products, such as ROS, which require an additional set of processes to compensate for collateral damage. Although T-cells have differential metabolic preferences throughout their lifespan, they display limited plasticity or compensating pathways to deal with the 'metabolic waste' from cancer cells, resulting in 'exhausted' states in the TME (93, 101). For example, high levels of ROS in the TME are toxic for T-cells (180–182). Central to these effector function insufficiencies is

mitochondrial function, which shows hyperpolarization, fragmentation, and increased ROS production in the TME (35, 59, 114, 130, 183). Furthermore, intratumoral hypoxia also limits T-cell migration away from the blood vessels into the tumor micro-environment, creating hypoxic immune privileged niches within the tumor (184). Thus, in addition to the limited availability of glucose itself, hypoxia further restricts T-cells' capacity to perform aerobic glycolysis (paragraph 2.3), hampers T-cell infiltration and hypoxia-related waste products directly affects T-cell viability.

## 3.4 How T-Cells Respond to Hypoxic Conditions

As mentioned above, induction of glycolysis is essential for T-cell effector functions and this induction is under control of mitochondrial ROS signaling and HIF-1α under *normoxic* conditions (6, 94) In particular Th17, Th1 CD4+ T-cells and CD8 + T-cells rely on increased glycolysis, whereas regulatory T-cells show less glycolysis dependency (93). For example, upon activation of CD3/CD28 on CD8+ T-cells, the expression of HIF-1α increases *via* PI3K/AKT/mTOR pathways to allow for increased glycolysis and effector functions such as IFN-γ and TNF-α secretion (185, 186). Under *hypoxic* conditions, HIF-1α induces downregulation of IFN-γ production by Th1 cells (187). These observations suggest a complex dual role for HIF-1α signaling in T-cells, which is environment and stimulus dependent. While glycolysis is required for T-cell effector functions, glutaminolysis and the pentose phosphatase pathway are necessary for biosynthesis. T-cell receptor triggering increases amino-acid transporters, along with upregulation of glucose metabolism, and therefore contributes to T-cell activation. However, given its different role glutaminolysis does not compensate for the dependency on glycolysis under hypoxic conditions. In fact, depletion of amino acids in the TME such as L-arginine by myeloid derived suppressor cells, inhibits T-cell proliferation (101). Perhaps the most important alternative metabolic pathways for T-cells in the TME to meet their metabolic demands is fatty acid oxidation (188). T-cell effector function is partially preserved by upregulating PPAR-a signaling to metabolize fatty acids under hypoxic and hypoglycemic conditions (39). Promotion of fatty acid metabolism could synergize with PD-1 blockade to control tumor growth, as shown in a preclinical melanoma model.

## 3.5 Hypoxia Blunts Efficacy of Anti-Cancer Treatment

Several preclinical and human studies have identified roles of hypoxia in blunting treatment efficacy, as a longstanding notion across cancer types (106, 189, 190), and in particular in radiotherapy (191). Radiosensitivity starts to decrease at oxygen tensions below 2% oxygen, most directly by decreased availability of molecules for radiolysis to produce ROS by ionizing radiation. The hypoxia found in cancer also leads to downregulation of the type I IFN pathway, while this pathway is necessary for an adequate immune response.

In addition to directly reducing the therapeutic potential of ionizing radiation, the downregulated type I IFN pathway due to hypoxia impairs immune activation upon immunogenic cell death, a phenomenon that is observed for radio- as wells as chemotherapy (192). Furthermore, regulatory T-cells and memory CD8+ T-cells largely depend on oxidative phosphorylation, which is also restricted under hypoxia (101), and at least partly explains the arduous task of immune activation in hypoxic tumor regions. Lastly, the disturbed vascularization in tumors is known to hamper the intra-tumoral delivery of therapeutic agents, resulting in sub-therapeutic intra-tumoral concentrations (193, 194). To this end, anti-angiogenic treatments have been introduced in adjunct to radiotherapy (191, 195) targeted- or chemotherapy (196, 197). The overall results over combination treatments targeting VEGF in NSCLC so far have been disappointing (198).

More recently, other processes involving tumor vasculature associated endothelial cells have been identified, which act in addition to the typical vessel sprouting induced by hypoxia-driven or mutation-driven PI3K/Akt signaling. These processes include vessel co-option and vascular mimicry and may partly explain previous ambiguous results of combination treatments in NSCLC. These alternative angiogenic process also illustrate the complex network between NSCLC, supporting stromal cells, such as endothelial cells and pericytes, and mobile immune cell populations. It is generally accepted that angiogenesis factors drive an immune suppressive microenvironment (16, 184). In preclinical models VEGF inhibition resulted in enhanced T-cell infiltration and improved anti-cancer immune responses (199) and help the induction of tertiary lymphoid structures. These studies sparked the interest in combining anti-angiogenic treatment with immune checkpoint inhibitors (200).

## 3.6 Imaging Targets Related to Oxygen Availability

Most of the current clinical hypoxia PET tracers are $^{18}$F-fluorinated nitroimidazole compounds, which target the altered redox status in cancer cells and its uptake is increased in hypoxic cells. The mechanism of fluorinated nitroimidazoles is based on an oxygen-reversible single-electron reduction of the nitro group, resulting in the formation of oxygen radicals which covalently bind to macromolecules in hypoxic cells (201), resulting in intracellular trapping of the tracer. In clinical setting, $^{18}$F-fluoromisonidazole ([$^{18}$F]FMISO) is the most widely used tracer for hypoxia (202, 203). However, [$^{18}$F]FMISO has slow clearance and low tumor uptake (204), which led to the development of second generation 2-nitroimidazole tracers, [$^{18}$F]fluoroazomycinarabinofuranoside ([$^{18}$F]FAZA), [$^{18}$F]FETNIM, [$^{18}$F]EF3, [$^{18}$F]EF5 (205). Even a third generation 2-nitroimidazole hypoxia tracer ([$^{18}$F]HX4, **Figure 4**) has been developed and clinically tested, showing more favourable pharmacokinetic and clearance properties than other $^{18}$F-fluorinated nitroimidazole compounds (206, 207). [$^{18}$F]HX4 is for these reasons favored over previous hypoxia tracers for response monitoring to (chemo-)radiation therapy (208–210).

Besides nitroimidazole analogues, other compounds that target the redox status in cancer cells are diacetyl-bis(N (4)-

methylthiosemicarbazone (ATSM), radiolabeled with different copper radioisotopes, or ionic copper (II) (211). [$^{64}$Cu]ATSM has several advantages over other nitroimidazole derivative hypoxia markers, including rapid tumor uptake and faster clearance from normoxic tissues (212). Several studies in lung cancer have shown that radiolabeled ATSM targets different regions within a tumor as compared to [$^{18}$F]FDG (213, 214), and enable prediction of response to radiotherapy (215). Similar findings have been observed in patients with locally advanced HNSCC, in which [$^{62}$Cu]ATSM was evaluated as a predictor of response (216), with results paralleling [$^{18}$F]HX4.

As hypoxia upregulates expression of CAIX on cancer cells, multiple radiotracers have been identified and tested pre-clinically for the imaging of CAIX, such as the anti-CAIX monoclonal antibody (mAb) G250, girentuximab (cG250), girentuximab antibody fragment Fab' and F(ab')2, and more recently affibody molecules. In a recent comparative preclinical study, the affibody ZCAIX:2, antibody fragment girentuximab-F(ab')2, and a complete antibody-based tracer were evaluated for imaging upregulation of CAIX in head and neck cancer xenograft models (217). Radiolabeled girentuximab, girentuximab Fab' and F(ab')2 fragments are also evaluated in human colorectal cancer xenografts (218). According to these studies the complete girentuximab IgG tracer showed the most promising results in both human tumor xenografts. In the clinical setting, the chimeric mAb girentuximab is mostly tested for targeting of CAIX in clear cell renal cell carcinoma (ccRCC) (219), but no clinical studies have been performed on primary lung cancer.

Alternatively to molecular imaging tracers with a particular target in a hypoxia related pathway, multi-modal imaging that combines tissue characteristics, using dynamic contrast enhanced CT, and glucose metabolism, using routine [$^{18}$F]FDG PET, was shown to accurately predict the presence of intra-tumoral regions with hypoxia (as defined by [$^{18}$F]HX4 accumulation (208)).

### 3.7 Hypoxia Imaging to Monitor Response to Immune Checkpoint Inhibition

As the agreement among different hypoxia-related tracers for PET imaging, or agreement with regional [$^{18}$F]FDG uptake in NSCLC is modest (220–224), it remains critical to obtain tissue validation or solid clinical endpoints (225) when incorporating hypoxia tracers in NSCLC studies. However, the most extensively tested hypoxia-related imaging tracer for response prediction in the clinical setting is [$^{18}$F]FMISO. In early stage NSCLC, the combined pattern of high [$^{18}$F]FDG and high [$^{18}$F]FMISO uptake was associated with an increased risk of recurrence after stereotactic radiotherapy (226). Such metabolic profile based in molecular imaging could help in guiding intensity-modulated treatment, as demonstrated in locally advanced NSCLC to avoid deleterious effects on organs-at-risk (227–229).

No studies have yet been performed regarding hypoxia imaging and immunotherapy in NSCLC, but in HNSCC [$^{18}$F]FMISO imaging was used pre-clinically in combined anti-PD-1 and anti-CTLA-4 treatment to monitor changes in the TME during treatment. Preliminary data shows the potential to predict response to checkpoint blockade with anti-PD-1 and anti-CTLA-4 therapy [Reeves et al. *J Nucl Med* 2020, volume 61, supplement 1; 407, meeting report]. In HNSCC patients, increased lymphocyte infiltration is seemingly determined by a hypoxia-dependent response to chemoradiation (230), and persistent hypoxia during definitive chemoradiation treatment correlated with persistent PD-L1 expression and reduced outcomes (230), illustrating the potential of hypoxia related imaging to probe the tumor microenvironment. Several clinical trials are ongoing with [$^{18}$F]FMISO as read-out in radiotherapy trials. One phase IB/II trial is ongoing to examine the feasibility and safety of the combination of two immune checkpoint inhibitor therapies (nivolumab and ipilimumab) in the neoadjuvant setting in resectable HNSCC. In this study, hypoxia measured by [$^{18}$F]FMISO PET imaging is investigated as determinant for the effect of immune checkpoint inhibitors on the intratumoral T cell capacity (NCT03003637).

## 4 GLUTAMINE METABOLISM

### 4.1 Glutaminolysis in Cancer Cells

In addition to glucose, most tumor types also display increased uptake of amino acids, such as glutamine, to meet their high demands in biosynthesis and macromolecular synthesis (79, 231). Glutaminolysis is the intracellular conversion of glutamine to glutamate by glutaminase (GLS). This process is facilitated by the upregulation of the alanine-serine-cysteine transporter 2 (ASCT2, also known as SLC1A5) receptors in different cancer types (231), including lung cancer (232). In particular under low-oxygen conditions, glutamine becomes a carbon source for proliferating cancer cells to perform lipogenesis *via* reductive carboxylation (142), taking over up to 80% of *de novo* lipogenesis in A549 lung carcinoma cells (233). *Via* several other routes, glutaminolysis provides a back-up for metabolic pathways that are usually sustained by glucose metabolism; by providing a source of NADPH (234) and the glycolytic intermediate PEP when gluconeogenesis can no longer be performed (235). Thus, increased glutaminolysis in most cancer types illustrates their metabolic plasticity and provides an alternative source to glycolysis for intracellular bioenergetics. This dual reliance of lung cancer is further illustrated by the upregulation of glutaminolysis once glycolysis is suppressed (236).

Another important role for glutamate in cancer cells is its conversion into glutathione, a critical intracellular redox buffer, which is necessary to counteract the oxidative stress inflicted by aerobic glycolysis (237).

Similar to glycolysis, increased glutaminolysis is driven by increased signaling in the PI3K and/or Akt, which results in increased signaling of mTOR. Lung cancer frequently harbors mutations in the receptor tyrosine kinases or further downstream (238), and some of the metabolic heterogeneity observed in lung cancer cell lines can be attributed to mutations

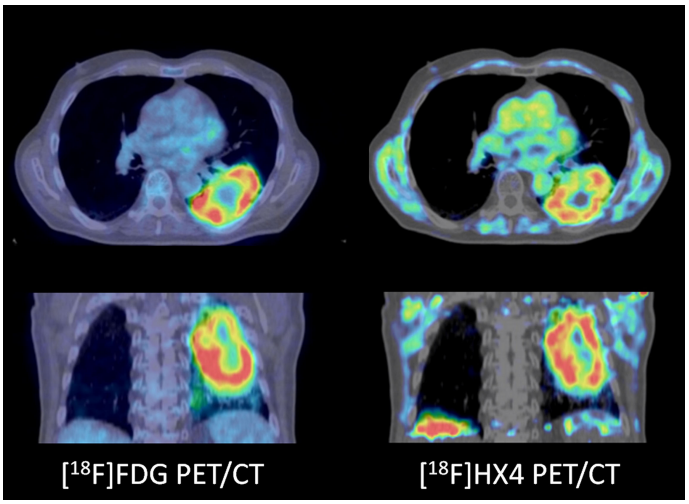


**FIGURE 4** | A patient with a cT3N2M0 non-small cell lung cancer not otherwise specified. PD-L1 status or molecular analyses was not performed. The tumor showed increased [$^{18}$F]FDG uptake (left panels) as well as increased [$^{18}$F]HX4 uptake (right panels), indicative of increased hypoxic stress. Note the regional differences of metabolic profiles in the tumor, for example the cranial part ([$^{18}$F]HX4 more than [$^{18}$F]FDG) versus the caudal part (both [$^{18}$F]HX4 and [$^{18}$F]FDG increased).

in KRAS or Trp53, apart from their histological subtype being adenocarcinoma (239) or squamous cell carcinoma (240).

## 4.2 How Glutaminolysis in Cancer Cells Affect T-Cells

Engagement of the T-cell receptor and the co-stimulatory molecule CD28 triggers pathways under the control of transcription factors HIF-1α and mTOR, which not only increase glycolysis, but also upregulate the expression of amino acid transporters (7). Thus activated and proliferating T-cells also display increased glycolysis and glutaminolysis (94, 100, 241), which associates with the increased expression of SCL1A5 for glutamine (242), similar to cancer cells. *In vitro* experiments demonstrated that glutamine deprivation indeed reduces T-cell proliferation, suppresses differentiation towards Th1 phenotypes but stimulates regulatory FoxP3+ phenotypes (243). In addition to its role as intracellular antioxidant similar to cancer cells, glutathione in T-cells also supports mTOR and NFAT activation, thus driving glycolysis and glutaminolysis (92) and promoting inflammatory responses.

Blocking glutaminolysis in lung cancer cell lines results in upregulation of PD-L1 expression *via* NF-κB activity and dampened T-cell activation, but when glutaminolysis is inhibited together with PD-L1 blockade, the balance tips towards T-cell mediated cancer cell death (37).

Besides glucose, and glutamine, T cells also consume tryptophan. Deprivation of tryptophan can impair the function of these T cells (244). Pathologic conditions as hypoxia induce the presence of IDO on tumors, resulting in a significantly increased tryptophan metabolism by the kynurenine pathway (245). This increase of the metabolic product kynurenine is toxic for T-cells and leads to immunosuppression (246). Tryptophan 2,3-dioxygenase (TDO) is like IDO as it also catalyzes tryptophan into kynurenine (247, 248). Since IDO and TDO both convert tryptophan into kynurenine, they are both important targets to image this tryptophan metabolism.

## 4.3 Imaging Targets Related to Glutamine Metabolism

### 4.3.1 Glutamine Metabolism

Glutamine metabolism in the TME can be visualized using glutamine radiolabelled with $^{18}$F or $^{11}$C (249–251). In preclinical experiments that studied the interplay between glutaminolysis and glycolysis, by using specific inhibitors in squamous cell lung cancer mouse models, PET imaging using [$^{18}$F]FDG or [$^{11}$C]Gln was used to quantify tumor metabolic profiles (240). In a lung cancer xenograft model, as well as in genetically engineered EGFR-mutant lung cancer model, increased [$^{18}$F]Gln correlated with expression levels of SLC1A5 (252). Besides the fluorinated glutamine analogue, another PET tracer has been developed and tested *in vitro* and in animal models, namely L-[5-$^{11}$C]-glutamine ([$^{11}$C]Gln) (250). In contrast to [$^{18}$F]Gln, this tracer is subjected to glutamase activity, converted to glutamic acid and further metabolized.

A clinical study in different cancer types, including lung cancer, supports the preclinical data that [$^{18}$F]Gln (**Figure 5**) can be used as a biomarker of glutamine flux and metabolism in the TME (253–255). However, these studies focus on tumor detection and at present no clinical studies have incorporated glutamine-tracers to classify TME or monitor responses to immunotherapy. One clinical study showed a decrease in [$^{18}$F]Gln uptake in the bone marrow upon chemotherapy with doxorubicin/rituximab, associated with a decrease in number of leukocytes (256). No clinical imaging studies are performed so far with [$^{11}$C]Gln.

Another tracer that can be a potential marker of glutamine metabolism is [$^{18}$F]Fluciclovine, which is predominantly

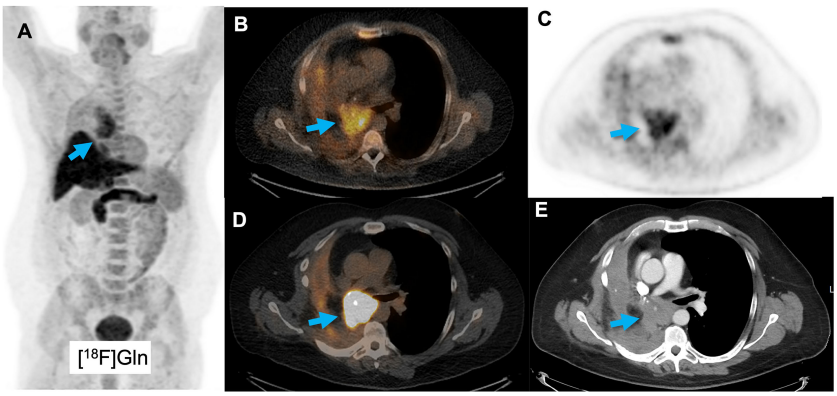


**FIGURE 5** | A patient with a squamous cell lung cancer lesion (arrow) scanned with [$^{18}$F]Gln, showing increased uptake **(A–C)**. Corresponding [$^{18}$F]FDG images show increased uptake as well **(D, E)**.

transported by the glutamine transporter SLC1A5. It is approved by the FDA as radiotracer for prostate malignancies (257), but its uptake is also increased e.g. breast cancer (258, 259) and it has preliminary been investigated to discriminate inflammatory lung lesions from lung cancer (260), with limited success. However, increased [$^{18}$F]Fluciclovine uptake is anecdotally reported in squamous cell carcinoma and adenocarcinoma lung cancer (261), and complementary to [$^{18}$F]FDG PET (**Figure 6**). Also, for this tracer, no studies in the context of immune therapy have yet been performed.

### 4.3.2 Tryptophan Metabolism

Imaging of tryptophan metabolism and presence of IDO in the tumor metabolism is performed by using the clinical available α-[$^{11}$C]methyl-L-tryptophan (AMT) PET tracer (262), in the context of breast, lung cancer and gliomas (263). One phase II study is enlisted on clinicaltrials.gov to investigate [$^{11}$C]AMT as a predictive imaging biomarker of response to immunotherapy with the PD-1 inhibitor Pembrolizumab in melanoma patients (NCT03089606), but this study is not yet recruiting. As its short half-life of this tracer limits clinical application, other tryptophan analogues were developed and tested pre-clinically, such as 1-L-[$^{18}$F]FETrp (264, 265), which will likely be translated to clinical setting.

## 5 DISCUSSION

The incremental use of advanced technologies, such as metabolomics (51) or optical imaging (68), that yield in-depth information on a cellular level, has deepened our understanding of the complexity of tumor metabolism and its impact on other components of the tumor microenvironment. Metabolic adaptation is now an established hallmark of cancer (1) and NSCLC is no exception to this. Prevailing metabolic pathways in lung cancer, its' counterpart in tumor infiltrating T-cells and its'

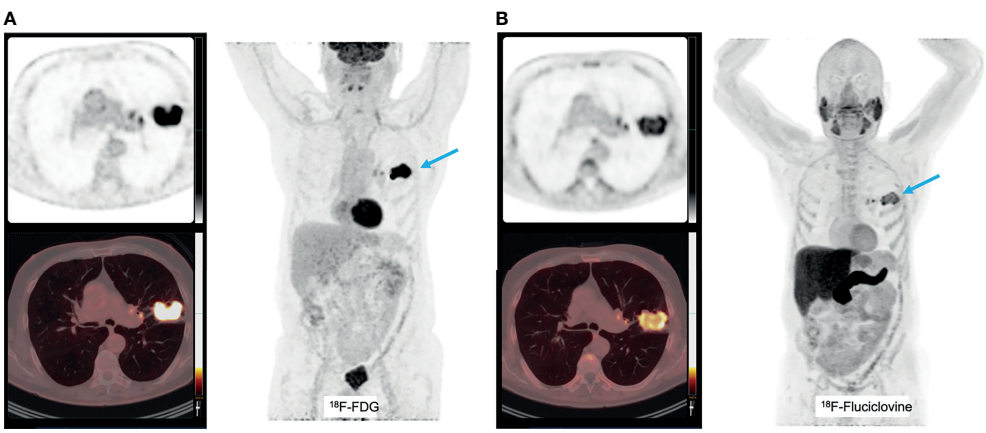


**FIGURE 6** | A patient with a T2bN0 primary adenocarcinoma of the left upper lobe, accidently detected on a [$^{18}$F]Fluciclovine PET/CT scan for prostate cancer staging **(A)**. This tumor was PD-L1 negative and molecular analyses detected mutations in KEAP1, amplification in HER2 and CDK12 and no micro-satellite instability. The corresponding [$^{18}$F]FDG PET images show increased uptake as well **(B)**.

underlying regulatory mechanisms, including the role of immune checkpoint molecules, have been described in this review. Apart from advancing our insights in metabolic pathways in lung cancer cells and T-cells, these high-throughput cell-based technologies applied in *in vitro* studies implicitly pointed towards a role for *in vivo* molecular imaging in translating mechanistic insights into clinical applications. These *in vitro* studies illustrate that the complex interplay between cancer cells and immune cells cannot be fully recapitulated by cell cultures alone, as different metabolic processes might occur in the multi-cellular TME (266), as opposed to mono-cellular cultures. Studies in lung cancer have for example demonstrated that the source of carbon used to fuel mitochondrial metabolism is context dependent. *In vitro*, glutamine is the predominant carbon source for mitochondrial metabolism, whereas *in vivo*, glucose carbon contributes to a greater degree (22, 103, 239, 267). Furthermore, immune cells can to a certain extent adapt their metabolic pathways to tissue specific preferences (74), which is highly relevant when designing novel metabolic interventions to manipulate the TME to enhance anti-cancer immunity. Lastly, intra-tumoral co-existence of clones with differential metabolic dependencies is frequently observed in preclinical models, and mostly relates to impaired treatment outcomes (73). Both these assets, tissue specific immune metabolism and intra-tumoral heterogeneity, can best be investigated with the use of *in vivo* imaging.

As molecular imaging using PET has the potential to complement the current body of knowledge with information on *in vivo* processes in live subjects, tissue specific characteristics and the impact of regional differences in tumor metabolism, radiolabeled metabolic substrates are attractive tracers in the setting of a clinical study. These small molecules have the capacity to rapidly diffuse into tissues, accumulate intracellularly in target cells, often in direct relation to transporter expression and enzyme activity allowing easy kinetic modelling, and rapid clearance. These features translate to simple radiochemistry with short-lived tracers, such as $^{18}$F, with favorable target-to-background ratios obtained within short time frames of minutes to an hour and thus low effective dose for subjects. However, the complicating disadvantage of *in vivo* PET imaging of metabolic pathways in lung cancer is that in fact it quantifies the net result of the targeted metabolic pathway at rather low spatial resolution (268). It does not allow thorough assessment of relative contributions of cancer cells, supportive or immune cells.

Despite this limitation, we envision a clear role for *in vivo* molecular imaging to advance the development of effective treatment for lung cancer in two domains. First, an imaging-based metabolic profile of a lung cancer lesion with conserved spatial information can optimize the efficacy of current standard of care treatments. The rapid clearance and short half-lives of tracers currently in use allow to perform consecutive PET scans with different tracers and thus providing a spatial profile of its dominant metabolic pathways (**Figure 7**). Such multi-modal imaging approach requires solid image registration techniques (269) as well as methods to quantify the correlative data. Although these required imaging processing techniques are yet under development, in principle such technology can be standardized and broadly implemented within current image processing platforms.

Instead of providing merely a summation of glucose metabolism in a lung cancer lesion, measured by its' maximum uptake value ($SUV_{max}$), [$^{18}$F]FDG should be complemented with e.g.[$^{18}$F]Gln or [$^{18}$F]FMISO. When overlaying these quantitative PET-derived datasets, these measures of the downstream net results of regional metabolic interactions in lung cancer provide

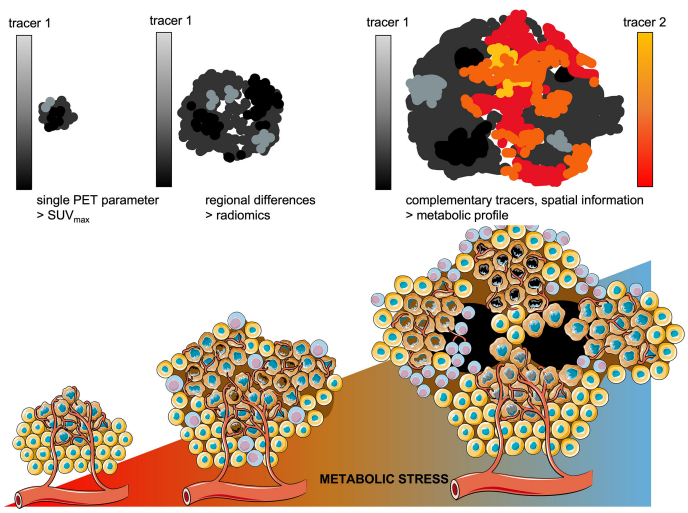


**FIGURE 7** | Towards metabolic profiling of lung cancer using PET/CT imaging. As cancer lesions progress, the metabolic stress increases which enforces metabolic competition between cancer cells and T-cells and drives further diversification of intra-tumoral regional differences. Whereas in smaller lesions single PET parameters might be sufficient to differentiate benign from malignant lesions. As the tumor lesions grow, radiomics are currently applied to quantitate the increasing intra-tumoral heterogeneity. Using complementary tracers, serial PET imaging would allow to address regional differences in dominant metabolic pathways, with conserved spatial information.

an impression whether the metabolic balance is tipped towards glucose dominant metabolism (tracer 1, e.g. [$^{18}$F]FDG) or alternative/compensating metabolic pathways are active (tracer 2, e.g. [$^{18}$F]Gln).

Current approach to assess intra-tumoral (metabolic) heterogeneity is *via* radiomics, which provides quantitative features that describe the distribution of signal intensities in a particular volume-of-interest. Indeed, increased intra-tumoral heterogeneity is inevitably linked to reduced overall survival (73, 270, 271) and this heterogeneity can be traced back to single cell level (272), providing a solid conceptual base for radiomics in lung cancer. Radiomics studies on intra-tumoral (contrast-enhanced) differences in tissue density on CT or differences in glucose metabolism on [$^{18}$F]FDG PET, often identify a correlation between radiomics features and mutation status in lung cancer. Most studies have been insufficient to provide solid prediction upfront of responses to treatment (273–275). This can be explained by the complex interactions of regionally located sub-clones of lung cancer with other cellular components in the TME, as described in this review, which lack a direct link with radiomics-based measures of heterogeneity. Moreover, radiomics analyses lose spatial information, which is necessary to guide local treatments. Thus, imaging-based metabolic profiling of lung cancer based, with conserved spatial information of regional differences within a lesion, will therefore be complementary to radiomics and allow tailoring treatment on a regional level in the tumor (276).

For example, in individualized radiotherapy planning, such information would enable radiotherapy planning based on intra-tumoral regional differences and adapt the radiation portal prior to treatment (277) or during treatment (278). Since 'dose-painting' is increasingly applied in lung cancer, especially in early-stage lung cancer (62, 279) local ablative (stereo-tactic) radiotherapy is considered a reasonable alternative to surgery. The imaging-based metabolic profile of an individual lung tumor may allow personalized dose prescription resulting in minimal toxicity with maximal chance of control in lung cancer. For the locally advanced stage, comprehensive metabolic profiling of lung cancer using a dual-tracer approach might allow selection of patients who will benefit from metabolic interventions accompanying chemoradiotherapy. Previous studies failed to demonstrate benefit in a randomized, unselected approach (280), and the existence of metabolic heterogeneity in a lung cancer lesion is deemed one of the underlying reasons underscoring the necessity to select patients based on the intervention that is addressed.

Second, the metabolic TME is one of the major determinants of an immune suppressive microenvironment for tumor-infiltrating T-cells, and T-cell metabolism is regulated by druggable immune checkpoint molecules such as PD-1. Therefore, complementary to immune imaging, imaging-based metabolic profiling also holds potential in metastatic setting. During PD-1/PD-L1 targeting therapy, tumor-infiltrating T-cells find themselves entangled between the metabolic constraints of the TME and the unleashed potential to accelerate cellular metabolism and execute their cytotoxic function. The incomplete understanding of which metabolic pathways are actual in a particular patient with lung cancer and its' intra-tumoral regional differences, is likely one of the reasons why current response rates are usually below 50%, and for most patients, long-term survival is not the reality (281). For example, if hypoxia is dominating the metabolic TME, adding CD28 blockade by anti-CTLA4 monoclonal antibody to anti- PD-1 therapy might yield higher clinical benefit than in patients where hypoxia is relatively less, and PD-1 inhibition is sufficient to reinvigorate T-cells. In the first line setting, monotherapy immunotherapy, chemo-immunotherapy with and without angiogenesis inhibition (282), chemo-immunotherapy (283) as well as immunotherapy doublets have become available (284). Except for PD-L1 status, current selection for a certain treatment regimen is usually based on national/local standards and preferences. We postulate that imaging-based metabolic profiling can provide an additional role to rationally choose first-line treatment, increase its' efficacy and avoid unnecessary exposure to potential adverse effects.

In addition, the trial-and-error approach in developing novel (combination) immunotherapies is failing (285) and new tools for smarter drug-development pipelines are mandatory. Upon progression on first-line therapy, multiple studies with new immunomodulatory compounds are ongoing, including metabolic interventions (56), usually in a "one-size-fits-all" approach. Complementary to platform trials (e.g. HUDSON (NCT03334617)), attrition rates can probably be improved the metabolic TME is taken into consideration, and results from the few studies that incorporated molecular imaging of metabolic pathways are eagerly awaited.

In conclusion, to advance the treatment landscape of lung cancer, molecular imaging of the metabolic TME should be integrated, as a biomarker tool to support the rational select current treatments and design of next generation of clinical trials.

## AUTHOR'S NOTE

The figures are originally created with use of open-source templates from Servier Medical Art under Creative Commons Attribution 3.0 Unported License, *via* smart.servier.com

## AUTHOR CONTRIBUTIONS

LH and EA drafted the outline of the review. EG and JW performed the literature search and reviewed the retrieved articles. All authors participated in analyzing and writing. All authors contributed to the article and approved the submitted version.

## FUNDING

SH received Dutch Cancer Society grant KWF-YIG10099. EA received Dutch Cancer Society grant KWFYIG12493. MK received funding from Cluster of Excellence iFIT (EXC 2180) "Image Guided and Functionally Instructed Tumor Therapies", University of Tuebingen, Tübingen, Germany.

## ACKNOWLEDGMENTS

We would like to thank prof. Dirk de Ruysscher (Maastro, The Netherlands) for kindly providing an example [$^{18}$F]HX4 PET image, and prof. Jason Lewis and prof. Mark Dunphy (Memorial Sloan Kettering Cancer Center, US) for providing an example on [$^{18}$F]Gln PET imaging in lung cancer.

## REFERENCES

1. Hanahan D, Weinberg RA. Hallmarks of Cancer: The Next Generation. *Cell* (2011) 144(5):646–74. doi: 10.1016/j.cell.2011.02.013
2. Pavlova NN, Thompson CB. The Emerging Hallmarks of Cancer Metabolism. *Cell Metab* (2016) 23(1):27–47. doi: 10.1016/j.cmet.2015.12.006
3. Dowling CM, Zhang H, Chonghaile TN, Wong KK. Shining a Light on Metabolic Vulnerabilities in Non-Small Cell Lung Cancer. *Biochim Biophys Acta Rev Cancer* (2021) 1875(1):188462. doi: 10.1016/j.bbcan.2020.188462
4. Vanhove K, Graulus GJ, Mesotten L, Thomeer M, Derveaux E, Noben JP, et al. The Metabolic Landscape of Lung Cancer: New Insights in a Disturbed Glucose Metabolism. *Front Oncol* (2019) 9:1215. doi: 10.3389/fonc.2019.01215
5. Kumar D, New J, Vishwakarma V, Joshi R, Enders J, Lin F, et al. Cancer-Associated Fibroblasts Drive Glycolysis in a Targetable Signaling Loop Implicated in Head and Neck Squamous Cell Carcinoma Progression. *Cancer Res* (2018) 78(14):3769–82. doi: 10.1158/0008-5472.CAN-17-1076
6. McGettrick AF, O'Neill LAJ. The Role of HIF in Immunity and Inflammation. *Cell Metab* (2020) 32(4):524–36. doi: 10.1016/j.cmet.2020.08.002
7. Wang W, Zou W. Amino Acids and Their Transporters in T Cell Immunity and Cancer Therapy. *Mol Cell* (2020) 80(3):384–95. doi: 10.1016/j.molcel.2020.09.006
8. Ringel AE, Drijvers JM, Baker GJ, Catozzi A, Garcia-Canaveras JC, Gassaway BM, et al. Obesity Shapes Metabolism in the Tumor Microenvironment to Suppress Anti-Tumor Immunity. *Cell* (2020) 183(7):1848–66 e26. doi: 10.1016/j.cell.2020.11.009
9. Lyssiotis CA, Cantley LC. Acetate Fuels the Cancer Engine. *Cell* (2014) 159(7):1492–4. doi: 10.1016/j.cell.2014.12.009
10. Adekola K, Rosen ST, Shanmugam M. Glucose Transporters in Cancer Metabolism. *Curr Opin Oncol* (2012) 24(6):650–4. doi: 10.1097/CCO.0b013e328356da72
11. Amendola CR, Mahaffey JP, Parker SJ, Ahearn IM, Chen WC, Zhou M, et al. KRAS4A Directly Regulates Hexokinase 1. *Nature* (2019) 576(7787):482–6. doi: 10.1038/s41586-019-1832-9
12. Kerr EM, Gaude E, Turrell FK, Frezza C, Martins CP. Mutant Kras Copy Number Defines Metabolic Reprogramming and Therapeutic Susceptibilities. *Nature* (2016) 531(7592):110–3. doi: 10.1038/nature16967
13. Kawada K, Toda K, Sakai Y. Targeting Metabolic Reprogramming in KRAS-Driven Cancers. *Int J Clin Oncol* (2017) 22(4):651–9. doi: 10.1007/s10147-017-1156-4
14. Zaslona Z, O'Neill LAJ. Cytokine-Like Roles for Metabolites in Immunity. *Mol Cell* (2020) 78(5):814–23. doi: 10.1016/j.molcel.2020.04.002
15. Virga F, Ehling M, Mazzone M. Blood Vessel Proximity Shapes Cancer Cell Metabolism. *Cell Metab* (2019) 30(1):16–8. doi: 10.1016/j.cmet.2019.06.011
16. Rahma OE, Hodi FS. The Intersection Between Tumor Angiogenesis and Immune Suppression. *Clin Cancer Res* (2019) 25(18):5449–57. doi: 10.1158/1078-0432.CCR-18-1543
17. Zhang W, Bouchard G, Yu A, Shafiq M, Jamali M, Shrager JB, et al. GFPT2-Expressing Cancer-Associated Fibroblasts Mediate Metabolic Reprogramming in Human Lung Adenocarcinoma. *Cancer Res* (2018) 78(13):3445–57. doi: 10.1158/0008-5472.CAN-17-2928
18. Jeong H, Kim S, Hong BJ, Lee CJ, Kim YE, Bok S, et al. Tumor-Associated Macrophages Enhance Tumor Hypoxia and Aerobic Glycolysis. *Cancer Res* (2019) 79(4):795–806. doi: 10.1158/0008-5472.CAN-18-2545
19. Meijer TWH, Looijen-Salamon MG, Lok J, van den Heuvel M, Tops B, Kaanders J, et al. Glucose and Glutamine Metabolism in Relation to Mutational Status in NSCLC Histological Subtypes. *Thorac Cancer* (2019) 10(12):2289–99. doi: 10.1111/1759-7714.13226
20. Meijer TW, Schuurbiers OC, Kaanders JH, Looijen-Salamon MG, de Geus-Oei LF, Verhagen AF, et al. Differences in Metabolism Between Adeno- and Squamous Cell Non-Small Cell Lung Carcinomas: Spatial Distribution and Prognostic Value of GLUT1 and MCT4. *Lung Cancer* (2012) 76(3):316–23. doi: 10.1016/j.lungcan.2011.11.006
21. Schuurbiers OC, Meijer TW, Kaanders JH, Looijen-Salamon MG, de Geus-Oei LF, van der Drift MA, et al. Glucose Metabolism in NSCLC is Histology-Specific and Diverges the Prognostic Potential of 18FDG-PET for Adenocarcinoma and Squamous Cell Carcinoma. *J Thorac Oncol* (2014) 9(10):1485–93. doi: 10.1097/JTO.0000000000000286
22. Mayers JR, Vander Heiden MG. Nature and Nurture: What Determines Tumor Metabolic Phenotypes? *Cancer Res* (2017) 77(12):3131–4. doi: 10.1158/0008-5472.CAN-17-0165
23. Faubert B, Vincent EE, Griss T, Samborska B, Izreig S, Svensson RU, et al. Loss of the Tumor Suppressor LKB1 Promotes Metabolic Reprogramming of Cancer Cells *via* HIF-1alpha. *Proc Natl Acad Sci U.S.A.* (2014) 111(7):2554–9. doi: 10.1073/pnas.1312570111
24. Bonanno L, Zulato E, Pavan A, Attili I, Pasello G, Conte P, et al. LKB1 and Tumor Metabolism: The Interplay of Immune and Angiogenic Microenvironment in Lung Cancer. *Int J Mol Sci* (2019) 20(8):1874. doi: 10.3390/ijms20081874
25. Watson MJ, Vignali PDA, Mullett SJ, Overacre-Delgoffe AE, Peralta RM, Grebinoski S, et al. Metabolic Support of Tumour-Infiltrating Regulatory T Cells by Lactic Acid. *Nature* (2021) 591(7851):645–51. doi: 10.1038/s41586-020-03045-2
26. Chang CH, Qiu J, O'Sullivan D, Buck MD, Noguchi T, Curtis JD, et al. Metabolic Competition in the Tumor Microenvironment Is a Driver of Cancer Progression. *Cell* (2015) 162(6):1229–41. doi: 10.1016/j.cell.2015.08.016
27. Coleman CN, Eke I, Makinde AY, Chopra S, Demaria S, Formenti SC, et al. Radiation-Induced Adaptive Response: New Potential for Cancer Treatment. *Clin Cancer Res* (2020) 26(22):5781–90. doi: 10.1158/1078-0432.CCR-20-0572
28. Frauwirth KA, Thompson CB. Regulation of T Lymphocyte Metabolism. *J Immunol* (2004) 172(8):4661–5. doi: 10.4049/jimmunol.172.8.4661
29. Pearce EL, Poffenberger MC, Chang CH, Jones RG. Fueling Immunity: Insights Into Metabolism and Lymphocyte Function. *Science* (2013) 342(6155):1242454. doi: 10.1126/science.1242454
30. Frauwirth KA, Riley JL, Harris MH, Parry RV, Rathmell JC, Plas DR, et al. The CD28 Signaling Pathway Regulates Glucose Metabolism. *Immunity* (2002) 16(6):769–77. doi: 10.1016/S1074-7613(02)00323-0
31. Xu K, Yin N, Peng M, Stamatiades EG, Shyu A, Li P, et al. Glycolysis Fuels Phosphoinositide 3-Kinase Signaling to Bolster T Cell Immunity. *Science* (2021) 371(6527):405–10. doi: 10.1126/science.abb2683
32. Palsson-McDermott EM, O'Neill LA. The Warburg Effect Then and Now: From Cancer to Inflammatory Diseases. *Bioessays* (2013) 35(11):965–73. doi: 10.1002/bies.201300084
33. Yu YR, Imrichov a H, Wang H, Chao T, Xiao Z, Gao M, et al. Disturbed Mitochondrial Dynamics in CD8(+) TILs Reinforce T Cell Exhaustion. *Nat Immunol* (2020) 21(12):1540–51. doi: 10.1038/s41590-020-0793-3
34. Vardhana SA, Hwee MA, Berisa M, Wells DK, Yost KE, King B, et al. Impaired Mitochondrial Oxidative Phosphorylation Limits the Self-Renewal of T Cells Exposed to Persistent Antigen. *Nat Immunol* (2020) 21(9):1022–33. doi: 10.1038/s41590-020-0725-2
35. Corrado M, Edwards-Hicks J, Villa M, Flachsmann LJ, Sanin DE, Jacobs M, et al. Dynamic Cardiolipin Synthesis Is Required for CD8(+) T Cell

Immunity. *Cell Metab* (2020) 32(6):981–95 e7. doi: 10.1016/j.cmet.2020.11.003
36. King A, Gottlieb E. Glucose Metabolism and Programmed Cell Death: An Evolutionary and Mechanistic Perspective. *Curr Opin Cell Biol* (2009) 21 (6):885–93. doi: 10.1016/j.ceb.2009.09.009
37. Byun JK, Park M, Lee S, Yun JW, Lee J, Kim JS, et al. Inhibition of Glutamine Utilization Synergizes With Immune Checkpoint Inhibitor to Promote Antitumor Immunity. *Mol Cell* (2020) 80(4):592–606 e8. doi: 10.1016/j.molcel.2020.10.015
38. O'Sullivan D, van der Windt GJW, Huang SCC, Curtis JD, Chang CH, Buck MD, et al. Memory CD8(+) T Cells Use Cell-Intrinsic Lipolysis to Support the Metabolic Programming Necessary for Development (Vol 41, Pg 75, 2014). *Immunity* (2018) 49(2):375–6. doi: 10.1016/j.immuni.2018.07.018
39. Zhang Y, Kurupati R, Liu L, Zhou XY, Zhang G, Hudaihed A, et al. Enhancing CD8(+) T Cell Fatty Acid Catabolism Within a Metabolically Challenging Tumor Microenvironment Increases the Efficacy of Melanoma Immunotherapy. *Cancer Cell* (2017) 32(3):377–91 e9. doi: 10.1016/j.ccell.2017.08.004
40. Wang Y, Gudikote J, Giri U, Yan J, Deng W, Ye R, et al. RAD50 Expression Is Associated With Poor Clinical Outcomes After Radiotherapy for Resected Non-Small Cell Lung Cancer. *Clin Cancer Res* (2018) 24(2):341–50. doi: 10.1158/1078-0432.CCR-17-1455
41. Binder DC, Fu YX, Weichselbaum RR. Radiotherapy and Immune Checkpoint Blockade: Potential Interactions and Future Directions. *Trends Mol Med* (2015) 21(8):463–5. doi: 10.1016/j.molmed.2015.05.007
42. Grassberger C, Ellsworth SG, Wilks MQ, Keane FK, Loeffler JS. Assessing the Interactions Between Radiotherapy and Antitumour Immunity. *Nat Rev Clin Oncol* (2019) 16(12):729–45. doi: 10.1038/s41571-019-0238-9
43. Singh SV, Chaube B, Mayengbam SS, Singh A, Malvi P, Mohammad N, et al. Metformin Induced Lactic Acidosis Impaired Response of Cancer Cells Towards Paclitaxel and Doxorubicin: Role of Monocarboxylate Transporter. *Biochim Biophys Acta Mol Basis Dis* (2021) 1867(3):166011. doi: 10.1016/j.bbadis.2020.166011
44. Dong Q, Zhou C, Ren H, Zhang Z, Cheng F, Xiong Z, et al. Lactate-Induced MRP1 Expression Contributes to Metabolism-Based Etoposide Resistance in Non-Small Cell Lung Cancer Cells. *Cell Commun Signal* (2020) 18(1):167. doi: 10.1186/s12964-020-00653-3
45. Kim J, Lee HM, Cai F, Ko B, Yang C, Lieu EL, et al. The Hexosamine Biosynthesis Pathway is a Targetable Liability in KRAS/LKB1 Mutant Lung Cancer. *Nat Metab* (2020) 2(12):1401–12. doi: 10.1038/s42255-020-00316-0
46. Pupo E, Avanzato D, Middonti E, Bussolino F, Lanzetti L. KRAS-Driven Metabolic Rewiring Reveals Novel Actionable Targets in Cancer. *Front Oncol* (2019) 9:848. doi: 10.3389/fonc.2019.00848
47. Xia M, Li X, Diao Y, Du B, Li Y. Targeted Inhibition of Glutamine Metabolism Enhances the Antitumor Effect of Selumetinib in KRAS-Mutant NSCLC. *Transl Oncol* (2021) 14(1):100920. doi: 10.1016/j.tranon.2020.100920
48. Wang T, Liu G, Wang R. The Intercellular Metabolic Interplay Between Tumor and Immune Cells. *Front Immunol* (2014) 5:358. doi: 10.3389/fimmu.2014.00358
49. Skoulidis F, Goldberg ME, Greenawalt DM, Hellmann MD, Awad MM, Gainor JF, et al. STK11/LKB1 Mutations and PD-1 Inhibitor Resistance in KRAS-Mutant Lung Adenocarcinoma. *Cancer Discovery* (2018) 8(7):822–35. doi: 10.1158/2159-8290.CD-18-0099
50. Boshuizen J, Peeper DS. Rational Cancer Treatment Combinations: An Urgent Clinical Need. *Mol Cell* (2020) 78(6):1002–18. doi: 10.1016/j.molcel.2020.05.031
51. Kaymak I, Williams KS, Cantor JR, Jones RG. Immunometabolic Interplay in the Tumor Microenvironment. *Cancer Cell* (2021) 39(1):28–37. doi: 10.1016/j.ccell.2020.09.004
52. Passarelli A, Aieta M, Sgambato A, Gridelli C. Targeting Immunometabolism Mediated by CD73 Pathway in EGFR-Mutated Non-Small Cell Lung Cancer: A New Hope for Overcoming Immune Resistance. *Front Immunol* (2020) 11:1479. doi: 10.3389/fimmu.2020.01479
53. Passiglia F, Reale ML, Cetoretta V, Novello S. Immune-Checkpoint Inhibitors Combinations in Metastatic NSCLC: New Options on the Horizon? *Immunotargets Ther* (2021) 10:9–26. doi: 10.2147/ITT.S253581
54. Wolf DA. Is Reliance on Mitochondrial Respiration a "Chink in the Armor" of Therapy-Resistant Cancer? *Cancer Cell* (2014) 26(6):788–95. doi: 10.1016/j.ccell.2014.10.001
55. Chang A, Liu L, Ashby JM, Wu D, Chen Y, O'Neill SS, et al. Recruitment of KMT2C/MLL3 to DNA Damage Sites Mediates DNA Damage Responses and Regulates PARP Inhibitor Sensitivity in Cancer. *Cancer Res* (2021) 81 (12):3358–73. doi: 10.1158/0008-5472.CAN-21-0688
56. Boreel DF, Span PN, Heskamp S, Adema GJ, Bussink J. Targeting Oxidative Phosphorylation to Increase the Efficacy of Radio- and Immune-Combination Therapy. *Clin Cancer Res* (2021) 27(11):2970–8. doi: 10.1158/1078-0432.CCR-20-3913
57. Chu H, Zhou J, Wong BH, Li C, Chan JF, Cheng ZS, et al. Middle East Respiratory Syndrome Coronavirus Efficiently Infects Human Primary T Lymphocytes and Activates the Extrinsic and Intrinsic Apoptosis Pathways. *J Infect Dis* (2016) 213(6):904–14. doi: 10.1093/infdis/jiv380
58. Chuang CH, Dorsch M, Dujardin P, Silas S, Ueffing K, Holken JM, et al. Altered Mitochondria Functionality Defines a Metastatic Cell State in Lung Cancer and Creates an Exploitable Vulnerability. *Cancer Res* (2021) 81 (3):567–79. doi: 10.1158/0008-5472.CAN-20-1865
59. Topper MJ, Vaz M, Marrone KA, Brahmer JR, Baylin SB. The Emerging Role of Epigenetic Therapeutics in Immuno-Oncology. *Nat Rev Clin Oncol* (2020) 17(2):75–90. doi: 10.1038/s41571-019-0266-5
60. Kunimasa K, Nagano T, Shimono Y, Dokuni R, Kiriu T, Tokunaga S, et al. Glucose Metabolism-Targeted Therapy and Withaferin A are Effective for Epidermal Growth Factor Receptor Tyrosine Kinase Inhibitor-Induced Drug-Tolerant Persisters. *Cancer Sci* (2017) 108(7):1368–77. doi: 10.1111/cas.13266
61. Vasan K, Werner M, Chandel NS. Mitochondrial Metabolism as a Target for Cancer Therapy. *Cell Metab* (2020) 32(3):341–52. doi: 10.1016/j.cmet.2020.06.019
62. Skwarski M, McGowan DR, Belcher E, Di Chiara F, Stavroulias D, McCole M, et al. Mitochondrial Inhibitor Atovaquone Increases Tumor Oxygenation and Inhibits Hypoxic Gene Expression in Patients With Non-Small Cell Lung Cancer. *Clin Cancer Res* (2021) 27(9):2459–69. doi: 10.1158/1078-0432.CCR-20-4128
63. Wiley CD, Campisi J. From Ancient Pathways to Aging Cells-Connecting Metabolism and Cellular Senescence. *Cell Metab* (2016) 23(6):1013–21. doi: 10.1016/j.cmet.2016.05.010
64. Braumuller H, Wieder T, Brenner E, Assmann S, Hahn M, Alkhaled M, et al. T-Helper-1-Cell Cytokines Drive Cancer Into Senescence. *Nature* (2013) 494(7437):361–5. doi: 10.1038/nature11824
65. Brenner E, Schorg BF, Ahmetlic F, Wieder T, Hilke FJ, Simon N, et al. Cancer Immune Control Needs Senescence Induction by Interferon-Dependent Cell Cycle Regulator Pathways in Tumours. *Nat Commun* (2020) 11(1):1335. doi: 10.1038/s41467-020-14987-6
66. Wu C, Li F, Niu G, Chen X. PET Imaging of Inflammation Biomarkers. *Theranostics* (2013) 3(7):448–66. doi: 10.7150/thno.6592
67. Di Gialleonardo V, Wilson DM, Keshari KR. The Potential of Metabolic Imaging. *Semin Nucl Med* (2016) 46(1):28–39. doi: 10.1053/j.semnuclmed.2015.09.004
68. Ntziachristos V, Pleitez MA, Aime S, Brindle KM. Emerging Technologies to Image Tissue Metabolism. *Cell Metab* (2019) 29(3):518–38. doi: 10.1016/j.cmet.2018.09.004
69. Krekorian M, Fruhwirth GO, Srinivas M, Figdor CG, Heskamp S, Witney TH, et al. Imaging of T-Cells and Their Responses During Anti-Cancer Immunotherapy. *Theranostics* (2019) 9(25):7924–47. doi: 10.7150/thno.37924
70. O'Connor JP, Aboagye EO, Adams JE, Aerts HJ, Barrington SF, Beer AJ, et al. Imaging Biomarker Roadmap for Cancer Studies. *Nat Rev Clin Oncol* (2017) 14(3):169–86. doi: 10.1038/nrclinonc.2016.162
71. de Vries EGE, Kist de Ruijter L, Lub-de Hooge MN, Dierckx RA, Elias SG, Oosting SF. Integrating Molecular Nuclear Imaging in Clinical Research to Improve Anticancer Therapy. *Nat Rev Clin Oncol* (2019) 16(4):241–55. doi: 10.1038/s41571-018-0123-y
72. Fruhwirth GO, Kneilling M, de Vries IJM, Weigelin B, Srinivas M, Aarntzen E. The Potential of *In Vivo* Imaging for Optimization of Molecular and Cellular Anti-Cancer Immunotherapies. *Mol Imaging Biol* (2018) 20(5):696–704. doi: 10.1007/s11307-018-1254-3
73. Robertson-Tessi M, Gillies RJ, Gatenby RA, Anderson AR. Impact of Metabolic Heterogeneity on Tumor Growth, Invasion, and Treatment Outcomes. *Cancer Res* (2015) 75(8):1567–79. doi: 10.1158/0008-5472.CAN-14-1428

74. Varanasi SK, Kumar SV, Rouse BT. Determinants of Tissue-Specific Metabolic Adaptation of T Cells. *Cell Metab* (2020) 32(6):908–19. doi: 10.1016/j.cmet.2020.10.013
75. Ma EH, Verway MJ, Johnson RM, Roy DG, Steadman M, Hayes S, et al. Metabolic Profiling Using Stable Isotope Tracing Reveals Distinct Patterns of Glucose Utilization by Physiologically Activated CD8(+) T Cells. *Immunity* (2019) 51(5):856–70 e5. doi: 10.1016/j.immuni.2019.09.003
76. Warburg O. On Respiratory Impairment in Cancer Cells. *Science* (1956) 124 (3215):269–70. doi: 10.1126/science.124.3215.269
77. Gatenby RA, Gillies RJ. Why do Cancers Have High Aerobic Glycolysis? *Nat Rev Cancer* (2004) 4(11):891–9. doi: 10.1038/nrc1478
78. Teicher BA, Linehan WM, Helman LJ. Targeting Cancer Metabolism. *Clin Cancer Res* (2012) 18(20):5537–45. doi: 10.1158/1078-0432.CCR-12-2587
79. Vander Heiden MG, Cantley LC, Thompson CB. Understanding the Warburg Effect: The Metabolic Requirements of Cell Proliferation. *Science* (2009) 324(5930):1029–33. doi: 10.1126/science.1160809
80. Wu J, Hu L, Wu F, Zou L, He T. Poor Prognosis of Hexokinase 2 Overexpression in Solid Tumors of Digestive System: A Meta-Analysis. *Oncotarget* (2017) 8(19):32332–44. doi: 10.18632/oncotarget.15974
81. Alfarouk KO. Tumor Metabolism, Cancer Cell Transporters, and Microenvironmental Resistance. *J Enzyme Inhib Med Chem* (2016) 31 (6):859–66. doi: 10.3109/14756366.2016.1140753
82. Warburg O. Iron, the Oxygen-Carrier of Respiration-Ferment. *Science* (1925) 61(1588):575–82. doi: 10.1126/science.61.1588.575
83. Maddocks OD, Vousden KH. Metabolic Regulation by P53. *J Mol Med (Berl)* (2011) 89(3):237–45. doi: 10.1007/s00109-011-0735-5
84. White E. Exploiting the Bad Eating Habits of Ras-Driven Cancers. *Genes Dev* (2013) 27(19):2065–71. doi: 10.1101/gad.228122.113
85. Zhao J, Lin X, Meng D, Zeng L, Zhuang R, Huang S, et al. Nrf2 Mediates Metabolic Reprogramming in Non-Small Cell Lung Cancer. *Front Oncol* (2020) 10:578315. doi: 10.3389/fonc.2020.578315
86. Mohammad HP, Barbash O, Creasy CL. Targeting Epigenetic Modifications in Cancer Therapy: Erasing the Roadmap to Cancer. *Nat Med* (2019) 25 (3):403–18. doi: 10.1038/s41591-019-0376-8
87. You JS, Jones PA. Cancer Genetics and Epigenetics: Two Sides of the Same Coin? *Cancer Cell* (2012) 22(1):9–20. doi: 10.1016/j.ccr.2012.06.008
88. Saggese P, Sellitto A, Martinez CA, Giurato G, Nassa G, Rizzo F, et al. Metabolic Regulation of Epigenetic Modifications and Cell Differentiation in Cancer. *Cancers (Basel)* (2020) 12(12):3788. doi: 10.3390/cancers12123788
89. Gupta V, Gopinath P, Iqbal MA, Mazurek S, Wellen KE, Bamezai RN. Interplay Between Epigenetics & Cancer Metabolism. *Curr Pharm Des* (2014) 20(11):1706–14. doi: 10.2174/13816128113199990536
90. Fox CJ, Hammerman PS, Thompson CB. Fuel Feeds Function: Energy Metabolism and the T-Cell Response. *Nat Rev Immunol* (2005) 5(11):844–52. doi: 10.1038/nri1710
91. Buck MD, Sowell RT, Kaech SM, Pearce EL. Metabolic Instruction of Immunity. *Cell* (2017) 169(4):570–86. doi: 10.1016/j.cell.2017.04.004
92. Mak TW, Grusdat M, Duncan GS, Dostert C, Nonnenmacher Y, Cox M, et al. Glutathione Primes T Cell Metabolism for Inflammation. *Immunity* (2017) 46(6):1089–90. doi: 10.1016/j.immuni.2017.06.009
93. Bantug GR, Galluzzi L, Kroemer G, Hess C. The Spectrum of T Cell Metabolism in Health and Disease. *Nat Rev Immunol* (2018) 18(1):19–34. doi: 10.1038/nri.2017.99
94. Pearce EL, Pearce EJ. Metabolic Pathways in Immune Cell Activation and Quiescence. *Immunity* (2013) 38(4):633–43. doi: 10.1016/j.immuni.2013.04.005
95. Kareva I, Berezovskaya F. Cancer Immunoediting: A Process Driven by Metabolic Competition as a Predator-Prey-Shared Resource Type Model. *J Theor Biol* (2015) 380:463–72. doi: 10.1016/j.jtbi.2015.06.007
96. Kareva I, Hahnfeldt P. The Emerging "Hallmarks" of Metabolic Reprogramming and Immune Evasion: Distinct or Linked? *Cancer Res* (2013) 73(9):2737–42. doi: 10.1158/0008-5472.CAN-12-3696
97. Lim S, Phillips JB, Madeira da Silva L, Zhou M, Fodstad O, Owen LB, et al. Interplay Between Immune Checkpoint Proteins and Cellular Metabolism. *Cancer Res* (2017) 77(6):1245–9. doi: 10.1158/0008-5472.CAN-16-1647
98. Chang CH, Curtis JD, Maggi LBJr., Faubert B, Villarino AV, O'Sullivan D, et al. Posttranscriptional Control of T Cell Effector Function by Aerobic Glycolysis. *Cell* (2013) 153(6):1239–51. doi: 10.1016/j.cell.2013.05.016
99. Cham CM, Driessens G, O'Keefe JP, Gajewski TF. Glucose Deprivation Inhibits Multiple Key Gene Expression Events and Effector Functions in CD8+ T Cells. *Eur J Immunol* (2008) 38(9):2438–50. doi: 10.1002/eji.200838289
100. Olenchock BA, Rathmell JC, Vander Heiden MG. Biochemical Underpinnings of Immune Cell Metabolic Phenotypes. *Immunity* (2017) 46(5):703–13. doi: 10.1016/j.immuni.2017.04.013
101. Biswas SK. Metabolic Reprogramming of Immune Cells in Cancer Progression. *Immunity* (2015) 43(3):435–49. doi: 10.1016/j.immuni.2015.09.001
102. Cascone T, McKenzie JA, Mbofung RM, Punt S, Wang Z, Xu C, et al. Increased Tumor Glycolysis Characterizes Immune Resistance to Adoptive T Cell Therapy. *Cell Metab* (2018) 27(5):977–87 e4. doi: 10.1016/j.cmet.2018.02.024
103. Fischer K, Hoffmann P, Voelkl S, Meidenbauer N, Ammer J, Edinger M, et al. Inhibitory Effect of Tumor Cell-Derived Lactic Acid on Human T Cells. *Blood* (2007) 109(9):3812–9. doi: 10.1182/blood-2006-07-035972
104. Vander Heiden MG, DeBerardinis RJ. Understanding the Intersections Between Metabolism and Cancer Biology. *Cell* (2017) 168(4):657–69. doi: 10.1016/j.cell.2016.12.039
105. Kato Y, Ozawa S, Miyamoto C, Maehata Y, Suzuki A, Maeda T, et al. Acidic Extracellular Microenvironment and Cancer. *Cancer Cell Int* (2013) 13 (1):89. doi: 10.1186/1475-2867-13-89
106. Brizel DM, Schroeder T, Scher RL, Walenta S, Clough RW, Dewhirst MW, et al. Elevated Tumor Lactate Concentrations Predict for an Increased Risk of Metastases in Head-and-Neck Cancer. *Int J Radiat Oncol Biol Phys* (2001) 51 (2):349–53. doi: 10.1016/S0360-3016(01)01630-3
107. Pilon-Thomas S, Kodumudi KN, El-Kenawi AE, Russell S, Weber AM, Luddy K, et al. Neutralization of Tumor Acidity Improves Antitumor Responses to Immunotherapy. *Cancer Res* (2016) 76(6):1381–90. doi: 10.1158/0008-5472.CAN-15-1743
108. Husain Z, Huang Y, Seth P, Sukhatme VP. Tumor-Derived Lactate Modifies Antitumor Immune Response: Effect on Myeloid-Derived Suppressor Cells and NK Cells. *J Immunol* (2013) 191(3):1486–95. doi: 10.4049/jimmunol.1202702
109. Bengsch B, Johnson AL, Kurachi M, Odorizzi PM, Pauken KE, Attanasio J, et al. Bioenergetic Insufficiencies Due to Metabolic Alterations Regulated by the Inhibitory Receptor PD-1 Are an Early Driver of CD8(+) T Cell Exhaustion. *Immunity* (2016) 45(2):358–73. doi: 10.1016/j.immuni.2016.07.008
110. Boussiotis VA. Molecular and Biochemical Aspects of the PD-1 Checkpoint Pathway. *N Engl J Med* (2016) 375(18):1767–78. doi: 10.1056/NEJMra1514296
111. Sharpe AH, Pauken KE. The Diverse Functions of the PD1 Inhibitory Pathway. *Nat Rev Immunol* (2018) 18(3):153–67. doi: 10.1038/nri.2017.108
112. McKinney EF, Smith KGC. Metabolic Exhaustion in Infection, Cancer and Autoimmunity. *Nat Immunol* (2018) 19(3):213–21. doi: 10.1038/s41590-018-0045-y
113. Choueiri TK, Fishman MN, Escudier B, McDermott DF, Drake CG, Kluger H, et al. Immunomodulatory Activity of Nivolumab in Metastatic Renal Cell Carcinoma. *Clin Cancer Res* (2016) 22(22):5461–71. doi: 10.1158/1078-0432.CCR-15-2839
114. Rivadeneira DB, Delgoffe GM. Antitumor T-Cell Reconditioning: Improving Metabolic Fitness for Optimal Cancer Immunotherapy. *Clin Cancer Res* (2018) 24(11):2473–81. doi: 10.1158/1078-0432.CCR-17-0894
115. Boellaard R, O'Doherty MJ, Weber WA, Mottaghy FM, Lonsdale MN, Stroobants SG, et al. FDG PET and PET/CT: EANM Procedure Guidelines for Tumour PET Imaging: Version 1. *0 Eur J Nucl Med Mol Imaging* (2010) 37(1):181–200. doi: 10.1007/s00259-009-1297-4
116. Wahl RL, Jacene H, Kasamon Y, Lodge MA. From RECIST to PERCIST: Evolving Considerations for PET Response Criteria in Solid Tumors. *J Nucl Med* (2009) 50(Suppl 1):122S–50S. doi: 10.2967/jnumed.108.057307
117. Usmanij EA, de Geus-Oei LF, Troost EG, Peters-Bax L, van der Heijden EH, Kaanders JH, et al. 18f-FDG PET Early Response Evaluation of Locally Advanced Non-Small Cell Lung Cancer Treated With Concomitant Chemoradiotherapy. *J Nucl Med* (2013) 54(9):1528–34. doi: 10.2967/jnumed.112.116921
118. Brown RS, Leung JY, Fisher SJ, Frey KA, Ethier SP, Wahl RL. Intratumoral Distribution of Tritiated-FDG in Breast Carcinoma: Correlation Between

Glut-1 Expression and FDG Uptake. *J Nucl Med* (1996) 37(6):1042–7 https://jnm.snmjournals.org/content/37/6/1042.long.
119. Avril N, Menzel M, Dose J, Schelling M, Weber W, Janicke F, et al. Glucose Metabolism of Breast Cancer Assessed by 18F-FDG PET: Histologic and Immunohistochemical Tissue Analysis. *J Nucl Med* (2001) 42(1):9–16 https://jnm.snmjournals.org/content/42/1/9.long.
120. Hansen AE, Gutte H, Holst P, Johannesen HH, Rahbek S, Clemmensen AE, et al. Combined Hyperpolarized (13)C-Pyruvate MRS and (18)F-FDG PET (hyperPET) Estimates of Glycolysis in Canine Cancer Patients. *Eur J Radiol* (2018) 103:6–12. doi: 10.1016/j.ejrad.2018.02.028
121. Lopci E, Toschi L, Grizzi F, Rahal D, Olivari L, Castino GF, et al. Correlation of Metabolic Information on FDG-PET With Tissue Expression of Immune Markers in Patients With Non-Small Cell Lung Cancer (NSCLC) Who are Candidates for Upfront Surgery. *Eur J Nucl Med Mol Imaging* (2016) 43 (11):1954–61. doi: 10.1007/s00259-016-3425-2
122. Takada K, Toyokawa G, Okamoto T, Baba S, Kozuma Y, Matsubara T, et al. Metabolic Characteristics of Programmed Cell Death-Ligand 1-Expressing Lung Cancer on (18) F-Fluorodeoxyglucose Positron Emission Tomography/Computed Tomography. *Cancer Med* (2017) 6(11):2552–61. doi: 10.1002/cam4.1215
123. Hu B, Chen W, Zhang Y, Shi H, Cheng D, Xiu Y. (18)F-FDG Maximum Standard Uptake Value Predicts PD-L1 Expression on Tumor Cells or Tumor-Infiltrating Immune Cells in Non-Small Cell Lung Cancer. *Ann Nucl Med* (2020) 34(5):322–8. doi: 10.1007/s12149-020-01451-0
124. Kaira K, Shimizu K, Kitahara S, Yajima T, Atsumi J, Kosaka T, et al. 2-Deoxy-2-[Fluorine-18] Fluoro-D-Glucose Uptake on Positron Emission Tomography is Associated With Programmed Death Ligand-1 Expression in Patients With Pulmonary Adenocarcinoma. *Eur J Cancer* (2018) 101:181–90. doi: 10.1016/j.ejca.2018.06.022
125. Grizzi F, Castello A, Lopci E. Is it Time to Change Our Vision of Tumor Metabolism Prior to Immunotherapy? *Eur J Nucl Med Mol Imaging* (2018) 45(6):1072–5. doi: 10.1007/s00259-018-3988-1
126. Mitchell KG, Amini B, Wang Y, Carter BW, Godoy MCB, Parra ER, et al. (18)F-Fluorodeoxyglucose Positron Emission Tomography Correlates With Tumor Immunometabolic Phenotypes in Resected Lung Cancer. *Cancer Immunol Immunother* (2020) 69(8):1519–34. doi: 10.1007/s00262-020-02560-5
127. Ottensmeier CH, Perry KL, Harden EL, Stasakova J, Jenei V, Fleming J, et al. Upregulated Glucose Metabolism Correlates Inversely With CD8+ T-Cell Infiltration and Survival in Squamous Cell Carcinoma. *Cancer Res* (2016) 76 (14):4136–48. doi: 10.1158/0008-5472.CAN-15-3121
128. Na KJ, Choi H. Tumor Metabolic Features Identified by (18)F-FDG PET Correlate With Gene Networks of Immune Cell Microenvironment in Head and Neck Cancer. *J Nucl Med* (2018) 59(1):31–7. doi: 10.2967/jnumed.117.194217
129. Singer K, Kastenberger M, Gottfried E, Hammerschmied CG, Buttner M, Aigner M, et al. Warburg Phenotype in Renal Cell Carcinoma: High Expression of Glucose-Transporter 1 (GLUT-1) Correlates With Low CD8 (+) T-Cell Infiltration in the Tumor. *Int J Cancer* (2011) 128(9):2085–95. doi: 10.1002/ijc.25543
130. Siska PJ, Beckermann KE, Mason FM, Andrejeva G, Greenplate AR, Sendor AB, et al. Mitochondrial Dysregulation and Glycolytic Insufficiency Functionally Impair CD8 T Cells Infiltrating Human Renal Cell Carcinoma. *JCI Insight* (2017) 2(12):e93411. doi: 10.1172/jci.insight.93411
131. Nobashi T, Baratto L, Reddy SA, Srinivas S, Toriihara A, Hatami N, et al. Predicting Response to Immunotherapy by Evaluating Tumors, Lymphoid Cell-Rich Organs, and Immune-Related Adverse Events Using FDG-PET/Ct. *Clin Nucl Med* (2019) 44(4):e272–e9. doi: 10.1097/RLU.0000000000002453
132. Cho SY, Lipson EJ, Im HJ, Rowe SP, Gonzalez EM, Blackford A, et al. Prediction of Response to Immune Checkpoint Inhibitor Therapy Using Early-Time-Point (18)F-FDG PET/CT Imaging in Patients With Advanced Melanoma. *J Nucl Med* (2017) 58(9):1421–8. doi: 10.2967/jnumed.116.188839
133. Ito K, Teng R, Schoder H, Humm JL, Ni A, Michaud L, et al. (18)F-FDG PET/CT for Monitoring of Ipilimumab Therapy in Patients With Metastatic Melanoma. *J Nucl Med* (2019) 60(3):335–41. doi: 10.2967/jnumed.118.213652
134. Sachpekidis C, Anwar H, Winkler J, Kopp-Schneider A, Larribere L, Haberkorn U, et al. The Role of Interim (18)F-FDG PET/CT in Prediction of Response to Ipilimumab Treatment in Metastatic Melanoma. *Eur J Nucl Med Mol Imaging* (2018) 45(8):1289–96. doi: 10.1007/s00259-018-3972-9
135. Dimitrakopoulou-Strauss A. Monitoring of Patients With Metastatic Melanoma Treated With Immune Checkpoint Inhibitors Using PET-Ct. *Cancer Immunol Immunother* (2019) 68(5):813–22. doi: 10.1007/s00262-018-2229-6
136. Aide N, Hicks RJ, Le Tourneau C, Lheureux S, Fanti S, Lopci E. FDG PET/CT for Assessing Tumour Response to Immunotherapy : Report on the EANM Symposium on Immune Modulation and Recent Review of the Literature. *Eur J Nucl Med Mol Imaging* (2019) 46(1):238–50. doi: 10.1007/s00259-018-4171-4
137. Iravani A, Hicks RJ. Imaging the Cancer Immune Environment and Its Response to Pharmacologic Intervention, Part 2: The Role of Novel PET Agents. *J Nucl Med* (2020) 61(11):1553–9. doi: 10.2967/jnumed.120.248823
138. Prigent K, Lasnon C, Ezine E, Janson M, Coudrais N, Joly E, et al. Assessing Immune Organs on (18)F-FDG PET/CT Imaging for Therapy Monitoring of Immune Checkpoint Inhibitors: Inter-Observer Variability, Prognostic Value and Evolution During the Treatment Course of Melanoma Patients. *Eur J Nucl Med Mol Imaging* (2021) 48(8):2573–85. doi: 10.1007/s00259-020-05103-3
139. Seith F, Forschner A, Weide B, Guckel B, Schwartz M, Schwenck J, et al. Is There a Link Between Very Early Changes of Primary and Secondary Lymphoid Organs in (18)F-FDG-PET/MRI and Treatment Response to Checkpoint Inhibitor Therapy? *J Immunother Cancer* (2020) 8(2):e000656. doi: 10.1136/jitc-2020-000656
140. Wong A, Callahan J, Keyaerts M, Neyns B, Mangana J, Aberle S, et al. (18)F-FDG PET/CT Based Spleen to Liver Ratio Associates With Clinical Outcome to Ipilimumab in Patients With Metastatic Melanoma. *Cancer Imaging* (2020) 20(1):36. doi: 10.1186/s40644-020-00313-2
141. Nakamoto R, Zaba LC, Liang T, Reddy SA, Davidzon G, Aparici CM, et al. Prognostic Value of Bone Marrow Metabolism on Pretreatment (18)F-FDG PET/CT in Patients With Metastatic Melanoma Treated With Anti-PD-1 Therapy. *J Nucl Med* (2021) 62(10):1380–3. doi: 10.2967/jnumed.120.254482
142. Vander Heiden MG, Lunt SY, Dayton TL, Fiske BP, Israelsen WJ, Mattaini KR, et al. Metabolic Pathway Alterations That Support Cell Proliferation. *Cold Spring Harb Symp Quant Biol* (2011) 76:325–34. doi: 10.1101/sqb.2012.76.010900
143. Rademakers SE, Span PN, Kaanders JH, Sweep FC, van der Kogel AJ, Bussink J. Molecular Aspects of Tumour Hypoxia. *Mol Oncol* (2008) 2(1):41–53. doi: 10.1016/j.molonc.2008.03.006
144. DeBerardinis RJ, Chandel NS. Fundamentals of Cancer Metabolism. *Sci Adv* (2016) 2(5):e1600200. doi: 10.1126/sciadv.1600200
145. Semenza GL, Jiang BH, Leung SW, Passantino R, Concordet JP, Maire P, et al. Hypoxia response elements in the aldolase AEnolase 1, and Lactate Dehydrogenase A Gene Promoters Contain Essential Binding Sites for Hypoxia-Inducible Factor 1. *J Biol Chem* (1996) 271(51):32529–37. doi: 10.1074/jbc.271.51.32529
146. Busk M, Walenta S, Mueller-Klieser W, Steiniche T, Jakobsen S, Horsman MR, et al. Inhibition of Tumor Lactate Oxidation: Consequences for the Tumor Microenvironment. *Radiother Oncol* (2011) 99(3):404–11. doi: 10.1016/j.radonc.2011.05.053
147. Hong WX, Hu MS, Esquivel M, Liang GY, Rennert RC, McArdle A, et al. The Role of Hypoxia-Inducible Factor in Wound Healing. *Adv Wound Care (New Rochelle)* (2014) 3(5):390–9. doi: 10.1089/wound.2013.0520
148. Nathan SD, Barbera JA, Gaine SP, Harari S, Martinez FJ, Olschewski H, et al. Pulmonary Hypertension in Chronic Lung Disease and Hypoxia. *Eur Respir J* (2019) 53(1):1801914. doi: 10.1183/13993003.01914-2018
149. Glasauer A, Chandel NS. Targeting Antioxidants for Cancer Therapy. *Biochem Pharmacol* (2014) 92(1):90–101. doi: 10.1016/j.bcp.2014.07.017
150. Nogueira V, Hay N. Molecular Pathways: Reactive Oxygen Species Homeostasis in Cancer Cells and Implications for Cancer Therapy. *Clin Cancer Res* (2013) 19(16):4309–14. doi: 10.1158/1078-0432.CCR-12-1424
151. Kumar S, Sharife H, Kreisel T, Mogilevsky M, Bar-Lev L, Grunewald M, et al. Intra-Tumoral Metabolic Zonation and Resultant Phenotypic Diversification Are Dictated by Blood Vessel Proximity. *Cell Metab* (2019) 30(1):201–11 e6. doi: 10.1016/j.cmet.2019.04.003
152. Gorrini C, Harris IS, Mak TW. Modulation of Oxidative Stress as an Anticancer Strategy. *Nat Rev Drug Discov* (2013) 12(12):931–47. doi: 10.1038/nrd4002

153. Kakkad S, Krishnamachary B, Jacob D, Pacheco-Torres J, Goggins E, Bharti SK, et al. Molecular and Functional Imaging Insights Into the Role of Hypoxia in Cancer Aggression. *Cancer Metastasis Rev* (2019) 38(1-2):51–64. doi: 10.1007/s10555-019-09788-3
154. Semenza GL. Targeting HIF-1 for Cancer Therapy. *Nat Rev Cancer* (2003) 3 (10):721–32. doi: 10.1038/nrc1187
155. Peyssonnaux C, Zinkernagel AS, Schuepbach RA, Rankin E, Vaulont S, Haase VH, et al. Regulation of Iron Homeostasis by the Hypoxia-Inducible Transcription Factors (HIFs). *J Clin Invest* (2007) 117(7):1926–32. doi: 10.1172/JCI31370
156. Tannahill GM, Curtis AM, Adamik J, Palsson-McDermott EM, McGettrick AF, Goel G, et al. Succinate is an Inflammatory Signal That Induces IL-1beta Through HIF-1alpha. *Nature* (2013) 496(7444):238–42. doi: 10.1038/nature11986
157. Carmeliet P, Dor Y, Herbert JM, Fukumura D, Brusselmans K, Dewerchin M, et al. Role of HIF-1alpha in Hypoxia-Mediated Apoptosis, Cell Proliferation and Tumour Angiogenesis. *Nature* (1998) 394(6692):485–90. doi: 10.1038/28867
158. McFate T, Mohyeldin A, Lu H, Thakar J, Henriques J, Halim ND, et al. Pyruvate Dehydrogenase Complex Activity Controls Metabolic and Malignant Phenotype in Cancer Cells. *J Biol Chem* (2008) 283(33):22700–8. doi: 10.1074/jbc.M801765200
159. Lu H, Forbes RA, Verma A. Hypoxia-Inducible Factor 1 Activation by Aerobic Glycolysis Implicates the Warburg Effect in Carcinogenesis. *J Biol Chem* (2002) 277(26):23111–5. doi: 10.1074/jbc.M202487200
160. Cui W, Wu F, Ma L. Hypoxia Associated Biomarkers in Lung Cancer - an Update. *Eur Rev Med Pharmacol Sci* (2017) 21(3 Suppl):43–6 https://www.europeanreview.org/article/13047.
161. Ullah MS, Davies AJ, Halestrap AP. The Plasma Membrane Lactate Transporter MCT4, But Not MCT1, is Up-Regulated by Hypoxia Through a HIF-1alpha-Dependent Mechanism. *J Biol Chem* (2006) 281(14):9030–7. doi: 10.1074/jbc.M511397200
162. McDonald PC, Dedhar S. Carbonic Anhydrase IX (CAIX) as a Mediator of Hypoxia-Induced Stress Response in Cancer Cells. *Subcell Biochem* (2014) 75:255–69. doi: 10.1007/978-94-007-7359-2_13
163. van Kuijk SJ, Yaromina A, Houben R, Niemans R, Lambin P, Dubois LJ. Prognostic Significance of Carbonic Anhydrase IX Expression in Cancer Patients: A Meta-Analysis. *Front Oncol* (2016) 6:69. doi: 10.3389/fonc.2016.00069
164. Giatromanolaki A, Harris AL, Banham AH, Contrafouris CA, Koukourakis MI. Carbonic Anhydrase 9 (CA9) Expression in Non-Small-Cell Lung Cancer: Correlation With Regulatory FOXP3+T-Cell Tumour Stroma Infiltration. *Br J Cancer* (2020) 122(8):1205–10. doi: 10.1038/s41416-020-0756-3
165. Li J, Zhang G, Wang X, Li XF. Is Carbonic Anhydrase IX a Validated Target for Molecular Imaging of Cancer and Hypoxia? *Future Oncol* (2015) 11 (10):1531–41. doi: 10.2217/fon.15.11
166. Alevizakos M, Kaltsas S, Syrigos KN. The VEGF Pathway in Lung Cancer. *Cancer Chemother Pharmacol* (2013) 72(6):1169–81. doi: 10.1007/s00280-013-2298-3
167. Bonnesen B, Pappot H, Holmstav J, Skov BG. Vascular Endothelial Growth Factor A and Vascular Endothelial Growth Factor Receptor 2 Expression in Non-Small Cell Lung Cancer Patients: Relation to Prognosis. *Lung Cancer* (2009) 66(3):314–8. doi: 10.1016/j.lungcan.2009.02.013
168. Korpanty G, Smyth E, Sullivan LA, Brekken RA, Carney DN. Antiangiogenic Therapy in Lung Cancer: Focus on Vascular Endothelial Growth Factor Pathway. *Exp Biol Med (Maywood)* (2010) 235(1):3–9. doi: 10.1258/ebm.2009.009191
169. Hendriksen EM, Span PN, Schuuring J, Peters JP, Sweep FC, van der Kogel AJ, et al. Angiogenesis, Hypoxia and VEGF Expression During Tumour Growth in a Human Xenograft Tumour Model. *Microvasc Res* (2009) 77 (2):96–103. doi: 10.1016/j.mvr.2008.11.002
170. Folkman J, Watson K, Ingber D, Hanahan D. Induction of Angiogenesis During the Transition From Hyperplasia to Neoplasia. *Nature* (1989) 339 (6219):58–61. doi: 10.1038/339058a0
171. de Mello RA, Costa BM, Reis RM, Hespanhol V. Insights Into Angiogenesis in Non-Small Cell Lung Cancer: Molecular Mechanisms, Polymorphic Genes, and Targeted Therapies. *Recent Pat Anticancer Drug Discovery* (2012) 7(1):118–31. doi: 10.2174/157489212798357994
172. Herbst RS, Johnson DH, Mininberg E, Carbone DP, Henderson T, Kim ES, et al. Phase I/II Trial Evaluating the Anti-Vascular Endothelial Growth Factor Monoclonal Antibody Bevacizumab in Combination With the HER-1/Epidermal Growth Factor Receptor Tyrosine Kinase Inhibitor Erlotinib for Patients With Recurrent Non-Small-Cell Lung Cancer. *J Clin Oncol* (2005) 23(11):2544–55. doi: 10.1200/JCO.2005.02.477
173. Hudson CC, Liu M, Chiang GG, Otterness DM, Loomis DC, Kaper F, et al. Regulation of Hypoxia-Inducible Factor 1alpha Expression and Function by the Mammalian Target of Rapamycin. *Mol Cell Biol* (2002) 22(20):7004–14. doi: 10.1128/MCB.22.20.7004-7014.2002
174. Watson JA, Watson CJ, McCann A, Baugh J. Epigenetics, the Epicenter of the Hypoxic Response. *Epigenetics* (2010) 5(4):293–6. doi: 10.4161/epi.5.4.11684
175. Iommarini L, Porcelli AM, Gasparre G, Kurelac I. Non-Canonical Mechanisms Regulating Hypoxia-Inducible Factor 1 Alpha in Cancer. *Front Oncol* (2017) 7:286. doi: 10.3389/fonc.2017.00286
176. Zhao Y, Wang XX, Wu W, Long H, Huang J, Wang Z, et al. EZH2 Regulates PD-L1 Expression *via* HIF-1alpha in Non-Small Cell Lung Cancer Cells. *Biochem Biophys Res Commun* (2019) 517(2):201–9. doi: 10.1016/j.bbrc.2019.07.039
177. Hua X, Chu H, Wang C, Shi X, Wang A, Zhang Z. Targeting USP22 With Mir305p to Inhibit the Hypoxiainduced Expression of PDL1 in Lung Adenocarcinoma Cells. *Oncol Rep* (2021) 46(4):215. doi: 10.3892/or.2021.8166
178. Giatromanolaki A, Tsolou A, Daridou E, Kouroupi M, Chlichlia K, Koukourakis MI. iNOS Expression by Tumor-Infiltrating Lymphocytes, PD-L1 and Prognosis in Non-Small-Cell Lung Cancer. *Cancers (Basel)* (2020) 12(11):3276. doi: 10.3390/cancers12113276
179. Koh YW, Lee SJ, Han JH, Haam S, Jung J, Lee HW. PD-L1 Protein Expression in Non-Small-Cell Lung Cancer and Its Relationship With the Hypoxia-Related Signaling Pathways: A Study Based on Immunohistochemistry and RNA Sequencing Data. *Lung Cancer* (2019) 129:41–7. doi: 10.1016/j.lungcan.2019.01.004
180. Ando T, Mimura K, Johansson CC, Hanson MG, Mougiakakos D, Larsson C, et al. Transduction With the Antioxidant Enzyme Catalase Protects Human T Cells Against Oxidative Stress. *J Immunol* (2008) 181(12):8382–90. doi: 10.4049/jimmunol.181.12.8382
181. Chen W, Jia Z, Pan MH, Anandh Babu PV. Natural Products for the Prevention of Oxidative Stress-Related Diseases: Mechanisms and Strategies. *Oxid Med Cell Longev* (2016) 2016:4628502. doi: 10.1155/2016/4628502
182. Cen J, Zhang L, Liu F, Zhang F, Ji BS. Long-Term Alteration of Reactive Oxygen Species Led to Multidrug Resistance in MCF-7 Cells. *Oxid Med Cell Longev* (2016) 2016:7053451. doi: 10.1155/2016/7053451
183. Rambold AS, Pearce EL. Mitochondrial Dynamics at the Interface of Immune Cell Metabolism and Function. *Trends Immunol* (2018) 39(1):6–18. doi: 10.1016/j.it.2017.08.006
184. Manaster Y, Shipony Z, Hutzler A, Kolesnikov M, Avivi C, Shalmon B, et al. Reduced CTL Motility and Activity in Avascular Tumor Areas. *Cancer Immunol Immunother* (2019) 68(8):1287–301. doi: 10.1007/s00262-019-02361-5
185. Doedens AL, Phan AT, Stradner MH, Fujimoto JK, Nguyen JV, Yang E, et al. Hypoxia-Inducible Factors Enhance the Effector Responses of CD8(+) T Cells to Persistent Antigen. *Nat Immunol* (2013) 14(11):1173–82. doi: 10.1038/ni.2714
186. Palazon A, Tyrakis PA, Macias D, Velica P, Rundqvist H, Fitzpatrick S, et al. An HIF-1alpha/VEGF-A Axis in Cytotoxic T Cells Regulates Tumor Progression. *Cancer Cell* (2017) 32(5):669–83 e5. doi: 10.1016/j.ccell.2017.10.003
187. Shehade H, Acolty V, Moser M, Oldenhove G. Cutting Edge: Hypoxia-Inducible Factor 1 Negatively Regulates Th1 Function. *J Immunol* (2015) 195 (4):1372–6. doi: 10.4049/jimmunol.1402552
188. O'Sullivan D, van der Windt GJ, Huang SC, Curtis JD, Chang CH, Buck MD, et al. Memory CD8(+) T Cells Use Cell-Intrinsic Lipolysis to Support the Metabolic Programming Necessary for Development. *Immunity* (2014) 41 (1):75–88. doi: 10.1016/j.immuni.2014.06.005
189. Hockel M, Knoop C, Schlenger K, Vorndran B, Baussmann E, Mitze M, et al. Intratumoral Po2 Predicts Survival in Advanced Cancer of the Uterine Cervix. *Radiother Oncol* (1993) 26(1):45–50. doi: 10.1016/0167-8140(93)90025-4

190. Brizel DM, Sibley GS, Prosnitz LR, Scher RL, Dewhirst MW. Tumor Hypoxia Adversely Affects the Prognosis of Carcinoma of the Head and Neck. *Int J Radiat Oncol Biol Phys* (1997) 38(2):285–9. doi: 10.1016/S0360-3016(97)00101-6
191. Meijer TW, Kaanders JH, Span PN, Bussink J. Targeting Hypoxia, HIF-1, and Tumor Glucose Metabolism to Improve Radiotherapy Efficacy. *Clin Cancer Res* (2012) 18(20):5585–94. doi: 10.1158/1078-0432.CCR-12-0858
192. Miar A, Arnaiz E, Bridges E, Beedie S, Cribbs AP, Downes DJ, et al. Hypoxia Induces Transcriptional and Translational Downregulation of the Type I IFN Pathway in Multiple Cancer Cell Types. *Cancer Res* (2020) 80(23):5245–56. doi: 10.1158/0008-5472.CAN-19-2306
193. Jain RK, Stylianopoulos T. Delivering Nanomedicine to Solid Tumors. *Nat Rev Clin Oncol* (2010) 7(11):653–64. doi: 10.1038/nrclinonc.2010.139
194. Stylianopoulos T, Munn LL, Jain RK. Reengineering the Physical Microenvironment of Tumors to Improve Drug Delivery and Efficacy: From Mathematical Modeling to Bench to Bedside. *Trends Cancer* (2018) 4(4):292–319. doi: 10.1016/j.trecan.2018.02.005
195. Stegeman H, Span PN, Peeters WJ, Verheijen MM, Grenman R, Meijer TW, et al. Interaction Between Hypoxia, AKT and HIF-1 Signaling in HNSCC and NSCLC: Implications for Future Treatment Strategies. *Future Sci OA* (2016) 2(1):FSO84. doi: 10.4155/fso.15.84
196. Daum S, Hagen H, Naismith E, Wolf D, Pircher A. The Role of Anti-Angiogenesis in the Treatment Landscape of Non-Small Cell Lung Cancer - New Combinational Approaches and Strategies of Neovessel Inhibition. *Front Cell Dev Biol* (2020) 8:610903. doi: 10.3389/fcell.2020.610903
197. Cantelmo AR, Dejos C, Kocher F, Hilbe W, Wolf D, Pircher A. Angiogenesis Inhibition in Non-Small Cell Lung Cancer: A Critical Appraisal, Basic Concepts and Updates From American Society for Clinical Oncology 2019. *Curr Opin Oncol* (2020) 32(1):44–53. doi: 10.1097/CCO.0000000000000591
198. Jayson GC, Kerbel R, Ellis LM, Harris AL. Antiangiogenic Therapy in Oncology: Current Status and Future Directions. *Lancet* (2016) 388 (10043):518–29. doi: 10.1016/S0140-6736(15)01088-0
199. Schmittnaegel M, De Palma M. Reprogramming Tumor Blood Vessels for Enhancing Immunotherapy. *Trends Cancer* (2017) 3(12):809–12. doi: 10.1016/j.trecan.2017.10.002
200. Khan KA, Kerbel RS. Improving Immunotherapy Outcomes With Anti-Angiogenic Treatments and Vice Versa. *Nat Rev Clin Oncol* (2018) 15 (5):310–24. doi: 10.1038/nrclinonc.2018.9
201. Nunn A, Linder K, Strauss HW. Nitroimidazoles and Imaging Hypoxia. *Eur J Nucl Med* (1995) 22(3):265–80. doi: 10.1007/BF01081524
202. Bell C, Dowson N, Fay M, Thomas P, Puttick S, Gal Y, et al. Hypoxia Imaging in Gliomas With 18F-Fluoromisonidazole PET: Toward Clinical Translation. *Semin Nucl Med* (2015) 45(2):136–50. doi: 10.1053/j.semnuclmed.2014.10.001
203. Rajendran JG, Krohn KA. F-18 Fluoromisonidazole for Imaging Tumor Hypoxia: Imaging the Microenvironment for Personalized Cancer Therapy. *Semin Nucl Med* (2015) 45(2):151–62. doi: 10.1053/j.semnuclmed.2014.10.006
204. Sorger D, Patt M, Kumar P, Wiebe LI, Barthel H, Seese A, et al. [18f] Fluoroazomycinarabinofuranoside (18FAZA) and [18F]Fluoromisonidazole (18FMISO): A Comparative Study of Their Selective Uptake in Hypoxic Cells and PET Imaging in Experimental Rat Tumors. *Nucl Med Biol* (2003) 30 (3):317–26. doi: 10.1016/S0969-8051(02)00442-0
205. Krohn KA, Link JM, Mason RP. Molecular Imaging of Hypoxia. *J Nucl Med* (2008) 49(Suppl 2):129S–48S. doi: 10.2967/jnumed.107.045914
206. Dubois LJ, Lieuwes NG, Janssen MH, Peeters WJ, Windhorst AD, Walsh JC, et al. Preclinical Evaluation and Validation of [18F]HX4, a Promising Hypoxia Marker for PET Imaging. *Proc Natl Acad Sci U.S.A.* (2011) 108 (35):14620–5. doi: 10.1073/pnas.1102526108
207. Chen L, Zhang Z, Kolb HC, Walsh JC, Zhang J, Guan Y. (1)(8)F-HX4 Hypoxia Imaging With PET/CT in Head and Neck Cancer: A Comparison With (1)(8)F-FMISO. *Nucl Med Commun* (2012) 33(10):1096–102. doi: 10.1097/MNM.0b013e3283571016
208. Even AJG, Reymen B, La Fontaine MD, Das M, Jochems A, Mottaghy FM, et al. Predicting Tumor Hypoxia in Non-Small Cell Lung Cancer by Combining CT, FDG PET and Dynamic Contrast-Enhanced CT. *Acta Oncol* (2017) 56(11):1591–6. doi: 10.1080/0284186X.2017.1349332
209. Reymen BJT, van Gisbergen MW, Even AJG, Zegers CML, Das M, Vegt E, et al. Nitroglycerin as a Radiosensitizer in Non-Small Cell Lung Cancer: Results of a Prospective Imaging-Based Phase II Trial. *Clin Transl Radiat Oncol* (2020) 21:49–55. doi: 10.1016/j.ctro.2019.12.002
210. Sanduleanu S, Wiel A, Lieverse RIY, Marcus D, Ibrahim A, Primakov S, et al. Hypoxia PET Imaging With [18F]-HX4-A Promising Next-Generation Tracer. *Cancers (Basel)* (2020) 12(5):1322. doi: 10.3390/cancers12051322
211. Liu T, Karlsen M, Karlberg AM, Redalen KR. Hypoxia Imaging and Theranostic Potential of [(64)Cu][Cu(ATSM)] and Ionic Cu(II) Salts: A Review of Current Evidence and Discussion of the Retention Mechanisms. *EJNMMI Res* (2020) 10(1):33. doi: 10.1186/s13550-020-00621-5
212. Bourgeois M, Rajerison H, Guerard F, Mougin-Degraef M, Barbet J, Michel N, et al. Contribution of [64Cu]-ATSM PET in Molecular Imaging of Tumour Hypoxia Compared to Classical [18F]-MISO–a Selected Review. *Nucl Med Rev Cent East Eur* (2011) 14(2):90–5. doi: 10.5603/NMR.2011.00022
213. Takahashi H, Ukawa K, Ohkawa N, Kato K, Hayashi Y, Yoshimoto K, et al. Significance of (18)F-2-Deoxy-2-Fluoro-Glucose Accumulation in the Stomach on Positron Emission Tomography. *Ann Nucl Med* (2009) 23 (4):391–7. doi: 10.1007/s12149-009-0255-3
214. Lohith TG, Kudo T, Demura Y, Umeda Y, Kiyono Y, Fujibayashi Y, et al. Pathophysiologic Correlation Between 62Cu-ATSM and 18F-FDG in Lung Cancer. *J Nucl Med* (2009) 50(12):1948–53. doi: 10.2967/jnumed.109.069021
215. Dehdashti F, Mintun MA, Lewis JS, Bradley J, Govindan R, Laforest R, et al. *In Vivo* Assessment of Tumor Hypoxia in Lung Cancer With 60Cu-ATSM. *Eur J Nucl Med Mol Imaging* (2003) 30(6):844–50. doi: 10.1007/s00259-003-1130-4
216. Minagawa Y, Shizukuishi K, Koike I, Horiuchi C, Watanuki K, Hata M, et al. Assessment of Tumor Hypoxia by 62Cu-ATSM PET/CT as a Predictor of Response in Head and Neck Cancer: A Pilot Study. *Ann Nucl Med* (2011) 25 (5):339–45. doi: 10.1007/s12149-011-0471-5
217. Garousi J, Huizing FJ, Vorobyeva A, Mitran B, Andersson KG, Leitao CD, et al. Comparative Evaluation of Affibody- and Antibody Fragments-Based CAIX Imaging Probes in Mice Bearing Renal Cell Carcinoma Xenografts. *Sci Rep* (2019) 9(1):14907. doi: 10.1038/s41598-019-51445-w
218. Carlin S, Khan N, Ku T, Longo VA, Larson SM, Smith-Jones PM. Molecular Targeting of Carbonic Anhydrase IX in Mice With Hypoxic HT29 Colorectal Tumor Xenografts. *PloS One* (2010) 5(5):e10857. doi: 10.1371/journal.pone.0010857
219. Lau J, Lin KS, Benard F. Past, Present, and Future: Development of Theranostic Agents Targeting Carbonic Anhydrase Ix. *Theranostics* (2017) 7(17):4322–39. doi: 10.7150/thno.21848
220. Bollineni VR, Kerner GS, Pruim J, Steenbakkers RJ, Wiegman EM, Koole MJ, et al. PET Imaging of Tumor Hypoxia Using 18F-Fluoroazomycin Arabinoside in Stage III-IV Non-Small Cell Lung Cancer Patients. *J Nucl Med* (2013) 54(8):1175–80. doi: 10.2967/jnumed.112.115014
221. Kinoshita T, Fujii H, Hayashi Y, Kamiyama I, Ohtsuka T, Asamura H. Prognostic Significance of Hypoxic PET Using (18)F-FAZA and (62)Cu-ATSM in Non-Small-Cell Lung Cancer. *Lung Cancer* (2016) 91:56–66. doi: 10.1016/j.lungcan.2015.11.020
222. Di Perri D, Lee JA, Bol A, Hanin FX, Janssens G, Labar D, et al. Correlation Analysis of [(18)F]fluorodeoxyglucose and [(18)F]fluoroazomycin Arabinoside Uptake Distributions in Lung Tumours During Radiation Therapy. *Acta Oncol* (2017) 56(9):1181–8. doi: 10.1080/0284186X.2017.1329594
223. Mapelli P, Bettinardi V, Fallanca F, Incerti E, Compierchio A, Rossetti F, et al. 18f-FAZA PET/CT in the Preoperative Evaluation of NSCLC: Comparison With 18F-FDG and Immunohistochemistry. *Curr Radiopharm* (2018) 11(1):50–7. doi: 10.2174/1874471010666171108162319
224. Cherk MH, Foo SS, Poon AM, Knight SR, Murone C, Papenfuss AT, et al. Lack of Correlation of Hypoxic Cell Fraction and Angiogenesis With Glucose Metabolic Rate in Non-Small Cell Lung Cancer Assessed by 18F-Fluoromisonidazole and 18F-FDG PET. *J Nucl Med* (2006) 47(12):1921–6 https://jnm.snmjournals.org/content/47/12/1921.long.
225. Sorace AG, Elkassem AA, Galgano SJ, Lapi SE, Larimer BM, Partridge SC, et al. Imaging for Response Assessment in Cancer Clinical Trials. *Semin Nucl Med* (2020) 50(6):488–504. doi: 10.1053/j.semnuclmed.2020.05.001
226. Watanabe S, Inoue T, Okamoto S, Magota K, Takayanagi A, Sakakibara-Konishi J, et al. Combination of FDG-PET and FMISO-PET as a Treatment Strategy for Patients Undergoing Early-Stage NSCLC Stereotactic Radiotherapy. *EJNMMI Res* (2019) 9(1):104. doi: 10.1186/s13550-019-0578-6

227. Thureau S, Dubray B, Modzelewski R, Bohn P, Hapdey S, Vincent S, et al. FDG and FMISO PET-Guided Dose Escalation With Intensity-Modulated Radiotherapy in Lung Cancer. *Radiat Oncol* (2018) 13(1):208. doi: 10.1186/s13014-018-1147-2
228. Vera P, Mihailescu SD, Lequesne J, Modzelewski R, Bohn P, Hapdey S, et al. Radiotherapy Boost in Patients With Hypoxic Lesions Identified by (18)F-FMISO PET/CT in Non-Small-Cell Lung Carcinoma: Can We Expect a Better Survival Outcome Without Toxicity? [RTEP5 Long-Term Follow-Up]. *Eur J Nucl Med Mol Imaging* (2019) 46(7):1448–56. doi: 10.1007/s00259-019-04285-9
229. Askoxylakis V, Dinkel J, Eichinger M, Stieltjes B, Sommer G, Strauss LG, et al. Multimodal Hypoxia Imaging and Intensity Modulated Radiation Therapy for Unresectable Non-Small-Cell Lung Cancer: The HIL Trial. *Radiat Oncol* (2012) 7:157. doi: 10.1186/1748-717X-7-157
230. Nicolay NH, Ruhle A, Wiedenmann N, Niedermann G, Mix M, Weber WA, et al. Lymphocyte Infiltration Determines the Hypoxia-Dependent Response to Definitive Chemoradiation in Head-And-Neck Cancer: Results From a Prospective Imaging Trial. *J Nucl Med* (2021) 62(4):471–8. doi: 10.2967/jnumed.120.248633
231. Yang L, Venneti S, Nagrath D. Glutaminolysis: A Hallmark of Cancer Metabolism. *Annu Rev BioMed Eng* (2017) 19:163–94. doi: 10.1146/annurev-bioeng-071516-044546
232. Goodwin J, Neugent ML, Lee SY, Choe JH, Choi H, Jenkins DMR, et al. The Distinct Metabolic Phenotype of Lung Squamous Cell Carcinoma Defines Selective Vulnerability to Glycolytic Inhibition. *Nat Commun* (2017) 8:15503. doi: 10.1038/ncomms15503
233. Lukey MJ, Wilson KF, Cerione RA. Therapeutic Strategies Impacting Cancer Cell Glutamine Metabolism. *Future Med Chem* (2013) 5(14):1685–700. doi: 10.4155/fmc.13.130
234. Lunt SY, Vander Heiden MG. Aerobic Glycolysis: Meeting the Metabolic Requirements of Cell Proliferation. *Annu Rev Cell Dev Biol* (2011) 27:441–64. doi: 10.1146/annurev-cellbio-092910-154237
235. Leithner K, Hrzenjak A, Trotzmuller M, Moustafa T, Kofeler HC, Wohlkoenig C, et al. PCK2 Activation Mediates an Adaptive Response to Glucose Depletion in Lung Cancer. *Oncogene* (2015) 34(8):1044–50. doi: 10.1038/onc.2014.47
236. Momcilovic M, McMickle R, Abt E, Seki A, Simko SA, Magyar C, et al. Heightening Energetic Stress Selectively Targets LKB1-Deficient Non-Small Cell Lung Cancers. *Cancer Res* (2015) 75(22):4910–22. doi: 10.1158/0008-5472.CAN-15-0797
237. Cairns RA, Harris IS, Mak TW. Regulation of Cancer Cell Metabolism. *Nat Rev Cancer* (2011) 11(2):85–95. doi: 10.1038/nrc2981
238. Ding L, Getz G, Wheeler DA, Mardis ER, McLellan MD, Cibulskis K, et al. Somatic Mutations Affect Key Pathways in Lung Adenocarcinoma. *Nature* (2008) 455(7216):1069–75. doi: 10.1038/nature07423
239. Davidson SM, Papagiannakopoulos T, Olenchock BA, Heyman JE, Keibler MA, Luengo A, et al. Environment Impacts the Metabolic Dependencies of Ras-Driven Non-Small Cell Lung Cancer. *Cell Metab* (2016) 23(3):517–28. doi: 10.1016/j.cmet.2016.01.007
240. Momcilovic M, Bailey ST, Lee JT, Fishbein MC, Braas D, Go J, et al. The GSK3 Signaling Axis Regulates Adaptive Glutamine Metabolism in Lung Squamous Cell Carcinoma. *Cancer Cell* (2018) 33(5):905–21 e5. doi: 10.1016/j.ccell.2018.04.002
241. Zhang L, Romero P. Metabolic Control of CD8(+) T Cell Fate Decisions and Antitumor Immunity. *Trends Mol Med* (2018) 24(1):30–48. doi: 10.1016/j.molmed.2017.11.005
242. Nakaya M, Xiao Y, Zhou X, Chang JH, Chang M, Cheng X, et al. Inflammatory T Cell Responses Rely on Amino Acid Transporter ASCT2 Facilitation of Glutamine Uptake and Mtorc1 Kinase Activation. *Immunity* (2014) 40(5):692–705. doi: 10.1016/j.immuni.2014.04.007
243. Metzler B, Gfeller P, Guinet E. Restricting Glutamine or Glutamine-Dependent Purine and Pyrimidine Syntheses Promotes Human T Cells With High FOXP3 Expression and Regulatory Properties. *J Immunol* (2016) 196(9):3618–30. doi: 10.4049/jimmunol.1501756
244. Lemos H, Huang L, Prendergast GC, Mellor AL. Immune Control by Amino Acid Catabolism During Tumorigenesis and Therapy. *Nat Rev Cancer* (2019) 19(3):162–75. doi: 10.1038/s41568-019-0106-z
245. Saito K, Markey SP, Heyes MP. Effects of Immune Activation on Quinolinic Acid and Neuroactive Kynurenines in the Mouse. *Neuroscience* (1992) 51 (1):25–39. doi: 10.1016/0306-4522(92)90467-G
246. Katz JB, Muller AJ, Prendergast GC. Indoleamine 2,3-Dioxygenase in T-Cell Tolerance and Tumoral Immune Escape. *Immunol Rev* (2008) 222:206–21. doi: 10.1111/j.1600-065X.2008.00610.x
247. Taniguchi T, Sono M, Hirata F, Hayaishi O, Tamura M, Hayashi K, et al. Indoleamine 2,3-Dioxygenase. Kinetic Studies on the Binding of Superoxide Anion and Molecular Oxygen to Enzyme. *J Biol Chem* (1979) 254(9):3288–94. doi: 10.1016/S0021-9258(18)50757-2
248. Batabyal D, Yeh SR. Human Tryptophan Dioxygenase: A Comparison to Indoleamine 2,3-Dioxygenase. *J Am Chem Soc* (2007) 129(50):15690–701. doi: 10.1021/ja076186k
249. Lieberman BP, Ploessl K, Wang L, Qu W, Zha Z, Wise DR, et al. PET Imaging of Glutaminolysis in Tumors by 18F-(2S,4R)4-Fluoroglutamine. *J Nucl Med* (2011) 52(12):1947–55. doi: 10.2967/jnumed.111.093815
250. Qu W, Oya S, Lieberman BP, Ploessl K, Wang L, Wise DR, et al. Preparation and Characterization of L-[5-11C]-Glutamine for Metabolic Imaging of Tumors. *J Nucl Med* (2012) 53(1):98–105. doi: 10.2967/jnumed.111.093831
251. Zhu L, Ploessl K, Zhou R, Mankoff D, Kung HF. Metabolic Imaging of Glutamine in Cancer. *J Nucl Med* (2017) 58(4):533–7. doi: 10.2967/jnumed.116.182345
252. Hassanein M, Hight MR, Buck JR, Tantawy MN, Nickels ML, Hoeksema MD, et al. Preclinical Evaluation of 4-[18F]Fluoroglutamine PET to Assess ASCT2 Expression in Lung Cancer. *Mol Imaging Biol* (2016) 18(1):18–23. doi: 10.1007/s11307-015-0862-4
253. Dunphy MPS, Harding JJ, Venneti S, Zhang H, Burnazi EM, Bromberg J, et al. *In Vivo* PET Assay of Tumor Glutamine Flux and Metabolism: In-Human Trial of (18)F-(2s,4r)-4-Fluoroglutamine. *Radiology* (2018) 287 (2):667–75. doi: 10.1148/radiol.2017162610
254. Grkovski M, Goel R, Krebs S, Staton KD, Harding JJ, Mellinghoff IK, et al. Pharmacokinetic Assessment of (18)F-(2s,4r)-4-Fluoroglutamine in Patients With Cancer. *J Nucl Med* (2020) 61(3):357–66. doi: 10.2967/jnumed.119.229740
255. Xu X, Zhu H, Liu F, Zhang Y, Yang J, Zhang L, et al. Dynamic PET/CT Imaging of (18)F-(2S, 4R)4-Fluoroglutamine in Healthy Volunteers and Oncological Patients. *Eur J Nucl Med Mol Imaging* (2020) 47(10):2280–92. doi: 10.1007/s00259-019-04543-w
256. Zhu H, Liu F, Zhang Y, Yang J, Xu X, Guo X, et al. (2s,4r)-4-[(18)F] Fluoroglutamine as a PET Indicator for Bone Marrow Metabolism Dysfunctional: From Animal Experiments to Clinical Application. *Mol Imaging Biol* (2019) 21(5):945–53. doi: 10.1007/s11307-019-01319-4
257. Ulaner GA, Schuster DM. Amino Acid Metabolism as a Target for Breast Cancer Imaging. *PET Clin* (2018) 13(3):437–44. doi: 10.1016/j.cpet.2018.02.009
258. Tade FI, Cohen MA, Styblo TM, Odewole OA, Holbrook AI, Newell MS, et al. Anti-3-18f-FACBC (18f-Fluciclovine) PET/CT of Breast Cancer: An Exploratory Study. *J Nucl Med* (2016) 57(9):1357–63. doi: 10.2967/jnumed.115.171389
259. Teoh EJ, Tsakok MT, Bradley KM, Hyde K, Subesinghe M, Gleeson FV. Recurrent Malignant Melanoma Detected on 18F-Fluciclovine PET/CT Imaging for Prostate Cancer. *Clin Nucl Med* (2017) 42(10):803–4. doi: 10.1097/RLU.0000000000001789
260. Amzat R, Taleghani P, Miller DL, Beitler JJ, Bellamy LM, Nye JA, et al. Pilot Study of the Utility of the Synthetic PET Amino-Acid Radiotracer Anti-1-Amino-3-[(18)F]fluorocyclobutane-1-Carboxylic Acid for the Noninvasive Imaging of Pulmonary Lesions. *Mol Imaging Biol* (2013) 15(5):633–43. doi: 10.1007/s11307-012-0606-7
261. Nguyen NC, Muthukrishnan A, Mountz JM. Differential 18f-FDG and 18F-Fluciclovine Uptake Pattern in a Patient With Poorly Differentiated Adenocarcinoma of the Lung and Prostate Cancer Biochemical Recurrence. *Clin Nucl Med* (2020) 45(1):e63–e4. doi: 10.1097/RLU.0000000000002781
262. Juhasz C, Chugani DC, Muzik O, Wu D, Sloan AE, Barger G, et al. *In Vivo* Uptake and Metabolism of Alpha-[11C]Methyl-L-Tryptophan in Human Brain Tumors. *J Cereb Blood Flow Metab* (2006) 26(3):345–57. doi: 10.1038/sj.jcbfm.9600199
263. John F, Muzik O, Mittal S, Juhasz C. Fluorine-18-Labeled PET Radiotracers for Imaging Tryptophan Uptake and Metabolism: A Systematic Review. *Mol Imaging Biol* (2020) 22(4):805–19. doi: 10.1007/s11307-019-01430-6
264. Henrottin J, Lemaire C, Egrise D, Zervosen A, Van den Eynde B, Plenevaux A, et al. Fully Automated Radiosynthesis of N(1)-[(18)F]fluoroethyl-Tryptophan and Study of Its Biological Activity as a New Potential Substrate for Indoleamine 2,3-Dioxygenase PET Imaging. *Nucl Med Biol* (2016) 43(6):379–89. doi: 10.1016/j.nucmedbio.2016.03.001

265. Yue X, Xin Y, Zhang S, Nikam R, Kandula V, Choudhary AK, et al. Automated Production of 1-(2-[(18)F]fluoroethyl)-L-Tryptophan for Imaging of Tryptophan Metabolism. *Appl Radiat Isot* (2020) 156:109022. doi: 10.1016/j.apradiso.2019.109022
266. Ma X, Zou F, Yu F, Li R, Yuan Y, Zhang Y, et al. Nanoparticle Vaccines Based on the Receptor Binding Domain (RBD) and Heptad Repeat (HR) of SARS-CoV-2 Elicit Robust Protective Immune Responses. *Immunity* (2020) 53 (6):1315–30 e9. doi: 10.1016/j.immuni.2020.11.015
267. Hensley CT, Faubert B, Yuan Q, Lev-Cohain N, Jin E, Kim J, et al. Metabolic Heterogeneity in Human Lung Tumors. *Cell* (2016) 164(4):681–94. doi: 10.1016/j.cell.2015.12.034
268. Bussink J, van Herpen CM, Kaanders JH, Oyen WJ. PET-CT for Response Assessment and Treatment Adaptation in Head and Neck Cancer. *Lancet Oncol* (2010) 11(7):661–9. doi: 10.1016/S1470-2045(09) 70353-5
269. Matsumoto KI, Mitchell JB, Krishna MC. Multimodal Functional Imaging for Cancer/Tumor Microenvironments Based on MRI, EPRI, and PET. *Molecules* (2021) 26(6):1614. doi: 10.3390/molecules26061614
270. Kessler DA, Austin RH, Levine H. Resistance to Chemotherapy: Patient Variability and Cellular Heterogeneity. *Cancer Res* (2014) 74(17):4663–70. doi: 10.1158/0008-5472.CAN-14-0118
271. McGranahan N, Swanton C. Biological and Therapeutic Impact of Intratumor Heterogeneity in Cancer Evolution. *Cancer Cell* (2015) 27 (1):15–26. doi: 10.1016/j.ccell.2014.12.001
272. Miller A, Nagy C, Knapp B, Laengle J, Ponweiser E, Groeger M, et al. Exploring Metabolic Configurations of Single Cells Within Complex Tissue Microenvironments. *Cell Metab* (2017) 26(5):788–800 e6. doi: 10.1016/j.cmet.2017.08.014
273. Rossi G, Barabino E, Fedeli A, Ficarra G, Coco S, Russo A, et al. Radiomic Detection of EGFR Mutations in NSCLC. *Cancer Res* (2021) 81(3):724–31. doi: 10.1158/0008-5472.CAN-20-0999
274. Dercle L, Fronheiser M, Lu L, Du S, Hayes W, Leung DK, et al. Identification of Non-Small Cell Lung Cancer Sensitive to Systemic Cancer Therapies Using Radiomics. *Clin Cancer Res* (2020) 26(9):2151–62. doi: 10.1158/1078-0432.CCR-19-2942
275. Lee G, Lee HY, Park H, Schiebler ML, van Beek EJR, Ohno Y, et al. Radiomics and Its Emerging Role in Lung Cancer Research, Imaging Biomarkers and Clinical Management: State of the Art. *Eur J Radiol* (2017) 86:297–307. doi: 10.1016/j.ejrad.2016.09.005
276. Ling CC, Humm J, Larson S, Amols H, Fuks Z, Leibel S, et al. Towards Multidimensional Radiotherapy (MD-CRT): Biological Imaging and Biological Conformality. *Int J Radiat Oncol Biol Phys* (2000) 47(3):551–60. doi: 10.1016/S0360-3016(00)00467-3
277. La Fontaine M, Vogel W, van Diessen J, van Elmpt W, Reymen B, Persson G, et al. A Secondary Analysis of FDG Spatio-Temporal Consistency in the Randomized Phase II PET-Boost Trial in Stage II-III NSCLC. *Radiother Oncol* (2018) 127(2):259–66. doi: 10.1016/j.radonc.2018.03.020
278. Meijer TWH, Wijsman R, Usmanij EA, Schuurbiers OCJ, Kollenburg PV, Bouwmans L, et al. Stereotactic Radiotherapy Boost After Definite Chemoradiation for Non-Responding Locally Advanced NSCLC Based on Early Response Monitoring (18)F-FDG-PET/Ct. *Phys Imaging Radiat Oncol* (2018) 7:16–22. doi: 10.1016/j.phro.2018.08.003
279. Brown JM, Diehn M, Loo BWJr. Stereotactic Ablative Radiotherapy Should be Combined With a Hypoxic Cell Radiosensitizer. *Int J Radiat Oncol Biol Phys* (2010) 78(2):323–7. doi: 10.1016/j.ijrobp.2010.04.070
280. Scarantino CW, McCunniff AJ, Evans G, Young CW, Paggiarino DA. A Prospective Randomized Comparison of Radiation Therapy Plus Lonidamine Versus Radiation Therapy Plus Placebo as Initial Treatment of Clinically Localized But Nonresectable Nonsmall Cell Lung Cancer. *Int J Radiat Oncol Biol Phys* (1994) 29(5):999–1004. doi: 10.1016/0360-3016(94)90394-8
281. Liu L, Bai H, Wang C, Seery S, Wang Z, Duan J, et al. Efficacy and Safety of First-Line Immunotherapy Combinations for Advanced NSCLC: A Systematic Review and Network Meta-Analysis. *J Thorac Oncol* (2021) 16 (7):1099–117. doi: 10.1016/j.jtho.2021.03.016
282. Socinski MA, Nishio M, Jotte RM, Cappuzzo F, Orlandi F, Stroyakovskiy D, et al. IMpower150 Final Overall Survival Analyses for Atezolizumab Plus Bevacizumab and Chemotherapy in First-Line Metastatic Nonsquamous NSCLC. *J Thorac Oncol* (2021) 16(11):1909–24. doi: 10.1016/j.jtho.2021.07.009
283. Reck M, Rodriguez-Abreu D, Robinson AG, Hui R, Csoszi T, Fulop A, et al. Five-Year Outcomes With Pembrolizumab Versus Chemotherapy for Metastatic Non-Small-Cell Lung Cancer With PD-L1 Tumor Proportion Score >/= 50. *J Clin Oncol* (2021) 39(21):2339–49. doi: 10.1200/JCO.21.00174
284. Planchard D, Popat S, Kerr K, Novello S, Smit EF, Faivre-Finn C, et al. Metastatic Non-Small Cell Lung Cancer: ESMO Clinical Practice Guidelines for Diagnosis, Treatment and Follow-Up. *Ann Oncol* (2018) 29(Suppl 4): iv192–237. doi: 10.1093/annonc/mdy275
285. Tang J, Shalabi A, Hubbard-Lucey VM. Comprehensive Analysis of the Clinical Immuno-Oncology Landscape. *Ann Oncol* (2018) 29(1):84–91. doi: 10.1093/annonc/mdx755


**Conflict of Interest:** MH received research grants from AstraZeneca, BristolMeyerSquibb, Janssen Pharmaceutica, Stichting Treatmeds, Merck, MSD, Novartis, Pamgene, Pfizer, Roche, Roche diagnostics, and received fees from Abbvie, Astrazeneca, BMS, Lilly,MSD, Novartis, Pfizer, Roche, none related to this manuscript.

The remaining authors declare that the research was conducted in the absence of any commercial or financial relationships that could be construed as a potential conflict of interest.

**Publisher's Note:** All claims expressed in this article are solely those of the authors and do not necessarily represent those of their affiliated organizations, or those of the publisher, the editors and the reviewers. Any product that may be evaluated in this article, or claim that may be made by its manufacturer, is not guaranteed or endorsed by the publisher.

# Advantages of publishing in Frontiers

**OPEN ACCESS**
Articles are free to read for greatest visibility and readership

**FAST PUBLICATION**
Around 90 days from submission to decision

**HIGH QUALITY PEER-REVIEW**
Rigorous, collaborative, and constructive peer-review

**TRANSPARENT PEER-REVIEW**
Editors and reviewers acknowledged by name on published articles

**Frontiers**
Avenue du Tribunal-Fédéral 34
1005 Lausanne | Switzerland

**Visit us:** www.frontiersin.org
**Contact us:** frontiersin.org/about/contact

**REPRODUCIBILITY OF RESEARCH**
Support open data and methods to enhance research reproducibility

**DIGITAL PUBLISHING**
Articles designed for optimal readership across devices

**FOLLOW US**
@frontiersin

**IMPACT METRICS**
Advanced article metrics track visibility across digital media

**EXTENSIVE PROMOTION**
Marketing and promotion of impactful research

**LOOP RESEARCH NETWORK**
Our network increases your article's readership